



Engineering of multiparticulate systems to modify the drug release across orally disintegrating tablets

Nihad Al-Hashimi

**A thesis submitted in fulfillment of the requirements for the degree of
Doctor of Philosophy (PhD)**

**Kingston University London,
United Kingdom
September, 2021**

Summary and work novelty

Orally disintegrating tablets (ODTs) or orally dispersible tablets are a new dosage that can degrade within less than 3 minutes once they contact the patients' saliva in the mouth. ODTs are considered an effective dosage form in delivering the drug for patients suffering from swallowing difficulty known as dysphagia. The drug is released and absorbed through the mouth's mucosal tissue, allowing a rapid onset of action because the tissue has a high blood supply. Besides, ease of ingestion made the ODTs popular among geriatrics and paediatrics. Nevertheless, administering multiple daily doses of medication for long-term conditions affects patient adherence and can lead to hospitalisation and health complications.

Therefore, the use of modified-release formulations (prolonged and delayed-release dosage forms) offers several advantages over the immediate release formulations, including lowering drug-level fluctuations in plasma, minimising the local side effect of drug release reducing the dose frequency enhancing patient compliance.

Indomethacin (IND) and propranolol hydrochloride (PRH) were applied as model drugs to evaluate their release profile. Both model drugs are widely used by many patients of different ages, elderly or young. However, IND use is associated with gastric side effects, including heartburn, gastric irritation, stomach pain, and vomiting (FDA, 2008). The side effect of immediate drug release associated with IND could influence patient compliance. On the other hand, as referred to earlier, reducing the dose frequency associated with chronic medication use such as propranolol is significantly essential. Propranolol is a widely used treatment for high blood pressure, irregular heartbeat, migraine, or angina 2-3 times a day, depending on the health issue (NHS, 2018).

Therefore, in this thesis novel, approaches were applied to

1. The delay indomethacin (IND) release reduces the gastric side effect via multiparticulates (microparticles and pellets) using ODTs.
2. The modification of propranolol hydrochloride (PRH) release reduces dose frequency and enhances patient adherence using pellets embedded in ODTs.

Keywords: multiparticulates, indomethacin, propranolol, compaction, ODTs

Abstract

Background and Aim: Orally disintegrating tablets (ODTs) combined with multiparticulate formulations of modified-release (MR) properties are considered more efficient medicinal options than traditional immediate-release formulations. ODTs & MR multiparticulates provide ease of medicinal use for dysphagic patients allowing a modified drug release to reduce the undesirable side effects, and the frequent daily dose would be eliminated, thus enhancing patient compliance. Nevertheless, the compaction of multiparticulates is challenging, causing polymeric damage leading to a loss in integrity and a rapid drug release. This project aims to prepare ODTs-MR of indomethacin (IND) and propranolol hydrochloride (PRH) by enhancing mechanical properties and the parameters of ODTs and multiparticulates production.

Methods: Two developed and validated HPLC methods (according to ICH guidelines) were utilized to detect and quantify indomethacin (IND) and propranolol hydrochloride (PRH) release from the prepared formulations. The direct compression method was used to prepare ODTs, extrusion spheronization and spray drying to prepare the multiparticulates. The mechanical properties of ODTs and multiparticulates were assessed using texture analysis and hardness testing. Through the project, all formulations were examined using disintegration time, dissolution studies (pH 1.2 and 6.8), thermogravimetric analysis (TGA), differential scanning calorimetry (DSC), scanning electron microscopy (SEM) and stereomicroscope.

Results and discussion: IND loaded microparticles of Eudragit L100 were successfully delayed IND release in pH 1.2 buffer using acetone as a solvent. The low value of YM, using the appropriate solvent type and setting feed concentration at 5% w/v, was appropriate for modifying IND release. Similarly, Eudragit L100 was used to prepare IND loaded pellets. Lactose and mannitol (63, 125 and 500 μm) ODTs comprised of IND loaded pellets disintegrated in less than 30 seconds with acceptable mechanical properties of less than 1.5 MPa and an adequate elastic profile. Also, ODTs-pellets from lactose and mannitol delayed IND release in acidic media to less than 1.07% at 120 minutes while released more than 93% at 120 minutes in phosphate buffer (pH 6.8). Furthermore, the tensile strength of IND-pellets of Eudragit L100 (45, 63 and 90 μm) was directly proportional to YM ($p < 0.05$),

offering enough support to maintain their integrity under compression. In addition, the *in vitro* release study showed a delayed release of IND in the acidic media (pH 1.2) and an immediate release in the buffer media (pH 6.8). On the other hand, the matrix system was unapplicable to delay PRH release from Eudragit RS based pellets despite changing the ratio and type of plasticisers. However, PRH pellets of reservoir system using Eudragit RS, Eudragit RL and combination of Eudragit RS: RL (1:1) w/w showed that the mechanical properties of the coated pellets differ significantly from the uncoated batch ($p < 0.05$). Besides, ODTs reservoir-pellets were able to modify PRH release to $\leq 53.9\%$ in acidic media and $\leq 47.2\%$ in phosphate buffer for 30 minutes, while the uncoated pellets released $> 75\%$ of PRH. Alongside, EDEM® successfully simulated the compaction process and showed that increasing compression force at the beginning of compression strengthens the interparticulate bonds at the surfaces resulting from the low surface roughness.

Conclusion: Matrix system to sustain IND release was achieved using Eudragit L100 microparticles and pellets embedded in the ODTs. The lowest percentage of propranolol release was attained from the reservoir system of Eudragit RS and RL pellets embedded in the ODTs. All formulations of ODTs disintegrated in less than 30 seconds. A balance between Young's modulus and tensile strength is essential to enhance the integrity of the multiparticulates and, eventually, drug release

Keywords: multiparticulates, compaction, ODTs, pellets, IND, PRH

Dedication

For all their absolute love and support and putting my dreams and wishes before theirs, I would never be able to accomplish all this without you. No words can be enough to thank you for being there at every stage of my life and for believing in me even when I had no faith in myself. Mother, your love, support, prayers, and numerous sacrifices are the reason I keep advancing. The PhD studies would not have been feasible without my family's enormous encouragement and support throughout the years.

Especially my father that I have lost him before making him to observe this important moment of my life. I hope he would be proud of what I have accomplished. Father, you could have never been a better role model for a daughter than you already were.

I hope I live up to your anticipations. May your pure loving soul rest in endless peace.

To people who supported me, friends, siblings and for infinite support

Professor Mehmet Dorak, Professor Reem Kayyali, Dr Carline Kim, Dr Liz Osaba, and my friends Dr Najma Easa, Dr Sarah Fawaz, Amtul Bhunnoo, Mai Babenko and Wafa for being the best cheerleading squad understanding.

To the one who always supported, encouraged, and motivated me during difficult times, and I lost during PhD, my aunt Dr Kawakib Jaber.

Acknowledgement

All the praises and thanks be to Almighty God, who has guided me to fulfil my research with protection and ability to do work.

Thanks, is not enough to express my gratitude and appreciation to my supervisors.

Dr Amr Elshaer without your guidance and support I would not be able to carry on with my studies. Your supervision brought this work towards a completion.

Prof Raid Alany I am so grateful to your guidance and supervision, and I am so proud that I have been one of your students all the last years.

Dr Mohammed Khoder I am thankful for your supervision and grateful for your support, knowledge, and involvement.

My special and heartily thanks to Prof Foot, Dr Huda Morgan, Dr Siamak Soltani, Dr Lauren Mulcahy, Richard Giddens and Wendy Brosnan. I thank all who in one way or another contributed to the completion of this thesis from family and at Kingston university.

Thank you all for consistently guiding this work in the direction to be completed and for steering me in the right direction.

Oral/Poster presentations

1. Enhancement of microparticles compaction properties for the sustained release Orodispersible tablets. Nihad AL-hashimi¹, Dania Hussein², Raid Alany¹, Mohammed Khoder², Amr Elshaer². Poster presentation at UKICRS conference, university of Strathclyde, Glasgow 2017
2. The correlation between particles size and elastic properties of pharmaceutical polymers. Nihad AL-hashimi¹, Abyan Hodon², Raid Alany¹, Mohammed Khoder², Amr Elshaer². Poster presentation at UKICRS conference, university of Strathclyde, Glasgow 2017
3. Orodispersible tablets of modified propranolol hydrochloride release across the particulate system. Nihad Al-Hashimi, Rona Faizy, Raid Alany, Mohammed Khoder, Amr Elshaer. Oral presentations at Chemistry & Pharmacy Research Group, Kingston university London, 2019
4. Modification of indomethacin release across Orodispersible tablets using pH dependent polymers. Nihad Al-hashimi¹, Raid Alany¹, Mohammed Khoder¹, Amr Elshaer¹. Poster presentation at Sheffield university workshop in Lausanne, Switzerland, 2019
5. Orodispersible tablets of modified indomethacin release across the particulate system. Nihad Al-hashimi¹, Raid Alany¹, Mohammed Khoder¹, Amr Elshaer¹. Poster presentation in the APS International PharmSci Conference, University of Greenwich, 2019
6. Modification of indomethacin release using Orodispersible tablets through Eudragit L100 pellets. Nihad Al-hashimi¹, Raid Alany¹, Mohammed Khoder¹, Amr Elshaer¹. Poster presentation at Royal Society of Chemistry event, Kingston University London, 2019

Publications/Manuscripts

1. Al-Hashimi, N., Babenko, M., Saaed, M., Kargar, N. and ElShaer, A., 2021. The Impact of Natural and Synthetic Polymers in Formulating Micro and Nanoparticles for Anti-Diabetic Drugs. *Current Drug Delivery*, [online] 18(3), pp.271-288. Available at: <<https://www.eurekaselect.com/184724/article>>.

2. Al-Hashimi, N., Begg, N., Alany, R., Hassanin, H. and Elshaer, A., 2018. Oral Modified Release Multiple-Unit Particulate Systems: Compressed Pellets, Microparticles and Nanoparticles. *Pharmaceutics*, [online] 10(4), p.176. Available at: <<https://www.mdpi.com/1999-4923/10/4/176>>.
3. Modification of propranolol release via time-dependent polymers and different plasticisers (in progress)
4. Delay indomethacin release using pH-dependent polymers via orally disintegrating tablets (in progress)

Awards and honours

1. Best poster award winner from GSK, Lausanne, Switzerland, 2019
2. Achievement Award Winner from Kingston University, 2019

Professional membership

1. Member of the Academy of Pharmaceutical Sciences, UK, 2021-2022
2. Editorial Board Member of the International Journal of Pharmacy and Chemistry 2019 and 2020
3. Peer-reviewing for Pharmaceutical Development & Technology 2018, 2019 & 2021
4. Associate Member of the UK higher education academy 2019- Current
5. Member of United Kingdom and Ireland Controlled Release Society 2017- Current

Table of contents

Chapter 1 General introduction	1
1.1 Background.....	2
1.2 Modified drug release particles via oral disintegrating tablets (MR-ODTs)	3
1.3 MR-formulations and the associated challenges.....	4
1.3.1 Polymers used in the preparation of MR-ODTs	5
1.3.2 Plasticisers and the enhancement of the formulation's mechanical properties	6
1.4 Introduction to the literature review	7
1.5 Challenges of the compression of multiparticulates	8
1.6 Compaction process	9
1.7 Compaction of microparticulate systems into MR Tablets.....	10
1.7.1 Microcapsules and Microspheres	10
1.7.2 Tablets of coated nanocapsules.....	10
1.8 Microspheres & Microcapsules MR tablets	12
1.8.1 The coating layers	12
1.8.2 The coating layer: thickness and polymeric quantity	13
1.8.3 Excipients: an additional role in enhancing the mechanical properties of the tablets.....	14
1.8.4 The compaction forces	15
1.9 Multiparticulate Drug Delivery Systems: Pellets.....	15
1.9.1 Compression of pellets into tablets.....	17
1.9.2 Role of the plasticisers.....	24
1.9.3 Pellet size	25
1.9.4 Pellets' porosity.....	25
1.10 Assessment of the compaction performance of multiparticulate systems	26
1.11 Aim and objectives	28
Chapter 2 Experimental: General materials and methods.....	29

2.1 Experimental	30
2.2 Materials	30
2.3 Methods	30
2.3.1 Pellet's preparation	31
2.3.1.3 Spheronization of extrudates.....	31
2.3.2 Physical characterization	32
2.3.3 Mechanical properties.....	34
2.3.4 Thermal analysis.....	36
2.3.5 Preparation of ODTs	37
2.3.6 Morphology, shape and size	38
2.3.6.2 Scanning electron microscope (SEM)	39
2.3.7 High-performance liquid chromatography (HPLC) Analysis.....	40
2.3.8 Dissolution tests.....	40
2.3.9 Compressibility of powder batches	40
2.4 Statistical methods.....	41
Chapter 3 Screening synthetic and natural polymers in the preparation of multiparticulates	42
3.1 Introduction	44
3.1.1 Polymers' suitability to modify the drug release	44
3.2 Aim and objectives	48
3.3 Experimental	49
3.3.1 Materials	49
3.3.2 Methods	49
3.4 Results and Discussion.....	54
3.4.1 Raw polymers	54
3.4.2 Effect of spray-drying on polymers' characteristics.....	73
3.5 Conclusion	88

Chapter 4 Method development and validation for detection and quantification of indomethacin and propranolol hydrochloride.....	90
4.1 Introduction	92
4.1.1 Model drugs: indomethacin (IND) and propranolol hydrochloride (PRH) ..	92
4.2 Analytical methods.....	93
4.2.1 High-performance liquid chromatography (HPLC)	94
4.3 Aim and objectives.....	101
4.3.1 Aim	101
4.3.2 Objectives	101
4.4 Experimental	102
4.4.1 Materials	102
4.4.2 Methods.....	102
4.5 Method validation.....	107
4.5.1 Standard solutions	107
4.5.2 Preparation of IND standard solutions	107
4.5.3 Preparation of PRH standard solutions.....	107
4.5.4 Validation	107
4.5.5 Linearity and range	108
4.5.6 Specificity.....	108
4.5.7 Accuracy	108
4.5.8 Precision	108
4.5.9 Robustness.....	109
4.5.10 Detection Limit (LOD) and Quantitation Limit (LOQ).....	109
4.6 Statistical analysis.....	110
4.7 Results and discussion	111
4.7.1 Method validation and optimisation of IND.....	111
4.7.2 Method validation and optimisation of PRH	116

4.8 Conclusion	121
Chapter 5 Delaying of indomethacin release through pH-dependent polymeric microparticles embedded in the orally disintegrating tablets	122
5.1 Introduction	124
5.1.1 Microparticles and ODTs combination	124
5.1.2 Overview of of spray drying parameter settings.....	126
5.2 Aim and objectives.....	128
5.2.1 Aim	128
5.2.2 Objectives	128
5.3 Experimental	129
5.3.1 Materials	129
5.3.2 Methods.....	129
5.3.2.11 Melt quench cooling.....	132
5.4 Results and discussion	134
5.4.1 Powder properties: Flowability and bulk density	134
5.4.2 Particle size and morphology.....	136
5.4.3 Mechanical properties: Elasticity profile for SD-IND particles	143
5.4.4 Tablet hardness and disintegration time	145
5.4.5 Thermal analysis DSC and TGA.....	149
5.4.6 Dissolution	154
5.5 Conclusion	160
Chapter 6 Effect of excipients particle size on IND release from ODTs containing pellets.....	161
6.1 Overview	163
6.1 Pellets	163
6.1.1 Pellets production methods.....	164
6.1.2 Extrusion-Spheronisation technique	165
6.2 Delayed-release pellets in orally disintegrating tablets (DRP-ODTs)	165

6.3 ODT matrix.....	167
6.3.1 Excipients of ODTs	168
6.3.2 Low-substituted Hydroxypropyl Cellulose (LHPC)	169
6.3.3 Magnesium Stearate.....	169
6.3.4 Lactose	169
6.3.5 Mannitol	170
6.4 Aims.....	172
6.5 Objectives	172
6.6 Experimental	173
6.6.1 Materials	173
6.6.2 Methods.....	173
6.7 Results and discussion of the first study	177
6.7.1 Preparation and evaluation of pellets.....	177
6.7.2 Flow properties analysis	178
6.7.3 Pellet's size and morphology	179
6.7.4 Pellets mechanical properties	183
6.7.5 Porosity.....	185
6.7.6 Thermal Analysis	186
6.7.7 Physical characterisation and particle size analysis	189
6.7.8 Mechanical properties of pellets and powder mix	191
6.7.9 Hardness of tablets.....	193
6.7.10 Lactose and mannitol ODTs morphology after compression	198
6.7.11 Disintegration of tablets	201
6.7.12 Dissolution	203
6.8 Results and discussion of the second study	211
6.8.1 Powder characterization	211
6.8.2 Powder flowability and density.....	211

6.8.3 Morphology and size of powder particles.....	213
6.8.4 Texture analysis.....	216
6.8.5 Porosity.....	217
6.8.6 Pellet's characterization and micrometric properties.....	217
6.8.7 Thermal analysis.....	227
6.8.8 Tablet's characterization	230
6.8.9 IND release analysis.....	234
6.8.10 Dissolution test	234
6.9 Conclusion	239
Chapter 7 Evaluation of propranolol hydrochloride release via matrix and reservoir pellets of time-dependent polymer	240
7.1 Background.....	243
7.1.1 Pellets excipients and core materials.....	243
7.1.2 Polymers of modified-release properties	244
7.1.3 Effect of plasticizers.....	245
7.1.4 Direct compression for tablets preparation	252
7.2 Aim and objectives.....	254
7.2.1 Aims.....	254
7.2.2 Objectives	254
7.3 Experimental	255
7.3.1 Materials	255
7.3.2 Methods.....	255
7.4 Results and discussion of the first study	260
7.4.1 Preparation of pellets.....	260
7.4.2 Tablets mechanical strength	273
7.5 Results and discussion of the second study	284
7.5.1 Pellets formulations and optimisation process parameters	284

7.5.2 Differential scanning calorimetry (DSC) and Thermogravimetric analysis (TGA).....	296
7.5.3 Tablet's characterisation.....	299
7.5.4 Dissolution studies.....	302
7.6 Conclusion.....	308
Chapter 8 Modelling trials in understanding compression performance of pellets to be used in the orally disintegrating tablet.....	309
8.1 Overview.....	311
8.1.1 Pellets in modified release dosage forms.....	313
8.1.2 Software simulation.....	315
8.1.3 Theory of Discrete Element Method.....	318
8.2 Aim and objective.....	321
8.2.1 Aim.....	321
8.2.2 Objectives.....	321
8.3 Experimental.....	322
8.3.1 Materials.....	322
8.3.2 Methods.....	322
8.4 Results and discussion.....	332
8.4.1 Micrometric data of pellets.....	332
8.4.2 Mechanical properties.....	334
8.4.3 Morphological characterization.....	337
8.4.4 Thermal analysis.....	340
8.4.5 Software simulation.....	342
8.5 Conclusion.....	351
Chapter 9 The summary, conclusions, and future perspectives.....	352
9.1 Summary and a general conclusion.....	353
9.2 Conclusion.....	354
9.3 Future studies.....	362

Chapter 10 Appendix.....	364
10.1 Appendix chapter 3	364
10.2 Appendix chapter 4	368
10.3 Appendix chapter 5	380
10.3.1 Hot stage microscopy method	380
10.4 Appendix chapter 6	383
10.5 Appendix chapter 8	386
10.5.1 Thermography analysis in detail DSC of all batches without PRH.....	386
10.5.2 Simulation trials showing the stages of simulation.....	386
Chapter 11 References	390

List of Figures

Figure 1.1 Simplified administration of ODT with immediate disintegration in the oral cavity for dysphagic patients (Dentagama, 2020)	3
Figure 1.2 Combination of ODT with different MR formulations(A. Elwerfalli <i>et al.</i> , 2015).....	4
Figure 1.3 Microspheres and microcapsules matrix and reservoir systems are drawn using Microsoft office 2018 (Al-Hashimi <i>et al.</i> , 2018)	10
Figure 1.4 Nanospheres and nanocapsules loaded with API drawn using Microsoft office 2018 (Al-Hashimi <i>et al.</i> , 2018)	11
Figure 1.5 Diagram showing the extrusion spheronisation technique steps of pellets preparation are drawn using Microsoft office 2018 (Al-Hashimi <i>et al.</i> , 2018) ..	16
Figure 1.6 Diagram showing of matrix and reservoir pellet and ODT containing pellets from one of our formulations consisting of Eudragit L100, sorbitol and indomethacin hydrochloride (IND) using SEM, stereomicroscope, and Microsoft office 2018 (Al-Hashimi <i>et al.</i> , 2018)	16
Figure 2.1 The steps of pellets preparation extrusion and collecting the extrudates (A), spheronization (B) and pellets formation using the Caleva Multi Lab extrusion spheronization instrument.....	32

Figure 2.2 Texture analysis graph (extracted from the exponent software) after testing the hardness of one pellet from Eudragit L100 90 μm showing the first notch (hardness value) and maximum force applied.....	36
Figure 3.1 Büchi Mini Spray Dryer, B-290, Switzerland (1), function principle (2): hot inlet gas (A), droplet formation from the nozzle (B), gas-droplet drying chamber (C), particles collection (D), filter protecting user and environment, drying gas (D).....	50
Figure 3.2 Scanning electron microscopy apparatus (Zeiss Evo50, UK).....	51
Figure 3.3 SEM images top view for the raw powder of pharmaceutical polymers at low magnification and high magnification 100 -10 μm sodium alginate (A), PVA (B), MC (C), PAA(D) and Eudragit L100 (E).....	59
Figure 3.4 Adsorption/Desorption isotherm of the pharmaceutical polymers: Eudragit L100 (A), showing Type 4 isotherm, and MC (B) showing Type 3 isotherm at adsorption temperature 77 K and relative pressure <0.9	61
Figure 3.5 DSC graph of 5 raw pharmaceutical polymers examined at (20 - 340) $^{\circ}\text{C}$ with 10 $^{\circ}\text{C}/\text{min}$ heating rate, (A) sodium alginate, (B) PVA, (C) methylcellulose, (D) PAA acid and (E) Eudragit L100	66
Figure 3.6 TGA analysis results of 5 raw pharmaceutical polymers A sodium alginate, B PVA, C MC, D PAA and E Eudragit L100, from 20 to 400 $^{\circ}\text{C}$ with 10 $^{\circ}\text{C}/\text{min}$ heating rate under nitrogen atmosphere	66
Figure 3.7 Young's modulus (MPa) reflects the elasticity profile of raw polymers sodium alginate, PVA, MC, PAA and Eudragit L100, the results obtained from the texture analysis (TA-XT Plus stable micro systems) all data were presented as mean \pm SD (n=3).....	69
Figure 3.8 Tableability results presenting in Tensile strength (MPa) against the compaction pressure (MPa) for tablets prepared in different compression pressure (36, 74, 148, 221, 295 and 443 MPa) of raw polymers: sodium alginate, PVA, MC, PAA and Eudragit L100.....	71
Figure 3.9 SEM images for the tablets of pharmaceutical polymers sodium alginate (A), PVA (B), MC (C), PAA (D) and Eudragit L100 (E) 20 and 200 -100 μm , high magnification and low magnification, respectively.....	72
Figure 3.10 SEM images spray-dried powder of pharmaceutical polymers sodium alginate(A), PVA (B), MC (C), PAA (D), Eudragit L100 (E)	77

Figure 3.11 Thermal analysis DSC of 4 spray-dried pharmaceutical polymers sodium alginate (A), PVA (B), MC (C), PAA (D) and Eudragit L100 (E) from 20 to 300°C temperature and 20 °C/min heating rate using METTLER software	81
Figure 3.12 TGA graph of the 4 spray-dried polymers (A) sodium alginate, (B) PVA, (C) MC, (D) PAA and (E) Eudragit L100 at heating range from 20 -350°C with 10°C/min heating rate in a nitrogen atmosphere using STARe software	81
Figure 3.13 Texture analysis results of spray-dried polymers illustrating Young's modulus under 300 Kg force mean ± SD (n=3).....	83
Figure 3.14 Tensile strength values (MPa) for tablets of spray-dried polymers sodium alginate, PVA, MC, PAA and Eudragit L100 under the maximum compaction pressure 443 MPa.....	86
Figure 3.15 SEM images of tablets after hardness test the tablets of spray-dried polymers sodium alginate (A), PVA (B), MC (C), PAA (D) and Eudragit L100 (E)	87
Figure 4.1 IND calibration curve showing the linearity $R^2 = 0.9994$ for all concentrations range with linear curve equation $y=58.778x-13.524$	112
Figure 4.2 Excipients and drug as showing the specificity of the method for IND pellets.....	113
Figure 4.3 One of the quality control concentrations 5 µg/mL showing high peak sharpness and detection specificity for IND with no interference	114
Figure 4.4 Calibration curve of PRH 1 – 40 µg/mL showing linearity $R^2 = 0.9974$ and equation $y = 23.945x - 0.2463$	117
Figure 4.5 Matrix of the used excipients in PRH formulations in blank samples using mobile phase as a solvent.....	118
Figure 4.6 Chromatogram of PRH with 20 µg/mL showing a sharp peak with 1.952 min retention time.....	118
Figure 5.1 SEM images showing a general overview of the particles of ODTs with low magnification.....	138
Figure 5.2 SEM images of A1 and A2 batches showing the difference of strands number and particles shape with high and low magnification	139
Figure 5.3 SEM images of B1 and B2 showing fewer strands formation with the effect of the parameters the images in low and high magnification	140
Figure 5.4 Images of SEM for C1 and C2 batches showing the formation of the high number of strands in both groups.....	142

Figure 5.5 SEM images for D1 and D2 showing the difference in strands and morphology of the microparticles	143
Figure 5.6 Results of disintegration time in seconds and tensile strength (MPa) (mean +/- SD) (n=3) for tablets of IND powder as a control (ODT) and DRM-ODTs.....	145
Figure 5.7 Two-way ANOVA results showing the type of interaction between the solvent type with temperature and aspiration for B, C and D batches of low and high parameters in mean \pm standard error	147
Figure 5.8 DSC thermogram showing the endothermic peak of IND (DRUG) and the Tg of the polymer in the formulation (A1, A2, B1, B2, C1, C2, D1 and D2) with 10 °C/min heating rate showing a decomposition after 230°C (Vlachou <i>et al.</i> , 2019).....	149
Figure 5.9 TGA results showing the low moisture content of A1, A2 & B1 and high moisture content of B2, C1, C2, D1 and D2 and Eudragit L100 raw powder (E) within range of 40-400 °C and 20 °C heating rate.....	150
Figure 5.10 DSC results of powder melted quench-cooled of physical mixture IND and polymer (A), IND alone (B) and one of the SD- INDE formulation B2 (C) showing a similar melting point of IND.	154
Figure 5.11 IND release results of DRM-ODTs and IND tablets as a control in acidic media pH 1.2, all results in mean +/- SD (n=3)	156
Figure 5.12 IND release results of DRM-ODTs and IND tablets as a control in pH 6.8 media, all results in mean +/- SD (n=3).....	157
Figure 5.13 Dissolution test in buffer media showing the IND release from all DRM-ODTs batches and IND ODs within the first 30 minutes (mean +/- SD) (n=3).	158
Figure 5.14 SD-INDE particles graph presenting the content uniformity of IND within the batches tested in two positions for each batch first (sample) and second (chamber) position (50 µg/mL), IND recovered from each position and standard deviation of the total IND amount in each sample (n=3)	159
Figure 6.1 SM images A and B showing the shape and morphology of the pellets, area, and diameter measurements	181
Figure 6.2 SM image processed showing applied in ImageJ software (A), SEM micrograph display the rough surface and AR of the pellet (B)	182

Figure 6.3 SEM images showing pellets embedded in lactose ODTs with AR (A), measured area using SEM (B), top view of tablet after hardness test showing pellets within in the tablet after compression (C).....	182
Figure 6.4 Thermogravimetric analysis showing the results of TGA (A) and DSC (B) for the raw powder of Eudragit L100, IND and the produced pellets.....	187
Figure 6.5 Sieve analysis results of lactose (A) and mannitol (B) raw powders with particles sizes of mid-points (C) presenting the cumulative oversize and the retained powders collected from each sieve	190
Figure 6.6 Elasticity profile represented by YM of tablets mix of ODTs (control), indomethacin (IND), pellets using lactose and mannitol 63, 125 and 500 μm particles.....	193
Figure 6.7 Tensile strength (MPa) values of Control (ODT), indomethacin (IND) mixed with ODT, and pellets embedded in the ODTs of lactose and mannitol	195
Figure 6.8 Micrographs of radial cross-sections from ODTs-pellets of lactose 63 μm (A), 125 μm lactose (B), 500 μm lactose cross-section (C), top view ODTs-pellets of 63 μm lactose (D), ODTs-pellets of mannitol 63 μm (E), 125 μm mannitol (F), 500 μm mannitol cross-section (G)	200
Figure 6.9 ODTs-pellets images from SM showing the distribution of the pellets within the radial cross-section tablets of lactose and mannitol A, B and C & D, respectively	201
Figure 6.10 disintegration time of lactose and mannitol ODTs only (control), tablets of IND and pellets.....	202
Figure 6.11 IND release profile from ODTs of lactose LM-pellets & LM-IND and mannitol DM-pellets & DM-IND in acid (A & B)	204
Figure 6.12 IND release profile from ODTs of lactose LM-pellets & LM-IND and mannitol DM-pellets & DM-IND in phosphate buffer pH 6.8 (A& B) using 63, 125 and 500 μm particles.....	208
Figure 6.13 Relationship between the cumulative oversize (%) and net powder retained from each sieve using sieving analysis	211
Figure 6.14 powder of Eudragit L100 with particle sizes of 45 μm (A), 63 μm (B), 90 μm (C) using a stereomicroscope	214
Figure 6.15 SEM images of low and high magnification showing the particles Eudragitl100 powder with particle size of 45 μm (A1, A2), 63 μm (B1, B2) and 90 μm (C1, C2.....	215

Figure 6.16 Pellets of 45 μm Eudragit L100 showing compressed pellets with texture analysis (A) general pellets image (B) & AR (C &D)	221
Figure 6.17 Different SEM images for 63 μm batch showing pellets after compression with texture analysis (A), general overview for pellets (B) and top view AR (C & D).....	222
Figure 6.18 SEM images of 90 μm batch showing pellets after compression with texture analysis (A), general overview (B) and top view for pellets with AR (C &D).....	222
Figure 6.19 Top overview for pellets of 90 μm batch embedded in ODT showing AR using SEM.....	223
Figure 6.20 Graph of mechanical properties of pellets prepared from 45, 63, 90 μm and raw powder of Eudragit L100 (control) showing YM and tensile strength in mean \pm SD	226
Figure 6.21 DSC graph of indomethacin (A), pellets of 90 μm (B), 63 μm (c), 45 μm (D) EudragitL100 powder using Mettler Toledo and STARe software.....	228
Figure 6.22 TGA Thermogram of EudragitL100 pellets of 63 (A) & 90(B) 45(C) μm showing the moisture content orderly and the degradation temperature.....	229
Figure 6.23 Tablet matrix showing in A the powder of ODT, B the compressed ODT top view and C cross section of the ODT (high and low magnification respectively).....	231
Figure 6.24 Stereomicroscope images of DRP-ODTs showing cross section view and top view of the tablets of 45 μm batch (A1&A2) 63 μm (B1&B2) 90 μm (C1 &C2) batches accordingly	231
Figure 6.25 SEM and stereomicroscope images show cross-sections DRP-ODTs after hardness and the top view of the tablet indicating the embedded pellets for 63 μm batch (A1, 2&3) and 90 μm (B1,2 &3)	232
Figure 6.26 Dissolution test results of pellets and DRP-ODTs in acid media A1 &A2, respectively	235
Figure 6.27 Dissolution test results of pellets and DRP-ODTs in buffer (pH6.8) B1 &B2, respectively	238
Figure 7.1 SEM images of PRH pellets produced from different types and ratios of plasticizers F1 (a), F2 (b), F3 (c), F4 (d), F5(e) and F6 (f)	266
Figure 7.2 YM (Mpa) and tensile strength (MPa) of pellets produced from different amounts and type of plasticizers	270

Figure 7.3 DSC thermogram of Eudragit RS raw powder and PRH using STAR ^e software within temperature range 20-400 °C	271
Figure 7.4 DSC thermograms of PRH pellets contained in the 15% sorbitol (F1), 30% sorbitol (F2), 3% TEC (F3), 5% TEC (F4), 3% ATEC (F5) and 5% ATEC (F6) and PRH (drug)	272
Figure 7.5 TGA results of all produced batches 15% sorbitol (F1), 30% sorbitol (F2), 3% TEC (F3), 5% TEC (F4), 3% ATEC (F5) and 5% ATEC (F6) and Eudragit RS and PRH (Drug)	273
Figure 7.6 Tablet preparation for SEM analysis with a diagram showing the distribution of the pellets within ODT	275
Figure 7.7 SEM images cross-section and top views detecting PRH pellet in the broken side of ODT surface; tablets of F1(1), F2(2), F3(3), F4(4), F5(5) and F6(6)	276
Figure 7.8 Tensile strength and disintegration time of ODTs contained in the pellets and control of PRH.....	277
Figure 7.9 Contact angle between the liquid droplet and tablet surface actual image and drawing illustrating the angle measurements	278
Figure 7.10 PRH release profiles of tablets contained in the prepared pellets in acidic media pH 1.2.....	280
Figure 7.11 PRH release profiles from tablets of the prepared pellets in phosphate buffer pH 6.8 (A and B) within 24 hrs and 2 hrs	281
Figure 7.12 Stereomicroscope images showing AR and general morphology for uncoated pellets (F1) and coated pellets (F2, F3 and F4).....	289
Figure 7.13 SEM images of all batches F1 (uncoated pellets) showing rough surfaces (A1 and A2) and coating layers with the smooth surfaces of the coated pellets for F2 (B1 and B2), F3 (C1&C2) and F4 (D1&D2), F5 matrix pellets (E1&E2) showing the surface irregularity	292
Figure 7.14 SEM images of F0 (A) showing the surface roughness and the presence of MCC crystals as distributed within F0 pellets in image B	293
Figure 7.15 One of the hardness test results showing force (N) against time (seconds), first notch as the crushing force (N) and the maximum force (F) at the end of the test for F5	293

Figure 7.16 The tensile strength and YM results (mean \pm SD) of uncoated drug pellets (F1), coated pellets with Eudragit RS (F2), coated pellets with Eudragit RL (F3) and coated pellets with Eudragit RS/RL (F4) and matrix pellets (F5).	294
Figure 7.17 DSC thermogram A: uncoated drug pellets (F1), coated pellets with Eudragit RS (F2), coated pellets with Eudragit RL (F3), coated pellets with Eudragit RL: RS (F4) and the pure drug PRH and B uncoated pellets of RS matrix (F5).....	298
Figure 7.18 TGA results of uncoated pellets F1 and coated pellets F2, F3, F4 and matrix Eudragit RS pellets F5 showing the degradation after 260°C for all batches	299
Figure 7.19 Tensile strength and disintegration results for tablets (n=3) (mean \pm SD) ODTs (without pellets), uncoated drug pellets (F1), coated pellets with Eudragit RS (F2), coated pellets with Eudragit RL (F3) and coated pellets with Eudragit RS/RL (F4) and uncoated pellets with Eudragit RS (F5).....	301
Figure 7.20 The dissolution profiles in acidic media of pH 1.2 for tablets of ODTs containing PRH, F1, F2, F3, F4 and F5	307
Figure 7.21 The dissolution profiles of ODT formulations PRH, F1, F2, F3, F4 and F5 in buffer media (pH 6.8)	307
Figure 8.1 Microcrystalline cellulose (MCC) of 370.35 (g/mol) molecular weight showing chemical structure (C ₁₄ H ₂₆ O ₁₁) in 3D format (A) and normal structure with atomic names (B) by ACDlab software (NCBI, 2015)	314
Figure 8.2 Contact forces effect on particles interaction and their behaviour during compression showing the used contact model (Yeom et al., 2019)	319
Figure 8.3 Starting window of the EDEM® creator showing tree, viewer, and toolbar	325
Figure 8.4 Hypothesized illustration of two particles showing the physical radius (R), contact radius (C.R), and bonds formation at the overlap of the contact radius drawn using Microsoft software 2018.....	327
Figure 8.5 Tableting machine with a manual hydraulic press and upper punch to compress the powders (SPECAC Ltd, UK)	328
Figure 8.6 Simulated tableting press showing upper and lower punch modelled by EDEM®.....	329
Figure 8.7 EDEM® Simulator, representing the simulation processing of the pellets	330

Figure 8.8 EDEM® analyst window showing tree, viewer, and toolbar	331
Figure 8.9 Mechanical properties of pellets showing the YM (n=3) and tensile strength (n=30) in mean +/- SD.....	336
Figure 8.10 SEM images of MCC batches with a general overview of low magnification showing AR batch 1 (A), batch 2 (B), batch 3 (C), batch 4 (D)..	339
Figure 8.11 SEM images of high magnification showing the surface of each batch 1 (A), batch 2 (B), batch 3 (C), batch 4 (D)	339
Figure 8.12 DSC thermograms of batches 1 (A), 2 (B), 3(C), 4(D) and drug (E) indicating the presence of the drug melting peak within batches 2,3 and 4	341
Figure 8.13 TGA results showing the moisture content of all batches 1(A),2(B),3(C),4(D) and the PRH in E	341
Figure 8.14 Simulation of compaction process demonstrated step by step according to the order of tablet preparations images extracted from EDEM	343
Figure 8.15 Bond strength between particles under compaction (top view)	345
Figure 8.16 Bond formations between particles upon compaction blue and pink particles represent ODT particles and the pellets, respectively, weak bonds are shown in cyan, and those in yellow, orange and red were stronger, orderly ...	346
Figure 8.17 EDEM® image showing the particle filling during tablet compression before applying the pressure with no bond's formation	347
Figure 8.18 Compressive force (N) against time (S) for pellets under compression	348
Figure 8.19 Pellets and ODTs particles after compression during simulation trials showing the weak interaction with cyan colour	349
Figure 8.20 Low compaction force during simulation trials represented by force (N) against time (seconds)	350
Figure 10.1 Porosity results showing adsorption desorption isotherms for raw and spray dried powders.....	365
Figure 10.2 The isotherms of the 4 polymers PAA, MC, sodium alginate and MC showing type3 isotherm	367
Figure 10.3 A and B BJH- plot from the preliminary studies of the raw and spray dried powder	367
Figure 10.4 statistical analysis using t-test (p<0.05) to detect the difference between Young's modulus results of raw powders.....	367

Figure 10.5 one of the particle size results of spray-dried polymers: sodium alginate, PVA, MC, and PAA using Laser diffraction technique showing the cumulative distribution (%) against particle size (μm)	368
Figure 10.6 PRH UV-vis calibration curve at 291 nm showing good peak linearity 0.9997 and range 5 – 50 $\mu\text{g}/\text{mL}$	369
Figure 10.7 IND stability of 100 $\mu\text{g}/\text{mL}$ stored at 5 $^{\circ}\text{C}$ – 8 $^{\circ}\text{C}$ for one year from calibration curve points showing method rigidity	372
Figure 10.8 PRH HPLC chromatogram 1 $\mu\text{g}/\text{mL}$	377
Figure 10.9 Robustness chromatogram of 20 $\mu\text{g}/\text{mL}$ PRH showing sharp peak with mobile phase ratio 50:30:20 of acetonitrile, methanol, and buffer respectively	377
Figure 10.10 Spray dried particles of Eudragit L100 with IND showing the drug release in buffer (pH 6.8) with no interference	378
Figure 10.11 Calibration curve concentration and retention time PRH using another Agilent HPLC using same samples of calibration curve contractions with adjusted range 5-50 $\mu\text{g}/\text{mL}$ showing high linearity and acceptable absorbance for the 291 nm wavelength.....	378
Figure 10.12 One of the trials of HPLC column (1) for IND and unsuitability of detection	379
Figure 10.13 Trials of using another C18 column (2) HPLC IND.....	379
Figure 10.14 One of the calibration curve concentration 5 $\mu\text{g}/\text{mL}$ of IND showing peak sharpness and area the run.....	380
Figure 10.15 Raw IND (a) and melted IND after 165 $^{\circ}\text{C}$, then slowly cooled melted IND (c) showing start of crystallization at 30 $^{\circ}\text{C}$	381
Figure 10.16 IND release from all batches of ODTs with obtained spray dried particles in pH 1.2 media with 100 bounds in Y axis	381
Figure 10.17 Lactose SEM image with low magnification showing a general size of particles.....	382
Figure 10.18 Mannitol image of SEM showing the shape and size of the particles	382
Figure 10.19 Sorbitol SEM image showing shape irregularity and surface roughness	383
Figure 10.20 IND SEM showing the similarity with mannitol particles	383
Figure 10.21 PRH release in buffer media pH 6.8 from ODTs of PRH, F1, F2, F3 and F4 for 24 hours.....	385

Figure 10.22 DSC thermogram of all batches showing a clear melting point (MP) of PHC in batches 2(B),3(C), 4(D) and missing from the batch1 of MCC only (A) along with a distinct T_g of MCC in all combinations (E)	386
Figure 10.23 Drawing the geometries	386
Figure 10.24 Compression simulation	387
Figure 10.25 Adjusting the cylinders shapes to match the real compression instrument	387
Figure 10.26 Particle's simulation trail without pellets	388
Figure 10.27 The issue with few quantity of particles and small sizes	388
Figure 10.28 The compaction force for compaction fine particles only during the trials	389
Figure 10.29 Pellet's simulation trial and shape parameters	389

List Of Tables

Table 1.1 Examples of Eudragit polymers of MR properties, application, and chemical structures(Gupta, Kumar and Sachan, 2015a)(Thakral, Thakral and Majumdar, 2013a)(Rowe, Raymond C., Paul Sheskey, 2009)	5
Table 1.2 Chemical structures of common pharmaceutical polymers used in coated multiparticulates and their elongation values (Al-Hashimi et al., 2018)	18
Table 1.3 Direct and indirect method of pharmaceutical compact characterisation..	27
Table 2.1 Compressibility index and Hausner ratio references (Kalal <i>et al.</i> , 2018) ..	41
Table 3.1 Particle size data (μm) for 5 raw pharmaceutical polymers sodium alginate, PVA, MC, PAA and Eudragit L100 (n=3, mean \pm standard deviation)	55
Table 3.2 Surface area analysis results of single run of raw powders sodium alginate, PVA, MC, PAA, and Eudragit L100 illustrating mean pore diameter (nm), surface area (m^2/g) and total pore volume (cm^3/g) in the range of 0.05– 0.35 N_2 relative pressure using BET model.....	63
Table 3.3 Particle size results of spray-dried powder presenting VMD \pm SD of PAA, MC, Sodium alginate and PVA obtained from laser diffraction (n=3)	75
Table 3.4 Surface area and porosity measurements for spray-dried powders using Belsrop.....	79

Table 4.1 pharmaceutical classification of drug showing solubility and permeability in the biological system(Savjani Ketan, Gajjar Anuradha and Savjani Jignasa, 2012; Shah and Amidon, 2014; Aulton and Taylor, 2018a).....	92
Table 4.2 Literature’s summary for HPLC methods of analysing IND	96
Table 4.3 Literature’s summary for HPLC methods for PRH.....	98
Table 4.4 Analytical method parameters for IND.....	104
Table 4.5 Analytical method parameters for PRH	106
Table 4.6 Accuracy and Intraday precision parameters for IND according to the proposed HPLC method (n=6) showing the theoretical concentration (T.C) and calculated concentration (C.C)	115
Table 4.7 Inter-day precision of IND HPLC method (n=6+6+6) represented by Mean \pm SD, %RSD, and %Recovery	115
Table 4.8 Robustness testing for the proposed HPLC method for IND of one of the quality controls points 3 μ g/mL concentration (n=6).....	116
Table 4.9 Results of accuracy and intraday precision of PRH HPLC method (n=6), showing T.C and C.C relationship.....	119
Table 4.10 Inter day precision showing T.C and C.C analysis according to PRH HPLC method (n=6+6+6).....	120
Table 4.11 Robustness of HPLC method of PRH showing mobile phase ratio and flow rate effect on 20 μ g/mL concentration	120
Table 5.1 Spray-dried particles of IND and Eudragit L100 using two settings of parameters inlet temperature and aspiration with each of feed concentrations	129
Table 5.2 Compressibility index and Hausner ratio references (Kalal <i>et al.</i> , 2018)	131
Table 5.3 Powder properties results and micrometric characterisation of SD-INDE particles of all batches.....	134
Table 5.4 Particles sizes result from laser diffraction showing volume median diameter (VMD) (μ m) and the span as x10 (10%), x50 (50%) and x90 (90%) are particles sizes of the volume distribution of the SD- INDE particles.....	137
Table 5.5 Elasticity profile of all the formulations showing YM (Mean \pm SD) (n=3) and the p values for every two batches indicating the statistical difference between the high and low parameters with % yield and moisture content according to t-test	144

Table 6.1 pellets aspect ratios (AR) (mean \pm SD) examined using a calliper, stereomicroscope (SM) and SEM	180
Table 6.2 Mechanical properties of the pellets using texture analysis showing pellets YM (n=3), hardness (n=30) and tensile strength (n=30)	184
Table 6.3 Pellets mean pore volume, total pore volume and surface area results using BELSORP software	186
Table 6.4 Statistical analysis of <i>t</i> -test ($p < 0.05$) for ODTs-lactose of 63, 125 and 500 μm with pellets in 30- and 120-minutes time in acid media (pH 1.2) (vs: versus)	205
Table 6.5 Statistical comparison between ODTs-lactose and mannitol with pellets of same particle size powders 63, 125 and 500 μm in 30 and 120 minutes in acidic media according to one-way ANOVA ($p < 0.05$)	207
Table 6.6 Compressibility index and flow properties of Eudragit L100 45, 63, 90 μm powder	213
Table 6.7 Texture analysis results for Eudragit L100 powder 45, 63 and 90 μm (n=3) showing the YM as elasticity profile analysed with exponent software.....	216
Table 6.8 Porosity measurements for Eudragit L100 raw powder, 63 μm and 90 μm particles using Belsorp analysis and BET equation.....	217
Table 6.9 Pellets physical and micrometric properties, pellets named according to the size of Eudragit L100 powder prepared from	220
Table 6.10 Porosity and surface area data for all batches of pellets prepared from raw Eudragit L100 particles (45,63 and 90 μm), pellets are named according to the size of Eudragit L100 prepared from	224
Table 6.11 TGA data of Eudragit L100 pellets and other batches (45, 63 & 90 μm) showing the moisture content and the residual	229
Table 6.12 Relationship between the disintegration time and hardness of the tablets with the embedded pellets and the control tablet of ODTs matrix only.....	233
Table 7.1 Examples of popular plasticizers in the pharmaceutical formulations.....	250
Table 7.2 The produced batches and different excipients ratios and the trial batch of Eudragit RS only	255
Table 7.3 Contents of pellets before pellets coating (F1-F5).....	256
Table 7.4 The prepared pellets of different plasticizers sorbitol, TEC and ATEC showing yield (%), amount of water (mL), moisture content (%) and bulk density (mean \pm SD and n=3).....	261

Table 7.5 The aspect ratio results for all batches in mean \pm SD (n=30) and relative standard deviation (%RSD).....	265
Table 7.6 Surface area, mean pore diameter and total pore volume of the sorbitol, TEC and ATEC pellets from the BET plot	268
Table 7.7 Hardness results of the produced pellets (n=30) (mean \pm SD).....	269
Table 7.8 Contact angle measurement using the sessile drop method (n=3)	279
Table 7.9 Physical characteristics of the pellets of all formulations: F1 (uncoated pellets), coated pellets F2 (RS), F3 (RL), F4 (RS RL) and F5 (uncoated pellets with RS)	288
Table 8.1 Examples of significant techniques to prepare orally disintegrating formulations (Badgujar and Mundada, 2011; Ghosh, Ghosh and Prasad, 2011; Arora and Sethi, 2013)	311
Table 8.2 Examples of simulation software and designed companies (Yeom et al., 2019).....	317
Table 8.3 Composition of each batch used in the preparation of PRH pellets (% w/w)	322
Table 8.4 Micrometric results showing bulk, tap density and the yield before drying with pellets sphericity in AR (n=30) and moisture content from TGA results...	332
Table 10.1 Structures of the polymers used in our study according to sigma Aldrich	364
Table 10.2 Columns of HPLC used for method development	368
Table 10.3 UV-vis accuracy and intra-day precision for PRH (n=6) using wavelength 291 nm.....	369
Table 10.4 Inter day precision for PRH using UV-vis confirming acceptable wavelength 291 nm showing acceptable rang (n=9)	370
Table 10.5 Accuracy and intra-day precision according the HPLC methods for additional quality control 15, 35 and 45 μ g/mL (n=3)	370
Table 10.6 Inter-day precision according to proposed HPLC method for quality control 15, 35 and 45 μ g/mL for IND (n=9).....	371
Table 10.7 IND method Robustness using 45 μ g/mL (n=3) with \pm 4 wavelength 248 nm.....	371
Table 10.8 readings of stability for IND HPLC method showing %RSD and %Recovery within the range 80-120% for 100 μ g/mL (n=3) as in the peak of Figure 10.7	371

Table 10.9 Method suitability and reproducibility using 10 (µg/mL) of the calibration curve points tested on another Agilent HPLC instrument with same conditions and column	372
Table 10.10 Raw data for IND inter day precision and accuracy over three consecutive days (n=9)	372
Table 10.11 Raw data of calibration curve equation for IND showing CC within acceptable range 80-120% according to ICH guidelines.....	374
Table 10.12 Raw data of the calibration curve PRH showing CC within acceptable range 80-120% according to ICH guidelines.....	374
Table 10.13 Raw data of Inter day accuracy and precision PRH (n=9).....	375
Table 10.14 P values obtained from all pellets batches using ANOVA illustrating the significant differences between the results.....	383

List Of Equations

Equation 2-1	33
Equation 2-2	33
Equation 2-3	33
Equation 2-4	35
Equation 2-5	35
Equation 2-6	37
Equation 2-7	38
Equation 2-8	41
Equation 2-9	41
Equation 3-1	50
Equation 3-2	52
Equation 3-3	53
Equation 4-1	109
Equation 4-2	109

List of abbreviations

%	Percentage
°C	Degree Celsius
µg	Microgram
µm	Micrometre
A	Area
ANOVA	Analysis of variance
API	Active pharmaceutical ingredient
AR	Aspect Ratio
ATEC	Acetyl triethyl citrate
BCS	Biopharmaceutics Classification System
BET	Brunauer-Emmett-Teller
BJH	Barrett-Joyner-Halenda
BP	British Pharmacopeia
C.C	Calculated concentration
C.R	Contact Radius
CFD	Computational Fluid Dynamics
COX	Cyclooxygenase
CPU	Central Processing Unit
CR	Controlled release
CS	Chitosan
D	Diameter
DBP	Dibutyl phthalate
DBS	Dibutyl sebacate
DCP	Dicalcium phosphate dehydrate
DEM	Discrete element method
Df	Diameter of Freret
DM	D-Mannitol
DPC	Drucker-Prager Cap
DR	Delayed Release
DRM	Delayed release microparticles
DRP-ODTs	Delayed Release Orally Disintegrated Tablets
DSC	Differential scanning calorimetry
EC	Ethylcellulose
EDEM	Discrete Element Modelling
ER	Extended release
F	Force
FDA	United States Food and Drug Administration
FEA	Finite Element Analysis
FEM	Finite element method
FTIR	Fourier transform infrared
g	Gram

GIT	Gastrointestinal tract
HCl	Hydrochloride
HPLC	High-performance liquid chromatography
HPMC	Hydroxypropyl methylcellulose
ICH	International Council for Harmonisation
IER	Ion-Exchange Resin
IER-ODT	Ion-Exchange Resin Orally Disintegrating Tablets
IND	Indomethacin
INDE	Indomethacin -Eudragit L100
IR	Immediate Release
IUPAC	International Union of Pure and Applied Chemistry
KG	Kilo Gram
LHB1	Pharmaceutical Grade of LHPC
LHPC	Low-substituted hydroxypropyl cellulose
LM	Lactose Monohydrate
LOD	Detection Limit
LOQ	Quantification Limit
mA	milliampere
mAU	Milli Astronomical Unit
MC	Methylcellulose
MCC	Microcrystalline cellulose
MDT	The mean dissolution time
MFT	Minimum film-forming temperature
mg	Milligram
mL	Millilitre
mm	Millimetre
MPa	Mega pascal
MR	Modified release
MR-ODTs	Modified drug release orally disintegrating tablets
MUDF	Multiple unit dosage forms
MUPS	Multiple unit pellet system
N	Newton
N ₂	Nitrogen
NICE	National Institute for Health and Care Excellence
NIMS	Novel nanoparticles-in-microparticles system
nm	Nano Meter
NSAID	Nonsteroidal anti-inflammatory drug
ODF	Oral disintegrating film
ODT	Orally Disintegrating Tablet
ODTs	Orally disintegrating tablets
OTC	Over The Counter
p	perimeter
P ₀	Saturation pressure
PAA	Polyacrylic acid

PDE	Partial Differential Equations
PEG	Polyethylene glycol
pH	Potential hydrogen
pKa	Acid Dissociation constant
PRH	Propranolol hydrochloride
PVA	Polyvinyl alcohol
PVP	Polyvinylpyrrolidone
r	Radius
RPM	Round per minute
RSD	Relative standard deviation
SD	Standard deviation
SD- INDE	Spray-dried Indomethacin -Eudragit L100
SEM	Scanning electron microscopy
SM	Stereomicroscope
SR	Sustained release
SUDF	Single-unit dosage form
T	Thickness
T.C	Theoretical concentration
TA	Texture Analysis
TBC	Tributyl citrate
TEC	Triethyl citrate
Tg	Glass transition temperature
TGA	Thermogravimetric analysis
TMUP	Tablets multi-unit pellet system
TMUPS	Tablet of multi-unit pellet system
US	United States
USP	United States Pharmacopoeia
UV	Ultraviolet visible spectroscopy
VH	Polyvinyl pyrrolidone
VMD	Volume median diameter
w/w	Weight by weight
WT%	Weight Percent
YM	Young's modulus

Chapter 1 General introduction

1.1 Background

Drug delivery through the oral route remains the desired drug administration route in today's market. The difficulty in swallowing, called dysphagia, was reported in patients of all age groups. Nevertheless, it was most widespread amongst children and older people (Sastry, Nyshadham and Joseph A. Fix, 2000).

The clinical studies for 50 to 69 age proved that 35% of patients suffered from dysphagia (Lindgren and Janzon, 1991). Furthermore, studies showed that 20% of patients avoid taking their medicines due to swallowing difficulty (Lindgren and Janzon, 1991; Krause and Breitzkreutz, 2008)

The solid dosage form of orally disintegrating tablets (ODTs) has recorded an impact of great extent on patient compliance (Alġin Yapar, 2014).

ODTs are defined by Food and Drug Administration (FDA) as solid formulations that disintegrate quickly within seconds when administered orally, releasing an active pharmaceutical ingredient (API) (Figure 1.1). The disintegration time is counted as the time required for an ODT to break down completely. The European Pharmacopoeia used the term Oro-dispersible tablet to disintegrate within 3 minutes in the oral cavity (Fu *et al.*, 2004; Alġin Yapar, 2014). Also, fast disintegrating tablets, mouth dissolving tablets, rapid dissolving tablets, porous tablets are other names for ODTs. However, oral disintegrating tablets was suggested and accepted over the other names by United States Pharmacopoeia (USP) (Hirani, Rathod and Vadalía, 2009; Hiraram Choudhary *et al.*, 2012).

The manufacturing technology ODTs considerably influences the quality of the prepared tablets. The main requirement for ODT is to dissolve rapidly in contact with saliva, which avoids water use.

Generally, ODTs should possess unique characteristics, including the ability to disintegrate and dissolve in the oral cavity in seconds to minutes without the need to administer with water. Adequate strength is necessary for ODTs to tolerate handling after manufacturing. ODTs should be stable against conditions such as temperature and humidity. Besides, ODTs should allow high drug loading and be of pleasant taste and cost-efficient (Hirani, Rathod and Vadalía, 2009; Hiraram Choudhary *et al.*, 2012).



Figure 1.1 Simplified administration of ODT with immediate disintegration in the oral cavity for dysphagic patients (Dentagama, 2020)

1.2 Modified drug release particles via oral disintegrating tablets (MR-ODTs)

The global ODTs market is growing around 11.4 billion US dollars in 2017 to an estimated 27 billion US dollars by the end of 2025. The high patient compliance was the main reason for this stipulated rise in the development of ODTs (Research, 2018). Combining ODTs with modified-release (MR) particulates (MR-ODTs) is another approach to developing ODTs of oral drug delivery (Figure 1.2). The MR system can be formulated as a multi-particulate system that can be prepared using several technologies. Technologies that could be utilised include micro or nanoparticles formation, pellets, or stimuli-responsive polymers to incorporate the API. These multi-particulate systems can be compressed to form tablets. The MR-ODTs disintegrate in the oral cavity, completely releasing the active pharmaceutical ingredient (API) in a controlled/sustained release pattern. This revolutionary formulation would decrease dosing frequency, enhance patient compliance, and eventually improve the patient's health state (Quinten *et al.*, 2012; A. M. Elwerfalli *et al.*, 2015a; Yassin *et al.*, 2015).

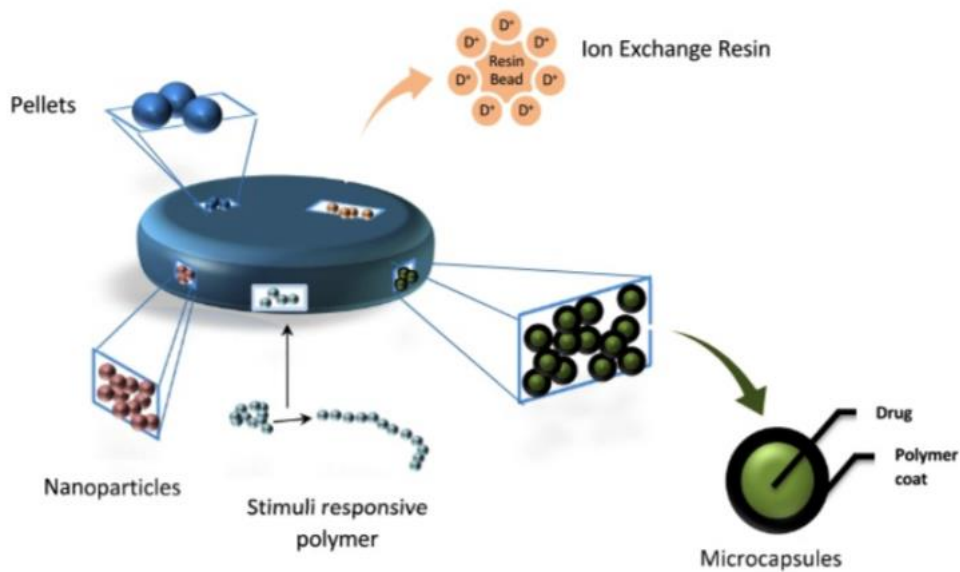


Figure 1.2 Combination of ODT with different MR formulations(A. Elwerfalli *et al.*, 2015)

1.3 MR-formulations and the associated challenges

Multiparticulates dosage forms (e.g., microparticles or pellets) are becoming increasingly essential in the pharmaceutical market. The multi-unit dosage forms offer several solutions compared to single units (e.g., tablets or capsules) (Asghar and Chandran, 2006). The multiparticulates dosage forms can be filled into hard gelatin capsules (Chopra *et al.*, 2002; Varshosaz *et al.*, 2012) or compacted forming tablets (Maganti and Çelik, 1994).

Compaction of the multiparticulates without negatively affecting the particulates integrity is a major challenge in the production of MR-ODTs (Maganti and Çelik, 1994). Hence, the fragmentation of the particles under compaction has major issues with the drug release (Tunón, 2003).

Therefore, the multiparticulate systems based on suitable polymers as monolithic or reservoir matrix systems can be a significant approach to achieving a delayed or extended-release system. However, the other significant factor to consider is investigating and observing the integrity of multiparticulates, including microparticles and pellets, after compaction of the ODT loaded multiparticulates by examining the used excipients mechanical properties and assessing the final drug release profiles.

1.3.1 Polymers used in the preparation of MR-ODTs

Selecting suitable polymer and excipients is an essential step to achieve the study aims.

Whether natural or synthetic, a polymer acts as a substance combined with API pre-designed (Singh and SI, 2009). The selection of polymers to be employed should possess certain properties such as biocompatibility, biodegradability, and economical (Joshi, 2013). The frequently employed polymers in the formation of multiparticulate systems are cellulosic and acrylic polyvinyl acetate. Ethylcellulose, MCC and hydroxypropyl methylcellulose (HPMC) are examples of cellulosic polymers (KOO and HENG, 2001; Iglesias *et al.*, 2020).

Eudragit polymers are acrylic polymers that possess suitable mechanical properties and elongation values that retain the integrity of the prepared microcapsules and pellets under compression. Therefore, acrylic polymers are preferable to cellulosic polymers to modulate drug release (Maejima and McGinity, 2001; Al-Hashimi *et al.*, 2018).

Eudragit was initially marketed in Germany in the 1950s. Eudragit is prepared by polymerising acrylic and methacrylic acids or esters, e.g., butyl ester or dimethyl aminoethyl ester (Rowe, Raymond C., Paul Sheskey, 2009; Gupta, Kumar and Sachan, 2015a). Different examples of the commonly used Eudragit are available for the MR formulations, as illustrated in Table 1.1.

Table 1.1 Examples of Eudragit polymers of MR properties, application, and chemical structures (Gupta, Kumar and Sachan, 2015a) (Thakral, Thakral and Majumdar, 2013a) (Rowe, Raymond C., Paul Sheskey, 2009)

Trade Name	Physical attributes	Applications	Chemical structure
Eudragit E PO	Yellow powder Soluble in gastric fluid- to pH 5	Film coating and taste masking	

Eudragit NE 30 D	Aqueous dispersion Swellable, permeable	MR matrix and enteric coating	$\left[\begin{array}{c} \text{H} \qquad \qquad \text{CH}_3 \\ \qquad \qquad \\ \text{---CH}_2\text{---C---CH}_2\text{---C---} \\ \qquad \qquad \\ \text{C=O} \qquad \text{C=O} \\ \qquad \qquad \\ \text{O} \qquad \qquad \text{O} \\ \qquad \qquad \\ \text{CH}_3 \qquad \text{C}_2\text{H}_5 \end{array} \right]_n$
Eudragit L 100	White powder Soluble in intestinal- fluid from pH 6	Enteric coatings	$\left[\begin{array}{c} \text{CH}_3 \qquad \qquad \text{CH}_3 \\ \qquad \qquad \\ \text{---CH}_2\text{---C---CH}_2\text{---C---} \\ \qquad \qquad \\ \text{C=O} \qquad \text{C=O} \\ \qquad \qquad \\ \text{OH} \qquad \qquad \text{O} \\ \qquad \qquad \qquad \\ \qquad \qquad \qquad \text{CH}_3 \end{array} \right]_n$
Eudragit RL PO	High permeability- time dependent	MR	$\left[\begin{array}{c} \text{CH}_3 \qquad \qquad \text{H} \\ \qquad \qquad \\ \text{---CH}_2\text{---C---CH}_2\text{---C---} \\ \qquad \qquad \\ \text{C=O} \qquad \text{C=O} \\ \qquad \qquad \\ \text{O} \qquad \qquad \text{O} \\ \qquad \qquad \\ \text{CH}_2 \qquad \text{CH}_3 \\ \qquad \qquad \\ \text{H}_2\text{C---N}^+ \text{---CH}_3 \\ \qquad \qquad \\ \qquad \qquad \text{CH}_3 \end{array} \right]_n$
Eudragit RS PO	Low permeability time-dependent	MR	$\left[\begin{array}{c} \text{CH}_3 \qquad \qquad \text{CH}_3 \\ \qquad \qquad \\ \text{---CH}_2\text{---C---CH}_2\text{---C---} \\ \qquad \qquad \\ \text{C=O} \qquad \text{C=O} \\ \qquad \qquad \\ \text{O} \qquad \qquad \text{O} \\ \qquad \qquad \\ \text{CH}_2 \qquad \text{C}_2\text{H}_5 \\ \qquad \qquad \\ \text{H}_2\text{C---N}^+ \text{---CH}_3 \\ \qquad \qquad \\ \qquad \qquad \text{CH}_3 \end{array} \right]_n$

1.3.2 Plasticisers and the enhancement of the formulation's mechanical properties

Plasticisers are the essential excipients utilised in a drug-polymer system to improve the elastic-plastic attributes of the polymers, such as reducing glass transition temperature and enhancing the flexibility of the polymeric molecules (Lim and Hoag, 2013a).

In general, plasticisers produce formulations with enough strength to resist the applied pressure during tablets formation but deform elastically with no fragmentation. Therefore, toughness and flexibility are observed using plasticisers (Zhu *et al.*, 2002; Rahman and Brazel, 2004). For instance, low concentrations plasticisers provide a softening effect rather than an increase in the rigidity of the formulations, which is called the anti-plasticisation effect. This effect can be applied differently in pharmaceutical systems, as it can change the drug permeability of polymers (Carvajal, Chamarthy and Pinal, 2006).

Different studies have implemented plasticised polymers due to their vital properties in drug delivery (Snejdrova and Dittrich, 2012). The plasticisers can be categorised into hydrophilic such as Glycerin/glycerol, polyethylene glycols, polyethylene glycol Monomethyl Ether, Sorbitol, and hydrophobic plasticisers such as acetyl tributyl/ acetyl triethyl citrate, castor Oil, triacetin and tributyl/triethyl citrate (Kim *et al.*, 2018).

The prepared formulations using specific excipients: polymers, fillers, and plasticisers were explored in the literature review in detail and findings were employed in every chapter according to their properties to approach each study's main aim and objectives.

1.4 Introduction to the literature review

Conventional dosage forms of immediate-release (IR) require frequent daily dosing. In addition, the multi-daily dose treatment is suitable for a few days treating acute or short-term health conditions such as colds and migraines. However, frequent dosing is undesirable for treating chronic conditions requiring longer treatment periods that can be months or even years. Also, it can result in missed doses (Felton, 2013).

High expenses reach billions of dollars are estimated to spend yearly due to patient noncompliance in the United States (US). Nevertheless, this surpasses the financial impact to cause a high mortality rate in patients with the worsened condition after ignoring taking their medicine or forgetting many doses.

The yearly estimation of deaths is more than 120,000 due to patient noncompliance. A study conducted by Martin *et al.* placed patients suffering from high blood pressure on a three and one times daily dose treatment. The treatment of one-time dose

showed around 84% patient compliance while 59% of patients complied with the three times dose treatment (Martin *et al.*, 2005; Walters-Salas, 2012). Therefore, the effectiveness of the oral MR dosage forms in enhancing patient compliance and treating chronic conditions is becoming increasingly popular as an alternative to solid oral formations of IR. The rationale for using the modified release (MR) dosage forms is to achieve a gradual or slow drug release. Therefore, MR dosage forms include an extended-release (ER) and sustained-release (SR) system (Siegel and Rathbone, 2012).

MR dosage formulations can be administered orally in single-unit dosage form (SUDF) or multiple-unit dosage form (MUDF). The multiparticulate dosage form is another name of MUDF. SUDF consists of a single tablet or capsule containing the drug. On the other hand, the MUDF consists of several discrete particles, including microparticles, nanoparticles, or pellets, as a single dosage system (Abdul, Chandewar and Jaiswal, 2010).

Coating the multiparticulates with a polymeric layer can be an effective approach for modification the drug release. Hence, these coated multiparticulates can be included in capsules or compacted as tablets (Xu, Heng and Liew, 2016).

Tablets are the most common solid oral dosage forms offering cost-efficient and high production speed. Tablets are mechanically stronger than hard gelatin capsules. However, both tablets and hard gelatin capsules correspond to swallowing issues impacting the elderly and geriatrics, eventually the patient compliance to medication (Cole, 1998). Combining MUDF with matrices of orally disintegrating tablets (ODTs) can offer an ingenious solution for many patients, especially dysphagia patients.

1.5 Challenges of the compression of multiparticulates

The combination of ODT with MR multiparticulates (micro/nanoparticles, uncoated pellets (matrix) or coated pellets (reservoir)) is expected to provide a rapid disintegration of the tablet after oral administration and release the particulates individually. The small size of the multiparticulates facilitates the spreading and the distribution of the particles over a large surface area along the gastrointestinal tract (GIT). This avoids high local drug concentrations and diminishes possible local irritation (especially with weak acids)(Meyer A.S. Hussain, 2005; Easterling and

Robbins, 2008; Kelly and Wright, 2009). The active pharmaceutical ingredient (API) is present in each particulate; thus, the total API is distributed into these subunits. This reduces the risk of side effects and the toxicity related to 'dose dumping' (Meyer A.S. Hussain, 2005).

Nevertheless, during tablet manufacturing, the compression of the particulate systems can be challenging (A. Elwerfalli et al., 2015). The presented review aims to critically assess the previous studies that investigated the compression of multiparticulates into tablets and provide a comprehensive understanding for future improvements in this field. Three different types of multiparticulates (microparticles, nanoparticles and pellets) are assessed accordingly. Considerable formulation parameters are discussed, involving the type of polymer used in the coating (e.g., cellulosic or acrylic), the quantity of polymer coating used, the effect of excipients in addition to other process variables such as the effect of compression force on protecting the integrity of the polymer coat. Numerous compaction theories were also evaluated, summarising the compaction behaviour of the multiparticulate systems.

1.6 Compaction process

The compaction process of powders is influenced by the type of the materials and physical properties of the particles, including size, morphology, and compaction forces. The porosity of particles and powder blend can be another essential factor (Ghori, 2016).

The volume and the amount of air between the particles decrease under compaction pressure over powder or granules, and this process requires energy uptake (Kuno and Okada, 1982; Ghori, 2016). The amount of pressure applied during compaction and the powder properties can affect the strength of the bond formation. The powder compaction reduces the distances between the particles leading to the formation of the interparticulate bond; hence, the compaction process is accompanied by heat release (Šantl et al., 2011; Ghori, 2016)

On the other hand, pellets compaction consists of two stages. The rearrangement and deformation of pellets occur in the first stage. The pellets crushing is in the second stage. The second stage is influenced by the porosity and deformability of pellets (Mallick et al., 2011; Šantl et al., 2011).

1.7 Compaction of microparticulate systems into MR Tablets

1.7.1 Microcapsules and Microspheres

Microparticles, microcapsules and microspheres are multi-unit particles consisting of a polymeric system and API. Microparticles generally possess a size range of 1-1000 μm consisting of a polymeric matrix with homogeneously distributed API. Microcapsules are coated microparticles of less than 800 μm size, containing API in the core and surrounded by the polymeric coat forming a reservoir system (Ju and Chu, 2019; Lengyel *et al.*, 2019). Therefore, microspheres and microcapsules are considered microparticles with smaller sizes; hence each can be prepared according to the formulation type and route of administration, like orally or parenterally (Yang and Alexandridis, 2000)(Vhora, Khatri and Misra, 2021).

The microparticles microspheres and microcapsules can also be compressed into tablets, similar to pellets, producing MR formulation. However, these multiparticulates are smaller than pellets in size; the typical diameter of microcapsules ranges between 100–150 μm (Bansode *et al.*, 2010). In simple words, microcapsules are based on a polymeric reservoir system, while microspheres are polymeric matrix systems containing the dispersed API (Figure 1.3).

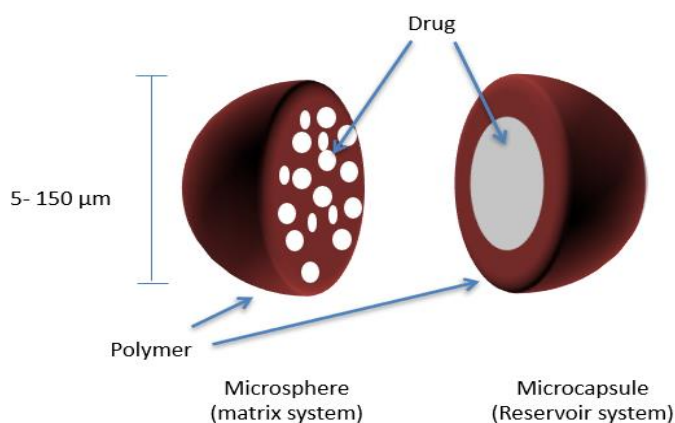


Figure 1.3 Microspheres and microcapsules matrix and reservoir systems are drawn using Microsoft office 2018 (Al-Hashimi *et al.*, 2018)

1.7.2 Tablets of coated nanocapsules

The compressed polymeric nanoparticles (nanospheres and nanocapsules) into tablet forming MR multiparticulates is an interesting application in drug delivery development. The nanoparticles are particles of size $<1 \mu\text{m}$ in which the drug either dispersed within the polymeric matrix making nanospheres or exist in the core and is surrounded by a polymeric layer making nanocapsules, as shown in Figure 1.4.

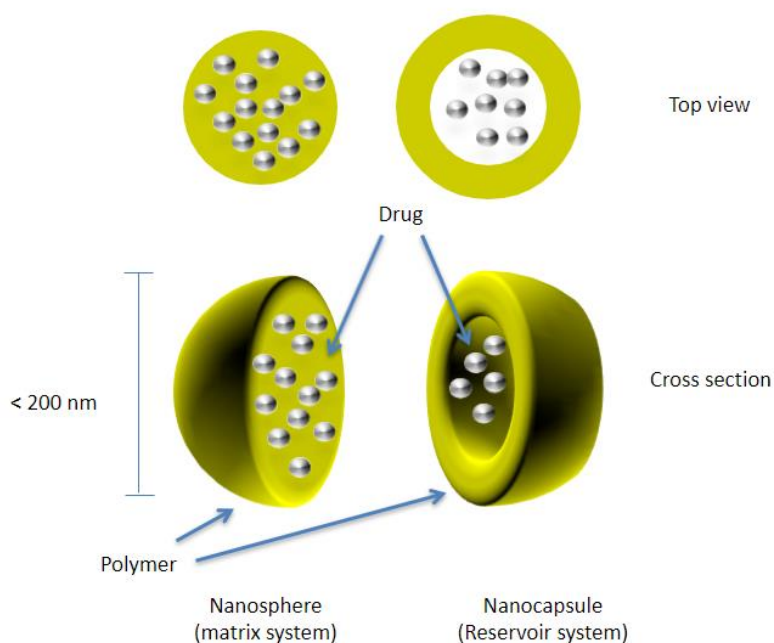


Figure 1.4 Nanospheres and nanocapsules loaded with API drawn using Microsoft office 2018 (Al-Hashimi *et al.*, 2018)

Like microparticles, the use of nanoparticles as an MR system within ODTs should provide a short disintegration time without influencing drug release within the multiparticulate system upon oral administration.

Hence, ODTs disintegrate in the mouth, causing the release of drug-loaded nanocapsules that distribute along with the GIT, providing a modified drug release. Compared to microparticles and pellets, the small size of nanoparticles provides wider distribution in the GIT, thus reducing the risk of local drug concentration and toxicity (A. M. Elwerfalli *et al.*, 2015a).

Friedrich *et al.* studied the effect of the coating layer on the compacted drug-loaded polymeric nanocapsules containing dexamethasone. Tablets were prepared to form nanocapsules (reservoir) to produce oral MR tablets and control tablets with no nanoparticles (Friedrich *et al.*, 2010). The *in vitro* drug release studies showed that

nonencapsulated tablets slowly released the dexamethasone compared to the controlled tablets. This indicates that the drug released was reserved from coated nanoparticles, and the coating layer was strong enough to resist the applied pressure during compression (Friedrich *et al.*, 2010).

1.8 Microspheres & Microcapsules MR tablets

1.8.1 The coating layers

The rationale for applying a coating layer around the API in the microcapsules is to achieve a modified drug release profile. Similar to reservoir pellets, microcapsules must be coated with a polymer of good mechanical properties to promote enough support for the compact under compaction.

In addition, the polymer should be chemically compatible with other microcapsule ingredients. The optimum coating layer provides a cohesive film with a suitable thickness around the microcapsule. Therefore, the ideal polymer coat should possess sufficient elastic-plastic properties to keep the compact undamaged after compaction (Bansode *et al.*, 2010).

One of the polymers that are widely used in particulate coating is alginate. This polymer possesses good mechanical properties; forming a thick solution and crosslinking it with calcium chloride can achieve modified drug release. Hence, alginates dissolve in alkaline media and precipitate at pH lower than its residues pKa values the mannuronic and guluronic acid 3.38 and 3.65, respectively. Therefore, alginate can easily be broken down in the intestinal but stable in gastric media (Chuang *et al.*, 2017)

Different studies prepared pellets and microparticles with a coating layer consisting of sodium alginates with other time or pH-dependent polymers (Abletshauser, Schneider and Rupprecht, 1993) (Gürsoy, Kalkan and Okar, 1998) (Silva *et al.*, 2006). However, using sodium alginate alone provides lower plastic properties than potassium alginate. Therefore, tablets with low rigidity can be prepared from sodium alginate (Rahim, Carter and Elkordy, 2015).

Compression of coated microcapsules was studied by Sawicki, Mazgalski and Jakubowska, using the hot tableting method to modify tramadol hydrochloride release. The authors studied different mixtures of coating polymers using ethylcellulose (EC) and Eudragit® RS/Eudragit® RL. The drug-loaded microcapsules were coated by fluid bed coating. The polymeric films were evenly distributed, covering the drug. However, the aqueous dispersion of the Eudragit® RS/Eudragit® RL mixture was difficult to apply.

Tablets of the microcapsules were prepared under low compression force 1kN and hot tableting method (56°C). Also, tablets were prepared using the traditional method of compression under 10 kN and 25°C temperature. The results showed that hot tableting microparticles had a sufficient coating layer to modify the drug release compared to the obtained tablets from the normal tableting method. Hence, the hot tableted microcapsules were comparable to the commercial brands(Sawicki, Mazgalski and Jakubowska, 2010). Therefore, the suitability of the compression method could depend on the polymeric mixture either in the matrix or coating layer of microparticles.

1.8.2 The coating layer: thickness and polymeric quantity

The other essential factor influencing the quality of microcapsules is the quantity and thickness of the polymeric membrane. The mechanical characteristics of the coated microcapsules can be influenced by the type and thickness of the coating layer upon compaction. A thicker coating layer could provide elastic-plastic behaviour. Therefore, elastic, and plastic deformation can be observed if the number of polymers increases. Hence, the high coating layer thickness makes the drug gradually diffuse through the thick coating layer over a long time, thus affecting the drug release. When the ODTs consist of coated microparticles of modified drug release, the tablets disintegrate after oral administration, and the individually coated microparticles should gradually release the drug over a longer time.

Three tablet formulations of diclofenac sodium microcapsules were prepared by Naveed (2011) to modify the drug release. The EC was coating polymer in three ratios to the diclofenac sodium of 1:1, 1:2, and 1:3. The results showed that increasing the coating layer ratio from 1:1 to 1:3 of EC provided modified drug release. Hence, increasing the EC generated thicker coating layer withstand the

applied pressure under compaction(Naveed, 2011). Although EC has low mechanical properties, the increased EC effectively rendered the microcapsule protected from the dissolution media.

On the other hand, Chourasia and Jain (2004) prepared a multiparticulate system of chitosan matrix-based microspheres coated with Eudragit L100 and Eudragit S100 for achieving colonic metronidazole delivery for amoebiasis treatment (Chourasia and Jain, 2004). Chitosan was crosslinked with glutaraldehyde to protect early degradation of microspheres protecting drug. The results showed that coated microspheres system successfully delayed metronidazole release until it reached the colon (Chourasia and Jain, 2004). Therefore, using Eudragit L100 effectively controlled drug release at low pH (1.2).

1.8.3 Excipients: an additional role in enhancing the mechanical properties of the tablets

The excipients promote different advantages during tablet preparation. The main purpose of using fillers is to add bulk to low-dose tablets forming a conveniently sized tablet. However, another essential purpose of using fillers is acting as a cushioning layer to protect the coating layer of the compressed microcapsules from rupturing upon compression (Bürki, 2016).

The plastic deformation of the cushioning agent should occur during the compression process with no fragmentation, as discussed earlier. Therefore, elastic-plastic deformation of the cushioning layer could provide enough support to protect coated microparticles; thus, modification of drug release can be achieved. The adequate mechanical strength of fillers could allow rapid disintegration upon oral administration without affecting the drug release (Habib, Augsburg and Shangraw, 2002).

On the other hand, lubricants can enhance particles flow by reducing inter-particle friction. The magnesium stearate as a lubricant is favoured in tablet manufacturing. However, the lubricant effect depends on the type of API used. Therefore, it should be added wisely. Zarnpi et al. found that the solubility of drugs (metformin, paracetamol, sulfamethoxazole, furosemide, carbamazepine, dipyridamole,

ibuprofen and itraconazole) decreased in the presence of magnesium stearate (2 and 5%) significantly due to its hydrophobic nature (Zarmpi *et al.*, 2020).

1.8.4 The compaction forces

Kim *et al.* (2010) also studied the mechanical characteristics of microcapsules prepared from alginate-chitosan protein. The elasticity modulus and the releasing rate of the protein were evaluated for the coated multiparticulates. Using a compression analysis, three ratios of chitosan coating layers, 1%, 2%, and 3%, were tested. The results indicated microcapsule elastic modulus increase with increasing the ratio of chitosan layer as the values were 11.8 ± 4.9 , 32.6 ± 11.4 , and 42.8 ± 14.4 kPa of for 1%, 2%, and 3% of chitosan, respectively (Kim *et al.*, 2010). Hence, the delayed protein release was associated with the increase in elasticity modulus.

1.9 Multiparticulate Drug Delivery Systems: Pellets

The pellets possess a typical size range between 0.5–2 mm (Yadav and Verma, 2016). The pellet is loaded with API, and the total drug dose is distributed within the pellets (Muley, Nandgude and Poddar, 2016).

Extrusion–spheronisation is the most common technique of multiple steps for preparing pellets, as shown in Figure 1.5 (Al-Hashimi *et al.*, 2018). On the contrary, other used techniques of preparing pellets, such as hot melt extruder, are associated with long steps process, high energy required and expenses for storing low melting point binders (Bhairy *et al.*, 2015; Yadav and Verma, 2016).

The Extrusion- spheronisation process consists of mixing the powder blend of API and excipients with a granulation fluid. This wet mass is then transferred into an extruder, forming long extrudates. The last step is the formation of the pellets by breaking up the extrudates using the spheronizer. The drug-loaded pellets can then be used as a matrix system or coated with a polymer (Phale and Gothoskar, 2011; Šantl *et al.*, 2011; Muley, Nandgude and Poddar, 2016).

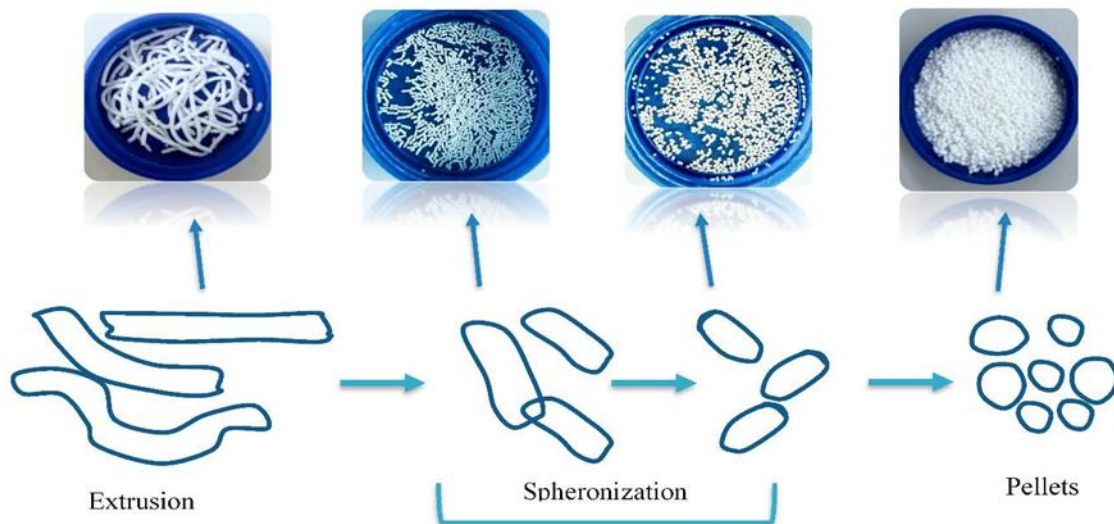


Figure 1.5 Diagram showing the extrusion spheronisation technique steps of pellets preparation are drawn using Microsoft office 2018 (Al-Hashimi *et al.*, 2018)

The matrix and the coated pellets, as shown in Figure 1.6, afterwards can be compressed into MR tablets (Kibria, Akhter and Ariful Islam, 2010; Phale and Gothoskar, 2011)(Al-Hashimi *et al.*, 2018).

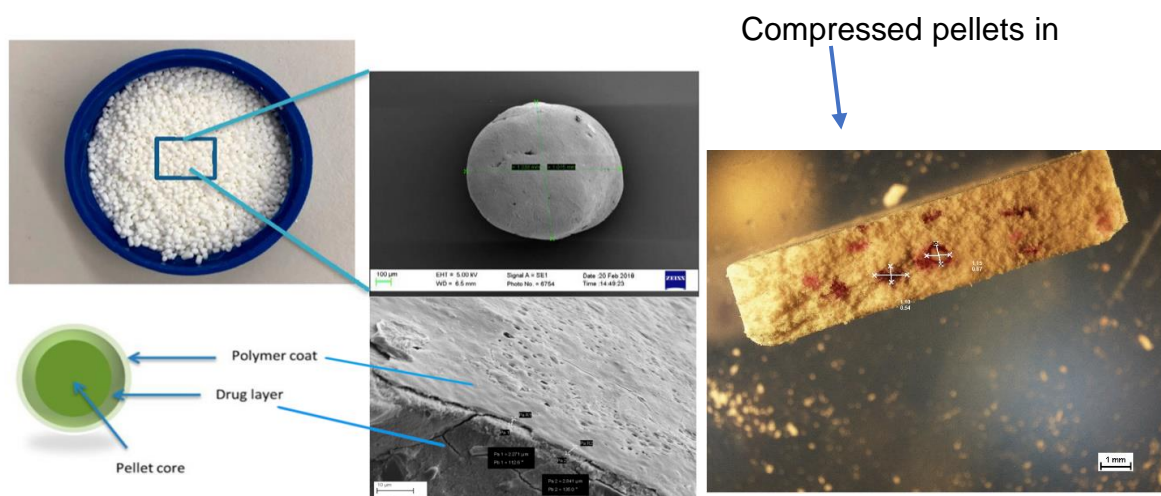


Figure 1.6 Diagram showing of matrix and reservoir pellet and ODT containing pellets from one of our formulations consisting of Eudragit L100, sorbitol and indomethacin hydrochloride (IND) using SEM, stereomicroscope, and Microsoft office 2018 (Al-Hashimi *et al.*, 2018)

1.9.1 Compression of pellets into tablets

There are different factors to be considered during the compression of pellets into tablets, as discussed in the following sections.

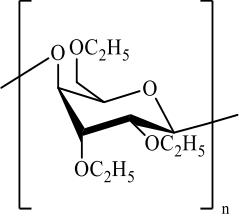
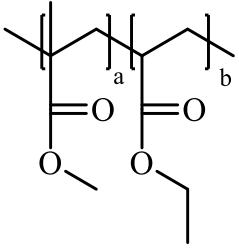
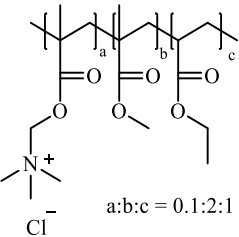
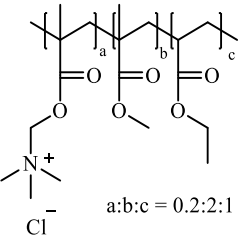
1.9.1.1 The choice of suitable coating layers

The choice of coating material is essential to withstand the compressing pressure in pellet production. The coating polymers must have enough elasticity, plasticity, and thickness without rupturing under compression (Tunón, 2003). Aqueous or organic polymeric solutions can be used. Aqueous polymeric solution is preferred, as there are minimum toxicity hazards compared to organic solutions; also, these polymers are less costly (Sadeghi, Shahabi and Afrasiabi Garekani, 2011). However, organic polymeric solutions are widely used for methacrylic polymers to modify drug release in multiparticulates preparation (Sadeghi, Shahabi and Afrasiabi Garekani, 2011). Also, organic solvents evaporate in a shorter time with fewer facilities producing pellets with low moisture content compared to aqueous solvents. Hence, moisture can act as a plasticiser that influences pellets' mechanical properties and drug release profile. Therefore, it is necessary to consider a suitable solution depending on the polymer and the drug type (Sadeghi, Shahabi and Afrasiabi Garekani, 2011).

1.9.1.2 The coating layer mechanical properties

The thickness of the coating layer is an essential parameter for retaining pellet shape during compression by protecting film integrity. As the coating layer thickness increases, the mechanical strength of the coated pellets improves. Hence, elastic and plastic properties of the pellets enhance, resulting in protecting the coating polymer from rupturing under compression, thus prolonging drug release (Murthy Dwibhashyam and Ratna, 2008). There are several semisynthetic and synthetic polymers used to prepare the MR system. These polymers differ in their mechanical properties. The common examples of these polymers are summarised along with their chemical structures in Table 1.2.

Table 1.2 Chemical structures of common pharmaceutical polymers used in coated multiparticulates and their elongation values (Al-Hashimi et al., 2018)

Polymer class	Coating polymer	Chemical structure	Elongation value
Cellulosic Polymers	EC		<5%
Acrylic polymers	Eudragit NE 30 D	 <p>a:b= 1:2</p>	≥365%
	Eudragit RS 30 D	 <p>a:b:c = 0.1:2:1</p>	<50%
	Eudragit RL 30 D	 <p>a:b:c = 0.2:2:1</p>	<50%

Verapamil hydrochloride pellets (40mg) were produced by Sawicki and Lunio (2005), dispersion of polyvinyl acetate was used as coating polymer and propylene glycols as a plasticiser to improve the pellets flexibility.

Correspondingly, the coating polymer was used to prepare two films A and B, with thicknesses 35 μm and 50 μm . The study found that pellets with film A (35 μm) could

not resist the compression force during tablet compaction. Also, a rapid drug release was caused by the rupturing of the coated polymer. In contrast, it has been noticed that film B of polymer thickness 50 µm caused the slower release of verapamil hydrochloride. Therefore, the thicker coat resists the compression force during tablet preparation (Sawicki and Łunio, 2005). Therefore, the coating layer dimensions should be considered during pellet preparation.

1.9.1.3 Examples of polymers used in the preparation of compacted pellets

1.9.1.3.1 Cellulosic Polymers

Cellulose is a natural polysaccharide polymer synthesised by plants (Ansell and Mwaikambo, 2009). Ethylcellulose polymers (EC) are semisynthetic, biodegradable, biodegradable and thermally stable polymers (Kraisit *et al.*, 2017)(EFSA, 2004). EC polymer is commonly used in the preparation of MR formulations. Nevertheless, this polymer is fragile with low elongation (<5%) thus low mechanical properties (Kraisit *et al.*, 2017)(Łunio *et al.*, 2008).

Hosseini, Körber and Bodmeier, (2013) prepared pellets of propranolol hydrochloride coated with EC. The authors used a cushioning layer to absorb the compaction energy protecting the coating layer from destruction under compression. The cushion layer consisted of MCC, lactose and sorbitol, where these excipients covered the top of the pellets. It was noticed that the coating layer ruptured under compression, despite the cushioning layer's presence and the EC coat's integrity was affected along with drug release. Nevertheless, the addition of glidant (such as magnesium stearate) to the cushion layer enhanced the mechanical strength of the pellets leading to reduce the effect of the compression pressure on coating polymer (Łunio *et al.*, 2008)(Hosseini, Körber and Bodmeier, 2013a)

Microcrystalline cellulose (MCC) is another widely used cellulosic copolymer in pellets' preparation by extrusion spheronisation(Sadeghi, Shahabi and Afrasiabi Garekani, 2011). MCC possesses plastic attributes supporting the prepared pellets and offering variation in drug release, particularly for drugs with low water solubility. However, MCC could be incompatible with some drugs (Muley, Nandgude and Poddar, 2016)(Kranz *et al.*, 2009).

On the other hand, hydroxypropyl methylcellulose (HPMC) is a water-soluble polymer used as a binder in coated pellets. Nguyen et al. showed that pellets were mechanically strong with the addition of HPMC. Hence, the higher the HPMC concentrations, the high resistance of the pellets for the applied compaction pressure. Moreover, the use of HPMC in the pellets provided a delayed glipizide release. Interestingly, glipizide was released through the pores within HPMC after water penetration into the pellets (Nguyen, Christensen and Ayres, 2014).

1.9.1.3.2 Acrylic Polymers

These polymers are commonly used compared to cellulose polymers because of their elastic properties, giving them a lower chance to deform under compression of the coated pellets. The elongation principles determine the elasticity of these polymers. An example of an aqueous copolymer is Eudragit NE 30 D as a dispersion of ethyl acrylate and methyl methacrylate in a ratio of 2:1 and an elongation rate of $\geq 365\%$ (Murthy Dwibhashyam and Ratna, 2008). These elongation values indicate that the polymer flexibility is relatively high. Therefore, it can withstand deformation under applied pressure during compression (Arno *et al.*, 2002; Murthy Dwibhashyam and Ratna, 2008; Ragnarsson *et al.*, 2008; Al-Hashimi *et al.*, 2018). In this case, the plasticisers are less required to improve the film flexibility due to the high elasticity of polymers (Murthy Dwibhashyam and Ratna, 2008).

The flexibility of Eudragit NE 30 D is related to the missing of strong hydrogen bonds in its chemical structure, as in Table 1.2. On the contrary, plasticiser was necessary with Eudragit RS and RL30D. It was found that the elongation value was $< 50\%$ in the absence of plasticiser or a little quantity added (10% w/w) for Eudragit® RS and RL 30D. Nevertheless, when the plasticiser quantity reaches 20%, the elongation value elevated to 300%. This results in enhancing the ability of polymer's film to endure compressive forces during the manufacturing of the tablets (Murthy Dwibhashyam and Ratna, 2008; Abdul, Chandewar and Jaiswal, 2010)

Three acrylic polymers were studied by Akhter and Kibria (2009), investigating their effect on drug release rate and its release kinetics. Eudragit RL 30 D, Eudragit RS 30

D and Eudragit NE 30 D coat ambroxol hydrochloride as MR pellets. *In vitro* dissolution tests of pH 1.2 and 6.8 mediums were used to test the prepared pellets from the three acrylic polymers. The drug release in acidic media from Eudragit RL 30 D, Eudragit RS 30 D, and Eudragit NE 30 D coated pellets was 35%, 13.75%, and 2.43%, respectively, at the first hour. The low drug release of Eudragit RS 30 D and Eudragit NE 30 D coated pellets could be associated with the low water permeability of both polymers (Akhter and Kibria, 2009). Hence, the high initial drug release from the Eudragit RL 30 D-coated pellets may be due to the high-water permeability of the film, causing the drug to dissolve and diffuse.

Eudragit RS contains a low ratio of quaternary ammonium groups compared to Eudragit RL. On the other hand, the carboxylic groups in Eudragit NE 30 D promoted a high water resistance (Akhter and Kibria, 2009). Therefore, it can be assumed that Eudragit NE 30 D and Eudragit RS 30D possess suitable retarding properties for the drug.

It is critical to prepare pellets of uniform size and shape to provide a consistently accepted mechanical property. Matrix or reservoir-based pellets can be produced efficiently using the extrusion spherulisation technique to prepare pellets of uniform shape with narrow size distribution (Asghar and Chandran, 2006). However, the use of suitable excipients affects the quality of pellets, the pellets' physical or mechanical properties, and drug release profile (Issa *et al.*, 2017). The widely used polymers to prepare multiparticulate systems are methacrylic acid copolymers, including Eudragit L100 and Eudragit S100 with dissolution above pH 6.0 (Khan, Prebeg and Kurjaković, 1999). It was reported that the addition of Eudragit L100 to the Eudragit S100 based multiparticulates provides controlling the drug release efficiently more than using Eudragit s100 alone (Asghar and Chandran, 2006).

The technique was utilised by Krogars *et al.* (2000) to make a matrix comprising ibuprofen, a commercially available anti-inflammatory drug (Krogars *et al.*, 2000). The matrix consisted of Eudragit S100, then coated by an aqueous citric acid and hydroxypropyl methylcellulose (HPMC) layer. Eudragit S100 and citric acid were applied as pH controlling agents. The results showed that the physical properties of the pellets were influenced significantly by the ingredients; for instance, the pellets sphericity and size were enhanced using Eudragit S100 and citric acid (Krogars *et al.*,

2000). Nevertheless, Eudragit S100 alone showed a limited effect on delaying drug release in the acidic media (pH 1.2) (Asghar and Chandran, 2006).

1.9.1.4 Pellet Composition

Generally, pellets or granules undergo two types of deformation during the compression process: elastic and plastic deformation. When pellets possess elastic deformation, they deform temporary and return to their initial shape after removing the applied stress. In contrast, the permanent shape change refers to plastic deformation after removing the applied stress.

To avoid reversible deformation and manufacturing failure, the applied pressure should be high during tablet compaction, exceeding the elastic limit. Hence, when low pressure is applied, elastic deformation occurs. Also, if the applied pressure during the tablet's compaction is low, the formed tablets could be brittle. Therefore, plastic deformation is necessary to manufacture mechanically resilient compacted pellets or tablets (Tunón, 2003; Murthy Dwibhashyam and Ratna, 2008). However, the compact with plastic properties should maintain its shape and mechanical properties with no fragmentation. Therefore, elastic-plastic equilibrium is necessary (Anbalagan, Liew and Heng, 2017). In addition, for a successful MR formulation considering suitable excipients/components contained in the pellet's matrix is essential. The inactive excipients should possess elastic-plastic deformation to assist in successful tableted pellet formation (Anbalagan, Liew and Heng, 2017).

The common excipients used in tablets manufacturing are MCC and lactose as fillers, hydroxypropyl methylcellulose (HPMC), and starch as binders. The excipients are incorporated with the API in the pellet preparation (Tan and Hu, 2016b; Tank *et al.*, 2018). On the other hand, stearic acid can be utilised in pellets preparation to eliminate the possible damage caused by the compression with no effect on the disintegration time of ODTs (Li *et al.*, 2016).

Chin, Chan, and Heng studied the effect of the lactose particle size and its use as a cushioning layer to support the compressed pellets' integrity. The coarse lactose particles showed high voids and offered weak protection, while micron-sized lactose with a median particle size of 2.3 μm supported by the pellet integrity with no

damage (Chin, Chan and Heng, 2016). However, the study used different grades of lactose that also possess without considering the shape factor of the particles.

The plastic deformation of the MCC made it favourable during pellets compression. MCC also offers good binding properties rendering the pellets mechanically strong and cohesive, making them suitable for tablet compression. Therefore, the good rheological and mechanical properties considered MCC a gold standard for pellets manufacturing (Murthy Dwibhashyam and Ratna, 2008; Dukić-Ott *et al.*, 2009). It was found that using MCC and HPMC provides good compaction properties and produce MR tablets (Ghori and Conway, 2016).

However, MCC has high plasticity and mixing it with other excipients can further enhance the compressibility of pellets and deform without fragmentation (Gómez-Carracedo *et al.*, 2008).

Although MCC is considered the gold standard excipient in the pellet formulation, some API may be chemically incompatible with MCC (Gómez-Carracedo *et al.*, 2008; Wu *et al.*, 2011). However, this varies with MCC grades and is also associated with other excipients. Therefore, consider this interaction when incorporating the API in pellet preparation (Gorain *et al.*, 2018).

Krueger *et al.* examined the extrusion spherulisation process variables, including spherulizer load, speed, and time on pellet properties, using two grades of MCC (I and II). The results showed that the spherulisation speed and time significantly affected the formed MCC II pellets' characteristics. The pellet weight and diameter increased while the pellet aspect ratio and porosity decreased during the spherulisation step. In contrast, MCC I pellets weight remained constant and decreased in diameter (Krueger, Thommes and Kleinebudde, 2013). Besides, in the extrusion spherulisation other than MCC, chitosan, pectin acid, polyethylene oxide, HPMC, and k-carrageenan can be used (Steckel and Mindermann-Nogly, 2004)(Jess and Steckel, 2007).

Three different types of commercial carrageenan (kappa, iota, and lambda) were examined by Bornhöft *et al.* as a potential alternative for MCC in pellets formation. The iota and lambda type of carrageenan failed to prepare uniformly shaped pellets and had good mechanical strength. The pellets were fragile with poor

plasticity, thus unsuitable to be compacted. On the other hand, pellets prepared from kappa-carrageenan demonstrated high mechanical strength and good plasticity. Therefore, kappa-carrageenan can be considered a another substitute for MCC (Bornhöft, Thommes and Kleinebudde, 2005)(Thommes and Kleinebudde, 2006).

Yang *et al.* used Eudragit NE 30 D to prepare pellets with good mechanical properties and modified Metoprolol Succinate release. It was found that using a coating layer of talc to Eudragit NE 30D in a ratio of 1:4 was ideal for preventing coalescence and obtaining pellets with enhanced mechanical attributes. Hence, the coating film possesses enough elastic and plastic properties to withstand the compaction pressure during the tablet preparation (Yang *et al.*, 2016).

1.9.2 Role of the plasticisers

Plasticisers are one of the pharmaceutical excipients that are used in solid dosage forms. When adding the plasticiser to compact, the flexibility enhances. In general, if the polymers are brittle at room temperature, they may damage under compaction leading to faster drug release from the tablets. Therefore, plasticisers enhance the polymeric film-forming attributes, leading to uniform distribution of the polymeric layer around the coated pellets (Chen *et al.*, 2017).

Osei-Yeboah et al. prepared pyridoxine-loaded pellets coated with EC aqueous dispersion. The pellets were further coated with an additional layer of plasticiser polyvinylpyrrolidone (PVP) (10%, 15%, and 20% w/w) as a protective layer prolonging the pyridoxine release over time. The prepared pellets were then compacted into tablets of multiple units. The results showed that drug release from compressed PVP coated pellets was maintained over 2 hrs from all coated pellets with PVP and EC, enhancing the polymer's flexibility to retain the intact pellets. This was not the case for coated pellets without the extra layer of PVP as rapid pyridoxine release was detected within the 2 hrs resulting from rupturing EC coat upon compaction (Osei-Yeboah, Lan and Sun, 2017). Also, Rajsharad and Kamble coated pellets with polyvinyl alcohol (PVA) in the aqueous polymeric suspension (Rajsharad and Kamble, 2006). The results showed that pellets were protected from cracking and damage after the film drying. Similarly, Laboulfie *et al.* found that the

elasticity of the HPMC coating layer was enhanced when adding polyethylene glycol (PEG) (Laboulfie *et al.*, 2013).

1.9.3 Pellet size

Pellet's compaction /properties are influenced by pellets shape and size. Thus, coated pellets integrity and the drug release pattern from the compacted pellets can be changed (Murthy Dwibhashyam and Ratna, 2008). This was investigated by Dashevsky *et al.*, assessing the effect of pellet size of coated pellets with polyvinyl acetate on propranolol HCl release. The results indicated that the smaller pellets provided a larger surface area and had a thinner coating. Therefore, the polymer coat was insufficiently coating the small pellets leading to their fragmentation and ruptured polymer coat. Moreover, the compromised polymer coat integrity influenced the drug release leading to a fast release pattern with no MR properties. However, the larger pellets resisted the compaction force preserving the polymer coat integrity and prolonging the drug release rate (Dashevsky, Kolter and Bodmeier, 2004) (Murthy Dwibhashyam and Ratna, 2008).

1.9.4 Pellets' porosity

Porosity as voids between pellets or within pellets affects the characteristics of the pellets, including mechanical properties, the polymer coat integrity and tablet tensile strength of the compressed pellets. The porous pellets tend to deform under compression, flattening with no fragmentation. However, the high porosity level could induce fragile pellets with low mechanical properties hence low contact points for interparticulate bonds (Choudhary and Avari, 2013).

Tunón, Gråsjö and Alderborn (2003) prepared three batches of pellets with varying intragranular porosities (low, intermediate, and high porosity). The study examined the compression performance and the subsequent drug release rate for all batches. The different porosities were attained using different amounts of ethanol and water in the granulation fluid, then a thin layer of EC was applied to coat the pellets. The authors concluded that the compaction force minimally influenced the pellets of high porosity during tablet preparation, therefore maintaining the integrity of the polymeric coat and a modified drug release was not diminished. Pellets with

high porosity promoted the increment of deformation and densification upon compression. Consequently, the drug of MR properties was unaffected. While the low porosity pellets were only slightly deformed and densified, thus drug release was relatively high (Tunón, Gråsjö and Alderborn, 2003).

1.10 Assessment of the compaction performance of multiparticulate systems

The compaction process consists of three main stages for the pharmaceutical powder: powder filling, compression, and ejecting and collecting the final compact.

Firstly, low pressure enables the particles-particle interaction and compresses with a reduced volume. The higher pressure applied to powder results in an additional reduction in volume and the particles' size. This process continues until the particles attain the final structure without further movement (Persson *et al.*, 2016). The examination of particle behaviour in each phase provides a complete understanding of the powder mechanical properties. Examples of direct and indirect methods of pharmaceutical compact characterisation for testing powder's physical and mechanical properties (Table 1.3) (Samimi, Hassanpour and Ghadiri, 2005). However, the experimental data can be predicted using simulation analysis, such as the discrete element method (DEM). Samimi, Hassanpour and Ghadiri used the experimental data of yield pressure and Young's modulus for individual granules to simulate and analyse the bulk compression process by DEM. Hence, the obtained numerical data were compared with the experimental result (Samimi, Hassanpour and Ghadiri, 2005). The DEM results showed the relationship between bulk compression and mechanical properties of individual granules. The experimental and simulated results agreed with the low ratio of the Heckel parameter to the yield pressure (<1), indicating the single granules softness result (Samimi, Hassanpour and Ghadiri, 2005).

Table 1.3 Direct and indirect method of pharmaceutical compact characterisation

	Evaluation	Method	Characterization	Reference(s)
DIRECT METHOD	Microscopic Evaluation	Scanning Electron Microscopy	Morphology and surface characteristics of multiparticulate and powders	(Park <i>et al.</i> , 2016) (Hirjau <i>et al.</i> , 2020)
	Particle Size Analysis	Sieve Analysis	Size of multiparticulate and powders of pharmaceutical materials	(Sarkar, Ang and Liew, 2014a)
INDIRECT METHOD	Analytical Procedures	Dissolution Studies	Release profile(s) of API	(Ghanam and Kleinebudde, 2011)
	Texture Analysis	Texture Analyser	<ul style="list-style-type: none"> ◆ Elastic-plastic properties of multiparticulate and powders ◆ The disintegration of compacts of rapid dissolving ingredients ◆ Mucoadhesion properties of polymers ◆ Hardness testing of pellets and tablets 	(Ahmat, Ugail and Castro, 2011) (Abdelbary <i>et al.</i> , 2005) (Cespi <i>et al.</i> , 2007)
	Compression Analysis	Heckle Model	<ul style="list-style-type: none"> ◆ Powder compressibility - porosity relationship ◆ Elastic-plastic deformation 	(ElShaer <i>et al.</i> , 2017) (Khomane and Bansal, 2014)
	Compression Analysis	Kawakita Equation	<ul style="list-style-type: none"> ◆ Flowability and cohesiveness of fluffy/smooth powders ◆ Volume-compressibility relationship ◆ Powder rearrangement at low pressure 	(Persson <i>et al.</i> , 2016)
	Compression Analysis	Partial Differential Equations	<ul style="list-style-type: none"> ◆ Prediction and appraisal of the variables influencing mechanical properties ◆ Determine shape model of pharmaceutical tablets 	(Ahmat, Ugail and Castro, 2011)
	Numerical Compression Analysis	Finite Element Method	<ul style="list-style-type: none"> ◆ Assessment of tablets shape and their mechanical properties 	(Frenning, 2010)

1.11 Aim and objectives

This thesis aims to design new orally disintegrating tablets with modified-release capabilities. This approach will boost patient compliance by easing ingestion and reducing dosing frequency. Manufacturing a multiparticulate system (microparticles/pellets) embedded within the matrix of an ODT was used to achieve this aim. The following objectives were set:

1. To evaluate the mechanical characteristics of excipients such as sodium alginate, PVA, MC, PAA, and EudragitL100 and evaluate their use in developing compressible pellets and microparticles.
2. To formulate and develop multiparticulate systems using optimised excipients, including polymers, plasticisers, and tablets fillers/bulking agents of sufficient mechanical and physical properties to maintain the integrity of the microparticles and pellets under compression when implemented in the formulation.
3. To reduce the number of excipients to provide environmentally friendly preparation methods.
4. To prepare ODTs with a short disintegration time using different fillers sizes.
5. To maintain the properties of ODTs after incorporating the modified release microparticles/pellets in the ODTs matrices.
6. To develop and validate two HPLC methods for quantifying IND and PRH release from the formulations.
7. To prepare IND and PRH loaded multiparticulates independently.
8. To optimise the preparation methods parameters achieving good mechanical properties of multiparticulates.
9. To formulate a modified released system via embedding the multiparticulates within the ODT matrix.
10. To maintain the integrity of pellets/microparticles under compression, protecting the drug release.
11. To delay the release rate of IND and modify the PRH release using matrix and reservoir system via microparticles and pellets.
12. To simulate the compaction behaviour of the multiparticulate loaded ODTs using simulation software to offer cost and time-efficient methods.

Chapter 2 Experimental: General materials and methods

2.1 Experimental

The experimental part includes the materials and general experimental for formulation preparations and characterization.

2.2 Materials

The materials were purchased from different companies and suppliers, as indicated in this section. Also, other used materials were available in the university laboratory. According to the prepared formulation, detailed material use is illustrated in each chapter according to its specific application.

In general, the ingredients used in our projects were as follow:

For formulation preparation: Indomethacin (IND) and propranolol hydrochloride (PRH) (Tokyo Chemical Industry, Japan). Eudragit L100, Eudragit RS and Eudragit RL (Evonik Industries, Germany), sorbitol (Sigma-Aldrich, France). Triethyl Citrate (TEC) (Sigma-Aldrich, Germany), Acetyl Triethyl Citrate (ATEC) (Sigma-Aldrich, USA), Rhodamine B (Research Chemicals Ltd., UK). Low-substituted hydroxypropyl cellulose powder (LHPC) (Shin-Etsu Chemical Co., Japan). MCC (Avicel® PH-101) (Sigma-Aldrich, Japan). Magnesium Stearate (Fluka, Germany), Lactose monohydrate (Sigma-Aldrich, Netherlands) and d-Mannitol (Sigma-Aldrich, China).

The following materials were used for HPLC and *in vitro* release studies: Acetic acid glacial (VWR International, France). Acetonitrile (HPLC – SUPER GRADIENT, VWR chemicals, France). Methanol (VWR chemicals, France). Disodium hydrogen phosphate (Alfa Aesar, Great Britain).

Sodium hydroxide and sodium chloride (Fischer Scientific, UK). Hydrochloric Acid (VWR chemicals, France). Potassium phosphate monobasic (Honeywell Fluka, Spain).

2.3 Methods

The method and experimental of the prepared formulations were performed according to British, European, and the United States (US), pharmacopoeia (Pharmacopoeia,

2013)(USPC, 2014)(USP, 2014) FDA/CDER, 1997; Council of Europe, 2005; British Pharmacopoeia, 2017).

2.3.1 Pellet's preparation

The extrusion spheronization was used to prepare the pellets using Caleva multi-lab instrument (Caleva process solutions Ltd, UK).

2.3.1.1 Preparation of wet mass

First, all the dry excipients were put into the mixer (Caleva Multi Lab, process solutions Ltd, UK). The powders were mixed for 10 minutes at a speed of 180 rpm before adding water. After adding water, the wet mass was mixed for 10 minutes simultaneously until the texture of the wet mass became like breadcrumbs.

2.3.1.2 Extrusion of wet mass

The wet mass was transferred to the extrusion platform that contains a single screw extruder set at 60 rpm. The wet mass was slowly poured into the extruder during the movement of the screw. The material was pushed towards the extruder screen, which is vertical to the screw. The screen contains holes of 1.0 mm x 1.0 mm in diameter and 26 holes in total. Cylinder-shaped rods called extrudates were formed and collected in a container at the end of the extrusion step.

2.3.1.3 Spheronization of extrudates

The collected extrudates were poured into the spheronizer to prepare pellets with spherical shapes. The spheronizer contains a metal die with a truncated pyramids disc. Once the disc rotates, friction is generated on the extrudates, and pellets form. The spheronization speed was set at 1200rpm for 10 minutes Figure 2.1.



Figure 2.1 The steps of pellets preparation extrusion and collecting the extrudates (A), spheronization (B) and pellets formation using the Caleva Multi Lab extrusion spheronization instrument

2.3.1.4 Drying process

The final stage of pellets preparation was drying the produced pellets. The pellets were collected in a glass petri dish, distributed as a monolayer, and then placed in the oven (Copley Termaks, Norway) at 40-50°C for 2 hours. After drying, the products were put in sealed vials and kept in dictators to prevent any possible interactions with the atmospheric moisture.

2.3.2 Physical characterization

The used expedients, pellets and tablets were examined comprehensively. The selective detail for each formulation characterization is included with each study individually.

2.3.2.1 Size and sphericity

Pellet sphericity, shape and size were determined using a calliper (Carbon Fiber Composite Digital Caliper, China). Two diameters of 30 pellets from each batch were measured with the calliper, and the aspect ratio (AR) was then calculated as in Hence $AR = \frac{x}{y}$ Equation 2-1, x is the longest diameter, and y is the shortest (Saripella *et al.*, 2016a)(Santos *et al.*, 2005).

$$AR = \frac{x}{y} \quad \text{Equation 2-1}$$

2.3.2.2 Percentage yield

The total yield of the obtained pellets was measured for each batch as in Equation 2-2. The weight of the prepared pellets was measured then divided by the theoretical weights of all used excipients and drugs.

$$\% \text{ Yield} = \frac{\text{weight of obtained pellets}}{\text{weight of drug and Excipients}} \times 100 \quad \text{Equation 2-2}$$

2.3.2.3 Bulk density

Bulk density is an essential property of powders, pellets, and other particles like solid substances(Santos *et al.*, 2005). Bulk density is the mass of a material divided by the volume occupied by that material (Šibanc *et al.*, 2013)(Issa *et al.*, 2017). The bulk density was measured for powders and the obtained pellets prepared from each batch as in Equation 2-3. Using a 10 mL graduated cylinder and 3-5 g of the sample weight was used.

$$\text{Bulk density} = \frac{\text{weight of pellets or powder}}{\text{bulk volume of pellets or powder}} \quad \text{Equation 2-3}$$

2.3.2.4 Flowability

Flow property is an important factor in assessing the properties of powders and pellets used in tablet preparations (Šibanc *et al.*, 2013)(Issa *et al.*, 2017). Flowability was measured by weighing 5 g of each sample using Erweka GTL Powder and granulate flow tester (Erweka, Germany). Results were recorded amount of poured sample (g) per second.

2.3.2.5 Porosity

The compressibility of the primary particles and the produced pellets is markedly affected by physical properties such as porosity. Porosimeter, Belsorp II (Belsrop mini, BEL Japan Inc., Japan) was used to evaluate the porosity of powders and the produced pellets(Santos *et al.*, 2005). The pre-weighed sample was poured into the sample's cells to be tested. All samples were subjected to pre-treatment for 2 hrs at 40°C to purge any form of moisture found within particles and interfere with the process of nitrogen adsorption in particles. The cells were purged by using helium gas due to the low molecular weight of helium compared to nitrogen(Zielinski and Kettle, 2013). The samples were weighed following pre-treatment, the weight of the accurate sample was recorded. The samples cells were exposed to liquid nitrogen (77K). The adsorption-desorption curve was plotted at the end of the measurement by removing nitrogen. The isotherms of the produced data were collected using Belsrop software and applying Brunauer–Emmett–Teller equation to show the relationship between the adsorption volume and the relative pressure from nitrogen adsorption. The nitrogen adsorption temperature was constant, and gas pressure was specified to obtain consistent results according to the property of the samples (Santos *et al.*, 2005; Particle Analytical - Analysis for the Pharmaceutical Industry, 2020)(Pharmacopoeia, 2005).

2.3.3 Mechanical properties

The elasticity and hardness of the powders and the prepared compacts were measured as detailed in the following sections.

2.3.3.1 Elasticity and deformation

The elasticity of powders and pellets was evaluated using the texture analyser (Stable Micro Systems, UK) and exponent software (Stable Micro Systems, UK). The elasticity was measured for each batch (n=3) by placing the sample into the die. The powder compaction rig- probe was selected. The parameters were set as the following strain height (20 mm), stress area (28.26 mm²) and die diameter (6 mm). The upper punch moves down at a 1.00 mm/second speed to compress the samples with force up to 300 kg. The results were recorded as a graph of the applied stress (MPa) as force per unit area against deformation, the strain (%). Data were interpreted using the gradient value, Young's modulus (YM), as expressed in Equation 2-4 (Wang *et al.*, 1997).

$$\text{Young's modulus} = \frac{\Delta \text{Stress}}{\Delta \text{Strain}} \quad \text{Equation 2-4}$$

2.3.3.2 Pellet hardness

The other property measured for all batches of pellets is hardness using the texture analyser (Stable Micro Systems, UK) and exponent software (Stable Micro Systems, UK). Pellets (n=25-30) were examined by placing each one on a flat base of stainless steel then subjected to 5 kg force at a rate of 0.5 mm/second by using stainless steel cylindrical probe of 35 mm diameter. Data were extrapolated as tensile strength, the maximum force the material can resist before breakage. According to Cespi *et al.*, hardness was measured by detecting the first notch of the texture analysis graph as in Figure 2.2 (Cespi *et al.*, 2007). Equation 2-5 was applied for the pellets where crushing force is F (N), the radius of the pellets is r (mm) (C. Salas-Bringas1 *et al.*, 2007; Bialleck and Rein, 2011; Šibanc *et al.*, 2013; Podczeck and Newton, 2014; Issa *et al.*, 2017).

$$\text{Tensile Strength} = \frac{0.4F}{\pi r^2} \quad \text{Equation 2-5}$$

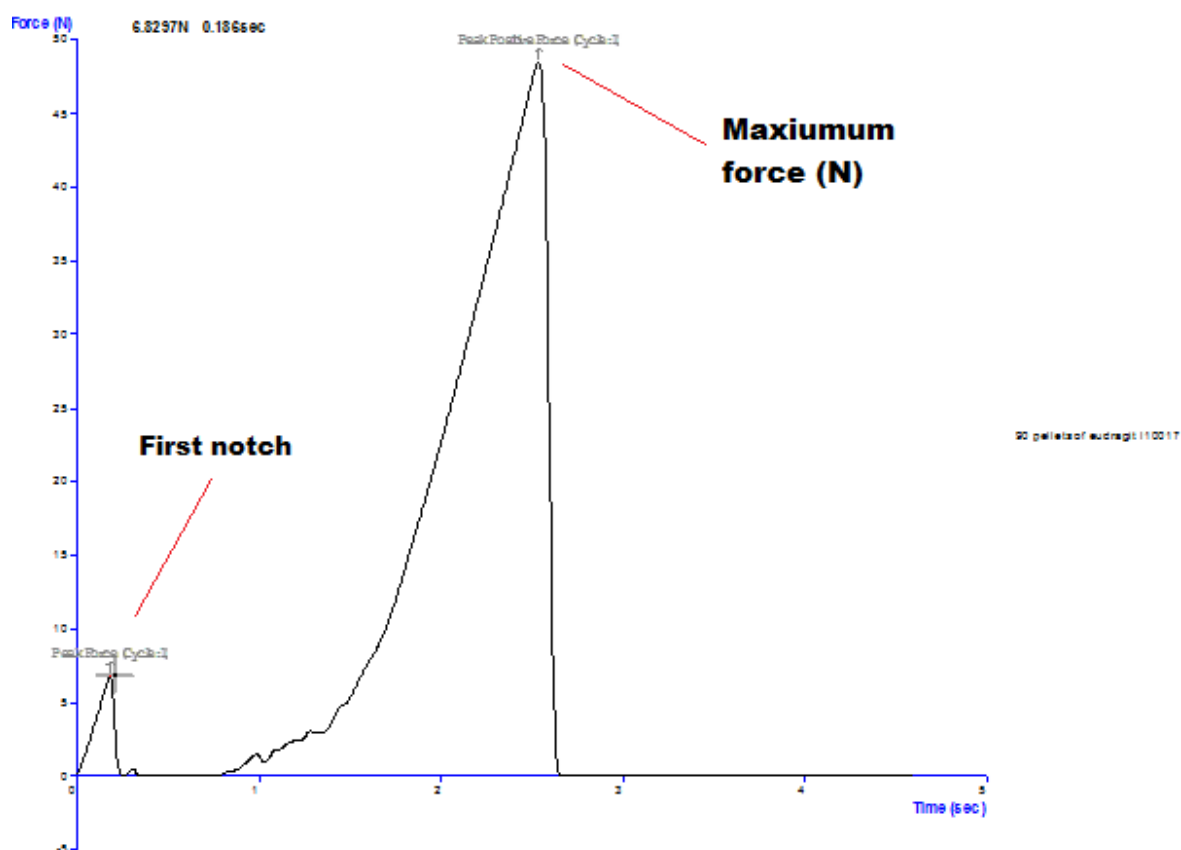


Figure 2.2 Texture analysis graph (extracted from the exponent software) after testing the hardness of one pellet from Eudragit L100 90 μm showing the first notch (hardness value) and maximum force applied

2.3.4 Thermal analysis

All materials were analysed according to their thermal behaviour as follow

2.3.4.1 Differential Scanning Calorimeter (DSC)

DSC system (Mettler Toledo, DSC822e, Switzerland) was used for detecting moisture content, glass transition temperature (T_g) and the melting point of all powders and pellets. An empty aluminium crucible was used as a reference. The pre-weighed samples were placed in an aluminium crucible (45 μm) then sealed with the corresponding lid using a manual sealing press. All samples were tested under the nitrogen atmosphere and temperatures between 25 to 300°C and 10°C/minute heating rate. The data were analysed using STAR^e software (Mettler Toledo, Switzerland).

2.3.4.2 Thermogravimetric analysis (TGA)

The decomposition/ degradation temperature and moisture content of powders and pellets were measured using TGA (Mettler Toledo SDTA/TGA 851e, Switzerland). All samples were analysed at heat flow 10 °C/minute and temperature range 20°C to 400°C under a nitrogen atmosphere by placing 5–10 mg of each sample in an open alumina crucible. Thermograms were collected using STAR[®] software (Mettler Toledo, Switzerland).

2.3.5 Preparation of ODTs

Matrix of ODTs was prepared by using three fillers according to the formulation using different fillers Lactose monohydrate, mannitol, or microcrystalline cellulose. LHPC was used as a disintegrant, and 1% Mg-stearate lubricant during tablet compression. Each pellets batches were mixed with ODTs matrices by including 10% - 20 % pellets and 80% - 90% ODT excipients to achieve 500 mg. A Turbula[®] mixer (Willy A. Bachofen AG, Switzerland) was utilized to mix the ODTs matrices and the prepared pellets at 50 rpm for 10 minutes. Similarly, the control tablets were prepared yet without pellets, and the model drug only was added as powder.

2.3.5.1 Tableting

The pellets and ODTs mixture were prepared in 500 mg from each batch. The pellets with ODTs mix were compressed using a manually controlled uniaxial hydraulic press (Specac tablet presser, UK). The mixture was poured into the die of a barrel to be compressed with a punch of 13 mm size and a one-ton compression force applied for 10 seconds, which is approximately equal to 74 MPa pressure as in Equation 2-6 (Sedlock and Engineering, 2016). All tablets were weighed after preparation to detect the final weight of 500 mg. The shape and morphology of tablets were evaluated using SEM and stereomicroscope, as mentioned previously in SEM.

$$pressure = \frac{Force}{area} \quad \text{Equation 2-6}$$

2.3.5.2 Mechanical properties

The mechanical properties of ODTs containing pellets were evaluated by testing tablets hardness. The tablet's thickness and diameter were measured using a digital calliper. All tablets (n=3) were placed individually on a tablet hardness tester (Pharmatron AG, Switzerland), and results of crushing force were recorded for each tableted formulation (Juban *et al.*, 2017)(Jarosz and Parrott, 1982). The values represent the applied force (N) to break a tablet. The hardness of tablets and the tablet dimensions were recorded to calculate tensile strength as in Equation 2-7

Where F is the force, D and T are the diameter and thickness of the tablet.

$$\text{Tensile strength} = \frac{2F}{\pi DT} \quad \text{Equation 2-7}$$

2.3.5.3 Disintegration test

Disintegration time is defined as the time required for tablets to disintegrate entirely without leaving any solid residues. A disintegration tester (Erweka ZT3, Germany) was used to measure the disintegration time (n=3) in the deionised water of 500 mL. The medium temperature was adjusted to $37 \pm 0.5^\circ\text{C}$ and kept constant during the test. Each tablet was placed in a specific position in a basket then covered with plastic disks to hold the tablets from floating. The disintegration time was measured for each formulation and the control tablets.

2.3.6 Morphology, shape and size

Evaluating the shape of the prepared pellets is an essential factor that affects the pellets' physical properties, such as porosity and compressibility.

2.3.6.1 Stereomicroscope

The microscope (Nikon Corporation, Japan) was used to assess the pellets (n= 30) shapes and sizes. The images were identified using a high and low-resolution imaging system (Nikon Digital Sight DS-Fi3, Nikon Corporation, Japan). The image acquisition

and measurements were applied using NIS-elements series software connected the microscope to the computer. The microscope was connected to a digital capturing system (Nikon Digital Sight, Japan) to examine and visualize the tested pellets and study the AR (n=25-30 pellets). The images were analysed via the installed software (NIS-Elements Viewer, Nikon Corporation, Japan).

2.3.6.2 Scanning electron microscope (SEM)

SEM (Zeiss Evo50- Oxford instrument, UK) was the other method to examine the morphology of raw materials and the prepared formulation. The method applied a beam of electrons that scans the sample going side-to-side and detecting all dimensions. In comparison to the light microscope, in which visible light is used, electrons provide the imaging in SEM. The low to high magnifications of greater than 100,000X and high-resolution images provided a clear view of the samples. All samples were prepared by applying some of the samples on a clean stub then coating them with gold at a low vacuum for 3 minutes using the sputtering coater (Polaron Equipment, Watford, UK) in the presence of argon as a noble gas (Echlin, 2009). Micrographs were collected for powders, pellets, and tablets at high and low magnifications, showing all samples' morphology, surface, and particles size using SmartSEM software (Zeiss Evo50- Oxford instrument, UK).

2.3.6.3 Laser diffraction

Laser diffraction was one of the methods applied to assess particle size. The particles were assessed using laser diffraction type HELOS /BF, Rodos dispenser (Sympatec GmbH, Germany) with 0.5/0.9 to 175 μm particles size measuring range. The Sympatec WINDOX software was used with a primary pressure of 1.0 bar (Air).

The following settings were applied; air pressure was set to 1.0 bar at a feeding rate of 20%. A specific amount of each polymer (0.2 - 0.5 g) was placed on the metal tray of (the VIBRI system) where the machine preceded the analysis. The particles were diffracted with the light beam directed by a lens over a photodetector (Babenko *et al.*, 2019). The particle size was assessed using average particle size, and volume means diameter (Keck and Müller, 2008). This calculation is based on fine particles scattering the laser beam, making larger angles and smaller angles with larger particles (Raval

et al., 2019)(Mlacker *et al.*, 2016). The used software to analyse the data was WINDOX (HELOS/Sympatec, Germany). All the examinations were done in triplicate and represented as mean \pm SD.

2.3.7 High-performance liquid chromatography (HPLC) Analysis

As detailed in the HPLC chapter.

2.3.8 Dissolution tests

Dissolution profiles were prepared according to British and US pharmacopoeia protocols using type II paddle apparatus for tablets and pellets (FDA/CDER, 1997; Council of Europe, 2005; British Pharmacopoeia, 2017). All samples were run with 50 rpm speed in 900 mL of the used media at $37^{\circ}\text{C} \pm 0.5^{\circ}\text{C}$.

The drug quantified in ODTs the control and ODTs containing pellets. The *in vitro* release studies in acid media (pH 1.2) were performed, and samples were collected at five sequential times 5 minutes, 15 minutes, 30 minutes, 1 hour and 2 hours. Similarly, all formulations were tested in buffer media (pH 6.8), yet the samples were collected at 8 sequential times 5 minutes, 15 minutes, 30 minutes, 1 hour, 2 hours, 4 hours, 8 hours, and 24 hours. A volume of 5 mL was withdrawn from each sample, then replaced with the same volume from the *in vitro* release media. The samples were filtered using a 45 μm micropore filter into HPLC vials before the analysis. All the samples were analysed using the established HPLC method (n=3).

2.3.9 Compressibility of powder batches

According to the study aim and objectives, some powders were characterised according to flow and compressibility characteristics.

Compressibility index, Hausner's ratio and tapped density were used to assess the flowability and the ability of the particles to settle during pellets preparation and select the powder of good values to prepare the pellets. Compressibility index and Hausner's ratio were calculated for the collected particles using a graduated measuring cylinder (100 mL) and around 10 g of powder. Also, tapped density was measured using Erweka tapped density tester (ERWEKA GmbH, Germany) applying 10, 500 and 1250

strokes according to the United States Pharmacopeia (USP) method 1 volume readings were recorded until no to little further volume change was noticed.

The method was also used to select good-sized particles to prepare the final formulations. Compressibility index and Hausner ratio were calculated according to Equation 2-8 and Hausner ratio = Untapped apparent volume /Final Tapped volume Equation 2-9, respectively. The results were compared to the referenced values in Table 2.1.

$$\text{Compressibility index} = 100 * \frac{(\text{untapped apparent volume} - \text{Final tapped volume})}{\text{untapped apparent volume}} \quad \text{Equation 2-8}$$

$$\text{Hausner ratio} = \text{Untapped apparent volume} / \text{Final Tapped volume} \quad \text{Equation 2-9}$$

Table 2.1 Compressibility index and Hausner ratio references (Kalal *et al.*, 2018)

Compressibility index (%)	Flow character	Hausner ratio
less than or equal to 10	Excellent	1.00-1.11
11-15	Good	1.12-1.18
16-20	Fair	1.19-1.25
21-25	Passable	1.26-1.34
26-31	Poor	1.35-1.45
32-37	Very poor	1.46-1.59
> 38	Very, very poor	> 1.60

2.4 Statistical methods

Results were analysed using Microsoft Excel software. Analyses of variance and t-test to compare the batches were applied at significance level 0.05. The statistical analysis results for all formulations are presented as Mean ± SD. All samples were run ≥3 times.

Chapter 3 Screening synthetic and natural polymers in the preparation of multiparticulates

Scope of the study:

This project evaluated polymers' mechanical properties to formulate modified-release multiparticulates embedded in orally disintegrating tablets (ODTs). The targeted polymer should have adequate elastic-plastic properties in a multiparticulate system during manufacturing. The good mechanical properties of the multiparticulate system can effectively aid in retaining the shape of the particles from being affected under applied compression pressure during the formulation process and tablets preparations. Therefore, the formulation should have good mechanical attains and drug release modification embedded in ODT. Five polymers, namely: sodium alginate, polyvinyl alcohol (PVA), methylcellulose (MC), polyacrylic acid (PAA) and Eudragit L100, were used. Polymers in raw form were characterised using different analysis techniques: Differential scanning calorimetry (DSC), Thermogravimetric analysis (TGA), Scanning electron microscopy (SEM), Tablet Hardness, Texture Analysis, Particle Size Analysis and Surface Area Analysis. PAA had the lowest Young's modulus of 5.375 MPa, and MC showed the highest value of 14.738 MPa. Polymers were spray-dried at a concentration of 5% w/v. The texture analysis data showed that Young's modulus was higher for the spray-dried powder of PAA 13.69 MPa.

Keywords: DSC, ODTs, Microparticles, Compression pressure, Young's modulus

3.1 Introduction

3.1.1 Polymers' suitability to modify the drug release

In order to choose the compact ingredients optimally, it is necessary to examine the powders' elastic tendencies. Hence, if the compaction pressure is not enough to pass the material's elastic limit and has high elastic properties, the particles return to their shape after removing the applied pressure (Choudhary and Avari, 2013; Chen *et al.*, 2017). Therefore, it is essential to choose a good balance between elastic-plastic properties showing plastic deformation with no fragmentation to retain compact integrity. Also, applying an optimum compaction pressure achieves the final compact with the desired properties without affecting drug release.

This study aims to evaluate different pharmaceutical polymers' physical and mechanical properties to test the suitability of combining them in the modified release system. The polymers used were as follow: water-soluble pharmaceutical polymers are sodium alginate, polyvinyl alcohol (PVA), methylcellulose (MC), polyacrylic acid (PAA) and non-water-soluble polymer Eudragit L100 (Appendix-Table 10.1).

3.1.1.1 Sodium alginate

Alginate is a polysaccharide with an ionic unbranched molecule (Malik *et al.*, 2017). According to the extraction method, there are different types of alginates salt, such as sodium alginate with 216.12 g/mol molecular weight (Kusumawati, Basmal and Utomo, 2018). It can be extracted from natural sources: brown algae such as *Laminaria digitata* (Gombotz and Wee, 2012). The extracted material endures a filtration process to precipitate alginate, followed by purifying powder, after which sodium alginate is obtained and can be used for commercial purposes in different types (Rinaudo, 2014).

The chemical structure of alginate consists of G and M units. These units influence the polymer physical and chemical properties (Appendix-Table 10.1). Also, G and M ratio in the polymer impacts the intermolecular crosslinking tendency of alginate with divalent cations (Hay *et al.*, 2010). The alginate's physical and mechanical properties are influenced by incrementing G block length and molecular weight (Lee and Mooney, 2012). Sodium alginate is a vital polymer with different pharmaceutical applications

due to its properties, such as adherence to the biological tissue called bio-adhesive property. This property is widely used in the formulation of modified drug release dosage forms and biomedical application (Kassem *et al.*, 2015).

The pKa for M and G are 3.38 and 3.65, respectively (Meng *et al.*, 2010). Therefore, gel formation of the soluble polymer occurs at pH lower than its monomeric parts pKa. However, the high viscosity and gel formation properties could offer good mechanical properties to the compact and retain their integrity under pressure (Kassem *et al.*, 2015). Therefore, raw or spray-dried sodium alginate can be mixed with other pH dependent or time-dependent polymers to improve the polymeric system's mechanical attains.

3.1.1.2 Polyvinyl alcohol (PVA)

PVA is a synthetic, water-soluble, pH-independent polymer with biodegradable properties with 44.05 g/mol - 31,000 g/mol molecular weight (Umemoto *et al.*, 2020). The polymer is highly stable with thermoplastic properties. Also, PVA holds the distinctive property of having hydrophilic and hydrophobic groups: hydroxyl and acetyl, respectively. As a biocompatible polymer and good mechanical properties, it is widely used in coating-based formulations (Deshmukh *et al.*, 2017). It can be mixed with other ingredients to enhance formulation flexibility. The PVA excellent film-forming and adhesive properties have led to wide use in film coating in pharmaceutical applications (Seo *et al.*, 2020). Also, it is commonly blended with other polymers. Additionally, PVA has been applied to improve the physical and mechanical properties and offer reduced cost formulation processes (Porter, Sackett and Liu, 2017).

These PVA properties were applied in different studies, as in Morita, Honda and Takahashi's study. The authors prepared controlled-release tablets consisting of drug-loaded granules of PVA and swelling control agent in the matrix, then coated with a mixture of ethylcellulose and one of MC grades compressed eventually into tablets. The model drug was water soluble antihistamine emedastine difumarate. The results showed a controlled drug release over 6 hrs in pH 1.2 and 6.8. This finding occurred due to reducing the swelling ability of PVA by adding salt and using a coating layer of water-soluble and insoluble polymers (Seo *et al.*, 2020). However, the study results show no data about the mechanical stability of PVA or the effect of compression pressure on the formulation (Morita, Honda and Takahashi, 2000).

3.1.1.3 Methylcellulose (MC)

MC is a water-soluble cellulosic polymer with 658.7 g/mol (PubChem, 2021). It is stable at room temperature with suitable physical and mechanical properties (Nasatto *et al.*, 2015). MC is highly viscous and shows a thermal behaviour at a temperature higher than 29 ± 2 °C forming an elastic gel, and its viscosity decreases below that temperature. MC has wide application in solid formulations as binder or stabiliser and thickener for film or coated formation (Hillier, 2007). In general, MC is a stable polymer that can be mixed with other polymers such as PVA. The polymer has stable viscosity at pH 3 to 11 and tends to reduce at very low or high pH of strong acids or base. MC can be applied in film-forming for coated formulations showing high stability and strength layers (Villetti *et al.*, 2011)(Nasatto *et al.*, 2015).

It was reported by Nasatto *et al.* that elastic modulus for MC gel at high temperatures (more than its critical temperature of 29°C depends highly on the polymer concentration (Hillier, 2007). The polymer shows good flow and plastic tendencies (Brady *et al.*, 2017).

In a study conducted by Mitchell *et al.* (2003), there was a difference in compaction properties of tablets prepared from different medical compounds (carbamazepine, naproxen and nifedipine). The addition of hydroxypropyl methylcellulose (HPMC) improved the compaction properties of produced tablets. Also, this was noticed by using microcrystalline cellulose (MC) in the preparation of metronidazole tablets. It was concluded that HPMC and MC have good compaction properties (Ghori and Conway, 2016).

3.1.1.4 Polyacrylic acid (PAA)

PAA is a water-soluble natural and biodegradable polymer. It has pH-dependent properties affecting its swelling behaviour (Swift *et al.*, 2016). PAA is liquid at pH 5 and gel at pH7 of 1800 - 5,100 g/mol molecular weight (Tseng *et al.*, 2018) (Kadajji and Betageri, 2011). This property made PAA a vehicle in ocular drug delivery to the corneal epithelium (Kadajji and Betageri, 2011). PAA is widely used in oral and mucosal contact formulations, such as controlled-release tablets and suspensions (Kadajji and Betageri, 2011). Also, it can be used as a thickening and stabilizing agent in emulsions for systems with little viscosity (Kadajji and Betageri, 2011).

This polymer can absorb or retain water and swell. PAA has wide pharmaceutical applications such as controlled release formulations (Ritthidej, 2011).

The polymer's hygroscopic properties make it elastic and adsorb moisture (Tjipangdjara and Somasundaran, 1992). Therefore, blending PAA with other polymers could be applied to improve the mechanical properties. At low pH, PAA is responsible for the mucoadhesion since its pKa is 4.5 (Tjipangdjara and Somasundaran, 1992). PAA viscosity can increase the hydrogen bond between its –COOH groups and glycoprotein sialic –COOH groups. Therefore, PAA combinations can also be used as hydrogels to treat ocular irritations (Soni *et al.*, 2019)(Ritthidej, 2011).

3.1.1.5 Eudragit L100

Eudragit® are polymers derived from acrylic and methacrylic acid esters. Functional groups in the polymers determine their physicochemical properties from pH to time-dependent release(Singh *et al.*, 2015). These polymers are widely used for coating pharmaceutical formulations to control the drug's release and protective layer with good mechanical properties (Pearnchob and Bodmeier, 2003). Eudragit L100 is used to protect the drug's effectiveness by modifying the drug release in gastric fluid and maintaining formulation integrity under compaction (Patra *et al.*, 2017)(Singh *et al.*, 2015)

The blend of Eudragit L100 with polymers to enhance compact mechanical properties could be applied to different formulations such as tablets, pellets and microparticles(Alotaibi *et al.*, 2019). Eudragit L100 is compactable and can be used in ocular insertion, nanoparticles or coated pellets with other polymers such as sodium alginate, PAA, MC (Taghe *et al.*, 2020)(Mohammadi *et al.*, 2019)(Cetin, Atila and Kadioglu, 2010). Multiparticulates of polymeric matrix based on Eudragit L100 is time-efficient, requiring fewer processing steps and low cost in modifying drug release. However, the polymer physical and elastic-plastic properties must be examined to achieve compact with the desired properties. Therefore, we aimed to examine and evaluate all suggested polymers' physical and mechanical properties to provide a comprehensive insight for future applications. Besides, our preliminary studies examined in-depth polymers properties to provide a clear view of the suitable polymers.

3.2 Aim and objectives

Despite the significant advantages of dispersing particulate systems in an ODT matrix, particles might not withstand compression pressure during the manufacturing of ODTs. Therefore, the current chapter aims to:

Screen 5 pharmaceutical polymers, namely sodium alginate, PVA, MC, PAA, and EudragitL100, to understand the tablet compression process and its effect on polymers mechanical properties. Our objectives are:

- Evaluate the polymers particle size using laser diffraction and characterisation of the polymer's morphology using a Scanning Electron Microscope
- Investigate the 5 polymers thermal behaviour with heating within specific heating rate and temperature by using Differential scanning calorimetry (DSC) thermogravimetric analysis (TGA)
- Prepare microparticulate systems using the spray drying technique
- Evaluate the mechanical properties of the raw and spray dried polymer by measuring Young's modulus
- Measuring the tensile strength of the prepared tablets from both powder types
- Shortlisting polymers with a desired elastic-plastic profile for future application in particulate systems

3.3 Experimental

3.3.1 Materials

Sodium alginate (5.0 – 40.0 cPs viscosity), PVA (average Mw 31,000) PAA (average Mw 5,100) were purchased from Sigma Aldrich (UK). Methylcellulose (viscosity 15 cups) and Eudragit L100 (125000 g/mol) were purchased from Alfa Aesar (UK) and Evonik Industries (Germany), respectively.

3.3.2 Methods

3.3.2.1 Spray Drying

This technique was used to produce a small particle size powder from raw polymers, with a particle diameter of about 5 to 100 μm microparticles (Jain *et al.*, 2012)(Malamatari *et al.*, 2020). The Mini Spray Dryer Büchi®B-290 (Switzerland) was used with the following settings: inlet temperature at 120-130°C, outlet at 78°C, the aspiration at 100%, drying gas flow rate was 35 m³/h, and the pump set at 20%. Nitrogen was used as the inert drying gas (Gunjal, 2020). In the spray drying process, the polymers aqueous solutions were prepared at a concentration of 5% w/v, where the solution was sprayed through a nozzle into high-temperature vapour steam to be evaporated, leaving the solid particles to collect in a drum (Figure 3.1). Eudragit L100 differed only with drying temperatures 85°C, outlet temperature 65-70°C and ethanol: water 9:1 (v/v). Other settings were identical to other powders. The yield was calculated for all the formulations working out the actual yield ratio to the theoretical yield percentage (Equation 3-1) (Gunjal, 2020). The settings were obtained after different trials and optimised according to the literature (Babenko *et al.*, 2019) (Jain *et al.*, 2012)(Malamatari *et al.*, 2020).

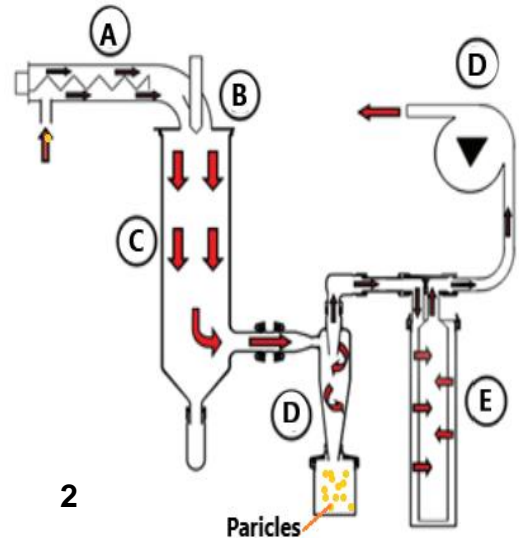
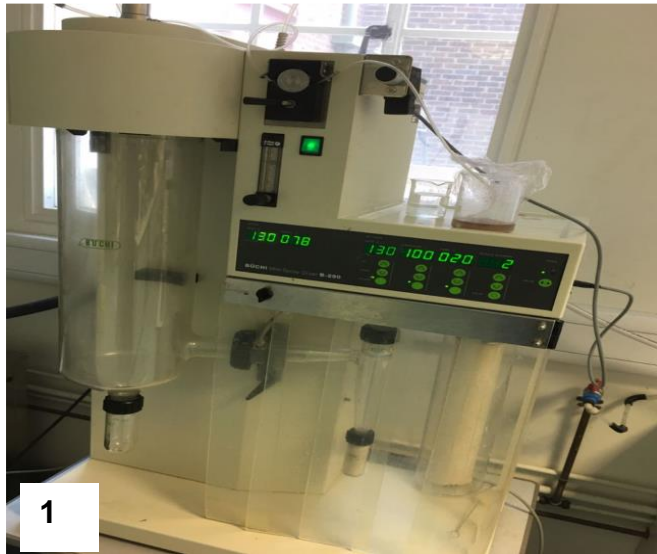


Figure 3.1 Büchi Mini Spray Dryer, B-290, Switzerland (1), function principle (2): hot inlet gas (A), droplet formation from the nozzle (B), gas-droplet drying chamber (C), particles collection (D), filter protecting user and environment, drying gas (D)

$$\%Yield = \frac{Actual (g)}{Theoretical (g)} * 100 \quad \text{Equation 3-1}$$

3.3.2.2 Characterisation of polymers (spray-dried and raw material)

3.3.2.2.1 Scanning Electron Microscopy (SEM)

The particles' shape and surface morphology of the five raw polymers and spray dried powders were examined using a scanning electron microscope (SEM, Zeiss Evo50-Oxford instrument, UK). Adequate amount of each sample spread over surfaces of the specimen stubs made of aluminium. The samples were then coated with gold to facilitate the electrical conduction. This step was done using a sputter coater (Polaron SC7640, UK) (Figure 3.2). The detailed method is explained in the experimental chapter.



Figure 3.2 Scanning electron microscopy apparatus (Zeiss Evo50, UK)

3.3.2.2.2 Differential Scanning Calorimetry

Samples were analysed using DSC (Mettler Toledo, Switzerland) to determine their thermal characteristics, such as glass transition, melting point, chemical reactions, and degradation (Mettler-Toledo, 2015). The method is detailed in the experimental chapter.

3.3.2.2.3 Thermogravimetric Analysis

TGA analysis (Mettler Toledo TGA 851e, UK) was applied to measure the samples' mass loss over time with temperature change for the 5 raw polymers and their spray-dried powders (Mettler-Toledo, 2019). The method is detailed in the experimental chapter.

3.3.2.2.4 Particle Size Examination

Laser diffraction (HELOS/Sympatec, Germany) was used to study the polymers' particle size distribution and then spray dried powders. The method is detailed in the experimental chapter.

3.3.2.2.5 Surface Area Examination

The porosity can be detected by measuring the specific surface area, pore size and pore size distribution (Amador and Martin de Juan, 2016). Hence, the measurement of specific surface area for material is applied by the physical adsorption using adsorption/desorption of a gas such as N₂ (Amador and Martin de Juan, 2016). Nitrogen is widely used for the adsorption/desorption method since it can be used to detect the pore size accurately of the material with micropores (<2 nm) and mesopores (2–50 nm) (Fu, Lin and Xu, 2017). Also, it is cheaper than other costly gases used like Argon. Surface area analysis is determined using Brunauer-Emmett-Teller (BET) equation for mono and multilayer adsorption as reported by Brunauer et al., 1938 (Amador and Martin de Juan, 2016; Fu, Lin and Xu, 2017). Depending on the relative pressure (partial to saturation pressure), the surface adsorption of gas changes for the material on a solid surface and under liquid nitrogen temperature. Hence, when the pressure increases, the adsorbed gas volume increases to an extent depending on the material porosity (Amador and Martin de Juan, 2016; Fu, Lin and Xu, 2017).

Porosimeter (Belsrop mini, JAPAN) was used to study the total porosity and the powders' specific surface area in the raw and spray-dried form. An equal amount of all the samples were weighed (0.2-0.5 g). The process consisted of two stages, the pre-treatment stage, where the samples were exposed to a temperature of 40-70°C for a 60-minute vacuum around 5 kPa for two hours. The second stage measurement was based on N₂ gas adsorption; this was for 5 hours with adsorption temperature 77 K and saturated vapour pressure 102.50 kPa. All the results were evaluated using the BET model as in Equation 3-2. BET graphs and the following equations were used to calculate the surface area of the samples:

$$a = \frac{V_m}{22414} LT \quad \text{Equation 3-2}$$

Avogadro constant is L, monolayer volume is V_m, and the cross-section area of the Adsorbate is T (ElShaer *et al.*, 2017)(Elsayed *et al.*, 2017).

The BET model principle depends on the relationship between adsorbed gas and the increase in relative pressure as in Equation 3-3. The equation shows the relationship between relative pressure and adsorbed gas amount (Lapham and Lapham, 2019).

$$\frac{\frac{P}{P_0}}{n(1-\frac{P}{P_0})} = \frac{1}{nmC} + \frac{C-1}{nmC} * (\frac{P}{P_0}) \quad \text{Equation 3-3}$$

As n is the amount of the adsorbed gas at the relative pressure P/P_0 , nm is the monolayer adsorption capacity, C is a constant of BET affected by the monolayer adsorption energy.

3.3.2.3 Tablet's preparation

Tablets were prepared from the spray-dried and raw polymers to study the powder's capacity to compact and its mechanical properties. A manual hydraulic presser (Specac tablet presser, UK) was used by applying different compression pressures 36, 74, 148, 221, 295 and 443 MPa, equivalent to 0.5, 1, 2, 3, 4, 6 tons, respectively. The pressure was applied for 10 sec on each run. The tablets of 0.5 g weight were made from each compression pressure. The obtained tablet had ~13 mm diameter. All tablets were kept in a desiccator to protect the tablets from atmospheric moisture before characterisation.

3.3.2.3.1 Tablet hardness

All tablets were examined by measuring the maximum force that each tablet can withstand before breaking (USP37-NF32, 2014). The method is detailed in the experimental chapter.

3.3.2.4 Texture analysis

Raw and spray dried powders were analysed using texture analysis (TA-XTPlus stable microsystems, UK). The method is detailed in the experimental chapter.

3.3.2.5 Statistical analysis

All experiments were analysed in triplicate, and the data were expressed in mean and SD. One-way & two-way ANOVA and t -test at a significance level of $p < 0.05$ were applied to detect the difference between the results.

3.4 Results and Discussion

The selected pharmaceutical polymers were assessed for intensive manufacturing characterisation using different analyses to measure their mechanical and thermal characteristics regarding their tablets' formulation ability. The polymers are sodium alginate, PVA, MC, PAA and Eudragit L100. These polymers have hydrophilic and hydrophobic properties and are widely used in ODTs to achieve a desirable drug profile. Also, these biocompatible polymers are cost-effective (Prajapati, Krunal and Patel, 2010). The 5 polymers are biodegradable with minimum toxicity effect; they have been used in different pharmaceutical applications such as film coatings preparation, binders, and coating of modified-release tablets combined with other polymers, microencapsulation, and tissue engineering (Jones, 2004). Furthermore, these polymers have mechanical properties that can be used to prepare tablets to enhance tablet strength, such as elastic and plastic properties.

The mechanical properties of the 5 polymers are essential and are characterised in their raw and spray-dried form. Also, the tablets are made of both forms were characterised. A suitable polymer would be applied for further studies depending on the mechanical properties and the drug modification effect.

3.4.1 Raw polymers

The raw powders were characterised using particle size analysis, scanning electron microscopy, surface area, and thermal analysis. The 5 polymers were then employed to prepare tablets under different compaction pressure. The tablets mechanical properties and morphological changes were also characterised.

3.4.1.1 Particle size analysis

Particle size is an essential factor affecting the powder compaction properties during tablet manufacturing. The smaller the particle size, the larger the surface area provides many binding sites enhancing inter-particulates bonds. Almaya and Aburub reported that decreasing the initial particle size of MC improved the tablet tensile strength compared to larger particles, where the tablets of small particles had 2.31 MPa, and large particles had 1.93 MPa (Almaya and Aburub, 2008).

Moreover, the fine particles' large surface increases the material's capability to withstand the applied pressure during tablet manufacturing, as reported by ElShaer (A. Patel *et al.*, 2015; Arvaniti *et al.*, 2015; ElShaer *et al.*, 2017)

Determination of particles size was carried out using laser diffraction; this technique has examined the polymers particle size. The SEM images of the particles also provided size measurement results to work out the average particle size. The results showed the particle sizes ranging between 54.58 μm , the smallest Eudragit L100, and 402.60 μm , the largest MC (Table 3.1). It was noticed that the rough surfaces of the particles and irregular shape affected the particles size measurement (Mühlenweg and Dan Hirleman, 1998). Hence, broad size distributions generated by irregular particle shape as particle's width and length cause the signal scattering (Malvern Panalytical, 2019). Therefore, several runs were necessary to take the average and minimize the error (n=3). Also, the results were supported by further measurements using SEM, as in the next section.

Table 3.1 Particle size data (μm) for 5 raw pharmaceutical polymers sodium alginate, PVA, MC, PAA and Eudragit L100 (n=3, mean \pm standard deviation)

Polymer	Particle size average (μm)
Sodium alginate	146.88 \pm 0.26
PVA	402.60 \pm 2.04
MC	302.30 \pm 2.51
PAA	101.00 \pm 1.51
Eudragit L100	54.58 \pm 0.74

3.4.1.2 Scanning electron microscope (SEM)

The SEM photomicrographs were taken to investigate the particles morphology, size and surface characteristic of the raw powder (Choudhary and Choudhary, 2017). It can be noticed that sodium alginate particles had irregular shapes with rough surfaces (Figure 3.3: A1 and A2). Smaller particles were also noticed, resulting in a wide range between 120 - 140 μm , in line with laser diffraction results. The surface roughness could provide enough surface area to enhance inter particulate bonding. Hence, a

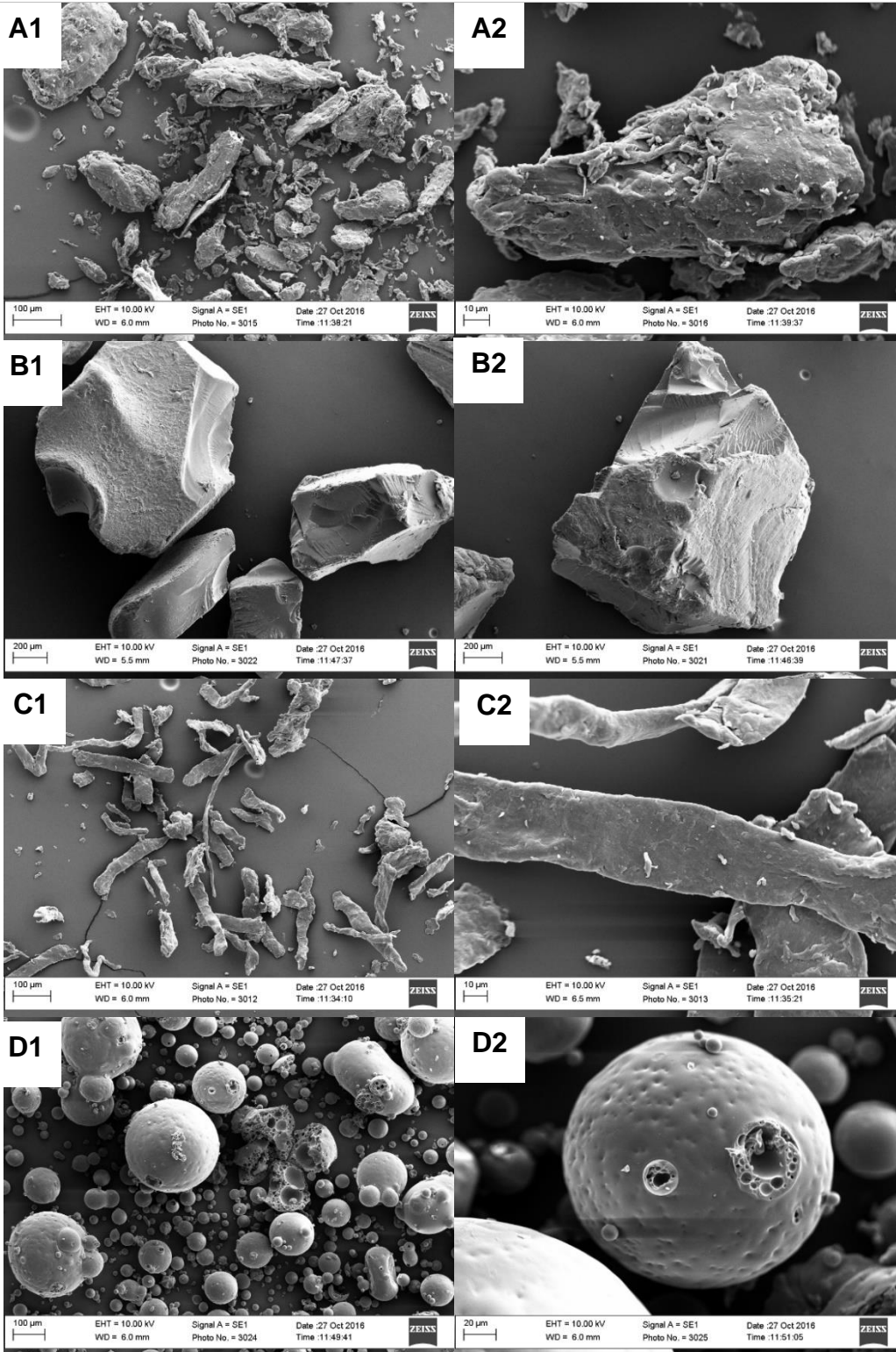
rough surface provides particles interlocking and generating good compact (Morin and Briens, 2013; ElShaer *et al.*, 2017).

The particles of PVA had coarse sizes with an asymmetrical surface. Similar irregularity was seen in sodium alginate. However, PVA showed smoother surfaces than sodium alginate, with a larger particle size around 400 μm (B1 and 2, Figure 3.3). Although particles of smooth surfaces provide fewer contact points for inter particulate bonds, particles could have higher adhesion strength with increasing the compaction pressure leading to fusing the particles and forming good compact. Nevertheless, this depends on the particles size and compaction pressure (Sun, 2017) as PVA showed poor compact strength, later in the discussion, influenced by the particle's shape irregularity and smoothness of the surfaces.

On the other hand, MC particles (Figure 3.3: C1 and C2) were elongated with a rod-like shape. It was noticed by Noronha et al. that film produced by MC showed smooth surface and good strength owing to the original powder properties (Noronha *et al.*, 2014). Also, MC particles were bigger than PAA. As mentioned earlier, the MC particle size was $302.3 \mu\text{m} \pm 2.51$. On the contrary, PAA showed spherical uniformly shaped particles of $101 \mu\text{m} \pm 1.51$. Also, PAA had a smoother surface than MC, with large pores that can be seen on the particle's shell (Figure 3.3: D1, D2).

Conversely, Eudragit L100 particles (Figure 3.3: E1 and E2) had the smallest size among other polymers. The particles displayed a spherical shape with apparent uniformity, as confirmed in laser diffraction results. Powders with smooth surfaces could enhance the flowability by reducing the particles' adhesion to the surface, as reported in the literature (Morin and Briens, 2013). This finding can be explained by the compaction process that starts with placing powder in the die between the punches (upper and lower). Then particles start to form a compact by migrating and interlocking. Further increase in the compaction pressure causes first elastic, then plastic deformation depending on the material type (Paluch *et al.*, 2013). However, further increment in the compaction pressure could cause cracking or crushing of the particles; thus, larger particles can form by merging smaller particles (Paluch *et al.*, 2013).

Another examination of particles physical properties was required to assess the surface area and porosity of the particles.



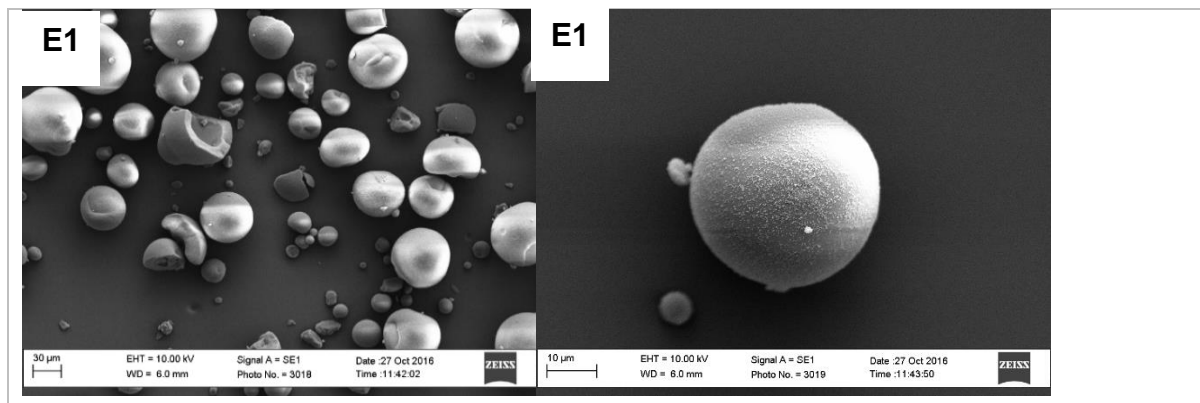


Figure 3.3 SEM images top view for the raw powder of pharmaceutical polymers at low magnification and high magnification 100 -10 μm sodium alginate (A), PVA (B), MC (C), PAA(D) and Eudragit L100 (E)

3.4.1.3 Surface Area Analysis

The tablet formulation process consists of powders of particles of different sizes. The larger particles can be formed from the aggregation of smaller sized particles. However, granular particles or large particles tend to form porous compact. In general, the powders particles constitute different types of pores according to their location, located within the particles (intra-particulates) or between the particles (inter-particulate) pores, which can be called voids (Nordström *et al.*, 2013). The particles maintain their integrity under tablet compaction to keep limited fragmentation under compression (Tan and Hu, 2016b). Examination of powder properties before and after compression is critical to assess the degree of powder compression. Hence, compression strength is influenced by several processes, such as particle deformation and fragmentation (Tan and Hu, 2016b). Thus, particles shape, size and porosity can change during compression.

It was reported that the primary particles porosity and the additional soft material such as lubricants influence the tablet properties during compression (Almaya and Aburub, 2008; Morin and Briens, 2013). Also, pharmaceutical powders' surface area and porosity can influence the tablets hardness and mechanical strength (ElShaer *et al.*, 2017). Therefore, studying porosity is an essential factor affecting the initial particles' properties (Nordström *et al.*, 2013).

The gas adsorption method is frequently used to examine powder surface area and porosity (Gibson *et al.*, 2020). The method comprises exposing powder particles to an inert gas then measuring the adsorbed volume of gas in the powder's sample using an adsorption/desorption isotherm. The data provided by this method illustrate the physical properties of the powder particles, such as surface area and total pore volume

(De Lange *et al.*, 2014). The suitable equation to measure powders surface and porosity, including single and multilayer adsorption, is Brunauer, Emmett and Teller (BET) (Bolis, 2013). The preferable gas is N₂ to assess the physical adsorption; hence a low temperature of liquid nitrogen represents the gas's boiling point (77 Kelvin) (Zielinski and Kettle, 2013). This analysis offers a wide range of pore size distribution and surface area (Ambroz *et al.*, 2018) (Sing, 2001). According to the BET method, the surface area is measured depending on the nitrogen-relative pressure and the adsorbed gas volume (De Lange *et al.*, 2014) (Sing, 2001). Also, the results were further processed to detect the pore distribution using Barrett, Joyner and Halenda (BJH), applying numerical equation involving pore volume and radius (Bardestani, Patience and Kaliaguine, 2019)(Sing, 2001)(De Lange *et al.*, 2014) (Appendix-Figure 10.3).

In general, five types of isotherm are commonly detected according to the adsorption of the gas. Type 1 displays a monolayer of gas adsorption and narrow micropore (<2 nm diameter). This result can be seen in the adsorption of nitrogen on charcoal at around 1800°C temperature(Sing, 2001). The graph of Type 2 displays a big draft from a model of gas adsorption demonstrating the non-porous materials of macropores (>50 nm diameter), as in the adsorption of nitrogen on iron (Bardestani, Patience and Kaliaguine, 2019). Type 3 graph shows low interaction between the surface and adsorbed gas, while Type 4 displays mesopores materials (2-50 nm diameter) with high affinity to adsorb gas (Figure 3.4). Type 5 isotherm is similar to Type 3, displays non-porous materials(Sing, 2001)(De Lange *et al.*, 2014).

The isotherms of N₂ adsorption/desorption were collected for all raw powders (Appendix-Figure 10.2). Sodium alginate, PVA, MC and PAA isotherms displayed Type 3 isotherm as they had a nonporous structure (Figure 3.4). This type of isotherm shows a low surface affinity to the adsorbed gas. (Sing, 2001) (Vlab.amrita.edu, 2017). While Eudragit L100 showed Type 4 isotherms indicating higher surface affinity to the gas (Bardestani, Patience and Kaliaguine, 2019) (Sing, 2001).

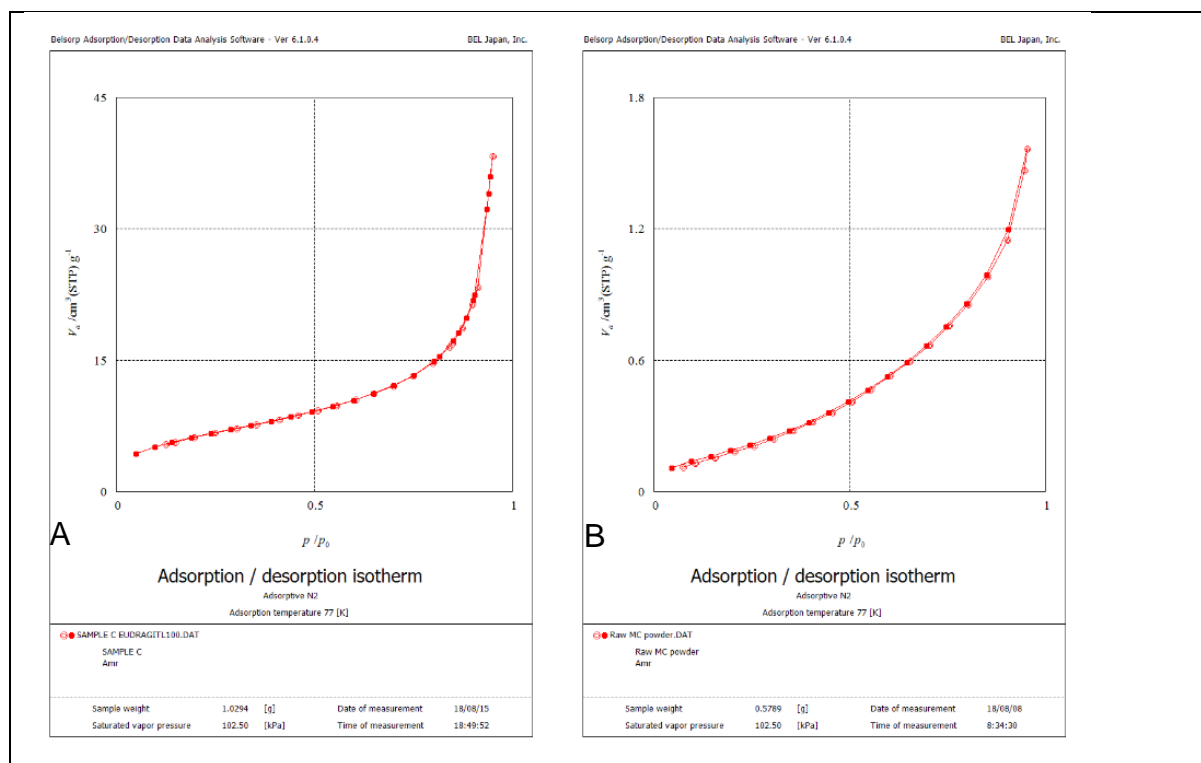


Figure 3.4 Adsorption/Desorption isotherm of the pharmaceutical polymers: Eudragit L100 (A), showing Type 4 isotherm, and MC (B) showing Type 3 isotherm at adsorption temperature 77 K and relative pressure <0.9

The detected surface area from the lowest to the highest was as follow PVA, sodium alginate, PAA, MC and Eudragit L100. Also, Eudragit L100 had the highest total pore volume, $5.12 \times 10^{-2} \text{ cm}^3 \text{ g}^{-1}$ and the lowest values reported were for sodium alginate and PVA $1.75 \times 10^{-3} \text{ cm}^3 \text{ g}^{-1}$, and $2.15 \times 10^{-3} \text{ cm}^3 \text{ g}^{-1}$, respectively (Table 3.2). The SEM images of sodium alginate demonstrated irregular shape with smooth to rough surfaces while the low surface area and the low total pore volume was detected. Hence, this type of isotherm correlates with the pores' specific shape, as reported in the literature (Zhang, 2016). Type 2 and 3 have narrow pores like ink-bottle and aggregate pores like long-narrow cuts, respectively (Zhang, 2016). Also, from the BJH data of detecting pore distribution, the pore diameter range is more than 2 nm (Ambroz *et al.*, 2018). It can be assumed that the presence of shadow or slit-shaped pores for sodium alginate correlates with the effect of different pore shapes and distribution (Zhang, 2016) (Ambroz *et al.*, 2018). Therefore, the mesopores sodium alginate showed weak interaction with adsorbed gas, offering a low surface area indicating almost low porosity (Zhang, 2016; Ambroz *et al.*, 2018). A similar trend was correlated with PVA offering low porosity. However, SEM showed that particles had smooth surfaces and irregular shapes offering low surface area of BET. PAA surfaces showed similar results of a relatively high number of pores and surface roughness, while MC

was difficult to assess according to SEM. This could be related to the nature of cellulose with high water holding capacity, thus showing high porosity (Ramasamy, Gruppen and Kabel, 2015). Also, SEM showed MC had elongated shaped particles that offered higher surface area for adsorption (Ramasamy, Gruppen and Kabel, 2015). It can be stated that the shape of the particle (regular or irregular) affects the surface area measurements and gas adsorption. PAA and Eudragit L100 particles appeared in a small spherical shape with porous surfaces. This could be related to the large surface area associated and a high number of pores with small particles (De Jesús *et al.*, 2002) (ElShaer *et al.*, 2017).

On the contrary, PVA particles surface was less porous, of large irregular shape, and particle size was large compared to other polymers. Therefore, PVA had a low surface area of value $0.05 \text{ m}^2/\text{g}$. The same trend was noticed in sodium alginate, which had a low surface area of $0.19 \text{ m}^2/\text{g}$. It should take that into account during powder compressibility as the highly compressible powder owns low porosity due to a high number of bonding sites (Ambroz *et al.*, 2018) (ElShaer *et al.*, 2017). The presence of voids in the porous powder could prevent powder compression resulting in obtaining brittle tablets (Ambroz *et al.*, 2018) (ElShaer, Hanson and Mohammed, 2013).

On the other hand, Eudragit L100 powder showed the highest surface area compared to the other powders. This was related to the small particles size that offered a high number of pores as detected using BET (De Jesús *et al.*, 2002). Hence, the smallest the pores, the high surface area (De Jesús *et al.*, 2002). However, this fact depends on the number of pores available in the tested sample. In our results, total pore volume demonstrated the highest value among other results.

Therefore, the surface area of BET was high, as reported in Table 3.2. Although Eudragit L100 showed higher porosity and surface area of BET, their effect was still constrained on the tablet's final mechanical properties owing to other powder properties such as elastic deformity, particle shape and size (De Jesús *et al.*, 2002). These findings could help us identify any defect during compactions of Eudragit L100 combined with other powders to enhance final product properties. Therefore, the shape and size of the particles supported by the porosity alter the final compact attains. Although small particles powder improves the desired mechanical properties of the final compact by cohesive forces, large particles powder could reduce particles friction and improve flowability (De Jesús *et al.*, 2002).

Table 3.2 Surface area analysis results of single run of raw powders sodium alginate, PVA, MC, PAA, and Eudragit L100 illustrating mean pore diameter (nm), surface area (m²/g) and total pore volume (cm³/g) in the range of 0.05–0.35 N₂ relative pressure using BET model

Polymer	Mean pore diameter (nm)	Surface area (m ² /g)	Total pore volume (cm ³ /g)
Sodium alginate	36.36	0.19	1.76 x10 ⁻³
PVA	23.88	0.05	2.15x10 ⁻³
MC	21.26	0.91	4.81x10 ⁻³
PAA	28.48	0.37	2.62x10 ⁻³
Eudragit L100	8.97	2.28	5.12x10 ⁻²

Moreover, according to some studies, spherical particles offer fewer adhesion forces with surfaces improving flowability (Brika *et al.*, 2020)(Bodhmage, 2006). Also, considering surface properties and internal porosity is significant during compact manufacturing. Therefore, preparing compact with good mechanical properties could be approached using powder of different particles size. Moreover, the thermal behaviour, particles deformity according to elastic or plastic properties were necessary to be investigated, providing a comprehensive understanding of initial particles properties on the final compact. Further characterisation was accomplished to evaluate the powder thermal behaviour and the tablets mechanical properties.

3.4.1.4 Thermal Analysis

DSC analysis is used to characterise the material's thermal behaviour with temperature change; it can be used to determine the polymers' physical properties such as melting point and crystallisation and glass transition temperature (T_g) (Menczel, J. D., & Prime, 2009). The complementary examination information can be obtained from TGA, where this technique can measure the amount of mass change as a function of temperature mixtures (Pyramides, Robinson and William Zito, 1995). TGA analysis determines the moisture content from the sample's weight loss then decomposition. Therefore, it can be used to study the powders or tablet mixtures (Pyramides, Robinson and William Zito, 1995) (Menczel, J. D., & Prime, 2009).

The thermal analysis of the polymers was essential to study the thermal behaviour of the 5 polymers. Water and moisture can influence hydrophilic polymers properties. Methylcellulose's mechanical properties are influenced by hydrogen bonding with

water, leading to plasticising the polymer and a good compacted tablet of high mechanical strength as suggested by Ford, J.L., 1999 (Ford, 1999).

The correlation between tensile strength and moisture content could be explained by solid bridges increase with the absorbed water and particle-particle interaction enhances with absorbed water layers at particle surfaces (Lordi and Shiromani, 2008) (Thapa *et al.*, 2017). Nevertheless, bulk water could also decrease the tablets' tensile strength by producing multiple layers of water at the particle's surface. Hence, the water layers may diminish intermolecular attraction forces, reducing the tablet's strength (Thapa *et al.*, 2017).

DSC results presented in Figure 3.5 (A) of sodium alginate showed dehydration peak around 100°C resulting from moisture loss. Also, the polymer's decomposition occurred at peak 240 - 260°C, represented by an exothermic peak, Soares *et al.* (2004) reported similar results (Soares *et al.*, 2004). TGA (Figure 3.6) showed sodium alginate dehydration around 100°C related to a moisture content of 2.89%, and the decomposition of the polymer was occurring at 240-260°C (Tripathi and Mishra, 2012). Similar results were reported by Tripathi and Mishra (2012), indicating that the decomposition of carbonaceous material can also occur above 300°C (Tripathi and Mishra, 2012).

The melting point was undetected in sodium alginate (Figure 3.5). According to the literature, this was also unclearly identified as Soares *et al.* suggested the melting point at different temperatures 185°C and 339°C while undetected in Tripathi and Mishra results (Soares *et al.*, 2004; Tripathi and Mishra, 2012). This could be related to the fast decomposition of sodium alginate (Soares *et al.*, 2004). Also, the moisture content and bounded water molecules may influence the detection (Menczel, J. D., & Prime, 2009). PVA, Figure 3.5(B), displayed dehydration around 60°C due to moisture loss of 1.73 % from the sample shown by TGA. The presence of an endothermic peak around 223°C indicated PVA partially melting then final melting point at 229°C similar trends was reported in the literature, indicating the semi crystallinity nature of the polymer (Thomas and Cebe, 2017). Also, degradation occurred at 280°C as in TGA (Figure 3.6).

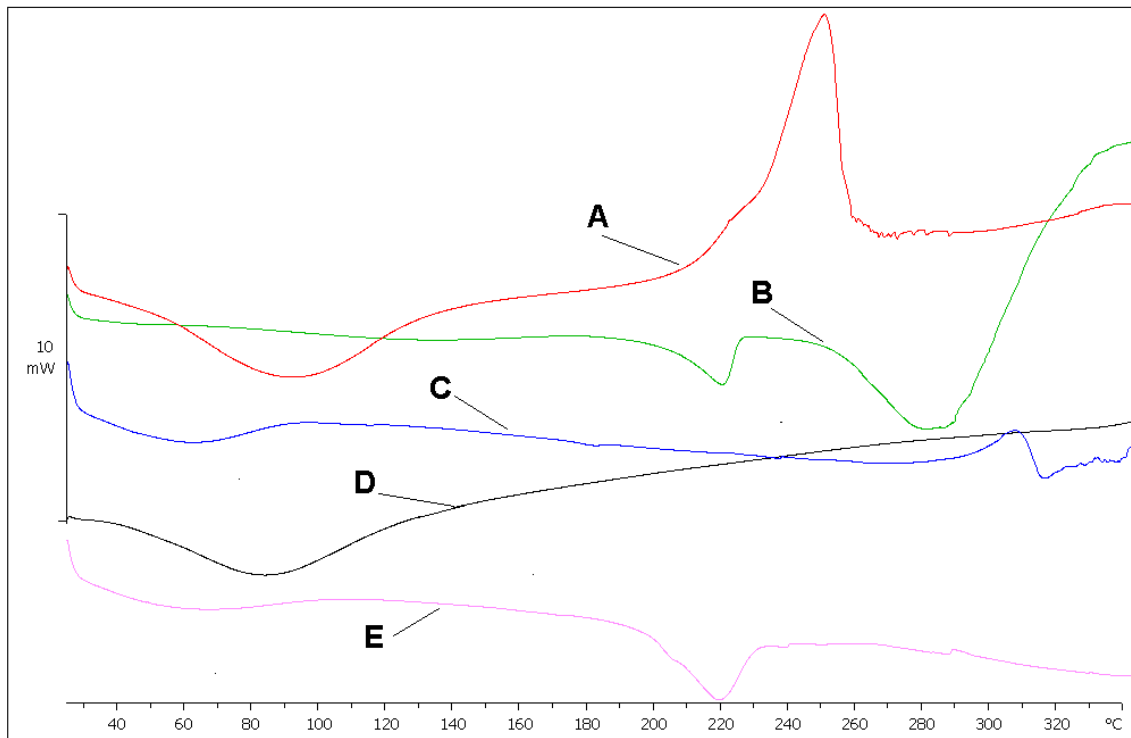
MC (Figure 3.5, C) displayed a broad endothermic peak that appeared around 70°C, representing dehydration (Oliveira *et al.*, 2015). This was correlated with TGA results (Figure 3.6), which showed a moisture content of 4.9%. It can be assumed around 310°C the degradation occurred. Also, the results displayed that some water was detected in the dry state with the powder. Ford J.L (1999) reported the same results

(Ford, 1999). On the other hand, PAA (Figure 3.5, D) demonstrated an endothermic peak between 58 - 80°C related to dehydration. Besides, it was reported that the polymer T_g at 106°C (Eisenberg, Yokoyama and Sambalido, 1969). Therefore, the peak resolution was affected by the moisture content (Moharram and Allam, 2007). The results were correlated with TGA, where the dehydration occurred at a region around 80 -100°C, and moisture content was around 4.6%. However, accurate detection of moisture content was complicated with the nature of PAA. The polymer is highly hygroscopic and was required multiple runs that even showed different moisture level according to our preliminary studies(Eisenberg, Yokoyama and Sambalido, 1969). It was reported that the polymer might display decomposition stages at temperature starting after 100°C (Moharram and Allam, 2007). Therefore, for the accuracy of the results, moisture content was only detected considering the free water molecules that evaporate quickly lower than 100°C.

Eudragit L100 DSC (Figure 3.5, E) showed a broad endothermic peak at 216.2°C and the lowest moisture content due to the polymer's amorphous nature and the absence of melting point. According to TGA, moisture content was lower than 2.6%. Also, T_g in the literature was reported differently at 30 - 70°C or 189 -200°C (Sharma, Sharma, A. K. Panda, *et al.*, 2011)(Parikh *et al.*, 2014)(Mudie *et al.*, 2020). This finding could be related to two possibilities start of decomposition or moisture content of bounded water (Figure 3.6-E) at the same temperature range.

Also, the sample colour in the crucible turned black at the end of the DSC analysis. This could be evidence of the degradation of Eudragit L100 over 300°C. The results and resolution may vary due to the difference in heating rate affected (Soares *et al.*, 2004) (Tripathi and Mishra, 2012).

^exo

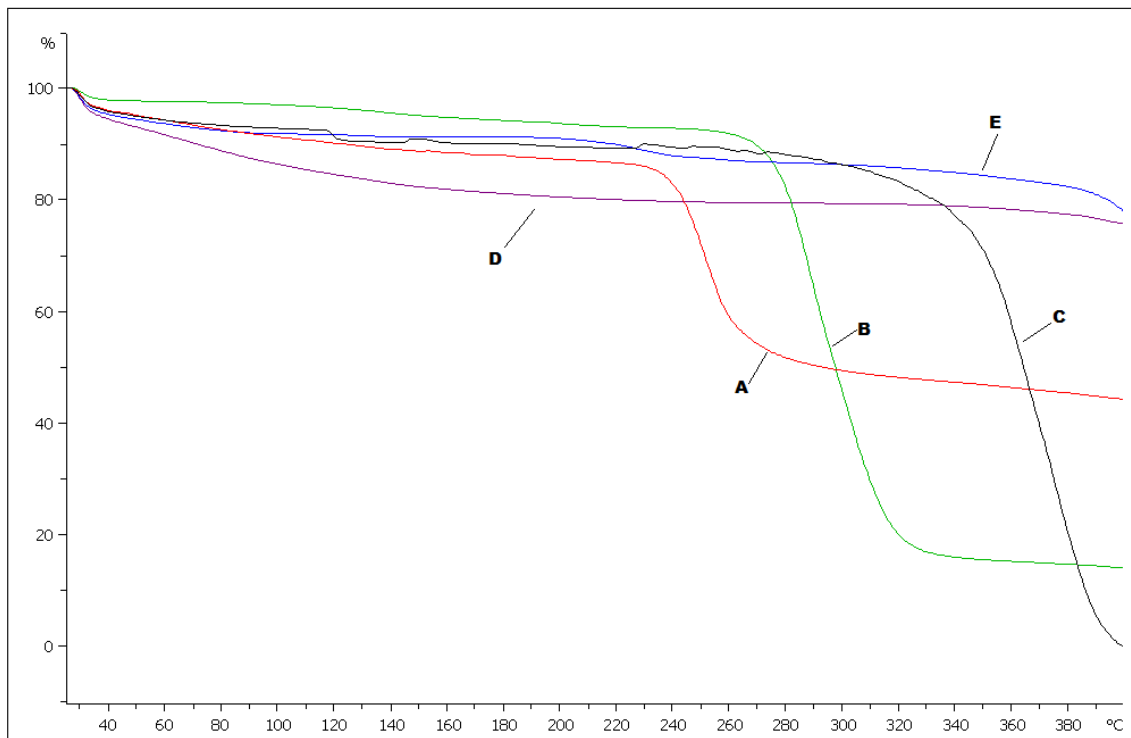


Lab: METTLER

STAR[®] SW 10.00

Figure 3.5 DSC graph of 5 raw pharmaceutical polymers examined at (20 - 340) °C with 10 °C/min heating rate, (A) sodium alginate, (B) PVA, (C) methylcellulose, (D) PAA acid and (E) Eudragit L100

^exo



Lab: METTLER

STAR[®] SW 10.00

Figure 3.6 TGA analysis results of 5 raw pharmaceutical polymers A sodium alginate, B PVA, C MC, D PAA and E Eudragit L100, from 20 to 400 °C with 10 °C/min heating rate under nitrogen atmosphere

3.4.1.5 Texture analysis for elasticity

The modulus of elasticity is an essential parameter in determining the degree of hardness, flexibility and stiffness of the polymeric tablet. This parameter can be calculated from the slope of the straight line of the stress-strain curve. If the modulus of elasticity increases, the plasticity increases, which, in turn, indicates the hardness of the tablet. However, passing the elastic limit, the material is considered brittle (Salama *et al.*, 2015). The elastic limit varies according to the material type (Tan and Hu, 2016b) (Sun, Kothari and Sun, 2018).

The five powders were tested using Stable Micro Systems texture analyser to measure Young's modulus using the stress (force per unit area) / strain (material deformation) correlation (Faridmehr *et al.*, 2014). A balance of elastic and plastic tendency in materials suffices to maintain particles integrity under compression, where the lowest Young's modulus's high elasticity (Tan and Hu, 2016b). According to One-way ANOVA, the results were significantly different between the powders ($p < 0.05$). Further statistical analysis was applied to show the difference between every two polymers using a *t*-test at a significant difference with $p < 0.05$. PAA and Eudragit L100 had the lowest Young's modulus of 5.37 ± 0.22 , 5.27 ± 0.19 MPa, respectively (Figure 3.7) with no significant difference ($p > 0.05$). In comparison, MC showed that highest elasticity modulus of 14.73 ± 0.23 MPa indicating the plasticity (Carnavas and Page, 1998). Similar trends were observed for the other two polymers. Young's modulus was 8.3 ± 0.25 MPa, and 6.6 ± 0.23 MPa for sodium alginate and PVA, respectively. The results indicated that when Young's modulus increases, the plastic deformation increases and elastic properties diminishes for sodium alginate, PVA and MC. On the contrary, as Young's modulus decreases, the elastic property of the material rises. Therefore, it can be suggested that PAA and Eudragit L100 demonstrated elastic tendency.

The results were correlated with the previous analysis data. Hence the particles size of PAA and Eudragit L100 were the lowest compared to the other polymers $101 \pm 1.51 \mu\text{m}$ and $54.58 \pm 0.74 \mu\text{m}$, respectively. Simultaneously, the particles' smooth surfaces (as in SEM analysis) resulted in the higher surface area providing high inter particulate bonding. Therefore, both polymers possess good compressibility, which can be seen in both polymers' texture analysis data (De Jesús *et al.*, 2002) (Brika *et al.*, 2020).

On the other hand, high MC particle size $302 \pm 2.51 \mu\text{m}$ and elongated shape and surface roughness could provide an interlocking bonding mechanism. This correlates with high elasticity modulus. Although Carnavas and Page (1998) stated that the

particles size ranges 50 - 300 μm have the lowest impact on Young's modulus, other factors should be considered, including surface roughness, particles shape and porosity (Carnavas and Page, 1998). It can be concluded that the surface roughness and particles shape irregularity affected the particle-particle interaction offering an interlocking mechanism as in sodium alginate, PVA and MC (Morin and Briens, 2013; ElShaer *et al.*, 2017). Nevertheless, the irregular shape of PVA and smooth surfaces diminished the particles compatibility resulting in low tensile strength. Although Eudragit L100 and PAA had low Young's modulus, the uniform shapes offered the lowest friction and cohesion forces, thus reducing the tensile strength (as in the next section) (De Jesús *et al.*, 2002) (Brika *et al.*, 2020). It can be stated that correlation between the Young's modulus and tensile strength could be applicable when the particles possess balance in elastic and plastic properties.

The initial powders mechanical properties could influence the final compact properties, i.e., tensile strength, as reported earlier by Mattsson, S. (2000). The materials' mechanical properties evaluated by measuring the plastic and elastic profile, which, in turn, can be affected by different features such as particles size, surface area, and porosity (Mattsson, 2000). The tableability, which is the powder's ability to be compressed into a tablet under applied force and the tensile strength were discussed in the next section (ElShaer *et al.*, 2017).

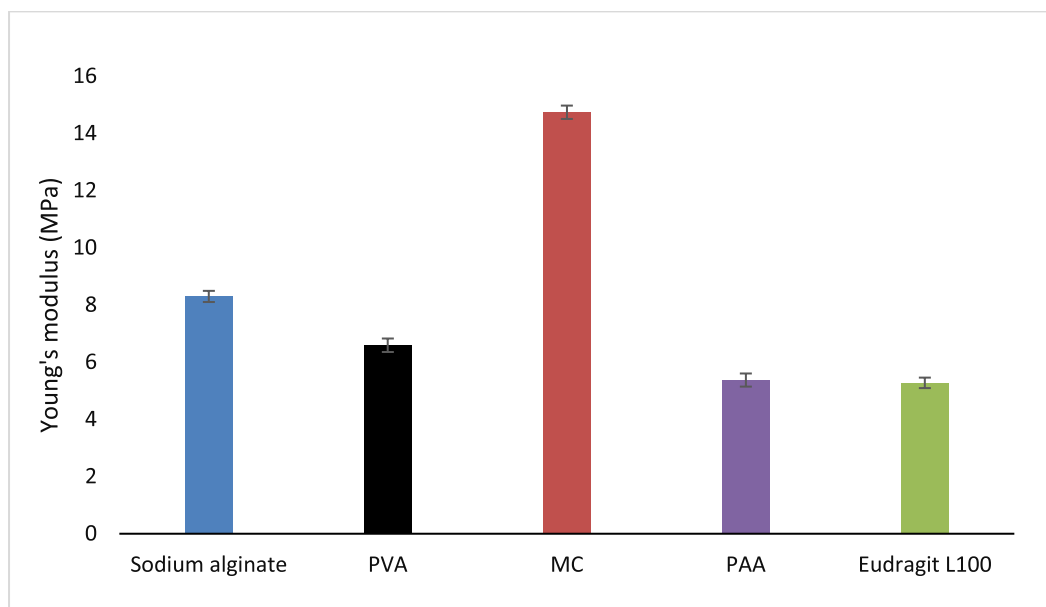


Figure 3.7 Young's modulus (MPa) reflects the elasticity profile of raw polymers sodium alginate, PVA, MC, PAA and Eudragit L100, the results obtained from the texture analysis (TA-Xt Plus stable micro systems) all data were presented as mean \pm SD (n=3)

3.4.1.6 Hardness test and Tensile strength

The last step in tablets manufacturing is the powder compaction by applying compression pressure over the powder bed. The particles rearrange and compress, tending to form a tablet with increasing the applied pressure. The tablets' inner structure and hardness can be assessed using tensile strength (Nordström *et al.*, 2013).

The powder tableability and compaction properties are important factors in studying a material's mechanical properties to cope with tablet manufacturing and packaging difficulties (Mattsson, 2000)(Ambroz *et al.*, 2018). Therefore, the hardness of the tablet along with tensile strength was determined. The tablets obtained under 5 different compaction forces (0.5, 1, 2, 3, 4, 6 ton equals to 74, 148, 221, 295 and 443 MPa accordingly) from each polymer. All tablets were tested for hardness and tensile strength, as in Figure 3.8.

The tensile strength of tablets of 5 polymers proportionally increased with compaction pressure; this can be attributed to the reduction in the porosity of the obtained tablets with the rise of the applied pressure. Hence, the bonding area increases resulting in enhanced inter particulate bonds, as reported by ElShaer, Hanson and Mohammed (2013). It was reported that the tableability of the powders enhances with addition applied pressure sites (Ambroz *et al.*, 2018)(ElShaer, Hanson and Mohammed, 2013).

Although sodium alginate and PVA had low porosity, particles surface, size, and shape were different, resulting in dissimilar behaviour under compression. PVA had poor tabletability with each compaction pressure, this can be attributed to smooth surfaces and irregular particles shape, decreasing the available binding sites for particles bonding resulting in poor compressibility sites (Ambroz *et al.*, 2018)(ElShaer, Hanson and Mohammed, 2013). Simultaneously, sodium alginate and MC had rough surfaces with smaller particles than PVA as detected in SEM and laser diffraction results. As explained earlier, the morphology of the particles influences the surface area. Thus, it can be assumed that the rough surfaces of sodium alginate and MC provided many binding sites for particles bonding, offering an interlocking mechanism. Therefore, these polymers showed consistent tensile strength increment with increasing the applied pressure (ElShaer *et al.*, 2017) (Arvaniti *et al.*, 2015).

Although PAA had smaller particles than sodium alginate, PVA and MC, the tensile strength increased significantly with applied pressure. A similar trend was detected with Young's modulus, as PAA had spherical particles with small size and noticeable surface roughness. These properties offered good particle-particle interaction (De Jesús *et al.*, 2002) (Brika *et al.*, 2020).

The t-test analysis showed that tablets produced from low compaction pressure 36, 74 and 148 MPa markedly differed between every two polymers ($p < 0.05$). However, at higher compaction pressure 221 MPa, the results showed similarity only between MC and PAA. Also, only sodium alginate and PAA increased the compaction pressure and showed no significant difference at 295 MPa and 443 MPa. This indicates a similar trend in particles behaviour for both sodium alginate and PAA at high pressure, and they remarkably differ at low pressure.

Therefore, it can be concluded that particles' shape and size influenced the tablets mechanical properties. This effect could reduce by increasing the pressure depending on the properties of the initial particles. Further characterization was accomplished to study the morphological changes after tablet compression.

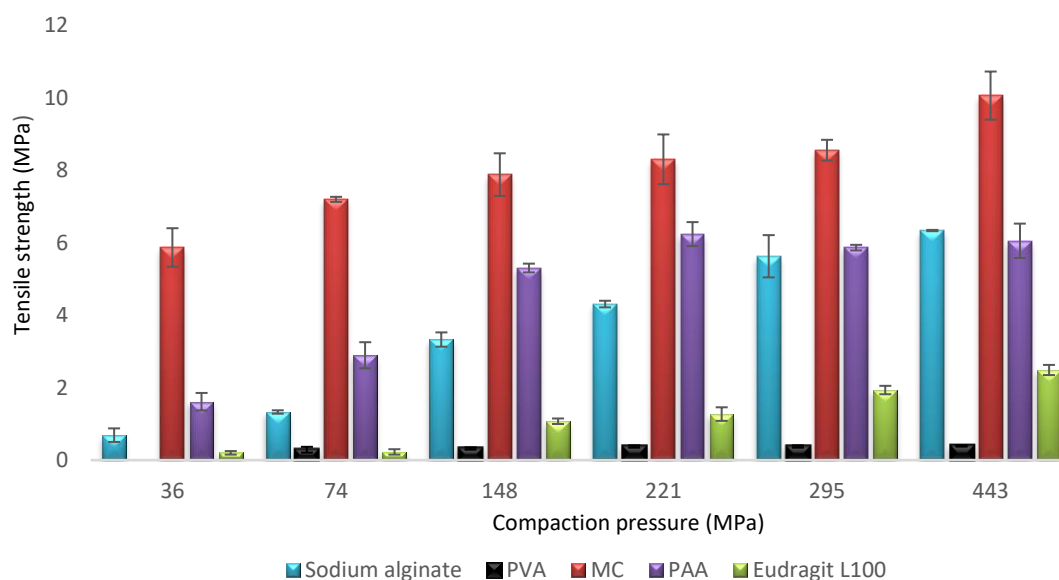


Figure 3.8 Tableability results presenting in Tensile strength (MPa) against the compaction pressure (MPa) for tablets prepared in different compression pressure (36, 74, 148, 221, 295 and 443 MPa) of raw polymers: sodium alginate, PVA, MC, PAA and Eudragit I100

On the other hand, the tablets were examined to assess the morphological changes using SEM. The tableability results were in accordance with SEM of the obtained tablets as in

Figure 3.9, where Sodium alginate demonstrated well-compacted tablets with retaining the same rough surface of the initial particles. However, the shape of the particles changed and deformed as compared with powder particles before compression.

Also, PVA tablets had a smooth surface with distinct voids within the tablet, indicating poor compact properties. On the other hand, MC particles retained their rough surface and relatively the same rod-shaped particles after tablet compression, which was seen in the particles' SEM results (ElShaer *et al.*, 2017) (Noronha *et al.*, 2014). PAA displayed that the initial particles' elastic properties helped to maintain their shape after compression. However, particles also deformed and fragmented to a smaller size. Eudragit L100 tablets (

Figure 3.9- E) were very smooth with no distinctly retaining initial particle shape. These findings indicate that the high porosity and elastic properties caused low compact properties.

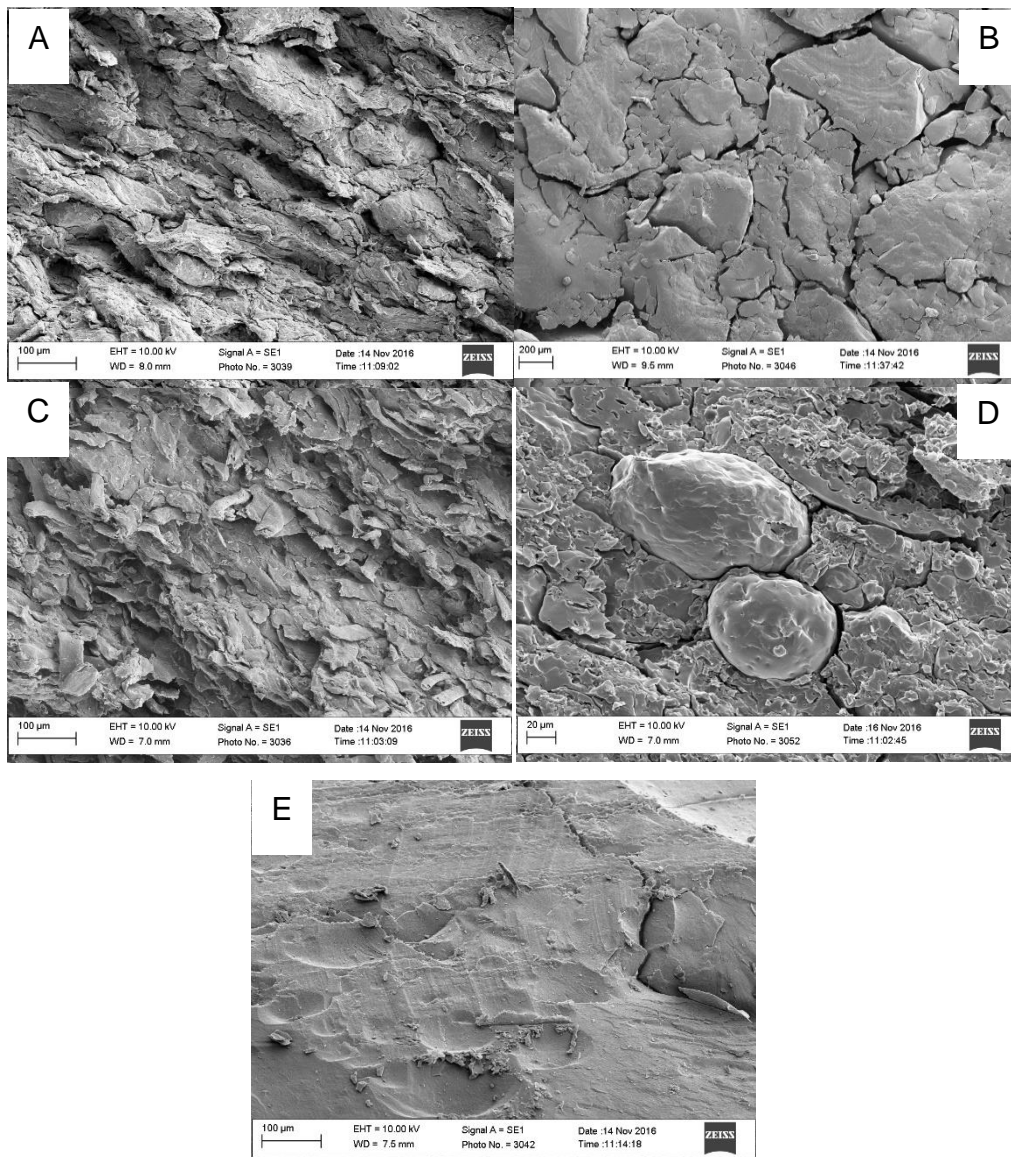


Figure 3.9 SEM images for the tablets of pharmaceutical polymers sodium alginate (A), PVA (B), MC (C), PAA (D) and Eudragit L100 (E) 20 and 200 -100 μm, high magnification and low magnification, respectively

3.4.2 Effect of spray-drying on polymers' characteristics

Spray drying consists of a continuous process based on a one-step contrary to other methods such as freeze-drying to prepare dry materials. This reduces preparation steps and time, which ultimately reduces costs (Zhou *et al.*, 2018).

Incorporating hydrophilic polymers in the spray-dried particles is an interesting approach to modifying the drug release profile. The hydrophilic polymer, such as cellulosic polymers MC or HPMC, enables fast gelation; thus, polymer hydrophilic tendency directly impacts the drug's encapsulation (Lee *et al.*, 2003) (Roy, 2011). Slowing the drug release rate can be achieved. However, hydrophilic polymers can also enhance the solubility of poorly water-soluble drugs (Sareen, Joseph and Mathew, 2012). Therefore, hydrophilic polymers either chemically modified or combined with hydrophobic polymers can be used to achieve modification of drug release. It was found that combination HPMC, Eudragit RS 30D and chitosan with alginate-based microparticles prevented a rapid drug release in the intestinal media from alginate microparticles (Lee *et al.*, 2003). Hence, sodium alginate microparticles could reduce the drug's burst effect as in hydrogels (Sosnik, 2014).

Moreover, polymeric particle size and particles shape uniformity significantly impact the compact mechanical properties, which should be enough to form microparticles with the desired properties (Kuriyama and Ozaki, 2014). Thus, it is essential to consider polymers' elastic and plastic properties using spray and raw powder (Lengyel *et al.*, 2019). Hence, both can be incorporated into the microparticulate system.

The sodium alginate, PAA, MC, PVA were spray-dried with a ratio of 5% w/v in water and similarly 5% w/v of Eudragit L100 using organic solvent ethanol/water 9:1. Overall, the yield was acceptable 55-60%. The characterisation of the collected particles was carried out similarly to the raw powders. This was done to compare the raw and spray dried powder to determine the polymer with the desirable properties that can be used to prepare microparticles and later in ODTs. To provide a consistent comparison in the same preparation ratio (5% w/v) of all polymers were applied yet different drying temperature only for Eudragit L100 (85 °C) from the other four polymers (120 °C).

3.4.2.1 Particle size analysis

The results showed that particle size significantly decreased compared with raw powders (Table 3.1) as in Table 3.3. This can be explained by the spray drying process that produced a smaller particle size of less than 100 μm (B. B. Patel *et al.*, 2015; Thirugnanasambandham and Sivakumar, 2017). The setting parameters such as the feed concentration, aspiration rate, and drying temperature affect particle size (Jain *et al.*, 2012; Santos *et al.*, 2018). The higher the inlet air temperature, the rapid moisture evaporation and more energy are provided. Also, the high feed viscosity hinders the proper droplet formation. This is related to the low viscosity solution, and the low solid content requires less energy (Patel, Patel and Suthar, 2009).

In general, the spray drying process produces hollow or solid spherical particles. There are different types of nozzles for atomisation of the feed solution, such as pressure nozzles, two-fluid nozzles, and rotary atomisers. Each nozzle produces particles with a specific size range. Two-fluid nozzles generally produce low particles sizes of 10 - 200 μm . In comparison, larger particle sizes produce by pressure nozzles up to 600 μm (Patel, Patel and Suthar, 2009; Jain *et al.*, 2012; B. B. Patel *et al.*, 2015).

According to one way-ANOVA, and t-test there is a significant difference between the polymers particle sizes before and after spray drying. Also, particle size may affect viscosity (Malvern Panalytical, 2015). The high solution viscosity was collected from Eudragit L100, PAA and sodium alginate. It was reported that particle size variation influenced by feed viscosity and inlet temperature (Mezhericher, Levy and Borde, 2010; Pietiläinen, 2013; Hadi, 2015; Grosshans *et al.*, 2016). Also, the impact of the inlet temperature was noticed while using the spray-dried Eudragit L100. Applying high temperature that similarly used for the other powders generated many filaments and sticky particles that agglomerated into larger particles. This could be related to the higher energy provided within a short time (Almeida e Sousa *et al.*, 2015). Therefore, reducing the temperature to 85°C instead of 120°C, which was optimised according to our experimental data, was suitable for spray drying Eudragit L100 (Lee, Kim and Kim, 1999; Pietiläinen, 2013). Although some of the particles showed collapsed shapes, generally, the collected particles had smooth surfaces and relative sphericity with fewer strands generated. Also, the low range of T_g of Eudragit L100 made selecting the suitable conditions critical to prepare uniform shaped microparticles, as reported earlier. Hence, particles of uniformed shapes are essential to prepare powder of good

flowability during tablet manufacturing (Amidon, Secreast and Mudie, 2009; Osei-Yeboah, Chang and Sun, 2016).

Similarly, Shepard et al. (2020) reported that reducing the inlet temperature from 117°C to 80°C during spray drying Eudragit L100 generated smaller particles and fewer filaments (Shepard *et al.*, 2020). This could be attributed to the fast-drying step that solidified the particles before droplet breaks up during the drying process. Hence, drying rate and atomisation should adequately be high to reduce rapid droplet breakup, which is polymer skinning. Therefore, considering the number of parameters to optimise spray drying settings: inlet temperature, polymer concentration, and solvent type as the slow evaporation solvent may generate the fewest filaments (Shepard *et al.*, 2020). However, reducing polymer concentration while using high drying temperature can improve the quality of the microparticles, i.e., integrity, shape and flowability (Büchi, 2002; BÜCHI Labortechnik AG, 2016; Lechanteur and Evrard, 2020).

Table 3.3 Particle size results of spray-dried powder presenting VMD ± SD of PAA, MC, Sodium alginate and PVA obtained from laser diffraction (n=3)

Polymer	Volume mean diameter (VMD) µm
Sodium alginate	8.56 ± 0.03
PVA	13.92 ± 0.02
MC	17.54 ± 0.04
PAA	7.26 ± 0.04
Eudragit L100	34.58 ± 0.2

3.4.2.2 Scanning electron microscope (SEM)

In spray-dried polymers' characterisation, all SEM images showed a reduction in particle sizes than the raw particles. Also, the results were correlated with particle size analysis. The sodium alginates particles showed hollow microparticles with different particles particle size; like PVA, the particles tend to agglomerate, forming larger particles (Figure 3.10-A and B). Simultaneously, MC particles had an irregular elongated shape structure and squashed surfaces (Figure 3.10-C). PAA particles displayed spherical shape and organised shaped structures (Figure 3.10-D). Eudragit L100 particles showed filaments generated (Figure 3.10-E). However, SEM also showed small-fine particles after spray drying. This could be attributed to the solution viscosity facilitated such finding. Hence, when the feed viscosity increases, the size of the produced particles increases. Also, using 5% solid concentration could be high influencing the particle size. The high concentration of ethanol (as an organic solvent) to solute reduced the feed concentration and eventually the particle size (Nolan *et al.*, 2011; Pietiläinen, 2013). Shepard *et al.* (2020) reported that particles sphericity enhanced at a higher drying temperature of 110 °C (Shepard *et al.*, 2020). However, further increment in the drying temperature may increase the particles size (Lechanteur and Evrard, 2020)(Wang, Dufour and Zhou, 2015).

Our preliminary studies showed similar findings applying other polymers parameters for Eudragit L100 produced a higher number of filaments with sticky particles. Although the yield increased using a lower inlet temperature, 85°C instead of 120°C, the yield is still low. This could be related to the particles' stickiness and low flowability during the drying process as detected during the spray drying process (Walton, 2000). Also, a higher evaporation rate may affect the yield (Goula and Adamopoulos, 2008). Moreover, it was noticed by Wang, Dufour and Zhou (2015), high cohesive particles generated when the drying temperature reached 180°C, which can be associated with elastic deformation of the flowing particles (Wang, Dufour and Zhou, 2015).

However, this finding varies depending on the solid content, type of the material, and the particles' drying energy, as discussed earlier. Therefore, shrinking, or hollow particles could be produced during the drying stage. It was also reported that spray-drying hydrophilic materials might generate smaller particle sizes due to higher water content in the particles, leading to shrinkage and decreased particle sizes (Rodrigues *et al.*, 2020).

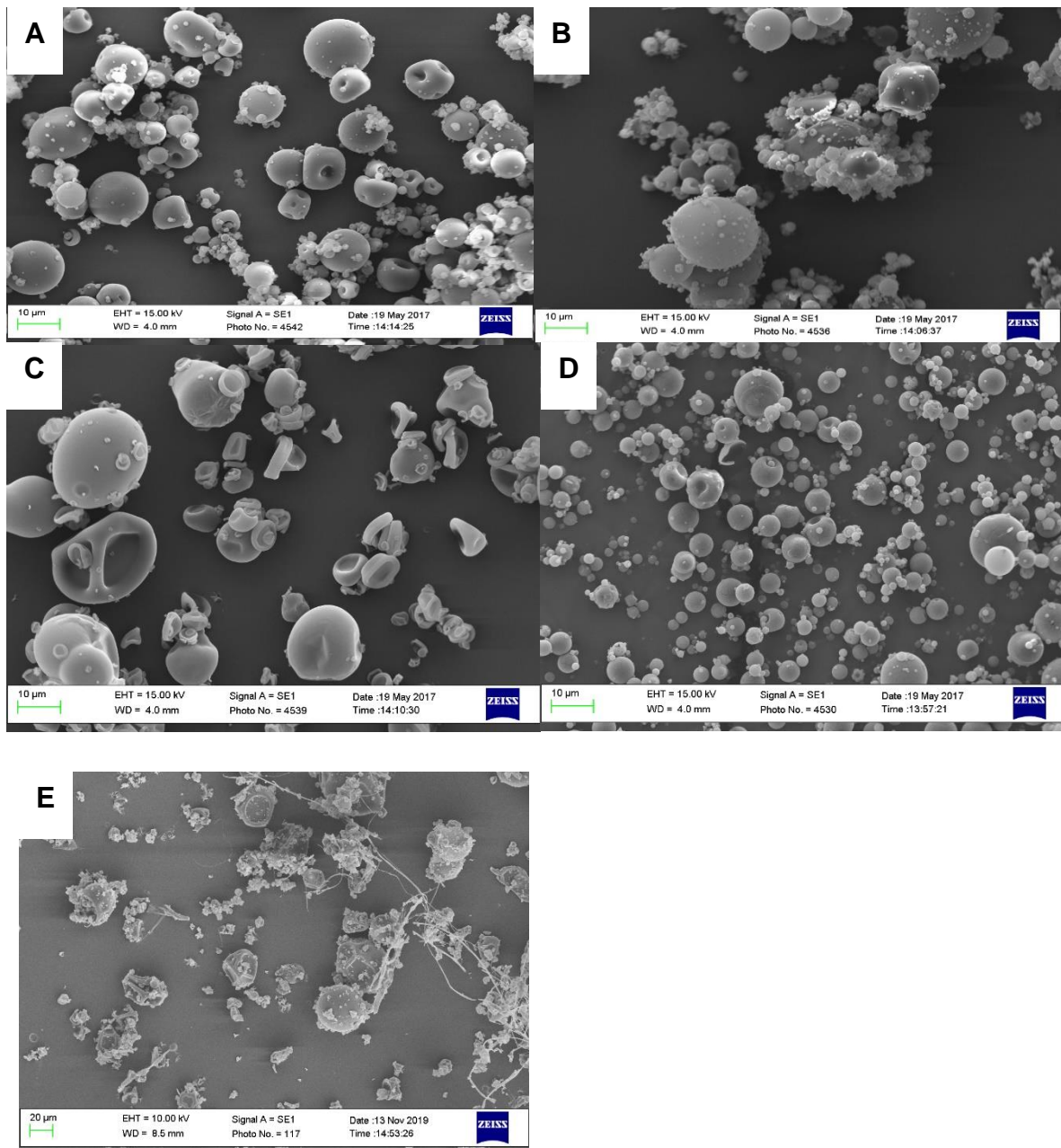


Figure 3.10 SEM images spray-dried powder of pharmaceutical polymers sodium alginate(A), PVA (B), MC (C), PAA (D), Eudragit L100 (E)

3.4.2.3 Surface area analysis

One of the commonly used methods to influence the material porosity and manipulating particle characteristics is spray drying(Zhou *et al.*, 2018). This can be directly related to the solvent evaporation and the adsorbed moisture at elevated temperature, leaving several inter and intra particles voids indicating high porosity (Chvatal *et al.*, 2019). Spray-dried powders are usually porous, appealing surface properties and particles with reduced size (Pietiläinen, 2013)(Nežić *et al.*, 2018).

It was reported that spray-dried powders enhance tablet compatibility due to the equal diameters of particles (Al-Zoubi *et al.*, 2021). This aids in uniform particle rearrangement during tablet compaction (Al-Zoubi *et al.*, 2021).

The studies showed that spray-dried powder tablets had high plastic deformation compared to raw and non-porous powders (Al-Zoubi *et al.*, 2021) (Zhou *et al.*, 2018). Hence, the voids provide enough space for particles to compress and form intra-particulate bonds resisting the applied pressure (Zhou *et al.*, 2018). However, the large surface area provided by small particle size and homogeneous surface properties also critically supports the compact's strength (Nežić *et al.*, 2018).

Nevertheless, materials with high porosity could generate fragile compact (ElShaer *et al.*, 2017) (Keleş *et al.*, 2015). This was reported by Zhou *et al.* in preparing tablets with improved compressibility yet still low hardness, which made them suitable for fast disintegration (Zhou *et al.*, 2018).

Like the raw powder, the spray-dried powders were analysed to detect the particles' porosity and surface area using a porosimeter. The results (Table 3.4) showed a general increment in porosity compared to the raw powders (Table 3.2). However, the detected surface area is also relatively low. The difference with raw powder was remarkably noticed in the isotherms (Appendix Figure 10.1 and

Figure 10.2). The adsorption-desorption isotherm of all samples exhibited Type IV curves, suggesting mesoporous structures. A similar trend was found by Jackcina Stobel Christy *et al.* (2020) in the isotherms of nanostructured polysaccharides, the inflation point was unclear, yet the results showed a mesopore structure with a Type IV curve (Zhou *et al.*, 2018; Jackcina Stobel Christy *et al.*, 2020).

On the other hand, owing to some technical issues, the Eudragit L100 porosity was undetected. Nevertheless, according to preliminary results, the bulk density showed that all spray dried polymers had bulk density 0.5-0.3 g/cm³, while the raw powders showed a consistent 0.5 g/cm³.

Similarly, the bulk density was low for spray-dried powder, indicating an increment in porosity. Hence higher the bulk density, the low porosity (Takeuchi *et al.*, 1998). Also, Shepard *et al.* found that Eudragit L100 bulk density was reduced after spray drying, indicating higher porosity (Shepard *et al.*, 2020). However, their reported results showed lower bulk density (0.1 g/mL) than our results. This could be related to particles' shape and surface properties, yet our bulk density range is still acceptable since no high variation. Further optimisation is necessary for a future approach.

On the other hand, the general difference between the polymers porosity and surface area could be attributed to some particles' shapes irregularity and the empty voids generated from the loss of water. A similar finding was reported by Paluch et al. (Paluch *et al.*, 2013).

Table 3.4 Surface area and porosity measurements for spray-dried powders using Belsrop

Polymer	Mean pore diameter (nm)	Surface area (m ² /g)	Total pore volume (cm ³ /g)
Sodium alginate	7.84	1.34	2.631 x10 ⁻³
PVA	8.10	2.12	4.296 x10 ⁻³
MC	8.25	2.58	5.335 x10 ⁻³
PAA	8.61	1.32	2.852 x10 ⁻³
Eudragit L100	NA	NA	NA

3.4.2.4 Thermal analysis

DSC and TGA analysis were performed on the spray-dried polymers (sodium alginate, PVA, MC, PAA, Eudragit L100). This was applied to characterise the polymers' thermal properties to understand their physical and chemical stability during the preparation of microparticles and tablet manufacturing. The powders moisture content after spray drying was measured using TGA. Hence, the moisture content and humidity may have a plasticising effect altering the tablets tensile strength and elastic recovery (NOKHODCHI *et al.*, 1996; Ghori and Conway, 2016).

In general, the results showed high similarity with the raw polymers. However, slight variations in DSC results (Figure 3.11) were detected. This could be related to moisture content and degree of crystallinity (Mathkar *et al.*, 2009). Hence, one of the spray drying effects is the formation of amorphous material (Nežić *et al.*, 2018). For instance, a disappeared melting peak in PVA thermograms indicates the polymer change into an amorphous form from the semi-crystalline structure of the raw form (Sambasivam, White and Cutting, 2016; Deshmukh *et al.*, 2017; Thomas *et al.*, 2018). On the other hand, it was noticed peak shifting in sodium alginate, MC and Eudragit L100. This could be related to the slight increase in the heating rate from 10 to 20°C /min. This might be related to the influence of a faster heating rate on the sample's heat capacity leading to shifting T_g to a higher temperature (Thomas, 2001).

Also, DSC results of spray-dried polymers (Figure 3.11) demonstrated sharper peaks compared to raw polymers (Figure 3.5). It can be assumed that the peaks sharpness resulted from the smaller particle sizes of the polymers obtained from spray drying, which was confirmed from the laser diffraction data (Mathkar *et al.*, 2009). Also, the particles' rearrangement within the sample pan may slightly impact the DSC thermograms (Faroongsarng, Kadejinda and Sunthornpit, 2000). In addition, smaller particles of polymers powder might aggregate together; this agglomeration may affect the results (van Dooren and Müller, 1984).

Consequently, particles size and agglomerates can cause sharper peaks; for instance, the sodium alginate (Figure 3.11- A) had a sharp exothermic peak around 240°C compare to the same raw powder polymer (Figure 3.5 - A). This may also be correlated with the polymers' hydrophilicity as the polymers showed an increment in the moisture content compared to the raw powder.

TGA (Figure 3.12) showed that all the polymers had moisture content lower than 5%. This indicates that water molecules and the spray drying process did not remove all the bulk water, which surrounded the surfaces of the particles (Tiefenbacher, 2017). Moreover, it was reported by García Mir *et al.* that moisture content could vary according to the process parameters (García Mir *et al.*, 2011). This was confirmed by the porosity results that showed higher porosity in spray-dried powder than the raw ones. Hence, this was related to the spray drying effect and evaporation of the water, leaving several voids among the particles. This also affects the tablets mechanical properties as in the next section (Young's modulus and tensile strength analysis) (Crouter and Briens, 2014).

Overall, spray-dried powders (Figure 3.12) agreed with the TGA results of raw powders showing similar degradation temperature. This confirms the limited effect on the chemical changes and the stability of the material's chemical properties. For instance, sodium alginate showed the same decomposition behaviour which was also reported by Soares *et al.* (Soares *et al.*, 2004).

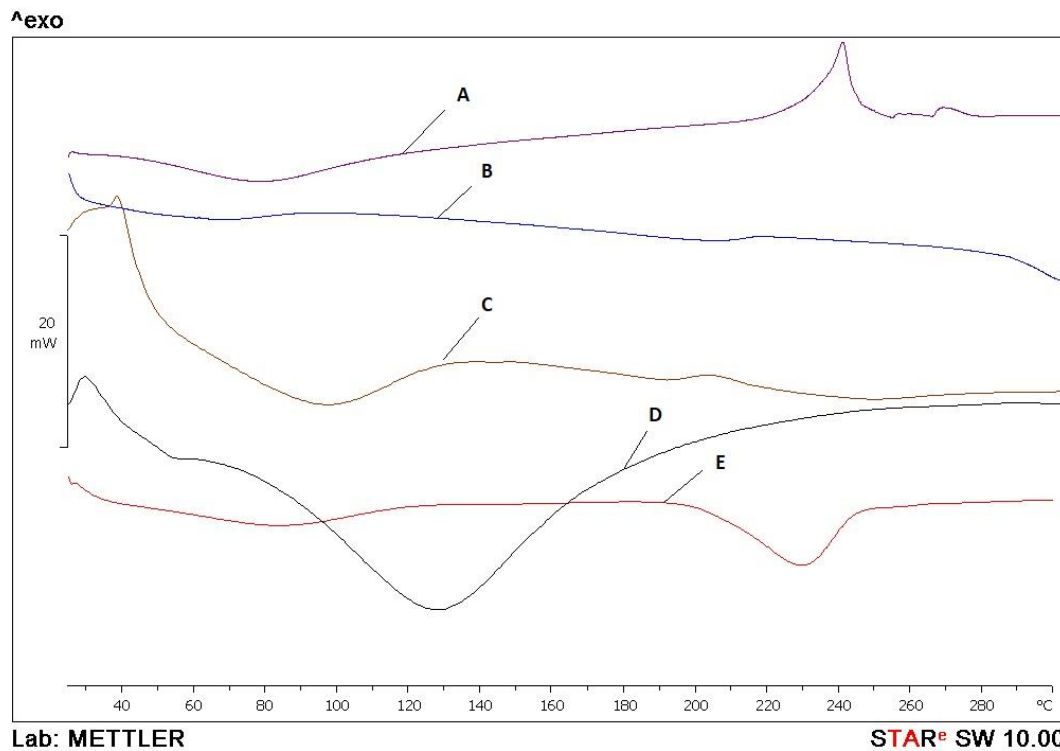


Figure 3.11 Thermal analysis DSC of 4 spray-dried pharmaceutical polymers sodium alginate (A), PVA (B), MC (C), PAA (D) and Eudragit L100 (E) from 20 to 300°C temperature and 20 °C/min heating rate using METTLER software

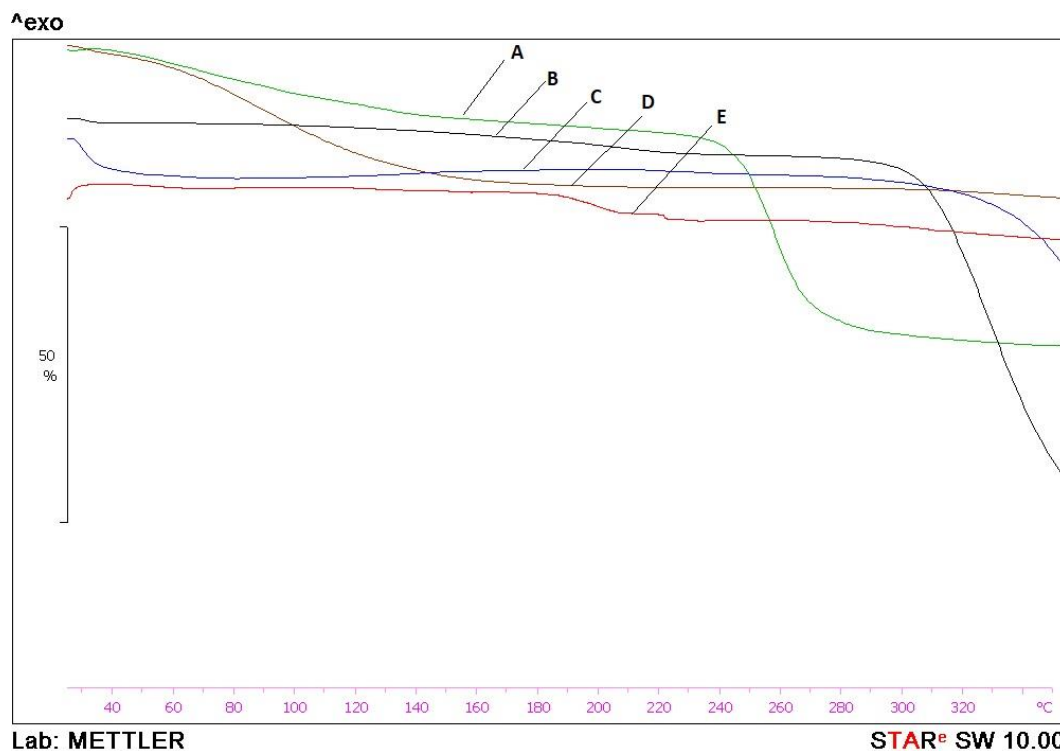


Figure 3.12 TGA graph of the 4 spray-dried polymers (A) sodium alginate, (B) PVA, (C) MC, (D) PAA and (E) Eudragit L100 at heating range from 20 -350°C with 10°C/min heating rate in a nitrogen atmosphere using STAR^e software

3.4.2.5 Texture analysis for elasticity

Young's modulus was measured for all the spray-dried particles using a texture analyser to detect the gradient of stress against the strain, representing the elasticity profile, i.e., Young's modulus (Faridmehr *et al.*, 2014)(Singaraju *et al.*, 2016).

In comparison to their raw form (Figure 3.7), Young's modulus for all spray dried polymers increased significantly ($p < 0.05$), as illustrated in Figure 3.13.

The elastic modulus values ranged between the lowest for Eudragit L100 9.72 MPa and the highest 23.71 MPa for MC. Young's modulus for the spray-dried powders showed that the particles were significantly different in their elastic profile according to One-Way ANOVA and t-test ($p < 0.05$). A similar trend was detected comparing raw powders together. This reflects the consistency of the difference in elastic profile between the powders before and after spray drying. However, only PAA and Eudragit L100 in raw form showed similar elastic tendencies with no significant difference. In contrast, that similarity disappeared after spray drying.

Two facts can explain the findings. Firstly, particle size reduction after spraying for all polymers, as in the particle size analysis (Table 3.3), generated high surface area. This, in turn, offered a high number of bonding sites enhancing the inter-particulate bonds; thus, the particles showed higher plasticity (Hiremath, Nuguru and Agrahari, 2019). However, as Young's modulus increases, the material's elasticity decreases and tablets become brittle (Salama *et al.*, 2015). Young's modulus' increment limit should provide a balance of elasticity and plasticity to be acceptable.

Secondly, alongside reducing powders' particle size after the spray drying, homogeneous particles surfaces were generated (Callard Preedy and Prokopovich, 2013). Therefore, the effect of particle size and shape dominated the high porosity associated with spray-dried powder.

However, small particles can easily sit within the pores between big particles, enhancing the packing density and showing a relative increment in the particles' plastic deformation (Wiącek and Stasiak, 2018). It was found by Kováčik the finer particle possess high packing properties owing to the higher porosity level and Young's modulus (Kováčik, 1999). Although in our results, porosity was relatively low even after spray drying, as discussed earlier, this could affect the final tablet compressibility and tensile strength, leading to a reduction in tensile strength and causing such variation in Young's modulus. Therefore, it is essential to accurately select the powder of

adequate balance between elastic and plastic tendencies either in raw or spray-dried form.

On the other hand, our results showed a significant effect of particles size after spray drying on Young's modulus. As sodium alginate and PAA had the smallest particle size and lowest Young's modulus and the opposite for PVA and MC. Kováčik (1999) reported that Young's modulus increased when the particle size differed within small particle size 0.5 - 2 μm demonstrating smaller elastic modulus value than larger sizes 2 - 4 μm . This could be attributed to the friction that could increase with decreasing particle size and deformation (Tanaka and Iizuka, 1991; Kováčik, 1999). Therefore, the particles size within slight variation could show a direct relationship with elastic modulus.

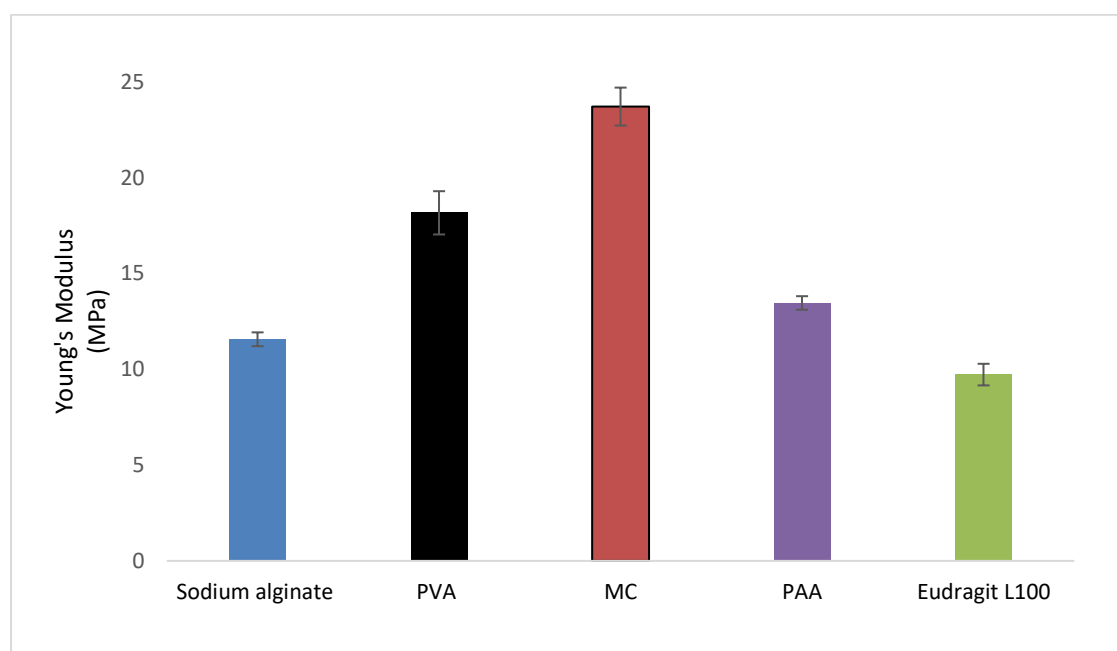


Figure 3.13 Texture analysis results of spray-dried polymers illustrating Young's modulus under 300 Kg force mean \pm SD (n=3)

Moreover, the moisture content increment could negatively affect the strength of the tablet. It was reported that water offered a lubrication effect with low moisture levels, thus improved particles flowability. However, the higher the moisture levels, the higher cohesion forces between the particles, thereby reducing particles flowability. As referred earlier, this was also detected in our preliminary data, showing acceptable flowability results (Sandler *et al.*, 2010; Crouter and Briens, 2014).

Therefore, compared to raw powders, the spray-dried powders showed a significant difference in elasticity profile with a general rise in all values. This showed the

correlation between the particles size reduction after spray drying and mechanical properties. As the smaller the particles, the higher the surface area available against the applied stress. Therefore, the particles showed plastic to brittle deformity. Further analysis for the tablets after compaction was necessary to provide comprehensive data.

3.4.2.6 Tablets tensile strength and morphological characterization

Tablets prepared from spray-dried polymers were examined for their hardness. All tablets prepared under 443 MPa compression pressure (Figure 3.14) as it was challenging to prepare tablets with the lowest compaction forces due to the tablets' friability.

The tensile strength results changed significantly compared to the raw powders at 443 MPa pressure according to One-way ANOVA and t-test ($p < 0.05$). Also, tablets produced from spray-dried particles showed a significant difference ($p < 0.05$), except sodium alginate and PVA showed similar tensile strength ($p > 0.05$). It can be noticed that the results showed a similar trend with Young's modulus for sodium alginate, PVA and MC increasingly. However, the results showed a reduction in all tablets' tensile strength after spray drying yet increased for Eudragit L100 tablets. For instance, MC was the highest 8 MPa among the four polymers (sodium alginate, PVA, PAA), while MC had a higher value in the raw form 10.07 MPa. It should be referred that the low Young's modulus value of raw powder PAA offered good tensile strength tablet compared to spray-dried PAA. Also, sodium alginate and PVA results were 5.7 MPa and 6.1 MPa, respectively, between PAA and MC strength.

SEM images of sodium alginate (Figure 3.15, image A) and PVA (image B) showed particles of tablets with change in shape and reduced size compared to tablets of raw powder. This explains the similar trend according to the statistical analyst between sodium alginate and PVA tensile strength ($p > 0.05$), as referred to in the text earlier. The results were in harmony with MC tablets' shape after the hardness test showing elongated irregular particle (Figure 3.15- C). On the other hand, the lowest tensile strength was 1.1 MPa for PAA, which was noticed from the SEM (Figure 3.15, image D). The particles maintained their shape after compression with a reduction in particle size. However, cracks were detected in the image within the tablet matrix, indicating low hardness.

Overall, the moisture content for the spray-dried powder increased compared to raw powders. Mattsson (2000) suggested that high moisture content can enhance particle-particle binding. However, this differs with material affinity to water and porosity (Mattsson, 2000; Almaya and Aburub, 2008; Wiącek and Stasiak, 2018). Although the applied pressure controls the impact of porosity, the particles' porosity influenced the tensile strength (Liu *et al.*, 2014; Zhou *et al.*, 2018). Therefore, it is necessary to consider particles porosity under the lowest compression pressure. According to the literature, 3-5% moisture content is an accepted value (Sun, 2008; Crouter and Briens, 2014; Liu *et al.*, 2014). It was reported that that Young's modulus and tensile strength primarily enhanced with increasing moisture content then reduced with further rises above 3.3% in moisture content (Sun, 2008). Therefore, moisture content could affect the particles' cohesion forces (Crouter and Briens, 2014). Also, it was reported that the tablets tensile strength was less affected by moisture content with a value of about lower than 5% (Amidon and Houghton, 1995). Nevertheless, the moisture effect could change according to materials type and the compaction pressure (Sun, 2008). It was reported that pellets of sodium alginate showed a high elastic profile compared to potassium alginate (Schmid and Picker-Freyer, 2009). Hence, this affected the drug release as plastic compact showed a higher release than more elastic alginates (Schmid and Picker-Freyer, 2009).

In contrast, the results of Eudragit L100 was different, showing an increment in tensile strength along with elastic modulus compared to the raw form. The results could be correlated with the low moisture content owing to the used highly volatile organic solvent. Also, Eudragit L100 hydrophobic polymer retaining or adsorb moisture is low compared to other polymers that show high hydrophilicity (Hillier, 2007; Braia *et al.*, 2012; Sigma-Aldrich, 2021). SEM results showed that Eudragit L100 correlated with good mechanical properties retaining the particles shape under compression (Figure 3.15- E).

The results indicate that Young's modulus below 9.7 MPa is desirable, and the low limit could vary depending on the physical structure and material types. Also, the desired moisture content is lower than 5 % (Sun, 2008; Crouter and Briens, 2014; Liu *et al.*, 2014).

Overall, the tablets showed sufficient tensile strength ranging from 1.12 – 14.01 MPa. Therefore, different formulations could be developed using the polymers such as pellets and microparticles to be compressed. However, the combination of the

polymers together could be applicable for future approach and require further investigation.

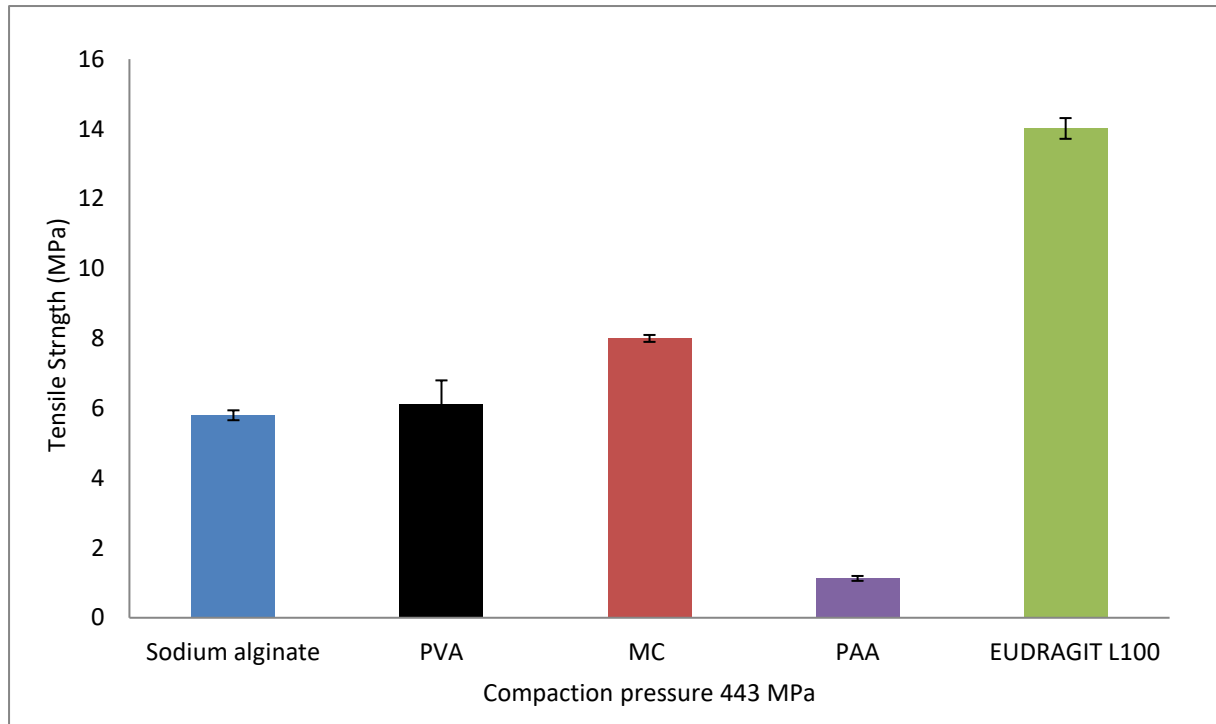


Figure 3.14 Tensile strength values (MPa) for tablets of spray-dried polymers sodium alginate, PVA, MC, PAA and Eudragit L100 under the maximum compaction pressure 443 MPa

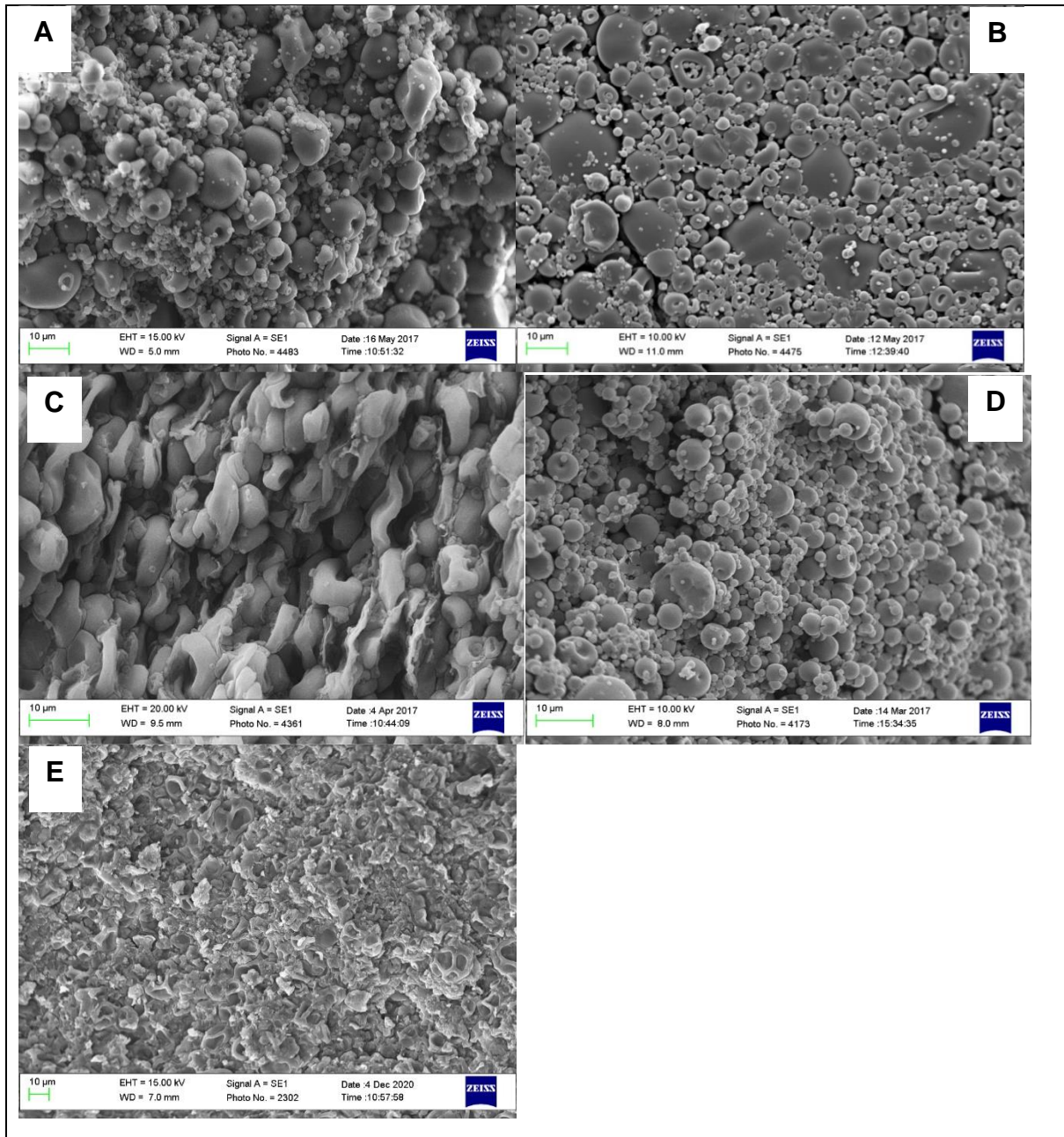


Figure 3.15 SEM images of tablets after hardness test the tablets of spray-dried polymers sodium alginate (A), PVA (B), MC (C), PAA (D) and Eudragit L100 (E)

3.5 Conclusion

The polymer properties were characterised in raw and spray dried status. Also, the tablets that obtained were analysed. Different analysis techniques have been used, including particle size characterisation, morphology examination using SEM, surface area analysis, thermal analysis, texture analysis, and hardness test.

It can be concluded from the obtained results the polymer with elastic-plastic balance provides suitable compaction property. SEM and surface area results showed a correlation with the mechanical findings. Several factors generated a difference between the mechanical properties of the powders before and after spray drying, including particles size, shape irregularity, surface smoothness and porosity. Also, moisture content differently affected the polymers depending on the type of the material and the affinity to water. Hence, water molecules could move over each other providing low compatibility and less available contact points within the powder particles. In general, our results of raw and spray dried powder showed good moisture content within the acceptable range lower than 5% according to the literature. Compared to raw powders, the increment in moisture content produced higher Young's modulus and tendency to fragility as confirmed from the low tensile strength values (lower than raw powders).

The particles size is one factor that remarkably affects the powders' mechanical properties and the obtained tablets. The smallest particle size has less elasticity modulus. Besides, it influenced the tablet's tensile strength differently and decreased the elastic recovery. Thus, PAA has more elasticity as compared to MC results of particle size analysis. Moreover, the spray drying process influenced the obtained powder properties. Also, there is a significant relationship between the particle's hardness and the applied pressure.

Moreover, the spray drying resulted in formation higher number of voids. The high number of voids caused reduction in tablets tensile strength. Eudragit L100 results showed lowest Young's modulus and highest tensile strength compared with the 4 hydrophilic spray dried polymers. As explained earlier owing to low affinity of the polymer to hold water and the possibility of intra-particle bonds provided adequately increment in Young's modulus of spray dried Eudragit L100 (9.7 MPa) compared raw

Eudragit L100 powder (5.2 MPa). The high tensile strength indicated good balance offered by the values of Eudragit L100. Overall, the tensile strength is still acceptable as recorded by the literature ranging between 0.1-4 MPa which was achieved with spray dried powder.

Therefore, Eudragit L100 was applied in the preparation of multiparticulate system as in the next chapters.

Chapter 4 Method development and validation for detection and quantification of indomethacin and propranolol hydrochloride

Scoop of HPLC methods

A valid method is needed to analyse the samples of tablets containing drug pellets from the dissolution studies. The validated method should be in acceptance with the validation specifications and parameters set by ICH. According to ICH, the parameters used for dissolution studies include linearity, specificity, accuracy, range, and precision. The methods for both model drugs indomethacin (IND) and propranolol hydrochloride (PRH) were modified from reported methods by Elshaer et al. and Aqil et al., respectively. The HPLC system selected for the dissolution studies (Liquid Chromatograph Agilent technologies II, USA) had a wavelength detector and fully functioned at room temperature. According to the ICH guideline, the methods were accurate and precise and were utilised to assess the drug release from the formulations with a low limit of quantification and detection.

Keywords: HPLC, ICH, IND, PRH

4.1 Introduction

4.1.1 Model drugs: indomethacin (IND) and propranolol hydrochloride (PRH)

Nonsteroidal anti-inflammatory drugs (NSAIDs) are considered the most used medications to treat pain and inflammatory diseases. The anti-inflammatory action of NSAIDs is based on inhibiting cyclooxygenase enzyme release, thereby inhibiting the synthesis of prostaglandin associated with undesired gastric side effects. According to their mechanism of action, NSAIDs are divided into nonselective NSAIDs that inhibit the release of both cyclooxygenase I & II and selective NSAIDs that inhibit cyclooxygenase II release only. (Savjani Ketan, Gajjar Anuradha and Savjani Jignasa, 2012)

IND is a nonselective NSAIDs that is widely used as a pain killer, antipyretic and anti-inflammatory product (Nalamachu and Wortmann, 2014; Ho *et al.*, 2018). Recent studies showed that NSAIDs with cyclooxygenase 2 inhibitor have activity against colonic cancer and can be a potential treatment by its antagonistic and anti-inflammatory effect (Ikawa *et al.*, 2012; Emam Kassab, 2019) . Specifically, IND can be used as a cost efficient future anticancer drug owing to its chemotherapeutic effect and reducing the colon cancer risk (Ikawa *et al.*, 2012; Seetha, Devaraj and Sudhandiran, 2020) According the Biopharmaceutics Classification System (Table 4.1), IND is a class II drug with half-life of 4-5 h and pKa of 4.5.

Table 4.1 pharmaceutical classification of drug showing solubility and permeability in the biological system(Savjani Ketan, Gajjar Anuradha and Savjani Jignasa, 2012; Shah and Amidon, 2014; Aulton and Taylor, 2018a)

Class I: Drugs have high permeability and solubility leads to fast absorption and hence high bioavailability	Class II: Drugs have high permeability and low solubility exhibiting limited absorption
Class III: Drugs have low permeability and high solubility, leading to limited permeability.	Class IV: Drugs have low permeability and low solubility leading to poor bioavailability.

Similarly to NSAIDs, IND causes gastric side effects that could be reversed by taking antihistamine drugs such as famotidine (Taha *et al.*, 1996; Assali *et al.*, 2020). However, this can influence patient adherence rendering the therapy challenging for long term conditions. Therefore, delaying the release of IND to bypass the stomach

and immediately release it in the small intestine was one of the aims of this project. In order to achieve this, a pH dependent polymers were used to delay the IND release from a multiparticulate system (pellets and microparticles) embedded in an orally disintegrated tablet matrix (ODTs) (Assali *et al.*, 2020).

On the other hand, the beta-blocker agent, propranolol (pKa 9.45), was used as a second model drug. In general, beta-blockers are agents used to treat high blood pressure as they block the release of two hormones known as adrenalin and noradrenaline. This results in slowing the heart rate and lowering blood pressure (British Heart Foundation, 2020). Propranolol is prescribed as a treatment for hypertension and heart diseases treatments as well as in controlling abnormal heart rate and tremor associated with certain diseases. According to BCS, PRH belongs to class I, as it has high solubility profile, and it gets adsorbed rapidly across the GIT(Pretorius and Bouic, 2009; Srikanth *et al.*, 2012; Papich and Martinez, 2015). There are different available dosage forms of PRH, including tablets, oral solutions, and syrups formulations. However, the frequency of dosing of PRH is a challenge, especially for patients with heart diseases that require long-term treatment or to combine more than one treatment regimen.

In order to achieve a prolonged release of PRH using suitable and novel formulations, PRH pellets based on a time-dependent polymeric system were manufactured to be released through ODTs. This would enable a modified release of PRH while minimising the frequency of dosing, thereby improving patients compliance (Srikanth *et al.*, 2012; Tanabe *et al.*, 2019)

4.2 Analytical methods

Different analytical techniques such as ultraviolet (UV), mass spectrometry (MS) and chromatography can be used to detect and identify various components in pharmaceutical formulations (Shabir, 2011)(El-Badry, Fetih and Fathy, 2009). One of the most common chromatographic techniques used to detect and quantify active pharmaceutical ingredient (API) is high-performance liquid chromatography (HPLC) (Coskun, 2016).

The high accuracy in detecting the analyte and the impurities is one of the main advantages of this technique. It is necessary to run the drug with excipients to detect

any influence on the drug quantification or method validation as different ingredients were used to prepare the formulation that may interfere with the detection of the analyte in the samples. HPLC with reversed-phase is a commonly used method for analysing the drugs and similarly applied in our HPLC methods (Coskun, 2016).

This chapter highlights the different characteristics and parameters investigated during HPLC method development and validation. The methods for the two active ingredients under analysis, the model drugs IND and propranolol hydrochloride (PRH), were established separately to allow for independent analysis in terms of drug release from the produced formulations for each drug.

The literature studied numerous methods that have previously been established to quantify IND and PRH (Nokhodchi *et al.*, 2005; Srikanth *et al.*, 2012). Although many methods were reported to detect IND and PRH release, our presented methods were developed and validated in detecting the drug incompatibility or interference with all excipients used in the prepared formulations.

Moreover, the methods were developed to quantify the low amount of drug by assessing LOD and LOQ in the formulation. Also, the methods were specifically detecting the drug combined with all the added excipients.

4.2.1 High-performance liquid chromatography (HPLC)

HPLC is an analytical procedure by which separation of the solutes is achieved. HPLC is a favoured analysis process amongst other analyses techniques as it offers high sensitivity, good resolution, accurate and reproducible data. The system consists of a mobile phase (mixed solutions) that is pumped through the stationary phase carrying the spiked analyte where separation occurs; then the spiked sample elutes out. The sample is then detected by UV/Vis detector that presents the data as a plot of absorbance against the elution time (Harshad V. Paithankar, 2013).

Depending on the affinity of the solute to the stationary phase, the separation occurs. Hence, the lower the affinity, the faster the elution (Harshad V. Paithankar, 2013). Therefore, the elution order of the components in a sample is influenced by their polarity; for example, the material with low polarity elutes rapidly from the polar stationary phase since the analyte shows minimum interaction with particles. Consequently, there are two modes of separation in the HPLC normal and reversed phase. In the normal-phase separation, a polar stationary phase with 100% organic

solvent with water traces as the mobile phase is used. Hence, polar analytes tend to bond with the polar stationary phase; thus, they show a long retention time (like attracts like). In contrast, the reversed-phase is performed using a polar mobile phase and a non-polar stationary phase (Betancourt and Gottlieb, 2018).

The reversed phase is a widely used HPLC method up to 75% preferable due to its reproducibility and applicability for analysis (Miyazaki, 2000; Welling and Welling-Wester, 2000; Lawson, 2008; Smith, 2014; Waters, 2018). Hence, the mobile phase can be a mixture of organic and aqueous solvent, such as acetonitrile or methanol, and water. This is necessary to provide good interaction between the analytes with the non-polar particles of the stationary phase. The commonly used reversed-phase HPLC column (stationary phase) is C18-bonded silica (Waters, 2018).

Moreover, either isocratic or gradient modes of elution can be used. Hence, gradient mode is run by changing the salt ratio or the ratios of the mobile phase constituents during the analysis to detect more than one analyte in the sample. While isocratic is a simple and easy separation mode since stable ratios and concentration of the mobile components are used. In addition, different reported methods provide good analysis for the model drugs, i.e., IND and PRH.

However, the major disadvantages of these methods are the complexity of instrumental application and the expensive analysis. Therefore, according to the comparison, as in the Table 4.2 and Table 4.3, our method development and validation for both IND and PRH were successfully achieved.

Table 4.2 Literature's summary for HPLC methods of analysing IND

Ref	Column	Mobile phase	Elution type	Wavelength (nm)	Flow rate (mL/min)	Elution time (min)	LOD & LOQ	Internal standard
(Roberts and Smith, 1987)	Spherisorb S5 ODS C ₁₈ (250 mm x 4.5 mm particle size 5 μ)	Methanol 70% with 30% Anhydrous sodium acetate 0.02 M solution pH 3.6	Isocratic	254	1.5	12	LOD 20 ng/mL, LOQ NA	Flufenamic acid
(Haq et al., 2014)	Lichrosphere reversed phase C ₈ column (250 x 4.0 mm, 5 μm)	Ethyl acetate (100 % v/v)	Isocratic	318	1.0	2.44	LOD 0.05 μg/mL and LOQ 0.15 μg/mL	NA
(Kim and Ku, 2000)	Reversed phase column Bondapak C ₁₈ (3.9 mm, id. x 30 cm)	Acetonitrile and 1 M acetic acid (1:1, v/v)	Isocratic	320	1.3	NA	NA	NA
(Tsvetkova et al., 2012)	LiChrosorb C ₁₈ (250 mm x 4.6 mm, 5 μm)	Mixture of 40 volumes 0.5 % v/v orthophosphoric acid, 20 volumes of methanol and 40 volumes of acetonitrile	Isocratic	240	2	9	LOD 0.05 μg/mL and LOQ 0.2 μg/mL	Indomethacin RS, 4-chlorobenzoic acid RS and 5-methoxy-2-indoleacetic acid RS
(Nováková et al., 2005)	Zorbax-Phenyl analytical column (75 mm x 4.6 mm, 3.5 μm)	Acetonitrile and 0.2% phosphoric acid (50:50, v/v)	Isocratic	237	0.6	7.5	NA	Ketoprofen or flurbiprofen

(Boon, Glass and Nimmo, 2006)	reversed-phase column C ₁₈ , 4.6 × 150 mm, 5 μm, 90Å (Varian Analytical Instruments)	Acetonitrile 60% in 0.02M sodium acetate buffer pH 3.6	Isocratic	320	1.0	Less than 7 min	LOD 10 ng/mL & LOQ 50 ng/mL in porcine plasma	Mefenamic acid
(Pai and Sawant, 2017)	Zorbax Eclipse Plus C ₁₈ , 3.5 μm, (4.6 mm × 100 mm)	Methanol: acetonitrile: 10 mM sodium acetate buffer pH 3, 10:50:40% v/v	Isocratic	254	1	5	LOD 1.036 μg/mL LOQ and 3.141 μg/mL	NA
(Hess et al., 2001)	C ₁₈ column, 250 mm × 4.6 mm with 10 nm pore diameter	Methanol 75% and 25% an aqueous solution of 0.2% v/v phosphoric acid	isocratic	320	1.5	2.7-16.4	LOQ 1 μg/mL and LOD NA	NA

Table 4.3 Literature's summary for HPLC methods for PRH

Ref	Column	Mobile phase	Elution type	Wavelength (nm)	Flow rate (mL/min)	Elution time (min)	LOD & LOQ	Internal standard
(Aqil et al., 2013)	Hypersil ODS C ₁₈ column (250x4.6 mm, i.d., 5 µm particle size)	Acetonitrile, methanol, and 0.01 M disodium hydrogen phosphate (pH 3.5) in the ratio of 50:35:15 v/v	Isocratic	250	1.0	6.62	LOD 0.27 µg/mL and LOQ 0.85 µg/mL	NA
(Meka et al., 2012)	reverse phase C ₁₈ column (3.9 mm x 300 mm, particle size 5 µm)	Acetonitrile: phosphate buffer (pH 4.5) (35:65) (v/v)	NA	214	1	6.6	NA	Diltiazem
(Tang et al., no date)	Phenomenex C ₁₈ column (150 mm x 4.6 mm, 5 µm)	Sodium dodecyl sulfate 1.6 g and 0.31 g tetrabutylammonium dihydrogen phosphate in a mixture of 1 ml sulfuric acid and 450 ml water and add 550 ml acetonitrile. Adjust to pH 3.30	isocratic	292	1.0	2.5-3	LOD 0.8 µg/mL and LOQ 2.0 µg/mL	NA

(Shaker et al., 2017)	BDS Hypersil C ₁₈ (150 mm x 4.6 mm and 5 μm)	Acetonitrile, methanol, and triethylammonium phosphate solution (15.0:32.5:52.5, v/v) as well as triethylammonium phosphate solution, pH 2.75	Isocratic elution	214	1.0	7.0	LOD 15 ng/mL and LOQ 50 ng/mL	Sildenafil
(Kim et al., 2001)	5 μm CAPCELL PAK analytical cyano column	Aqueous acetic acid 1% containing 0.2% triethylamine and acetonitrile (65:35, v/v; pH 3.8)	NA	column effluent was monitored with a fluorescence detector at an excitation wavelength of 230 nm and an emission wavelength of 340 nm	0.5	10.5	LOD 1.34 ng/mL and LOQ 2 ng/mL	Pronethalol
(Rani et al., 2011)	Waters C ₁₈ column (250 x 4.6 mm, i.d. 5 μ)	Acetonitrile: water (adjusted to pH 2.3 with ortho phosphoric acid) in the ratio 60:40 v/v	Isocratic HPLC	214	1.0	10	LOD 0.4 μg/mL and LOQ 1.2 μg/mL	NA
(Yadav and Majee, 2015)	Waters Acquity BEH C ₁₈ column (30 x 2.1 mm, 1.7 μm)	Trifluoroacetic acid (0.1%) and acetonitrile in the ratio 80:20 v/v	Isocratic	230	0.3	2.5	NA	NA

(Shabir, 2011)	Reversed phase C ₁₈ (150×4.6 mm, 5 μm) column	Pyrrolidine 50 mM (pH 11.5) - acetonitrile (50:50, v/v)	Isocratic	214	1	2.86	LOD 0.95 μg/mL and LOQ 2.5 μg/mL	NA
(Salman et al., 2010)	C ₁₈ end-capped (250 × 4.6 mm I.D., 5μm)	Water 160 mL, 180 mL methanol, 70 mL acetonitrile, 2.5 mL acetic acid, and 125 μl triethylamine (v/v)	NA	291	0.5	9.14	LOD 1 ng/mL and LOQ 10 ng/mL	Oxprenolol

4.3 Aim and objectives

4.3.1 Aim

This chapter aims to develop and validate HPLC methods for detection and quantification IND and PRH independently.

The objectives were as follow for both IND and PRH

4.3.2 Objectives

- To validate the HPLC method according to International Conference of Harmonization (ICH) guidelines
- To determine the accuracy, precision (inter and intraday precision)
- To detect the specificity, linearity, and range
- To examine the robustness of the method to be applied for the formulations

4.4 Experimental

4.4.1 Materials

IND and PRH were purchased from Tokyo Chemical Industry (Japan). Acetic acid glacial (ACS, Reag. Ph. Eur., VWR International, France), acetonitrile (HPLC – grade, VWR International, France) and methanol (VWR chemicals, France) and disodium hydrogen phosphate (Alfa Aesar, Great Britain) were used for the isocratic HPLC analysis to prepare mobile phases. Sodium hydroxide (Fischer Scientific, UK) and hydrochloric acid (VWR chemicals, France) were used to adjust the pH of the buffer.

4.4.2 Methods

Method development and validation for IND and PRH were achieved independently using HPLC (Agilent technologies II, USA) and Lab Software (Agilent OpenLab CDS, Agilent, USA) to analyse the obtained chromatograms. All samples were analysed using the column type 00F-4420-E0 HyperClone™ 5µm, BDS C18 130A° of dimensions 150 x 4.6 mm (Phenomenex, USA). The flow rate was set at 1 mL/min using 20 µL of sample volume to be injected. The validation of IND and PRH was in harmony with the ICH guideline, Q2 (R1), namely, accuracy, precision (inter and intraday precision), specificity, linearity, and range. HPLC analysis was set before running the samples and operated at room temperature. Ultraviolet-visible spectroscopy (UV) (Cary 100 Bio, United States) IND and PRH (10 µg mL⁻¹) concentration showed maximum absorbance at lambda max 248 nm and 291 nm, respectively.

4.4.2.1 HPLC method development of IND

The mobile phase of 0.1 M acetic acid and acetonitrile at a ratio of 30:70 (v/v) ratio was used to develop the IND method. The method was adapted by modifying parameters, namely mobile phase composition and retention time Elshaer et al. reported method (Table 4.4).

4.4.2.1.1 Column selection

Three columns were trialled for separation of IND, (HPLCing) column (1) xTera™ reversed-phase C₁₈ (4.6 mm x 100 mm, 3.5 μm) (Water, UK), column (2) Prodigy™ reversed Phase C₁₈ (4.6 mm x 250 mm, 5 μm) (Phenomenex, USA) , and column (3) HyperClone™ reversed-phase C₁₈ (4.6 mm x 150 mm, 5 μm) (Appendix Table 10.2). Column 1 was not considered sufficient as the analyte peak eluted before the solvent peak, indicating poor retention. Column 2 and column 3 displayed good analyte peaks. However, column 3 was selected as it demonstrated results superior to the other (column 2). Hence, tailing was detected with column 2 owing to the free OH-group in column 2, while deactivated OH-groups in column 3 reduced the peak tailing (Lesellier and Tchaplal, 2005).

4.4.2.1.2 Mobile phase

The literature has shown methods that have previously quantified IND using acetonitrile and acetic acid mobile phases. These mobile phases were trialled and adapted to develop a novel method. Mobile phase compositions trialled include 0.1 M acetic acid and acetonitrile at a ratio of 60:40, 55:45, 40:60 and 30:70 v/v. The mobile phase selected was 30:70 (v/v) of acetic acid (0.1 M) and acetonitrile, as it was most suitable with the selected stationary phase and displayed a good peak shape and height.

4.4.2.1.3 Wavelength selection

The maximum absorbance of IND was determined using UV analysis. The lambda max obtained was 248 nm. On the HPLC, the wavelength trialled were 235 nm, 320 nm, and 248 nm. The maximum absorbance was associated with 248 nm and gave the best detection of the analyte with good peak shape and peak height.

4.4.2.1.4 Flow rate

In the literature, 1 mL/min was the most frequently used flowrate. Thus, 0.8 mL/min, 1 mL/min and 1.2 mL/min were trialled. There was no difference between the three flow rates apart from retention time. Therefore 1 mL/min was selected.

4.4.2.1.5 Injection volume

The injection volume is an important parameter to investigate as the aim is to find a volume that gives good detection without overloading and blocking the column. Injection volumes trialled were 5, 10 and 20 μL (Pai and Sawant, 2017)(Assali *et al.*, 2020). The suitable injection volume 20 μL was selected, providing suitable volumes to load onto the column showing narrow peaks. Hence, optimal injection volumes are related to the column cross-sectional area ($A=\pi r^2$) and length (Bakalyar *et al.*, 1997).

Table 4.4 Analytical method parameters for IND

Parameters Investigated	Method Characteristics
Column	C ₁₈ of dimensions 150 x 4.6 mm, 5 μm (Phenomenex, USA)
Mobile Phase	0.1 M acetic acid and acetonitrile at a ratio of 30:70 (v/v)
Wavelength	248 nm
Injection Volume	20 μL
Flow rate	1 mL/min

4.4.2.2 HPLC method development of PRH

On the other hand, the used mobile phase for PRH analysis composed of 50:35:15 (v/v) of acetonitrile, methanol and 0.01M disodium hydrogen phosphate of pH 3.5, which was adjusted by hydrochloric acid and sodium hydrochloride adapted mobile phase ratio from a reported method (Aqil *et al.*, 2013)(Elshaer, Hanson and Mohammed, 2014). Before use, the mobile phase was degassed for 20 min and filtered (0.45 μm , Millipore, UK). The column was conditioned with acetonitrile (HPLC

grade) 100% (v) for 30 min, and the system was purged before and post-analysis. The selected parameters were optimised to develop a novel method, as in Table 4.5.

4.4.2.2.1 Column selection

Two columns were trialled for separation of PRH, including column (1) Prodigy™ reversed Phase C₁₈ (4.6 mm x 250 mm, 5 µm) (Phenomenex, USA), and column (2) Hyper Clone™ reversed-phase C₁₈ (4.6 mm x 150 mm, 5µm) (Appendix Table 10.2). It was found that the analyte peak eluted before the solvent peak showing poor retention with Column 1, and the column stabilisation was required for a longer time comparatively (Lesellier and Tchaplá, 2005). Column C₁₈ (150 x 4.6 mm, 5 µm) (Phenomenex, USA) displayed narrow analyte peaks with no tailing and demonstrated results enhanced to the other column. These columns were trialled and adapted to develop a novel method.

4.4.2.2.2 Mobile phase

According to the reported studies that have analysed PRH, the commonly used mobile phase composition was for PRH analysis composed acetonitrile, methanol, and buffer pH 3.5. Different ratios of mobile phase were tried to provide good resolution peak and system suitability. Mobile phase compositions include 30:55:15, 60:30:10, 50:35:15 v/v. The mobile phase 50:35:15 (v/v) of acetonitrile, methanol and 0.01M disodium hydrogen phosphate (pH 3.5) was the most suitable ratio with the used stationary phase displaying a good peak shape and height.

4.4.2.2.3 Wavelength selection

PRH absorbance was determined using UV analysis. The lambda max obtained was 291 nm. On the other hand, using HPLC, the wavelength trialled were 250 nm, 214 nm, and 291 nm. The wavelength 291 nm gave the best detection of the analyte showing good peak shape and peak height. Hence, different trialled was performed to develop a novel method using 291 nm selectively for PRH. Also, our preliminary

studies using UV–vis showed that 291 nm wavelength was suitable to detect PRH (Appendix-Figure 10.6& Table 10.3 and Table 10.4).

4.4.2.2.4 Flow rate

According to the reported studies, the most commonly used flow rate was 1 mL/min. However, 0.8 mL/min, 1 mL/min and 1.2 mL/min were trialled to choose the appropriate flow rate. The three flow rates showed similar peak resolution except for retention time; therefore, a 1 mL/min flow rate was selected.

4.4.2.2.5 Injection volume

Selecting a suitable injection volume is critical to consider during HPLC analysis to provide peak detection without overloading and blocking the column. Injection volumes trialled were 10, 20, 25 µL. The injection volume 20 µL was selected that provided suitable volumes to prevent overlading the column showing narrow peaks. Hence, larger injection volumes may be acceptable depending on the peaks shape and the column dimensions. For instance, if the peak showed broadening, so the volume is too large. The ideal injection volumes can be calculated depending on the column cross-sectional area ($A=\pi r^2$) and length (Bakalyar *et al.*, 1997). In general, with the used column dimensions, 20 µL is a widely used injection volume.

Table 4.5 Analytical method parameters for PRH

Parameters Investigated	Method Characteristics
Column	C ₁₈ of dimensions 150 x 4.6 mm, 5 µm (Phenomenex, USA)
Mobile Phase	50:35:15 (v/v) of acetonitrile, methanol and 0.01M disodium hydrogen phosphate of pH 3.5
Wavelength	291 nm
Injection Volume	20 µL
Flow rate	1 mL/min

4.5 Method validation

4.5.1 Standard solutions

Standard stock solutions of IND and PRH were freshly prepared every day during the analysis to construct and validate the calibration curve. All the standard solutions were prepared daily before the HPLC analysis. Three volumetric flasks of 10 mL were prepared of each standard solution and collected to construct the calibration curve.

4.5.2 Preparation of IND standard solutions

The stock solution was prepared by accurately weighing IND powder equivalent to 100 mg and poured into 100 mL volumetric flask of the mobile phase sonicated until completely dissolving the solid. From the IND stock solution, samples were diluted accurately with mobile phase to prepare calibration curve concentrations 1, 5, 10, 20, 30, 40, 50, 100 µg/mL of IND using 10 mL volumetric flasks for each. Each of these concentrations was prepared in three different vials to detect linearity and range. Measurements were run in triplicate for each concentration, and the chromatograms were collected to construct the calibration curve.

4.5.3 Preparation of PRH standard solutions

A standard stock solution of PRH with 1000 µg/mL concentration was prepared by collecting 50 mg of PRH powder in a 50 mL volumetric flask, then diluted with the mobile phase until achieving the required volume of complete solubility. The calibration curve was constructed by preparing serial dilutions of 1, 5, 10, 20, 30, 40 µg/mL using the stock solution. Each of these concentrations was prepared three times. The collected data were used to construct the calibration curve and validate the HPLC method.

4.5.4 Validation

The validation is an analytical procedure to determine if the developed method is suitable for its intended aim, such as detecting and/or quantifying the drug in the

formulations. The quality control samples with ranges of 80, 100, 120% (concerning the theoretical drug concentration) were prepared and used for validating the method (n=9). The validation was achieved following the ICH guideline and using the following procedure:

4.5.5 Linearity and range

The linearity was achieved through constructing the calibration curve using the collected data (chromatograms), which is directly related to the effective concentration of the drug. The method demonstrated linearity in the range of 1- 100 µg/mL and 1- 40 µg/mL for IND and PRH, respectively.

4.5.6 Specificity

The specificity was investigated by detecting the excipients used in the mobile phase and analysed using the developed method. The range, which refers to the interval between drug concentrations (upper to lower concentrations), was consequential to obtain an acceptable level of precision, accuracy, and linearity. The detected values should be within the range +/-20 % of the reference value.

4.5.7 Accuracy

The accuracy study was detected by measuring the closeness of the experimental concentrations of the drug to the true or actual value.

Accuracy was evaluated by preparing three fresh quality control samples daily: low, intermediate, and high (over three consecutive days). The samples were within the drug concentrations range 1 – 100 for IND µg/mL and 1 – 40 µg/mL for PRH. Each of the samples was prepared daily and analysed (n=6). The percentage error and %recovery was determined from all the samples. The three concentrations were selected to cover the quantity of the drug in the formulation. Therefore, IND contractions were 1, 3, 5 µg/mL and PRH contractions were 1 6, 20 and 24 µg/mL.

4.5.8 Precision

Precision refers to the closeness of each sample measurement from other samples values. The precision was presented by reproducibility, intermediate precision, and repeatability (ICH expert working group, 1995). Similarly, the inter-day precision was performed using the allocated concentrations of freshly prepared samples for the three consecutive days (n=6+6+6). The chromatograms were used to work out the concentrations of the samples by applying the values of the peak area in the linear equation of the constructed calibration curve. Reproducibility was assessed by comparing all the results over 3 consecutive days (inter-day) and running one of the quality controls samples after one month.

4.5.9 Robustness

According to ICH, robustness can be defined as the capability of a scientific or investigative method to withstand any small and deliberate changes in the method's parameters (Swartz and Krull, 2012).

This was performed by changing the mobile phase composition ($\pm 3\%$ v/v) and flow rate (± 0.1 mL/min) for IND. On the other hand, PRH robustness was achieved by changing two parameters: the mobile phase composition buffer to methanol ratio ($\pm 5\%$) and the flow rate (± 0.1 mL min⁻¹).

4.5.10 Detection Limit (LOD) and Quantitation Limit (LOQ)

LOD is defined as the minimum concentration of the drug in the samples that can be perceived. While the minimum quantified concentration of the drug can be identified by calculating the LOQ (Swartz and Krull, 2012). The LOD and LOQ values were identified from the standard calibration curves based on the standard deviation formula. LOD (Equation 4-1) and LOQ (Equation 4-2) were identified using the calibration curve points (n=6) by applying the values in the following equations:

$$LOD = (3.3\sigma/s) \quad \text{Equation 4-1}$$

$$LOQ = (10\sigma/s) \quad \text{Equation 4-2}$$

σ is the standard deviation of the response, s is the regression line slope (ICH expert working group, 1995).

4.6 Statistical analysis

Statistical analysis for HPLC method development and validation was achieved using standard deviation (SD), relative standard deviation (%RSD), %recovery, %relative error, t-Test with $P < 0.05$ for significance and regression of analysis of variance using Microsoft Excel.

4.7 Results and discussion

A valid method was required to detect and quantify drug concentration from the prepared tablets comprising IND or PRH in different dissolution media. The validated method was in accordance with the validation specifications and parameters set in the ICH since it details the validation of investigative methods. The parameters used for validation studies include linearity, range, specificity, accuracy, and precision and LOD & LOQ.

4.7.1 Method validation and optimisation of IND

4.7.1.1 Linearity and range

The calibration concentrations 1, 5, 10, 20, 30, 40, 50, 100 mg/mL of IND was used to develop an isocratic HPLC method for IND detection and quantification. This was to easily apply the equation to quantify a wide range of drug concentrations in the prepared formulations. The samples were run for 4 mins using the indicated mobile phase and reversed phase C₁₈ column, at room temperature 25 ± 0.5 °C. Linearity and range were detected using the collected samples, and they showed a high linearity relationship R²= 0.9994. Measurements were run in triplicate for each concentration to construct the calibration curve as in Figure 4.1 .

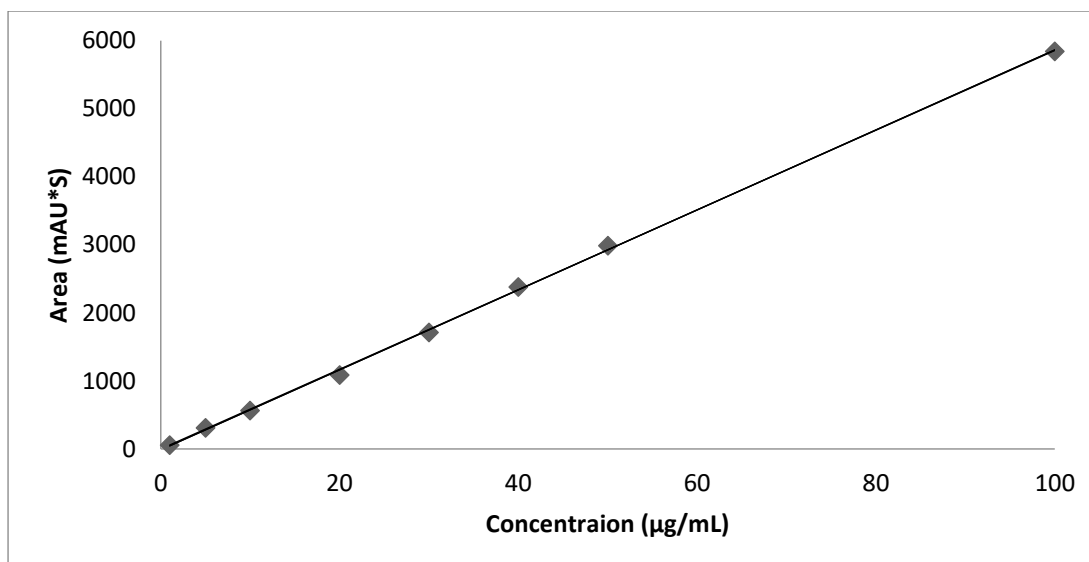


Figure 4.1 IND calibration curve showing the linearity $R^2 = 0.9994$ for all concentrations range with linear curve equation $y=58.778x-13.524$

4.7.1.2 Specificity and accuracy

The specificity was applied to detect the method's accuracy to quantify and detect drug peak with no interference from other excipients. As presented in Figure 4.2, samples showed the peaks for the solvent with no interfering with IND, whereas the IND chromatogram in Figure 4.3 demonstrated a sharp peak with no tailing for the drug and no interference with its absorbance.

The method's accuracy can also be observed for the theoretical concentration of IND 5 µg/mL as demonstrated in Figure 4.3, and the calculated concentration was worked out using the LabSolutions software within 2.39 - 2.4 min retention time.

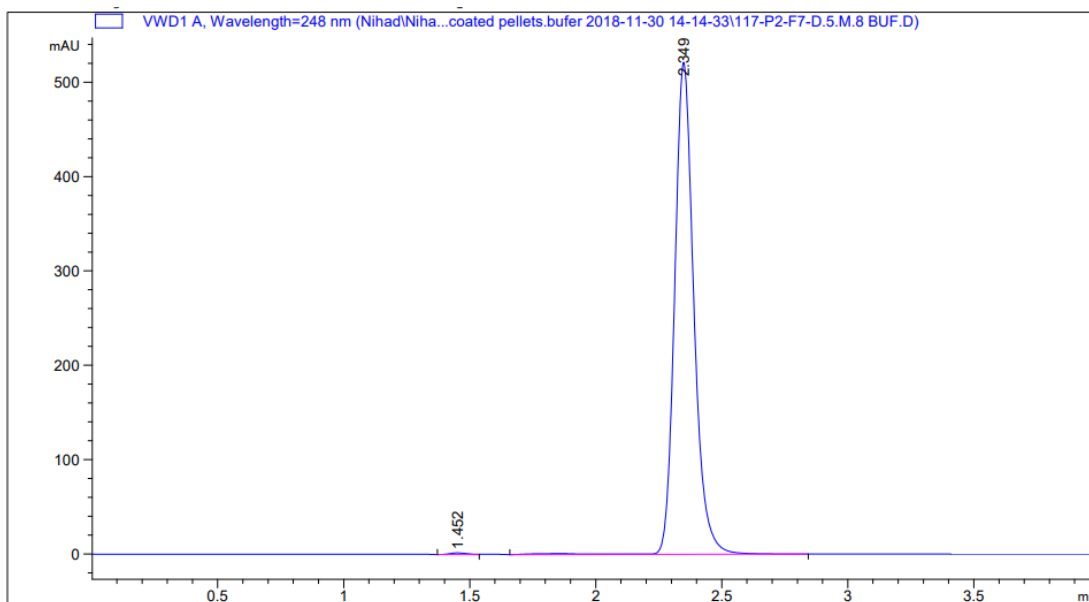
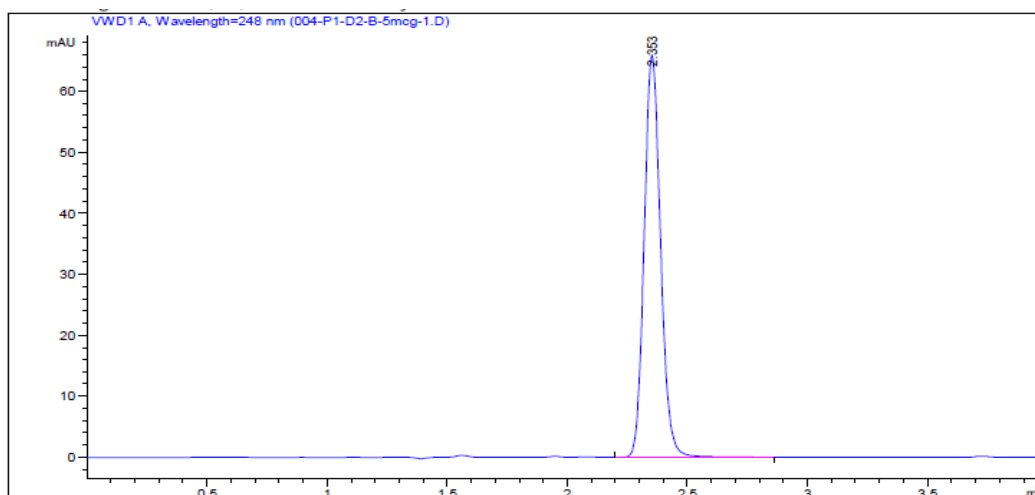


Figure 4.2 Excipients and drug as showing the specificity of the method for IND pellets



```

=====
                          Area Percent Report
=====

Sorted By      :      Signal
Multiplier     :      1.0000
Dilution       :      1.0000
Use Multiplier & Dilution Factor with ISTDs

Signal 1: VWD1 A, Wavelength=248 nm

Peak RetTime Type Width Area Height Area
# [min] [min] [min] [mAU*s] [mAU] %
-----|-----|-----|-----|-----|-----
  1  2.353 BB  0.0732  312.25214  65.97144 100.0000

Totals :                312.25214  65.97144

=====
                          *** End of Report ***
=====

```

Figure 4.3 One of the quality control concentrations 5 µg/mL showing high peak sharpness and detection specificity for IND with no interference

4.7.1.3 Accuracy and precision

The calculated concentration (C.C) was detected according to the calibration curve equation related to theoretical concentration (T.C). The freshly prepared samples of each quality control point were tested (n=6) according to the ICH guideline. The results demonstrated good accuracy, intraday & inter-day precision (Table 4.6 and Table 4.7). The results of the quality control point low, medium, and high concentrations (1, 3 and 5 µg/mL) showed that %recovery was between 89.20 - 99.89, indicating the acceptable range 80-120% according to ICH guideline. Although %relative error was 8.7% for low-quality control (1 µg/mL), this could be expected with low concentrations (United Nations Office on Drugs and Crime (UNODC), 2009). In addition, the results showed a %relative error for 3 and 5 µg/mL less than 2%, indicating the high accuracy of the method (Table 4.6) (EMA, 2009). On the other hand, good system precision was obtained as intra-day precision demonstrated %RSD ranged between 0.24% – 1.24% (Table 6) and inter-day precision obtained ranged between %RSD 0.95% - 2.07% over three consecutive days (Table 4.7).

According to ICH guideline, the intra and inter-day precision were within acceptance criteria as %RSD should not exceed 5%. Moreover, further analysis for three quality control samples 15, 35 and 45 µg/mL was performed to confirm the method accuracy and precision, which confirmed the low %relative error and %RSD for the reported data (Appendix Table 10.5 & Table 10.6). Also, one of the calibration samples, 100 µg/mL were tested after 1 year after storing the sample under cold condition 5-8°C. The results showed that %RSD was less than 1%, and %recovery was within the acceptable range (80 - 120%), showing method reproducibility (Appendix

Table 10.8 and Figure 10.7).

Table 4.6 Accuracy and Intraday precision parameters for IND according to the proposed HPLC method (n=6) showing the theoretical concentration (T.C) and calculated concentration (C.C)

T.C µg/mL	C.C µg/mL Mean± SD	%Relative error	%RSD	%Recovery
1	0.91 ± 0.01	8.70	1.24	91.30
3	3.04 ± 0.01	1.43	0.31	101.43
5	4.99 ± 0.01	0.18	0.24	99.82

Table 4.7 Inter-day precision of IND HPLC method (n=6+6+6) represented by Mean ± SD, %RSD, and %Recovery

T.C µg/mL	Day1	Day2	Day3	C.C µg/mL Mean± SD	%RSD	%Recovery
1	0.88	0.88	0.91	0.89 ± 0.02	2.07	89.20
3	2.98	2.97	3.04	3.00 ± 0.04	1.17	99.89
5	4.93	4.88	4.99	4.94 ± 0.05	0.96	98.73

4.7.1.4 Robustness

The robustness of the proposed method was detected by testing minor changes in the method parameters; the mobile phase composition (0.1 M acetic acid and acetonitrile at a ratio of 30:70 (v/v)) flow rate (± 0.3 mL/min) were applied while running 3 µg/mL IND sample. The results demonstrated that the IND method was robust and applicable to different conditions. The sample was run six times to demonstrate the rigidity, as in Table 4.8.

The deliberate changes displayed no significant difference in peak shape and peak area. %Recovery was within the acceptable range between 91.13 – 106.33% with an acceptable range of %RSD between 0.22 - 0.78%. According to the robustness study, the slight change in method parameters showed that the method could optimally be performed. Moreover, the method robustness was detected by testing one of

additional quality control 45 µg/mL (n=3) using deliberate change in the wavelength (± 4) and fixing other conditions (mobile phase and flow rate). The results demonstrated low %RSD as 0.08% and 97.93% of %recovery and 2.336 min retention time (Appendix Table 10.7).

Table 4.8 Robustness testing for the proposed HPLC method for IND of one of the quality controls points 3 µg/mL concentration (n=6)

Parameters	Ratio	Retention time	C.C µg/mL Mean \pm SD	%RSD	%Recovery
Acetonitrile ratio ($\pm 3\%$ v/v)	73:27	2.20	2.99 \pm 0.01	0.22	99.59
	67:33	2.49	2.99 \pm 0.02	0.30	99.56
Flow rate (± 0.1 mL/min)	1.1	2.12	2.73 \pm 0.02	0.78	91.13
	0.9	2.60	3.19 \pm 0.02	0.52	106.33

4.7.1.5 LOD and LOQ identification

Detection limits LOD and LOQ were extrapolated from the presented results of the IND HPLC method. The results were obtained by calculating the values according to the ICH guidelines using the indicated equations depending on the regression line of the calibration curve (n=6). It was found that LOD and LOQ values were 0.312 µg/mL and 0.947 µg/mL, respectively. The LOD and LOQ were lower than the lowest concentration in the calibration curve. Therefore, the method can detect and quantify IND in a low amount in the prepared formulations.

4.7.2 Method validation and optimisation of PRH

4.7.2.1 Linearity and range

The calibration curve was constructed using six concentrations of 1, 5, 10, 20, 30, and 40 µg/mL for PRH detection and quantification. Samples were run for 4 mins using the indicated mobile and reversed phase C18 column at temperature $25 \pm 0.5^\circ\text{C}$. The relationship between the concentrations of PRH samples and the peak areas was

linear for the range 1 – 40 µg/mL. The results demonstrated a good regression coefficient (R^2) = 0.997. The analysis of six concentrations, triplicate run for each sample, was used to attain calibration curve equation as shown in Figure 4.4. The chromatograms of the standard concentrations with retention time 1.9 - 2 mins were attained, demonstrating a good range and suitability of the equation.

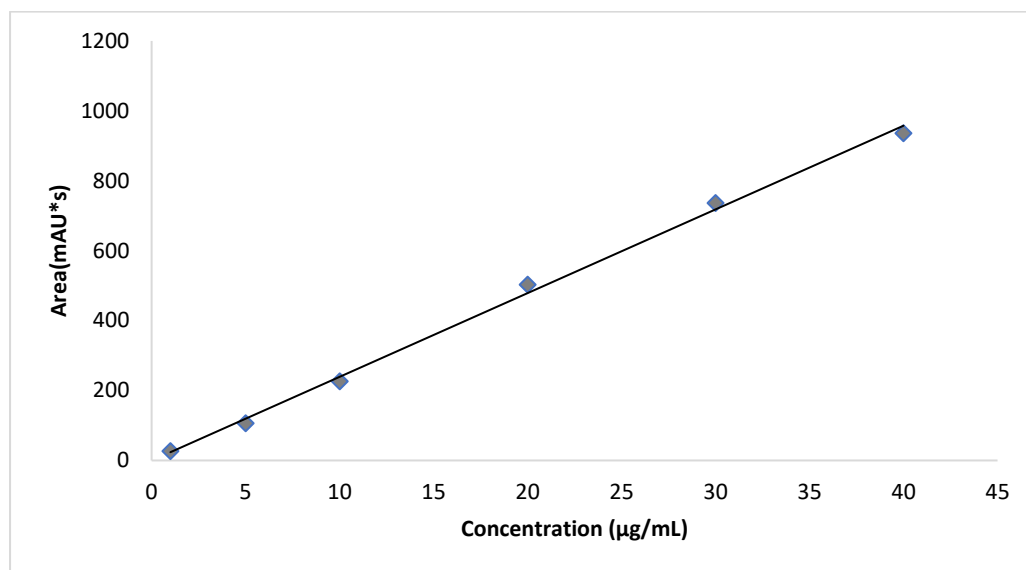


Figure 4.4 Calibration curve of PRH 1 – 40 µg/mL showing linearity $R^2 = 0.9974$ and equation $y = 23.945x - 0.2463$

4.7.2.2 Specificity and accuracy

The method specificity was determined using blank samples consist of the formulation excipients. This is essential to identify any interference with PRH peak during quantification and detection studies. The spiked samples showed no interference with PRH retention time and the suitability of the mobile phase of the HPLC method, as in Figure 4.5. Also, the chromatogram of PRH in Figure 4.6 demonstrated a sharp peak for 20 µg/mL with no tailing other chromatograms of low concentrations (e.g., 1 µg/mL) illustrated a consistent result (Appendix Figure 10.8). This was performed confirming the specific detection for PRH in the formulation with no interference with its absorbance. Therefore, the method demonstrated a distinct optimal peak from analyte and impurities.

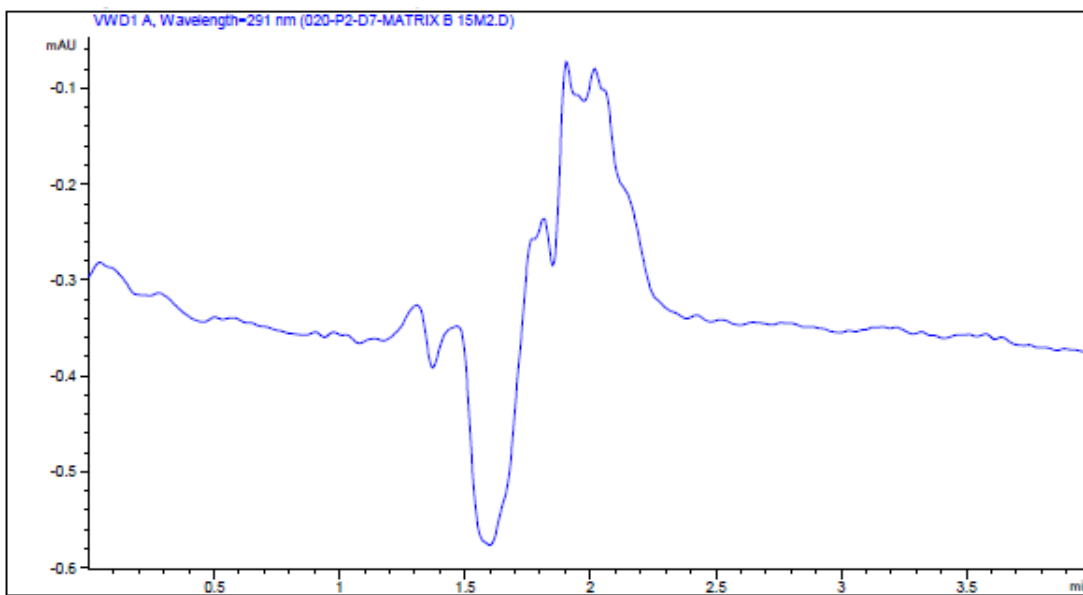


Figure 4.5 Matrix of the used excipients in PRH formulations in blank samples using mobile phase as a solvent

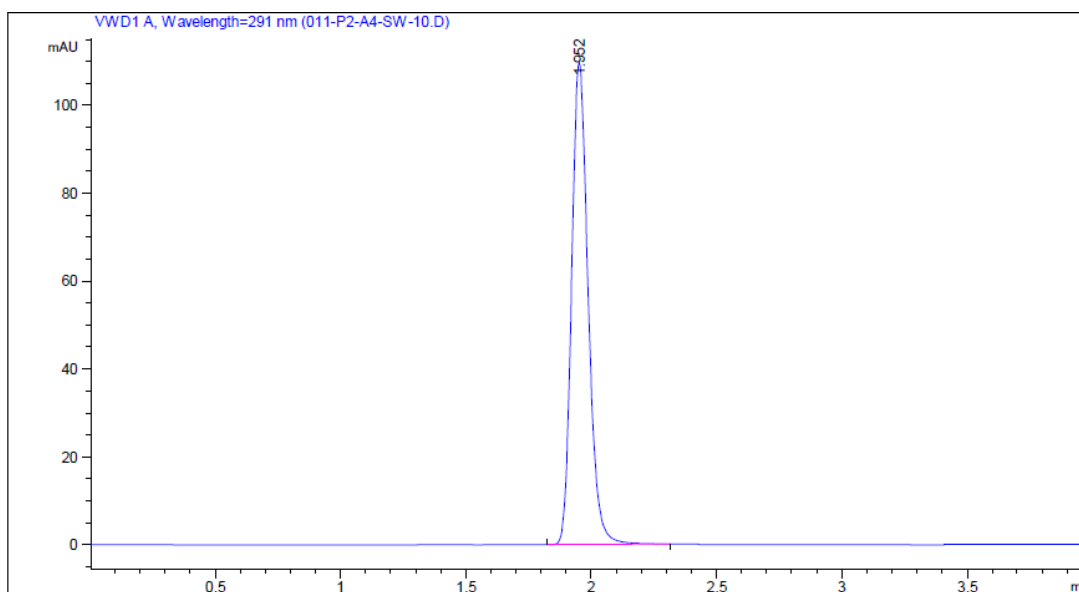


Figure 4.6 Chromatogram of PRH with 20 µg/mL showing a sharp peak with 1.952 min retention time

4.7.2.3 Accuracy and precision

Three quality control concentrations 16, 20 and 24 µg/mL (n=6) were run to assess the accuracy of the HPLC method. The fresh samples were prepared from the stock solution for three days consecutively and used to perform repeatability, inter-day

precision and accuracy on each day. According to the ICH guideline, the accuracy parameter was described as %relative error, %recovery and %RSD. The results showed high accuracy as %relative error was low lower than 5%, indicating the low difference between the T.C and C.C values (Table 4.9) (Cheng, Huang and He, 2007). Moreover, the acceptable range of %RSD between 0.26% – 0.91% was obtained for all determinations indicating a high precision (intra-day) as in Table 9.

On the other hand, inter-day precision for the PRH method showed good %Recovery within 80-120% (Table 4.10). Although the values obtained from the inter-day study demonstrated %RSD higher than %RSD of intraday precision, the range was acceptable because such differences could occur due to laboratory conditions on different days (Barwick, 1999, United Nations Office). Moreover, %relative error was lower than 1.66% for all the values. Therefore, %RSD ranging between 1.27-5.18% can be acceptable.

In addition, method reproducibility was also assessed by testing one of the calibration curve points 10 µg/mL of the calibration curve points on another Agilent HPLC instrument applying the same conditions (temperature, wavelength, and mobile phase) and same column C₁₈ (Appendix Table 10.9). According to ICH guidelines, %RSD (0.55%) and %Recovery (94.63%) data were within the acceptable range. The obtained data showed no significant difference compared to the old results using t-Test ($p>0.05$).

Table 4.9 Results of accuracy and intraday precision of PRH HPLC method (n=6), showing T.C and C.C relationship

T.C µg/mL	C.C µg/mL Mean ±SD	%RSD	%Relative error	%Recovery
16	16.09 ± 0.05	0.32	0.54	100.54
20	19.53 ± 0.05	0.26	2.33	97.67
24	23.49 ± 0.21	0.91	2.13	97.87

Table 4.10 Inter day precision showing T.C and C.C analysis according to PRH HPLC method (n=6+6+6)

T.C µg/mL	Day1	Day2	Day3	C.C µg/mL Mean ± SD	%RSD	%Recovery
16	16.49	16.09	16.22	16.27 ± 0.20	1.27	101.66
20	21.49	19.53	19.84	20.29 ± 1.05	5.18	101.44
24	25.18	23.49	23.34	24.01 ± 1.02	4.26	100.02

4.7.2.4 Robustness

Robustness was performed by deliberately changing two parameters, the mobile phase ratios ± 5 % of methanol and dipotassium hydrogen phosphate with a constant ratio of acetonitrile to see the effect of different ratio on the method robustness. Also, flow rate ± 0.1 was used to examine the robustness of the PRH validated method. The method showed good robustness with an undetectable effect on the quality control point 20 µg/mL of PRH. The obtained results of %RSD (0.09% – 1.17%) and %recovery (102.35 - 99.24) indicated that all values within the acceptable range (80-120%) with low SD as in Table 4.11. This was clearly detected in the chromatogram of 20 µg/mL of PRH demonstrating a sharp peak at mobile phase ratio of 50:30:20 of acetonitrile, methanol, and buffer, respectively (Appendix -Figure 10.9).

Table 4.11 Robustness of HPLC method of PRH showing mobile phase ratio and flow rate effect on 20 µg/mL concentration

Parameters	Ratio	Retention time	C.C µg/mL Mean ± SD	%RSD	%Recovery
Mobile phase (± 5% v/v)	50:30:20	1.869	19.85 ± 0.16	0.78	99.24
	50:40:10	2.035	20.47 ± 0.02	0.09	102.35
Flow rate (± 0.1 mL/min)	1.1	1.922	20.50 ± 0.24	1.17	102.52
	0.9	2.167	22.79 ± 0.20	0.89	113.93

4.7.2.5 LOD and LOQ identification

Detection and quantification of the lower limits within the HPLC method were performed, calculating LOD and LOQ of PRH (n=6). The results were obtained according to the ICH guideline equation indicated in the method. It was noticed that LOD was 0.324 µg/mL and LOQ was 0.982 µg/mL, showing the method's efficiency to detect very low drug concentration. The limit of detection and quantification should be lower than the lowest concentration of the calibration curve. According to the experimental trials, increasing the number of samples provided enhanced results with higher detection and low error. This could be related to minimising error that generates owing to the system or human error in pipetting (Kuselman and Pennechi, 2016). Therefore, this was considered with calculating LOD and LOQ.

Both validated methods were applied to quantify and detect IND and PRH release individually in all the prepared formulations comprising each drug (Appendix- Figure 10.10).

4.8 Conclusion

In summary, two accurate and reliable HPLC methods were developed to detect and quantify IND and PRH HPLC. The methods were validated according to ICH guidelines. IND intra-day precision showed raised % relative error, and similarly, %RSD in the inter-day precision of PRH. The limits are still acceptable (Barwick, 1999; EMEA, 2009; United Nations Office on Drugs and Crime (UNODC), 2009). This was confirmed by method robustness results showing low %RSD with the deliberate changes. The LOD and LOQ values were calculated in the dissolution release studies despite no indication in the ICH guideline. The values were lower than the lowest points on the calibration curves. The validated method for both IND and PRH was successfully applied to quantify drug in the formulations with no interference.

Chapter 5 Delaying of indomethacin release through pH-dependent polymeric microparticles embedded in the orally disintegrating tablets

Scoop of the study

The use of analgesic pharmaceutical ingredients has severe side effects. A better drug delivery system is provided to mitigate this challenge by using orally disintegrating tablets (ODT) combined with a multiparticulate system, such as microparticles. ODTs, which dissolve rapidly in the mouth, contain microparticles of a pH-dependent polymer to reduce indomethacin's gastric side effects. These microparticles are designed and developed through the implementation of the spray-drying method. Eight batches of Eudragit L100 based indomethacin microparticles were prepared and characterised to examine the effect of different spray-drying parameters: temperature, aspiration, and solvent type on the indomethacin (IND) release profile. The obtained batches using acetone and methanol solvents showed a consistent delayed-release indomethacin profile in the acidic media and immediate release in intestinal pH media. The batches prepared by ethanol showed inconsistent drug release compared to other batches.

Keywords: ODTs, Eudragit L100, microparticles, IND

5.1 Introduction

5.1.1 Microparticles and ODTs combination

Combining ODTs with a multiparticulate drug delivery system (microparticles, nanoparticles and pellets, etc.) is of great interest in developing optimized formulations with the advantages of both ODTs and microparticles. The multiparticulate systems promote different benefits in both clinical and industrial areas. These advantages include reducing side effects and local irritation from immediate drug release formulations and frequent drug dosing requirements, leading to improved patient compliance (Nadal *et al.*, 2016).

The microparticles (size range 1–1000 μm) are widely used multiparticulate that offer further advantages, including unpleasant taste masking, enhancing the drug's targeting effect and modifying the drug release. The method of microparticle preparation and the use of specific polymers and excipients needs to be considered to achieve the desired modified drug release formulation (Lengyel *et al.*, 2019).

Hence, polymers and excipients keep the active pharmaceutical ingredient (API) protected from the environment of the gastrointestinal tract (GIT) (Santos *et al.*, 2018). Different techniques to prepare microparticles include spray drying, emulsion-based methods, and solvent evaporation (Lassalle and Ferreira, 2007). The selection of the method depends on several factors, including method reproducibility, cost, and time efficiency.

Spray drying is a commonly used multistep process to produce microparticles (Lassalle and Ferreira, 2007). This method is suitable for hydrophobic and hydrophilic active compounds and heat-sensitive materials due to rapid drying and relatively short exposure to heat (Santos *et al.*, 2018) (Sosnik and K. Seremeta, 2015). The process produces a dry powder from dissolving dry ingredients in a suitable solvent system. The produced solution is then atomized into a hot drying gas/air environment (chamber). The product is usually of narrow size distribution, and homogeneous shaped particles are formed (Santos *et al.*, 2018) (Sosnik and K. Seremeta, 2015). On the other hand, the spray-drying technique has proven useful in developing ODTs on a massive scale. The method is fully automated and quick, allowing it to be applied on an industrial scale (Lou *et al.*, 2014).

Spray drying process is widely used in the food and pharmaceutical industry. This process involves continued drying energy within the hot gas flow leading to the atomisation of the liquid (solvent, active ingredients and excipients) and the production of micro or nanoparticles of uniform sizes within a short time (Wang, Dufour and Zhou, 2015)(Santos *et al.*, 2018). The main principle of the method is the dissolving of active ingredients and other excipients in a suitable solvent (aqueous or organic). Then the obtained feed (solution, gel, or suspension) is scattered by the atomiser nozzle into fine droplets with high temperature and high air pressure using a temperature higher than the solvent's boiling temperature. During the spray drying process, conversion of the molecular arrangement can occur, i.e. crystalline to amorphous state (Singh and Van den Mooter, 2016). Hence, the produced droplets are rapidly dried and collected as fine dried particles. The droplets diameters and ultimately physical properties of the produced particles vary depending on different factors, including inlet temperature, feed solution viscosity and pressure of the airflow (Ohshima and Makino, 2014)(Wang, Dufour and Zhou, 2015)(Santos *et al.*, 2018).

Microencapsulation via spray-drying technique is a modern method for compliant and non-compliant patients. According to Li *et al.*, perfecting microencapsulation would help control drug release rate, allowing the drug components to be released at the right time consistently with minimum bitterness. Further, the authors indicated that recent trends in microencapsulation have led to the development of a "novel nanoparticles-in-microparticles system" (NIMS) that continues to produce satisfying results based on entrapping a pharmaceutical drug particle, encapsulating its bitter elements, and releasing them at the right moment. However, insufficient literature further explores this system, thus inhibiting its approach and implementation to inform the general medical profession (Li *et al.*, 2011).

Generally, different polymeric systems are applied according to the type of the drug and its side effects. Li *et al.* note that chitosan, a polysaccharide, has been extensively used to develop drug delivery systems. The authors further indicate that additional studies have shown tremendous progress with incorporating chitosan in NIMS to increase drug release efficiency (Li *et al.*, 2011). These studies promise better results, with future improvements opening the doors to further research and experimentation as scientists continue to explore polymers and their different applications in ODTs, controlled drug release rates, modern taste-masking techniques, and drug delivery

systems to mitigate the side effects of the pharmaceutical materials (Bankars et al., 2014).

Our model drug IND is a widely used nonsteroidal anti-inflammatory drug to treat the pain and symptoms of joints swelling and stiffness caused by arthritis and gout (Ikawa *et al.*, 2012; Emam Kassab, 2019). However, IND side effects of gastric irritation, especially for elderly patients, limited its use (Goldstein and Cryer, 2014). Therefore, delaying IND release to bypass the stomach is an integral approach to minimize gastric disturbance.

5.1.2 Overview of of spray drying parameter settings

The original material properties can determine the applied spray drying parameters. Also, the quality of the collected particles using the spray drying technique is strongly associated with the instrumental settings. Himmetagaoglu and Erbay (2019) noticed that applying an aspiration rate of 75% improved the final product's physical properties (Himmetagaoglu and Erbay, 2019).

In our study, using different solvents was essential to produce particles with uniform size and mechanical attributes. Hence, solvent viscosity and volatility can determine the feed solution's quality (Shepard et al., 2020) (Esposito et al., 2000). Therefore, three solvents were used, methanol, acetone, and ethanol, as these are the most used solvents to prepare Eudragit L100 based microparticles. For instance, Shepard et al. used acetone and methanol as a solvent, while Esposito et al. used ethanol and methanol (Shepard et al., 2020)(Esposito et al., 2000).

Moreover, the settings parameters including inlet temperature, aspiration rate and feed concentration could influence the final product properties. The inlet temperature is the drying air temperature, which is measured before air flows into the chamber (Büchi, 2002). The temperature is required to be high enough to provide separation with no necessity to be higher than the solvent's boiling point (water or organic fluid). Hence, the solvent is vaporised and removed during spray drying the dispersion or emulsion as the surface to volume ratio would be enough to evaporate the individual drops (Ziaee *et al.*, 2019)(Büchi, 2002). When the dry particles start to enter the cyclone results in an uncontrolled temperature called outlet temperature, this temperature results from the intense heat and mass transfer (Büchi, 2002)(Santos *et al.*, 2018). Hence, the particles can have the same temperature as the gas; as a result, the outlet temperature can be considered product temperature. Therefore, increasing

the inlet temperature can improve the product yield and reducing the particles sticking (Santos *et al.*, 2018)(Büchi, 2002). In addition, the moisture content can increase when the large difference between the inlet and outlet temperature (Büchi, 2020)(Santos *et al.*, 2018).

On the other hand, the aspirator controls the dried gas or air entering the drying chamber under specific pressure conditions. The aspirator speed regulates the amount of heated drying air. Hence, the provided energy for vaporisation is influenced by the quantity of drying air. Therefore, the optimum aspirator setting can be determined experimentally (Büchi, 2002)(Aghbashlo *et al.*, 2012). For instance, the high aspirator speed can increase the separation time in the cyclone and enhance the yield. Also, the low aspiration can affect the final moisture content if the energy provided is enough to dry all the particles (Büchi, 2002)(Santos *et al.*, 2018).

In addition, larger particles can be generated when a high concentration of feed is used. However, keeping certain parameters stable is required when optimising the parameters and examining their effect on the final product properties(Büchi, 2002)(Sosnik and K. P. Seremeta, 2015)(Santos *et al.*, 2018). For instance, increasing the pump speed can reduce the outlet temperature, which may increase the difference between the inlet and outlet temperature, thus increasing the moisture content. Also, at a high aspiration speed, the residence time becomes shorter, yet the time can be not enough to produce a completely dry product; thus, moisture content increases (Büchi, 2002)(Büchi, 2020)(Kojima *et al.*, 2013).

Thus, optimisation of instrumental settings is necessary to investigate any quality error in the product.

5.2 Aim and objectives

5.2.1 Aim

To prepare delayed-release indomethacin (IND) microparticles to be used in orally disintegrating tablets (ODTs)

5.2.2 Objectives

- To prepare spray-dried particles using a pH dependent polymer Eudragit L100
- To study the effect of three different solvents on the spray-dried particles
- To assess the impact of parameters, namely aspiration speed and inlet temperature, on the product quality
- To evaluate IND release from spray-dried indomethacin-Eudragit L100 particles (SD-INDE)

5.3 Experimental

5.3.1 Materials

Listed in the experimental chapter.

5.3.2 Methods

5.3.2.1 Preparation of spray-dried IND-Eudragit L100 particles (SD- INDE)

The physical mixture of IND and Eudragit L100 was dissolved in the same quantity in three different solvents: acetone, methanol, and 97/3% v/v ethanol/water (Table1). Büchi Mini Spray Dryer B-290 (BÜCHI Labortechnik AG, Switzerland) was used to prepare the spray-dried particles (Babenko *et al.*, 2019). Two concentrations of the feed solution were prepared, 10% w/v and 5% w/v for an acetone-based solution and 5% w/v for the methanol and ethanol solutions. The IND concentration was maintained at 5% w/w with respect to the polymer in all batches as in Table 5.1. Two parameters' settings were applied independently; the first had a low inlet temperature of 75°C and a low aspiration speed of 75%. The second had a high inlet temperature at 85°C with a high aspiration speed of 100%. The corresponding outlet temperature ranges 55-63 ± 0.5 °C for low and high parameters, respectively.

Table 5.1 Spray-dried particles of IND and Eudragit L100 using two settings of parameters inlet temperature and aspiration with each of feed concentrations

Formulation	Ratio%	Solvent (100 mL)	Inlet temperature °C	Aspiration
A1	10%	Acetone	75	75
A2	10%	Acetone	85	100
B1	5%	Acetone	75	75
B2	5%	Acetone	85	100
C1	5%	Methanol	75	75
C2	5%	Methanol	85	100
D1	5%	Ethanol: water (9:1)	75	75
D2	5%	Ethanol: water (9:1)	85	100

After different trials, these parameters were applied to optimise the parameters and subsequent comparison to reported studies (Shepard *et al.*, 2020)(Esposito *et al.*, 2000). The other parameters were kept constant during the experiment, including feed

rate at 320 mL/h and the spray gas flow to atomise the feed solution set between 414 and 473 L/h with 5 and 8 bar for out and received pressure.

5.3.2.2 Tablet preparation

The spray dried particles were mixed with ODTs matrices to prepare delayed-release IND multiarticulate embedded in the ODTs. The matrix of ODTs was prepared by using 74% w/w of Lactose monohydrate as a bulking agent, LHPC as a disintegrant in 25% w/w and 1% w/w magnesium stearate as a lubricant during tablet compression. Spray-dried powder of each batch was mixed with ODTs matrices by including 10% w/w (equivalent to 2.5 mg of IND) of the spray-dried powder and 90% w/w of the ODT excipients. A TURBULA® mixer (WAB AG, Switzerland) was utilised to mix the ODTs matrices and the delayed release microparticles at 50 rpm for 10 minutes. Similarly, the control tablets were prepared in the same way with indomethacin added as a powder.

The delayed-release microparticles-ODTs (DRM-ODTs) mixture was weighed to 500 mg per sample and compressed using a manually controlled uniaxial hydraulic press (Specac tablet presser, Slough, UK). The mixture was poured into the die of a barrel to be compressed with a punch of 13 mm size and a one-ton compression force applied for 10 second, which is approximately equal to 75.07 MPa pressure. All tablets were weighed after preparation and confirmed to be 500 mg. Microparticles represented a 10% ratio of the DRM-ODTs.

5.3.2.3 Percentage yield

The batches were tested according to the detailed method in the experimental chapter.

5.3.2.4 Compressibility index

The Flowability of SD-INDE batches was measured to assess the ability of the particles to settle and compress according to the referenced data in Table 5.2. Compressibility index and Hausner ratio were used to assess the powder flow property as explained in the experimental chapter.

Table 5.2 Compressibility index and Hausner ratio references (Kalal *et al.*, 2018)

Compressibility index (%)	Flow character	Hausner ratio
less than or equal to 10	Excellent	1.00-1.11
11-15	Good	1.12-1.18
16-20	Fair	1.19-1.25
21-25	Passable	1.26-1.34
26-31	Poor	1.35-1.45
32-37	Very poor	1.46-1.59
> 38	Very, very poor	> 1.60

5.3.2.5 Bulk density

The bulk density was measured as detailed in the experimental chapter.

5.3.2.6 Flowability

Flowability was measured for the obtained spray-dried particles using Erweka GTL Powder and granulate flow tester (Erweka, Germany). The method was detailed in the experimental chapter.

5.3.2.7 Morphology and particles sizes

5.3.2.7.1 Scanning electron microscopy

Morphology and particle size of all spray dried batches were examined using scanning electron microscopy (SEM-ZEISS EVO®50, UK). For each sample, different images were collected. The method was detailed in the experimental chapter.

5.3.2.7.2 Laser diffraction

All eight batches of the sprayed dried particles were assessed for particle size using laser diffraction (HELOS /BF, Rodos dispenser) (Sympatec GmbH, Germany) according to the detailed method in the experimental chapter.

5.3.2.8 Mechanical properties

5.3.2.8.1 Elasticity and deformation

Determination of the elasticity of powders was evaluated using a Texture Analyser (Stable Micro Systems, UK) with the software Exponent. The method was detailed in the experimental chapter.

5.3.2.8.2 Tablet's hardness

The hardness of tablets was input to calculate tensile strength. The method was detailed in the experimental chapter.

5.3.2.9 Disintegration

DRM-ODTs disintegration time was carried out for each formulation and the control (n=3). The method was detailed in the experimental chapter.

5.3.2.10 Thermal analysis

5.3.2.10.1 Differential Scanning Calorimeter (DSC)

5.3.2.10.2 Thermogravimetric analysis (TGA)

All the spray-dried batches were examined using the detailed method in the experimental chapter.

5.3.2.11 Melt quench cooling

Quench cooling of SD-INDE particles was performed on one of the produced formulations to confirm the presence of IND in the formulation and to detect recrystallisation of the amorphous form. Samples The method was adapted from a previously reported method (Zimper *et al.*, 2010), with the same procedure of DSC for sample preparation as in our study for both samples of SD-INDE particles and raw IND. The only difference is that heating the sample to the upper-temperature limit above the 162.5°C melting point of IND, 166 °C, and quench cooling the sample by placing the sample crucible in a beaker inside a liquid nitrogen container followed by DSC analysis since this method showed no chemical degradation for IND according

to a reported study (Yoshioka, Hancock and Zografi, 1994). The thermograms were evaluated using STARe software after collecting the thermograms from DSC analysis (Mettler Toledo, UK).

5.3.2.12 Dissolution studies

All tablets were run in triplicate (n=3) to quantify IND in ODTs in control and SD-INDE tablets using *in vitro* release studies in acid media (pH 1.2) and buffer media (pH 6.8). All the samples were analysed using the established HPLC method in triplicate (n=3). The method was detailed in the experimental chapter.

5.3.2.13 Content uniformity

The content uniformity of all batches' SD-INDE particles was evaluated to measure the amount of drug in each sample and the even distribution of the drug within the sample. This was performed by taking similar quantities of each sample. Simultaneously, particles of the same sample were collected from different position within the spray drying chamber to compare with collected samples. The final concentration of 50 µg/mL was prepared using methanol as solvent. The results were analysed using the presented HPLC method for IND.

5.3.2.14 Statistical methods

Results were analysed using Microsoft Excel software. Analyses of variance ($p < 0.05$) and t-test to compare between the batches was applied. The results of the statistical analysis for all formulation are presented as Mean \pm SD.

5.4 Results and discussion

5.4.1 Powder properties: Flowability and bulk density

All formulations were prepared using a spray drying process. Compressibility index, Hausner ratio, and tapped density were used to assess the flowability and the ability of the particles to settle during tablets preparation (Table 5.3). The results showed different flow character passable, fair, and good according to the solvent and the aspiration settings. However, this variation could be related to the number of polymer strands in each sample, dimensions, and distribution of strands. This was confirmed when detecting the flowability through the orifice as the results showed similar flow with 0.7 g/sec with limited variation. The aspiration, which represents the volume of drying air per unit time, was set to 75% and 100% for the low and high settings, respectively. The aspiration effect was noticed on the particle size, as particles of smaller dimensions were produced with high aspiration settings. This can be seen in laser diffraction results, showing VMD reduced with high settings (aspiration and temperature). The difference between the values of particle sizes for each batch varied if the change in temperature and aspiration was small.

Table 5.3 Powder properties results and micrometric characterisation of SD-INDE particles of all batches

Batch	Compressibility index (%)	Hausner ratio	Bulk density gm/mL	Tapped density mg/mL	Flow character	%Yield
A1	20	1.25	0.5	0.63	Fair	58
A2	22.22	1.29	0.56	0.71	Passable	88
B1	15	1.17	0.62	0.73	Good	84
B2	16.25	1.19	0.63	0.75	Fair	92
C1	20	1.25	0.50	0.63	Fair	48
C2	22.22	1.28	0.55	0.71	Passable	46
D1	17.07	1.2	0.60	0.73	Fair	50
D2	21	1.26	0.5	0.63	Passable	48

Moreover, the effect on particle size was optimised by changing the feed concentration. For instance, comparing the same solvent batches 10% of A and 5%

of B, the particles size decreased to 63.73 μm and 61.64 μm in A2 and B2, respectively.

On the other hand, at the high aspiration setting, the time for the particles to transfer from the atomiser to the collecting tube became shorter. Consequently, the time for the particles to interact with the drying gas was also shortened. This resulted in a reduced rate of drying of the solvent and the formation of partially dry particles, which started to stick to each other and form aggregates and particles with larger sizes. Hence, particle size can increase through increasing different parameters such as; feed rate, concentration and temperature of spray drying (Hadi, 2015)(Shepard *et al.*, 2020).

Moreover, it was noticed that the yield increased with high temperature and aspiration settings (Table 5.3). The high velocity of the drying air could result in the efficiency of the cyclone being enhanced (Hadi, 2015)(Shepard *et al.*, 2020). Thus, allowing a high yield to be collected.

The aspiration parameter showed a positive effect on the produced yield for the formulations. However, the methanol and ethanol batches (C and D) showed a negative relationship with the yield. Hence, the high aspiration and inlet temperature increased the output to a certain point then started to decline. This can be attributed to the effect of the increased inlet temperature on reducing the required time for droplets to dry, yet the aspiration was high, which further shortened that time. Zhang and Youan noticed a similar trend (2010); when the inlet temperature and aspiration were high, the yield increased. Yet, after few minutes, the yield started decreasing, highlighting a negative effect of the high settings (Zhang and Youan, 2010). This can be explained by the inability of some particles to dry at the beginning of spray drying, leading to high yield until this process is overwhelmed with continuous high aspiration, which results in the production of clammy and sticky particles due to insufficient time for the particles to dry (Zhang and Youan, 2010). These particles are retained in the chamber, leaving a low quantity of dry powder to be collected.

The other reason for the particle's stickiness in the chamber and the low yield could be related to the low T_g . This enabled the conversion of the material from crystalline to an amorphous state. The amorphous materials of low T_g tend to stick to the chamber due to the change of the status from brittle to elastic (Hadi, 2015). Hence, different T_g was reported for Eudragit L100 as followed 60-70, 165 and 195°C (Shepard *et al.*, 2020)(Gupta, Solanki and Serajuddin, 2016)(Gupta, Kumar and Sachan, 2015b)

(Thakral, Thakral and Majumdar, 2013b)(AG, 2020a) (AG, 2020b). Therefore, it can be stated that the conversion of all particles into an amorphous state occurred.

On the other hand, the direct effect of these factors on the yield depended on particles physical properties, including particles flowability, density and shape. However, the shape of the particles with the presence of strands rendered measurements of flowability and the bulk density difficult.

Hence, in general, small-sized particles could have poor or passable flowability due to the high surface area that provides high cohesive forces(Barjat *et al.*, 2021). In addition to the flow properties of the particle, particles can be influenced by other factors, such as morphology, shape, particles size distribution and moisture content (Liu *et al.*, 2008)(Hart, 2015). The slight difference between the flowability of the batches from passable to fair and good flowability was demonstrated by one batch (B1).

Therefore, the adherence of the particles to the drying chamber and the formation of a high number of strands resulted in the agglomeration of the particles and poor flowability (Shepard *et al.*, 2020). However, reducing the feed concentration to 5% with the low settings as in B1 resulted in enhanced flowing particles. This can be explained by the large size of particles noticed in laser diffraction results (Table 5.4) and the lower number of strands, which was confirmed by the SEM images. Also, the presence of moisture at 1.65%, confirmed by TGA results, indicated the propensity of the particles to be sticky.

5.4.2 Particle size and morphology

5.4.2.1 Particle size analysis

The particle size analysis was assessed using VMD and the span of the produced batches through laser diffraction (Table 5.4). The results showed that particles that were noticeably different in sizes correlated to the solvent used rather than the change in parameters; for instance, A1 and A2 had 63.75 and 63.73 μm , respectively.

Table 5.4 Particles sizes result from laser diffraction showing volume median diameter (VMD) (μm) and the span as x10 (10%), x50 (50%) and x90 (90%) are particles sizes of the volume distribution of the SD- INDE particles

Batch	VMD (μm)	Span ((x90 -x10) / x50)
A1	63.75	3.74
A2	63.73	3.71
B1	63.12	2.34
B2	61.64	2.39
C1	78.51	1.63
C2	74.48	1.80
D1	40.96	5.05
D2	39.97	4.49

Similarly, other batches of methanol and ethanol particles showed smaller sizes of 78.51 μm , 74.48 μm , 40.96 μm and 39.97 μm for C1, C2, D1 and D1, respectively. However, all batches showed a broad particle size distribution related to the high span values. This suggests two outcomes that influence the particles size distributions. Firstly, the presence of a high number of strands in the samples and generating strands with different aspect ratios and thicknesses when changing the parameters (as in SEM results in the following section). The second one is that applying different parameters has less impact on particles sizes when compared to the effect of the solvent and solvent ratio. It was expected that using different solvents and modifications to parameters could have a synergistic impact on the particle size and thereby product mechanical properties. However, this assumption was different to the results and the statistical analysis (ANOVA and t-test). For instance, the results in the tensile strength showed no significant differences ($p>0.05$) in the same batches of different parameters (low and high) and the significant difference ($p<0.05$) when changing the solvent type was independent of the parameter modifications.

5.4.2.2 SEM analysis

The particles morphology, size and strands number were detected using SEM. Particles of the ODTs matrix was examined to detect the particles shape and size effect on the final combination of ODTs and the SD- INDE particles (Figure 5.1). SD-INDE particles were examined using SEM to differentiate between the size and morphology of each formulation.

In general, it was difficult to elucidate a considerable difference between SEM images of the batches, and the correlation was weak for the dimensions of the strands from SEM compared with other results.

In our study, we avoided using very high inlet temperatures to reduce the effect of the temperature on the number of strands formed. However, the trend observed was akin to the study by Shepard et al. (2020), as the filament abundance was higher when using methanol as a solvent. Simultaneously the yield was reduced compared to acetone batches A & B. Nevertheless, the trend was different between the batches of different solvents, dependent on the closeness of the inlet temperature to the evaporating temperature of the solvents. Also, it was reported that the high parameters lead to the evaporation of the solvent before the formation of particles, and subsequent formation of strands with small bead-like particles is observed (Shepard *et al.*, 2020).

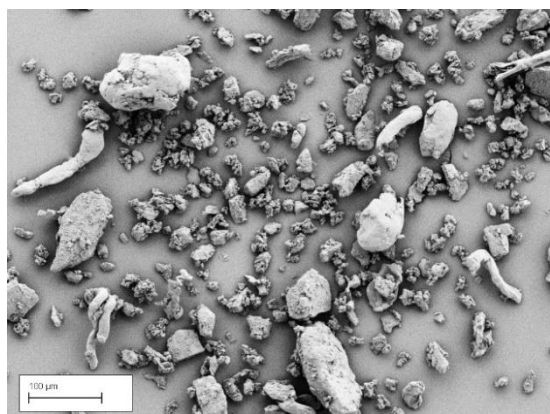


Figure 5.1 SEM images showing a general overview of the particles of ODTs with low magnification

Moreover, according to Esposito et al. (2000), the polymer ratio influenced the morphology and size of the microparticles. In our study, the SD-INDE particles were affected by the polymer ratio corroborating these findings. For instance, at a high polymer concentration (10% w/v), as in A1 & A2, the strands formed in high

abundance, which can be seen in the SEM images (Figure 5.2) compared to B1 and B2 SEM images (Figure 5.3). On the other hand, the abundance of microparticles was higher in A2 and fewer strands than A1 (Figure 5.2). Despite the lower polymer ratio of (5% v/w), B1 and B2 showed less effect on the microparticle sizes (according to laser diffraction results in Table 5.4). Yet, fewer strands were generated with a higher percentage of microparticles in B2 compared to B1 (Figure 5.3) (Esposito *et al.*, 2000) (Böhmer *et al.*, 2006). However, SEM results demonstrated that the highest ratio of strands appeared in C1 and C2 batches (Figure 5.4), explaining why this batch had low yields ($\leq 50\%$) (Table 5.3).

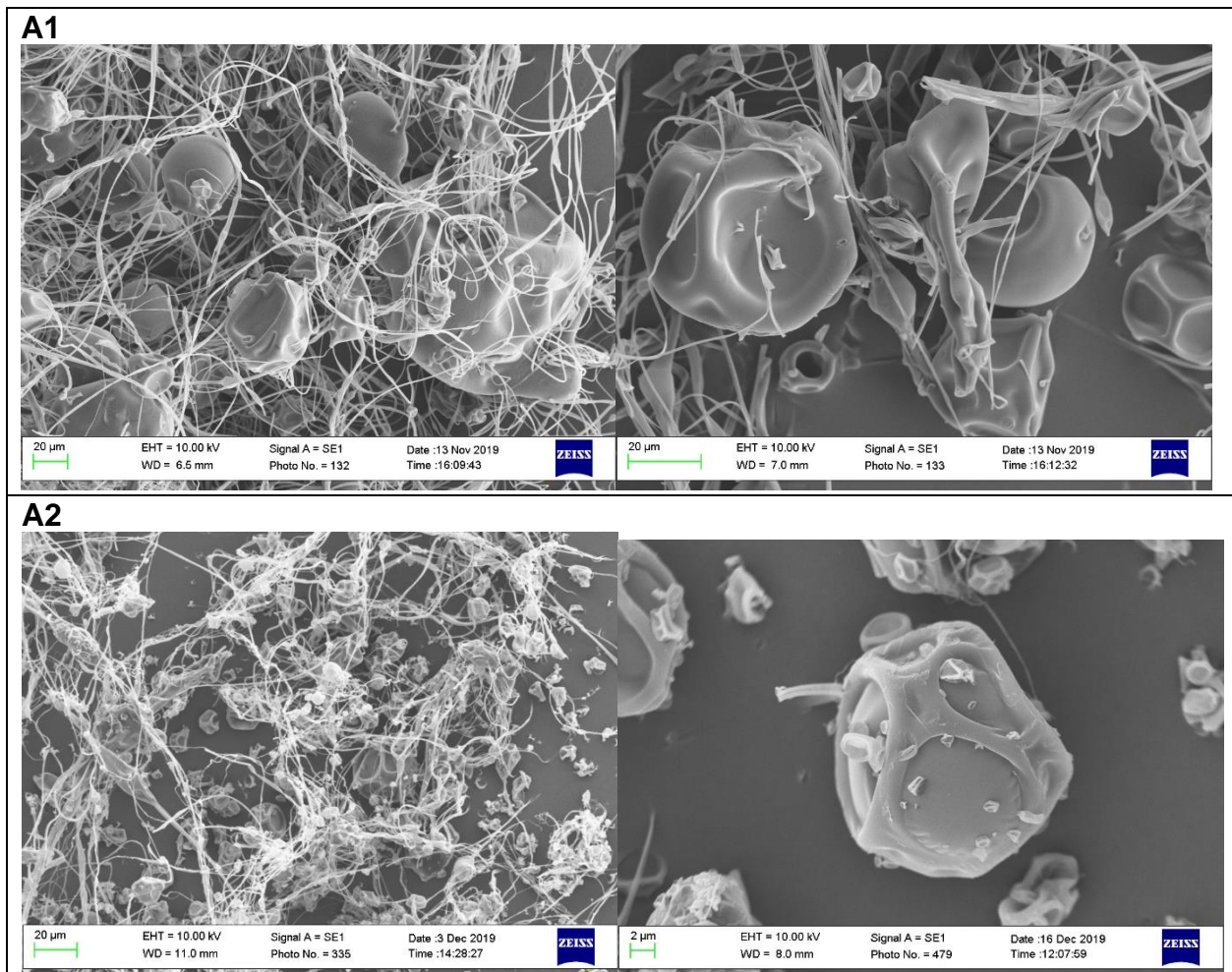


Figure 5.2 SEM images of A1 and A2 batches showing the difference of strands number and particles shape with high and low magnification

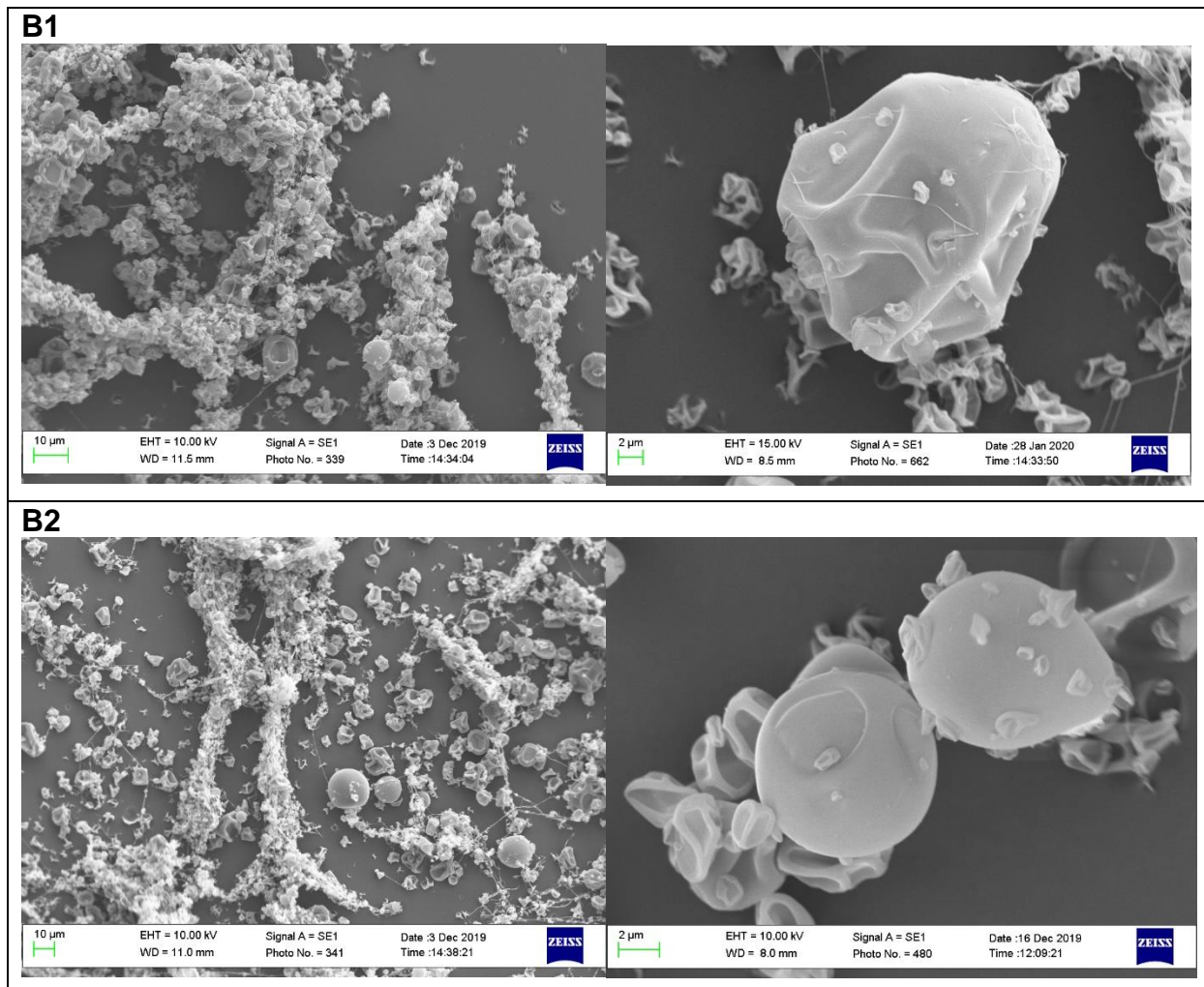


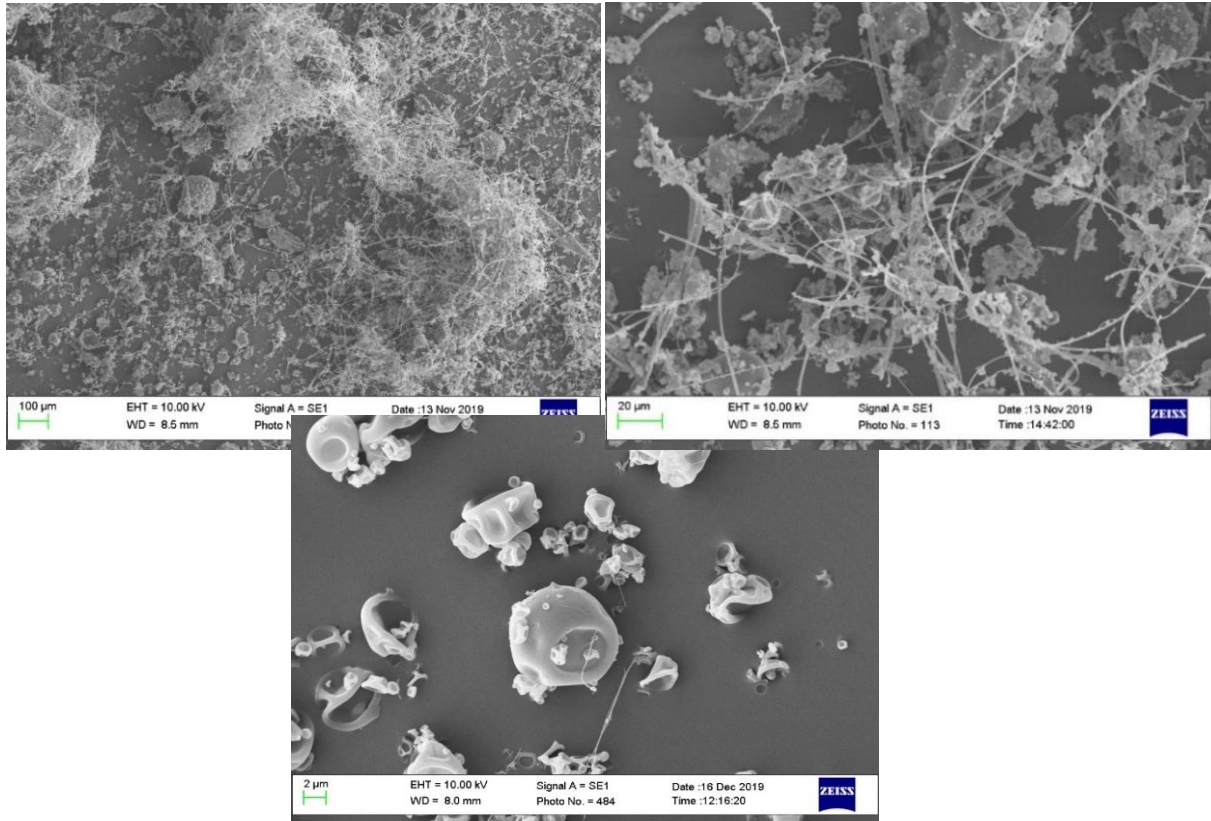
Figure 5.3 SEM images of B1 and B2 showing fewer strands formation with the effect of the parameters the images in low and high magnification

The irregular shape and the low yield can be explained by the adherence of the remaining particles to the wall of the drying chamber during spray drying. On the other hand, the strands were at a low abundance with ethanol batches D1 and D2 (Figure 5.5), demonstrating irregularly shaped microparticles which correlated with the dissolution studies that showed faster IND release from these batches in acidic media (as in the dissolution section). However, strands increased in abundance when using high parameters, as observed in C2 and D2. A similar trend was noticed by Shepard

et al. (2020). Their results showed that strands in the spray-dried Eudragit L100 particles were in low abundance at 100°C inlet temperature, while at the higher temperature of 110 °C, the strands increased, reducing the yield% from 85% to 42%. This was attributed to the increased droplet's drying energy and the short time set to dry the particles. Also, the authors stated that low volatility solvents could increase strand formation, which was noticed when using methanol as a solvent (Shepard *et al.*, 2020).

SEM results correlated with YM results (in the following section) as the highest YM was observed in the methanol batch (C) compared to other batches. This can be explained by the formation of a high number of strands in both batches C1 and C2, showing insignificant differences ($p>0.05$) when changing temperature and aspiration between C1 to C2 (Figure 5.4).

C1



C2

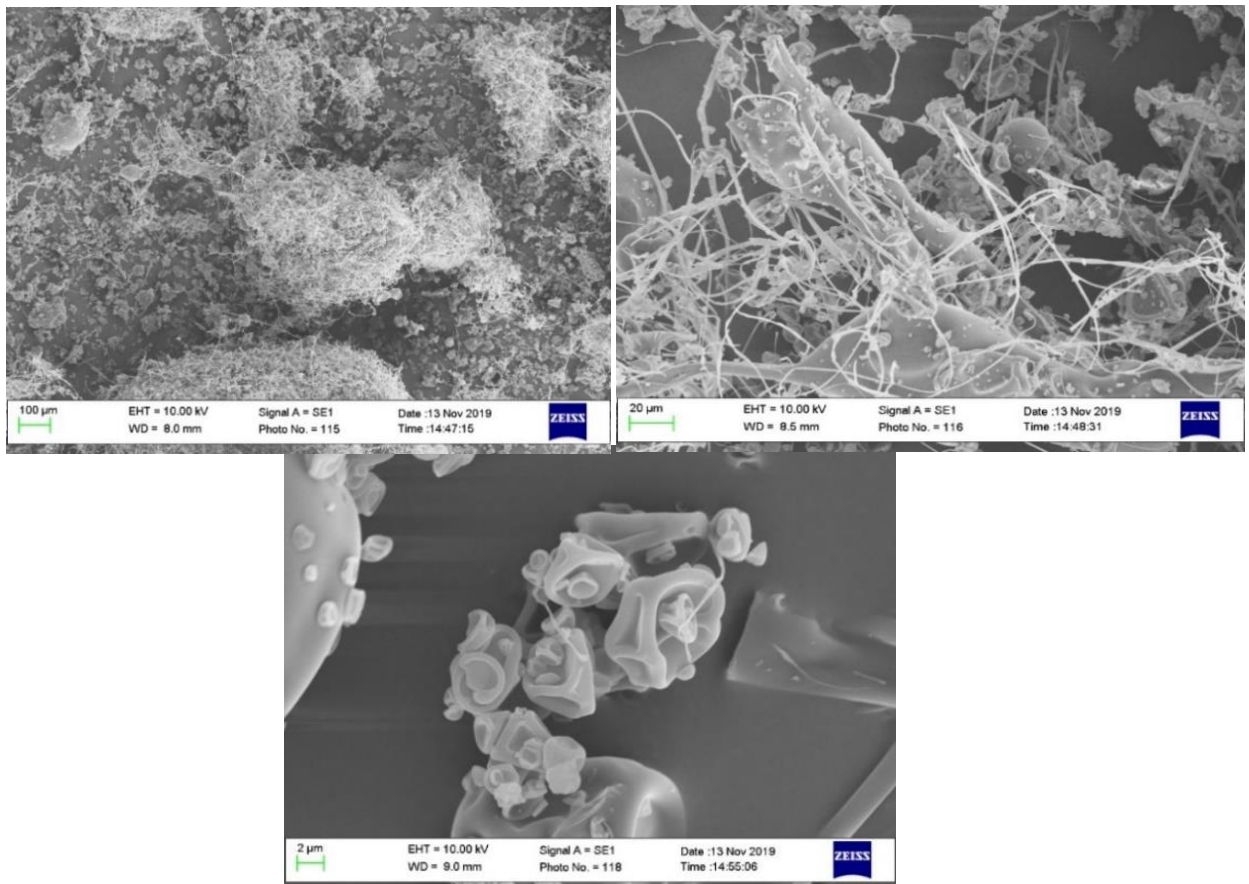


Figure 5.4 Images of SEM for C1 and C2 batches showing the formation of the high number of strands in both groups

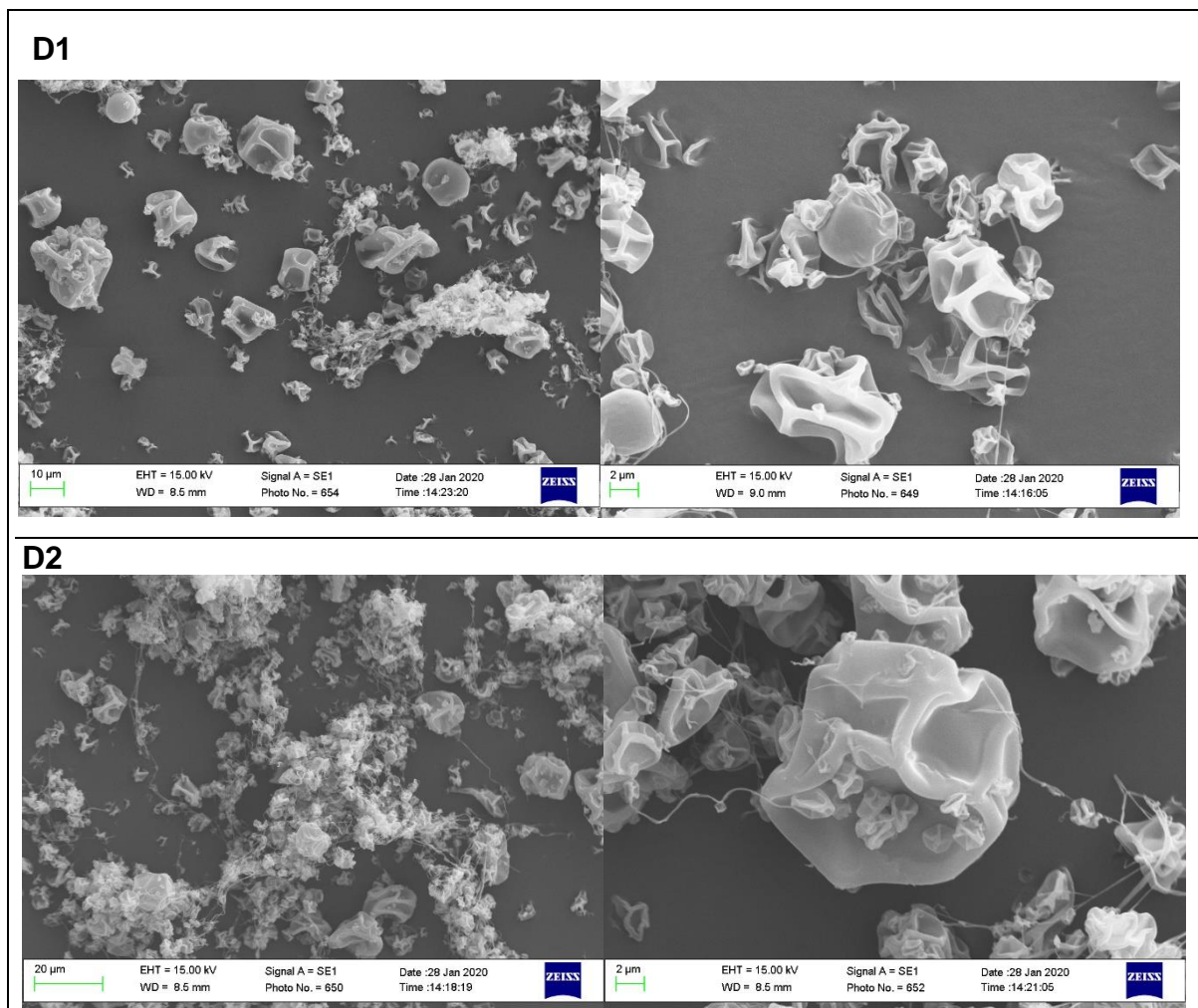


Figure 5.5 SEM images for D1 and D2 showing the difference in strands and morphology of the microparticles

5.4.3 Mechanical properties: Elasticity profile for SD-IND particles

Texture analysis was applied to examine the elastic properties of the particles, and YM represented the results (Table 5.5). The results showed a remarkable difference between YM of the same batch (high and low) correlating with the change in the parameters. Hence, YM significantly differed ($p < 0.05$) between B1 and B2, also between D1 and D2. However, the high feed ratio of 10% w/v in A1 and A2 showed no significant differences ($p > 0.05$) and similarly, when using methanol solvent as in C1 and C2, no significant differences were seen.

Table 5.5 Elasticity profile of all the formulations showing YM (Mean \pm SD) (n=3) and the p values for every two batches indicating the statistical difference between the high and low parameters with % yield and moisture content according to t-test

Formulation	YM (MPa) \pm SD	Mean P values / statistical difference	Moisture content
A1	9.20 \pm 0.53	0.2 (insignificant)	0.57
A2	8.09 \pm 0.92		0.11
B1	8.19 \pm 0.26	0.01 (significant)	1.65
B2	7.24 \pm 0.19		2.95
C1	10.79 \pm 0.92	0.08 (insignificant)	1.35
C2	10.61 \pm 1.38		1.23
D1	7.08 \pm 0.60	0.01 (significant)	5.21
D2	8.95 \pm 0.15		3.99

The low temperature and low aspiration settings increased YM more than the high settings in batches A, B, and C. However, D showed the opposite trend, as YM was higher with high settings.

Two reasons could explain this; firstly, this effect occurred due to changing the IND state from crystalline to amorphous while simultaneously passing T_g of the Eudragit L100; 30-70°C (Shepard *et al.*, 2020)(Santos *et al.*, 2018). The second reason is the effect of moisture content on T_g reduction and the subsequent reduction of YM. Since moisture content could have a plasticising effect on the microparticles, lowering the YM (Crouter and Briens, 2014).

Amidon and Houghton previously (1995) reported that moisture content above 5% had a remarkable plasticising effect while that of less than 5% (3.3–5%) showed almost no effect (Amidon and Houghton, 1995). This finding can be correlated with the highest moisture content value in D1 (5.21%) that demonstrated the lowest YM 7.08 MPa and the trend being different in D2 with 8.95 MPa YM and 3.99% MC. However, this difference could also be attributed to the high number of strands in D2 that affected the results.

Consequently, YM was significantly different ($p < 0.05$) between D1 and D2 batches resulting from the explained factors (moisture content and strands number). On the other hand, the highest YM was associated with C1 and C2 batches since the shape and the number of the formed strands were similar in both batches showing low moisture content values of 1.35% and 1.23% for low and high settings, respectively. This was akin to A1 and A2 results that demonstrated high YM with low MC. This correlation can be confirmed by the YM insignificant differences between the batches with low MC; A1 with A2 and C1 and C2 (Table 5.5).

5.4.4 Tablet hardness and disintegration time

All SD-INDE were combined with ODTs matrixes to prepare tablets by direct compression method. The obtained tablets were characterised by hardness and disintegration time determination (Figure 5.6). The results represented by the tensile strength corresponded with the maximum force that the tablets could withstand before breaking. The results showed that the difference between the batches of the same ratio was insignificant ($p > 0.05$) and independent of the change in parameters B1 & B2, C1 & C2 and D1 & D2. However, changing the solvent type made a significant difference ($p < 0.05$), as in B1, C1 and D1 $p = 5.54793E^{-08}$, similarly in B2, C2 and D2 $p = 2.7E^{-07}$.

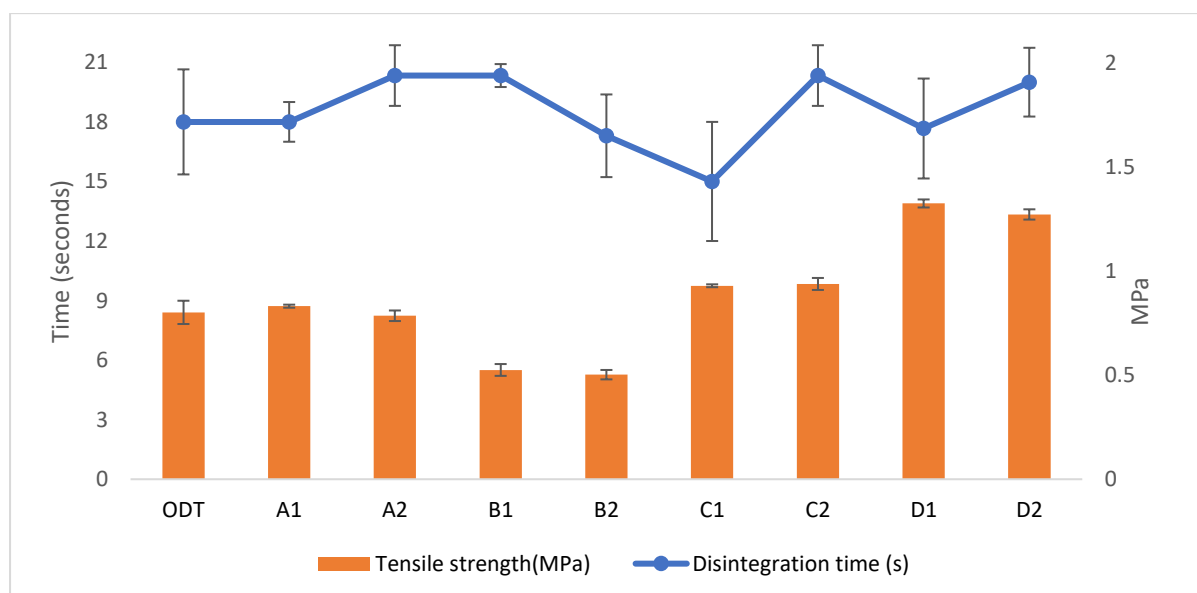


Figure 5.6 Results of disintegration time in seconds and tensile strength (MPa) (mean +/- SD) (n=3) for tablets of IND powder as a control (ODT) and DRM-ODTs

This can be explained by the shape and size of the microparticles and the strand abundance that affected tablets strength or hardness. The tensile strength depends on the crushing force applied per unit area of the tablet matrix and ingredients, including the microparticles and other constituents. Thus, the smaller the particles, the higher the surface area for particle-particle bonding leading to stronger tablets (Hart, 2015)(Khan *et al.*, 2019). However, particle roughness and porosity have different impacts on tensile strength. Eichie and Kudehinbu (2009) found that the porosity of tablets produced with particle sizes from 850–1700 μm was double that of tablets with particle sizes less than 212 μm . This can be explained by the tendency of the larger particles to form a void within the compact area under compression leading to higher porosity. In contrast, the opposite is true for small particles that show high tensile strength (Eichie and Kudehinbu, 2009) (Khomane and Bansal, 2013). Hence, the available binding sites between the particles increase with decreasing porosity, leading to more compact products with higher mechanical strength (Khan *et al.*, 2019). Moreover, VMD in the particles size analysis was the smallest for D1 and D2, yet the span was 5.05 and 4.49 μm , respectively, indicating a wide particle size distribution. Although C1 and C2 showed the largest particle sizes according to the results from laser diffraction, the tensile strength was high. This could be explained by the thickness effect and the low surface porosity of the strands that determine the particle-particle bonding (Hart, 2015). Hence, the span was low for C1 and C2, indicating narrow particle size distribution. Therefore, the mentioned factors earlier (thickness and the low surface porosity) could affect the tensile strength irrespective of the particle size of the strands.

Moreover, it can be assumed that the number of strands affects the inter-particulate bonds, which can be seen in SEM images of the C batch Figure 5.4), illustrating a high number of strands. Although the ratio of the spray-dried powder was low in the tablet matrix (10%), changing the solvent type made a significant difference ($p < 0.05$) on the tensile strength. Therefore, these assumptions are highly associated with the change of the solvent type rather than the parameters.

On the other hand, the comparison between the tensile strength of A (acetone) batch 10% w/v and B (acetone) 5% w/v was significantly different ($p < 0.05$) (t-test) (A1 with B1 and A2 with B2) when using similar parameters of high or low together. These findings indicate a notable effect of feed concentration on tablet strength. However,

according to one-way ANOVA, changing the parameters only in all batches showed no difference in the group of each batch (only the same solvent batches).

However, according to two-way ANOVA, there was no interaction between the solvent type and the parameters indicating that these were two independent variables ($p>0.05$), and variance between the group was very low, as seen in Figure 5.7. However, the results showed a remarkable difference between various solvent batches (same ratio) when keeping the parameters constant ($p<0.05$). Therefore, it can be concluded that changing solvent and powder to solvent ratio had a much greater effect than the spray drying parameters on tablet tensile strength. A similar trend was noticed with YM and particle size analysis results, where greater changes were afforded by changing the solvent and feed ratio.

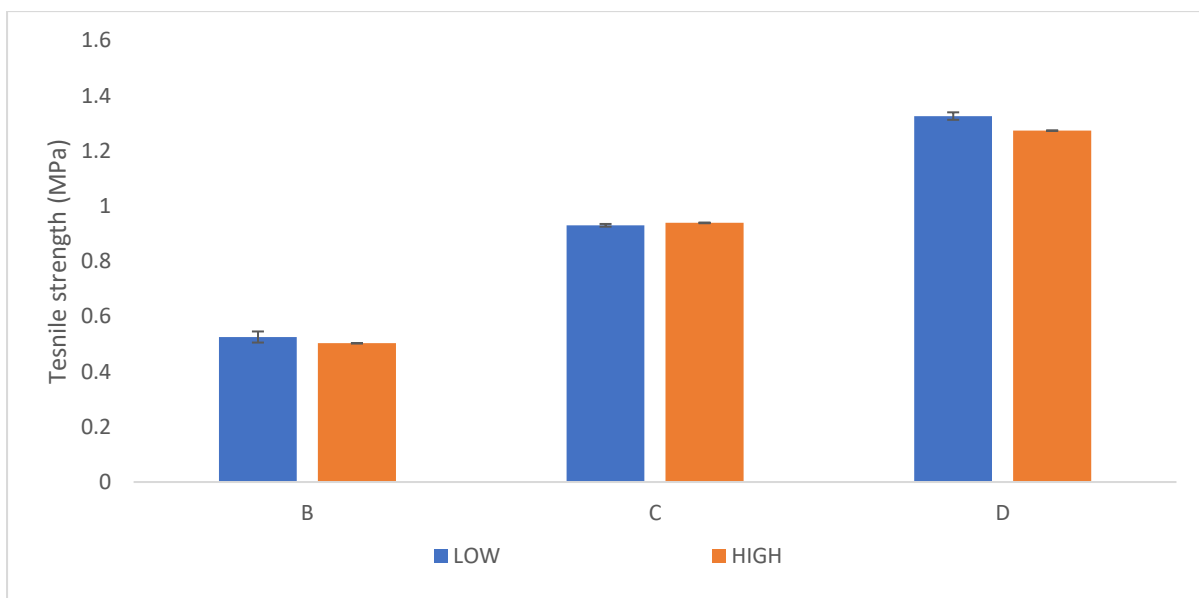


Figure 5.7 Two-way ANOVA results showing the type of interaction between the solvent type with temperature and aspiration for B, C and D batches of low and high parameters in mean \pm standard error

Hence, the effect of the parameters was studied precisely by keeping the peristaltic pump feed rate low (20%) to minimise the difference between the inlet and outlet temperature, therefore avoiding the effect of temperature variance on the final product properties. Also, using a low pump rate with a constant change in inlet temperature and aspiration speed helped to increase the dry content in the final product. Hence, increasing the peristaltic pump increases the feeding rate, which requires higher

energy to dry the particles, thus causing a reduction in dry powder quantity in the yield (Büchi, 2002) (Hadi, 2015).

On the other hand, the tablets showed a short disintegration time between 15-21 seconds, indicating the acceptable ODTs properties and successful combination of both ODT matrix and microparticles (Figure 5.6) (Hirani, Rathod and Vadalia, 2009)(U. FDA, 2008a). This can be explained by the excellent distribution of the SD-INDE particles within the ODT matrix. This was noticed in SEM images by detecting the small particle sizes for ODTs powder and SD- INDE particles. Hence, narrow size distribution facilitates the homogeneity of the mixture to form excellent compact properties (Szalay, 2015).

It was noticed that there was a slight difference between the disintegration time among the batches; for instance, tablets of C1 had a disintegration time of 15 seconds compared to C2, which had a time of 20.3 seconds. A similar trend was noticed among the batches as the disintegration time was higher with high settings (A2, C2 and D2) and lower for low settings batches (A1, C1 and D1) which correlated with the different number of strands of various aspect ratios within each ODT. Nevertheless, the difference was insignificant ($p>0.05$) within the group of different parameters with the same solvent, as well as the same parameters with different solvents of all batches ($p>0.05$). This could be attributed to the homogenous distribution of the particles within the tablets and the adequate mixing time (10 minutes) achieved during tablet preparation. Although these findings were different from B1 and B2 results that showed an opposite trend in disintegration time with the parameters, the difference was also insignificant ($p>0.05$) within batch B (B1 and B2). Therefore, the variance between all batches can be associated with the particle size and mechanical property differences that either enhance or diminish the disintegration time of the ODTs.

Moreover, the loading of only 10% of particles in ODTs provided a limited effect on the disintegration time.

It can be concluded that all DRM-ODTs showed a low disintegration time (<22 seconds), indicating there was a limited effect of DRM on the disintegration of the tablets. Although tensile strength differed significantly ($p<0.05$) between batches of different solvents (same parameters and same ratio), the disintegration time of these batches was low. This indicates that all batches were compatible to be used in the ODTs without affecting their disintegration properties.

5.4.5 Thermal analysis DSC and TGA

The batches of SD-IND, Eudragit L100 and IND, were analysed thermally to detect the physical changes in the formulations. DSC (Figure 5.8) and TGA results Figure 5.9) were collected. The IND melting point appeared in the DSC thermogram showing an endothermic peak at 162.5 °C (Cerchiara *et al.*, 2011). All SD-IND microparticles showed a thermal event between 30-70 °C corresponding to the T_g of Eudragit L100, indicating the predominant effect of the polymer (Shepard *et al.*, 2020). Simultaneously, the moisture loss occurred at the range of 80-120 °C, leading to a distinctly diminished T_g . This was correlated with TGA results in Figure 5.9.

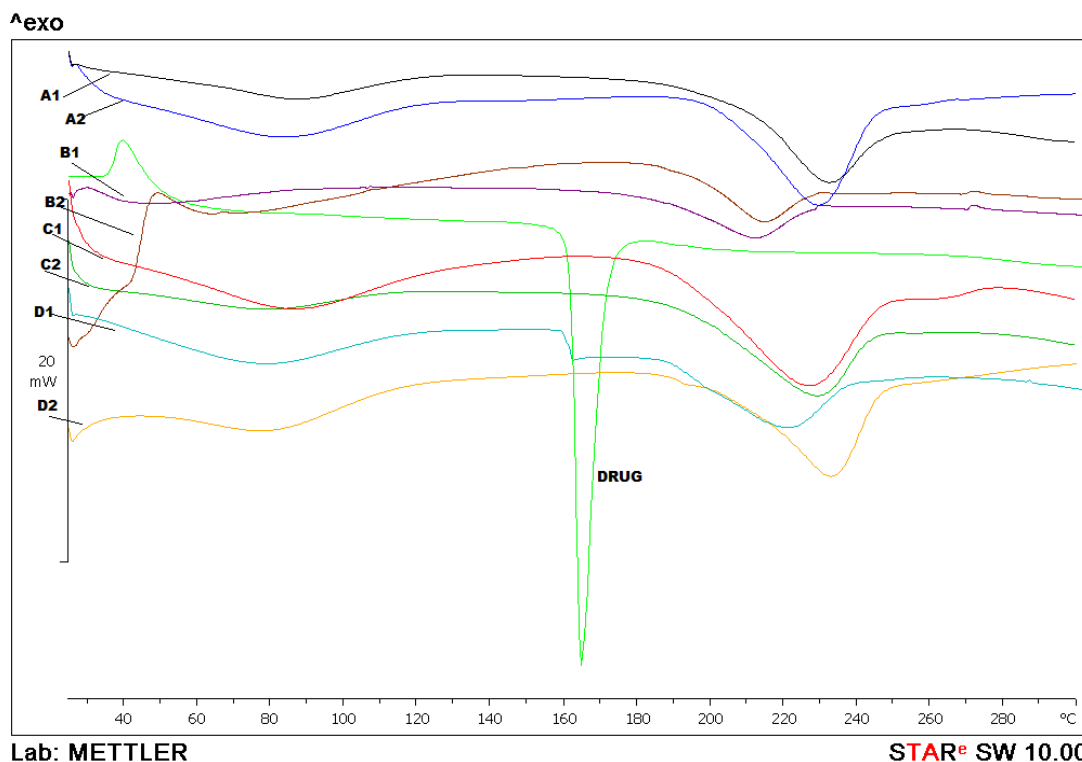


Figure 5.8 DSC thermogram showing the endothermic peak of IND (DRUG) and the T_g of the polymer in the formulation (A1, A2, B1, B2, C1, C2, D1 and D2) with 10 °C/min heating rate showing a decomposition after 230°C (Vlachou *et al.*, 2019)

On the other hand, all batches of SD-IND showed an endothermic peak at lower than 100°C. This could correspond to the moisture loss, which masks the thermodynamic effects of glass transition, as in Figure 5.8 (Amidon and Houghton, 1995). The thermodynamic effect of moisture loss is very broad and has a very strong response.

Thus, it can be noticed that this is the case by looking at the TGA curve (Figure 5.9). TGA shows mass loss started from start-up to a temperature of around 140°C.

This is followed by what looks like the onset of decomposition after 230 °C (Thapa *et al.*, 2017). Hence, the polymeric decomposition could result in simpler molecules by cracking of carbon-carbon bonds and releasing bounded water(Jelić, 2021).

Also, the decomposition peak was detected in raw Eudragit L100 within 220-240 °C as in TGA results (E in Figure 5.9). Also, all formulations showed a similar decomposition peak at 220-240 °C. Similarly, Vlachou *et al.* (2019) found that Eudragit polymers in raw status showed endothermic peak below 100 °C due to their amorphous state. Also, the decomposition of the polymers resulted in another endothermic event over 200 °C (Vlachou *et al.*, 2019). This could be another explanation of the gradual mass reduction of the polymer-drug thermograms as in TGA.

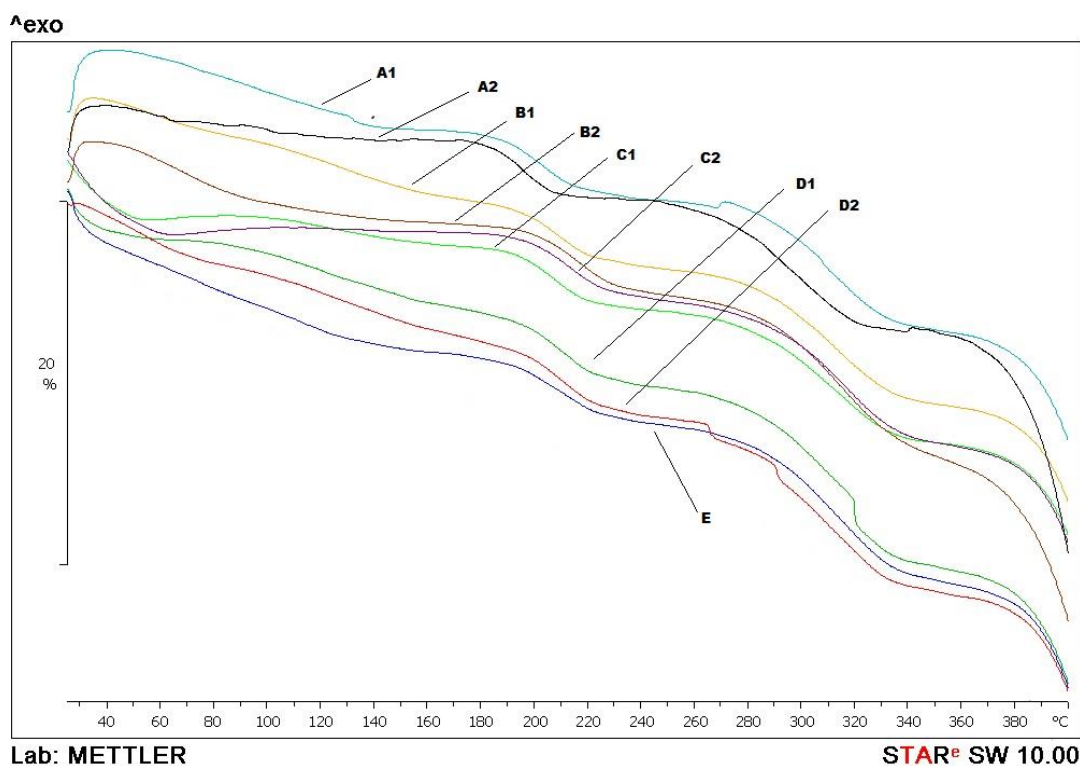


Figure 5.9 TGA results showing the low moisture content of A1, A2 & B1 and high moisture content of B2, C1, C2, D1 and D2 and Eudragit L100 raw powder (E) within range of 40-400 °C and 20 °C heating rate

Additionally, the results of moisture content in the TGA curve were correlated with DSC results showing the mass loss between 60-80 °C and between 80-100 °C corresponding to unbound water(Strasser, 2018).

On the other hand, the disappearance of the IND endothermic peak from the formulations can be attributed to the spray drying of IND, leading to changes in the crystalline status of IND from crystalline to amorphous. Similar findings were reported by Cerchiara et al. (2011) for nanospheres of albumin carrying IND-cyclodextrin complex to prepare enteric-coated formulations. In this study, the DSC results showed the disappearance of the IND endothermic peak, confirming the interaction with the carrier (albumin). Besides, the other reason was the polymorphic change of IND in spray drying from a crystalline to an amorphous state (Cerchiara *et al.*, 2011).

The results of high moisture content (TGA thermogram- Figure 5.9) in D1 were also associated with low YM since moisture content effect lowered T_g as discussed earlier, highlighting that moisture content above 5% showed a favourable plasticising impact (Amidon and Houghton, 1995). Although, the elastic properties were insufficient to support the integrity of all D batch microparticles leading to burst IND release, which shows IND release from both D batches being lower than the control IND. Hence, the elastic propensity is important for the particles to retain their shapes and to protect the drug from being released immediately (Al-Hashimi *et al.*, 2018).

Also, a small endothermic peak was noticed in the DSC results for D1 (100 and 200 °C). This could indicate the presence of water crystals and the start of decomposition, respectively. TGA showed a mass loss gradually for D1, which was confirmed from the highest moisture content compared to other batches. Lin et al. (1995) noticed in the analysis of Eudragit L100 thermal stability, a structural rearrangement occurred, and water loss took place after 176°C (Parikh *et al.*, 2014) (Lin, Liao and Hsiue, 1995). Also, the authors indicated that the mass loss after 176°C resulted from the conversion of methacrylic acids to anhydrides via water loss and structural rearrangement.

The melt quench cooling method was used to confirm the presence of IND in the formulation and the transformation from crystalline to amorphous after spray drying.

The results showed that the IND peak appeared within 156-162°C, close to the original peak of IND (162-165 °C) (Atef *et al.*, 2012) (Figure 5.10). However, the peak was shifted due to the change to the amorphous state requiring higher energy at low temperature to melt. This confirmed the findings of Cerchiara et al. (2011). As the melting point was passed, only the predominant effect of the polymer was seen using DSC in detecting the spray dried IND loaded nanospheres coated with Eudragit L100 and Eudragit S100. The prepared nanospheres showed higher IND release in pH 2

and 7.4 than the commercial IND due to the reduction in crystallinity after spray drying (Cerchiara *et al.*, 2011). This was similarly noticed in our SD-INDE release study.

On the other hand, the quench cooled amorphous IND was studied by Zimper *et al.* (2010), and the results showed that after quench cooling, recrystallisation and melting occurred, resulting in the IND alpha (α) form before the gamma (γ) form and the stability of each form causing crystallisation. IND has a polymorphic structure with α and γ forms (Greco and Bogner, 2010)(Atef *et al.*, 2012). Hence, the α form can recrystallize to the highly stable γ form during the DSC analysis of the melt quench-cooled samples leading to a slight reduction in the melting point. This was reported by Atef *et al.* showing the crystallisation of α to γ form during the thermal analysis of IND, and the melting point was affected by the amount of α and γ forms in the samples(Atef *et al.*, 2012). Where the melting point for pure α form was 151–154°C and for the pure γ form was 159–162°C and the observed difference in melting points of IND samples (mixed ratios) was corresponding to the quantity of the α and γ forms in the samples. Hence, DSC is a quantification method for thermodynamic steadiness for the compounds and affects by the amorphous/crystalline phase(Atef *et al.*, 2012)(Shah, Kakumanu and Bansal, 2006)(Phillips, 1997). However, the recrystallisation and detection of T_g may differ according to the type of compounds included in the formulation and preparation method (Zimper *et al.*, 2010)(Karmwar *et al.*, 2011). For instance, the detection of a T_g in the DSC of SD-INDE batches was difficult. This difficulty could relate to two reasons; either the low T_g or the effect of MC, which was noticed in all batches, that covered the small T_g .

However, the DSC results showed in B2 an exothermic peak around 40-50°C, similar to that in the IND peak (drug as in Figure 5.8) (Zimper *et al.*, 2010). This indicates the possible effect of the γ form of IND since it is stable with a melting point of 165°C. This means it can start to crystallise at a low temperature of 20-45°C.

It was reported that the crystallisation of IND under isothermal conditions occurred below T_g , demonstrating γ form crystallisation of IND and crystallisation of both γ and α start at a higher temperature or equal to T_g (Yoshioka, Hancock and Zografi, 1994). Similarly, crystallization was detected using hot stage microscopy in our study at around 30°C after melting the raw IND powder. However, IND is stable during the storage conditions, and such differences could result during the formation of amorphous form leading to a slight shifting of this exothermic event as in B2 compared

to IND thermograms in DSC (Yoshioka, Hancock and Zografi, 1994)(Corrigan, 1995)(Patterson et al., 2007).

The other reason might be that the sample distribution in the DSC crucible is slightly different, which was noticed while testing the samples by repeating the experiment at different times. However, such differences had a limited effect on the mechanical properties, as reported earlier in this study.

In addition, the difference in the endothermic peaks in Figure 5.10 for melt-quenched samples is normal within the monotropic system showing the stability as in γ form (high melting than α) over the entire temperature range, and IND polymorphs (α and γ) should be considered to be correlated, which was reported consistently previously with our findings (Urakami *et al.*, 2002)(Lee, 2014)

Although the melting point of IND was unclear in all the formulations, such events could prove the predominant effect of the polymer and the presence of the IND in the formulation, which was confirmed by the melt quench cooling method. These findings could be confirmed by the dissolution test results that showed differences between SD-INDE batches due to the formation of amorphous IND during spray drying. Also, IND could be partially undergoing crystallization; as a result, IND release may vary between the prepared batches (Greco and Bogner, 2010).

Also, the advantage of forming an amorphous form of IND could further develop to improve the drug solubility to be used in different drug formulations (Patterson *et al.*, 2007) (Novakovic *et al.*, 2018).

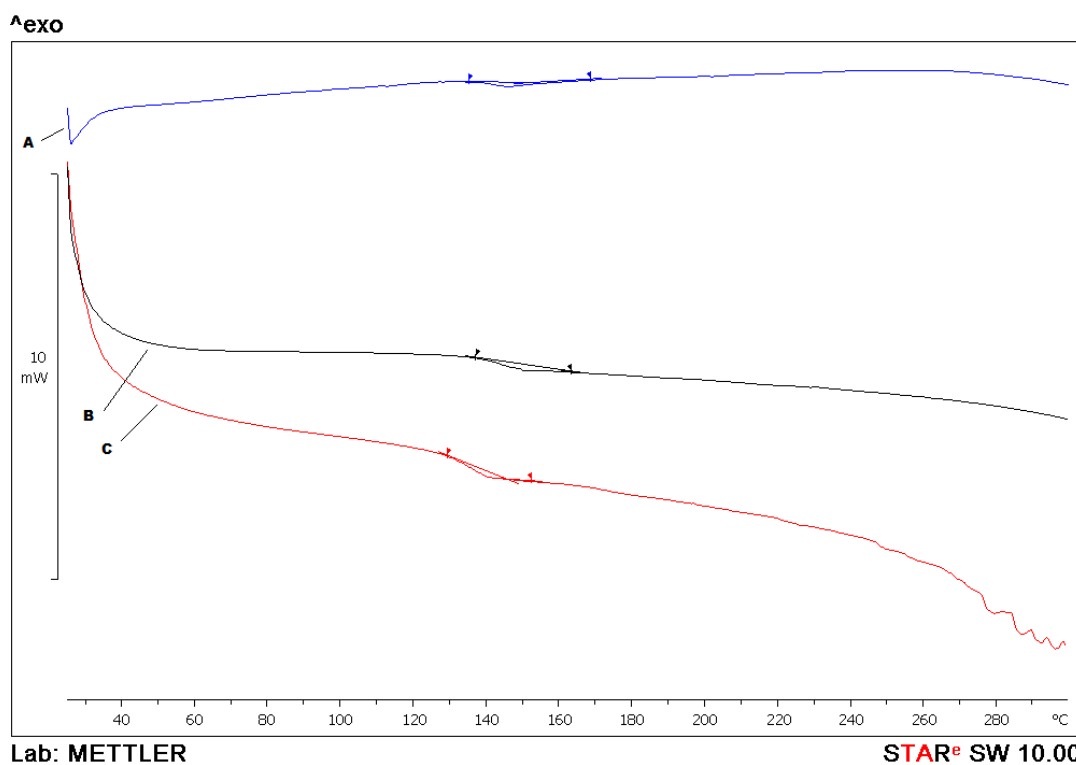


Figure 5.10 DSC results of powder melted quench-cooled of physical mixture IND and polymer (A), IND alone (B) and one of the SD- INDE formulation B2 (C) showing a similar melting point of IND.

5.4.6 Dissolution

The drug release was evaluated for all formulations in acidic pH 1.2 (Figure 5.11) and phosphate buffer media pH 6.8 (Figure 5.12 and Figure 5.13). IND tablets were used as a control containing the raw IND powder with ODTs matrix.

The results of SD-INDE ODTs in acidic medium showed the highest release of IND in D1, D2 and C2, indicating the weakness of these formulations in suspending IND release. It is noticed from the SEM images that D1 and D2 batches showed diffracted microparticles despite fewer strands being formed compared to the methanol batches. In general, the particles were irregular with squashed surfaces. The results in acidic media were significantly different ($p < 0.05$) at 60 minutes among batches of different solvents with the same parameters as in B2, C2 and D2 when considering IND release. Moreover, batches of the same solvent and different parameters were significantly different ($p < 0.05$), including batch A, C and D. The difference was insignificant ($p > 0.05$) between B batch formulations. However, changing the feed concentration affected the IND release through comparisons of the IND release at 60 minutes, as in A1 and B1, which showed a significant difference ($p < 0.05$) in contrast to A2 and B2

that showed no significant difference ($p > 0.05$). These differences can be attributed to different factors, including the differences in content uniformity for these batches, which was demonstrated in Figure 5.14, as the batches show a significant difference ($p < 0.05$). Besides, the impact of strands in each batch, as seen in SEM images, is less with a higher number of microparticles in A2 than A1 (Figure 5.2). Although A2 and B2 showed equivalent IND release at 60 minutes, IND release differed at 2 hrs demonstrating that B2 was relatively consistent in releasing IND, maintaining the delayed-release style.

On the other hand, it was noticed that the YM differently affected the ability of the particles to suspend IND release. Hence YM was significantly different ($p < 0.05$) between D1 and D2, and similar significance was seen for IND release. However, low YM had a low impact on improving the IND delaying property in D batches. A similar trend was noticed in B batches, where YM was low, with a significant difference ($p < 0.05$) between B1 and B2. Nevertheless, the difference in IND release showed no remarkable difference at 60 minutes in both batches of B. On the other hand, the control tablet of IND showed the highest IND release compared to all SD-INDE formulations, indicating these formulations had a delayed IND release property resulting from the polymeric pH dependent effect (Eudragit L100). Moreover, the rest of the SD- INDE formulations showed a consistent delay of IND release in pH 1.2.

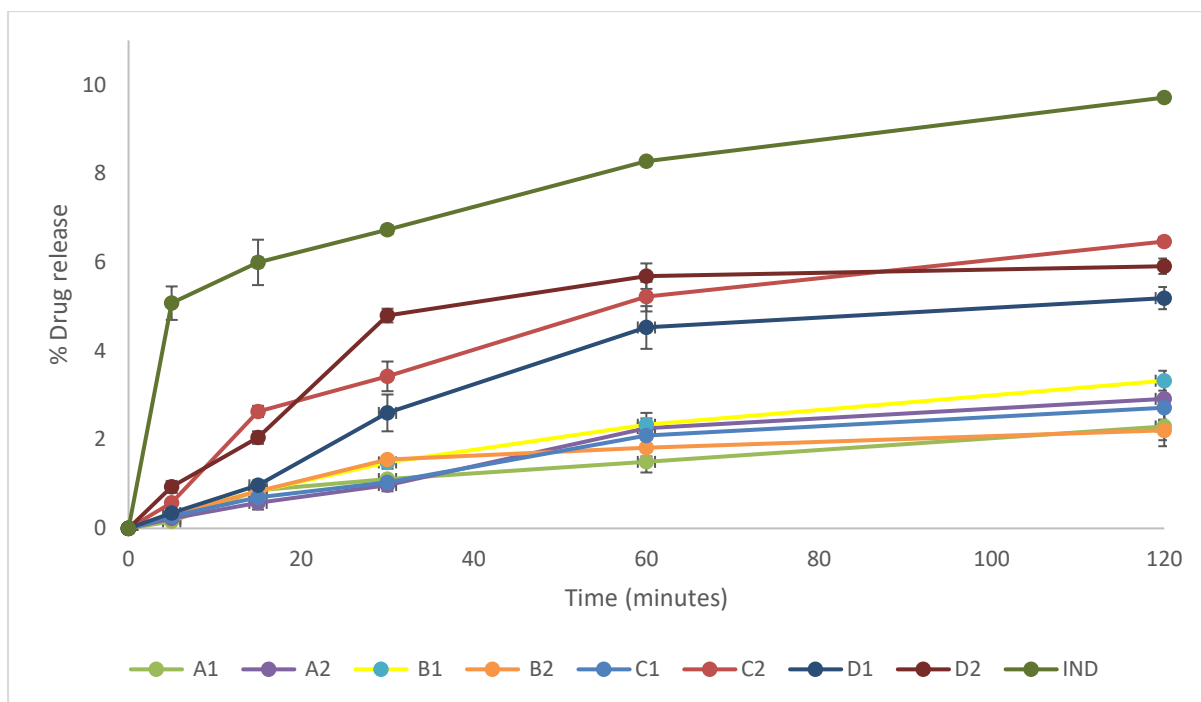


Figure 5.11 IND release results of DRM-ODTs and IND tablets as a control in acidic media pH 1.2, all results in mean \pm SD (n=3)

On the other hand, IND release in pH 6.8 was immediate from the SD-INDE formulations, as seen in Figure 5.12. Although the fluctuated release appeared in the acidic medium for D1, D2 batches and in pH 6.8, the release of IND was the lowest. In comparison, B2 showed constant and more stable release results in both media as it was continually controlling IND release in acidic medium and immediately released IND in intestine mimic medium (pH 6.8).

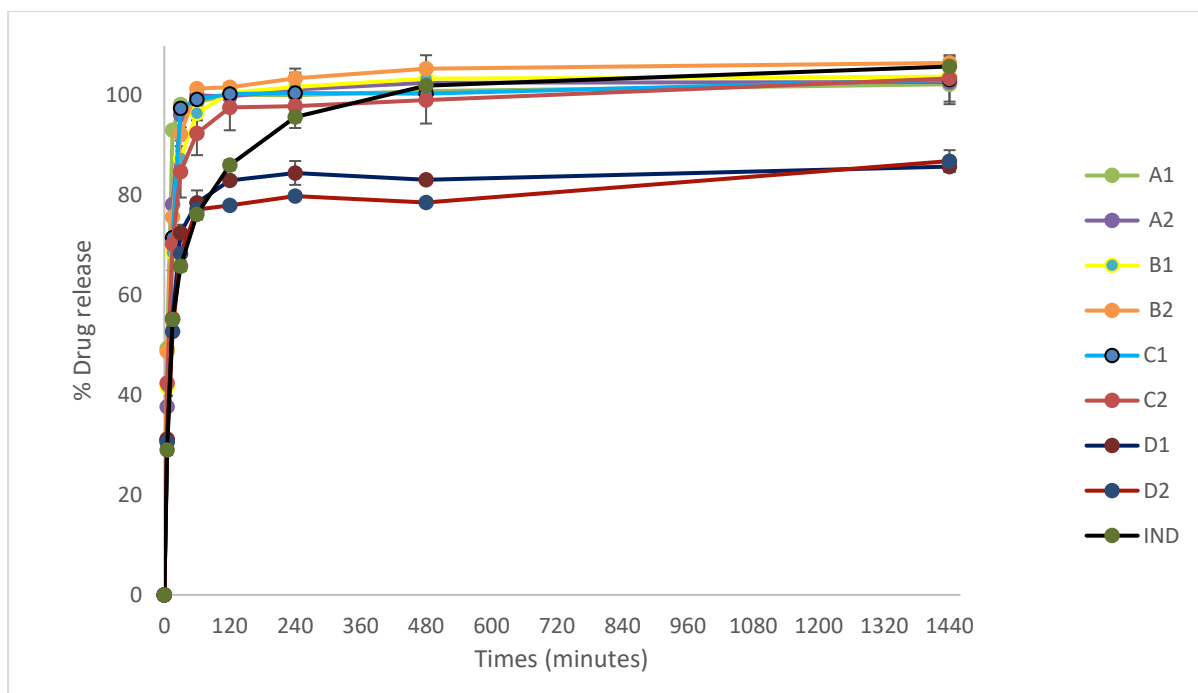


Figure 5.12 IND release results of DRM-ODTs and IND tablets as a control in pH 6.8 media, all results in mean \pm SD (n=3)

However, all batches showed a significant difference ($p < 0.05$) in IND release at 30 minutes, indicating different factors affecting the formulations' IND release. Firstly, YM impact was identified since the high YM of C1 and C2 rendered the SD- INDE plastic, which could affect the release of IND from the formulation. The results showed that in the buffer set at pH 6.8, C1 released 97.43% & 100.32% of IND after 30 min and 120 min (2 hrs), respectively and C2 released 84.74% & 97.65% after 30 min and 120 min (2 hrs) respectively. While C1 suspended IND release in acidic media as after 1 hr IND release was 2.09 %. However, IND release from C2 was 5.22%, indicating that the high plasticity of this batch had affected the integrity of the particles (Dave *et al.*, 2012) (Al-Hashimi *et al.*, 2018).

In general, the *in vitro* release studies for all the batches in pH 6.8 media indicate an improvement of IND release compared to the control batch. This confirmed the transformation of IND from crystalline to amorphous during the spray drying process, increasing the IND release from all batches at 30 min in pH 6.8 (Figure 5.13). However, the formulations were relatively successful in delaying the IND release in the amorphous form, indicating this method's possibility to be applied for delaying drug release.

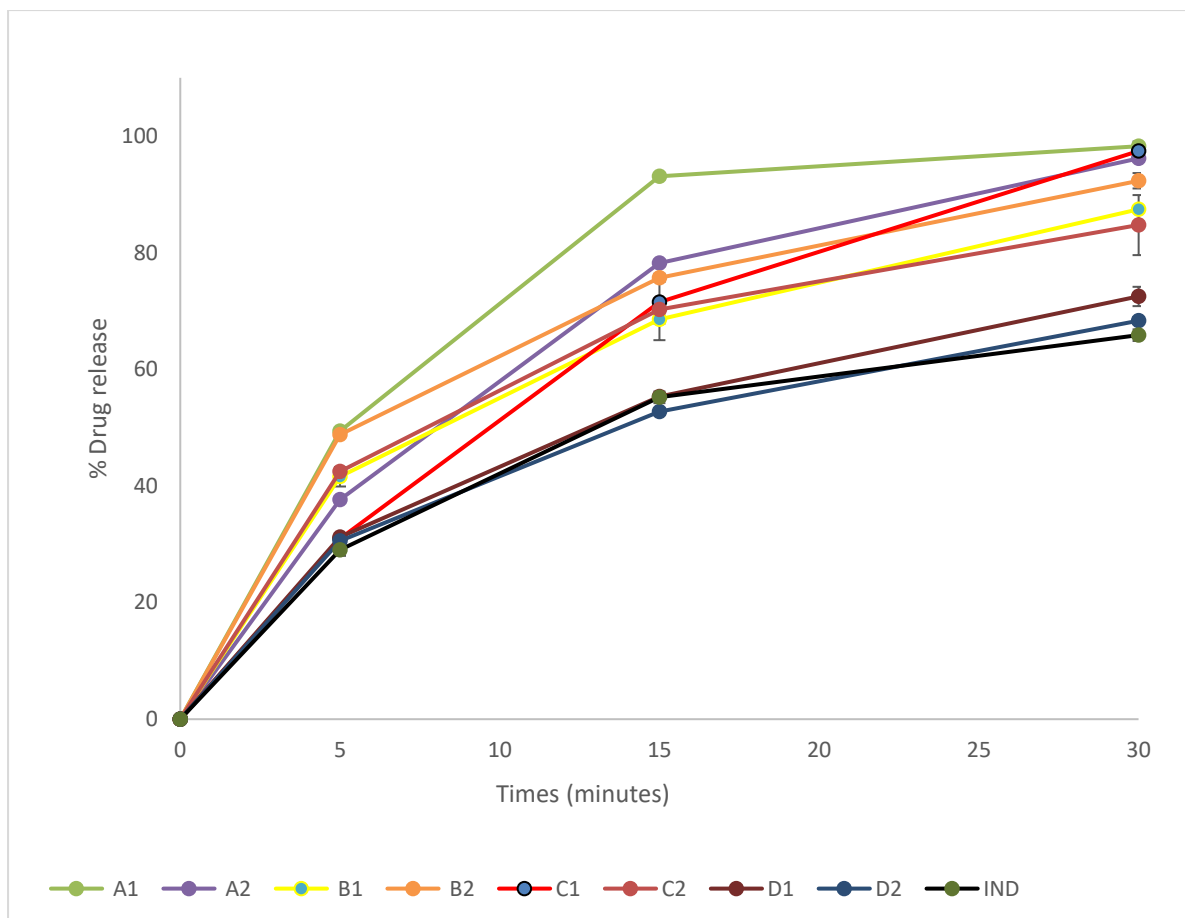


Figure 5.13 Dissolution test in buffer media showing the IND release from all DRM-ODTs batches and IND ODs within the first 30 minutes (mean +/- SD) (n=3)

Nevertheless, YM was not significantly different ($p>0.05$) between C1 and C2, and this can be attributed to the presence of a high number of strands in both batches, as seen from SEM images in Figure 5.4. As previously discussed, the YM impact on formulations was different among the batches and limited to affecting the drug release than other factors contributing to variance. The change in parameters settings showed a noticeable impact on the drug release, which was relatively absent in previous characterisations. Moreover, different solvents affected the properties of SD- INDE particles and, similarly, the drug release. For instance, these combined factors in batch B1 and B2, where acetone was set as a solvent with a 5% (w/v) feed concentration, the low value of YM was significantly different ($p<0.05$), and a change in parameters showed a significant difference at 30 min on IND in pH 6.8 media between batches. Therefore, the effect of low YM and appropriate solvent choice along with an appropriate concentration was sufficient to achieve modification of IND release.

Secondly, the other factor could be the content uniformity of the formulations, which measures differences in the IND content within the same formulation, as samples were taken from different positions first from the collected sample (n=3), second from the chamber (n=3) (Figure 5.14). Hence, all the batches showed a significant difference ($p < 0.05$) between IND concentrations from two positions of the same batch. However, the only batches with no significant difference ($p > 0.05$) were B1 and B2. This proposed factor correlated with IND release in both dissolution media. Hence, the B1 and B2 batches showed acceptable YM values (intermediate), and %recovery for B1 and B2 (first and second position) was 96.71, 96.56 and 99.34, 97.04%, respectively, indicating the ability of these formulations to successfully delay the IND release in pH 1.2 and immediately release IND in the buffer at intestinal pH (6.8). Also, according to content uniformity results, %recovery showed noticeable differences between the samples from first and second positions: 88.99 & 102.62 % in C2; 85.66 & 95.88 % in D1 and 70.43 & 93.91% in D2. The other batches had almost similar results, and all recovered with a 90% ratio in the samples.

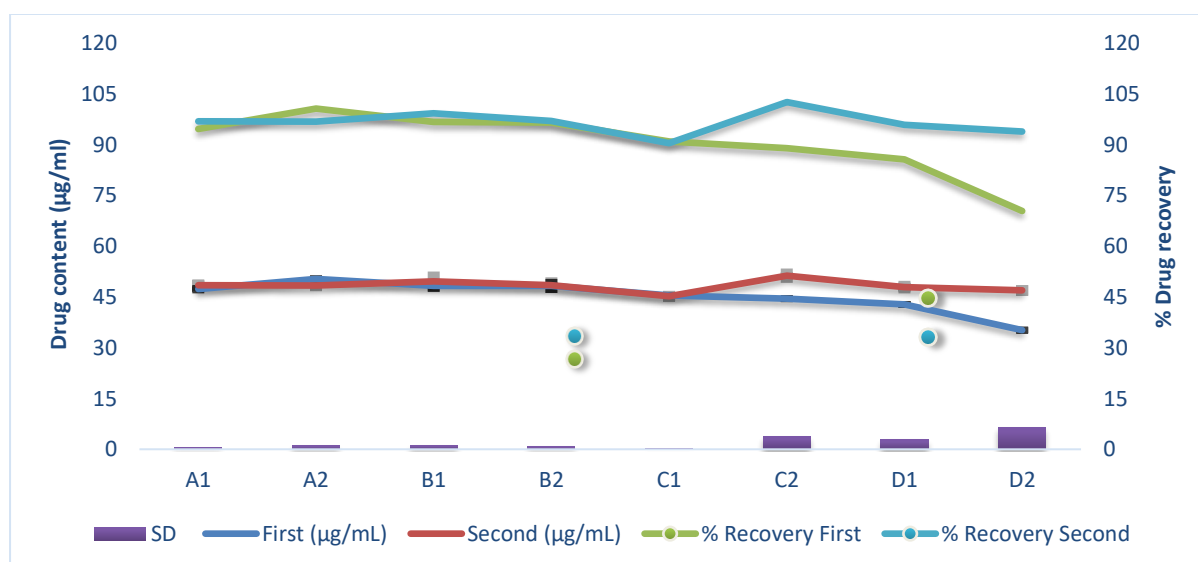


Figure 5.14 SD-INDE particles graph presenting the content uniformity of IND within the batches tested in two positions for each batch first (sample) and second (chamber) position (50 µg/mL), IND recovered from each position and standard deviation of the total IND amount in each sample (n=3)

5.5 Conclusion

In conclusion, spray drying parameters showed a high impact on the properties of produced microparticles. The IND release profile was affected by selecting the solvent and concentration of the solvent used to prepare the microparticles.

IND release in pH 6.8 showed a similar trend to the behaviour of the formulations in an acidic medium.

C2, D1 and D2 demonstrated the highest IND release in pH 1.2, while D1 and D2 had the lowest IND release in pH 6.8. B2 was the best formulation compared to other batches that could consistently control IND release in an acidic medium and induce immediate release in an intestine mimic medium. Different factors were evaluated, which demonstrated effects on the IND release from formulations, including the solvent type, number of strands, particles dimensions and YM.

It is suggested that the high YM of C1 and C2 renders the SD-INDE plastic, which in turn affects the release of IND from the formulation. Although C1 delayed IND release in acidic media, IND release from C2 was high, which correlates with the plasticity of this formulation. However, YM was not significantly different ($p>0.05$) between C1 and C2, and this can be attributed to the presence of a high number of strands in both batches. The YM showed a significant difference ($p<0.05$) between B1 & B2 with a low value for each, indicating that changing the parameters and using acetone as a solvent made it suitable when sprayed with 5% w/v feed concentration. Therefore, the low value of YM, using the appropriate solvent type and setting feed concentration at 5% w/v, was appropriate for modifying IND release. It can be concluded that B1 and B2 have acceptable mechanical properties that support the microparticles integrity and lead to a consistent delayed release of IND in acidic media.

Finally, all batches were compatible with the disintegration time, achieving low dispersible time within 21 seconds without significantly affecting the ODTs disintegration properties.

Chapter 6 Effect of excipients particle size on IND release from ODTs containing pellets

Scoop of the studies

Eudragit L100 based pellets were prepared using indomethacin (IND) as a model drug to fulfil this approach. The effect of particle size ODT matrices on DR-ODT was evaluated. Lactose and mannitol were used with different particles sizes 63 μm , 125 μm and 500 μm to prepare ODTs. Pellets within all ODTs showed good integrity and retaining their shapes under compression. All batches disintegrated in less than 30 seconds. The mechanical properties were acceptable, demonstrating less than 1.5 MPa tensile strength and an adequate elastic profile. The dissolution studies showed that both lactose and mannitol ODTs protected the pellets' morphology, shape, and dimensions under compression. All ODT-pellets from lactose and mannitol delayed IND release in acidic media, releasing less than 1.07% at 120 minutes and released more than 93% at 120 minutes in phosphate buffer (pH 6.8). Similarly, Eudragit L100 of different particle sizes (45, 63 and 90 μm) was used to formulate IND pellets by using the extrusion spheronisation technique. The pellets were embedded into the matrix of ODTs. Particle sizes were of good elastic properties as Young's modulus (YM) values were low, and no significant difference between the different sizes ($p > 0.05$). Testing the pellets' mechanical properties showed that the tensile strength was directly proportional to YM ($p < 0.05$), offering enough support to maintain their integrity under compression. The pellets hardness was associated with initial particles properties in each pellets batch. The pellets prepared from 63 μm Eudragit L100 showed a suitable mechanical properties balance compared to the other sizes.

Disintegration time was affected by the porosity of the pellets, and all tablets showed a low disintegration time of lower than 30 seconds. The results obtained from the in vitro release study showed delayed release of IND in the acidic media (pH 1.2) and an immediate release in the buffer media (pH 6.8).

Keywords: pellets, cushioning layer, IND, lactose, mannitol

6.1 Overview

6.1 Pellets

Pellets are dosage types in the form of beads that comprise the APIs and excipients, consisting of small and solid particles uniform in nature, nearly sphere-shaped with 2.5 mm of diameter (Tan and Hu, 2016b). Orally formulations based pellets can be administered in two forms: compressed into ODTs or filled into hard gelatin capsules (Allen L.V. and Ansel, 2014).

The pellets compaction is considered a critical dosage form. However, it is necessary to use suitable cushioning layers for DRP-ODTs. Therefore, reducing the compression effect on drug release is achieved and facilitating the manufacturing process (Hosseini, Körber and Bodmeier, 2013b). Chen et al. (2017) indicated that the challenge of manufacturing tablets comprising modified release pellets associated with maintaining desired drug release and obtaining uniform drug content after compression (Chen *et al.*, 2017). The compression process applied on the modified-release tablet for manufacturing tablets can rupture the pellets, interfering with the release profile and forming a slowly or non-disintegrating tablet. The mechanical characteristics of polymer are essential to maintain pellets integrity (Hosseini, Körber and Bodmeier, 2013b). Depending upon the rate and the release mechanism, multiparticulate formulations having pellets or microparticles can be obtained in various systems. The reservoir matrix structure comprises the active pharmaceutical ingredient in the inner centre covered with the polymerized system that controls the drug drainage via the substrate to the surrounding medium. The thickness of the coating layer and the coating film composition also determine the drug release. The second system consists of the drug particles embedded in a matrix composed of hydrophilic or hydrophobic polymers called a monolithic matrix system (Nokhodchi *et al.*, 2012). According to the study aim and type of drug delivery system (immediate or modified), both reservoir and matrix systems can be applied. However, the reservoir system is unfavourable compared to the matrix. This can be attributed to the complexity of the method to prepare the formulation, long coating time. Also, using hydrophobic excipients that require organic solvents could negatively affect the environment and make the process costly (Aulton and Taylor, 2018b). However, in controlled release formulations reservoir system is preferable, while the matrix system is applicable in delaying the drug release. The hydrophilic and hydrophobic polymers

can be used to achieve desired drug release. Hydrophilic polymers bloat and dissolve in the aqueous solutions, and the hydrophobic polymers disperse either with time or upon making contact with solvent or certain pH (Nokhodchi *et al.*, 2012) (Muley, Nandgude and Poddar, 2016).

In this particular research, we used a monolithic approach to investigate the contribution of this system to delaying the release time of IND. The polymeric system was prepared using pH-dependent polymer, Eudragit L100. Although highly spherical pellets are preferable for pharmaceutical applications, the less rounded pellets of irregular shape with homogeneous surfaces can still be used to achieve pellets with vital characteristics (Glatt GmbH, 2013). Therefore, in this project, the size and shape of the primary ingredients were considered in the pellet's preparation.

Pellet surfaces are necessary to be equally uniform when preparing tablets or filling capsules with pellets. Hence, the surface roughness of pellets increases the friction between these pellets and further reducing the flow rate (Glatt GmbH, 2013). These surface properties roughness or fissures indirectly produce interlocking pellets, enabling their agglomeration and may form coarse particles. As a result, formulation defects could occur during compression of the pellets, reflecting on drug release property (Rodriguez *et al.*, 2001; Thoorens *et al.*, 2014)(Kangulu, 2009).

On the other hand, the high surfaces roughness of reservoir pellets can affect the thickness consistency of the layer. This leads to an inconsistent drug release from the pellets due to the variation in coating thickness. In the same way, it was noticed that large quantities of coating solutions were used in preparing modified release pellets which also contributed to the roughening of the surfaces (Sarkar, Ang, and Liew, 2014).

Therefore, in the first part of this chapter, we aimed to prepare pellets based on a monolithic system using Eudragit L100 (raw powder) and in the second part different particle sizes of Eudragit L100 (45, 63 and 90 μm).

6.1.1 Pellets production methods

Muley, Nandgude and Poddar (2016) stated that there are few methods used to form pellets. The methods were identified to include: globalisation (e.g., spray congealing and spray drying), compaction (e.g., powder compression), agitation (e.g., balling),

and drug layering (e.g., solution/suspension, powder) (Sun *et al.*, 2012; Muley, Nandgude and Poddar, 2016).

6.1.2 Extrusion-Spheronisation technique

Extrusion and spheronisation is another technique widely used by pharmaceutical companies to produce strong pellets (Sun *et al.*, 2012; Muley, Nandgude and Poddar, 2016).

This technique includes several phases of frame pellets, of which the initial process begins with the blending of the powdered ingredients. For the homogenous matrix, a reasonable amount of fluid is usually added, making a wet mass. The wet mass is then expelled into the cylinders. The process of spheronisation then follows where the extrudate is broken and adjusted into particle shaped spheres. The last stage includes drying the produced pellets. In this process, pellets with a narrow size distribution, uniform roundness are maintained, and high API loading can be achieved. Two classifications of pellets are produced using this strategy; matrix and coated pellets (Muley, Nandgude and Poddar, 2016; M. Zhang, X.K. Li, D.I. Wilson, T.T. Yao, 2018).

Kondo *et al.* (2013) and Kathpalia *et al.* (2014) revealed that the use of a suitable granulation fluid producing perfect spheres (Kondo *et al.*, 2013; Kathpalia *et al.*, 2014). Moreover, spheronisation time was found to affect friability and the generated yields. It also influences the pellets' roundness and aspect ratio (AR), an indicator for the pellet sphericity (Tiwari, Agarwal and Tiwari, 2013). Sinha *et al.* (2009) and Woodruff and Nuessle (1972) indicated that uniformity and roundness of the pellets were directly proportional to the speed of spheronisation (Sinha *et al.*, 2009).

Gouldson *et al.* also revealed that sphericity and yield are directly related to the load and speed of spheronisation, while Sinha *et al.* (2009) stated that an increase in spheronisation inversely gives a return on the yield (Gouldson and Deasy, 1997; Sinha *et al.*, 2009). Lau *et al.* (2014) evaluated the shape and size of the pellet, suggesting the properties of the initial particle denote the ability of extrudate to break into particles with adequate plasticity (Lau *et al.*, 2014).

6.2 Delayed-release pellets in orally disintegrating tablets (DRP-ODTs)

DRP-ODTs are produced by incorporating API's multiunit dosage form (MUDF) as encapsulated or as dispersed API in a polymeric matrix. The current technologies used to formulate ODTs are vital in producing DRP-ODTs that incorporate spray drying, moulding, direct compression, freeze-drying, and application of a disintegrant (A. Elwerfalli *et al.*, 2015). Pellets, ion interchange resin system, nanoparticles, and the utilisation of microencapsulation are some of the many approaches that have been applied to retard API release across ODTs. These approaches have positive and negative effects. Hence, there is a need for their performance evaluation (A. M. Elwerfalli *et al.*, 2015b).

The production of DRP-ODTs containing betahistine dihydrochloride, an anti-vertigo drug, was pioneered by Shamma *et al.* in preparing a microencapsulated drug. The API resin complex was coated with Eudragit® RS100, then directly compressed to make a tablet. The result indicated that the DRP-ODTs release features were preserved, illustrating that the compression process had no damaging effect on the microcapsule coat (Shamma, Basalious and Shoukri, 2011). The spray drying technique is another method for microencapsulation preparation via a conventional organic or aqueous solvent (Ré, 2007). The produced product is composed of shell or other materials and a core of API. Therefore, the release of API could occur by diffusion via the matrix system or by osmosis via the reservoir system (Lengyel *et al.*, 2019). Kondo *et al.* used the spray drying method to produce multiple particles of modified release (Kondo *et al.*, 2013). When microcapsule was added to the tablet matrix, the results showed failure in drug release modification. The majority of formulations comprise brittle compounds; for instance, ethylcellulose was weak to resist compaction pressure during tableting. The authors revealed that this was the leading cause of drugs leaking through the damaged pellet (Kondo *et al.*, 2013).

Ion-exchange resin (IER) is another method used frequently to control drug release across the ODTs. The review process showed a new technological system to study DR-ODT using the IER cation system that helps in masking the bitter taste. The designed system facilitated a "Fickian" drug release, which was not dependent on the drug loading (Al-Hashimi *et al.*, 2018).

The change in the polymer is closely associated with the increased release of the drug. Smart or intelligent polymers are widely known with different names according to their properties, such as stimuli-responsive or environmentally sensitive (Peponi *et al.*, 2017). The polymers' response depends on environmental fluctuations and

physicochemical properties, including ionic strengths, enzymes, pH, and temperature (Depeursinge *et al.*, 2010). Eudragit and crosslinked hydrogels are examples of intelligent polymers; hence, the change in polymer properties can be caused by external forces (Almeida, Amaral and Lobão, 2012; Cabane *et al.*, 2012; Peponi *et al.*, 2017).

Wei, Yang and Luan, (2013) studied the modified ketoprofen release, an anti-inflammatory drug, using ODT (Miles, 2007)(Wei, Yang and Luan, 2013). In the process, ketoprofen was first spray-dried using starch, Eudragit® RS-30D and polyethylene glycol (PEG) 6000 at a rate of 1.5 mL/min and 100°C as inlet temperature. It was recorded that the compressed tablets of spray-dried granules with lactose, mannitol and super disintegrants achieved a short disintegration time of 30 seconds and modifying ketoprofen over 24 hrs showing this method's applicability. However, the authors found that cross-linked polyvinylpyrrolidone percentage as a super disintegrant influenced disintegration time with a limited examination of lactose and mannitol (Wei, Yang and Luan, 2013). Therefore, it is necessary to investigate the physical properties of ODT ingredients and the applicability of each one.

6.3 ODT matrix

Damage induced by compression has been the main problem preventing the development of MUPS as compressed ODTs instead of capsules. The use of excipients in the formulation assists in the compaction procedure and prevents cracking of the embedded pellet. Hence, it is significant in protecting pellet integrity, thereby enabling drug release properties (Chen *et al.*, 2017). The ideal excipients can prevent pellets' direct contact under compression. These excipients form a protective layer when pressure develops to monitor changes to the coatings and release of medication(Chen *et al.*, 2017). However, several factors influence the suitable powder properties to use in the compact preparation. These factors include particles' dimensions, shape and mechanical properties(Mohanty and Subrahmanyam, 2017)(Amidon, Secreast and Mudie, 2009) (Charoo, 2020). Hence, particles size affects the tablet's hardness remarkably since the lower the particles size, the higher the surface area (Rajani *et al.*, 2018).

Moreover, irregularity of particles shape could lead to tablet formation issues. The other factors could be polymorphism, degree of crystallinity and amorphousness (Trasi *et al.*, 2011; Paluch *et al.*, 2013). It was found that treating glucose at high temperatures for drying purposes led to amorphous segments formation within the material, resulting in improved compacting properties (Trasi *et al.*, 2011; Paluch *et al.*, 2013). Sebhatu and Alderborn reported a strong relationship between the available interparticle contact points and the tensile strength of lactose tablets of amorphous and crystalline states. It was found that tensile strength was higher for lactose tablets of amorphous form than crystalline lactose (Sebhatu and Alderborn, 1999). Besides, the excipients' particle size is a critical parameter to consider since the segregation problem could develop due to variation in shape, particles coherence, and bulk density (Leane *et al.*, 2015).

Therefore, using a cushioning filler within ODTs matrix of good mechanical properties and an acceptable particle size range is essential to support pellet integrity under tablet compression.

6.3.1 Excipients of ODTs

Excipients are pharmaceutical materials used to prepare well-compacted tablets with specific properties according to the desired aim (Tunón, 2003). In ODTs containing pellets, excipients' importance is to fill the intraparticle and Intra pellets voids forming good tablet strength with enough support as a cushioning agent by absorbing the compression pressure (Abdul, Chandewar and Jaiswal, 2010). These materials are used as fillers to separate and protect pellets from direct contact (Murthy Dwibhashyam and Ratna, 2008). For instance, the coated pellets' fusion could occur during tablet compaction, forming a thick layer around the pellets (Murthy Dwibhashyam and Ratna, 2008). Therefore, the inactive excipients should prevent the pellets from rupturing and damaged under compression without affecting the drug release. However, along with the previous properties, the excipients should provide acceptable hardness and rapid disintegration of tablets at low compression pressure (Chen *et al.*, 2017).

Also, blending uniformity is another factor to consider when selecting the excipients to avoid the components' segregation; thus, weight and content variation in the tablets (Ježerská *et al.*, 2006) (Alyami *et al.*, 2017). Therefore, to accurately select the tablet's

excipients, considering particles sizes is an essential parameter to assess initial particles effect on the final tablet's and pellets properties achieving the desired drug release (Abdul, Chandewar and Jaiswal, 2010; Abdel-Hamid, Alshihabi and Betz, 2011; Leane *et al.*, 2015).

6.3.2 Low-substituted Hydroxypropyl Cellulose (LHPC)

LHPC is a semisynthetic biodegradable hydroxypropyl ether of low cellulose substitute (Younes *et al.*, 2018). LHPC is an excipient of dual functionality owing to its ability to absorb water and swelling, facilitating its utilisation as both a binder and a disintegrant (Younes *et al.*, 2018). It helps in the quick disintegration of tablets, forming an effective diffusion that would increase the dissolution rate (ElShaer *et al.*, 2018). This phenomenon is beneficial since it promotes better dissolution due to disintegration into smaller particles. According to the tableting process, LHPC also provides anti-capping effects and enhances binding properties, as ElShaer *et al.* reported (ElShaer *et al.*, 2017). LHPC has a small number of hydroxypropyl groups in the cellulose backbone, making it water-insoluble and offering good compressibility properties (Kleinebudde, 1993) (Younes *et al.*, 2018). Although LHPC is water-insoluble, it is still a suitable disintegrant due to its water absorption capacity and volume expansion (Diós *et al.*, 2015).

6.3.3 Magnesium Stearate

Magnesium stearate is a pharmaceutical excipient widely used as a lubricant (Li and Wu, 2014). It possesses a light white precipitate, a faint odour of a particular stearic acid with a low density, that when touched, is greasy and adheres to the skin surface (Almaya and Aburub, 2008). A suitable amount of lubricant for direct compression of the tablet usually ranges between 0.25% and 5.0% w/w. (Rowe, Sheskey and Fenton, 2011).

6.3.4 Lactose

Lactose is a crystalline powder utilised as one of the pharmaceutical excipients. Lactose is considered to be odourless and contains a slightly sweet taste. The

excipient is used as tablet and capsule fillers, tablet binders, capsule, and tablet diluent (Committee for Human Medicinal Products, 2018)(Staurt, 2008).

Lactose can also be applied in the lyophilised products, which help in particles cohesion. Distinctive lactose physical properties include distribution, flow and particle sizes are considered. It was referred that fine lactose grades are preferred since the fine particles utilise binders efficiently and properly mix with other ingredients (Rowe, Sheskey and Fenton, 2011; Chen *et al.*, 2017). In other cases, lactose can be used in film-coating solutions to prepare sugar-coated formulations (Ando *et al.*, 2007). Lactose possesses various isomeric forms in the solid-state depending on its drying condition or crystallisation (Rowe, Sheskey and Fenton, 2011; Chen *et al.*, 2017).

Lin *et al.*, 2011 studied the impact of using micronized lactose as a cushioning agent in tablets preparation to protect the coated multi-particulates from rupture during tablets preparation and compression. The results showed that the lactose cushioning effect was mainly influenced by its particle size. Also, the physical and mechanical properties of lactose were improved using smaller sizes. However, the study did not investigate the particle size effect with a larger range of particle sizes and only covered spray-dried powders with micro sizes (~2 µm)(Lin *et al.*, 2011). Therefore, using a simple and unexpensive technique to investigate different particle sizes of lactose as a cushioning filler is necessary.

6.3.5 Mannitol

Mannitol as a multipurpose excipient has good chemical stability, low hygroscopicity, low solubility, and organoleptic properties. It is widely used in the formulation as a binder or filler (Ohrem *et al.*, 2014). Also, mannitol provides enhancement of tableting and offers good disintegrating properties (Yoshinari *et al.*, 2003). Mannitol has a sweet taste due to the sugar alcohol presence (Grembecka, 2015). For bitter taste masking, pharmaceutical companies have considered the use of mannitol (Fandino, 2019). Besides, lyophilisation can be applied to prepare mannitol to directly compressed tablets for oral dispersible formulations since it dissolves more quickly yet still provides porosity (Dey and Maiti, 2010)(Emami *et al.*, 2018).

Moreover, Mannitol promptly conveys first-rate sweetness achieved through the creamy mild sweetness and creamy texture(Dey and Maiti, 2010)(Emami *et al.*, 2018). The highlighted mannitol properties make it a suitable, perfect formulation

excipient with a patient-friendly oral dispersible dosage form. Siow, Heng and Chan, 2020, investigated the use of freeze-dried mannitol as a cushioning agent and the impact of the particle size on the mechanical properties on the protection of multiparticulates pellet system tablets compression. The combination of freeze-dried mannitol with hydroxypropyl methylcellulose in 3:1 ratio the excipients demonstrated the best cushioning effect. Hence, the fillers tend to rearrange around the coated pellets adsorbing the compressive forces. Thus, the contact between pellet-pellet was reduced, and the damaging effect of compressive forces was prevented (Siow, Heng and Chan, 2020).

Several studies explored different approaches to protect particle quality and improve tablet strength, considering different cushioning agents, pellets coating layer, compaction pressure, and tableting speed (Habib, Augsburger and Shangraw, 2002) (Tan and Hu, 2016b)(Xu, Heng and Liew, 2016). Increasing the number of excipients to support the mechanical properties of the multiparticulate system is costly and time-consuming. Limited data are provided to understand cushioning filler mechanical properties according to particle size. Therefore, exploring the effect of different particle sizes of lactose or mannitol was required to explore comprehensively.

6.4 Aims

Two studies were performed to achieve a delayed release of IND via ODTs.

The first study aimed to: evaluate the effect of ODT filler's (mannitol and lactose) on the integrity of IND pellets formulated using Eudragit L100.

The second study aimed to: investigate the effect of Eudragit L100 particle size on delaying IND release via ODTs.

6.5 Objectives

- To prepare pellets based on Eudragit L100 and IND
- To optimise the pellets achieving good mechanical properties
- To formulate DRP-ODTs via embedded pellets within the ODT matrix
- To maintain the integrity of pellets under compression protecting IND release
- Evaluate the effect of ODT powder particle size on the IND release
- Detecting IND in both acidic and alkaline media in all formulation

6.6 Experimental

6.6.1 Materials

As detailed in the experimental chapter

6.6.2 Methods

6.6.2.1 Preparation of matrix pellets

Three ingredients were used to prepare the pellets matrix (w/w) as follows: 5% IND, 30% sorbitol, and 65% of Eudragit L100 (raw powder, 45, 63 and 90 μm). The dry ingredients were mixed for 10 minutes using a food mixer (Tefal, France) at 100 rpm. Deionised water (1.3 mL) was added gradually as granulation fluid until the wet mass formed with a breadcrumb-like texture. This was with a total mixing time of 10-15 minutes.

The wet mass was transferred to the extrusion platform that contains a single screw extruder set at 60 rpm. The collected extrudates were poured into the spheronizer to prepare pellets with spherical shapes. The spheronisation speed was set at 1200 rpm for 10 minutes.

The final stage of pellets preparation was drying the produced pellets. The detailed method is in the experimental chapter.

6.6.2.2 Physical properties of pellets: Yield, flowability and bulk density

The percentage yield represents the produced amount of the pellets that were calculated as detailed in the experimental chapter.

Similarly, bulk density and flow property was assessed according to the detailed method in the experimental chapter.

6.6.2.3 Pellets shape and sphericity determinations

6.6.2.3.1 Manual method: Caliper

The longest and shortest diameter was measured for 30 pellets, and the values were recorded in units of a millimetre. The detailed method is in the experimental chapter.

6.6.2.3.2 Digital method: Stereomicroscope (SM)

The other method for detecting the pellets dimensions and shape was the stereomicroscope (Nikon Corporation, Japan). The AR was calculated similarly to the manual method. The detailed method is in the experimental chapter.

6.6.2.3.3 Scanning Electron Microscopy (SEM)

All pellets were evaluated with SEM (Zeiss Evo50- Oxford instrument, UK) to detect the pellets' morphology and size(Echlin, 2009). The recorded images were collected using SEM software. The detailed method is in the experimental chapter.

6.6.2.4 Pellets hardness

Data were extrapolated as detailed in the experimental chapter.

6.6.2.5 Porosity

The method details are in the experimental chapter.

6.6.2.6 Differential Scanning Calorimeter (DSC)

6.6.2.7 Thermogravimetric analysis (TGA)

The method details are in the experimental chapter.

6.6.2.8 Sieve analysis and particle size distribution

A. Lactose monohydrate (LM) and D-Mannitol (DM)

An equal amount of both lactose and mannitol powder was weighed (100g) individually. The sieving method was performed using a vibratory sieve shaker (Retsch, Germany) with mesh sizes from 1000 μm to 45 μm . The sieve shaker was vibrated at 1.5 mm amplitude for 10 min. The particles on each sieve were collected and weighted. This study's collected powders were 500 μm , 125 μm and 63 μm particle sizes from lactose and mannitol.

B. Sieve analysis of Eudragit L100

Pellets of IND were prepared from Eudragit L100 of different particle sizes raw, 45, 63 and 90 μm . The sieve analysis was applied using similar settings to the method explained in ODTs matrix in section A.

C. Preparation of powder mix

ODTs matrix was prepared using the following ingredients: 25% of the disintegrant LHPC and 1% of the lubricant magnesium stearate and 74% of the filler/diluent lactose and mannitol individually (63 μg , 125 μg and 500 μg). All dry ingredients were mixed using a Turbula mixer (Willy A. Bachofen AG, Switzerland) for 10 minutes.

6.6.2.9 Mechanical properties of pellets and powder mix

Determination of powders and pellets' elasticity was evaluated using Texture Analyser (Stable Micro Systems, UK) and exponent software. The method is detailed in the experimental chapter.

6.6.2.10 Tableting

Tablets were also prepared from all the particle sizes for each cushioning powder (lactose and mannitol) and the same quantity of the other excipients, as noted earlier. The method details are in the experimental chapter.

6.6.2.11 Stereomicroscope (SM) of ODTs

6.6.2.12 Scan electron microscope (SEM) for all ODTs

Tablet shape and morphology was evaluated using SEM and stereomicroscope as mentioned in the experimental chapter.

6.6.2.13 Hardness of tablets

The method details are in the experimental chapter.

6.6.2.14 Disintegration

The method details are in the experimental chapter.

6.6.2.15 HPLC analysis

Method development and validation are reported in the HPLC chapter.

6.6.2.16 Dissolution

The method details are in the experimental chapter.

6.6.2.17 Statistical analysis

Mean, SD, relative standard deviation (%RSD), *t*-test, and one-way analysis of variance (ANOVA) was applied to detect any significant difference between the results with a fixed confidence interval of $p < 0.05$. Statistical analysis of the data was performed using Microsoft Excel.

6.7 Results and discussion of the first study

6.7.1 Preparation and evaluation of pellets

The pellets (10 g) were prepared using the extrusion spheronisation technique. The pellet's matrix comprised IND 5% w/w, sorbitol 30% w/w and Eudragit L100 65% w/w. The prepared pellets were used for the pellet characterisation and tablets preparation. The produced pellets' yield was 75% before the drying step and then reduced to 70% due to moisture loss evaporating from pellets. Therefore, as discussed in the next sections of TGA, the reported moisture content could be associated with the amount of water added (Figure 6.4). Also, it was found that the bulk density of the pellets was 0.66 g/cm³ indicating an excellent bulk density as reported earlier (Kanwar, Kumar and Sinha, 2015; Zoubari, Ali and Dashevskiy, 2019). The bulk density was measured to assess the pellets' properties and the available voids that these pellets would occupy during tablets preparation (Organization, 2012a; Aher, Shelke and Patel, 2017). Hence, this micrometric property is an essential step in the formulation preparation and development by determining the pellets quantity that fits the space in the tablet, hooper or the die of tablet press during the dosage form manufacturing (Amidon, Meyer and Mudie, 2017; Kaur *et al.*, 2020).

On the other hand, water was used as granulation fluid in this study since the commonly used granulation fluid in the extrusion spheronisation is water, owing to its safety and the environment-friendly virtue (Vervaet, Baert and Remon, 1995). Zoubari, Ali and Dashevskiy reported that the granulation fluid's suitability in pellet preparation had a remarkable impact on the pellets' properties, including bulk density and hardness. When using isopropanol, a water mixture was used as a granulation fluid; the pellets showed low bulk density and hardness compared to the prepared pellets using water, irrespective of the drug quantity and the binder (Zoubari, Ali and Dashevskiy, 2019). This finding followed the bulk density results in our study showing water's suitability as granulation fluid and the adequate amount used in pellets preparation. Our experimental work showed that the amount of water had a noticeable impact on the pellets' quantity. Hence, adding a low amount of water (0.3 - 0.5 mL) made the wet mass of incohesive texture form very poor yield pellets.

Similarly, when a high quantity was used (> 2 - 2.5 mL), the low yield observed is due to the over-wetted mass, leading to the particles' aggregation and blocking the screen

during the extrusion step. This can be explained by strengthening the particles interparticulate bonds since solid bridges form between the particles by water filling ability in particles voids, leading to attract the particles and form good compact. Hence, the water increases the adhesion between the particles (ElShaer *et al.*, 2017). However, reducing or increasing the water in the pellet's matrix must be wisely adjusted since it affects the bulk water and bound water molecules. Hence, water is distributing within the particles or on their surfaces as bound water or bulk molecules, manipulating the produced mass's strength and physical properties and eventually pellets characteristics (Muley, Nandgude and Poddar, 2016).

Also, the granulation fluid quantity for pellet preparation depends on the amount, type of the drug, and the excipients in the formulation (Lustig-Gustafsson *et al.*, 1999) (Galland, Ruiz and Delalonde, 2009). Therefore, the required amount of water should be added wisely to prepare a good quality pellet.

6.7.2 Flow properties analysis

The flowability is an essential parameter in tablet making and capsule filling, providing uniformity of packing and pellet integrity (Bodagala, Jayaveera and Ambati, 2016). The good range of flowability depends on different factors, such as pellet diameter, surface roughness and sphericity. Pellets with smooth surfaces and the narrow distribution size could impact the flow rate; hence rough surface particles can adhere to each other, hindering the particles flow rate (Shah, Tawakkul and Khan, 2008). Also, the small-diameter particles provide a high surface-to-volume ratio, thus good tablet production. Hence, the ideal pellets' shape is essential for equality of active ingredients distribution within the prepared dosage form through the matrix system. Besides, pellet shapes' uniformity is necessary for the intended substrate coating to modify the API release (Beretzky *et al.*, 2002; Sinha *et al.*, 2007).

The pellets flowability was measured for pre-weighed pellets and tested using the flow tester (ERWEKA, Germany); the results were reported in triplicate (mean \pm SD). The pellets demonstrated a high flow rate of 4.6 ± 0.2 g/s. The pellets' accepted flowability is associated with shape, size, density, and the range of the pellet sizes also reflects the excellent flow properties for the obtained pellets as reported earlier (Sinha *et al.*, 2007; Bodagala, Jayaveera and Ambati, 2016). Also, pellet density has a significant

factor in the uniform distribution of tablets and other ingredients' weight and quantity. Hence, pellets with low flowability and equal densities may segregate from the excipients during tablet preparation (Gang *et al.*, 2010; Choudhary and Avari, 2013). Thus, pellets size and density play a role in tablets uniformity. The good physical properties of produced pellets are related to the appropriate extrusion-spheronisation settings. Thiry *et al.* and Sinha *et al.* reported that operational settings during pellets preparation, including speed and time of extrusion & spheronisation, affect the pellets' quality (Sinha *et al.*, 2009; Thiry, Krier and Evrard, 2015). Also, Lau *et al.* study showed that the operating parameters of the extrusion/spheronisation during pellet preparation as well as the optimal amount of granulation fluid (water) resulted in a high yield of 72% and low-density pellets of 0.66 g/cm³ (Lau *et al.*, 2014).

In addition, an adequate amount of particle mixing provided the accepted bulk density leading to formulate pellets with good compatibility since increasing the bulk density reduces the tablet's compatibility. (Kanwar, Kumar and Sinha, 2015). On the other hand, the free-flowing, spherical and small size pellets ranging between 500 to 1500 µm are typical for pharmaceutical applications. Therefore, pellets could confer good distribution of the formulation in the GIT (Dukić-Ott *et al.*, 2009).

6.7.3 Pellet's size and morphology

The pellet diameters and AR measurements were done on randomly selected pellets using different methods to assess the suitable method and compare the results. SEM was used to detect both the shape and the AR of pellets (n=12) and similarly SM (n=30) through a digital capturing system (Nikon Digital Sight, Japan). The measurements were compared with the results of pellets AR generated using the calliper. The results showed that pellets' AR using all techniques was low, close to the spherical ratio of 1 (Dukić-Ott *et al.*, 2009; Tiwari, Agarwal and Tiwari, 2013)

However, it was noticed that %RSD was high, ranging between 14.23-17.24% (Table 6.1) due to the size variance, as shown in Figure 6.1-A and Figure 6.1 B.

Table 6.1 pellets aspect ratios (AR) (mean \pm SD) examined using a calliper, stereomicroscope (SM) and SEM

	n	Mean AR \pm SD	%RSD
Caliper	30	1.30 \pm 0.25	14.25
SM	30	1.29 \pm 0.22	17.24
SEM	12	1.18 \pm 0.17	14.23

On the other hand, AR measurements showed high spherical pellets as literature reported the range of AR within 0.85-1.30; this demonstrates pellets had high sphericity (Figure 6.1) (Oluwabukola and Cheng Shu, 2015). However, the pellets differed in shape and size according to the morphological assessment using SM and SEM, either elongated or irregular. As such, the high %RSD was recorded (Table 6.1). The morphological differences between the pellets and AR values were discussed by Ronowicz et al. suggested that several factors, namely water content, extrusion screen orifices, spheronisation time and speed, could influence pellet's AR (Ronowicz *et al.*, 2015). Besides, Tiwari et al. disclosed that pellet's sphericity and roundness are influenced mainly by spheronisation time and speed (Tiwari, Agarwal and Tiwari, 2013). Therefore, observing AR results' similarities using SEM, SM, and the calliper indicates all the used technique's reliability.

The analysins of SM images using ImageJ program were correlated with SEM images showing almost spherical shaped pellets (Figure 6.2-A and B). However, the pellets had rough surfaces with irregular edges (Figure 6.2-B). Although surface roughness could be a defect factor affecting the tablet homogeneity, Leanne et al. indicated that smooth particles could segregate remarkably from the powder blend and emphasised the importance of the surface roughness for tablets content uniformity (Leane *et al.*, 2015). Therefore, this could offer an advantage in overcoming size variation between powder mix and pellets size, offering content uniformity in tablets.

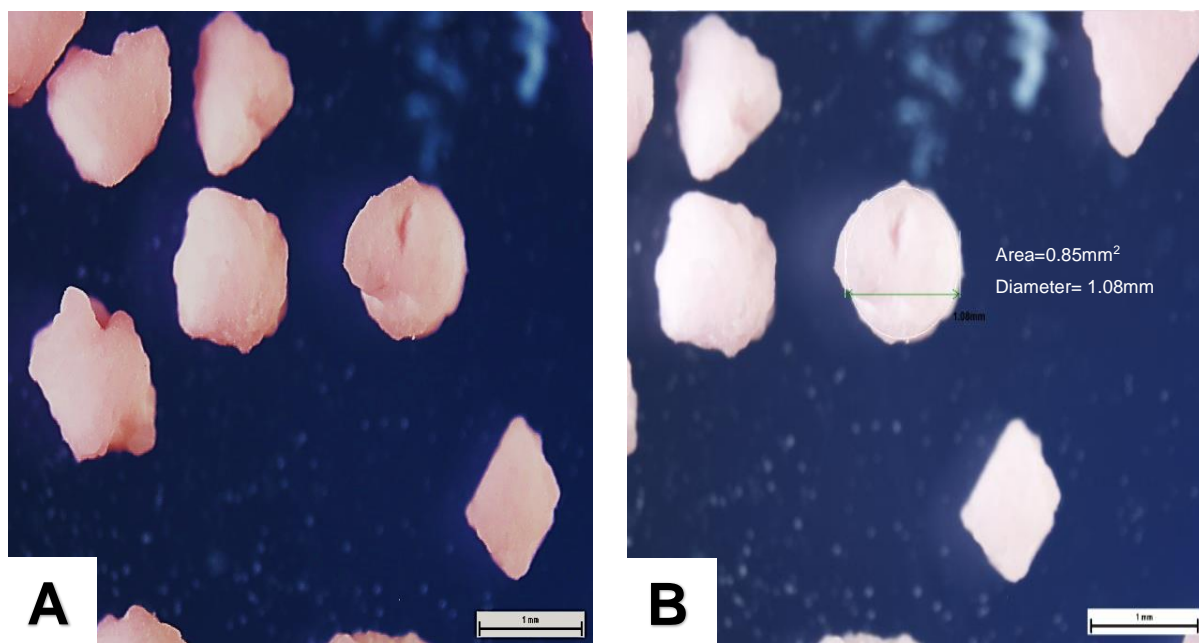


Figure 6.1 SM images A and B showing the shape and morphology of the pellets, area, and diameter measurements

On the other hand, pellets showed different behaviour under compression due to the mechanical properties discussed in the next section, showing high SD after hardness testing revealing a remarkable difference in the plastic tendency and the pellets' attribute to retain their shapes under compression. Hence, Figure 6.3- A showed the pellets' measured area and detected in the tablet (Figure 6.3-C) with limited deformity, while Figure 6.3- B showed the shape change of the deformed pellet in the ODT. Therefore, this reveals two facts; the first could be that some pellets possessed insufficient balance between plastic-elastic propensity leading to a weakened physical structure. Second, the cushioning filler's impact conferred with the ingredients and the properties of the ODT matrix.

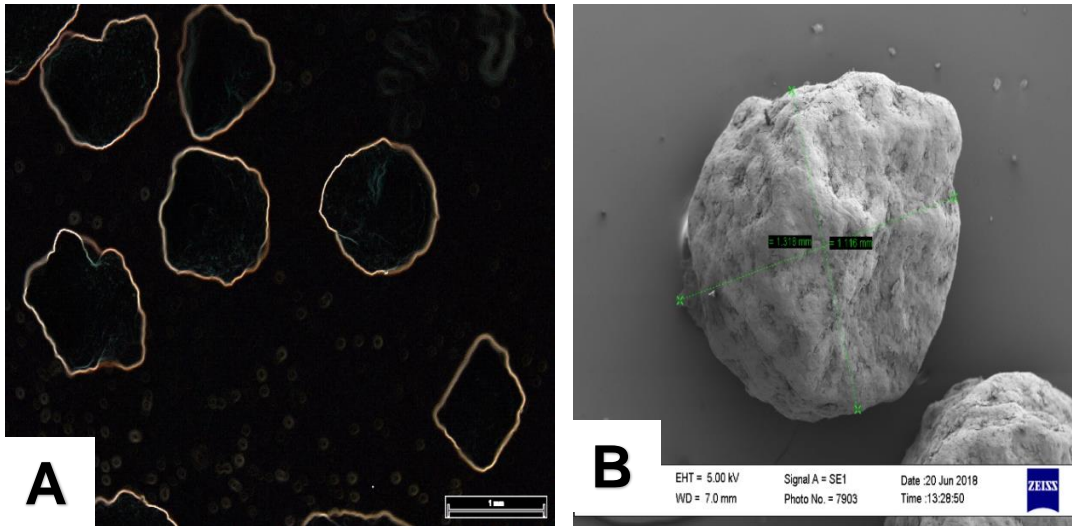


Figure 6.2 SM image processed showing applied in ImageJ software (A), SEM micrograph display the rough surface and AR of the pellet (B)

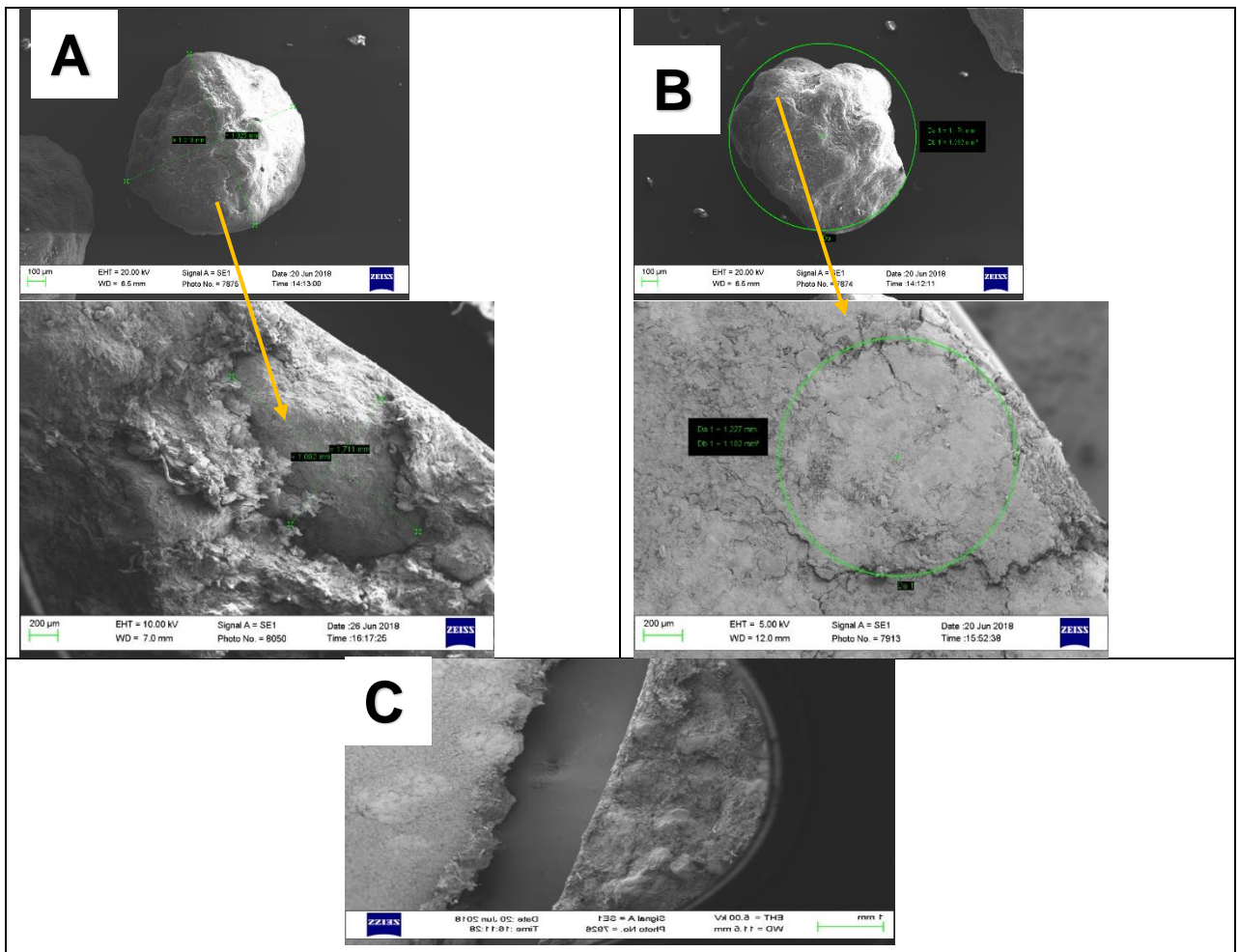


Figure 6.3 SEM images showing pellets embedded in lactose ODTs with AR (A), measured area using SEM (B), top view of tablet after hardness test showing pellets within in the tablet after compression (C)

6.7.4 Pellets mechanical properties

The Texture analyser was used to assess the pellets' hardness against the applied force, and the results were recorded as tensile strength (MPa). The results revealed that pellet diameters' variance influenced the hardness; hence, the average hardness was 4.92 ± 1.95 N with a high %RSD 52.13 % due to the variation in pellet's shape (Figure 6.1) and diameter as discussed earlier. The pellets mechanical strength is an essential parameter for further formulation processing, i.e., tableting. The pellets showed high tensile strength 2.16 ± 0.26 MPa (Table 6.2), providing enough support for the pellets during tablet manufacturing to adequate resistance for the applied pressure (Michie, Podczeczek and Newton, 2012; van den Ban and Goodwin, 2017). However, the pellets' tendency to preserve their shape with limited deformity is essential to retain the pellets integrity, thereby preserving the drug release (Thommes and Kleinebudde, 2007). Hence, YM, which describes the resilience or hardness of materials, is commonly used to assess the pharmaceutical powders' mechanical properties and compacts during the compression process (F Bassam *et al.*, 1990). Govedarica *et al.* stated that hardness and YM are fundamental methods for assessing the particles' deformation properties and measuring the intermolecular forces' stiffness of the materials. These properties can be measured either by stretching, twisting or compression depending on the samples type (Govedarica *et al.*, 2012). Different studies report controversial views regarding the tensile strength and YM relationship of materials in pharmaceutical applications. ROBERTS and ROWE with Payne *et al.* and agreed that an estimated value of the modulus of elasticity could be predicted from the crystal arrangement and physical structure of the raw pharmaceutical excipients; hence the tensile strength can be estimated depending on YM value (Payne *et al.*, 1996; ROBERTS and ROWE, 1999). However, the interatomic or intermolecular binding strength varies depending on the material type, particle size and surface properties; unpredictable changes in the mechanical properties could be generated (Govedarica *et al.*, 2012; Zhang *et al.*, 2017). Therefore, pellets' YM was measured to examine pellets' elasticity profile and behaviour during compaction in addition to the tensile strength.

The texture analysis was used to assess the pellets' elastic properties using the stress-strain relationship as YM (The proportional limit after which the relationship becomes

nonlinear). Hence the higher the YM, the stiffer the material (Govedarica *et al.*, 2012; Instron, 2017; Cabiscol *et al.*, 2018). The results showed that YM was 7.43 ± 0.14 MPa (Table 6.2), indicating a correlated result with the tensile strength since both values correspond to the materials' elastic-plastic behaviour. Although the tensile strength showed the pellets' high strength, the YM value could reveal that the pellets retained a good relative elastic-plastic ratio. Since under compression, the pellets retained their shape as in SEM (Figure 6.3-A).

Moreover, the value was correlated with the IND release behaviour where the pellets showed a delayed-release IND in the acidic media (pH 1.2) after being compressed in ODTs. This finding indicates the suitable physical property conferred by the adequate ratio of initial materials, granulation fluid, and good pellets AR. Nevertheless, increasing the granulation fluid amount could increase the moisture content and hence the plasticiser effect increases. This fact can be seen in the forthcoming sections of the moisture content, as detected with TGA. This could help confer a uniform balance between the elastic-plastic properties to avoid the inconsistency of pellets mechanical properties preserving their integrity under compression, as seen in deformed pellets detected with SEM (Figure 6.2-B).

Table 6.2 Mechanical properties of the pellets using texture analysis showing pellets YM (n=3), hardness (n=30) and tensile strength (n=30)

Physical properties	Value
Hardness	4.92 ± 1.95 N
Tensile strength	2.16 ± 0.26 MPa
YM	7.43 ± 0.14 MPa

6.7.5 Porosity

Measuring the pellets' surface area and porosity is an essential parameter in assessing pellets densification and degree of deformation depending on the available inter and intramolecular voids under compression (Tunón, Gråsjö and Alderborn, 2003). Hence, this could lead to a change in drug release due to the available surface area. Therefore, the relationship between physical and mechanical properties and the pellets' porosity was assessed (Szumilo *et al.*, 2017). Abdul, Chandewar and Jaiswal showed that low porosity pellets suffer limited permanent deformation during compression due to little porosity change in the limited available intraparticle void under the compression. Contrary to high pellets' porosity, showing a remarkable irreversible distortion (Abdul, Chandewar and Jaiswal, 2010). In our study, porosity was measured using the adsorption-desorption method using the BELSORP instrument for pre-weighed pellets. The sample was pre-treated for a specific time and temperature (40 °C – 2 hours) to remove traces of adsorbed gases or moisture from the pellets. There was a slight variance in pellets weight 0.0049 g after pretreatment, indicating that the pellets were contained in well-controlled containers (dictators) during the characterisation. Brunauer–Emmett–Teller (BET) equation using BELSORP software was the appropriate method to account for the physical adsorption of a gas on the surface area of solid samples and measuring the pore size distribution (Sinha *et al.*, 2019). The results showed that the isotherms were Type IV, showing mesoporous pores (Table 6.3)(Thommes *et al.*, 2015; Morishige, 2016). However, the loop shape indicates a weak interaction between the gas and the pores of the particle. This could be related to a number of facts suggested by the literature, including narrow mesopore size, irregular pore shape, and surface roughness (Grosman and Ortega, 2005; Rengasamy, 2006; Morishige, 2016; Bruschi *et al.*, 2018; Schmool and Markó, 2018). Another assumption suggests that particles pores with mesoporous diameters could show similar Type II isotherm (Thommes *et al.*, 2015). Therefore, it can be stated that the few numbers of big pores and small volumes of pores made the inflation or the change in the curve at the end of the first layer of adsorption short. Although surface roughness of the pellets could cause variation in mesopore diameter, the isotherm steepness indicates good characteristic material showing a consistent narrow mesopore size distribution (Thommes *et al.*, 2015)

Table 6.3 Pellets mean pore volume, total pore volume and surface area results using BELSORP software

Sample	Surface area (m ² g ⁻¹)	Total pore volume (cm ³ g ⁻¹)	Mean pore diameter (nm)
Pellets	4.249	0.007	7.481

6.7.6 Thermal Analysis

In our study, the moisture content was measured using TGA, as in Figure 6.4-A. The results showed that moisture content was 6.89%, 5.63%, 6.58% and 4.84% for IND, Eudragit L100, sorbitol, and pellets, respectively. This indicates that drying temperature and the duration of the drying step after pellets formation was adequate. Hence, pellets had moisture lower than 5% despite the high moisture content (>5%) of initial ingredients. Also, pellets showed a degradation that started after 220-240 °C, and a similar trend was noticed with Eudragit L100 after 230°C, yet the decomposition occurred first, then degradation (Giram *et al.*, 2018). This was correlated with the DSC results as an endothermic peak appeared after 230 °C, indicating the decomposition then started the degradation of Eudragit L100 (Figure 6.4-B) (Giram *et al.*, 2018).

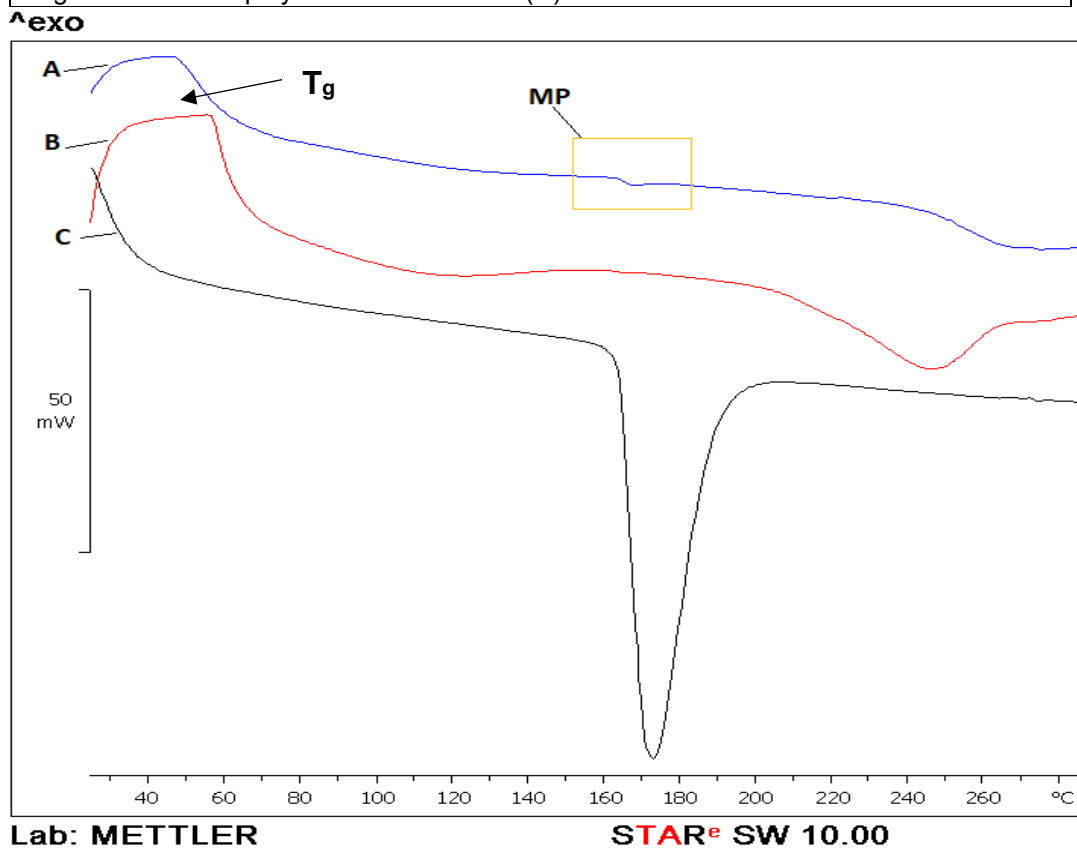
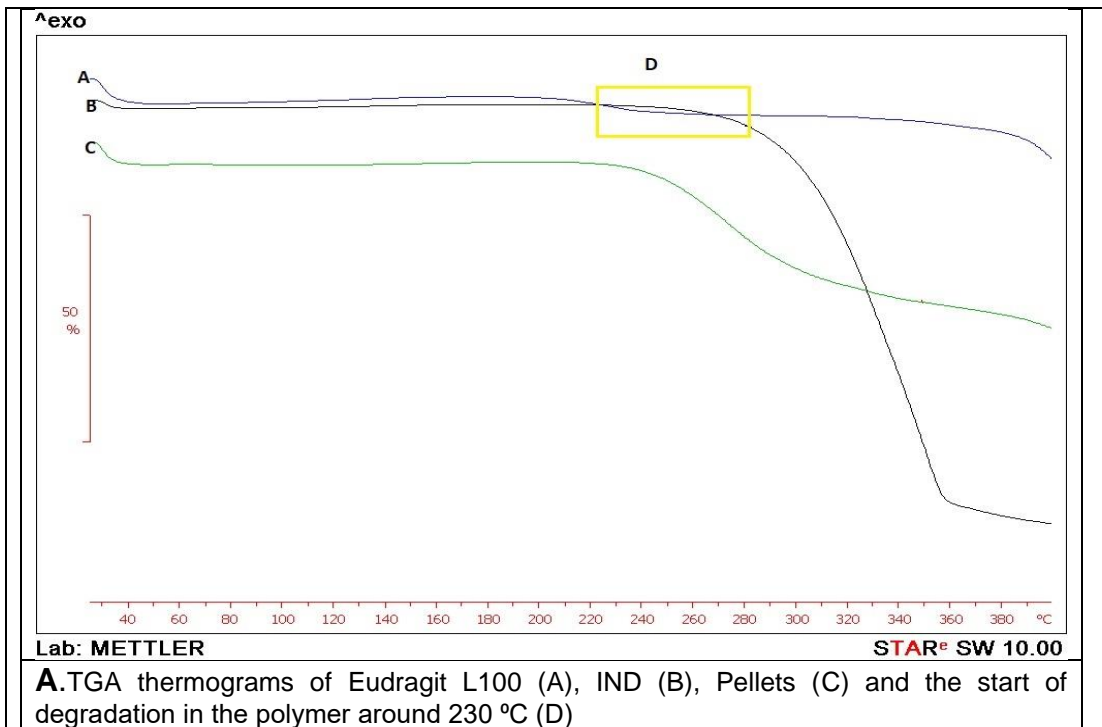


Figure 6.4 Thermogravimetric analysis showing the results of TGA (A) and DSC (B) for the raw powder of Eudragit L100, IND and the produced pellets

On the other hand, the moisture content was within an acceptable range aligning with the mechanical properties results discussed in the previous section; it showed a good balance between plastic and elastic properties. Hence, water molecules affect the formulation differently depending on their distribution within the compacts and the ingredients' water holding capacity. Using water as a granulation fluid could produce a plasticisation effect with an inversely proportional relation between T_g and moisture content. T_g elucidates the state's transition from glassy to rubbery (Bley, Siepmann and Bodmeier, 2009).

On the other hand, if the absorbed water acts as a surface restructuring vehicle or immobile water absorbed by particle surfaces, tensile strength increases proportionally to moisture content (Yohana Chaerunisaa, Sriwidodo and Abdassah, 2020) (Thapa *et al.*, 2017). Hence, the absorbed water raises the number of solid bridges between particles, and the absorbed immobile water improves the particle-particle inter-activity on particle surfaces.

When bulk water exists, generating several water layers remaining on the particles' surface tablet's tensile strength is reduced by hindering the intermolecular attraction (Thapa *et al.*, 2017). Therefore, explaining the moisture content effect is a controversial concept corresponding to the ratio of added granulation fluid, i.e., the excipients' water and properties. Besides, the water holding capacity is affected by the type of polymers used. For instance: MCC particles possess a water-retaining ability resulting in wide use as a filler in wet granulation with high moisture content (Yohana Chaerunisaa, Sriwidodo and Abdassah, 2020). Additionally, increasing inter-particles cohesion forces may become another role for moisture generating liquid or solid bridges (Yohana Chaerunisaa, Sriwidodo and Abdassah, 2020). This gives rise to another virtue for using Eudragit L100, polymer, in the pellets matrices as a pH-dependent hydrophobic soluble polymer only in organic solvents. Thus, it possesses less ability to retain the water compared to MCC. Besides, the pellets contain sorbitol with hygroscopic properties that may retain moisture in a high ratio.

On the other hand, DSC was applied to detect any modification in the materials' physical, chemical properties, and the interface between pellets' ingredients. The change in energy can be detected from and to materials and comparing to a reference. DSC thermograms of IND and pellets demonstrated endothermic peaks around 162.94-164.59 °C owing to the melting point of IND (Figure 6.4-B) (Wang *et al.*, 2007;

Parikh *et al.*, 2014). Also, sorbitol T_g was detected at 98.21 °C, similarly reported by Seo *et al.* (2005). According to Shepard *et al.*, Eudragit L100 possess T_g between 30-70 °C. Similarly, in this study, T_g of Eudragit L100 could be found at 50-60°C. However, the pellets showed lower and unclear T_g correlating to comprising sorbitol as a plasticiser in the formulation and the amount of water that acted as a plasticiser (Shepard *et al.*, 2020). Both of these factors reduced T_g lower than 50 °C hence the starting of degradation was reduced (Giram *et al.*, 2018).

Therefore, filling the voids within the polymeric structure could enhance the elastic-plastic properties of Eudragit L100 and the compact. Therefore, Eudragit L100 chains within the compacts/pellets can slide and move over each other, smoothly providing enough energy that lowers polymeric T_g (Jadhav *et al.*, 2009).

6.7.7 Physical characterisation and particle size analysis

Different lactose and mannitol sizes were collected using the sieving method, as in Figure 6.5 (A & B). The powders first were weighed equivalently and sieved to collect an adequate amount from each indicated particle size. The retained powders were then collected and used in tablet preparation to prepare ODTs with delayed IND pellets. Both lactose and mannitol showed the highest retained powder associated with low particle size > 90 μm . However, compared to lactose, mannitol showed the highest retained particles with $\leq 63 \mu\text{m}$ containing a higher number of fine particles than lactose. Nevertheless, collated particles from 63 μm were the highest for both lactose and mannitol, showing similar consistency in both materials. The chosen particle sizes were used to identify the differences between fine, medium, and coarse particles in the mechanical properties, disintegration, and dissolution properties of the prepared ODTs. Therefore, particles retained on 63, 125 and 500 μm sieves from both materials (Figure 6.5-C) were suitably selected to cover that range in tablets preparation and further characterisations.

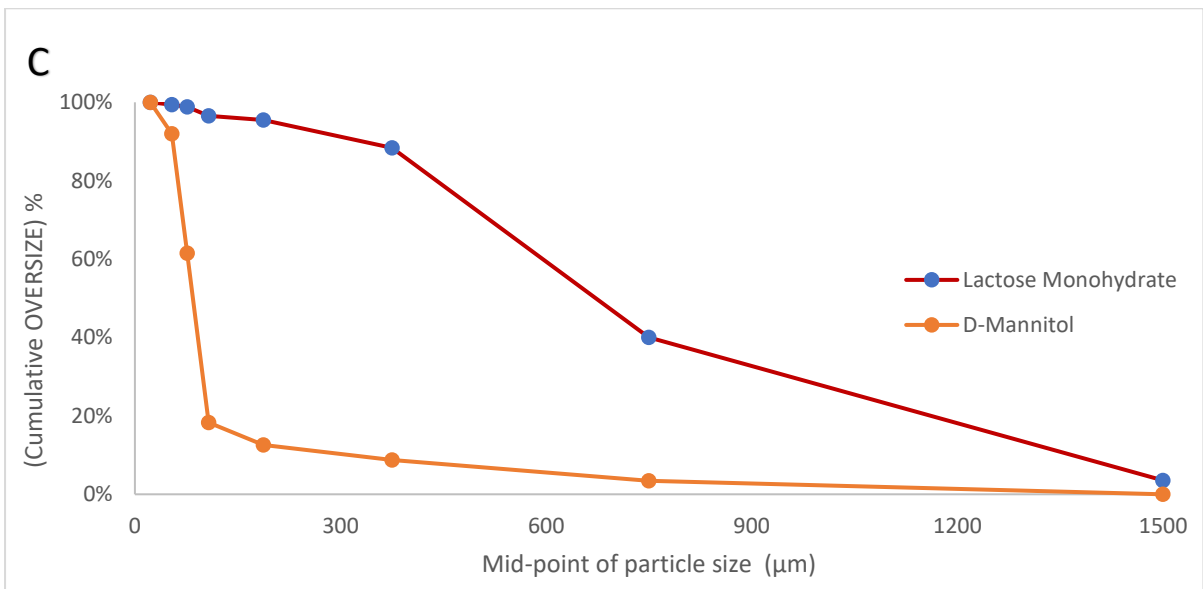
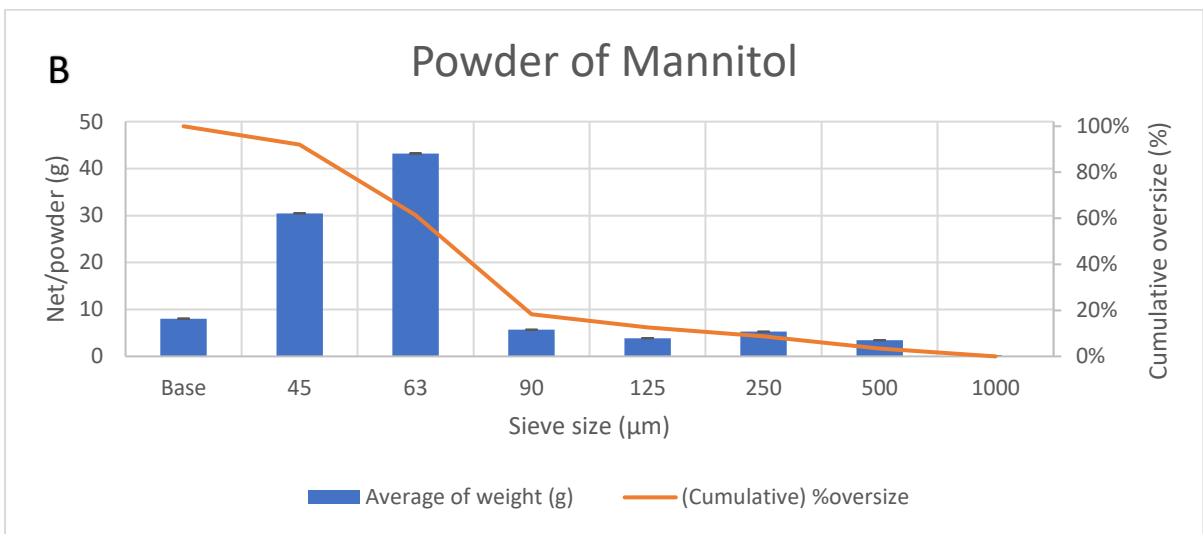
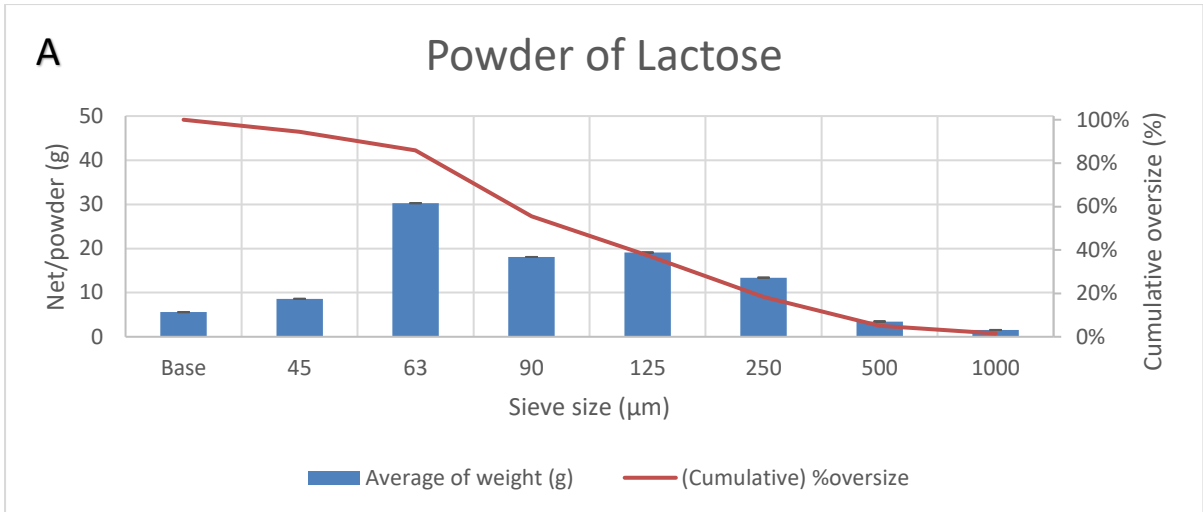


Figure 6.5 Sieve analysis results of lactose (A) and mannitol (B) raw powders with particles sizes of mid-points (C) presenting the cumulative oversize and the retained powders collected from each sieve

6.7.8 Mechanical properties of pellets and powder mix

Lactose and mannitol powders were used to prepare tablets using the three particle sizes 63, 125 and 500 μm . Three prepared batches from each particle size consisted of ODTs ingredients with lactose or mannitol as ODTs/control, the second and third batches comprising IND raw powder and pellets. The obtained mixture was initially characterised to assess elasticity using YM, and then the tensile strength was evaluated for all tablets. Hence, the higher the YM, the more plastic material properties (Sun, Kothari and Sun, 2018).

The elasticity analysis results showed a statistical difference among particle sizes 63, 125 and 500 μm of the same mixture of lactose ODTs-pellets matrix, IND, and raw powder (Figure 6.6). The detected variation was between 63 μm particle size batch with 125 and 500 μm sizes, and the later sizes showed a similar elasticity trend using the same mixtures. Hence, the homogeneity of particles' shape is improving by reducing the particle size while larger particles demonstrate a higher shape variety (Singaraju *et al.*, 2016). Therefore, the particles of 63 μm showed a similar trend in all the tested matrices of that size, including ODTs, ODT-IND, and ODT-pellets with no statical variation.

However, the only detected difference was comparing lactose raw powder with all 63 μm particle size batches. This finding indicates that the addition of ODTs ingredients improved the mixture's homogeneity showing limited to no difference for the obtained matrixes of the smallest particle size lactose that produced a similar elasticity profile.

On the other hand, all batches of 125 and 500 μm showed a noticeable variation in YM using the same particle sizes lactose of control, ODTs-IND, ODTs-pellets and similarly when including lactose powder of these sizes. This evidence confirms the limited variation within small particles powders compared to the bigger particles demonstrating limited coherence with the addition of ODTs to raw powder. A further comparison was conducted to assess the elastic behaviour of each two lactose ODTs, pellets and IND, using different particle sizes 63, 125 and 500 μm via *t*-test. The batches showed undetectable variation between 125 and 500 μm batches, and the difference was consistently related to the elastic behaviour of 63 μm lactose batches compared to batches of 125 and 500 μm of the less elastic tendency. Using specific

large particles sizes (125 and 500 μm) of lactose generated a consistent plastic behaviour with a predominant effect over other ingredients under compression even with the addition of ODTs components. Thus, a homogeneous elastic profile with 63 μm lactose matrices was occurred as in Figure 6.6. Hence, a similar trend was detected with tensile strength results (Figure 6.7), showing higher values with 125 and 500 μm batches than 63 μm , which express the predominant effect of initial particles behaviour over the particles size effect.

On the other hand, elasticity results of mannitol formulations of the same content with different particles size 63, 125 and 500 μm showed that raw powder and ODTs-pellets matrices behaved similarly with no detectable difference among each tested batch. However, in ODTs (control) batches and IND batches, the variation of elasticity values was significant among all the used particle sizes (63,125 and 500 μm). According to the *t*-test, this variation was correlated with 63 μm mannitol compared to 125 and 500 μm powders that showed an almost identical trend. Nevertheless, using the same particle size of mannitol with different formulation content showed identical performance in their elastic tendency demonstrating no difference between the compared results of ODTs, ODTs-IND, ODTs-pellets mixtures. The only variation was detected by including raw powder with other mixtures of the same used size of mannitol. Therefore, it can be assumed that the combination of ODTs ingredients with each particle size of mannitol generated a similar effect minimising the variation generated by raw powder.

Moreover, elastic properties' coherence using different mannitol sizes with ODT-pellets indicates the suitability of using mannitol without sieving and no necessity for a specific particle size to select. The comparison between similar size lactose and mannitol of the same mixtures of ODTs, IND, and pellets showed that the YM was significantly smaller in mannitol. However, the comparison of 63 μm particles of lactose with mannitol showed similar YM results, while particles of 125 and 500 μm were significantly different demonstrating plastic properties to that of mannitol. Overall, the YM in lactose was higher than mannitol for the comparable batches with the same particle size, reflecting the powder rigidity. Although the raw lactose's comparable sizes had higher YM than mannitol, mannitol raw powders, similar to lactose, were consistently the highest YM among the prepared mannitol batches. Hence, in the

following section, SEM showed a similar effect in protecting the pellets under compression using mannitol (Figure 6.8).

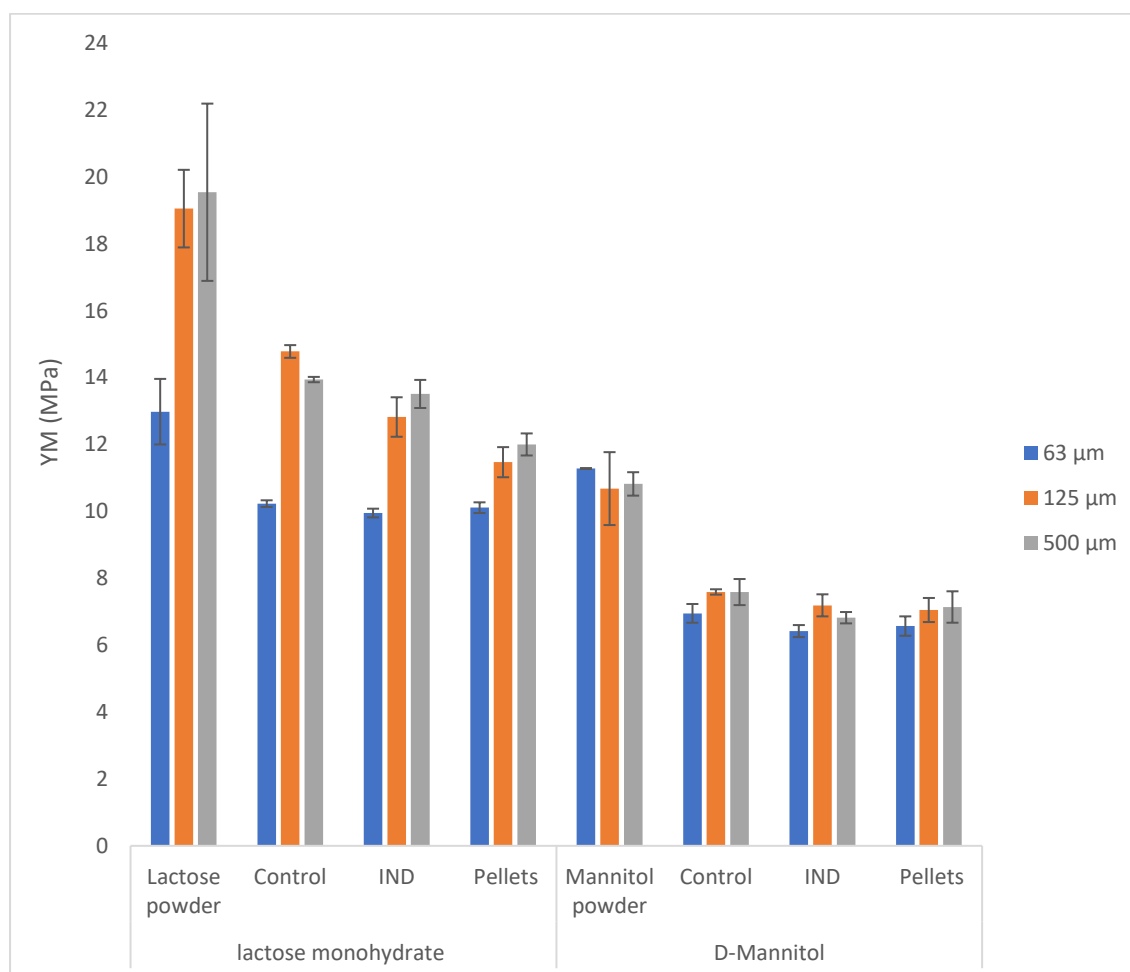


Figure 6.6 Elasticity profile represented by YM of tablets mix of ODTs (control), indomethacin (IND), pellets using lactose and mannitol 63, 125 and 500 μm particles

6.7.9 Hardness of tablets

A hardness test was used to evaluate the maximum force that tablets resist before breakage by extrapolating tensile strength(Sun, Kothari and Sun, 2018).

The tablet's tensile strength is an imperative characteristic of tablet mechanical strength to maintain integrity during processing, packaging, transport, and patient use (Pitt and Heasley, 2013).

Nevertheless, relative weakness in the tablet's mechanical strength is required to make a breakable tablet within a human body and release its contents. The accepted values of tensile strength differ according to the prepared formulation. Generally,

mechanical strength greater than 1.7 MPa is sufficient for tablets to withstand manufacturing processing, while some tablets are intended to be prepared with a low tensile strength that can be lower than 1 MPa (McCormick, 2005a; Pitt and Heasley, 2013).

The prepared formulations of ODTs-control, IND and pellets were tested using the hardness test. The dimensions for all tablets were recorded using the digital calliper and applied along with hardness values in tensile strength calculations as in Figure 6.7. Tablets' weights and dimensions were almost identical with no variations among the prepared tablets; for instance, 13.1 ± 2.8 mm and 13.1 ± 3 mm were the diameters and thickness of lactose and mannitol tablets, respectively.

Using one-way ANOVA, all lactose prepared tablets demonstrated accepted tensile strength with no significant difference using the same particle size lactose or different sizes. Similarly, no statistical difference was detected between hardness results indicating the uniformity of tablets dimension that can be achieved using all the particle sizes of lactose. These findings were in accordance with YM results (Figure 6.6), showing high initial particles plasticity for 125 and 500 μm batches compared to 63 μm batches that showed the same trend in tensile strength results (Figure 6.7). It can be assumed that particles' shape and surface roughness significantly affected mechanical properties. Hence, it was reported that the irregularity in shape and surface roughness of the particles aid in the bonding and interlocking of the particles (Abdel-Hamid, Alshihabi and Betz, 2011).

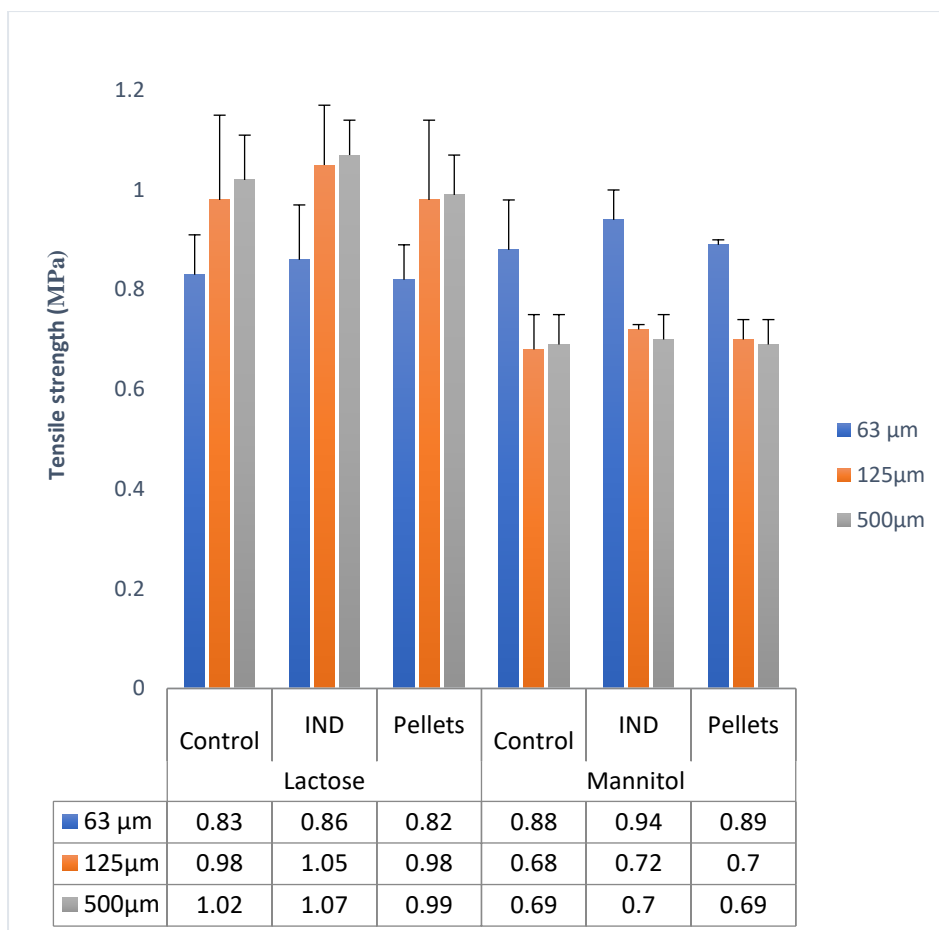


Figure 6.7 Tensile strength (MPa) values of Control (ODT), indomethacin (IND) mixed with ODT, and pellets embedded in the ODTs of lactose and mannitol

On the other hand, the tensile strength of the same particle size mannitol of different ODTs content had no difference demonstrating a similar trend with YM results. However, mannitol batches of 63 μm particle sizes behaved differently from 125 and 500 μm of the same ODTs content. Surprisingly, comparing lactose and mannitol tablets of the same particle size showed a significant difference between 125 and 500 μm batches, and only 63 μm particle size batches were consistently similar. Hence, the difference in tensile strength within mannitol batches was caused by 63 μm mannitol batch, while 125 and 500 μm showed harmonised results using *t*-test. These findings could be associated with different factors, including the particles' shape, physical and rheological characteristics of each particle size, surface roughness, particles arrangements, and particle distribution during tablet compression (Abdel-Hamid, Alshihabi and Betz, 2011; Deb *et al.*, 2018). However, the critical factor that is consistently causing the reported variations is mainly the particle size.

Generally, all YM results were > 6 MPa indicating that all formulations acquire a plastic tendency enough for tablet preparation. However, mannitol batches of larger particle size demonstrated the lowest YM causing difficulty for tablets preparation. Also, YM and tensile strength results showed that lactose batches generally possessed a higher plastic property than mannitol (Figure 6.6 and Figure 6.7). However, 63 µm mannitol batches presented a high tensile strength with low YM in 125 and 500 µm. This exciting finding indicates that the coherence between YM and tablets tensile strength could vary according to different factors such as particles composition, intra-porosity, surface roughness, elastic-plastic deformation and particle-particle contact points (Tho and Bauer-Brandl, 2011; Pitt and Heasley, 2013; Cabiscol *et al.*, 2018). However, such variation could be reduced and showing no difference as detected from the similarity of lactose and mannitol 63 µm tensile strength that was coherent with the YM comparison of lactose mannitol 63 µm raw powder. Therefore, it can be stated that limited variation could be generated in the mechanical properties of tablets using small particle size powder rather than the larger one (Singaraju *et al.*, 2016) (Ziffels and Steckel, 2010; Vanhoorne *et al.*, 2016).

These findings indicate that mannitol and lactose's cushioning filler was good enough to protect the embedded ingredients (pellets). Also, the materials within tablets could suffer the uniformity distribution problem owing to different surfaces properties. However, pellets sizes were bigger than ODTs matrix. Therefore, a higher number of pellets in the matrices is expected depending on the particles surfaces properties. The quantification of IND amount in the final formulation revealed such a relationship in the dissolution test.

This variation could be related to two facts: firstly, the difference between mannitol and lactose's physical structure in the degree of crystallinity. It was reported that mannitol possesses a crystalline structure of alpha, beta, and delta phases. Subsequently, the presence of three phases within mannitol provide different behaviour under compression depending on the degree of each phase within the structure (Fronczek, Kamel and Slattery, 2003). Although lactose can exist in both amorphous or crystalline form, lactose tends to crystallise over time, associated with high plasticity to brittle tablets under compression (Listiohadi *et al.*, 2009) (Murphy, Prescott and Larson, 2005). Secondly, surface roughness and particles shape could affect the tablet's hardness; hence, Zhang *et al.* reported that lactose particles had higher strength than mannitol and required higher compression effort. The reason behind that was the high

surface smoothness associate with mannitol compared to lactose. Besides, mannitol tablets expansion after ejection was the other reason correlated with high elasticity compared to lactose (Zhang *et al.*, 2017).

Similarly, this was associated with our results showing the high tensile strength and YM related to all particles sizes of lactose compared to that of mannitol.

Also, owing to the difference in the hygroscopic property that is higher in lactose compared to mannitol, these two materials could behave differently owing to their original properties, which was detected with higher particle sizes showing additional differences contributed to the shape of the particles (Shiga *et al.*, 2014)(Listiohadi *et al.*, 2009)

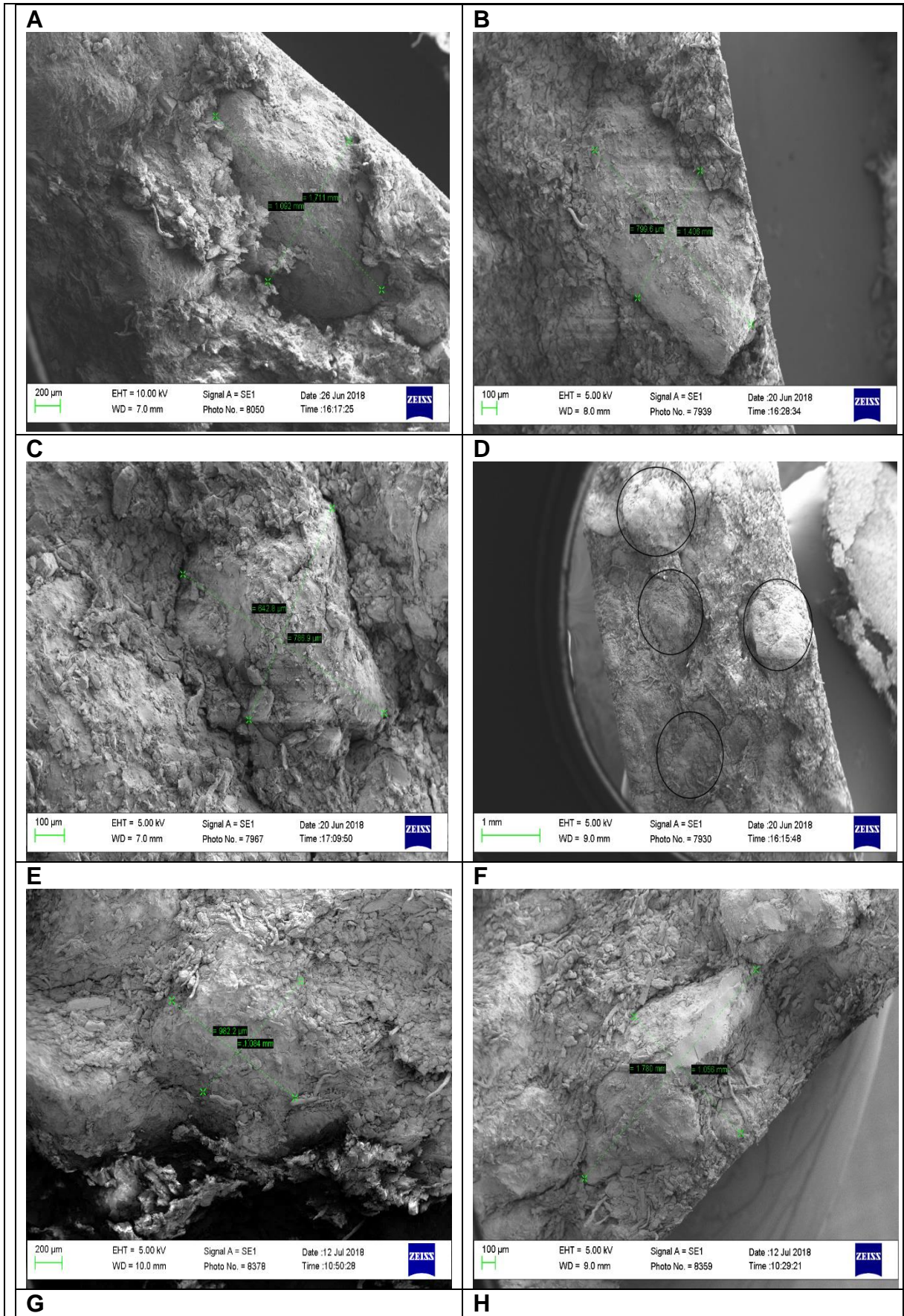
The molecules of water available within the particles in the form of crystals can affect the compact's tensile strength under the compression, leading to enhanced interparticle bonding more than that of low moisture content. Paluch *et al.* study showed that the tablets of hydrated particles demonstrated high tensile strength compared to tables of dehydrated particles; hence the bonds in the latter tablets formed either due to interlocking forces or thermal fusion, making a permanent deformation. Moreover, the study showed that the high ratio of the amorphous phase in the particles produced high tensile strength tablets compared to the anhydrous crystalline particles (Paluch *et al.*, 2013).

It was found by Westermarck *et al.* the tablets made of powder particles of mannitol showed an increase in surface area under compression from 0.58 to 0.61 m²/g with a reduction in porosity. On the contrary, the tablets based on granulated mannitol particles showed a reduction in the porosity, and ultimately surface area was reduced from 1.55 to 1.26 m²/g due to the particles' fusion (Paluch *et al.*, 2013)(Westermarck *et al.*, 1998). On the other hand, Busignies *et al.* study discussed the compression of tablets consisting of lactose, and the results demonstrated that the surface area of tablets increased with increasing the compression pressure and it then started to decrease with applying higher pressure indicating that the initial behaviour under compaction was owing to plastic deformation and further compaction resulting in the fusion of particles (Busignies *et al.*, 2011). When increasing the pressure, the particles placed between the punches migrate and start to form interlocking bonds, and further pressure can lead to elastic deformation of the particles then permanently deform plastically. The higher the pressure, the more particles' deformation leading to crushing or cracking particles then fuse, making larger particles (Paluch *et al.*, 2013).

Therefore, the large particles tend to break into small particles that can fuse, forming a larger surface area.

6.7.10 Lactose and mannitol ODTs morphology after compression

All ODTs of lactose and mannitol were evaluated using SEM and SM to detect the change in pellets integrity after compression of all particle sizes (Figure 6.8 and Figure 6.9). The results showed that both lactose and mannitol protected the pellets from being distorted by providing a supportive cushioning filler Figure 6.8 and Figure 6.9. Although different particle sizes were used to prepare ODTs, there was no considerable variation in the morphology between different sizes of both lactose and mannitol batches. However, 63 μm lactose and mannitol tablets showed coherent surface demonstrating good compatibility correlated with tensile strength results that showed the similarity between these batches. Also, the particles' variation after compression confirms the difference in particles sizes and their mechanical properties. Therefore, owing to the physical structure of lactose and mannitol that conveys a different degree of crystallinity, such variation in the reported results (mechanical and morphological findings) could be detected, indicating that lactose of physical structure possessed consistent mechanical properties with unnoticeable differences (Ziffels and Steckel, 2010; Vanhoorne *et al.*, 2016). Although pellets were detected similarly retaining their shape under compression from all batches, there was slight deformation in the pellets embedded in lactose 500 μm tablets than mannitol (Figure 6.8). However, the smaller the particle size, the less detected the difference between the two powders. Similar findings were reported by Paul *et al.* in assessing the effect of different grades of lactose and mannitol on tablets strength, and their results showed that the large particles exhibited a noticeable variation in plastic properties while using of equivalent particle size, which was obtained in small particles, had a similar degree of crystallinity (Paul *et al.*, 2019).



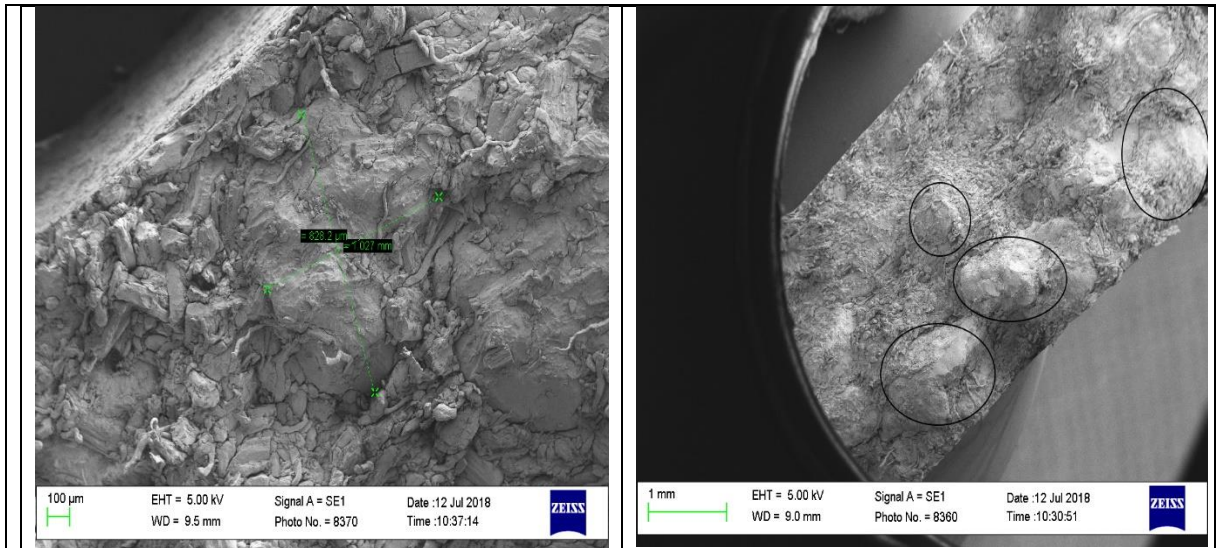
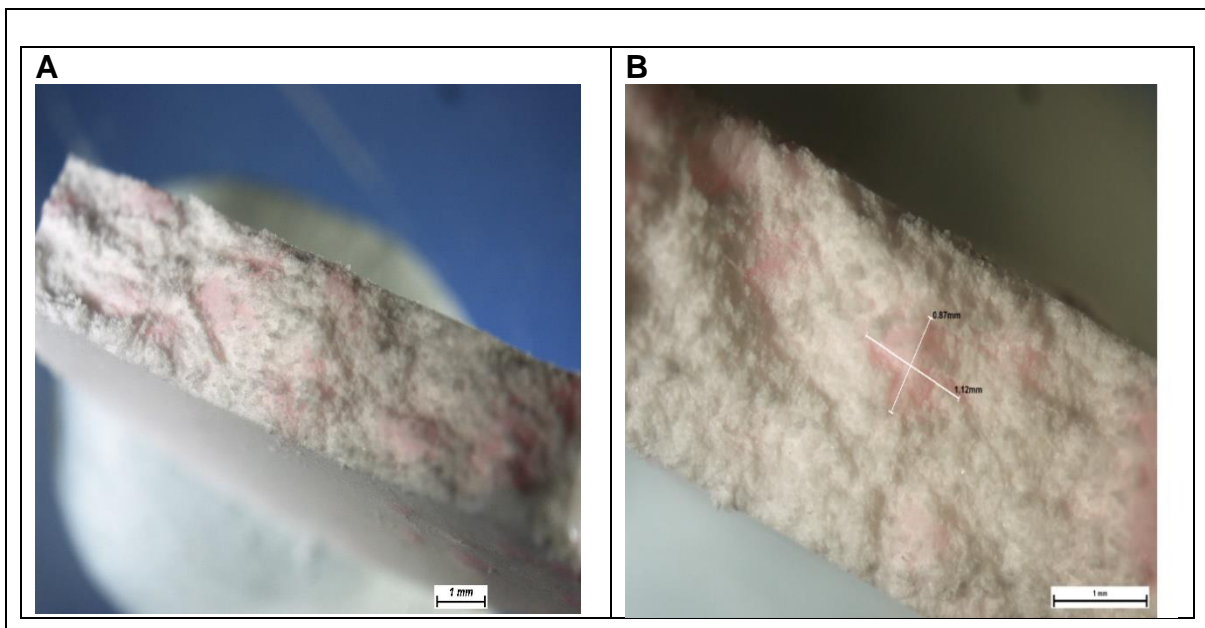


Figure 6.8 Micrographs of radial cross-sections from ODTs-pellets of lactose 63 μm (A), 125 μm lactose (B), 500 μm lactose cross-section (C), top view ODTs-pellets of 63 μm lactose (D), ODTs-pellets of mannitol 63 μm (E), 125 μm mannitol (F), 500 μm mannitol cross-section (G)



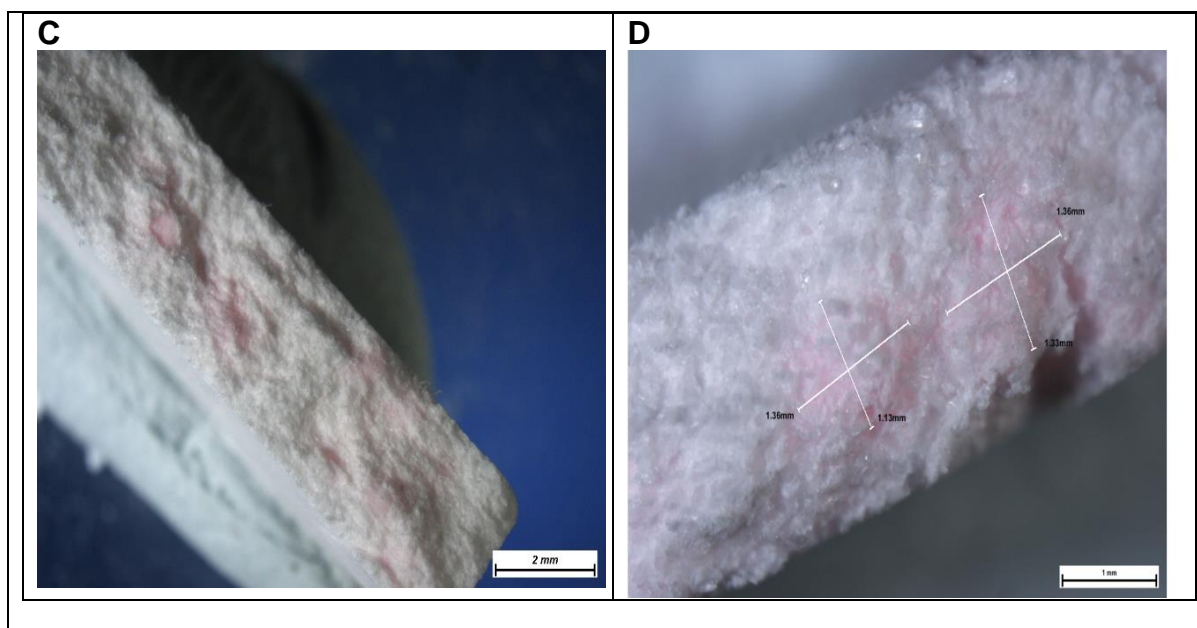


Figure 6.9 ODTs-pellets images from SM showing the distribution of the pellets within the radial cross-section tablets of lactose and mannitol A, B and C & D, respectively

6.7.11 Disintegration of tablets

Different factors affect disintegration time, including ingredients, the porosity of the tablets, and their weight. However, in our results, tablets demonstrated no significant variation in the tablets' weight and dimensions. Therefore, in this case, the disintegration time could be independent of porosity when using the same ODTs mixtures and thus correlated with tablets hardness. Harada *et al.* stated that disintegration time decreases when the porosity increases. They noticed that with increasing tablets weight, the disintegration time elongates (Harada *et al.*, 2010).

Moreover, the authors concluded that the disintegration time could be estimated by tablets hardness independently ODTs weight (Harada *et al.*, 2010). In our study, tablet hardness showed a similar trend between batches of the same particle size and different contents for lactose and mannitol. It can be stated that disintegration time could be predicted regardless of the porosity of the tablet. The results showed that the disintegration time of mannitol ODTs was not markedly different between different particle size ODTs of the same mixture (Figure 6.10). However, disintegration time was significantly different in the same size ODTs of different contents. This finding demonstrates ODTs components' influence on disintegration time than mannitol's particle size, as Hoag reported (Hoag, 2017).

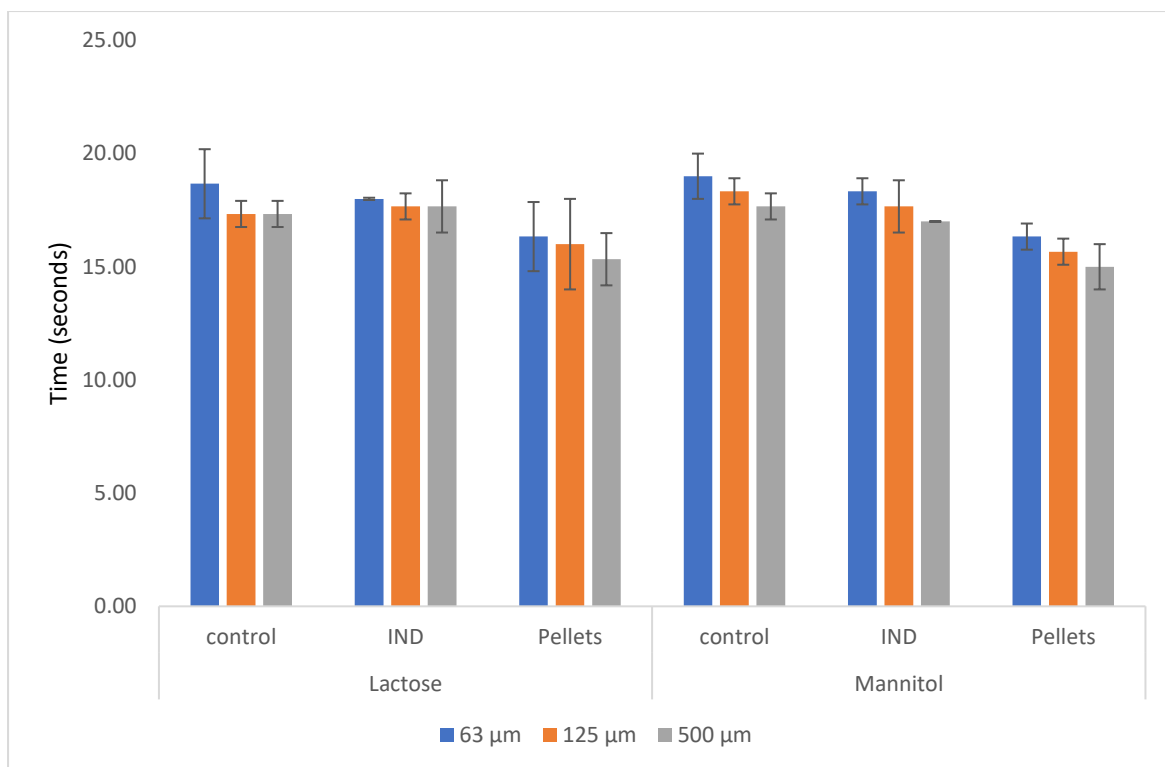


Figure 6.10 disintegration time of lactose and mannitol ODTs only (control), tablets of IND and pellets

Similarly, Daraghmeh *et al.* referred to the improved mannitol compressibility by adding other ingredients to enhance tablets formation and mechanical properties (Daraghmeh *et al.*, 2011)(Bansal, Balwani and Sheokand, 2019). The results of mannitol ODTs batches were in correlation with tensile strength evaluation. For instance, ODTs-pellets demonstrated the highest tensile strength from 63 μm, then 125 μm and the lowest from 500 μm of mannitol. The longest disintegration time was also recorded with 63 μm, 125 μm and the shortest with 500 μm mannitol of ODTs-pellets. Similarly, 63 μm mannitol showed the longest disintegration time in the other batches of ODTs alone (control) and ODTs-IND.

However, this trend was undetected with lactose that showed consistently short disintegration time equally with no statistical variation. Similarly, this finding was recorded by comparing the tensile strength of lactose batches that was coherent with no statistical variation. This correlation could confirm the adequate strength of lactose tablets and the homogeneous distribution of the materials within the produced ODTs producing the same effect consistently. In general, lactose and mannitol batches showed that the tablet's disintegration time was shortened with particle size increase. This can be explained by the high tendency of hydrophilic bond formation with larger particles (Hiremath, Nuguru and Agrahari, 2019). Besides, lactose batches showed a

shorter disintegration time than mannitol tablets. Kraciuk and Sznitowska detected a similar trend by recording faster tablet disintegration from lactose-containing tablets than with mannitol (Kraciuk and Sznitowska, 2011).

On the other hand, all lactose and mannitol particles sizes used in tablets preparation had no considerable influence on tablets water uptake capacity and water distribution. Therefore, using different particle sizes to prepare tablets is suitable, showing no significant difference in tablets disintegration exhibiting similar water interactions. Even Though different particle sizes were used to prepare tablets of lactose and mannitol, the tablets' water uptake capacity and water distribution were similar; thus, disintegration time was not significantly different. Similarly, Saripella, Mallipeddi and Neau reported that water interactions were equally detected from all corresponding samples of different particle sizes due to similar thermal properties (Saripella, Mallipeddi and Neau, 2014). This evidence supports lactose and mannitol tablets' good mechanical properties from all used particle sizes (Kraciuk and Sznitowska, 2011). Nevertheless, in our study, both lactose and mannitol showed a fast disintegration time < 30 seconds from all ODTs mixtures with no statistical variation between the batches of similar particle sizes (Figure 6.10).

6.7.12 Dissolution

According to British and US pharmacopoeia, IND release in both acidic (pH 1.2) (Figure 6.11 A and B) and phosphate buffer media (pH 6.8) (Figure 6.12-A and B) was measured (FDA/CDER, 1997; Council of Europe, 2005; British Pharmacopoeia, 2017). The results were recorded for all ODTs comprising IND and pellets using lactose and mannitol of all particle sizes 63,125 and 500 μm .

In acidic media, both lactose and mannitol ODTs of all particle sizes with pellets showed a similar trend of delaying IND release from the prepared tablets than ODTs-IND batches that showed a higher release of IND (Figure 6.11-A & B). Hence, all formulations of pellets released between 0.44 - 1.07% of IND at 120 minutes, while ODTs-IND batches showed a higher release profile of more than 9% at the same time point, demonstrating a significant difference between ODTs of pellets with the same particle size ODTs-IND ($p < 0.05$) using *t*-test. Moreover, ODTs-IND of lactose and similarly that of mannitol showed a remarkable difference in IND release at 120 minutes from all particle sizes ODTs. A similar trend was detected between IND

release from each different particle size of the ODTs-IND batches (according to *t*-test). However, that variation was undetectable by comparing ODTs-IND of lactose with mannitol of the same particle size demonstrating no difference in the release profile.

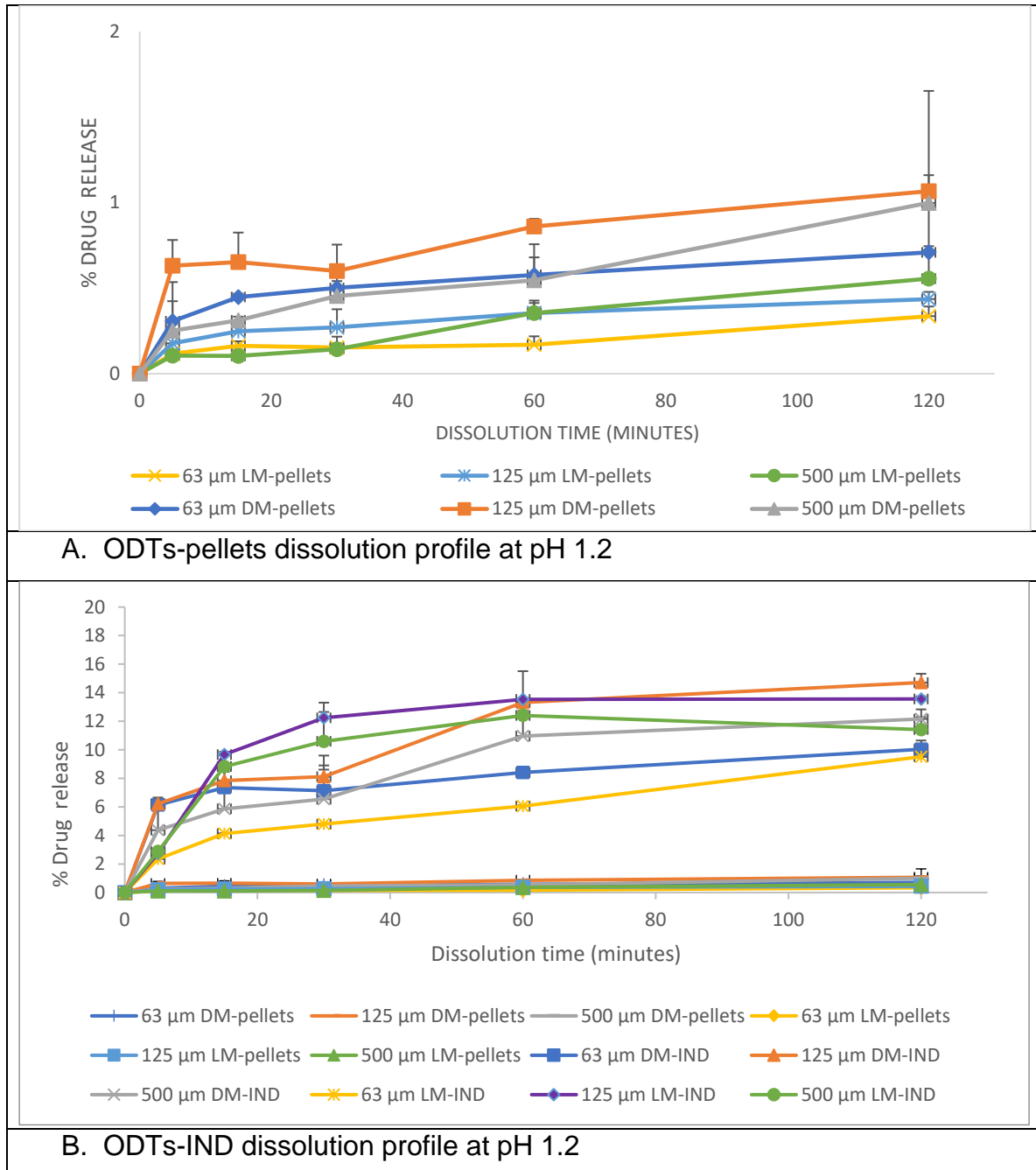


Figure 6.11 IND release profile from ODTs of lactose LM-pellets & LM-IND and mannitol DM-pellets & DM-IND in acid (A & B)

These findings indicate two facts; firstly, the distribution of IND powder within ODTs tablets was equivalent between lactose and mannitol, showing a similarity in the release profile with no statistical difference. Secondly, the sieving method effectively

collated an almost similar particle size range with minimum variation, indicating the analysis's reproducibility.

On the other hand, even though IND release was similarly delayed from all mannitol ODTs -pellets, there was no remarkable difference in IND release profile using different particle sizes of mannitol at time points 30 and 120 minutes. Therefore, using different mannitol particle size powder as a cushioning filler to prepare ODTs had no significant effect on IND release from all pellets. On the contrary, according to one-way ANOVA, IND release showed a significant difference using lactose ODTs of 63, 125 and 500 μm with pellets after 120 minutes (Table 6.4). These results agreed with the elasticity profile for mannitol and lactose. Hence, ODTs-IND of mannitol showed a significant difference in YM values of all particle sizes ODTs-IND, and no such variation detected in ODTs with pellets. Moreover, lactose showed a remarkable variation of YM results in ODTs-pellets and ODT-IND batches; hence 125 and 500 μm batches showed a similar trend, and the variation was owing to 63 μm particle size batches. This was correlated with dissolution results that showed a significant difference between IND release from 63 μm ODTs with pellets compared to 125 and 500 μm batches and similarly to ODTs-IND powders (Table 6.4). However, IND release was continually delayed within 30 minutes from all lactose-pellets batches with no remarkable difference.

Table 6.4 Statistical analysis of *t*-test ($p < 0.05$) for ODTs-lactose of 63, 125 and 500 μm with pellets in 30- and 120-minutes time in acid media (pH 1.2) (vs: versus)

Tablets of lactose (μm)	Time (minutes)	Statistical difference ($p < 0.05$)
63 vs 125	30	Not significant
63 vs 125	120	Significant
63 vs 500	30	Not significant
63 vs 500	120	Significant
125 vs 500	30	Not significant
125 vs 500	120	Not significant

The consistency in controlling IND release from lactose and mannitol batches indicates the validity of any particle's sizes to prepare the cushioning filler for preparing DRP-ODTs. Although all lactose batches demonstrated a delay in IND release, a significant difference was detected in the 63 μm particle size batch after 2 hours. Two assumptions can be revealed from these facts; first, the difference in IND release from lactose ODTs at 2 hours is associated with pellets' incompetence mechanical properties to withstand the applied pressure under compression. The second is that lactose tablets of 63 μm were sufficient to protect the pellets during tablet compression, maintaining their integrity. Hence, IND release was the lowest from that batch associated with YM variation from 125 and 500 μm batches. Nevertheless, the first assumption is weaker than the second since such variance should be detected in mannitol batches, indicating consistent behaviour correlated to the sufficient mechanical attribute. Therefore, we accept the second fact of using a suitable cushioning filler that provides enough pellets support to reduce the compaction pressure's deformation effect during tablet preparation.

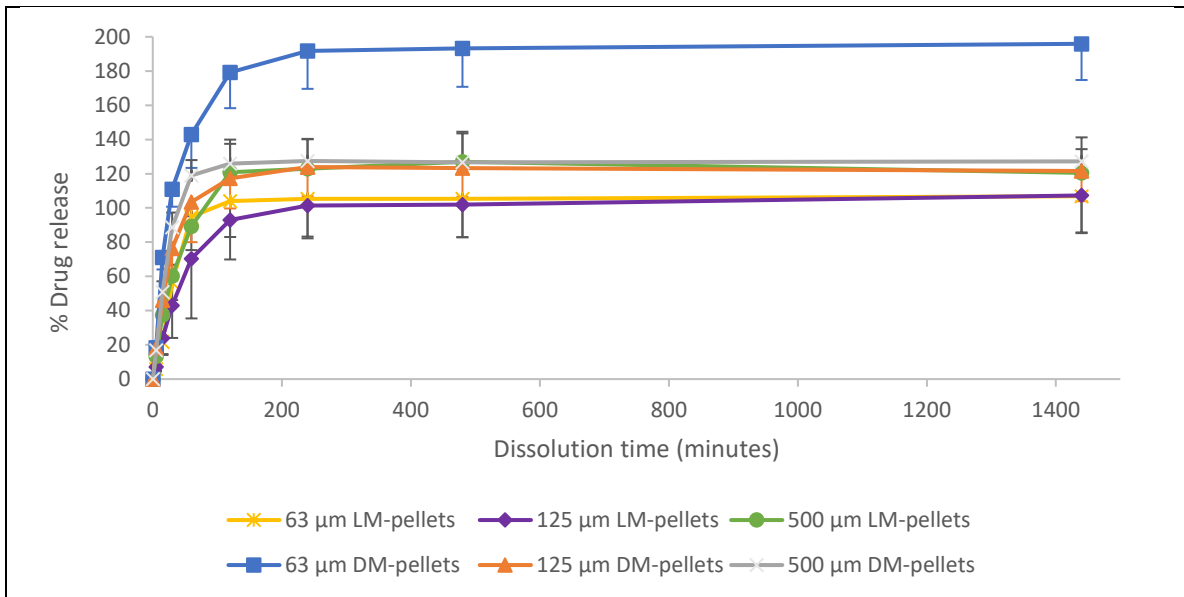
At the same time, mannitol with lactose 125 μm batches showed a significant difference in IND release (

Table 6.5). Therefore, detecting the lowest IND release, 63 μm particle size was the suitable batch that showed consistency in the statistical analysis first among mannitol batches 125 and 500 μm , second with lactose batches (125 and 500 μm) and third in the comparison between mannitol and lactose tablets of 63 μm . These findings correlate with the hardness results that showed no difference in comparing lactose and mannitol ODTs with pellets using 63 μm particle size. Moreover, mannitol ODTs-pellets demonstrated a significant difference between 125 and 500 μm tensile strength with 63 μm . This finding indicates that 63 μm particles adequately support the pellets to maintain their function under compression. This can be explained by the smaller the particle sizes, the larger the surface area, and the higher the strength (Hu *et al.*, 2020). Besides, the homogeneity of smaller particle sizes of powder can be associated with the desired drug release profile and final batch properties (Singaraju *et al.*, 2016). Furthermore, there is a necessity to assess the pellets integrity using different Eudragit L100 particle sizes and select the suitable size for optimizing the formulation.

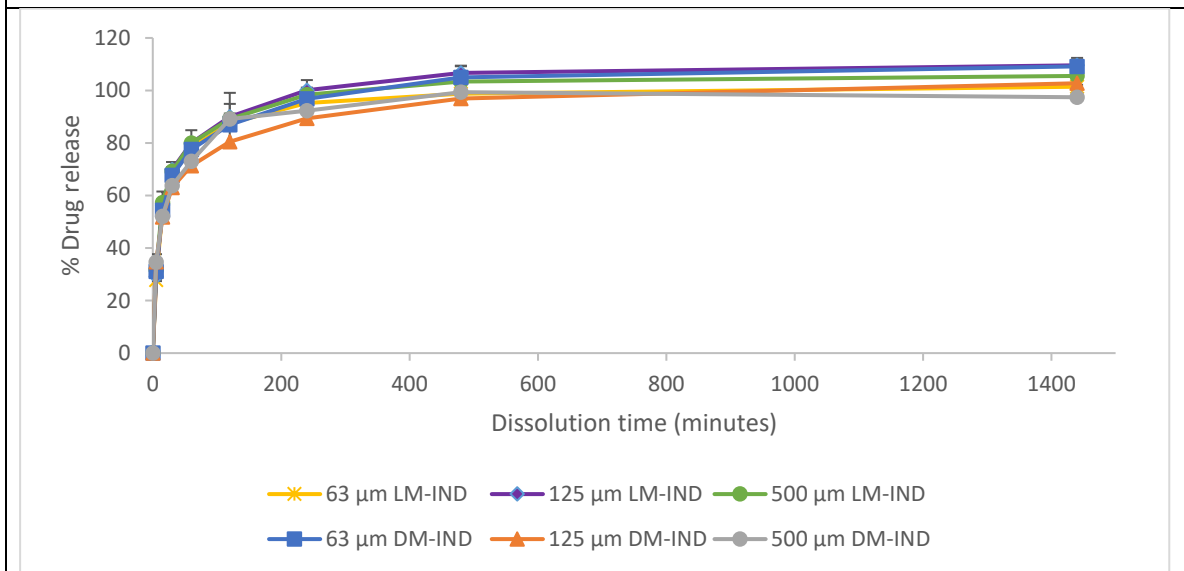
Table 6.5 Statistical comparison between ODTs-lactose and mannitol with pellets of same particle size powders 63, 125 and 500 μm in 30 and 120 minutes in acidic media according to one-way ANOVA ($p < 0.05$)

Tablets of lactose and mannitol (μm)	Time (minutes)	Statistical difference ($p < 0.05$)
63	30	Significant
63	120	Not Significant
125	30	Significant
125	120	Significant
500	30	Significant
500	120	Not significant

On the other hand, ODTs-IND and ODTs-pellets of lactose and mannitol of all particle sizes were evaluated in phosphate buffer (pH 6.8) to detect IND release as in Figure 6.12-A and B. One-way ANOVA for detecting IND release from the dissolution test of all lactose ODTs-IND at 30, 120, and 480 minutes showed a significant difference in IND release from all particle sizes. The same trend was detected between each two ODTs-IND of different particle size powder, according to the t -test ($p < 0.05$).



A. ODTs-pellets dissolution profile at pH 6.8



B. ODTs-IND dissolution profile at pH 6.8

Figure 6.12 IND release profile from ODTs of lactose LM-pellets & LM-IND and mannitol DM-pellets & DM-IND in phosphate buffer pH 6.8 (A & B) using 63, 125 and 500 μm particles

On the other hand, the comparison of ODTs-IND mannitol batches at 30, 120 and 480 minutes showed no noticeable difference between IND release from all particle sizes showing no evidence of using different particle sizes to generate a difference. The closeness of IND powder particle size from mannitol particles could generate these findings. However, YM and tensile strength results showed a significant difference between 63, 125 and 500 μm ODTs-IND.

Also, a significant difference was detected in acidic media from mannitol ODTs-IND, as reported earlier. Therefore, the other explanation to consider is the relative resemblance between mannitol and IND particles surfaces provided a high homogeneity of IND distribution during tablet preparation that affects the particles rearrangements and performance (Descamps *et al.*, 2007; Aubrey-Medendorp, Swadley and Li, 2008; Vanhoorne *et al.*, 2016; Su *et al.*, 2017). It can be assumed that the remarkable variance in IND release from lactose control compared to mannitol is related to the particle shape and the homogenised distribution of IND within mannitol compared to that of lactose. Therefore, sieving of IND powder could overcome such defects in distribution and provide minor variance. The comparison between lactose and mannitol showed that ODTs-IND demonstrated a similar IND release from 63 μm batches only at all proposed time points. However, 125 and 500 μm batches showed a significant difference. These findings followed tensile strength results that showed similarity between only 63 μm tablets of lactose and mannitol. Also, lactose-mannitol ODTs-IND comparison in acidic media equivalently released IND from 63 μm particle size tablets at a 120-minute time point. Besides, this similarity could be related to the homogeneity of both materials' small particle sizes; hence, raw powders of 63 μm of both materials showed similar YM. Moreover, all batches from lactose and mannitol ODTs control demonstrated consistent IND release > 80% within 120 minutes releasing time.

Therefore, two points could be concluded; the first is to use mannitol powder with no need for sieving nor using different particle size powder to prepare ODTs-IND.

Secondly, IND particles shape variation with lactose particles affected the IND distribution within ODTs and thus the necessity of using IND of similar particle size when combined with sieved lactose particles to even drug distribution within ODTs.

On the other hand, all lactose and mannitol ODTs-pellets showed more than 90% IND release within 120 minutes. All lactose batches of ODTs-pellets showed a significant difference at time points 30 and 120 minutes. However, that difference was undetectable at 480 minutes. Similarly, IND showed a similar trend at 480 minutes in comparing lactose batches ODTs-pellets and ODTs-IND of similar particle sizes. This indicates a significant effect of particles shape and the available contact points between pellets and all particle sizes embedded in ODTs. A similar reason was

discussed earlier regarding the difference in mechanical properties (Tho and Bauer-Brandl, 2011; Pitt and Heasley, 2013; Cabiscol *et al.*, 2018). Although lactose ODTs-pellets showed significant IND release at 30 and 120 minutes, ODTs-pellets showed a similar IND release at 480 minutes. The reason behind that could also be related to the difference in particles shape and particle size effect. However, such variation in the initial release profile has a limited effect on the final IND release.

On the contrary, Lactose ODTs-IND showed consistent differences between all the used lactose sizes at 30, 120 and 480 minutes. The opposite trend was detected from ODTs-IND of mannitol that showed IND released similarly from all batches. Also, the difference was detected with all mannitol ODTs- pellets at all time points. This finding is related to the high similarity with mannitol and IND particles, and the difference in particles surfaces suggested such difference in pellets batches.

Mannitol ODTs- pellets showed a statistical difference in IND release within 30 and 120 minutes in phosphate buffer media between 63 and the other 125 and 500 μm mannitol batches. Therefore, in harmony with previous results, the pellets' distribution is affected by particle size, particle shapes, and surface roughness. Hence, the variation was detected between small particles compared to the larger particles that showed similar trends as in 125 and 500 μm .

In mannitol ODTs-IND, variation was missing, which confirms the similarity of the particle's roughness and shapes that facilitated the homogenous distribution of the IND particles within mannitol of all particle sizes (Tho and Bauer-Brandl, 2011; Pitt and Heasley, 2013; Cabiscol *et al.*, 2018). However, all the prepared batches of IND and pellets from lactose and mannitol (63, 125 and 500 μm) showed IND release $\geq 80\%$ within 120 minutes in buffer media. Furthermore, the lactose-mannitol ODTs-pellets comparison showed a consistent release from all batches at 480 minutes. The only batch that showed a significant difference was mannitol ODTs-pellets of 63 μm .

The comparison of lactose ODTs-pellets to ODTs-IND of the same size and similarity in mannitol showed a consistent IND release after 480 minutes, yet only mannitol 63 μm batches were remarkably different. The 63 μm lactose can improve patients compliance with no taste disturbance (Kathpalia *et al.*, 2014)(Patil *et al.*, 2016)(Kakar, 2018). Therefore, it can be applied for future applications to prepare ODTs.

6.8 Results and discussion of the second study

6.8.1 Powder characterization

Solid oral dosage forms depend on the primary materials' properties to prepare the final formulation. In order to prepare a well-compacted system of delayed-release IND pellets to be used in the ODTs, we prepared the IND pellets from different Eudragit L100 particles sizes (45, 63 and 90 μm) and examined the effect of the particles sizes of the pH-dependent polymer and their physical/ mechanical properties. The collected powders using sieve analysis were characterized individually to examine the particle size effect (Figure 6.13).

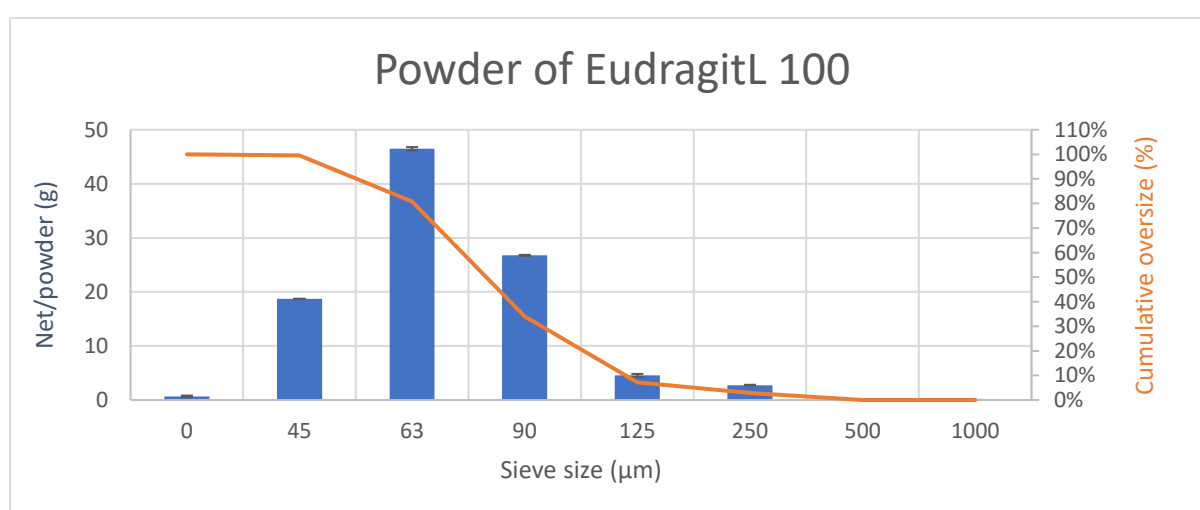


Figure 6.13 Relationship between the cumulative oversize (%) and net powder retained from each sieve using sieving analysis

6.8.2 Powder flowability and density

In pellets preparation, adhesive and cohesive forces can generate between the particles of Eudragit L100 and other excipients, causing agglomeration of the particles (Loh, Samanta and Sia Heng, 2014). Hence, adhesive forces occur between particles of different materials or surfaces, while cohesive forces occur between similar material particles (Li, 2005). These forces can include solid bridges between the particles due to a change in the particles' physical properties, such as elevating the temperature caused by friction or preparation process, particles attracting forces of differently charged surfaces and liquid bridges from the moisture content or water molecules (Li, 2005). The contribution of the mentioned forces can vary depending on different

factors such as particle size, shape, bulk density, surface area, and mechanical properties, which affect the quality of the pellets.

Furthermore, irregular surfaces lead to interlocking bonding and forming agglomerates (Loh, Samanta and Sia Heng, 2014). Hence, the particles agglomerate together through interlocking bonds when particles have rough surfaces or fissured (Yang and Zhang, 2017) (Kangulu, 2009). Therefore, evaluating powder particles physical properties is essential. Flowability for all particles of 45 μm , 63 μm , 90 μm size was measured to assess the ability of the particles to settle and compress. The compressibility index and Hausner's ratio of all Eudragit L100 particle sizes were studied in Table 6.6. It was found that the flow character of all particles was acceptable, ranging between excellent and fair, to be selected in pellets preparation. This is related to the fact that interaction is less significant between the particles of powders with good flowability as the values of bulk and tapped densities were close (Ortega-Rivas, Juliano and H, 2005). Although powder of 45 μm showed fair flowability, the bulk and tapped density were close to other sizes values and no remarkable difference between the results (SD was zero).

Moreover, only for the materials of poor flowability, a remarkable difference between bulk and tapped densities can be noticed as such, these materials are not preferable to be used in forming compacts (Sheehan, 2013).

Loh, Samanta and Sia Heng reported a similar trend. The particles lower than 30 μm tend to have more cohesive forces and reduced powder flow (Loh, Samanta and Sia Heng, 2014).

Table 6.6 Compressibility index and flow properties of Eudragit L100 45, 63, 90 µm powder

Sample name	Compressibility index (%)	Hausner's ratio	Bulk density gm/mL (n=3)	Tapped density gm/mL	Flow character
Eudragit L100 45 µm	16	1.19	0.50	0.59	Fair
Eudragit L100 63 µm	12	1.13	0.50	0.57	Good
Eudragit L100 90 µm	8	1.08	0.50	0.54	Excellent

6.8.3 Morphology and size of powder particles

Stereomicroscope and SEM analysis were used to detect all powder particles' sizes and morphological characteristics. The microscope images showed the difference in sizes of Eudragit L100 particles which was correlated with the sieve analysis confirming the accuracy of the method to collect the powders of variant sizes. Also, most of the particles had spherical shapes and smooth surfaces (Figure 6.14), which was a helpful factor in producing a wet mass of good consistency after that easily prepared pellets.

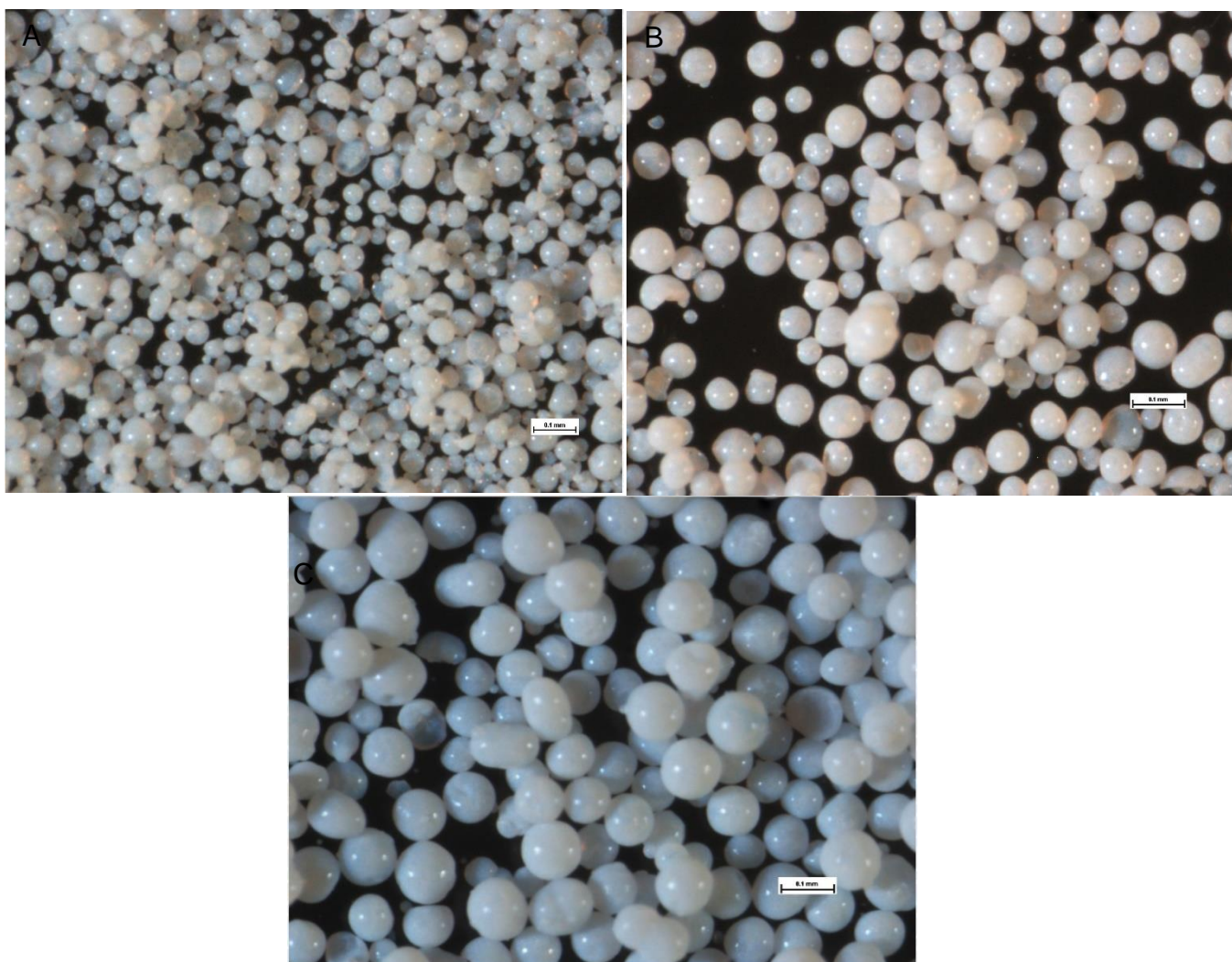


Figure 6.14 powder of Eudragit L100 with particle sizes of 45 μm (A), 63 μm (B), 90 μm (C) using a stereomicroscope

The other method to distinguish between the particles sizes and morphology was SEM (Figure 6.15). It can be observed from SEM images the differences in particle sizes of the powder particles and the presence of some other small particle sizes, which can be related to that the small particles can agglomerate and interlock during the sieving. Shi, Hao, et al. found that particles cohesiveness decreases with increasing particles sizes which was noticed with Eudragit L100 powder particles in our study (Shi *et al.*, 2018). Also, the other factor that can be considered for optimizing the sieving method is to increase the sieving time (Liu, 2009). However, the analysis was performed according to ICH guideline, and the findings were not markedly affecting the powder particles sizes properties due to the explicit differences between the compressibility

and flowability of the powder particles (Bp *et al.*, 2005)(ICH Harmonised Tripartite Guideline, 2010).

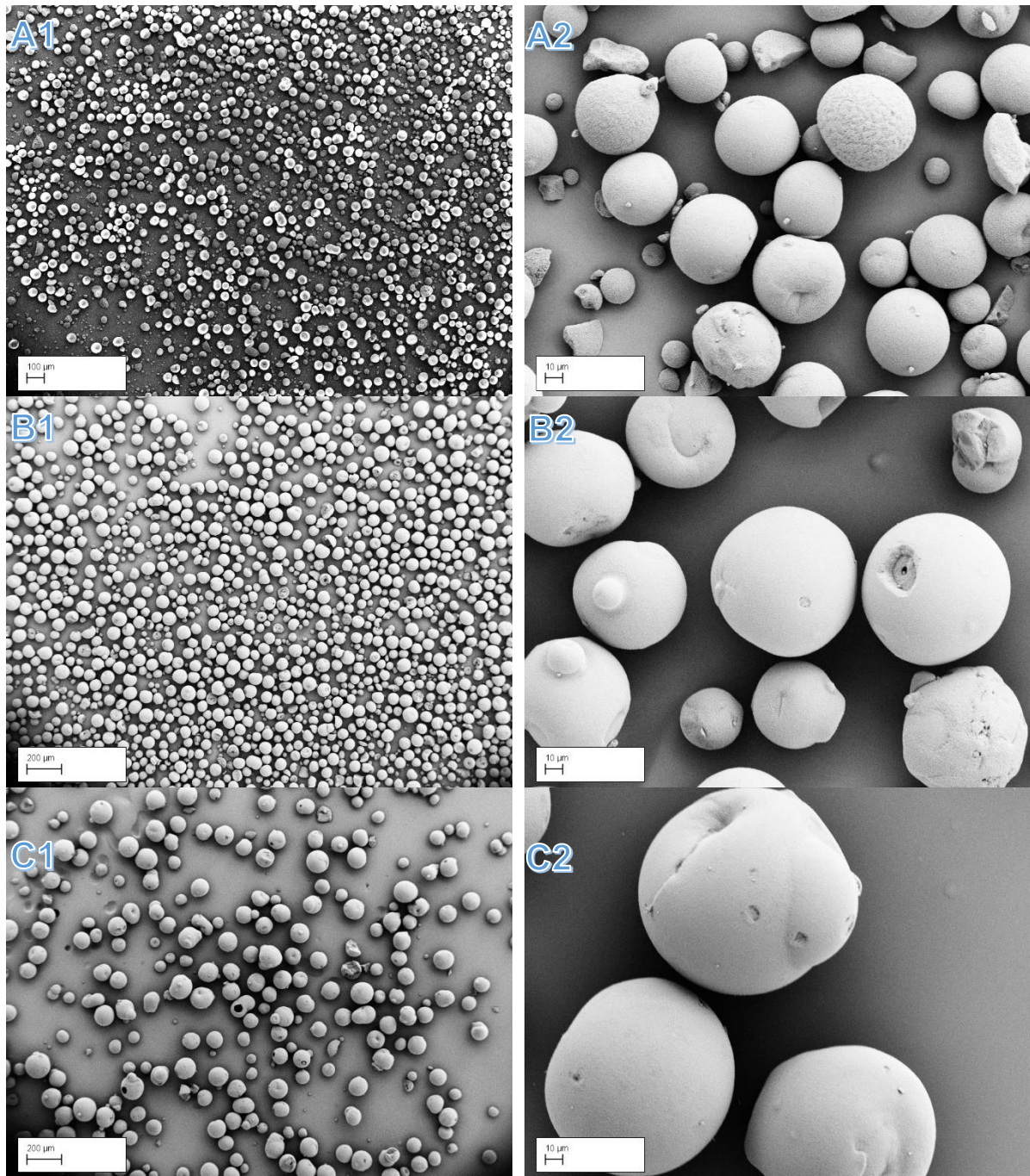


Figure 6.15 SEM images of low and high magnification showing the particles Eudragit L100 powder with particle size of 45 µm (A1, A2), 63 µm (B1, B2) and 90 µm (C1, C2)

6.8.4 Texture analysis

The other characterization was to study the elasticity profile of Eudragit L100 particles to calculate YM (Table 6.7). Hence, the ability of the material to form a compact depends on its tendency to deform permanently (plasticity) or temporary (elasticity). YM, which is the relationship between the applied stress on the martial particles and the strain (change in dimensions), was used to measure the elasticity of particles and their ability to protect their shapes under the applied force. The texture analyser with a maximum force of 300 kg was used, and the obtained graph extrapolated to get the gradient (stress/ strain)(F. Bassam *et al.*, 1990). All particle sizes showed low YM values contributing to good elastic properties as the lowest the YM's highest elasticity (F. Bassam *et al.*, 1990). Although the values were different, YM values were low, and there was no significant difference ($p>0.05$).

Bassam *et al.* examined the YM of the following excipients starch < MCC < sugars < inorganic fillers and divided them according to their stiffness 3.71 to 88.28 GPa ascendingly (F. Bassam *et al.*, 1990). The lowest value was considered elastic, and the highest had high stiffness. Therefore, our powders YM values reflected the good properties of Eudragit L100 particles to resist compression (Table 6.7). Thus, they considered being used in pellets preparations. In addition, for each batch, the standard deviation was low, indicating the analysis was consistent, and the minimum effect of the laboratory error could be detected (Table 6.7).

Table 6.7 Texture analysis results for Eudragit L100 powder 45, 63 and 90 μm (n=3) showing the YM as elasticity profile analysed with exponent software

Sample name	YM (MPa) (mean \pm SD)
Eudragit I100 45 μm	4.376 \pm 0.619
Eudragit I100 63 μm	4.751 \pm 0.502
Eudragit I100 90 μm	4.97 \pm 0.277

6.8.5 Porosity

The original excipients properties can affect the prepared pellets' physical and mechanical properties. Therefore, the porosity of the Eudragit L100 powder was measured for all particle sizes (Table 6.8). The 63 μm particles had almost similar porosity results to that of Eudragit L100 powder. This similarity was correlated with sieving data as the particles of 63 μm had the highest collected weight (retained) and high cumulative oversize, among other particles. Moreover, the porosity results are considered acceptable and showed a low effect on the powder mechanical properties. According to YM results, all particle sizes showed low YM with no significant difference ($p>0.5$). Similarly, all batches (45, 63, 90 μm) had low bulk densities with similar values ($p>0.5$), which was not affected by Eudragit L00 powder porosity. Nevertheless, the slight difference in porosity can be related to the difference in particle sizes, which can be seen in SEM images. Hence, the smaller the particle size, the more compacted surfaces could be noticed later in the pellets section (Ogolo *et al.*, 2015). Finally, the particles had a pore diameter between 2- 50 nm demonstrating mesoporosity. Hence, surface area and total pore volume are proportional (Table 6.8)(Suresh Kumar *et al.*, 2019).

Table 6.8 Porosity measurements for Eudragit L100 raw powder, 63 μm and 90 μm particles using Belsorp analysis and BET equation

Sample	Surface area ($\text{m}^2 \text{g}^{-1}$)	Total pore volume ($\text{cm}^3 \text{g}^{-1}$)	Mean pore diameter (nm)
Eudragit L100 Raw	2.280	0.051	8.97
Eudragit L100 63 μm	2.285	0.062	10.94
Eudragit L100 90 μm	2.249	0.059	10.53

6.8.6 Pellet's characterization and micrometric properties

Eudragit L100 powder of each particle size 45 μm , 63 μm and 90 μm was used in pellets preparation with sorbitol as a plasticizer and water as granulating fluid. Extrusion spheronization was used to prepare all the batches. The pellets were

evaluated according to the three batches' shape, size, and mechanical properties. Through the results, the pellets are named according to the size of Eudragit L100 prepared from, for instance, 45 μm pellets or batch of 45 μm indicated to the pellets prepared from Eudragit L100 45 μm particle size.

6.8.6.1 The effect of particle size on the yield, bulk density and flowability

The pellets prepared from particles sizes of Eudragit L100 powder 45, 63, 90 μm were successfully obtained with an acceptable % yield (Table 6.9). The pellets 45 μm had the lowest yield, 58%, while the highest was 66%, for the 90 μm batch among the prepared pellets from sieved powders. This difference can be related to the difference in particles sizes of the initial powder as the small-sized particles tend to aggregate, forming agglomerates of strong adhesion forces that were difficult to extrudate, which was noticed in our study (Ashraf *et al.*, 2018). Also, when particles sizes reduce, the surface area increases and inter particulate forces generate between the fine particles, as discussed in the introduction (Hart, 2015). Therefore, yield varied among the pellets of sieved batches, and the difference in sizes had a minimum effect on pellets prepared from raw powder, which showed a 72% yield.

Moreover, it was found that the AR of the pellets was lower than 2 mm and all of the batches showed acceptable sphericity (Table 6.9). However, the pellets with high sphericity were obtained from 90 μm batch (AR 1.25%) that was close to the reference value of raw powder pellets (AR 1.30%)

On the other hand, flow property can significantly affect pellets' quality in tablet preparation. This is because flow property depends mainly on bulk density and particle size, as small particles tend to flow less than bigger particles (Choudhary and Avari, 2015).

Besides, the material ability for packing is measured by its bulk density, and any difference in bulk density can influence packing volume (Organization, 2012b). In general, all batches showed a low value of bulk density between 0.53-0.66 g/cm^3 and a flow rate of 4.5 to 5.1 g/sec , as in Table 6.9. Although the values differed among the batches, the bulk density of all pellets showed an acceptable value. However, other factors, including particle shape and surface properties, offer different particle-particle adherence influencing the pellet's flowability and bulk density (Kudo, Yasuda and Matsusaka, 2020) (Bodhmaghe, 2006). Low bulk density could be related to large voids

between the packed particles of larger size surfaces. Simultaneously, the smaller particles can fill in the voids between bigger particles, rearranging powder density and occupying the unfilled voids (Bodhmaghe, 2006). It was stated that pellets of low bulk density $< 1.25 \text{ g/cm}^3$ indicate good flowability (Choudhary and Avari, 2015)(Kaur *et al.*, 2020). Therefore, in our study, the pellets showed good flow properties. Moreover, the obtained flowability is due to the pellets' good sphericity since AR for all pellets is lower than 2 mm. The difference between the batches can be attributed to the improved sphericity of pellets 90 μm compared to other batches with lower AR 1.25%. Hence AR values were significantly different between batches ($p < 0.5$) (45, 63 & 90 μm). Although 45 μm and 63 μm batches showed high AR 1.52% and 1.49%, the difference was insignificant ($p = 0.76$). Similarly, 45 μm and 63 μm batches had equivalent flow rates. The latter can be associated with similarity in bulk density values for both batches; hence density affects the flow rate in addition to the AR effect (Kanwar, Kumar and Sinha, 2015)(Choudhary and Avari, 2015).

Moisture content difference between the batches could be correlated to particles sizes variance and their ability to retain water. This ability depends mainly on the porosity and surface area of the particles. Therefore, it can be noticed that pellets 63 μm batch had higher moisture content (6.05%) compared to other batches, which is correlated with the high surface area of the original particles ($2.285 \text{ m}^2 \text{ g}^{-1}$). The value of moisture content is acceptable unless the value is less than 1%, indicating the low hardness of pellets and crush easily upon compression.

Table 6.9 Pellets physical and micrometric properties, pellets named according to the size of Eudragit L100 powder prepared from

Batch	Aspect ratio% (Mean \pm SD) (n=30)	Yield %	Moisture content %	Bulk densi ty gm/m L (n=3)	Flow rate (g/sec) (n=3)
EudargitL100 pellets	1.30 \pm 0.25	72 %	6.58%	0.66	4.5 \pm 0.50
45 μm pellets	1.52 \pm 0.37	58%	4.09%	0.53	4.3 \pm 0.02
63 μm pellets	1.49 \pm 0.26	61%	6.05%	0.53	4.3 \pm 0.10
90 μm pellets	1.25 \pm 0.17	66%	5.11%	0.56	4.93 \pm 0.40

6.8.6.2 Morphology and size

The pellets top overview and their AR were recorded for 45, 63 and 90 batches, as shown in Figure 6.16, Figure 6.17 and Figure 6.18, respectively. SEM images showed the pellet morphology and aspect ratios in harmony with the AR of the manual method (calliper). The pellets have a smooth surface and low AR. Also, the results showed the difference in porosity of the pellets as in the 90 μ m batch, and the pellet showed porous surfaces with high roughness. The results agreed with pellet porosity results as 90 μ m batch showed the highest specific surface area and pore volume $5.26 \text{ m}^2 \text{ g}^{-1}$ and $0.01 \text{ cm}^3 \text{ g}^{-1}$. The pellets were explicitly detected after compression within tablets, as in Figure 6.19, showing a pellet of the 90 μ m batch embedded in the ODTs.

In comparison, 45 μ m batch had very smooth surfaces, and minimum pores voids could be noticed within the pellet's surfaces. Similarly, these results were correlated with porosity results as 45 μ m batch demonstrated the lowest surface area ($3.26 \text{ m}^2 \text{ g}^{-1}$) and pore volume ($0.007 \text{ cm}^3 \text{ g}^{-1}$). However, the lowest porosity values for raw powder were noticed in 90 μ m particles and indirectly correlated with the produced pellets. The porosity of 63 μ m pellets was intermediate among pellets, while the initial powder 63 μ m had high porosity and specific surface area. However, the porosity of the initial particles had a limited effect on final compact mechanical properties. For instance, the YM of 63 μ m was higher for initial particles than the produced pellets of

that batch. Therefore, it can be suggested that the spherical shape homogeneity of the initial particles corresponded to minimize the negative effect of porosity on pellets mechanical properties. Furthermore, particle size tends to form dens compact due to large contact points with a high surface area of the small particles(Khan *et al.*, 2019)(Hart, 2015). Therefore, low voids were available between the initial particles during compression.

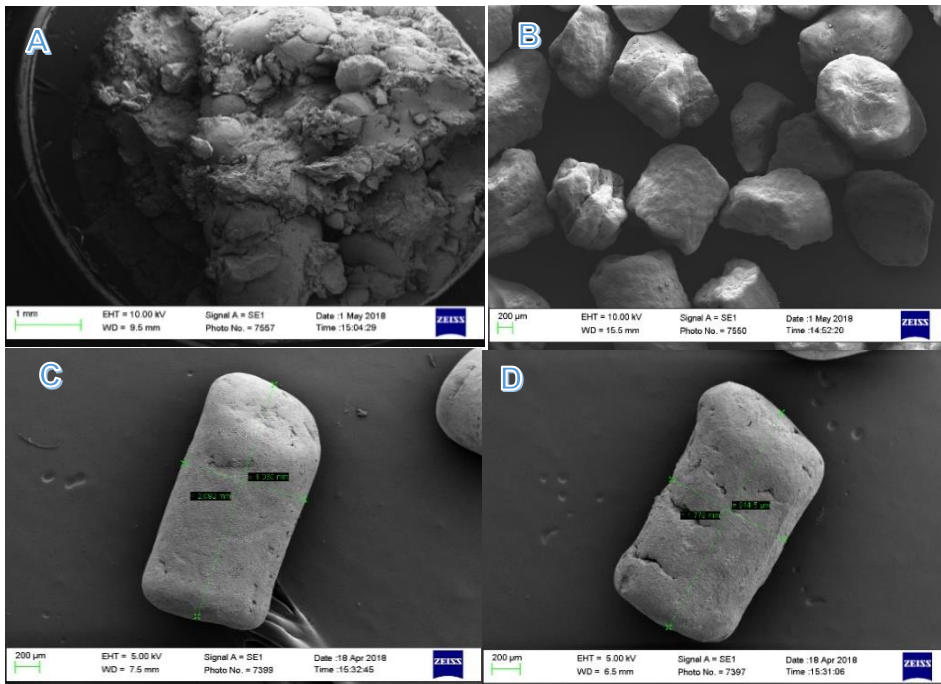


Figure 6.16 Pellets of 45 µm Eudragit I100 showing compressed pellets with texture analysis (A) general pellets image (B) & AR (C &D)

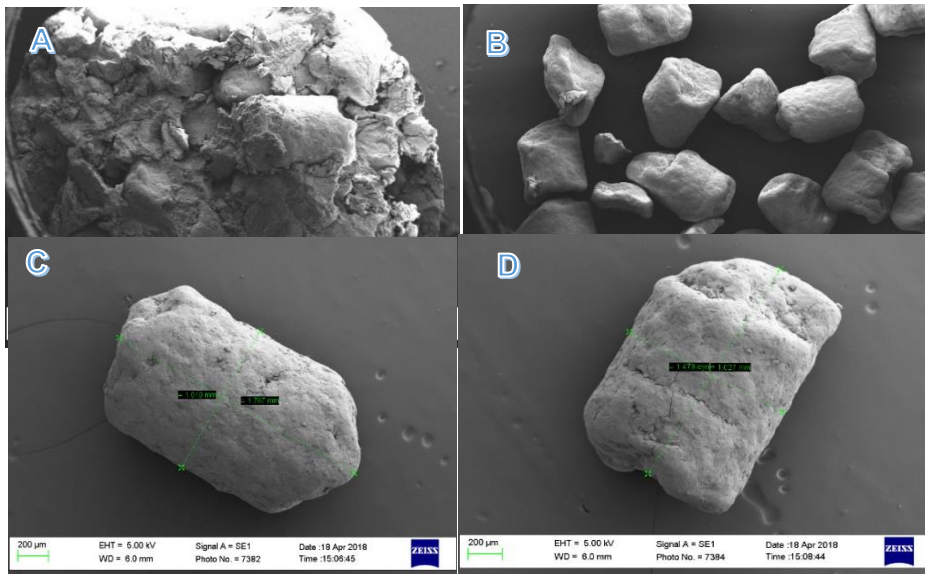


Figure 6.17 Different SEM images for 63 μm batch showing pellets after compression with texture analysis (A), general overview for pellets (B) and top view AR (C & D)

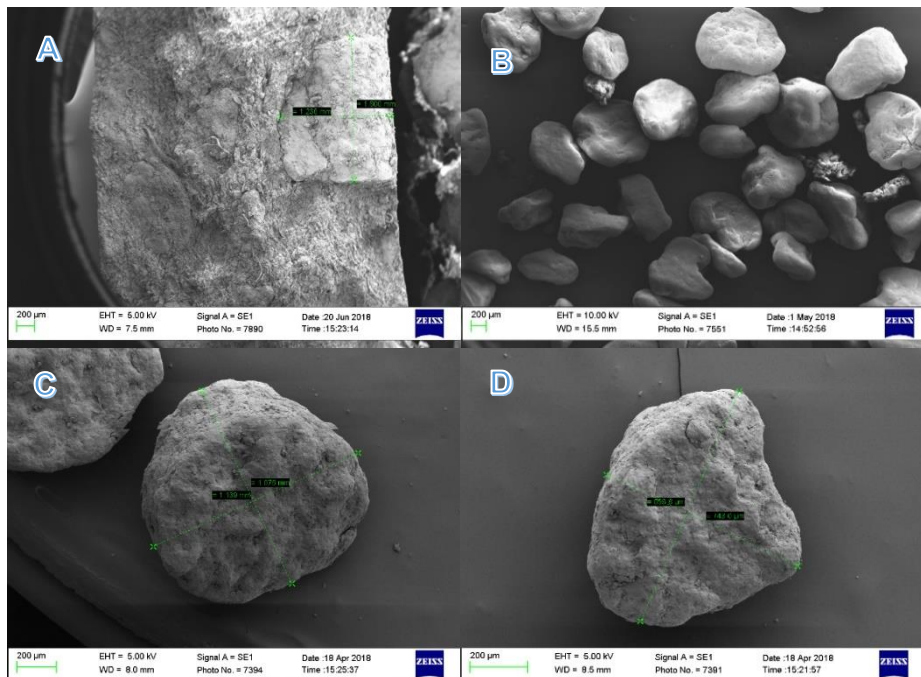


Figure 6.18 SEM images of 90 μm batch showing pellets after compression with texture analysis (A), general overview (B) and top view for pellets with AR (C & D)

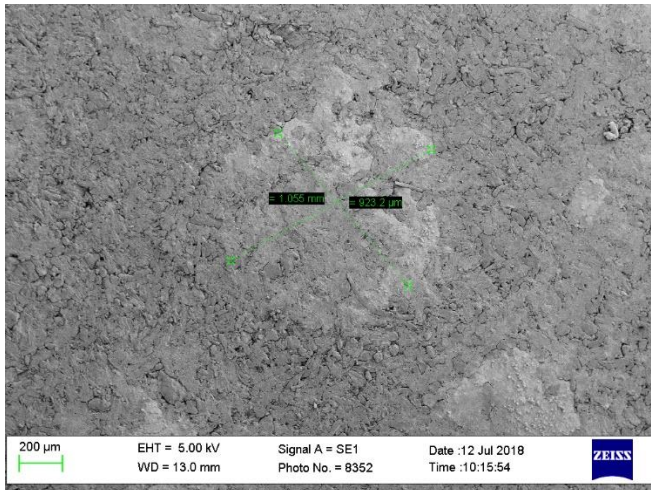


Figure 6.19 Top overview for pellets of 90 µm batch embedded in ODT showing AR using SEM

6.8.6.3 The porosity of the pellets

Pellet's porosity was measured for all the prepared batches as recorded in Table 6.10. According to the previously discussed and described powder data, the initial powder particles 63 µm has a higher porosity than 90 µm particles. This trend was inversely demonstrated for prepared pellets 63 µm batch. The pellets had a low surface area and pore volume of $4.44 \text{ m}^2 \text{ g}^{-1}$ and $0.009 \text{ cm}^3 \text{ g}^{-1}$, respectively, compared to other batches of sieved powders. This can be related to the fact that particles are subjected to compression during powder extrusion, reducing the particles' voids.

On the other hand, the starting material of 90 µm had low porosity, while 90 µm batch pellets had the highest surface area and porosity (as seen in Table 6.10). Thus large particles tend to agglomerate yet with porous structure as discussed earlier (inter and intra particulates voids between big particles) (Choudhary and Avari, 2015). It was reported that when pellets are prepared from brittle excipients of low porosity tablets and pellets compressibility can be influenced (Zainuddin *et al.*, 2014)(Thapa *et al.*, 2017). However, using primary powders with good elasticity is desirable to produce pellets of good mechanical properties and eventually tablets. Therefore, the low YM of primary particles minimized the effect of other parameters. Also, homogeneity particles' spherical shape helped produce pellets with good mechanical properties as in the texture analysis data(Li, 2006)(Shah *et al.*, 1995).

Moreover, other factors can change the porosity, such as AR, moisture content and parameters of extrusion spheronization such as time and speed. Hence, the lowest

AR (1.25%) correlated to a small diameter (1.21 ± 0.27) demonstrated by a 90 μm batch, leading to the high surface area. Also, since all materials had a mean pore diameter between 2-50 nm, these formulations are mesoporous. Therefore, the mesoporous material tend to show monolayer and multilayer as part of the Type IV isotherm.

Table 6.10 Porosity and surface area data for all batches of pellets prepared from raw Eudragit L100 particles (45,63 and 90 μm), pellets are named according to the size of Eudragit L100 prepared from

Sample	Surface area ($\text{m}^2 \text{g}^{-1}$)	Total pore volume ($\text{cm}^3 \text{g}^{-1}$)	Mean pore diameter (nm)
Pellets of Eudragit L100-raw	4.51	0.007	7.04
Pellets (45 μm)	3.26	0.007	8.24
Pellets (63 μm)	4.44	0.009	7.82
Pellets (90 μm)	5.26	0.01	7.67

6.8.6.4 Mechanical properties of pellets

The mechanical properties represented by YM, and tensile strength were measured using the texture analysis method for pellets.

6.8.6.4.1 The elasticity profile and hardness

The temporary deformation and fragmentation of pellets during compression are relatively correlated with the starting materials' fundamental mechanical properties such as elasticity and plasticity (Cespi *et al.*, 2007). It is necessary to consider the elastic-plastic properties of the material and determining the optimum batch. Hence, high tensile strength values could indicate brittle materials that suffer fragmentation. On the other hand, a high degree of plasticity provides irreversible compacts with deformed shapes (Mohan, 2012). While particles with elastic property irreversibly return to their shape after compression (Tunón, 2003) (Almaya and Aburub, 2008).

Therefore, a balance between elastic and plastic properties can improve the pellets compaction retaining their shape after compression with no fragmentation.

In addition, physical properties of the primary particles such as porosity, shape and density can affect the compression of the formed or compressed pellets (Aulton and Taylor, 2018b). Also, tensile strength increases with increasing packing density of particles due to the increase in the number and intensity of interparticle forces (adhesion, cohesion, interfacial, bridging and interlocking) (Frodeson and Berghel, 2018). Similarly, this was noticed in our results as the highest bulk densities were obtained from Eudragit L100 and 90 μm pellets 66 & 56 gm/mL, respectively. Although the 90 μm batch showed high porosity compared to the other batches, the porosity was still relatively low, showing the limited difference and showed no effect on IND release as in the following sections. Hence, if the porosity increases, we expect the contact points to decrease, leading to fragile compact and rapid drug release (Klose *et al.*, 2006)(Khan *et al.*, 2019). This was detected in the control batch that showed a good correlation with the low porosity and mechanical strength compared to the 90 μm batch. However, other factors could be considered, such as the pellets dimensions as the shortest diameter pellets could offer large surface area and provide high interparticulate binding sites resulting in strong bonds resisting the applied pressure (García-Triñanes, Luding and Shi, 2019). Therefore, 90 μm showed the highest tensile strength among the pellets of sieved powders, as in Figure 6.20. Also, the low AR, which is the largest diameter to smallest, and the small diameter of 90 μm batch rendered the pellets high surface area, leading to increased hardness and eventually tensile strength. A similar trend was noticed with the YM value, which is the relationship between the applied stress and strain, as the AR of the pellets indirectly affected YM (Cespi *et al.*, 2007).

This finding could explain the significant difference between 45, 63 & 90 μm batches ($p=2.78\text{E-}12$) in the hardness values while pellets 45 μm and 63 μm showed no statistical difference ($p= 0.666$) (Figure 6.20). On the other hand, the high pressure applied could lead to structural changes owing to the heat generated during compression (Khan *et al.*, 2019). Therefore, the mechanical properties of the batches can differ within the tablet matrix affected by the applied pressure leading to reduced porosity and fusion of the particles with structural changes (Khan *et al.*, 2019). In addition, the high surface roughness associated with the 90 μm batch could lead to an interlocking mechanism offering high strength with the tablets matrix or other pellets

(Frodeson and Berghel, 2018). This was detected in the tablet's mechanical strength section. However, the difference showed limited effect with low compression pressure.

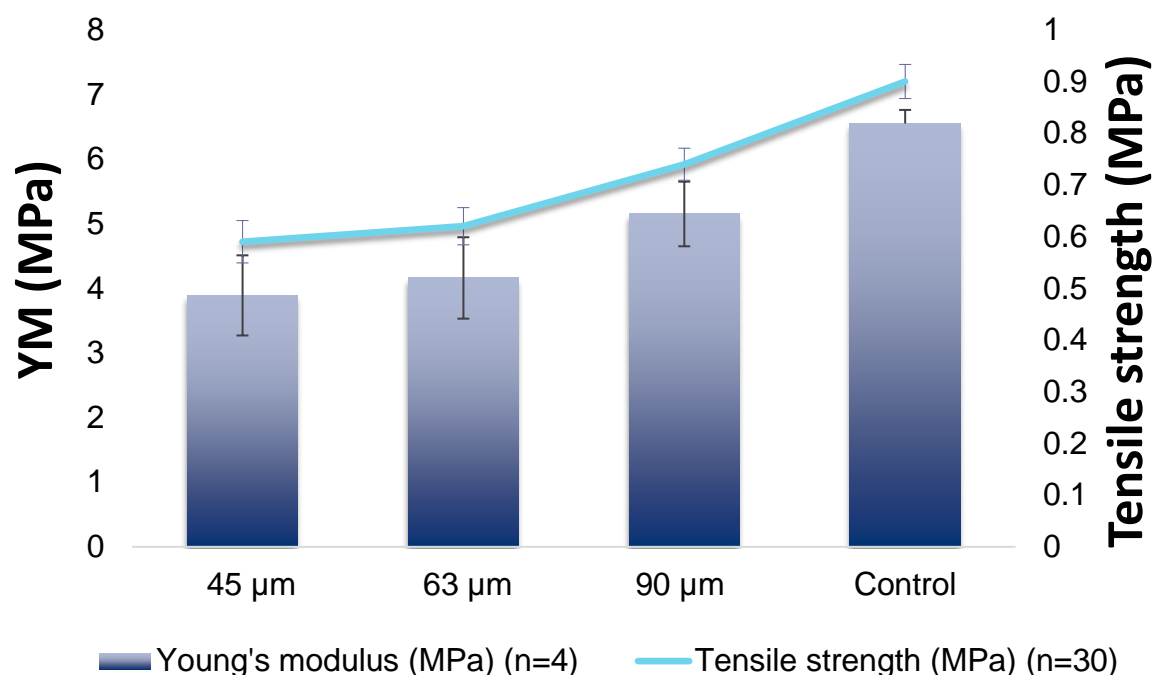


Figure 6.20 Graph of mechanical properties of pellets prepared from 45, 63, 90 µm and raw powder of Eudragit L100 (control) showing YM and tensile strength in mean ± SD

The p-value reflected the significant difference between 45, 63 and 90 µm batches in hardness, tensile strength, aspect ratio and YM (Appendix-Table 10.14). The proposed difference is correlated with the difference in aspect ratio between the batches. Hence, the tensile strength value depends on the dimensions of the pellets. A similar trend is associated with YM. Also, the surface area offered by the smallest diameter of 90 µm batch and surface roughness resulting in high YM (Narayan and Hancock, 2005). Other factors may generate that difference, including moisture content, porosity, and particle sizes of the powders. However, the difference was insignificant between YM of 63 & 45 batches and 63 µm & 90 µm batches. Sarkar, Ang and Liew reported that the initial powder particle size influenced the produced pellets roughness. Also, the authors indicated that initial powder particles of smaller size could compact well with lower deformation forming smoother surfaces of the pellets (Sarkar, Ang and Liew, 2014b).

On the other hand, the high tensile strength of the same batch is influenced by the small aspect ratio as it is inversely proportional with pellets dimensions (García-Triñanes, Luding and Shi, 2019). Also, moisture content can act as a plasticizer by enhancing molecular mobility and reducing T_g , thereby lowering YM (Roig *et al.*, 2011)(Kanwar, Kumar and Sinha, 2015). However, moisture may have a controversial effect on an anti-plasticizer as the higher moisture content (more than 5%) can generate intra molecular hydrogen bonding. Therefore, a strong compact generates with high YM and tensile strength, which was noticed with 63 and 90 batches of pellets (Roig *et al.*, 2011)(Kanwar, Kumar and Sinha, 2015) (Suresh Kumar *et al.*, 2019)(García-Triñanes, Luding and Shi, 2019).

6.8.7 Thermal analysis

The produced pellets of Eudragit L100 (45 μm , 63 μm & 90 μm) were characterized to examine their thermal behaviour using DSC and TGA analysis techniques to examine the crystallinity and the amorphous phase of the materials. Also, DSC was used to detect the melting point and degradation (Atef *et al.*, 2012).

DSC showed that the physical mixture of the formulations had no chemical interaction with IND (Figure 6.21). Hence, the melting point of IND 162 °C was detected in all tested pellets(Sukul *et al.*, 2017). Although the peak area of the pellets batches was different from that of the pure drug, the quantity of the IND used was low (5%) and the predominant effect of polymer (65%) correlated with the preparation method of pellets. Moreover, the slight deviation in the melting point of the formulation could be attributed to the plasticization effect of sorbitol that lower T_g .

It was noticed by Atef *et al.* in the DSC results that the melting point for gamma form of IND was between 160–162°C while alpha form had a melting point of 152–154°C (Atef *et al.*, 2012). Therefore, our IND formulation could be alpha form.

Moreover, Eudragit L100 amorphous state was confirmed by the absence of the endothermic peak of melting point(Sharma, Sharma, A. Panda, *et al.*, 2011). The peak around 230-240°C could be related to the degradation(Parikh *et al.*, 2014). It was reported that Eudragit L100 T_g around 200°C(Gupta, Simerdeep Singh, Nayan Solanki, 2016)(Parikh *et al.*, 2014). However, the value may vary depending on storage

conditions and the manufacturer. Hence, all pellets suffered degradation after 220°C as in the TGA thermogram (Figure 6.22). Therefore, the endothermic peak in the DSC graph is related to the starting of polymeric degradation (Sharma, Sharma, A. K. Panda, *et al.*, 2011)(Gupta, Simerdeep Singh, Nayan Solanki, 2016).

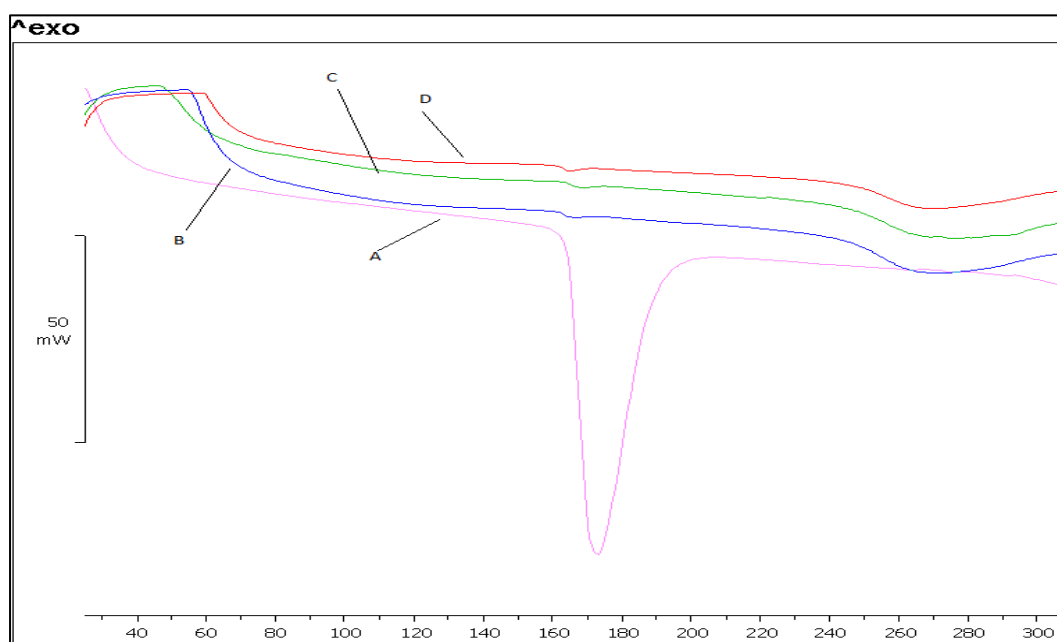


Figure 6.21 DSC graph of indomethacin (A), pellets of 90µm (B), 63µm (c), 45µm (D) EudragitL100 powder using Mettler Toledo and STARe software

On the other hand, the moisture content was measured using TGA, and the results of all batches showed the difference in moisture content (Table 6.11). This can be attributed to the behaviour of the primary materials and the difference in particle sizes. The high porosity of both raw powders of Eudragit L100 and that of 63 µm is associated with the ability of the particles to retain water, demonstrating high moisture content for the produced pellets 6.58 & 6.05% consecutively (Figure 6.22). ALL pellets had good moisture content (less than 7%), yet the excellent balance of 90 µm batch mechanical properties correlates with low moisture content. Although the 45 µm batch showed the lowest moisture content, the pellets showed the lowest mechanical properties.

This can be related to two explanations: firstly, the low surface area and pore volume of pellets (according to porosity results) shows minimum filled voids (with gas or water) between the particles, which was confirmed from the smooth surfaces SEM. Secondly,

the moisture content can behave differently among the particles. Thus, the moisture content is necessary to be within a specific range to produce pellets with the desired properties (as discussed earlier)(Thapa *et al.*, 2017). Briefly, moisture content can exist in three phases tightly bonded to the particles, weakly bonded or as bulk water. When moisture increases, the tensile strength of compact increases due to solid bridges between the particles or particle-particle interaction. However, when the water molecules exist at particles surfaces, acting as a lubricant can reduce the attraction of the particles, thereby tensile strength. Therefore, low moisture content can reduce the tensile strength seen in the 45 μm batch (Thapa *et al.*, 2017).

Table 6.11 TGA data of Eudragit L100 pellets and other batches (45, 63 & 90 μm) showing the moisture content and the residual

Sample	Residual	Moisture content
Eudragit L100 pellets	93.42%	6.58%
45 μm Eudragit L100 pellets	95.91%	4.09%
63 μm Eudragit L100 pellets	93.95%	6.05%
90 μm Eudragit L100 pellets	94.89%	5.11%

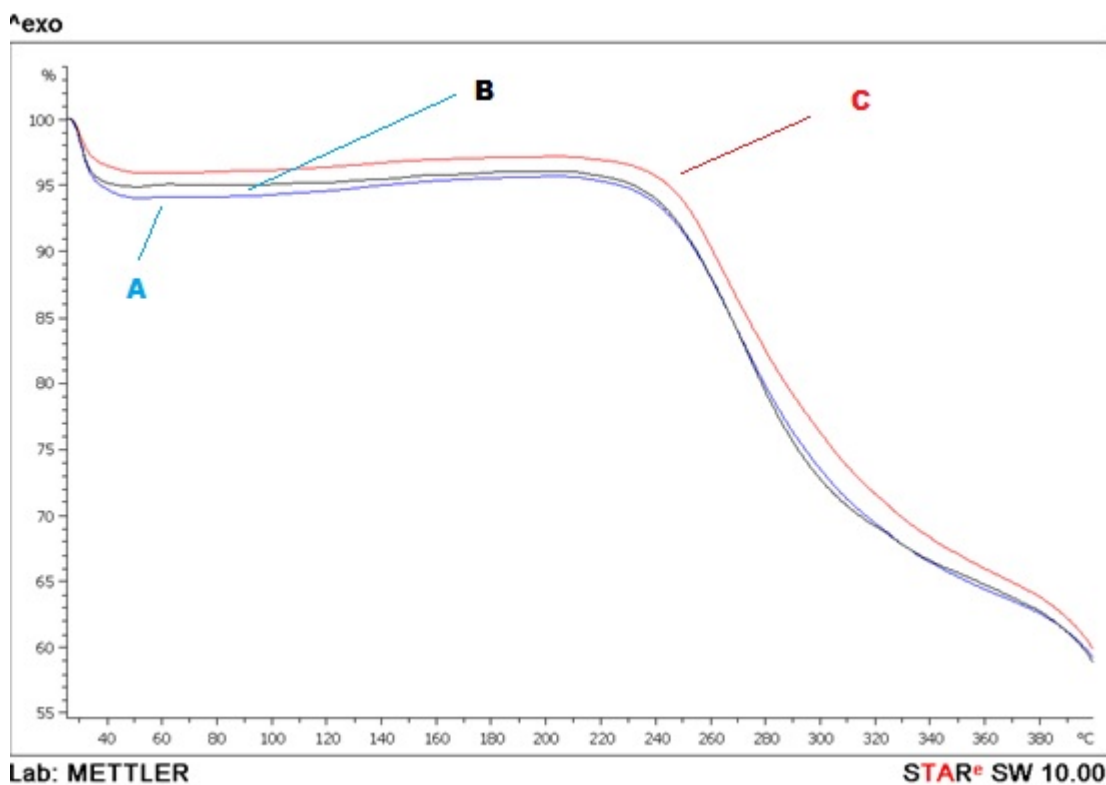


Figure 6.22 TGA Thermogram of EudragitL100 pellets of 63 (A) & 90(B) 45(C) μm showing the moisture

content orderly and the degradation temperature

6.8.8 Tablet's characterization

The obtained pellets from all Eudragit L100 sizes (45 μm , 63 μm and 90 μm) were used to prepare ODTs. The tablets included 10% (w/w) of pellets and compressed under the same pressure and method as described earlier. The prepared tablets were evaluated to assess the morphology, hardness, disintegration, and IND release profile.

6.8.8.1 SEM analysis and Stereomicroscope

The tablets were analysed under SEM to investigate the tablet matrix before and after compression (Figure 6.23). Also, a stereomicroscope was used to identify the pellets within the tablet's matrix and detect AR pellets (Figure 6.24). Also, the cross-section view for all batches was examined using SEM and stereomicroscope to detect the pellets within ODTs matrices, as in Figure 6.25.

The results showed the shape of the starting material as elongated particles with rough surfaces that can provide good disintegration time. Hence, the ODT matrix consists mainly of LHPC (disintegrant) and Lactose monohydrate (binder and diluent), which can be noticed from the rough surfaces of ODT. During DRP-ODTs preparation, the mixing of ODTs matrices and the pellets was challenging due to the difference in particle sizes of the ODT matrix, the large size of the pellets and the non-uniform shapes of initial particles forming the ODT matrix. Therefore, this was considered through increasing mixing time and evaluating IND release from the uncompacted pellets to be compared with the DRP-ODTs release independently, as in the next section. Moreover, stereomicroscope images indicated the presence of the pellets embedded in the matrix distinctly. Hence AR obtained from the microscope was correlated with the calliper results. All pellets were detected successfully within the ODTs matrix showing retained shape under compression as detected in Figure 6.25 for ODTs before and after the hardness test.

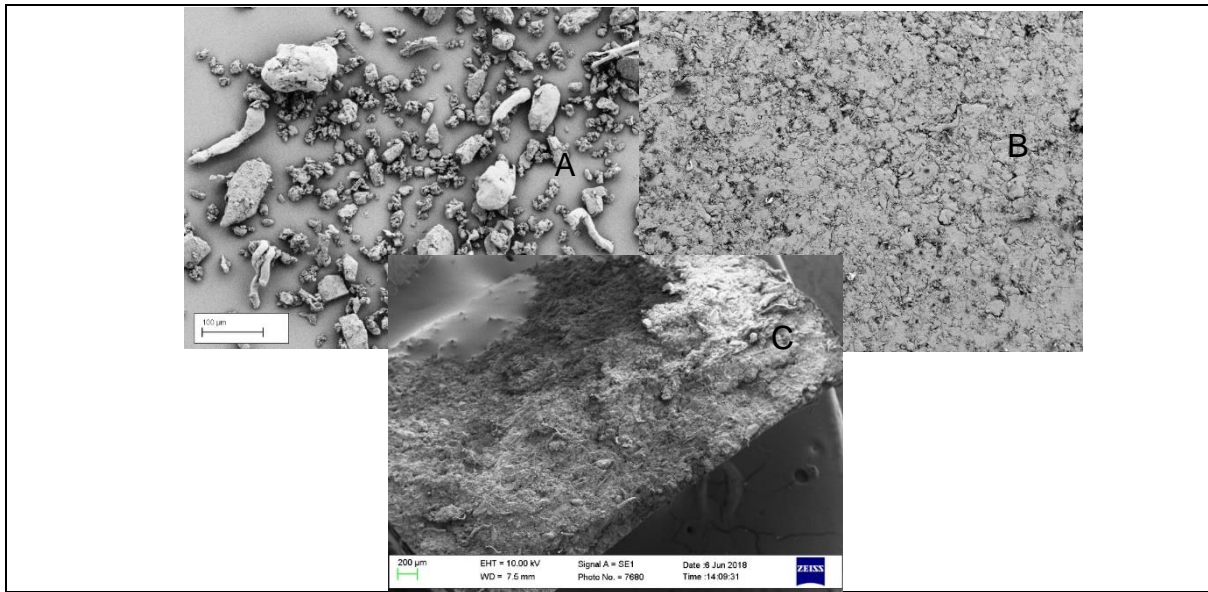


Figure 6.23 Tablet matrix showing in A the powder of ODT, B the compressed ODT top view and C cross section of the ODT (high and low magnification respectively)

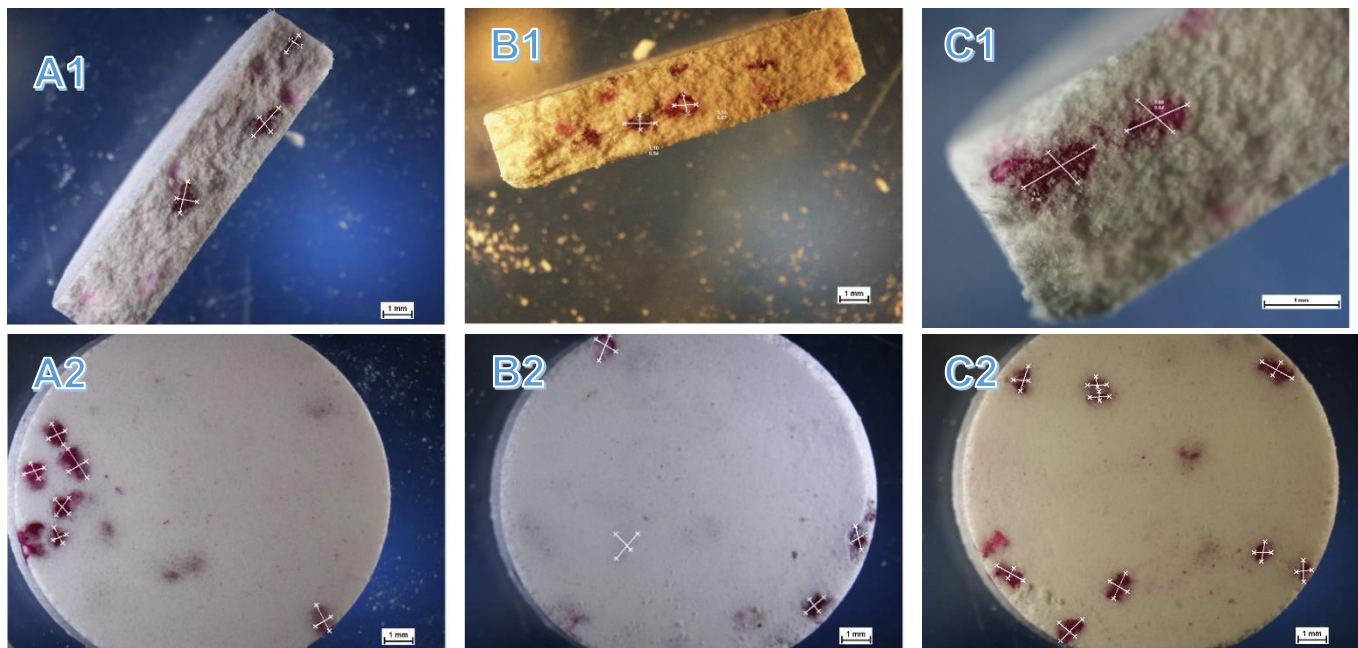


Figure 6.24 Stereomicroscope images of DRP-ODTs showing cross section view and top view of the tablets of 45 μm batch (A1&A2) 63 μm (B1&B2) 90 μm (C1 &C2) batches accordingly

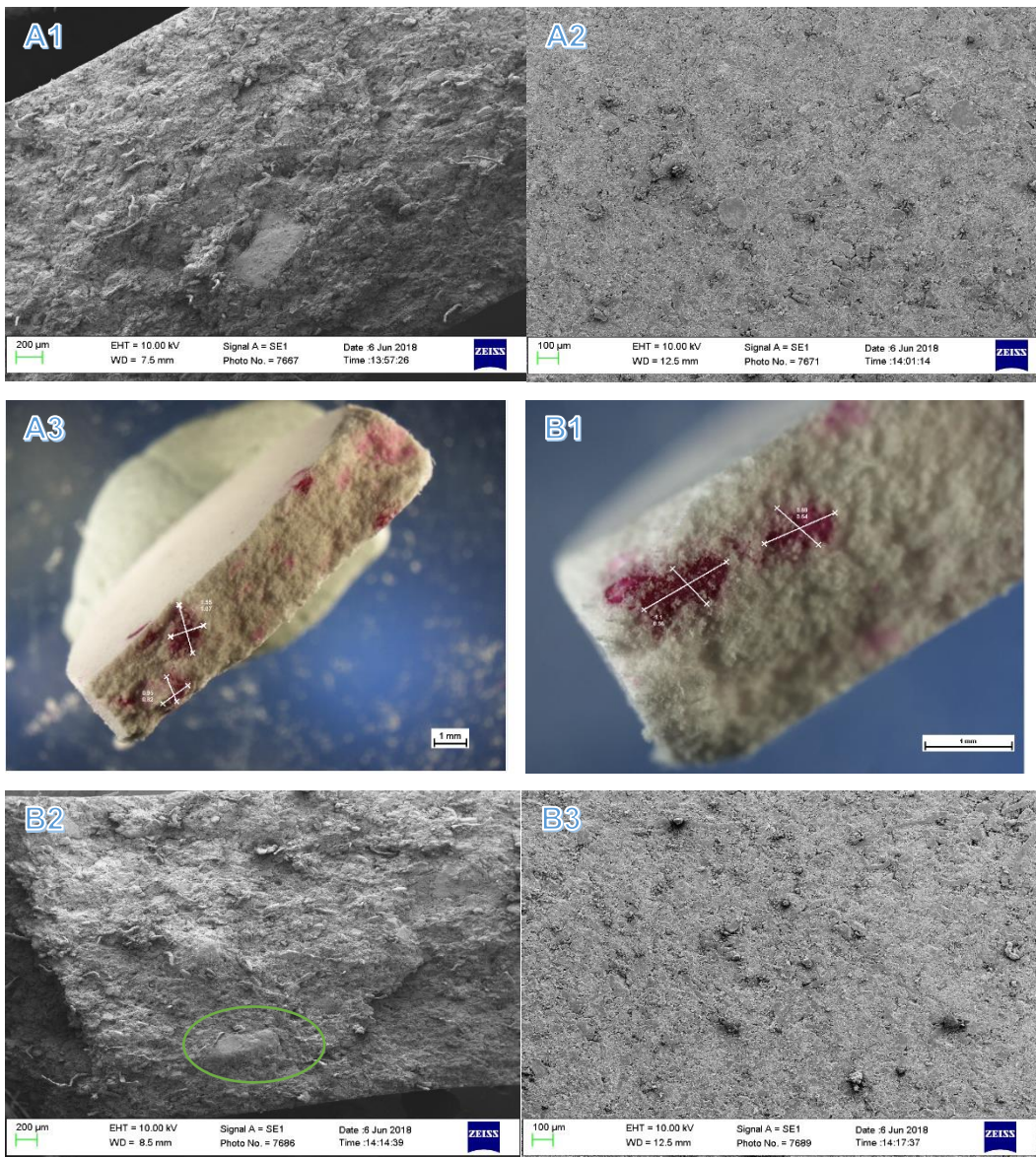


Figure 6.25 SEM and stereomicroscope images show cross-sections DRP-ODTs after hardness and the top view of the tablet indicating the embedded pellets for 63 µm batch (A1, 2&3) and 90 µm (B1,2 &3)

6.8.8.2 The hardness of the Tablets and disintegration time

The DRP-ODTs hardness was detected using the hardness tester, and the results were recorded for extrapolating tensile strength (Table 6.12) (Thapa *et al.*, 2017) (Cespi *et al.*, 2007). Also, all batches of DRP-ODTs were tested for the disintegration time (Table 6.12). Although DRP-ODTs showed higher tensile strength than the control, tensile strength was lower than 1 MPa for all tablets (García-Triñanes, Luding and Shi, 2019). This can be attributed to tablets matrices that contained 10% of the pellets, which enhanced mechanical properties. In addition, the results showed a

possible correlation with the properties of each batch as pellets of good strength influenced the ODT strength. For instance, 90 µm pellets (no compaction) showed the highest tensile strength. Similarly, tablets of that batch showed the highest strength. However, 45 µm batch behaved differently had 0.87 MPa strength tablets. The reason behind that could be the rough surfaces of 90 µm pellets allowing to generate mechanical interlocking with the particles of ODTs matrix, leading to stronger bonds compared to pellets of smoother surfaces (45&63)(EIShaer *et al.*, 2017).

Nevertheless, the difference was insignificant ($p>0.05$), and all batches considered of good strength. Therefore, the variation within tensile strength did not affect the disintegration time as all ODTs showed fast disintegration with less than 30 seconds (Table 6.12). Moreover, the fast disintegration of DRP-ODTs can be related to the possibility of voids formation between large embedded pellets and the small particles of the matrices (Tan and Hu, 2016b). Hence, this could be a positive factor providing cushioning layer supporting the pellets integrity under compression (Murthy Dwibhashyam and Ratna, 2008). Therefore, the values indicated adequate mechanical strength.

Table 6.12 Relationship between the disintegration time and hardness of the tablets with the embedded pellets and the control tablet of ODTs matrix only

Tablet	Tensile strength MPa (mean ±SD)	Disintegration time seconds (mean ±SD)
Control	0.80±0.060	20±0.3
45 µm ODT	0.87±0.23	16.3±0.5
63 µm ODT	0.84±0.03	14±0.6
90 µm ODT	0.89±0.08	14±0.6

6.8.9 IND release analysis

The prepared batches were evaluated to detect IND release in acidic (pH 1.2) and buffer (pH 6.8) media using HPLC for IND to be quantified. Also, ODTs containing IND as powder were tested as a control to compare with the obtained DRP-ODTs and uncompressed pellets from all batches. All tablets were tested to evaluate IND release in dissolution media acid and buffer, as shown in Figure 6.26 and Figure 6.27 (A&B).

6.8.10 Dissolution test

The pellets and DRP-ODTs were assessed independently to detect IND release in acidic (Figure 6.26-A1 and A2, respectively) and phosphate buffer media (Figure 6.27-B1 and B2, respectively) using the validated HPLC method, as detailed earlier (Elshaer, Hanson and Mohammed, 2014). This was applied to detect the difference between the compacted pellets within ODTs and the uncompacted pellets.

The IND release for both pellets and DRP-ODTs showed a delayed release in acidic media, as shown in Figure 6.26 in A1 and A2, respectively. The control of IND tablets showed more than 9% within 2 hrs, while DRP-ODTs showed less than 2%. However, the release from 90 μm (pellets and tablets) demonstrated a consistent delay in IND release compared to those of 45 μm showing a significant difference ($p < 0.05$). However, the difference was insignificant between 90 and 63 μm in both tablets & pellets, which can be correlated with the closeness of the results of these batches, including porosity and pellets mechanical properties (YM & tensile strength). On the other hand, 45 & 63 μm and 45 & 90 μm batches (tablets & pellets) showed a significant difference ($p < 0.05$) in IND release in the acidic media at 30 minutes. Similarly, the DRP-ODTs showed the same significant difference once between batches 45 and 63 μm and 45 with 90 μm while no remarkable difference between batches 63 μm and 90 μm of DRP-ODTs. This finding occurred due to the homogeneity resulting from pellets AR ($p > 0.05$), pore volume and powders mechanical properties of 63 & 90 μm . Moreover, the results indicated the good mechanical properties of the pellets as there was no significant difference in the IND

release from the pellets before and after compression from each batch (45, 63 and 90 μm) within the first 30 min according to One-way ANOVA and t-test ($p > 0.05$).

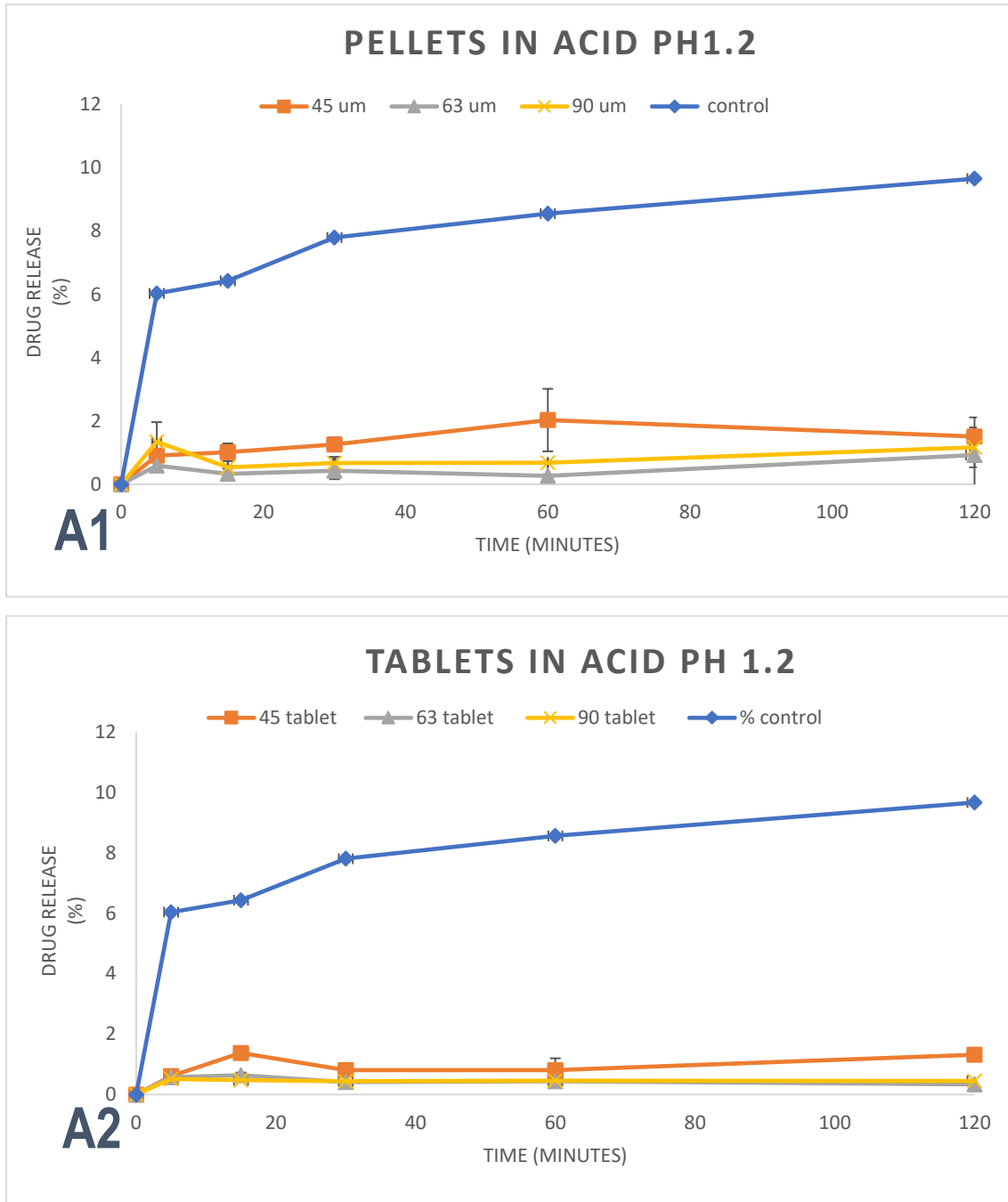


Figure 6.26 Dissolution test results of pellets and DRP-ODTs in acid media A1 &A2, respectively

On the other hand, there was a sudden release of IND from the 45 μm pellets between 5 and 20 minutes and similarly in the DRP-ODTs of 45 μm (no significant difference) ($p>0.05$). However, the second sudden release was associated only with 45 μm between 40-60 minutes, and this behaviour was absent in the same batch of tablets. This could be attributed to a formulation defect in the process, which did not appear in the tablets. Therefore, it can be concluded that pellets prepared from 63 μm and 90 μm showed a consistent delayed-release and good mechanical properties compared to the other batches in both non compacted pellets and DRP-ODTs. Moreover, they were offered good resistance under compression as the IND release was similar after tablet compression. Additionally, ODTs disintegration time and hardness were good enough compared to other batches. As a result, the pellets of 63 and 90 μm demonstrated maintained integrity, successfully achieving the aim of the study. However, further optimization to enhance pellets' shape and reduce pellet sizes by modulating the spheronization speed can be applied for future approaches (Li, 2006). IND release in the phosphate buffer showed immediate release for all formulations with more than 60% of IND release as in Figure 6.27. Although the IND release was higher than 100% for DRP-ODTs, the pellets with no compaction showed consistent, immediate IND release. Hence, all pellets showed no significant difference with control of IND tablets within 30 minutes in the buffer media. However, DRP-ODTs demonstrated a significant difference ($p<0.05$) compared to the control batch in the buffer media at 120 minutes (2 hours). There is possible segregation of powder and pellets during the tablet preparation as the particles had different sizes resulting in a higher number of pellets in the tablets than control (Tunón, 2003). Therefore, for optimization, the formulation granulation of the ODTs matrix or using different particle sizes could solve this issue as suggested by Tunón (2003). Hence, the excipients that are contained in the ODTs can be secondary agglomerates combined with pellets.

However, this difference did not affect the IND release in acidic media, indicating that the pellets could protect their integrity under the compression and delay the IND release. Therefore, the increment of IND release in buffered media can be only attributed to the homogeneity of pellets distribution. In addition, it was a remarkable coincidence indicating the ability of the system to protect the IND release in acidic media even there was a higher number of pellets within ODTs.

Furthermore, as shown in the DSC results, Eudragit L100 elastic properties were improved with sorbitol, which significantly helped retain the IND particles within the polymeric matrices due to the ratio of methacrylic acid and methyl methacrylate (Patra *et al.*, 2017). Nevertheless, the presence of IND particles on the surfaces of the pellets and the presence of hydrophilic plasticizer could result in the sudden IND release in acid, yet this effect was minimal as the delayed release continued until the end of the test. Finally, despite the low porosity demonstrated by the pellets of higher porosity showed good compaction properties offering a consistent drug release as in 63 and 90 batches (Phale and Gothoskar, 2011). A similar trend was reported by Tunón, Gråsjö and Alderborn, showing that the pellets with low porosity were compressed with minor densification increasing the drug release. Thus, compared to non-porous pellets, porous pellets showed no change in the drug release after compression (Tunón, Gråsjö and Alderborn, 2003). However, this finding is one of the factors that should be accompanied by the good mechanical properties of the pellets offering good compressibility and limited impact on drug release. Therefore, this confirms our statement for the necessity of demonstrating adequate elastic-plastic properties by pellets to support their integrity under compression and influentially modify the drug release.

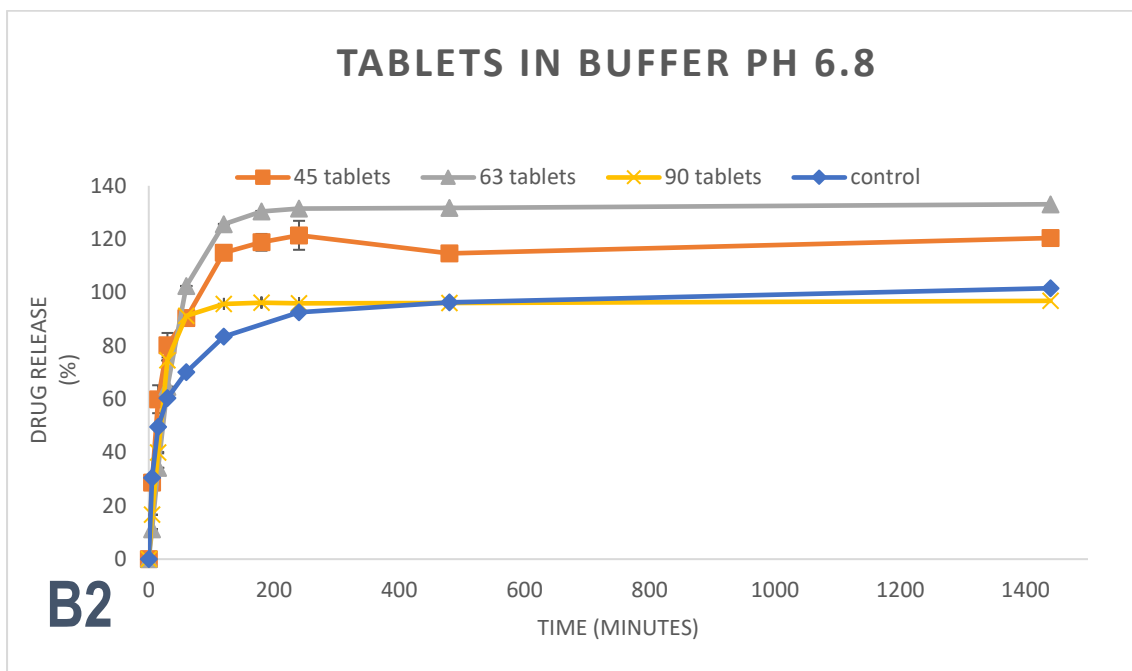
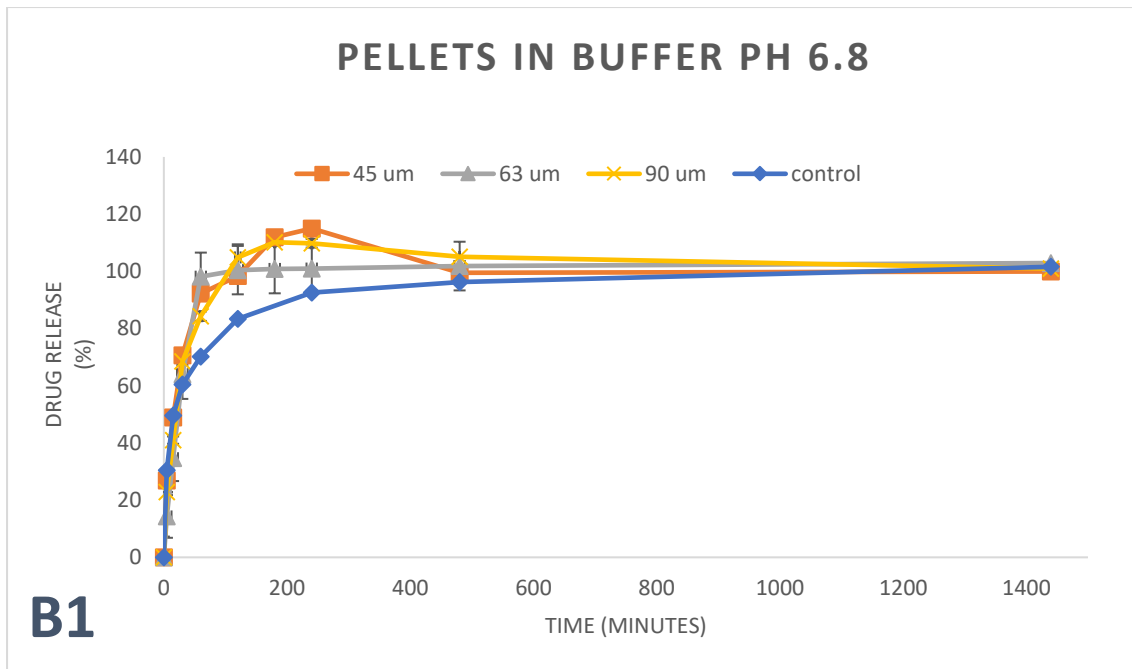


Figure 6.27 Dissolution test results of pellets and DRP-ODTs in buffer (pH6.8) B1 &B2, respectively

6.9 Conclusion

Particle size and shape could affect the compaction performance of lactose and mannitol, which ultimately can affect the mechanical properties of the final tablets and the pellets included in the tablet matrix.

The YM results were directly related tensile strength of the same materials. The lactose tablets demonstrated higher plasticity than mannitol. The additive materials performed differently at different particle sizes, and such variance was reduced with increasing the powder particle size. Also, adding ODTs ingredients, including LHPC (grade LHB1), magnesium stearate and IND, could bond differently.

The disintegration time was lower than 30 seconds for all batches, and the adequate tensile strength was lower than 1.5 MPa. Lastly, lactose was a suitable ingredient for ODTs to retain the pellet's integrity under compression.

The dissolution studies indicated that pellets distribution using lactose batches were more homogeneous than mannitol. Both lactose and mannitol ODTs-pellets delayed IND release in acidic media, releasing less than 1.07% at 120 minutes and released more than 93% at 120 minutes in phosphate buffer (pH 6.8). It can be concluded that there was no need for sieving mannitol powder nor using different particle size powder to prepare DRP-ODTs. Similarly, all lactose batches showed suitability to prepare ODTs and combining all particles with no sieving could be more beneficial to improve homogeneity. To conclude that factors affecting the pellets' mechanical properties were powder particle size, pellets' sphericity, and porosity. There was a significant relationship between the morphology and hardness of the pellets. Protecting pellets integrity was essential to delay the release in the acidic media to be immediately released in alkaline media. Finally, the IND release was modified in the acidic media and immediately released in the buffer media showing that pellets could delay the IND release to bypass the stomach and release in the small intestine. Further optimization for 60 and 90 μm pellets is expected to be considered for future studies as this batch can be used as an anticipated formulation. Improving pellet sizes and shape by modulating the spheronization time can be applied in future approaches (Li, 2006).

Chapter 7 Evaluation of propranolol hydrochloride release via matrix and reservoir pellets of time-dependent polymer

Scoop of the studies

Multiparticulate systems such as pellets (matrix and reservoir) contained inside orally disintegrating tablets (ODTs) garner great interest compared to other similar dosage forms. However, the weakness of coated pellets (reservoir) capacity to withstand pressure during tablet compaction brings about the damage of the polymer covering and subsequent loss of the adjusted delivery properties from this type of pellet. Thus, matrix pellets have been proposed to overcome this issue.

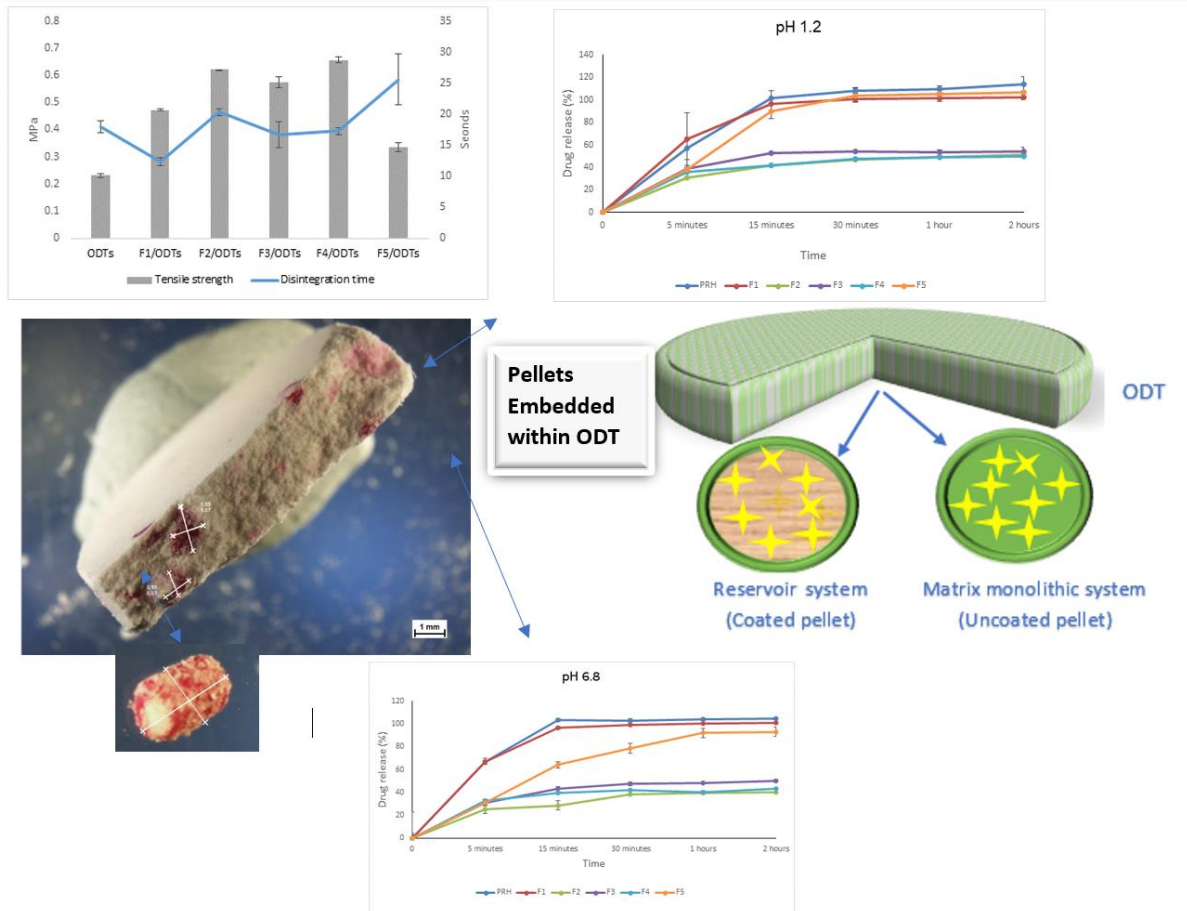
The first study aimed to apply matrix pellets for modified propranolol hydrochloride (PRH) delivery through ODTs and assessment of the impact plasticisers have on the modified delivery properties of fused pellets which utilise; Eudragit RS as a polymer, sorbitol, triethyl citrate (TEC) and Acetyl triethyl citrate (ATEC) as plasticisers.

Extrusion spheronization was used to produce six structured pellet comprising of 20%(w/w) PRH, 15% and 30% (w/w) sorbitol or 3% and 5% (w/w) TEC or 3% and 5% (w/w) ATEC with appropriate amounts of Eudragit RS up to 100 % (w/w) formulation.

The results showed that modifying PRH release from the prepared formulations in the acidic media (pH 1.2) was unachievable for all pellet batches. However, the coated or reservoir pellets of Eudragit RS, RL and RS: RL were successfully modified PRH release showing the suitability of Eudragit RS and RL for reservoir system.

Keywords: Eudragit RS PO, matrix pellets, PRH, extrusion-spheronisation, texture analysis

An illustration of the influence of ODT containing matrix and reservoir pellets on PRH release



7.1 Background

7.1.1 Pellets excipients and core materials

The pellets' core must possess specific mechanical properties such as elasticity to facilitate change of shape upon compression, without the coating layer suffering damage (Bodmeier, 1997) (Dashevsky, Kolter and Bodmeier, 2004). The drug release profile must not be altered during tableting (Bodmeier, 1997) (Beckert, Lehmann and Schmidt, 1998). In the case of insufficient elasticity on the coating film's part, the modified release profile of the drug would be lost due to tablet rupturing during the compression phase of the tableting process. Compression often leads to the deformation of pellets. Hence most attempts to incorporate particulate systems into modified release formulations have been unsuccessful.

The naturally found cellulose from the fibrous plant is microcrystalline cellulose (MCC), produced by the spray drying method. MCC can also be produced by different methods, such as reactive extrusion. MCC is a commonly used excipient in different applications, including in the food, medical and pharmaceutical industries. However, there are different grades of MCC, which differ according to the manufacturer and method of preparation. The grades are differentiated by moisture content, degree of crystallinity, porosity, and surface properties. Therefore, using MCC depends on the original properties of each type and the future result to be achieved.

Chen et al. (2017) claim that MCC is the most common excipient to formulate core pellets to obtain modified release dosage forms (Chen *et al.*, 2017). In addition, its disintegration pattern, compaction behaviour, and high drug loading make it a favourable choice (Patel *et al.*, 2010). However, the degree of crystallinity of MCC affects the formulation properties through the amorphous part possessing more hygroscopic properties than the crystalline part due to the polymer chain's irregular pattern. As a result, the higher the amorphous to crystalline ratio, the more significant the core pellet's hygroscopic property (Yohana Chaerunisaa, Sriwidodo and Abdassah, 2020). Also, MCC imparts suitable plasticity onto a wet mass, leading to its wide use for extrusion-spheronization (Sadeghi, Hijazi and Garekani, 2011). The most suitable binder to be used with MCC is water (Fielden, Newton and Rowe, 1992).

7.1.2 Polymers of modified-release properties

The choice of a polymer affects many aspects of the formulation, including the API's release pattern. The extended-release profile of a formulation is often due to Ethyl Cellulose and acrylic polymers. Eudragit® and Kollicoat® are popular brands of acrylic polymers and are preferred to Ethyl Cellulose since Ethyl Cellulose has less flexibility, rendering it less amenable to go through compression (Bodmeier, 1997).

Eudragit® comes in an array of varieties with different properties made for numerous applications. Out of these varieties, Eudragit RS PO, RS 100, RS 30D, and RS 2.5 are time-dependent polymers and are used in modified release dosage forms (Akhgari, Abbaspour and Moradkhanizadeh, 2013) (Patra *et al.*, 2017). Eudragit RS is a type of methacrylate polymer with time-dependent properties that consists of methyl methacrylate, ethyl acrylate, and methacrylic acid. This polymer also contains quaternary ammonium groups that provide the swelling potential for Eudragit RS with low permeability, no water solubility, and pH independent and biocompatible behaviour (Patra *et al.*, 2017).

Abbaspour, Sadeghi and Afrasiabi Garekani, studied Ibuprofen pellets made of Eudragit RL PO and RS. They used extrusion-spheronization and thermal heating to obtain the pellets. The resulting pellets with either 60 or 40% Ibuprofen displayed favourable mechanical properties before compression commenced. Under compression, the pellets changed from brittle to plastic (Abbaspour, Sadeghi and Afrasiabi Garekani, 2007). Comparing the two types of Eudragit used here, it was concluded that Eudragit RL PO had higher crushing strength than its counterpart and that elastic modulus remained unaffected by choice of Eudragit type. In the next step of their research in 2008, the authors coated their pellets with a 4:1 mixture of Eudragit Rs 30D and RL 30D plus 20% Triethyl Citrate (TEC). A coating level of 5% managed to achieve a modified release profile of the API. Combining compression force, the composition of excipients, and granulation of filler choice led to achieving modified-release tablets. These elements did not affect the drug release profile of the individual pellets, but they did influence tablet properties such as disintegration time and hardness. Studies showed no notable damage to the coating of the pellets, which

illustrates the importance of optimization of core pellet formulation (Abbaspour, Sadeghi and Afrasiabi Garekani, 2007)(Abbaspour, Sadeghi and Afrasiabi Garekani, 2008).

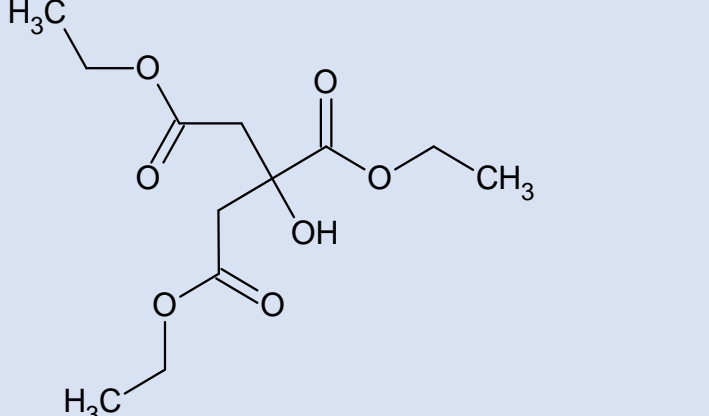
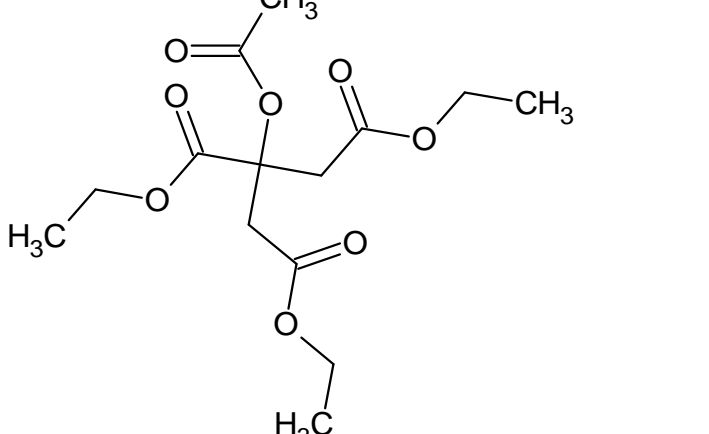
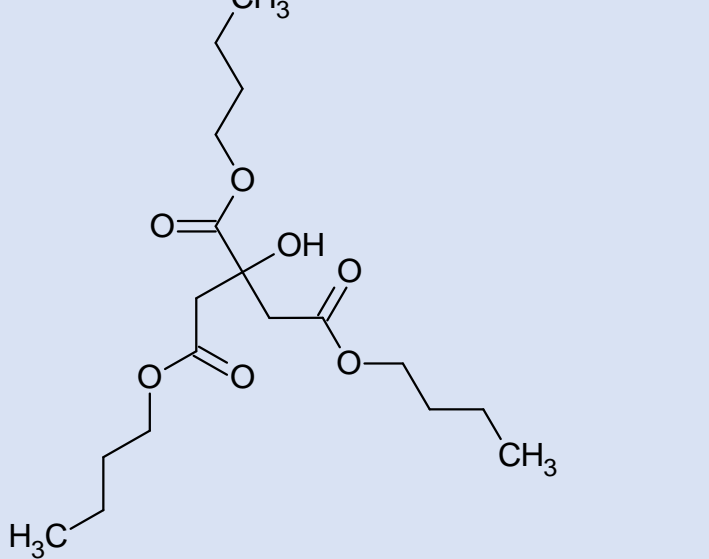
The use of Eudragit in modified release matrix pellets has recently been studied to tackle issues relating to compression-induced damage in pellets leading to loss of release properties. Pai, Kohli and Shrivastava used a combination of Eudragit L 30D 55 (or Eudragit NM 30D), Aquacoat® ECD 30 (ethylcellulose aqueous dispersion), and sodium alginate (Keltone® LV CR) to produce an extended-release formulation of sertraline hydrochloride pellets. The results indicated similar release profiles between compacted pellets and matrix pellets (Pai, Kohli and Shrivastava, 2012). A different study conducted on colonic delivery by controlled release of matrix pellets used a combination of Eudragit RS and RL PO and pectin. This matrix proved to control the release of 5-Amin Salicylic Acid in the upper GI, making it a suitable substitute for coated or reservoir-type pellets for the modified release of orally disintegrating tablets (Akhgari, Abbaspour and Moradkhanizadeh, 2013) (Pai, Kohli and Shrivastava, 2012).

7.1.3 Effect of plasticizers

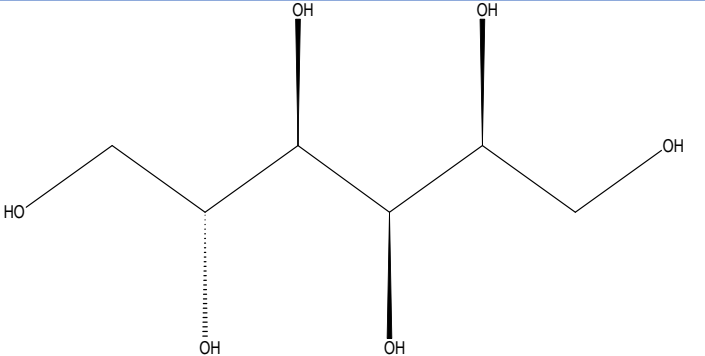
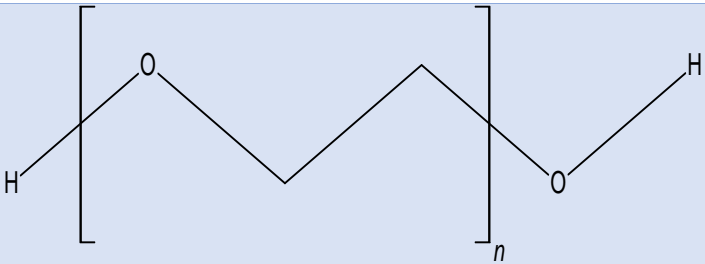
The mechanical, physicochemical, and thermal properties of polymers are directly affected by plasticizers. Polymers with incorporated plasticizers have better flexibility and lower viscosity, elastic modulus, tensile strength, and T_g . Employing low processing temperatures can improve the strength and flexibility of the polymer (Zhu *et al.*, 2002). Plasticizers can be categorized as traditional and non-traditional, as well as based on their chemical structure.

Failure to incorporate plasticizers into the formulation can render the polymers brittle, rendering them unfit to withstand compressive forces (Bodmeier, 1997). In such situations, flexibility can be modified by reducing the polymer's elastic modulus and tensile strength (Gutiérrez-Rocca and McGinity, 1994). Another study stated that plasticizer-free coating made of Kollicoat® was too brittle and eventually rupture during tableting. Enhanced flexibility was observed using 10% (w/w) of TEC in the mixture alongside better compaction properties (Dashevsky, Kolter and Bodmeier, 2004) (Chamarthy and Pinal, 2008). Brittleness was also seen in Eudragit RL based pellets of Ibuprofen, contained in the MCC, and 0-1% PEG 400, while those with 3-5% PEG 400 presented more plastic properties under compressive forces. The inclusion of PEG 400 drastically reduces elastic modulus while affecting the mechanical properties of the pellets in a way that makes them suitable for compression, such as increasing plastic behaviour (Abbaspour, Sadeghi and Afrasiabi Garekani, 2007).

Table 7.1 Examples of popular plasticizers in the pharmaceutical formulations

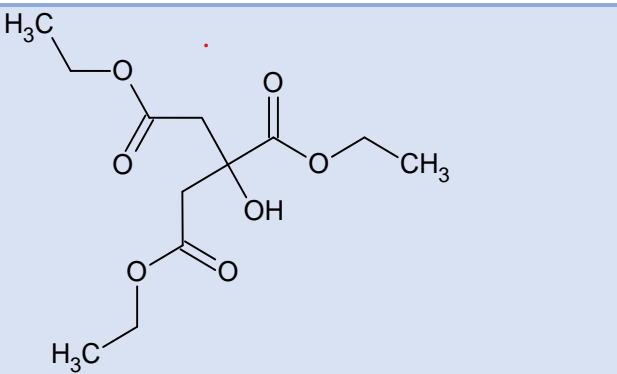
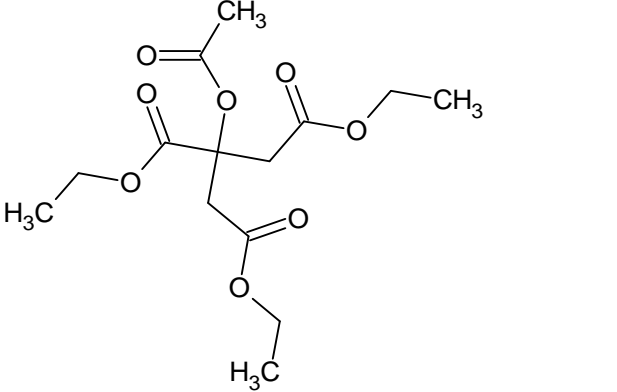
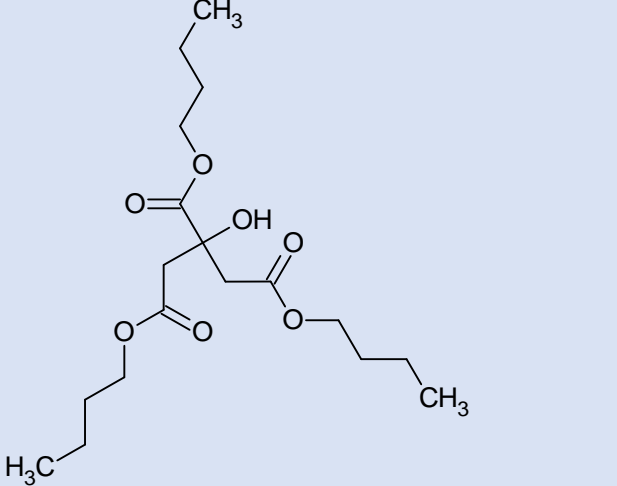
Plasticizer	Type	Structure
Triethyl citrate (TEC)	Hydrophilic	
Acetyl triethyl citrate (ATEC)*	Hydrophilic/ hydrophobic	
Tributyl citrate (TBC)	Hydrophobic	

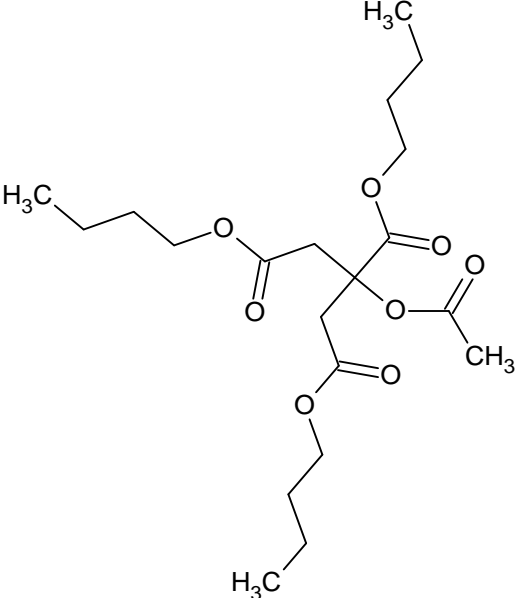
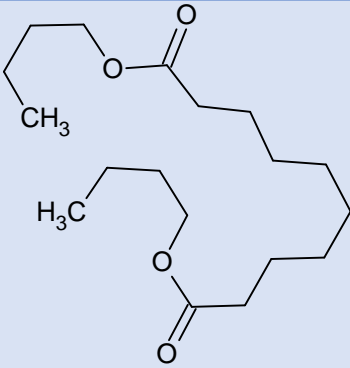
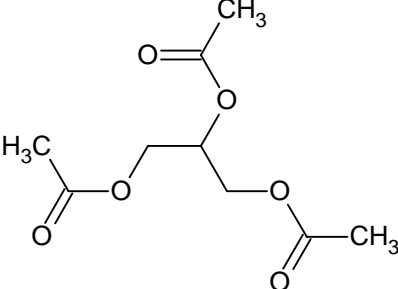
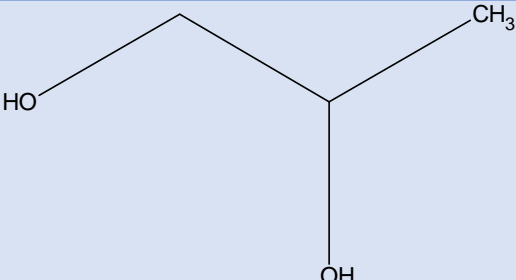
Acetyl tributyl citrate (ATBC)	Hydrophobic	
Dibutyl sebacate (DBS)	Hydrophobic	
Triacetin	Hydrophilic	
Propylene glycol	Hydrophilic	

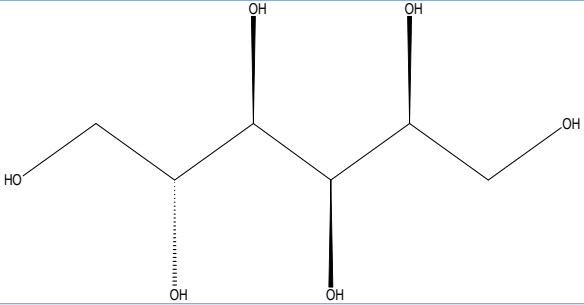
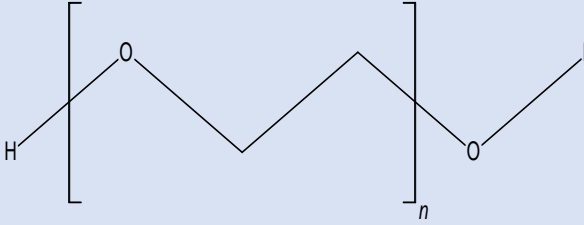
Sorbitol	Hydrophilic	 <p>The chemical structure of Sorbitol is a six-carbon polyol chain. From left to right, the carbons are: C1 (primary alcohol, HO-CH2-), C2 (secondary alcohol, -CH(OH)-), C3 (secondary alcohol, -CH(OH)-), C4 (secondary alcohol, -CH(OH)-), C5 (secondary alcohol, -CH(OH)-), and C6 (primary alcohol, -CH2-OH). The hydroxyl groups on C2, C3, and C4 are shown with different stereochemistry: C2 is dashed, C3 is solid, and C4 is solid.</p>
Polyethylene glycol (PEG)	Hydrophilic	 <p>The chemical structure of Polyethylene glycol (PEG) is a repeating unit of an ethylene glycol chain. It consists of a central carbon-carbon bond with two oxygen atoms attached to each carbon. The structure is shown as a zigzag line representing the carbon backbone, with oxygen atoms at the vertices. The chain is enclosed in large square brackets with a subscript 'n' at the bottom right. The terminal oxygen atoms are bonded to hydrogen atoms (H).</p>

Failure to incorporate plasticizers into the formulation can render the polymers brittle, rendering them unfit to withstand compressive forces (Bodmeier, 1997). In such situations, flexibility can be modified by reducing the polymer's elastic modulus and tensile strength (Gutiérrez-Rocca and McGinity, 1994). Another study stated that plasticizer-free coating made of Kollicoat® was too brittle and eventually rupture during tableting. Enhanced flexibility was observed using 10% (w/w) of TEC in the mixture alongside better compaction properties (Dashevsky, Kolter and Bodmeier, 2004) (Chamarthy and Pinal, 2008). Brittleness was also seen in Eudragit RL based pellets of Ibuprofen, contained in the MCC, and 0-1% PEG 400, while those with 3-5% PEG 400 presented more plastic properties under compressive forces. The inclusion of PEG 400 drastically reduces elastic modulus while affecting the mechanical properties of the pellets in a way that makes them suitable for compression, such as increasing plastic behaviour (Abbaspour, Sadeghi and Afrasiabi Garekani, 2007).

Table 7.1 Examples of popular plasticizers in the pharmaceutical formulations

Plasticizer	Type	Structure
Triethyl citrate (TEC)	Hydrophilic	
Acetyl triethyl citrate (ATEC)*	Hydrophilic/ hydrophobic	
Tributyl citrate (TBC)	Hydrophobic	

Acetyl tributyl citrate (ATBC)	Hydrophobic	
Dibutyl sebacate (DBS)	Hydrophobic	
Triacetin	Hydrophilic	
Propylene glycol	Hydrophilic	

Sorbitol	Hydrophilic	
Polyethylene glycol (PEG)	Hydrophilic	

7.1.4 Direct compression for tablets preparation

Numerous well-known advantages of direct compressions, such as having fewer steps, make it one of the most common tableting techniques. Elimination of moisture and heat effects in this technique make it favorable for drugs with heat and moisture sensitivities. This method is often chosen for medium-high potency compounds, having less than 30% drug composition (Jivraj, Martini and Thomson, 2000). Specific dry binders and fillers are necessary for this method. Excipients are divided into dry binder, disintegrant, filler, and lubricant. Excipients must resemble a cushion during compression to prevent damage to the pellets' integrity (Murthy Dwibhashyam and Ratna, 2008). The physical characteristics of pellets are required to be as similar to the cushioning excipients as possible (Murthy Dwibhashyam and Ratna, 2008). Also, the combination of the excipients of the modified release-ODTs should provide the required drug release rate, tablets strength, and disintegration with optimal compression force. The pellet ratio to filler directly affects the tablet's disintegration and strength, but without influencing the drug release rate from the pellets (Abbaspour, Sadeghi and Afrasiabi Garekani, 2008). On the other hand, Chen et al. claimed that this ratio not only affects strength, friability, the integrity of the coating, uniformity of drug content, and disintegration time, but it also influences the rate of drug release (Chen *et al.*, 2017).

Different excipients such as MCC, lactose, starch 1500, mannitol, sorbitol, and dicalcium phosphate dehydrate can be used in direct compression processes. Such excipients serve different purposes and functions based on the concentration in which they are used (Jivraj, Martini and Thomson, 2000). The most popular and most widely used direct compression excipients are MCC and lactose (Jivraj, Martini and Thomson, 2000). Lactose is most suited for formulations requiring fast disintegration due to its water-soluble nature. MCC used in concentrations of 20-90% (w/w) acts as a diluent, from 5-15% (w/w) it is a disintegrant, and from 5-20% (w/w) can be an anti-adherent. Magnesium stearate is an anti-adherent, glidant, or lubricant in 0.25-5% (w/w) concentrations (Rowe, Raymond C., Paul Sheskey, 2009).

7.2 Aim and objectives

Two studies were applied in this chapter to modify PRH release using pellets embedded in ODTs.

7.2.1 Aims

The first study aimed to modify PRH release via uncoated pellets based on time-dependent polymer (Eudragit RS) embedded in ODT using different types of plasticizers.

The second study aimed to modify PRH release via coated pellets embedded in ODTs using Eudragit RS, RL and RS: RL.

7.2.2 Objectives

1. To prepare PRH pellets using extrusion spheronization.
2. To optimise and use simple method of coating to save time and cost
3. To prepare coated pellets with different Eudragits ratios.
4. To examine the mechanical properties of the produced pellets utilizing the texture analysis technique.
5. To study the effect of Eudragit RS as a time-dependent polymer on modifying PRH release.
6. To evaluate the impact of different types and ratios of plasticizers sorbitol (15% & 30%), TEC (3% & 5%) and ATEC (3% & 5%) on PRH release profile.
7. To prepare ODTs consisting of PRH pellets using direct compression with complete characterization (dimensions, tensile strength, disintegration time, contact angle, and *in vitro* release test).

7.3 Experimental

The method and measurements were applied following the detailed method in the experimental chapter. The method, material and characterisation are briefly illustrated according to specific determinations in this study.

7.3.1 Materials

As detailed in the experimental chapter.

7.3.2 Methods

7.3.2.1 Pellets formulation

The multiple processes based on extrusion-spheronization (Caleva Multi Lab machine, England) was used to prepare 10 g powder comprising pellets excipients. The pellets matrix included PRH (20% w/w), MCC (20% w/w), Eudragit RS and plasticizer in suitable quantities to make 100% (w/w) (Table 7.2). All the ingredients were mixed using a kitchen mixer (Tefal, France) for 10 minutes and 100 rpm speed. The liquid components (water, ATEC or TEC) were added gradually to the desired amounts. The produced mass was then transferred to the extruder to prepare the extrudates (elongated shaped threads). The extruder was attached to a die of multiple holes of a 1 mm diameter with 20 rpm speed. In the other step, at a speed of 1200 rpm for 10 minutes, a spheroniser of a disc with cross-hatched patterns was set to break down the extrudate into small spherical shaped granules. The final step was drying the produced pellets using an oven set to 40°C for 2 hours (lower than the polymer's T_g). The pellets weight was recorded after the drying process then applied in the calculations of both the pellets yield and the moisture content. The obtained batches were stored in small vials placed in a desiccator.

Table 7.2 The produced batches and different excipients ratios and the trial batch of Eudragit RS only

<i>Material</i>	<i>F0</i>	<i>F1</i>	<i>F2</i>	<i>F3</i>	<i>F4</i>	<i>F5</i>	<i>F6</i>
<i>Plasticizer</i>	0%	15% sorbitol	30% sorbitol	3% TEC	5% TEC	3% ATEC	5% ATEC
<i>PRH</i>	0%	20%	20%	20%	20%	20%	20%

<i>MCC</i>	0%	20%	20%	20%	20%	20%	20%
<i>Eudragit RS</i>	100-60%	45%	30%	57%	55%	57%	55%
<i>Water (mL)</i>	3.0	1.3	1	3.1	2.4	3.1	2.6

Similarly, the coated pellets were prepared using the same parameters. The composition of the coated pellets is detailed in Table 7.3

Table 7.3 Contents of pellets before pellets coating (F1-F5)

Excipient	No drug pellets (F0)	Uncoated drug pellets (F1)	Coated pellets with Eudragit RS (F2)	Coated pellets with Eudragit RL (F3)	Coated pellets with Eudragit RL/RS (F4)	Uncoated Pellets of Eudragit RS (F5)
PRH (%w/w)	0	20	20	20	20	20
Eudragit RS	0	0	0	0	0	57
MCC (%w/w)	100	77.00	77.00	77.00	77.00	20
Acetyl triethyl citrate (%w/w)	0	3.00	3.00	3.00	3.00	3.00

7.3.2.2 Pellets coating

The formulated pellets were coated using Eudragit RS PO, Eudragit RL PO separately and a combination of Eudragit RS / RL (1:1). The coating solution was formulated using a magnetic stirrer to achieve a homogenous solution by dissolving 10% (w/v) of Eudragit RS PO and Eudragit RL PO in ethanol. Exactly 10 g of pellets were added into the coating pan (Erweka AR403, Germany) then sprayed with the coating solutions (10 mL) at two puffs/minute and pan rotation speed 400 rpm. The pellets were again dried at 40°C in the oven for 2 hours (Qiao *et al.*, 2010). Until further characterisation, the pellets were stored in a desiccator. The endpoint of the spray coating was the consumption of the full coating solution.

7.3.2.3 Examination of pellet morphological and physical and properties

A.Sphericity and shape

All pellets were examined to assess the sphericity by measuring each batch's aspect ratio (AR) of 30 pellets (Santos *et al.*, 2002). The method and measurement were applied following the detailed method in the experimental chapter.

B.Scanning electron microscopy SEM

The samples were prepared and detected following the detailed method in the experimental chapter.

C.Determination of bulk density of pellets

The bulk density of all pellets was measured for all batches using the detailed method in the experimental chapter.

D.Porosity measurements and surface area

The porosity and surface area were measured for all pellets using BELSORP-mini (BEL INC, Japan) and Bel-Master software. The method is detailed in the experimental chapter.

7.3.2.4 Mechanical testing of pellets

A.Elasticity and deformation

Determination of pellets' elasticity was evaluated using Texture Analyser (Stable Micro Systems, UK) and exponent software. The method is detailed in the experimental chapter.

B.Determination of pellet hardness

All pellets were examined as detailed in the experimental chapter.

7.3.2.5 Thermal analysis

A. Differential Scanning Calorimeter (DSC)

B. Thermogravimetric analysis (TGA)

The produced batches were examined using DSC and TGA (Mettler Toledo, Switzerland) as detailed in the experimental chapter.

7.3.2.6 Validation of the HPLC method for propranolol hydrochloride

The HPLC method is detailed in the HPLC chapter.

7.3.2.7 Preparation of tablets

All tablets were prepared using 20% (w/w) of pellets. The ODT matrix consisted of MCC 5% (w/w), magnesium stearate 1% (w/w) and lactose 74%(w/w). The pellets and ODT powder were mixed for 10 minutes using a tubular mixer (TURBULAR[®], Switzerland). The powder was weighed to prepare 500 mg per tablet from each batch (n=14). The powder was compressed using a manual tablet presser machine (SPECAC, UK). The method is detailed in the experimental chapter.

7.3.2.8 Scanning electron microscopy of tablets

The tablets' morphology and surface properties and the pellets within the produced tablets were detected using SEM. The method is detailed in the experimental chapter.

7.3.2.9 Determination of tablets hardness and tensile strength

All tablets were analysed according to the detailed method is in the experimental chapter.

7.3.2.10 Disintegration

DRM-ODTs disintegration time was carried out for each formulation and the control. The detailed method is explained in the experimental chapter.

7.3.2.11 Detection of tablets contact angle

The tablets were evaluated to examine their wettability (n=2) by measuring the contact angle and using the sessile drop method. The drop shape analyser (model DSA30S, Germany) was used to detect the wettability by applying one droplet of water from a prefilled syringe with distilled water. When the drop was placed on the tablet surface, several images were captured immediately. The DSA4 software was used to compute the angle.

7.3.2.12 Dissolution test

The produced tablets were tested in both media at acidic pH 1.2 and phosphate buffer at pH 6.8 (n = 3). The detailed method is illustrated in the experimental chapter.

7.4 Results and discussion of the first study

7.4.1 Preparation of pellets

PRH pellets were manufactured using the extrusion-spheronization technique. Six batches were successfully prepared. The pellets matrix consisted of Eudragit RS and PRH, yet the plasticisers' type or concentration were changed. The optimized plasticizers concentration was used to produce the adequately shaped pellets. The results showed that the yield was higher than 60% for all batches (Table 7.4). However, it was noticed that concentration and type of plasticizers affected the yield. For instance, the yield for F5 and F6 of ATEC was 87.56 and 92.66%, respectively. While sorbitol batches F1 and F2 showed yields of 66.00 and 87.10%, respectively.

Moreover, the yield increased when using a high ratio of the plasticizer. Although the yield differed between TEC and ATEC batches, F3 with F4 and F5 with F6, the yield varied slightly by less than 10%. This could indicate that the use of TEC and ATEC in the pellet formulations resulted in higher yields. Besides, the sorbitol at low ratios showed the minimum impact on yield.

On the other hand, water was required in low abundance in batches with high plasticizer concentration. Although similar amounts of water were added to ATEC and TEC batches at both concentrations, the sorbitol batch contained the lowest amount of water. This could be attributed to the differences in the states of the plasticizers and solubility. Hence, TEC and ATEC are liquid plasticizers, while sorbitol is solid. Since ATEC and TEC have low water solubility compared to sorbitol, a high quantity of water is required as that difference in solubility can render water molecules unbound in the matrix (Fadda *et al.*, 2008) (Fadda *et al.*, 2008) (National Center For Biotechnological Information, 202AD).

Moreover, moisture content's impact depends on the state and position of water molecules within the pellets matrix since water can exist in two forms; bulk water and anhydrous units bounded either strongly to the particles or absorbed to the surface of the particles. Therefore, mechanical properties, such as tensile strength, could also increase with increased moisture content since a higher number of solid bridges form between particles, thus minimizing the distance between them, allowing particle-particle attraction (Thoorens *et al.*, 2014). On the other hand, if water molecules exist

as bulk water within the particles, multiple water layers can exist on the particles' surfaces, leading to swelling of MCC particles. Thus, the existing distances between pellet particles gradually affect particle bonding by hindering the intermolecular attraction forces, decreasing the tensile strength (Thoorens *et al.*, 2014). These findings were in accordance with the tensile strength in this study, as shown later in the discussion.

On the other hand, the moisture content affected by the amount of water added increased with respect to the added quantities; for instance, F5 and F6 showed 2.54 % with 3.1 mL water and 2.00 % with 2.6 mL water of moisture content, respectively. Also, It was stated by Thoorens et al. that the fraction of amorphous to the crystalline state in the MCC structure affects the water sorption within the particles as water mainly retained in the amorphous part (Thoorens *et al.*, 2014). Therefore, such differences could occur during pellets preparation.

Table 7.4 The prepared pellets of different plasticizers sorbitol, TEC and ATEC showing yield (%), amount of water (mL), moisture content (%) and bulk density (mean \pm SD and n=3)

	F0	F1	F2	F3	F4	F5	F6
Yield (%)	NA	66.00	87.10	94.55	92.61	87.56	92.66
Moisture content (%)	NA	1.60	1.22	2.53	1.90	2.54	2.00
Bulk density	NA	0.53	0.42	0.58	0.57	0.59	0.57
\pm SD (kg m⁻³)		\pm 0.00	\pm 0.00	\pm 0.02	\pm 0.01	\pm 0.00	\pm 0.00

On the other hand, this kind of difference can occur due to certain factors: the extruder speed, plasticizer amount, drying time, and granulation fluid type used for pellet's formulation. Akhgari, Abbaspour and Moradkhanizadeh reported that extruder speed set at 120 rpm affected the quality and yield of extrudates. Therefore, in this study, the extrudates were produced smoothly using a low extrusion speed (20 rpm). Also, using high extrusion speed, the probability of losing moisture content is high and can affect the pellets' strength (Akhgari, Abbaspour and Moradkhanizadeh, 2013). It was stated

that there was heat generation during the extrusion step owing to the friction between the particles (Muley, Nandgude and Poddar, 2016).

Moreover, it was reported that during the drying process, the distribution of water could be rearranged within the polymer particles leading to inhibition of water evaporation during the drying step. When the matrix particles are combined, water evaporation is hindered, leading to the necessity of prolonging drying time (Vervaeet, Baert and Remon, 1995) (Voogt *et al.*, 2019). Therefore, it must be considered for future studies that different pellet constituents require different drying times. However, in this study, such parameters are kept consistent for all formulations to compare only the plasticisers' effect. Despite all the observed differences between the formulations, pellets were successfully prepared from F1, F2, F3, F4, F5, and F6, showing the importance of incorporating plasticizer in pellet matrices missing in F0 batches resulting in randomly shaped pellets and collection difficulty. Hence, the extruder screen was blocked, producing few extrudates.

A similar trend was noticed by Sadeghi *et al.* The prepared mass blocked the screen during the extrusion leading to no pellet formation; hence this batch contained no MCC and no plasticizer. This could be explained by the plasticizer influence on T_g of the polymer, leading to a reduction of the polymers' mechanical properties by the transition from glassy to rubbery state (Wang *et al.*, 1996) (Wang *et al.* Therefore, polymers without plasticiser were brittle and challenging to extrude. According to Muley, Nandgude and Poddar, using an adequate quantity of water in pellet preparation is an essential factor in achieving mass with good consistency without over wetting the mass and achieving good yield with minimum blockage to the extruder screen (Muley, Nandgude and Poddar, 2016). On the other hand, the plasticizer effect was reported differently according to its ratio. Hence, it was reported that low concentrations of ATEC and TEC (<10%) generated an anti-plasticizing effect with a low impact on the T_g of the polymer leading to increases in the tensile strength (Wang *et al.*, 1997). However, according to the same study, findings showed that a low concentration of plasticizers demonstrated a low impact on the YM due to pellets' porous structure (Wang *et al.*, 1997). This was similar to our finding, as discussed in the tensile strength section. Also, the porous structure of the pellets was demonstrated in the SEM images.

Moreover, it was reported that the high tensile strength is related to the anti-plasticizing effect that reduces the pellets permeability leading to a delay in drug release. This was required to achieve the delayed drug release as the aim of the study. As a result, the required amount of water and the plasticizers was optimised to prepare pellets with good mechanical properties (Chamarthy and Pinal, 2008). It can be assumed that the plasticizer in low concentrations (<10%) could fill the gaps between the polymer particles producing opportunities for interparticulate bonds and solid bridges to form, leading to improved formulation strength. Nevertheless, water could improve the pellets' elastic properties due to its plasticizing effect (Blasi *et al.*, 2005). Thus, these combinations could help produce pellets with good mechanical properties that resist the applied pressure and still have good flexibility to retain their shape.

On the other hand, owing to the low plasticization effect of ATEC and TEC, a higher quantity of water was required in their batches compared to sorbitol batches (Wang *et al.*, 1997). Therefore, in this study's experimental work, low quantities of both plasticizers were used and an appropriate amount of water to synergise the plasticizing influence on Eudragit RS and MCC (Chamarthy and Pinal, 2008).

Plasticizer concentration had an impact on the amount of granulation fluid required to prepare the wet mass. For instance, using a lower sorbitol concentration required a higher amount of water as recorded in F1 compared to F2. The results were similar for F3 and F5 compared to F4 and F6, respectively, as the composition of the pellets affects the required amount of water to prepare wet masses of a good consistency for the extrusion-spheronization technique (Blasi *et al.*, 2005) (Abbaspour, Sadeghi and Garekani, 2005). It can be stated that the higher the plasticizer concentration, the less water added and, therefore, lower moisture content.

Moreover, one of the important factors in the preparation of good pellet properties is bulk density. The bulk density of all batches indicated the packing properties of formulation particles related to the spherical-shaped pellets (Muley, Nandgude and Poddar, 2016).

7.4.1.1 Pellets morphology and dimensions

Pellets sphericity was assessed by measuring the AR of 30 pellets (longest and shortest diameter) from each batch (Table 7.5). Oval, cylindrical, and rounded shaped pellets were seen in all formulations. The results showed that AR (mean) was close to 1 for batch F1 (1.3) and increased with changes to the plasticizer type and concentration; for instance, the AR for the TEC batch was higher than the sorbitol batch with AR in $F3 > F1$, and similarly, the ratio increased with higher TEC concentration rendering AR in $F4 > F2$. However, the AR markedly increased with increasing TEC and ATEC concentrations compared to sorbitol; for instance, sorbitol in F1 was 15% (w/w), while in F3 and F5, the ratio of TEC and ATEC was 3% (w/w), respectively. According to Gandhi, Badgujar and Kasliwal, the spherical pellets with a good AR were 1.11, showing an acceptable range close to 1. Besides, Dukić et al. found that the comparison between pellets with and without sorbitol showed a remarkable impact of the plasticizer on the pellets' surface properties and the consistency of the wet mass, where pellets without sorbitol had fractured surfaces. In contrast, sorbitol pellets had fewer rough surfaces (Dukić *et al.*, 2007). These findings were similar to our study findings as the SEM images of F1 showed good sphericity with lower sorbitol concentrations. However, the higher concentration of sorbitol produced pellets with rough surfaces, which Goyanes noted, Souto and Martínez-Pacheco, the Pellets of MCC with 50% (w/w) sorbitol amount in the pellets showed faster drug release than the pellets of MCC with 50% (w/w) mannitol owing to the higher porosity and surface roughness of sorbitol pellets (Goyanes, Souto and Martínez-Pacheco, 2010). This indicates that the plasticiser's addition needs to be within a specific range without affecting the pellets' surfaces properties. In addition, each plasticizer has different effects depending on the amount of water added. It was found that the particle size of the primary materials plays a remarkable impact in the final roughness and surface structure of the pellets produced by extrusion spheronization (Sarkar, Ang and Liew, 2014b). Higher number of small particles will provide fewer voids providing high contact points (Sebhatu and Alderborn, 1999; Gochioco, 2014). Also, shape uniformity is high in small particles leading to form pellets of smooth surfaces in F1 and F2 batches (Bodhimage, 2006; Abdel-Hamid, Alshihabi and Betz, 2011). All ingredients in batches F1 and F2 were solid particles, while liquid plasticizers were included in F3, F4, F5 and F6. Although the results

showed that %RSD was high in all formulations in our study, the lowest %RSD was associated with the F1 batch at the lowest AR. This finding indicates that sorbitol provides good shape enhancing properties (Gandhi, Badgujar and Kasliwal, 2011).

Table 7.5 The aspect ratio results for all batches in mean \pm SD (n=30) and relative standard deviation (%RSD)

	F1	F2	F3	F4	F5	F6
Aspect ratio \pm SD	1.3 \pm 0.3	1.9 \pm 0.9	1.8 \pm 0.4	2.0 \pm 0.8	1.6 \pm 0.6	1.8 \pm 0.7
%RSD	22.9	45.1	24.4	41.1	34.8	37.7

The SEM images showed, in general, oval-shaped pellets. The SEM results of F2- F6 showed that pellets had irregular surfaces and elongated shapes. Also, all pellets in batches F1-F6 showed high surface porosity owing to the pellets' rough surfaces detected by SEM. The SEM results followed pellets measurements with AR as F1 showed the lowest AR with good sphericity in Figure 7.1-a. Simultaneously, the other batches showed elongated shaped pellets that agreed with high AR results for these batches (F2, F3, F4, F5 and F6).

Moreover, a shaggy like surface was noticed for F2, as seen in Figure 7.1-b. This observation could be related to the influence of drying temperature on the pellets surface structure. This can be explained by the lower moisture content of F2 (Table 7.4), exposing the particles to higher drying temperatures, leading to sticky pellets' formation after drying. The pellets stickiness could be generated by the presence of a high concentration of sorbitol (30%), leading to a change in the pellets' thermal properties and reducing T_g of the F2 batch (Snejdrova and Dittrich, 2012; Ma *et al.*, 2018). This was in harmony with the YM results in the following sections (

Figure 7.2), with F2 demonstrating lower YM than F1.

The results also indicate the accuracy of the AR measurement by using the calliper as an inexpensive, easy, and reproducible method compared to SEM software.

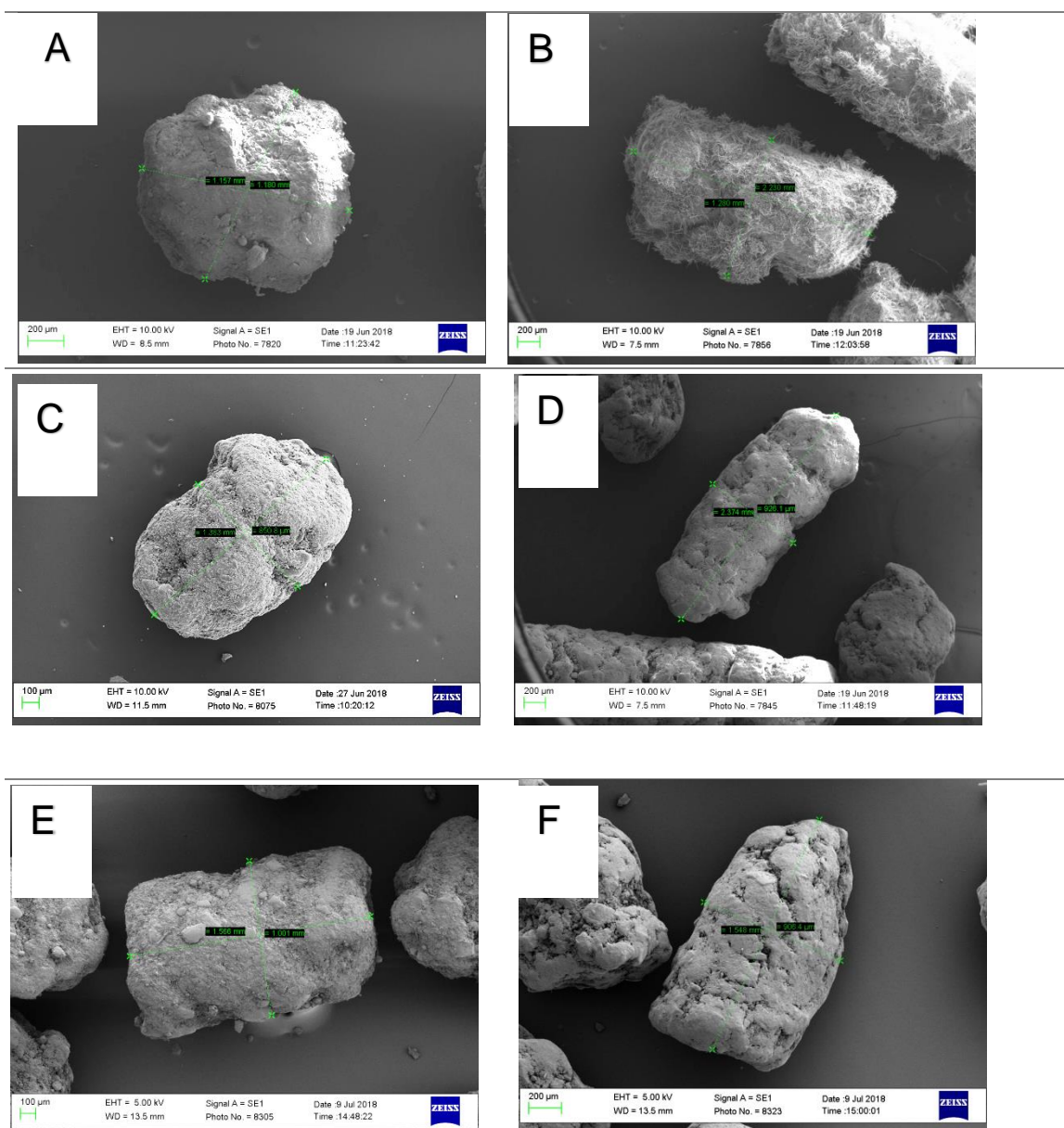


Figure 7.1 SEM images of PRH pellets produced from different types and ratios of plasticizers F1 (a), F2 (b), F3 (c), F4 (d), F5(e) and F6 (f)

7.4.1.2 Porosity and surface area

The Belsorp software was used to generate and analyse the adsorption/desorption results for all pellet batches (Table 7.6). Depending on the interaction between the gas and the exposed particles' surfaces, an amount of gas adsorbed. BET analysis was used to detect nitrogen adsorption, commonly utilized due to its high purity and interaction with the solids' particles. To provide enough interaction between the

particles, surfaces and the gas samples are cooled with liquid nitrogen. Then, adsorption layers are generated until no more absorption of nitrogen atmosphere occurs, leading to an increase in temperature and gas release via desorption (Raja and Barron, 2019). The BET isotherms showed the amount of gas adsorbed against temperature. According to the Union of Pure and Applied Chemistry (IUPAC), our results showed that F1, F2, F3 and F4 demonstrated mono-multilayer adsorption of type 4 isotherm (Donohue and Aranovich, 1998). Hence, the monolayer was the first layer of adsorption generated, followed by a multilayer of adsorption (Sing, 1982). This can be explained by filling the fine pores (micropore) initially with gas molecules at low pressure and then at high pressure, large pores (mesopores and macropores) were filled (Labani *et al.*, 2013). While isotherm type 3 was demonstrated by F5 and F6. The type 3 isotherm shows a strong interaction between the adsorbate molecules compared to the adsorbate particles interaction, which is weaker. According to IUPAC, there are three types of pore sizes; micropores (<2nm diameters), mesopores (2-50nm diameter) and macropores (>50nm diameters) (Sing, 1982).

All pellets showed a 9-16 nm pore size demonstrating a mesoporous structure. The added plasticizer can also be defined as mesoporous according to the definition from IUPAC. The change in plasticizer ratio affected the surface area slightly with proportional increments of plasticizer concentration. On the other hand, the drug release rate is affected by the surface area; hence, the larger the surface area, the faster the drug release seen in F1 and F2 batches. It can be assumed that the batch with the highest surface area affected PRH to release the greatest as in the sorbitol batches. However, the difference was less evident between TEC and ATEC batches (Muley, Nandgude and Poddar, 2016).

Nevertheless, the difference in the surface area results is correlated with the total pore volume and the mean pore diameter; hence if the surface area is low, it indicates that either of these parameters is high. For instance, in F5 and F6, the surface area for F5 was smaller ($0.23 \text{ m}^2\text{g}^{-1}$) than that of F6 ($0.28 \text{ m}^2\text{g}^{-1}$). Similarly, the total pore volume of F5 was smaller while observing that the mean pore diameter of F5 (11.06 nm) was larger than that of F6 (9.33 nm), indicating that these factors can affect the results of each batch. On the other hand, surface properties could contribute to porosity; for example, F5 and F6 showed high surface roughness. However, the pellets of F5 had greater surface roughness (Table 7.6) (Tunón, Gråsjö and Alderborn, 2003).

Table 7.6 Surface area, mean pore diameter and total pore volume of the sorbitol, TEC and ATEC pellets from the BET plot

Samples	Surface area (m ² g ⁻¹)	Mean Pore Diameter (nm)	Total Pore Volume (cm ³ g ⁻¹)
F1	1.45	12.72	0.00460
F2	0.87	9.91	0.00216
F3	0.31	14.11	0.00111
F4	0.32	15.62	0.00126
F5	0.23	11.06	0.00631
F6	0.28	9.33	0.00646

7.4.1.3 Pellets' Young's modulus and hardness

The tensile strength and YM results of pellets were measured for all batches (

Figure 7.2). The AR data was used to calculate pellets radius and length. According to a reported study, the first notch was detected as an indication of the pellets' hardness (Cespi *et al.*, 2007). The first notch was produced after applying pressure on the pellet. This second notch correlated with the completion of the test. The notch allowed determination of the hardness or crushing force of batches F1, F2, F5 and F6. However, the notch detection was challenging for several pellets of F3 and F4.

It was noticed that an increase of sorbitol concentration (F1 to F2) reduced hardness, while an incremental increase of TEC and ATEC as in F3 to F4 and F5 to F6 showed an increase in pellet hardness (Table 7.7). A similar trend showed by the tensile strength. These findings agreed with the results of wang et al. that concluded the effect was through ATEC and TEC's anti-plasticising effect when used in low concentration (Wang *et al.*, 1997). In contrast, the high ratio of sorbitol produced the expected plasticizing effect, but the tensile strength decreased with higher abundances (F2) than lower abundance batches (F1). This influence was unclearly demonstrated in the results of YM. This can be explained by the moisture content impact on the pellets' YM

since high moisture content improves their elasticity profile and renders them able to retain their shape under compression, as noticed in SEM images 4 and 10.

Table 7.7 Hardness results of the produced pellets (n=30) (mean \pm SD)

	F1	F2	F3	F4	F5	F6
Hardness	1.74	\pm 0.88	\pm 6.08	10.89	5.19	11.92
(N)	1.0	0.4	\pm 1.06	\pm 5.59	\pm 1.51	\pm 5.49

Moreover, the difference between the YM of F1 and F2 was significant ($p < 0.05$), with a similar trend between F5 and F6 ($p < 0.05$). However, F3 and F4 showed no statistically significant difference ($p > 0.05$) in the YM values. Similarly, Abbaspour et al. reported that the elastic modulus was insignificantly affected while using TEC in the coating layer of Eudragit RS 30 D and LR 30D pellets. In our results, we showed that the increase of plasticizer in the formulation reduced the YM. The pellets with sorbitol and ATEC in higher abundances demonstrated a remarkable effect on the elastic properties (Abbaspour, Sadeghi and Afrasiabi Garekani, 2007)(Abbaspour, Sadeghi and Afrasiabi Garekani, 2008). The differences between the batches could be attributed to the concentration and the type of plasticizer (Wang *et al.*, 1996) (Wang *et al.*, 1997). It was reported that T_g of Eudragit L 30D and 100-55 film reduced by using higher amounts (~30%) of hydrophilic plasticizers such as triacetin, TEC and ATEC instead of hydrophobic TBC and ATBC plasticizers where the T_g decreased with lower abundances of plasticizer (10%) with no advantages observed with increased plasticizer amounts (10 to 30%) (Gutiérrez-Rocca and McGinity, 1994; Wang *et al.*, 1996)

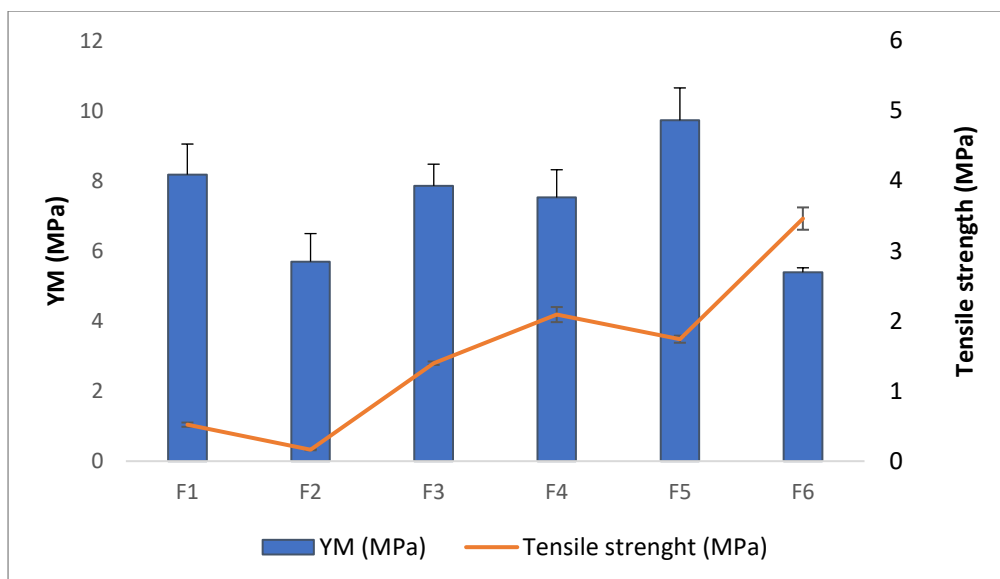


Figure 7.2 YM (Mpa) and tensile strength (MPa) of pellets produced from different amounts and type of plasticizers

7.4.1.4 Thermal analysis: DSC and TGA

To understand and detect the thermal properties of the prepared batches DSC and TGA were used. The DSC results showed that the T_g of the used polymer Eudragit RS was affected by plasticizers. Incoherence with Gupta, Kumar and Sachan's study, the T_g of Eudragit RS PO was reported at 65 °C in our study with the raw Eudragit RS PO powders T_g measured at 63-65 °C as seen in Figure 7.3 (Gupta, Kumar and Sachan, 2015b). Simultaneously, the DSC thermograms of all batches showed shifting in the original T_g range of 50-60 °C in a relatively ascending order of F4 and F6>F2. Two factors could explain this difference, firstly, the effect of different levels of plasticizing among the three plasticizers TCA, ATEC and sorbitol (Lim and Hoag, 2013b). Hence, T_g is an important parameter, and the addition of other components to the formulation could shift T_g of the polymer, demonstrating an interaction with that ingredient (Lim and Hoag, 2013b). Abbaspour, Sadeghi and Afrasiabi Garekani noticed this by adding ibuprofen to a Eudragit RS mixture reducing the T_g of Eudragit RS (Abbaspour, Sadeghi and Afrasiabi Garekani, 2007). Although the higher the plasticizer ratio, the greater change in polymer T_g was observed, there are exceptions to other properties such as the model drug and the moisture content (Khodaverdi et al., 2012). Therefore, the second factor is the plasticizing effect of moisture content. As a synergistic effect, this can cause a reduction in T_g . Thus, the moisture content in F4 and F6 was almost

the same yet higher than that of sorbitol in F2. The moisture content affects the MCC volume enlargement and ability to swell. A high number of water molecules leads to fewer hydrogen bonds in the MCC polymeric chain. Therefore, the polymer expands, facilitating the molecules' motion providing further mobility (Sahputra, Alexiadis and Adams, 2019). Therefore, moisture content can impact the stiffness of the batches by reducing the T_g of the polymer. This trend was also seen in the DSC results of F1, which showed lower T_g compared to F2. Similarly, F3 and F5 showed higher moisture content than F4 and F6, respectively; thus, T_g decreased in both. Although F2, F3 and F5 included lower ratios of polymers, the moisture content was synergistically reducing T_g as discussed earlier, and this can be confirmed even by the slight reduction in T_g observed with F1 since the moisture content is slightly higher than that in F2.

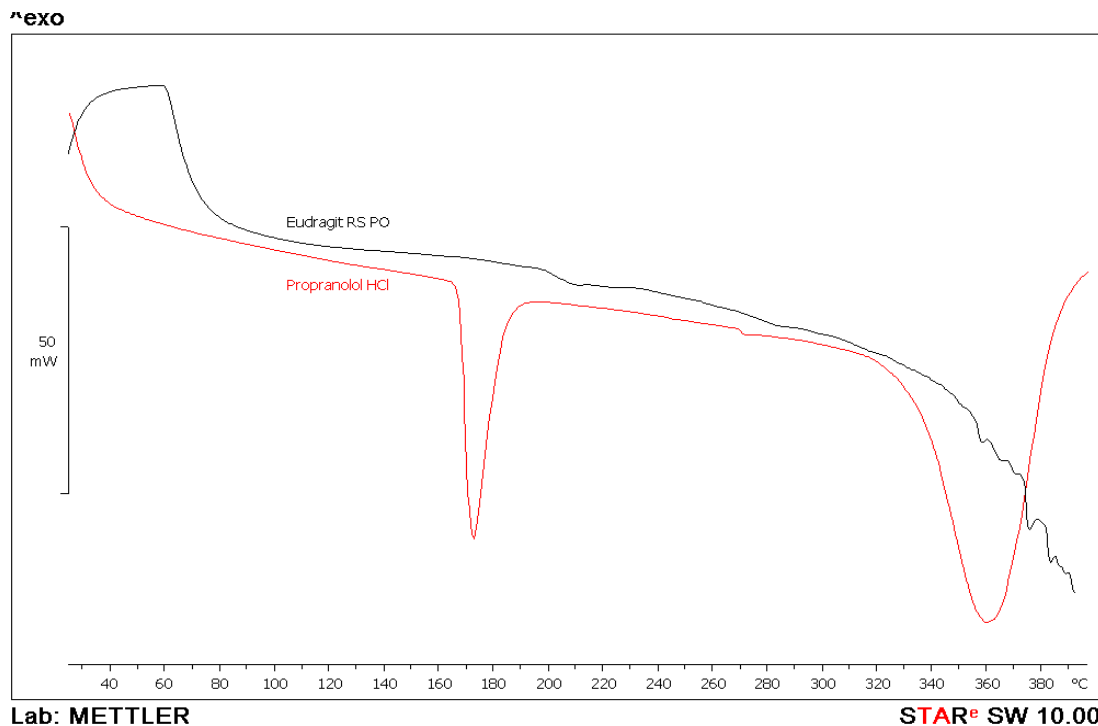


Figure 7.3 DSC thermogram of Eudragit RS raw powder and PRH using STAR^e software within temperature range 20-400 °C

Therefore, it can be stated that the drying temperature used during pellets preparation had no impact on the thermal properties of the formulations. For these adequately dried pellets, the plasticizer type and ratio in the pellets could affect these findings. Hence, the applied drying temperature was 40 °C, and Eudragit RS T_g was within 63-65 °C (Figure 7.3).

On the other hand, the melting point of PRH was 166 °C showing an endothermic peak in the DSC graph (Figure 7.4). The melting point was detected in all batches, F1 and F2, showed a minimal peak with slightly shifting to 158 °C. The plasticiser's predominant effect could explain this difference since F1 had 15% sorbitol (w/w) and F2 had 30% (w/w) sorbitol, with the melting point more evident in F1 than F2. The melting point of propranolol hydrochloride was 163-166 °C (National Centre for Biotechnology Information /PubChem., 2000; Thermofisher, 2018).

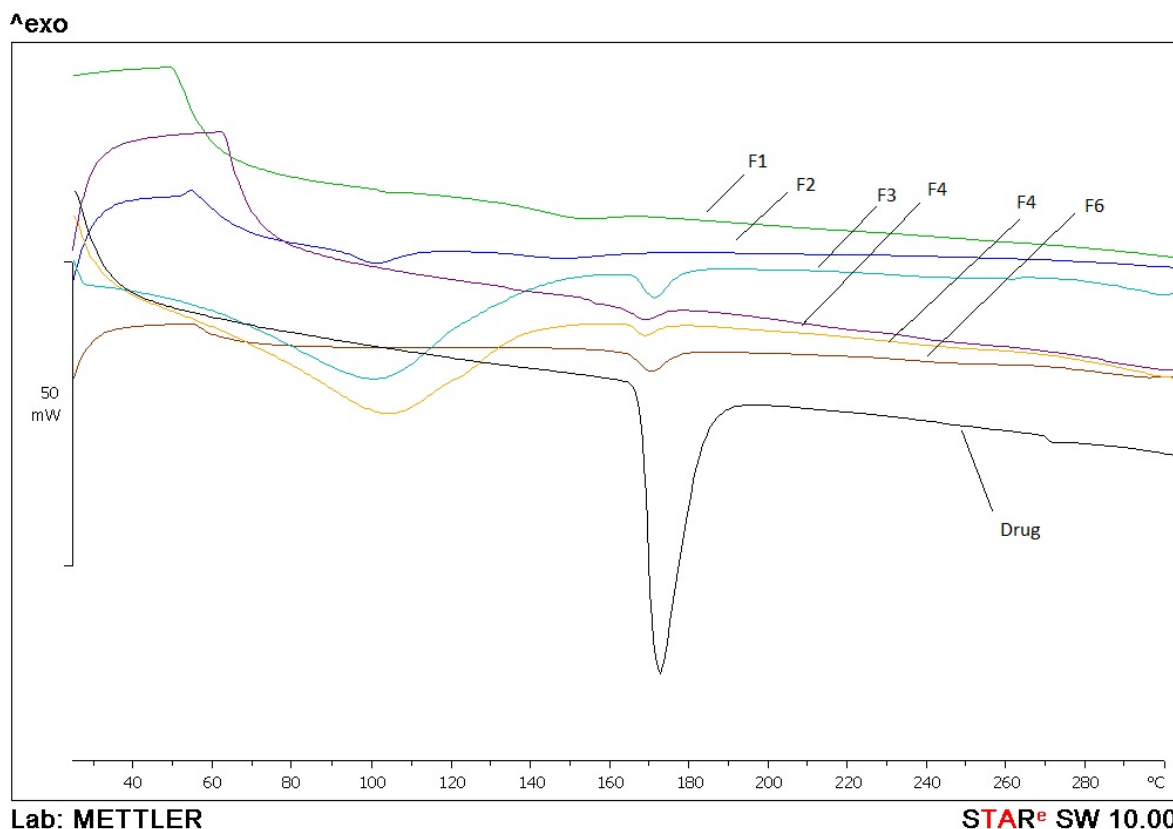


Figure 7.4 DSC thermograms of PRH pellets contained in the 15% sorbitol (F1), 30% sorbitol (F2), 3% TEC (F3), 5% TEC (F4), 3% ATEC (F5) and 5% ATEC (F6) and PRH (drug)

TGA results agreed with DSC findings. Hence, the TGA thermograms showed a moisture content generated a broad endothermic peak at 100 °C in the DSC graph. For instance, F5 and F6 batches made up of 3% and 5% ATEC pellets, shown in Figure 7.5, showed this correlation.

On the other hand, all batches suffered from the same decomposition temperature, which correlated with the Eudragit RS decomposition, starting at 280 °C. However, decomposition temperature is slightly affected by changing plasticizer type and concentration and including PRH. Pellets in sorbitol batches (F1 and F2) decompose

around 320 °C, which was different from TEC and ATEC batches (F3 and F6) that decompose at approximately 300°C. Hence, degradation occurred after the decomposition, as observed in the DSC and TGA graphs.

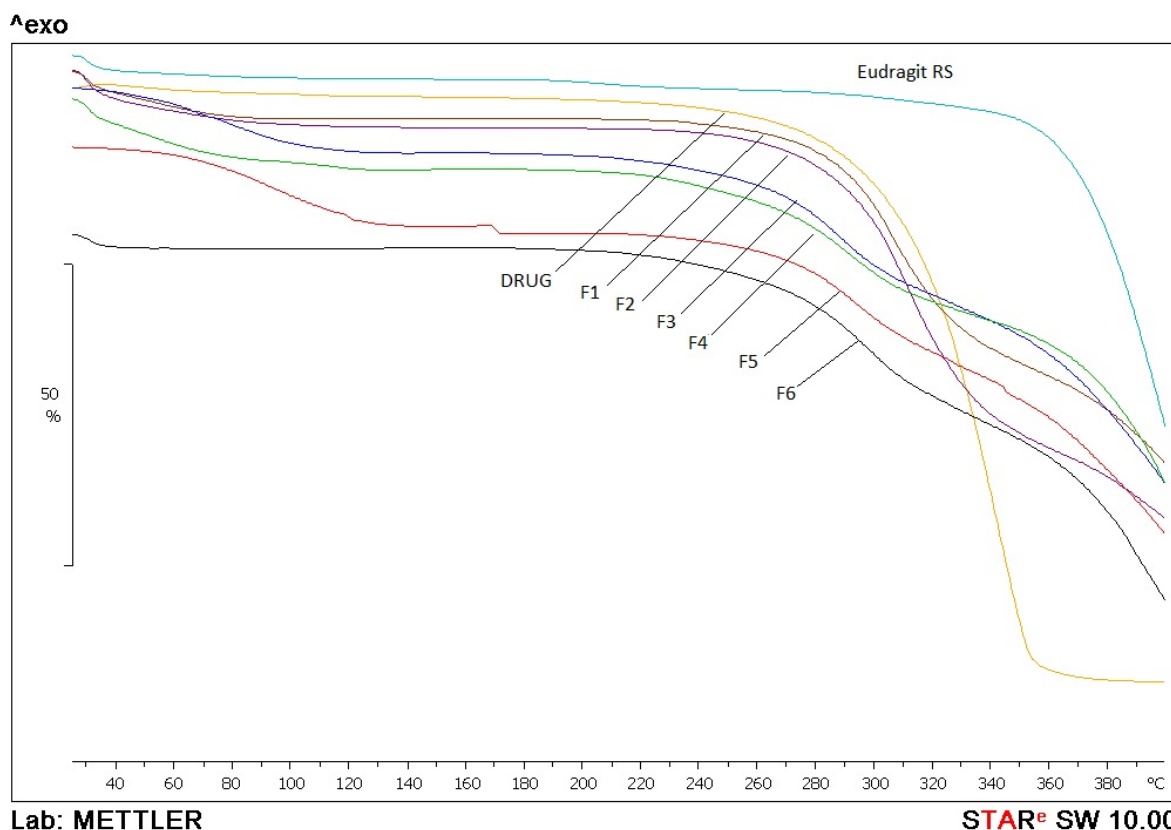


Figure 7.5 TGA results of all produced batches 15% sorbitol (F1), 30% sorbitol (F2), 3% TEC (F3), 5% TEC (F4), 3% ATEC (F5) and 5% ATEC (F6) and Eudragit RS and PRH (Drug)

7.4.2 Tablets mechanical strength

The prepared tablets from ODTs matrix and pellets were tested according to their mechanical and morphological properties. The tensile strength was calculated for all ODTs comprising 20% (w/w) pellets depending on each tablet's hardness, thickness, and diameter (Figure 7.8). Hence, maximum force before breaking was recorded (Sabri *et al.*, 2018). Similarly, tablets without pellets were tested. It was reported that the adequate tensile strength for tablets differs according to the type of formulation. Generally, mechanical strength greater than 1.7 MPa is sufficient for conventional tablets to withstand manufacturing processing, while other types of tablets, such as fast-dissolving, intended to be prepared with a low tensile strength that can be lower

than 1 MPa (McCormick, 2005a; Pitt and Heasley, 2013). This is important to provide adequate weakness to allow the breakdown of the tablets after ingestion. The results showed that all tablets had low tensile strength indicating the brittleness of the tablets. This could be related to the low mechanical properties of the ODTs starting materials, which can be seen from the control tablet results (no pellets). A similar trend was noticed in the results of pellet-based tablets indicating that inclusion pellets and varying the plasticizer ratio had a limited effect on the tablets' strength with no statistical difference ($p>0.05$) observed. However, a significant difference ($p<0.05$) was detected between the F5 and F6 tablets tensile strength. This can be correlated with the pellets' distribution that offers more support to that batch. Hence, according to SEM results in Figure 7.1 & Figure 7.7, the pellets with different surface roughness could offer mechanical interlocking during tablet compression with other particles, thus enhancing the tensile strength as reported by ElShaer et al. and Moon and Jang (Moon and Jang, 1999; ElShaer *et al.*, 2017). Our results suggested that all tablets possessed acceptable hardness ranging from 12 to 21N. This is important to enable a short disintegration time to enhance tablets disintegration orally (Velmurugan, S., 2010).

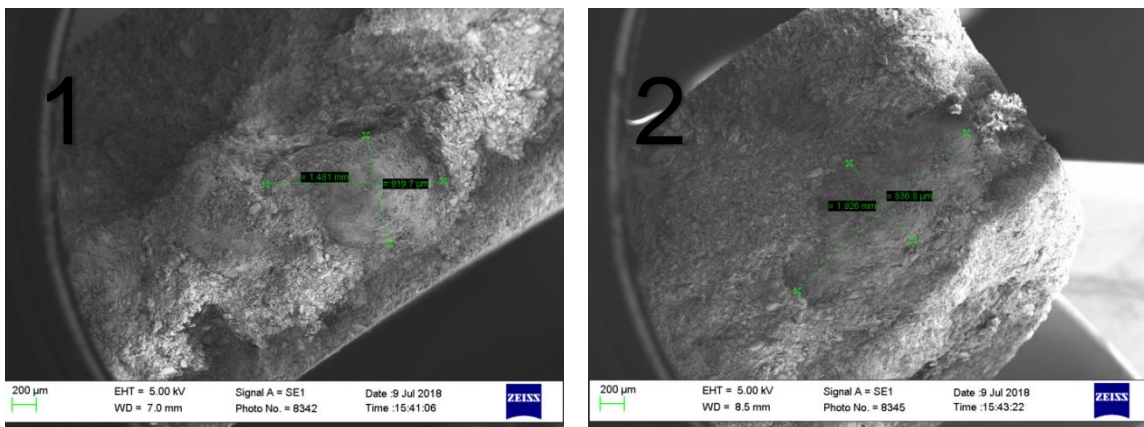
7.4.2.1 Scanning electron microscopy of tablets

SEM was used for all prepared tablets to detect the pellets' presence within the tablets matrices and to examine the change in pellets and particles shape after compression. The tablets were carefully prepared to distinguish between the tablet matrix and the embedded pellets, as in Figure 7.6. The SEM images showed that all tablets had a similar general look with the pellets' presence within the matrix detected. Although it was difficult to detect the pellets in tablet matrices in the images, the pellets were observed easily on the broken side of the tablets. Although pellets had flattened surfaces from the compression during tablet preparation, this was expected and determined according to their high YM results. However, some pellets did retain their shape under compression (Figure 7.7-4 and 5). The other reason could be that the number of pellets present near the tablet surface exposed to high pressure rendered the surfaces too flat, as Pai, Kohli and Shrivastava reported (Pai, Kohli and Shrivastava, 2012). These results were in harmony with the disintegration test and tensile strength tests that showed no significant difference between the tablets as in SEM images (Figure 7.7). However, the prepared tablets' release profiles showed that

the pellets under compression affected the PRH release, which could be one reason for inadequately controlled PRH release.



Figure 7.6 Tablet preparation for SEM analysis with a diagram showing the distribution of the pellets within ODT



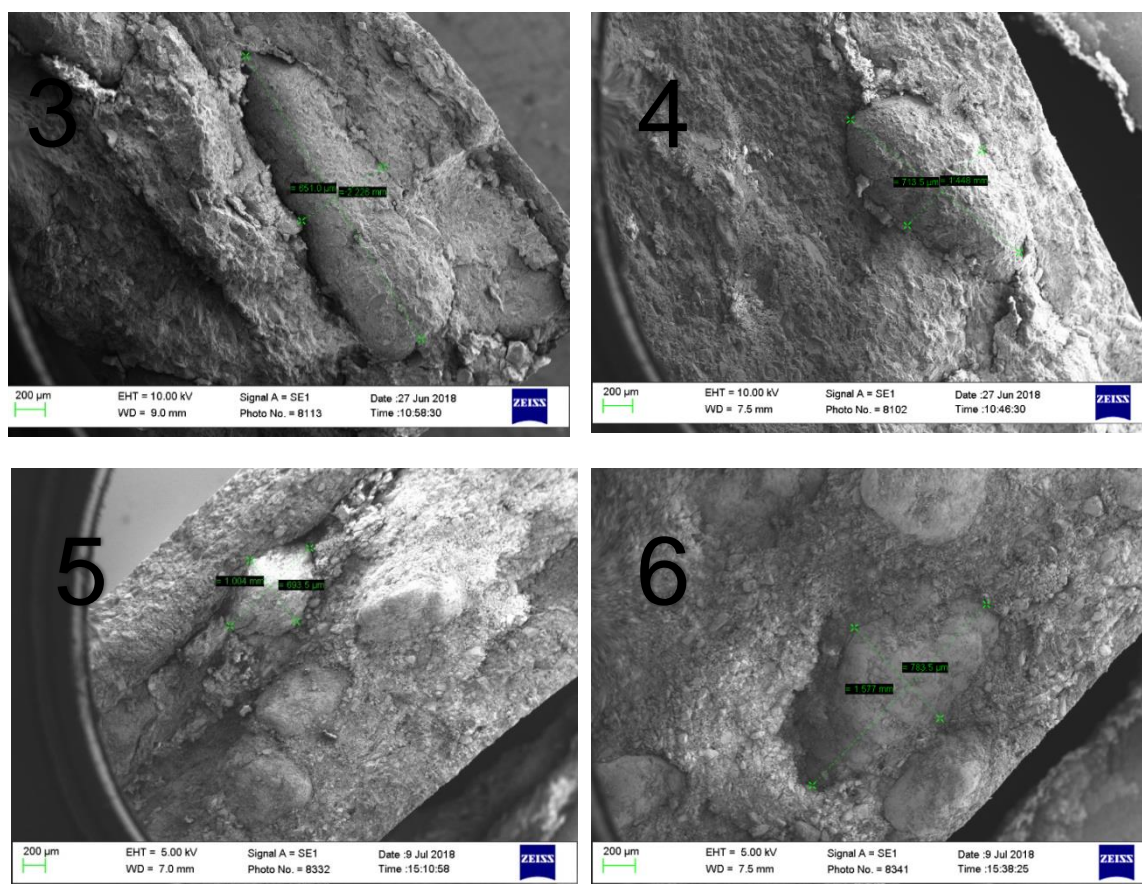


Figure 7.7 SEM images cross-section and top views detecting PRH pellet in the broken side of ODT surface; tablets of F1(1), F2(2), F3(3), F4(4), F5(5) and F6(6)

7.4.2.2 Disintegration test

The orally disintegrating tablets, known as rapidly melted or fast-dispersing dosage forms, disintegrate within seconds or less than 3 minutes (Sastry, Nyshadham and Joseph A Fix, 2000; Rowe, Raymond C., Paul Sheskey, 2009; A. Elwerfalli *et al.*, 2015). Disintegration time for all tablets was measured (n=3) to detect the tablets' breakup ability after pellets' inclusion (Figure 7.8). The tablets of all batches showed an acceptable disintegration time (<30 seconds) correlating with the results of the tensile strength (Sastry, Nyshadham and Joseph A Fix, 2000; Rowe, Raymond C., Paul Sheskey, 2009; A. Elwerfalli *et al.*, 2015). This indicates that pellets had a limited effect on the properties of ODTs and including them within the matrix is possible for future formulations.

Although the tablets showed similar values to the control, which disintegrated within 20 seconds, there was a difference in the disintegration time between the tablets contained in the PRH pellets. Hence, the time of the disintegration decreased with increasing plasticizer abundance in pellets. However, the difference between the disintegration times of the formulations was insignificant ($p>0.05$). Goyanes, Souto and Martínez-Pacheco reported that the high sorbitol ratio in pellets increased hydrochlorothiazide's dissolution rate (model drug). Therefore in our study, this could disturb the disintegration since a high plasticizer ratio would facilitate the diffusion of water into the pellets matrix owing to the higher hydrophilic elements of these plasticizers (Goyanes, Souto and Martínez-Pacheco, 2011).

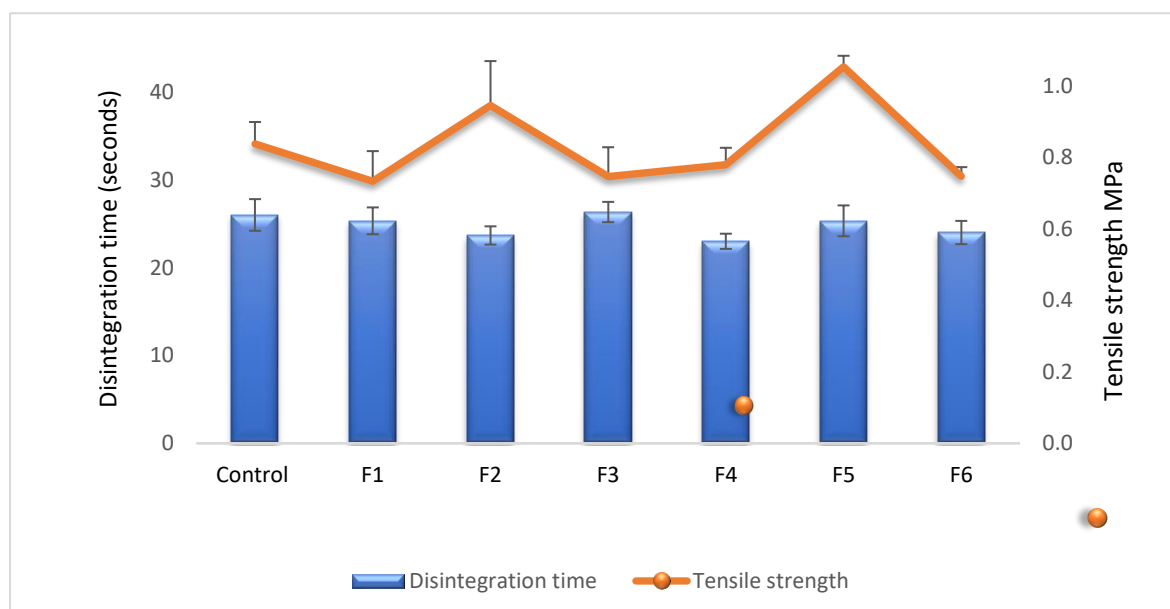


Figure 7.8 Tensile strength and disintegration time of ODTs contained in the pellets and control of PRH

7.4.2.3 Contact angle

A Wettability test was used to identify the ODT's ability to disintegrate along with the disintegration test (Nachajski *et al.*, 2019). The test depends on the contact angle generated between the fluid (distilled water) and the solid surface (tablet). In general, when the fluid and the other boundaries generate the contact angle are stable, the contact angle can be measured according to the sessile drop method, as illustrated in Figure 7.9 (Nachajski *et al.*, 2019). The sessile drop is a suitable method for particles and compressed powders showing simply the detected contact angle depending on

the tangent generated between the liquid and solid (Yuan and Lee, 2013; Yang *et al.*, 2018).

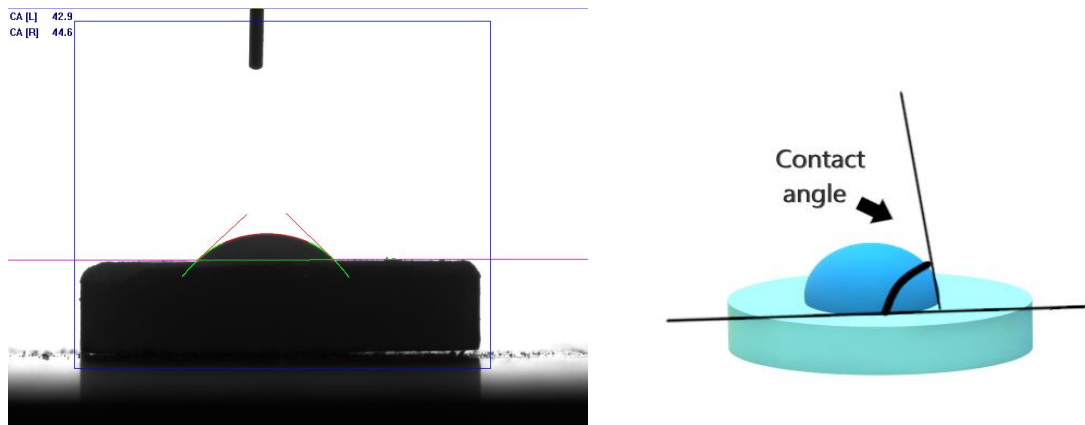


Figure 7.9 Contact angle between the liquid droplet and tablet surface actual image and drawing illustrating the angle measurements

Both methods, disintegration, and wettability, were used to determine the disintegration ability of the tablets. The results of contact angles showed that the formed tangent between the water droplet and the tablet was smaller than 40° (Table 7.8).

The low value of that tangent shows a high wettability propensity, which indicates the short disintegrating time. Hence the water droplet was spreading over the tablet surface evenly. On the other hand, if the tangent were high, the wettability is poor, and the tablets demonstrate long disintegration times (Dimitrov *et al.*, 1991). However, the results showed a slight difference between the formed tangents; this could be attributed to multiple factors; such as tablet porosity, particles and surface roughness, tablet and strength under compression (Yuan and Lee, 2013).

The wettability test results followed the disintegration results demonstrating a short disintegration time. Batch F4 (Figure 7.8) showed the smallest contact angle and the lowest disintegration time. It was reported by Yang *et al.* that a low contact angle ($<90^\circ$) indicates that tablets show good wettability, which was similar to our findings (Yang *et al.*, 2018). Hence, in this study, the disintegration time was close to the wetting rate.

According to Yang *et al.*, the correlation between the tangent of contact and the disintegration is unclearly studied. However, our showed a good correlation. Consequently, this study could be applied to estimate the wetting rate that shows the unpredictable disintegration of ODTs.

Table 7.8 Contact angle measurement using the sessile drop method (n=3)

Tablet	F1	F2	F3	F4	F5	F6
1	31.5	27.5	42.9	26.4	36.1	32.9
2	26.2	31.5	38.1	20.8	35.7	30.0
Mean ± SD	28.9 ± 3.7	29.5 ± 2.8	40.5 ± 3.4	23.6 ± 4.0	35.9 ± 0.3	31.5 ± 2.1

7.4.2.4 Dissolution

According to BP, the dissolution test was done using apparatus II with hydrochloric (acidic) and phosphate buffer media of pH 1.2 and 6.8, respectively mimicking the gastrointestinal fluid (FDA/CDER, 1997; Council of Europe, 2005; British Pharmacopoeia, 2017).

The test was performed independently in both media to observe any imperceptible change in PRH release profile without affecting the release study and to evaluate the formulation to modify PRH release. Therefore, the optimized formulation could be selected for further development and testing.

The results showed that PRH released entirely from all the formulations within 30 minutes in acidic media (Figure 7.10). On the other hand, in phosphate buffer media, all the formulations showed 100% release within 1 hr except F3, F4 and F5 that showed 89.83, 86.74, 91.98% of PRH was released, respectively. The exact formulations demonstrated a similar trend at 2 hrs of phosphate buffer dissolution test where F3, F4 and F5 released 93.93, 90.18 and 92.93% of PRH, respectively, with over 100% for the rest of the batches.

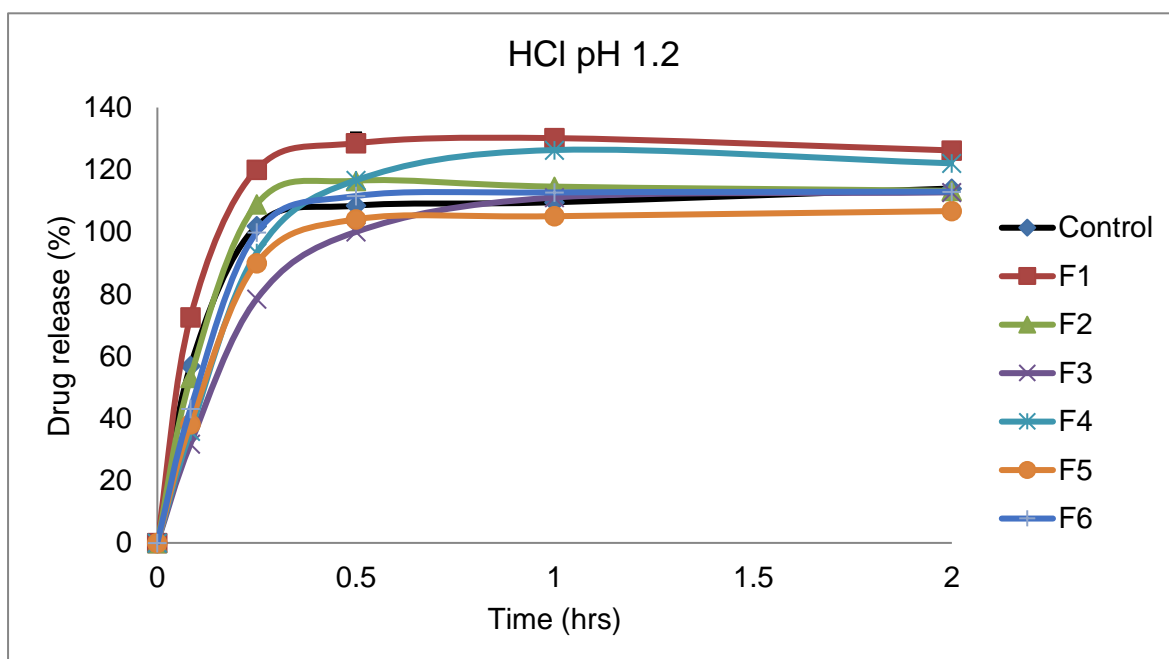


Figure 7.10 PRH release profiles of tablets contained in the prepared pellets in acidic media pH 1.2

Hence, it can be noticed from the dissolution study in Figure 7.11 (A and B) that at 2 hours in phosphate buffer media that F4 and F5 showed a stable release profile. However, 100% PRH was reached after 4hrs for all batches. PRH in acidic media reached over 110% from all batches except for F5 that released 106% PRH, and that batches stably releasing PRH reached 92.92% while indicating good surface properties of this batch. On the other hand, the other batches showed unequal distribution related to different factors, including the pellets diameter, surface roughness and porosity. This affects the particles bonding and leads to the segregation of the fine particles of ODTs from the large-sized pellets when preparing the tablets. Hence, the high porosity pellets could provide a low contact area and start to segregate from the matrix while surface roughness could generate particles interlocking (Moon and Jang, 1999; Tunón, Gråsjö and Alderborn, 2003; ElShaer *et al.*, 2017). For instance, F5 showed a low surface area of $0.23 \text{ m}^2\text{g}^{-1}$ and a high total pore volume ($0.00631 \text{ cm}^3\text{g}^{-1}$). Also, according to SEM (Figure 7.1), the high surface roughness and the lowest diameter were recorded for F5 (AR Table 7.5).

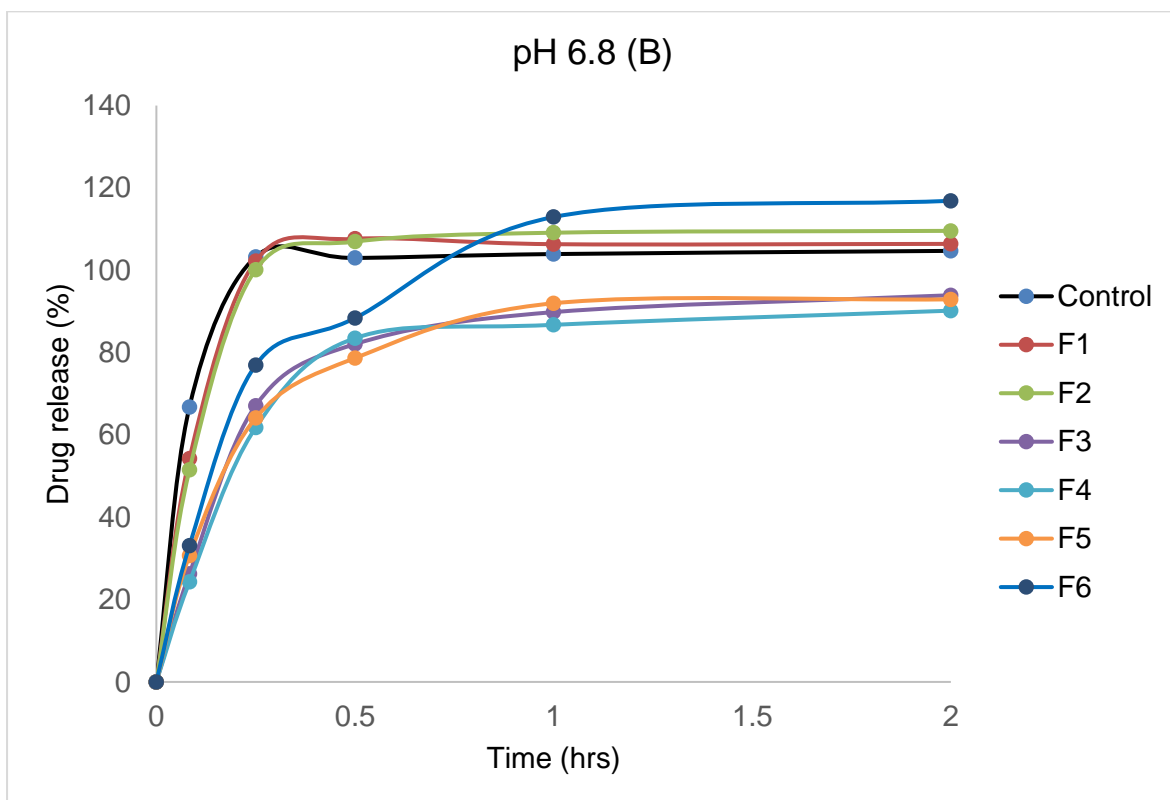
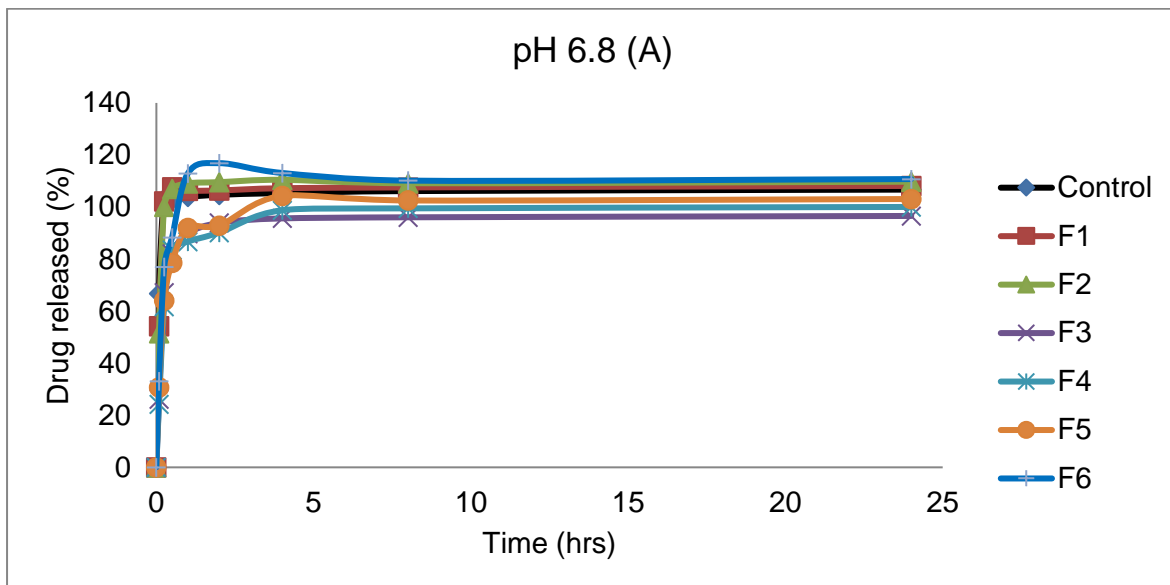


Figure 7.11 PRH release profiles from tablets of the prepared pellets in phosphate buffer pH 6.8 (A and B) within 24 hrs and 2 hrs

Nevertheless, the presented porosity in F5 showed limited effect and pellets predominantly influenced by the surface roughness and size. Hence, particle size, shape, and surface roughness affect the surface area, porosity and pore size distribution (Amador and Martin de Juan, 2016). Moreover, this finding could be confirmed by the tensile strength results as the F5 tablet showed the highest value compared to other tablets (Sabri *et al.*, 2018).

The batches' results in both media approached the study aim but showed minimal effects on PRH release control. It was expected that Eudragit RS modified PRH release when combined with other excipients in the pellets preparation since this polymer is time-dependent (Akhgari, Abbaspour and Moradkhanizadeh, 2013; Patra *et al.*, 2017). However, PRH released immediately at 30 minutes in the acidic media. Similarly, the release of PRH was almost immediate within 30 minutes in buffer media, with minor differences between the batches. Thus, the detected variations in both acidic and phosphate buffer media could be related to different types of plasticizers used in the pellets preparation ($p < 0.05$), while the change in ratios of plasticizers showed no statistically effect ($p > 0.05$). In addition, PRH is a weak base with pH-dependent solubility favoring to release in acidic media (Bolourchian and Dadashzadeh, 2008)(Calatayud-Pascual *et al.*, 2018).

Moreover, according to one-way ANOVA, at 30 minutes in both media (acidic and phosphate buffer) the difference in PRH release between the batches of TEC and ATEC for both ratios (3% and 5%) showed no significant difference ($p > 0.05$), while sorbitol batches (15% and 30%) were statistically different from each batch of TEC and ATEC for both ratios (3% and 5%).

However, according to the two-way ANOVA, the interaction showed no significant difference for all drug release analysis (30 mins in both media) when varying the plasticisers' ratio and type. This indicates there was no interaction between the two independent variables. On the other hand, although quaternary groups of ammonium in salt form provide pH-independent properties, it enhances the water permeability of Eudragit RS and affects the polymer's ability to swell and release PRH (Wagner and McGinity, 2002) (Aguilar-de-Leyva *et al.*, 2019).

Akhgari, Abbaspour and Moradkhanizadeh reported that the burst release of the model drug (mesalazine) from all batches of Eudragit RS based pellets in acidic media pH 1.2 took 15 minutes. Therefore, suggesting coated or reservoir-based pellets of Eudragit RS could address this issue (Akhgari, Abbaspour and Moradkhanizadeh, 2013). Therefore, replacing matrix system with reservoir system using a coating layer based on time-dependent polymers such as Eudragit RS or Eudragit RL could aid control of PRH. However, selecting one of these plasticizers either TEC or ATEC or their ratio is dependent on the mechanical and physical properties of the produced pellets and tablets since the drug release was insignificantly different between the distinguished plasticizers. ATEC of 3% ratio showed a good balance between elasticity and plasticity according to mechanical characterization results of pellets (YM and tensile strength). Therefore, the batch of sufficient strength for preparation, packing and handling with minor imperfection could be achieved using 3% ATEC with pellets (1.1 Mpa) of appropriate disintegration time (<30 seconds). Hence, the pellet's YM significantly differed between ATEC batches 3% and 5% of F5 and F6, respectively. Although YM was high for 3% of ATEC, the pellets were necessary to show moderate tensile strength, and this batch offered such balance in pellets and eventually the tablets. Simultaneously, the tablet's tensile strength between 3% of ATEC and TEC were statistically different ($p < 0.05$), while 5% ATEC and TEC showed no significant difference ($p > 0.05$). Hence, this was variation undetectable in all tablets except when adding 3% ATEC batch (one-way ANOVA). These findings were also supported with the best AR of 3% of ATEC pellets that was achieved.

7.5 Results and discussion of the second study

Formulation of coated pellets contained in ODTs is a challenging approach. It is essential to choosing suitable coating layers, type, and the coating materials' concentration (Kandela *et al.*, 2010; Mehta *et al.*, 2012)

Therefore, in our project, we aimed to investigate the effect of the coating layer and the ratio of the ingredients utilising an uncomplicated coating process. The method was applied, providing time and cost-saving with minimum effort. Trying different coating layers was an essential step in the pellets coating approach to modify the drug release. This was performed to initially facilitate the coating process independently from the other parameters, which could be considered for future studies. Therefore, the generated data would be considered to avoid the limitations and default of the obtained formulation for method optimisation. Also, it can examine the coating process and formulation properties without using expensive advanced coating techniques such as fluid bed coating.

7.5.1 Pellets formulations and optimisation process parameters

The time-dependent methacrylate's Eudragit RS and Eudragit RL were used to formulate the uncoated and coated pellets. However, our trials for the preparation of matrix pellets of Eudragit RS only were unsuccessful. Moreover, different trials to prepare uncoated pellets based on Eudragit RL were unsuccessful. Therefore, the uncoated pellets were prepared using Eudragit RS and the gold standard MCC matrices facilitating the formation of the pellets (Mehta *et al.*, 2012). Eudragits RS and RL were used in the coating layer as a reservoir system to be compared with the matrix system.

Four formulations of pellets were prepared with the same PRH loading (20% w/w). Three batches of pellets were coated with 10% w/v of polymers in ethanol; Eudragit RS, Eudragit RL or the combination of Eudragit RS: RL in the ratio of 1:1.

The process parameters were optimised in our study as the initial stage to avoid factors influencing the preparation of coated pellets using MCC, Eudragit RS and

Eudragit RL. Hence, the pellet's core could affect the physical and mechanical properties of the pellet, as discussed earlier in the introduction. The collective level of formulation variables includes replacing the mixer, testing the suitable speed of the extruder, the speed of spheronisation. These parameters' influence was considered to understand and provide a comprehensive overview of the method's reproducibility with the suitable settings. These parameters were trialled comparing with the literature according to the type of polymers and method of preparation (Lustig-Gustafsson *et al.*, 1999; Abbaspour, Sadeghi and Garekani, 2005; Kaur *et al.*, 2020).

The extrusion at 100-120 rpm speed produces fragile extrudates. Hence no pellets could be produced at this speed. The high-speed extrusion could increase the temperature, causing water evaporation and high friction between the particles (FIELDEN *et al.*, 1988; Muley, Nandgude and Poddar, 2016). Conversely, at a speed of 60 rpm, the extrudates demonstrated good textures and successfully formed after spheronisation (Thommes *et al.*, 2009). The optimised speed for spheronisation was 1200 rpm, resulting in obtaining pellets with a low AR that agrees with the literature (Muley, Nandgude and Poddar, 2016).

7.5.1.1 Coating process parameters and yield

Eudragit RS and RL were used as the coating layer to study their effect on the PRH release. Different studies applied these time-dependent polymers to prepare reservoir system formulations. Most studies used the laboratory-scale instrument fluidised bed system to coat the formulation and achieve a modified drug release (Friedman and Donbrow, 1978; Guignon, Duquenoy and Dumoulin, 2002; Stulzer *et al.*, 2008).

Since this facility was unavailable to be applied, our study aimed to use an uncomplicated and inexpensive coating method developed in our laboratory. We initially investigated specific coating parameters in this study to achieve an optimised formulation with modified drug properties. Consequently, this could provide a comprehensive understanding of the applicability and limitations of our coating method for future use. In addition, the observations would be helpful to be employed in the standard available coating method such as fluidised bed system, thus saving time and cost. Therefore, the final optimised formulation should be compared with the prepared

batch of the same parameters using the fluid bed coating method, which can be considered in further studies.

Eudragit RS and RL were used at three different levels with 10% w/v. The different concentrations of more than 10% w/v of coating layers were initially tried. However, the homogeneous solution was difficult to prepare without forming aggregation that may cause slow drying of the formulation under the experimental conditions. Similarly, the used concentration (10%) was trialled by Kaur et al. (2020) using Eudragit S100 to achieve colon-specific drug delivery. This concentration was suitable for coating layers with acceptable viscosity. Moreover, the authors found that the sphericity and morphology of the coated pellets were optimised using 10% w/v of polymer concentration (Kaur *et al.*, 2020).

On the other hand, MCC concentration was applied differently in the matrix and reservoir pellets at 20% w/v and 77% w/v, orderly. This was related to the difficulty of using the same amount of MCC in the matrix system with Eudragit RS. The coated pellets were prepared using the same ratio of MCC (77% w/w). According to our previous studies, ATEC of 3% w/w concentration was the suitable plasticiser.

The results showed that the concentration of MCC influenced the yield. MCC concentration at 20% w/w generated the highest yield, 87.56%. At the same time, the yield decreased to 64-69% with 77% w/w of MCC.

The 100% w/w concentration of MCC showed the lowest percentage yield 48-50% when using a similar amount of water (granulation fluid) among the other formulations. Therefore, a higher amount of water, 7 mL, was added to achieve enough pellets quantity. This batch was prepared to investigate the suitable percentage of MCC to prepare pellets with uniform shapes and surfaces. Hence, pellets' uniform shape and morphological properties are essential for a homogeneous distribution of the coating layer (Andersson *et al.*, 2000; Murthy Dwibhashyam and Ratna, 2008). Although the yield increased to around 80%, this batch cannot be applied for further comparison as the water amount differed remarkably from the other batches and only was examined for future application. Therefore, the yield was found to decrease with an increase in MCC concentration.

Similarly, Kaur et al. (2020) reported that MCC influenced remarkably the yield of the pellets showing that the lowest MCC concentration (47.8% w/v) produced the highest

yield when the amount of the other ingredients was constant (Kaur *et al.*, 2020). The other factor that may influence the pellets yield could be the mixing method. Hence, it necessary to use a bigger mixer container to facilitate the pellets preparation process. It also reduced the time consumed by changing the instrument parts during each preparation step (mixing, extrusion and spheronisation) (Muley, Nandgude and Poddar, 2016). According to our previous results, the mixing method was similarly used, and the obtained yield was consistently similar to the obtained pellets (F0 and F1). Therefore, ingredients and concentration can be considered essential factors are influencing the formulation yield (Dukić *et al.*, 2007).

However, the yield could be improved by examining the suitable quantity of water while keeping the other ingredients constant. It was found that the amount of water influenced the particles mechanical properties due to the formation of the bonding forces. Consequently, the formed dust during the spheronisation could be reduced (Amidon and Houghton, 1995; Singh, Pai and Kusum Devi, 2012; Crouter and Briens, 2014; Bhairy Srinivas, 2015; Saripella *et al.*, 2016b).

7.5.1.2 Physical properties of pellets

The physical properties of pellets, including flowability, bulk density, and AR, were evaluated for uncoated and coated batches (Table 7.9).

The flowability results (Table 7.9) were recorded for all batches. The results ranged between 4-5 g/second for all batches. The pellets were free-flowing with high flowability similar trend were reported by Šibanc *et al.* and Liu *et al.* (Liu *et al.*, 2008; Šibanc *et al.*, 2013). However, detected variations related to the surface properties of the pellets. Nevertheless, this was limitedly detected in our flowability results. This could be attributed to large dimensions of pellets as suggested by stereomicroscope and SEM analysis (Liu *et al.*, 2008). Hence, friction between surfaces can affect the flowability of the particles with dimensions smaller than 250 µm remarkably (Šibanc *et al.*, 2013). Therefore, the surface properties and pellets shape showed a limited effect and governed by pellets dimensions.

On the other hand, bulk density was between 0.59 – 0.65 g/mL. This variation could be generated from the difference in shape between the produced batches (Table 7.9).

The MCC concentration and the coating process could result in such variation. Similarly, Kaur et al. MCC and water content influenced the prepared pellets to shape differently (Kaur *et al.*, 2020). However, the adequate quantity of water used in our enhanced the extrusion spheronisation and the shape of the produced pellets as detected in the shape factor (Table 7.9) (Dukić-Ott *et al.*, 2009). Thoorens et al. (2014) stated that moisture content lower than 6% positively enhances the mechanical properties of the produced formulation (Thoorens *et al.*, 2014). Hence, this correlates with the initial amount of water that produces a plasticising effect on MCC particles; thus, ease of extrusion was enabled (Dukić-Ott *et al.*, 2009).

Table 7.9 Physical characteristics of the pellets of all formulations: F1 (uncoated pellets), coated pellets F2 (RS), F3 (RL), F4 (RS RL) and F5 (uncoated pellets with RS)

Formulation	Bulk density g/cm ³	AR (mean ± SD) (n=30)
F1	0.65	1.28±0.21
F2	0.63	1.46±0.24
F3	0.59	1.52±0.29
F4	0.63	1.42±0.30
F5	0.59	1.63±0.60

Further characterisation was necessary to assess the shape factor (AR) and morphological properties. Therefore, AR was measured for all batches (Table 7.9), and further examination for the pellets dimension and shape was detected using the stereomicroscope (Figure 7.12).

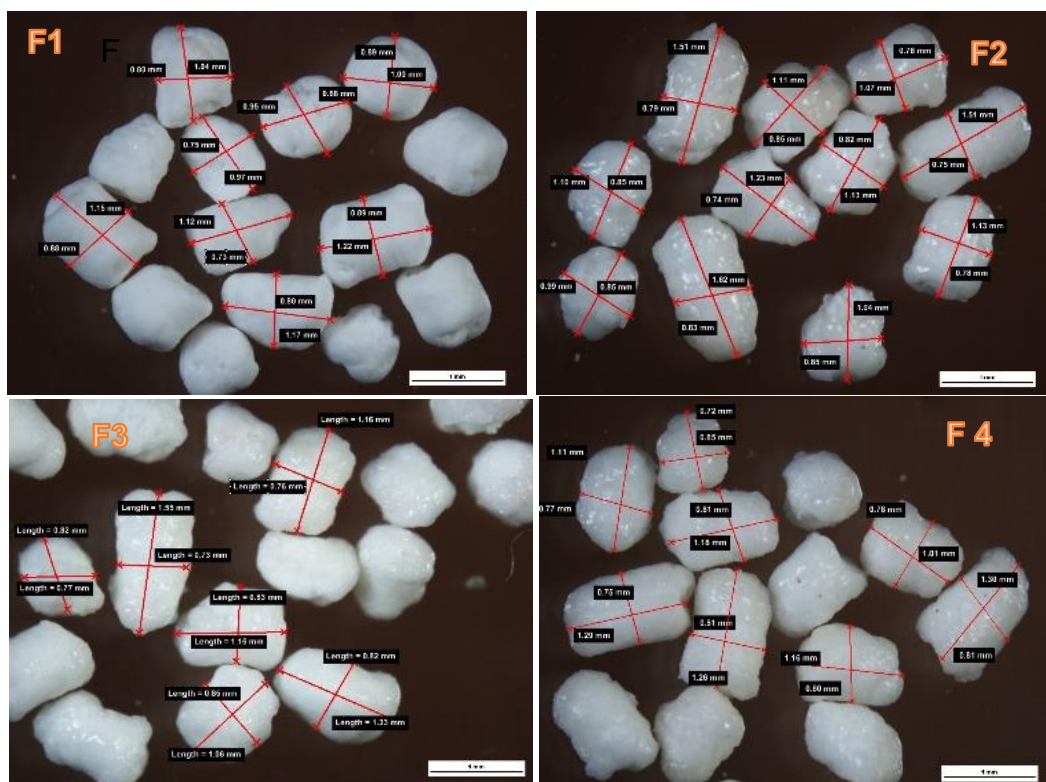


Figure 7.12 Stereomicroscope images showing AR and general morphology for uncoated pellets (F1) and coated pellets (F2, F3 and F4)

Hence, the pellets diameter and sphericity influence remarkably the packing properties, which is indicated by bulk density (Muley, Nandgude and Poddar, 2016). Vervaet, Baert and Remon, indicated that bulk density decreases with increasing the particle size; we also suggest that the shape factor controls the bulk density remarkably (Vervaet, Baert and Remon, 1995). In our results, the bulk density was associated with the sphericity factor as in Table 7.9, where the small AR the high bulk density and similarly reported in the literature (Kaur *et al.*, 2020). Therefore, AR correlates with the bulk density as both can provide an idea about the pellets size homogeneity.

Moreover, the spherical pellets provide an easier coating to attain a modified drug release and optimal pellet mass flow. Hence, the preferred pellets are spherical with a mean diameter between 0.5 and 1.5 mm, and pellets with less than 100 μm are not desirable. Hence, these pellets provide a large surface area and tend to agglomerate during the coating process due to the cohesive forces between the small particles.

This could result in uneven distribution of the coating material and thin coating film, which can cause an immediate drug release. Therefore, the preferable AR should be lower than 1.2 with narrow size distribution and smooth surfaces, allowing good flowability and less friable product (Wen and Park, 2010).

The AR was 1.57 ± 0.5 for F0 then reduced in F1 to 1.28 ± 0.21 , as shown in Table 7.9. This could be correlated with the adequate MCC concentration in F1 and the suitable water amount (3-4 mL) (Thoorens *et al.*, 2014). However, lower MCC contraction (20% w/v) in F5 and the AR was the highest 1.63 ± 0.57 . This could be attributed to the effect of Eudragit RS in the pellet's matrix, which was noticed in the difficulty of preparing pellets from Eudragit RS alone during our experimental work, as indicated earlier. It was reported by Kaur *et al.* that the AR of pellets reduced with increasing MCC content and the level of water (Kaur *et al.*, 2020). This was related to increasing interparticulate forces enough to reduce the pellets size during spheronisation (Kaur *et al.*, 2020).

A similar trend was detected in our results showing the combined effect of the low amount of MCC and water in F5, increasing the AR. Thus, a high amount of MCC and water level provided enhanced pellets shapes with F0. However, the MCC concentration and water amount were adequate as in F1, demonstrating the low AR. Hence, a higher quantity of water could dissolve the drug (PRH), forming a highly viscous solution interfering with the MCC function (Lustig-Gustafsson *et al.*, 1999).

The optimised concentration of MCC was used to prepare coated pellets in F2, F3 and F4. Therefore, 77% w/w of MCC concentration could be taken forward for a future approach.

On the other hand, the coated pellets' AR was higher than uncoated pellets of the same content (F1). Similarly, stereomicroscope images showed this shape difference (Figure 7.12). Hence, internal images of coated pellets (F2, F3 and F4) were glossy compared to the uncoated batch (F1).

According to the t-test, AR differed significantly ($p < 0.05$) between the same matrices' pellets, the uncoated pellets F1, and each coated batches F2, F3, and F4 accordingly. While F2, F3 and F4 demonstrated no statistical difference in their AR values according to one-way ANOVA and t-test ($p > 0.05$). These findings indicate the presence of the

coating layers, causing the difference in the pellets dimensions and reducing the sphericity (Tiwari, Agarwal and Tiwari, 2013).

However, further investigation is required for a future approach to improving the AR of the coated pellets to achieve the spherical range (≤ 1.2) (Manda, Walker and Khamanga, 2019). Hence, the pellets mechanical properties and modification of PRH release were the main focus in this stage.

7.5.1.3 Morphology examination using SEM

The pellets morphology, surface properties and coating layers were examined using SEM. The obtained images of the F1 batch (Figure 7.13-A1&A2) showed a rough surface for the pellets matrix with no coating layer applied compared to other formulations. In comparison, in Figure 7.13(B, C and D), the coated batches F2 (B1&B2), F3 (C1 &C2) and F4 (D1 &D2) showed smoother surfaces with outer layers surrounding the pellets. The coating layers were generally similar with slight variation associated with pellets shape and original surface roughness of the inner core as detected in F1. These findings were correlated with the AR results that showed no statistical variation between the coated batches. However, F4 showed a clear coating layer around the pellet compared to the other batches. Therefore, further investigation of pellets mechanical properties was necessary to assess the coating layer's quality and identify any undetectable defect in morphological characterisation. Similar to F1, F5 showed surface roughness and no coating layer (Figure 7.13-E). The MCC particles were detected in the F0 (Figure 7.14-A and B) batch, which was tested to detect the change in pellets shape and surface morphology. On the other hand, the rough surface of F0 could be correlated to the original particles of MCC (Figure 7.14-A) of crystal shape while it was undetected in F1 and F5 (Figure 7.13-A and E respectively)

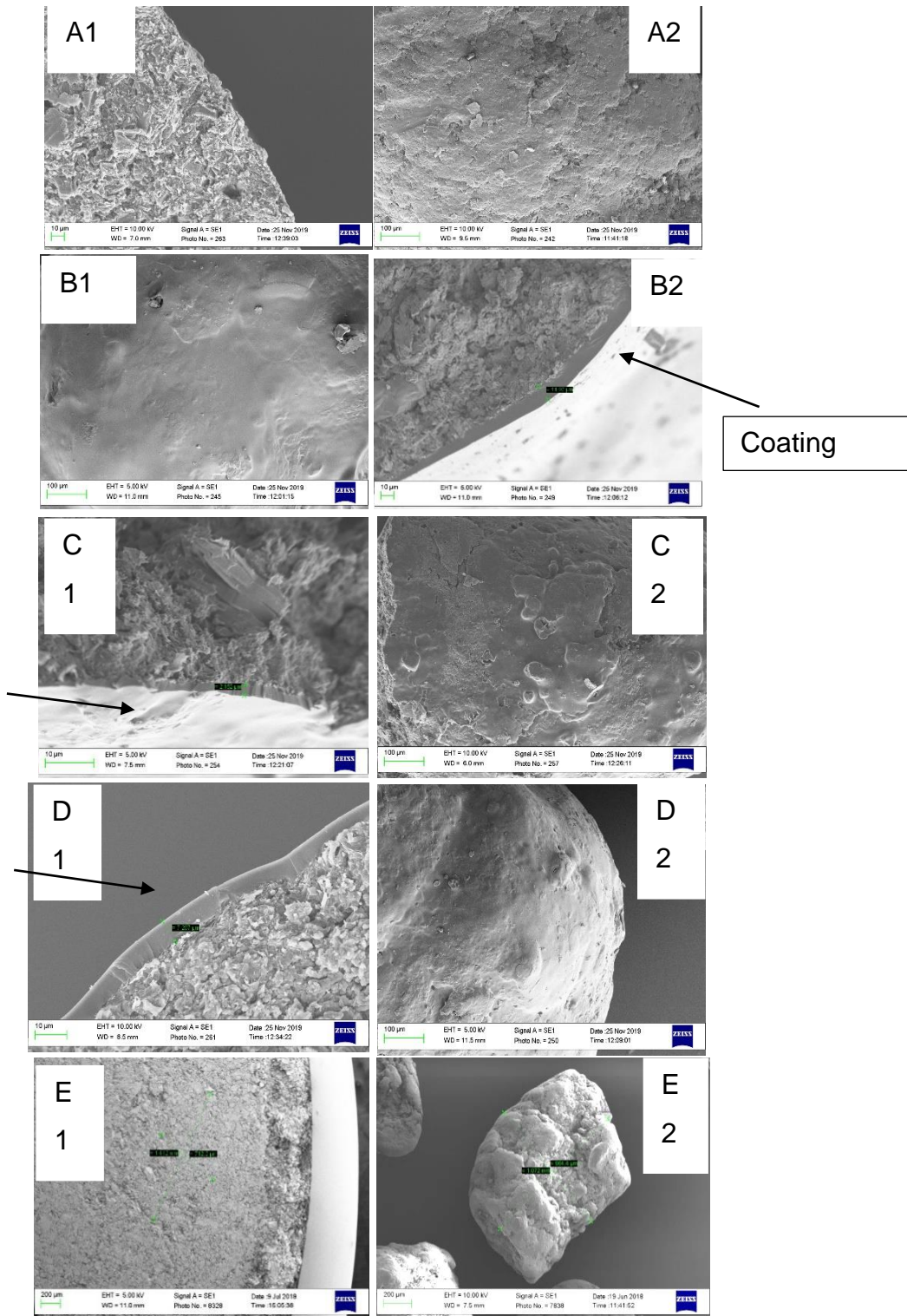


Figure 7.13 SEM images of all batches F1 (uncoated pellets) showing rough surfaces (A1 and A2) and coating layers with the smooth surfaces of the coated pellets for F2 (B1 and B2), F3 (C1&C2) and F4 (D1&D2), F5 matrix pellets (E1&E2) showing the surface irregularity

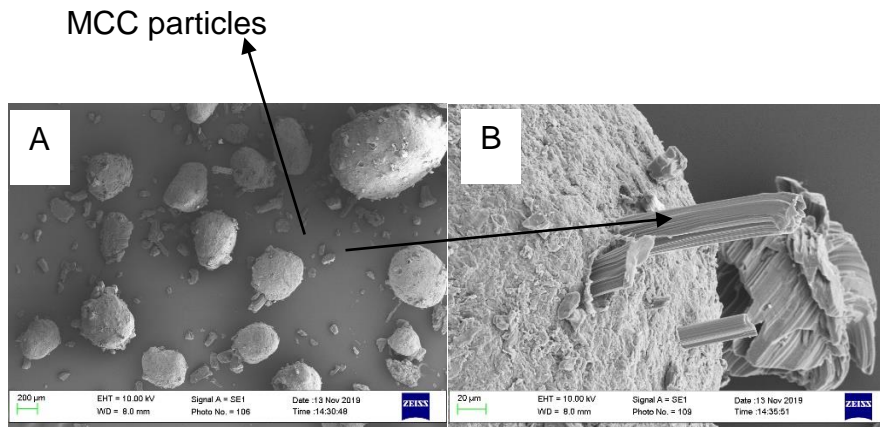


Figure 7.14 SEM images of F0 (A) showing the surface roughness and the presence of MCC crystals as distributed within F0 pellets in image B

7.5.1.4 Tensile strength and YM of pellets

The tensile strength and YM were the assessed mechanical properties of pellets using texture analysis. The tensile strength was calculated using the crushing strength obtained from the force against the time. Hence, the first notch or first peak with a drop of force was considered the crushing force. The notch represents the first crack of pellets deformation, and the highest peak in the graph is related to the max force to deform the pellets completely, represents the end of the test (Cespi *et al.*, 2007)(C. Salas-Bringas1 *et al.*, 2007). Therefore, the crushing strength was calculated using the first notch value during the hardness test for the formulations as in Figure 7.15.

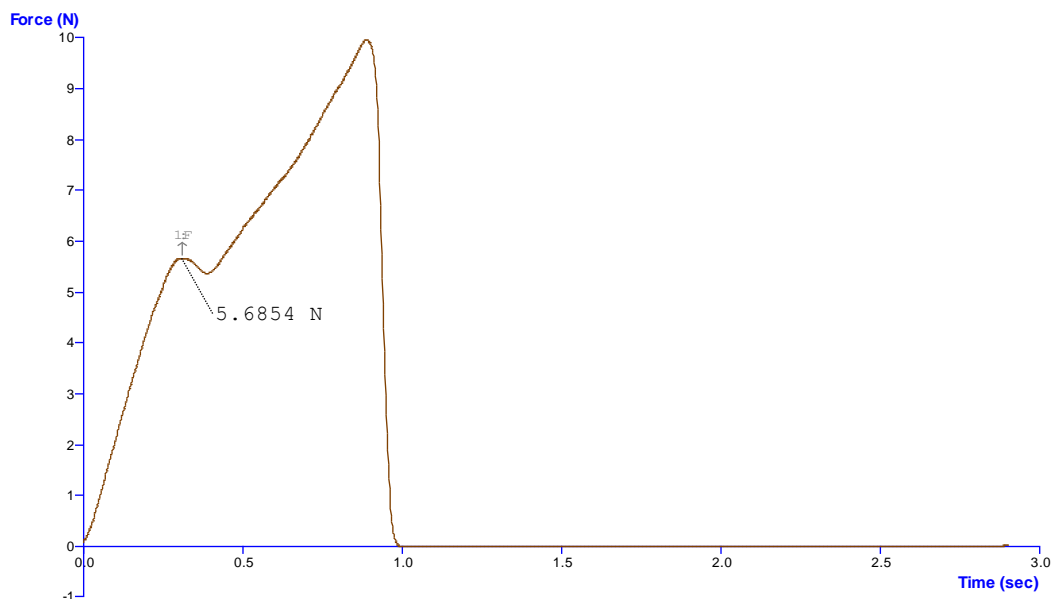


Figure 7.15 One of the hardness test results showing force (N) against time (seconds), first notch as the crushing force (N) and the maximum force (F) at the end of the test for F5

The tensile strength was measured for all pellets formulations (Figure 7.16). F1 showed the highest value then started to decrease after coating in F2, F3 and F4. In contrast, F5 had the lowest tensile strength among the batches. This could be associated with the difference in MCC ratio in the other batches and the addition of Eudragit RS (Sadeghi, Shahabi and Afrasiabi Garekani, 2011) (Patel *et al.*, 2016). F1 had the highest MCC ratio compared to F5 that contained the lowest.

Although the uncoated and coated pellets had the same MCC content, the coated layers remarkably reduced tensile strength. According to one-way ANOVA and t-test, the tensile strength of coated pellets was significantly different ($p < 0.05$) from the uncoated pellets (Figure 7.16). However, the coated pellets showed no significant difference between them ($p > 0.05$). This could be associated with the shape factor of the coated pellets as there was no difference between their AR ($p > 0.05$), yet AR differed significantly ($p < 0.05$) between the uncoated and coated pellets.

Moreover, the coating layer showed consistent mechanical behaviour indicating a stable coating process. Consequently, the deformation of these pellets is less affected by the applied force during the compaction, as the integrity of the pellets coating was maintained.

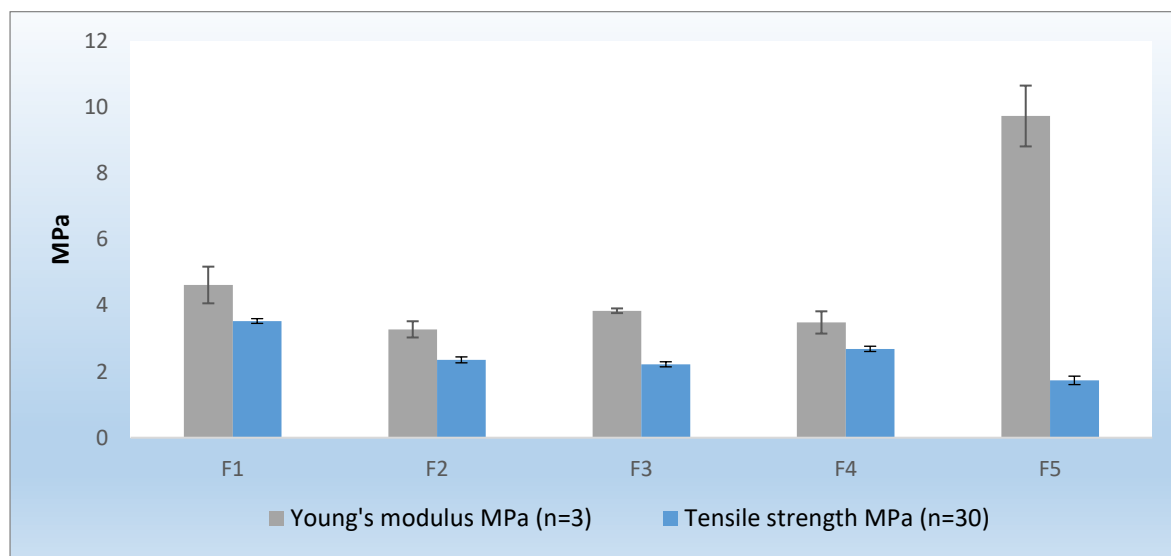


Figure 7.16 The tensile strength and YM results (mean \pm SD) of uncoated drug pellets (F1), coated pellets with Eudragit RS (F2), coated pellets with Eudragit RL (F3) and coated pellets with Eudragit RS/RL (F4) and matrix pellets (F5)

Murthy Dwibhashyam and Ratna (2008) stated that the coated pellets should possess enough hardness strength to deform under compression without fragmentation of the coating layer (Murthy Dwibhashyam and Ratna, 2008). Also, the inner core could provide supportive strength providing plastic deformation such as MCC (Murthy Dwibhashyam and Ratna, 2008) (Beckert, Lehmann and Schmidt, 1998). Therefore, all batches of 77% MCC (F1-F4) showed significant difference ($p < 0.05$) from 20% MCC batch (F5).

In addition, the difference in the mechanical properties between the formulations can be attributed to the moisture content; hence F1 were the highest. It was found by Cespi et al. the elastic and plastic properties of the pellets influenced by the moisture content and MCC amount. Where, higher MCC ratio resulted in elastic pellets (Cespi *et al.*, 2007).

Furthermore, the other factor can be the polymers powders' original characteristics, which offered additional support for the pellets. Eudragit RS powder demonstrated a YM value of 4.52 ± 0.46 MPa and 5.54 ± 0.32 MPa for Eudragit RL.

On the other hand, YM was recorded for all batches using the slope of the linear line of the stress against strain. The YM results were correlated with tensile strength results as F1 demonstrated YM higher than that of the coated batches (F2, F3 and F4) (Figure 7.16).

According to the t-test, the F1 differed significantly from the coated batches F2 and F4 ($p < 0.05$). Surprisingly, there was no significant difference ($p > 0.05$) between F1 and F3. Therefore, the core of the pellet of MCC and ATEC could produce a similar effect on the produced batches after coating (Abbaspour, Sadeghi and Garekani, 2005) (Gaith Zoubari, Ali and Dashevskiy, 2019). Moreover, the influence of the low T_g resulted in a rapid phase transition of the polymer from the brittle to the elastic state offering flexibility in the coating layers as demonstrated earlier in thermal analysis (Tan and Hu, 2016b).

Although F3 showed the highest YM compared to F2 and F4, there was no statistical difference according to one-way ANOVA between F2, F3 and F4. Similarly, this trend

was undetected in AR or tensile strength results ($p>0.05$). Therefore, this limited difference is related to the type and thickness of the coating layer around the pellets. On the other hand, YM of F5 differed remarkably from all batches. F5 demonstrated high YM and weak tensile strength indicating fragile pellets as suggested by YM. The desired mechanical properties of the pellets provide elastic-plastic balance resulting in flattened surfaces under compression with no fragmentation (Tunón, 2003) (Pai, Kohli and Shrivastava, 2012). Therefore, modification of PRH release through the formulation could depend on the pellets' mechanical properties. These findings were further examined in the drug release study, where F2 and F4 had the lowest PRH release and F1 had the highest values in acidic (pH 1.2) and buffer media (pH 6.8). In contrast, no modification of drug release was detected in F5. Consequently, the presence of polymers in the coating layer and the use of MCC as a core material in the pellets' matrices supported the plastic property during compression, making both tensile strength and YM close for the coated formulations. In comparison, the absence of coating had a remarkable effect on the formulation (Kiziltas *et al.*, 2014).

7.5.2 Differential scanning calorimetry (DSC) and Thermogravimetric analysis (TGA)

Thermal analysis was necessary to examine the thermal properties such as melting point and T_g and to detect the compatibility and the presence of the drug in the formulation (Dourado, 2019) (Saunders, 2008).

Hence, DSC detects the change in heat capacity and the energy transferred from and to the samples (Dourado, 2019) (Saunders, 2008). Also, measurement of the moisture content that could influence the formulation's mechanical properties was assessed by TGA (Ronowicz *et al.*, 2015).

The DSC results showed a sharp endothermic peak at 166-167 °C, which is related to the melting point of PRH (Figure 7.17-A) (Bp *et al.*, 2005) (CHMP, 2014). Similarly, all batches showed the same indicated endothermic peak. The results of F5 were attached separately to clearly show the difference and examine the results properly (Figure 7.17-B). Hence, the same endothermic peak of PRH was detected in F5.

In contrast, in the Sahoo et al. study, the combination of PRH with HPMC did not show the melting point of PRH (Sahoo *et al.*, 2008). Therefore, the combination in our study successfully showed the compatibility between the material with no chemical interaction, which was similarly reported by Venkata Srikanth et al. (Venkata Srikanth *et al.*, 2012). Moreover, the thermogram showed no different event indicating no incompatibility that may influence PRH therapeutic efficacy (Dourado, 2019).

The slight difference in the positions of the peaks could be attributed to the predominant effect of the polymers in the matrix and coating layers of higher quantity. In addition, MCC could show T_g between 117-120°C (Picker and Hoag, 2002). However, studies reported that only endothermic peaks could exist related to MCC around 66-100°C (Barboza *et al.*, 2009)(Li *et al.*, 2015). This could be related to the plasticiser effect that caused polymeric relaxation, thus hidden and weak T_g in our results (Picker and Hoag, 2002). On the other hand, PRH may influence the polymers T_g . Kidokoro et al. stated that ibuprofen was an effective plasticiser for the polymer Eudragit RS PO and decreased the T_g temperature of the polymeric matrix (Abbaspour, Sadeghi and Garekani, 2005). Although the T_g of MCC was unclearly detected in our batches, the uncoated batches F1 and F5 showed an endothermic peak around 80-100°C (Barboza *et al.*, 2009)(Li *et al.*, 2015). Hence, the presence of the coating layer in F2, F3 and F4 could dominate the MCC effect.

Further, according to the literature Eudragit RS and RL demonstrate T_g around 64°C and 63°C, respectively (Parikh *et al.*, 2014). However, this was also unclear in the coated batches. This could be attributed to the transition of polymer state from glassy to rubbery after the addition of ATEC that reduced T_g .

Moreover, moisture content could synergise the plasticizer effect making T_g further low. Hence, moisture content (lower than 5-6%) can play a remarkable role in reducing the tensile strength and improving the elasticity of the polymers providing a balance in the mechanical properties of the formulations (Kaur *et al.*, 2020) (Wu and McGinity, 2000)(Rujvapat and Bodmeier, 2012). Consequently, maintain the pellets integrity under compaction and protecting the coating layer from being ruptured (Zoubari, Ali and Dashevskiy, 2019).

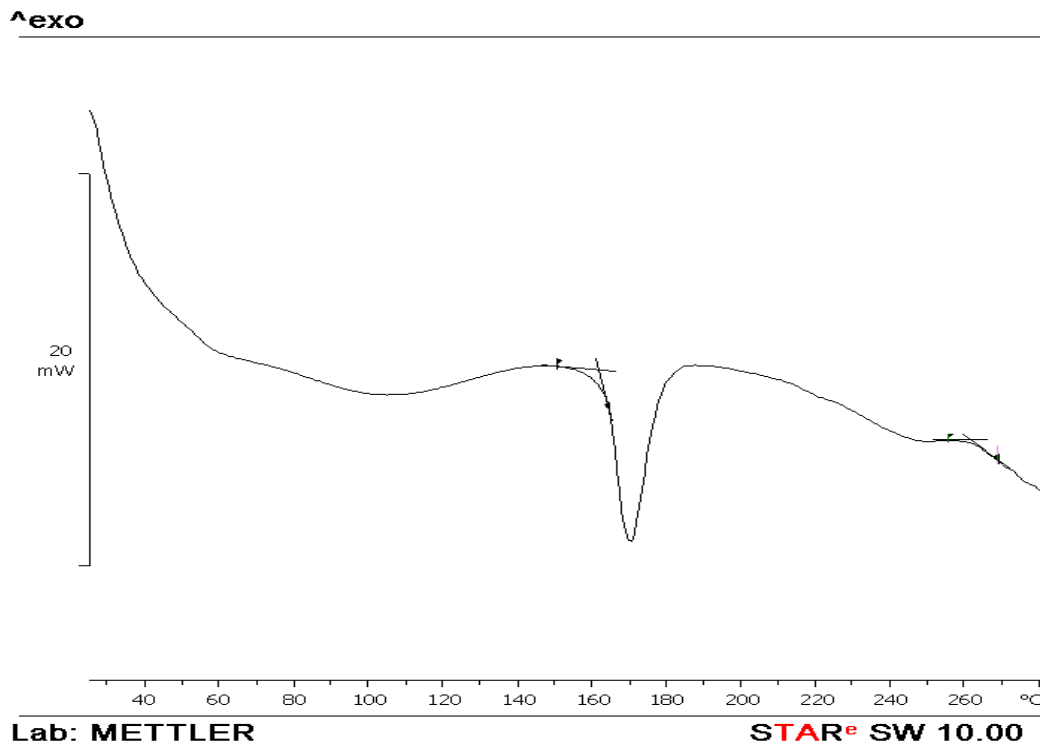
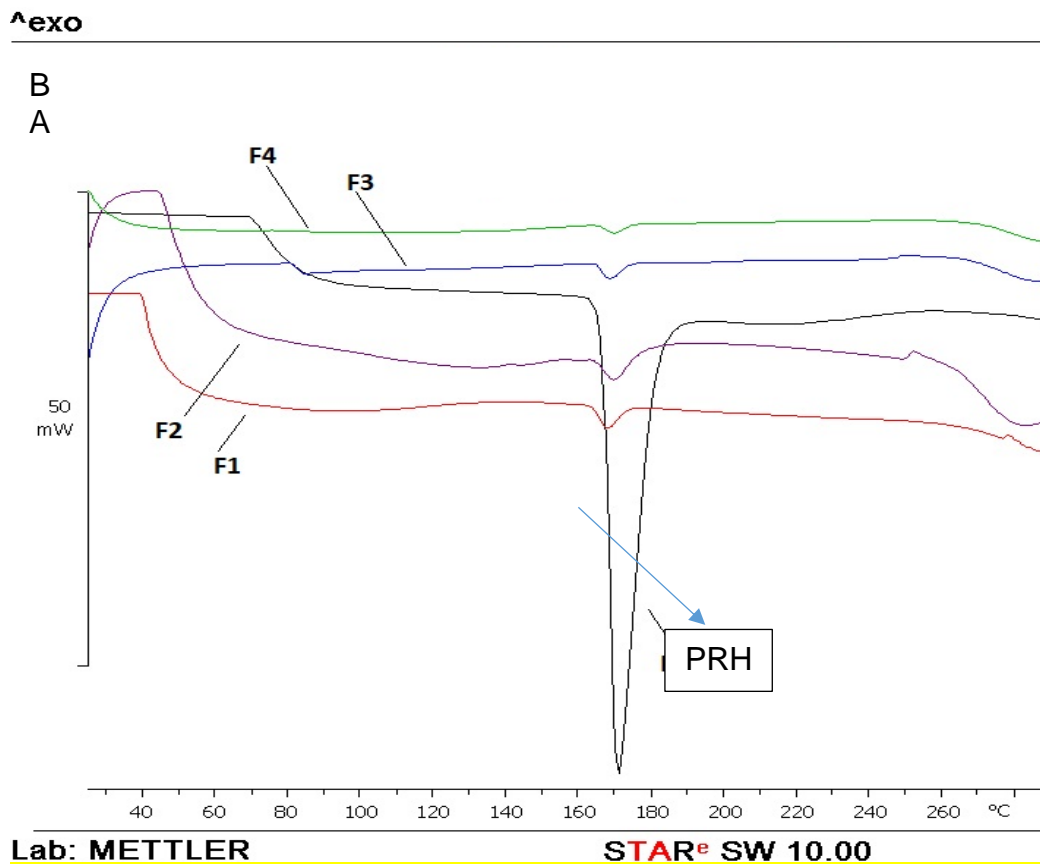


Figure 7.17 DSC thermogram A: uncoated drug pellets (F1), coated pellets with Eudragit RS (F2), coated pellets with Eudragit RL (F3), coated pellets with Eudragit RL: RS (F4) and the pure drug PRH and B uncoated pellets of RS matrix (F5)

Moisture content was detected using TGA for all batches (Figure 7.18). Although moisture content was lower than 5% for the coated batches, moisture content was the highest in F1 (5.2%). This could be related to the high holding capacity of MCC alone compared to the other incorporated polymers (Tomer *et al.*, 2001). The difference in moisture content could be correlated to the hydrophilicity of the excipients and the quantity of water and MCC (Kaur *et al.*, 2020).

In addition, all batches showed degradation after 260°C, which was confirmed in the TGA thermograms (Figure 7.18) (Picker and Hoag, 2002) (Barboza *et al.*, 2009).

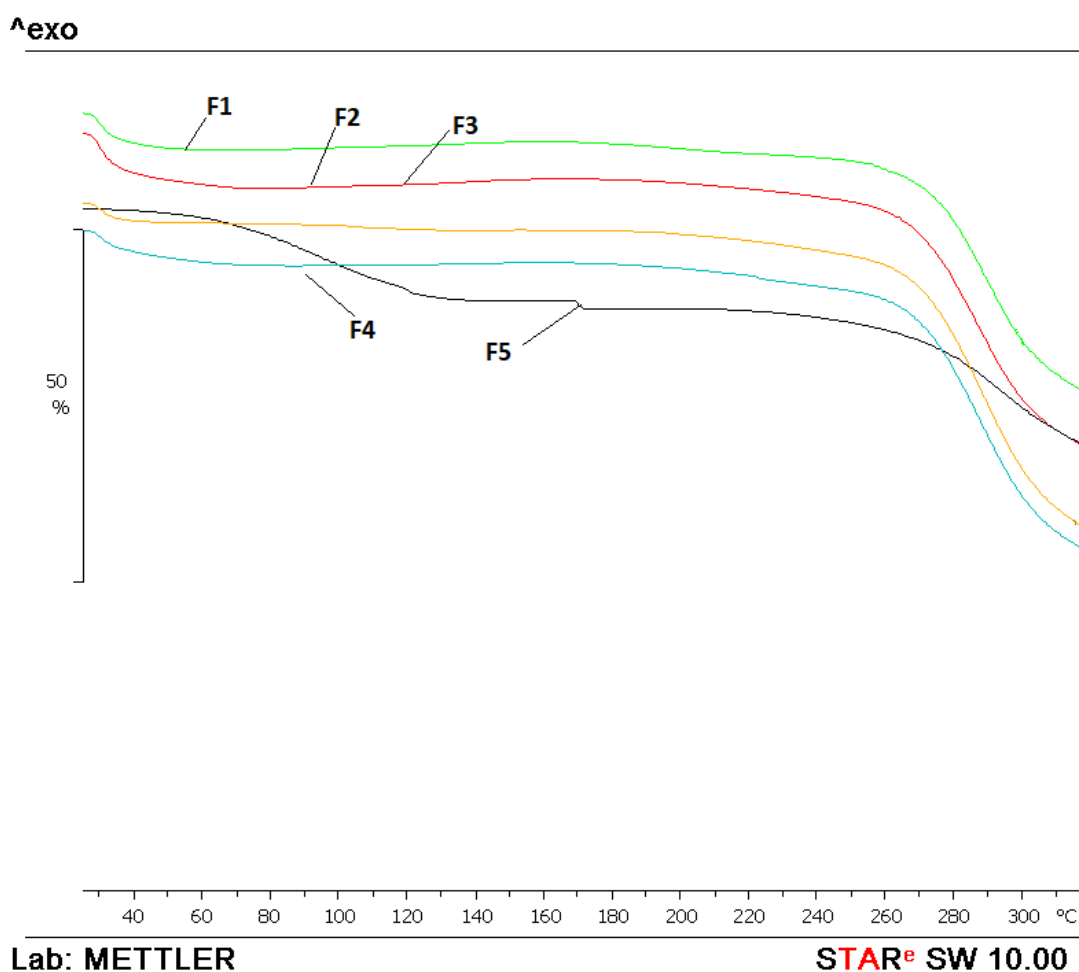


Figure 7.18 TGA results of uncoated pellets F1 and coated pellets F2, F3, F4 and matrix Eudragit RS pellets F5 showing the degradation after 260°C for all batches

7.5.3 Tablet's characterisation

The tablets were prepared using 20% w/w pellets and 80% w/w of ODT matrices. Also, tablets of 100% w/w ODT matrices were prepared to compare with the obtained results

in the tensile strength and disintegration tests. The control tablets of ODTs matrices and PRH powder were used to study the drug release profile in the dissolution test.

7.5.3.1 Tensile strength and Disintegration tests

The tensile strength is an important attribute of tablets mechanical properties (Pitt and Heasley, 2013). The tablets need to be strong enough to resist handling, such as packaging, transporting, and reaching the patients. However, tablets need to be weak to break and dissolve in GIT and release the ingredients. Generally, a tablet with a tensile strength of more than 1.7 MPa could be sufficient in ensuring good mechanical strength to withstand the manufacturing process (Pitt and Heasley, 2013). However, other tablets with tensile strength ≤ 1 MPa could be sufficient for the tablets are not exposed to high mechanical pressures according to their medical applications (McCormick, 2005b; Pitt and Heasley, 2013).

The tablet's dimensions (thickness and diameter) were measured before the hardness test. The crushing force of tablets was assessed using a hardness tester. The recorded force and tablets dimensions were applied to calculate the tensile strength (Pitt and Heasley, 2013).

The tensile strength was recorded for all batches (Figure 7.19). The tensile strength of obtained batches was significantly different ($p < 0.05$), as suggested by the t-test. This was associated with the difference between the pellets' mechanical properties and the coating layers' presence in the coated batches, as discussed earlier. Moreover, the variation could be attributed to the AR of the pellets and their diameters. Interestingly, F2-ODTs and F4-ODTs showed a similar trend with no remarkable difference ($p > 0.05$), while both batches differed significantly from F3-ODTs ($p < 0.05$). Also, the thickness of the coating layer could influence the final mechanical properties of the tablet. In general, the tensile strength of the ODTs containing pellets was higher than ODTs without pellets. The distance between the pellets and particles could decrease under compaction, strengthening the binding force between pellets and particles (Tan and Hu, 2016b). Thus, an increment in the hardness of the tablets is expected. In addition, when the materials of the pellets core mechanically strong enough, the tableting hardness can increase appropriately (Tan and Hu, 2016b). Tan and Hu (2016) stated that excipients play an important role in enhancing the tablets compressibility of MCC-containing pellets. Therefore, variation in the tensile strength

was expected due to the difference in the used materials. Firstly, in the pellet's core as in F1 compared to F5, secondly, in the coating layers around the coated batches. According to our results, an acceptable hardness range should offer short disintegration with no interference in each function (Tan and Hu, 2016b). Therefore, the disintegration test was performed to examine the time required for a tablet to break completely without leaving solid residues is called disintegration time (Beckert, Lehmann and Schmidt, 1998).

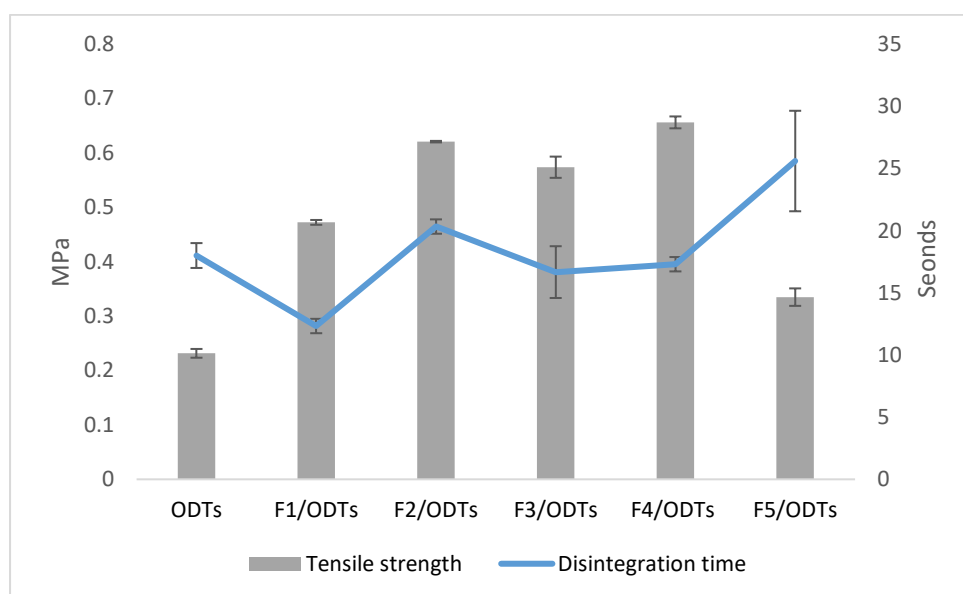


Figure 7.19 Tensile strength and disintegration results for tablets (n=3) (mean \pm SD) ODTs (without pellets), uncoated drug pellets (F1), coated pellets with Eudragit RS (F2), coated pellets with Eudragit RL (F3) and coated pellets with Eudragit RS/RL (F4) and uncoated pellets with Eudragit RS (F5)

The good disintegration time, according to European pharmacopoeia, is less than 3 minutes or within seconds according to FDA (Koner *et al.*, 2019)(U. FDA, 2008b)(EP, 2021). All the prepared ODTs demonstrated a significant difference between their disintegration time ($p < 0.05$), as suggested by the t-test. However, all batches disintegrated rapidly within less than 30 seconds (Figure 7.19). This could be related to the suitable mechanical strength of tablets and pellets in harmony, offering a short disintegration time. Therefore, the obtained formulations achieved the characteristic of ODTs (Koner *et al.*, 2019).

Moreover, the difference in the disintegration time can be attributed to the pellets' mechanical properties and the strength of binding forces between the particles and

pellets. Therefore, the particles interparticulate forces were influenced, thereby affecting the quality of the tablet (Anthony Armstrong, Patel and Jones, 1988).

However, the combination of ODTs matrix with pellets had no negative effect on ODTs properties. Interestingly, the mechanical properties enhanced, offering a short disintegration time. Therefore, it can be stated that the ODTs containing pellets were mechanically strong enough to resist the stress conditions during the manufacturing. Examination of the PRH release from the prepared batches was necessary to assess pellets quality and modify the PRH release.

7.5.4 Dissolution studies

According to the British pharmacopoeia method, the drug release profile was evaluated using the dissolution test mimicking the stomach and intestinal medium (British Pharmacopoeia, 2017). All formulations were tested in two media, acid media of pH 1.2 (Figure 7.20) and phosphate buffer media of pH 6.8 (Figure 7.21) (EMA, 2008).

The PRH release from the prepared batches was compared to the PRH only tablet as a control to study the release difference. The results of PRH release in acidic media showed 100% after 15 minutes for PRH tablets. Also, ODTs of F1 and ODTs of F5 released 96.2% and 89.9%, respectively. Simultaneously, the coated pellets released 42%, 52.5% and 42.4% of PRH from ODTs of F2, F3 and F4, respectively.

The statistical analysis was performed to study the PRH release from the formulation accurately in 15 minutes, 30 minutes, and 2 hours. All uncoated batches (PRH control, F1 and F5) were significantly different from the coated batches (F2, F3 and F4) according to t-test ($p < 0.05$). According to one-way ANOVA, the results showed that the PRH release showed no statistical difference ($p < 0.05$) between batches of uncoated pellets (F1 and F5) and the tablets of PRH at suggested timings.

However, further analysing the data with t-test, this difference turned to be significant ($p < 0.05$) at 30 minutes and 2 hours only between PRH and F1 batches.

This finding indicates two possibilities. First, the MCC based matrix of high ratio (77%) influenced PRH released. Hence, the F1 batch showed a remarkable difference over 30 minutes and 2 hours. Therefore, the similarity in PRH release between PRH and F1 batch at 15 minutes could be related to the presence of some PRH particles

unbounded from the matrices. MCC is frequently used in pellets preparation owing to its high elastic properties and tensile strength (Tan and Hu, 2016b). Therefore, the difference between MCC concentration in F1 and F5 influenced the mechanical properties of the pellets and eventually the PRH release. This was confirmed from our results as suggested by YM and tensile strength when comparing F1 to F5.

Kállai et al. (2010) stated that MCC pellets affected the PRH release compared to the sugar and isomalt-based pellets attributed to the insolubility of MCC in water and its poor disintegration when used in the matrix composition (Kállai et al., 2010). However, F1 mechanical properties were not good enough, making it a weak formulation to modify PRH release (Pitt and Heasley, 2013).

Although the F1 batch showed high PRH release, the pellet's core could provide additional support to maintain the modification of PRH release. Kállai et al. (2010) showed that the release rate from the coated pellets was affected by the type of the pellet's core in addition to the ratio of the coating polymers. This also explains the significant difference ($p < 0.05$) in PRH release between batches of coated pellets and uncoated pellets of F1 and F5 at the suggested timings.

This was correlated with the consistent mechanical properties of the coated pellets that showed a balance between elastic-plastic properties as suggested by YM and tensile strength. Therefore, maintaining the pellets integrity during compression helped the coating layers to modify PRH release efficiently.

Hosseini, Körber and Bodmeier (2013) noticed coated pellets with brittle EC deteriorated the pellets integrity during compression; thus, drug release was high. While layering the pellets with glidant, MCC and lactose supported the coated pellets without compromising the drug release (Hosseini, Körber and Bodmeier, 2013b).

The second possibility assumes that variation in the content of PRH within the pellets might occur. Nevertheless, the results showed the similarity between PRH, F1 and F5 batches. Then after 30 minutes, the F1 batch consistently differed from the PRH batch. Also, F2, F3, and F4 batches showed a remarkable difference in PRH release. While the F5 batch that had no coating layer and the lowest MCC content behaved similarly to the PRH batch. Therefore, the most relevant fact explaining these findings is the effect of the pellets core and the coating layer.

In order to further investigate PRH release from the coated pellets, a comparison was conducted between the batches of the coated pellets.

The results showed that F2 and F3 batches had significant differences ($p < 0.05$) at 15 and 30 minutes. However, at 2 hours, the batches reached to similar PRH release with no difference. Similarly, F3 and F4 differed only remarkably at 15- and 30-minutes timing. In contrast, F2 and F4 batches had a similar release of PRH at 15, 30 and 2 hours. These results were in accordance with the coated pellets' mechanical properties. Hence, the highest YM and lowest tensile strength were recorded by the F3 batch. Also, ODTs containing F3 showed the lowest tensile strength. Therefore, the pellets integrity might be influenced under compaction releasing higher PRH than F2 and F4 batches.

Also, these findings suggest that the coated pellets released PRH differently at different timing, reaching a similar manner after a specific time. This confirms the time-dependent attribute of Eudragit RS and RL (Torrado and Augsburger, 1994; Qiao *et al.*, 2010; Akhgari and Tavakol, 2016). This finding also could vary according to the amount/ ratio of the coating layer. Hence, the surfaces of the coated pellets varied according to SEM results. Nevertheless, the layers were detected on the pellets confirming the dissolution findings.

Further on studying PRH release, the batches showed a different release of PRH in buffer media (pH 6.2) (Figure 7.21).

A statistical comparison of PRH release from the same batch in two different media (acidic and alkaline) was achieved.

The comparison showed that the PRH batch released PRH significantly at 30 minutes ($p < 0.05$), while no difference was detected at 15 minutes and 2 hours in acidic and buffer media.

On the other hand, the F1 batch showed a consistent trend in both media at 15-30 minutes and 2 hours. Therefore, we considered 2 hours to compare the PRH release from the same batch in different media (pH 1.2 and 6.8).

At 2 hours, each of the following batches behaved similarly in acidic and buffer media F1, F3 and F5. While each of F2 and F4 released PRH differently in both media. This finding could be related to the difference in the coating layers distribution around the pellets.

It was found by Qiao et al.(2010) that the drying of the coated pellets with Eudragit RS and RL at 40 °C temperature for 120 minutes made the coating particles fuse firmly, forming uniform layers. In contrast to the cured pellets at 30 °C temperature for less than 60 minutes, the particles were separately distributed around the pellets (Qiao *et al.*, 2010). This finding was also confirmed by our preliminary results that showed weak control of PRH release due to the coating layer's weak distribution and consistency. Therefore, this variation could be experimentally based, as confirmed by the consistent PRH release from batches of PRH and the uncoated pellets F1 and F5. In addition, PRH is a weak base that tends to have a high release in acidic media (Bolourchian and Dadashzadeh, 2008). Therefore, the tendency for higher PRH release in acidic than buffer media indicates the presence of some PRH particles on the surfaces of the pellets. Thus, these uncoated PRH particles resulted in the rapid PRH release from the coated pellets. Hence, the difference at 30 minutes between F2 in acid and buffer was insignificant ($p>0.05$).

In general, the batches of the coated pellets showed higher PRH release in acidic media (pH 1.2) (Figure 7.20) than buffer media (pH 6.8) (Figure 7.21). A similar trend was noticed by Akhgari and Tavakol (2016) study that attributed the difference in the drug release from the coated pellets with Eudragit RS in acidic and buffered media to the distribution of the coating layer and its thickness (Akhgari and Tavakol, 2016). While the study of Wulff and Leopold (2014) reported that Eudragit RL coated pellets released the drug in acidic media higher than buffer media without giving any reason (Wulff and Leopold, 2014). Moreover, Qiao et al. (2010) found that the higher concentration of the coating layer, the higher resistance to the hydrostatic pressure that builds up inside the formulation core. Thus, the formation of premature cracks was reduced during the dissolution test. However, undesirable control of drug release occurred for 12 hours without reaching 100% release (Qiao *et al.*, 2010).

Our study agrees with Akhgari and Tavakol (2016), and Qiao et al. (2010) justify the burst release with the difference in the coating thickness and cracks formation in some pellets

Moreover, Beckert, Lehmann and Schmidt (1998) found that thicker coating layers of Eudragit L 30 D-55 and Eudragit NE on bisacodyl pellets influenced the mechanical properties of the formulation. Therefore, the liberation of the drug was only 4% w/w of the total amount of bisacodyl (acidic and buffer media). However, the coating layers did not dissolve to release the full amount (Beckert, Lehmann and Schmidt, 1998).

The study showed that the high elasticity of the coated pellets reduces the deformation of the pellets during compression.

In addition, film rupturing is a time-dependent process. Therefore, the elasticity of the coating layers and their thickness resulted in the drug release modification (Beckert, Lehmann and Schmidt, 1998). This finding agrees with our results that showed low YM from the coated pellets. Hence, our pellets core contains 3% w/w ATEC, further supporting the pellets' elasticity. Also, the provided coating layers enhanced the tensile strength due to the increased binding between the pellets core and the coating layers.

Furthermore, different studies reported similar effects of using Eudragit polymers RS and RL on retaining drug release. Their results indicated that the curing and fusion of pellets formed a protective layer providing further protection resistant to time (Kidokoro *et al.*, 2001; Azarmi *et al.*, 2002; Abdul, Chandewar and Jaiswal, 2010).

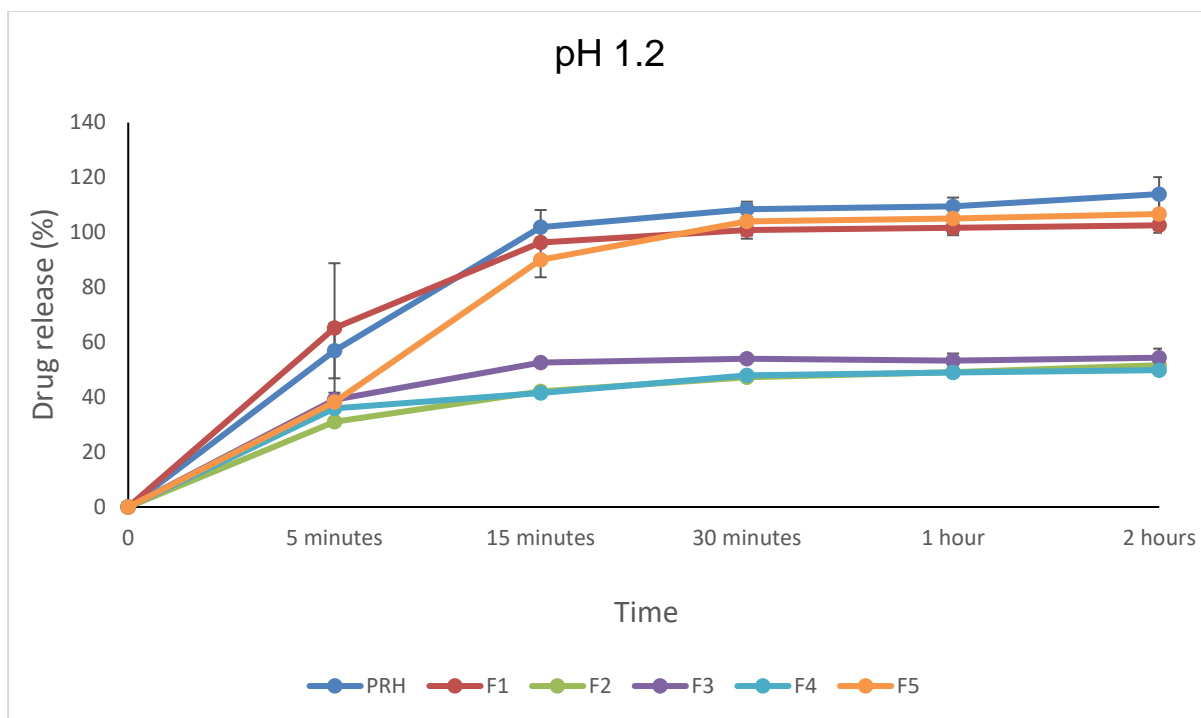


Figure 7.20 The dissolution profiles in acidic media of pH 1.2 for tablets of ODTs containing PRH, F1, F2, F3, F4 and F5

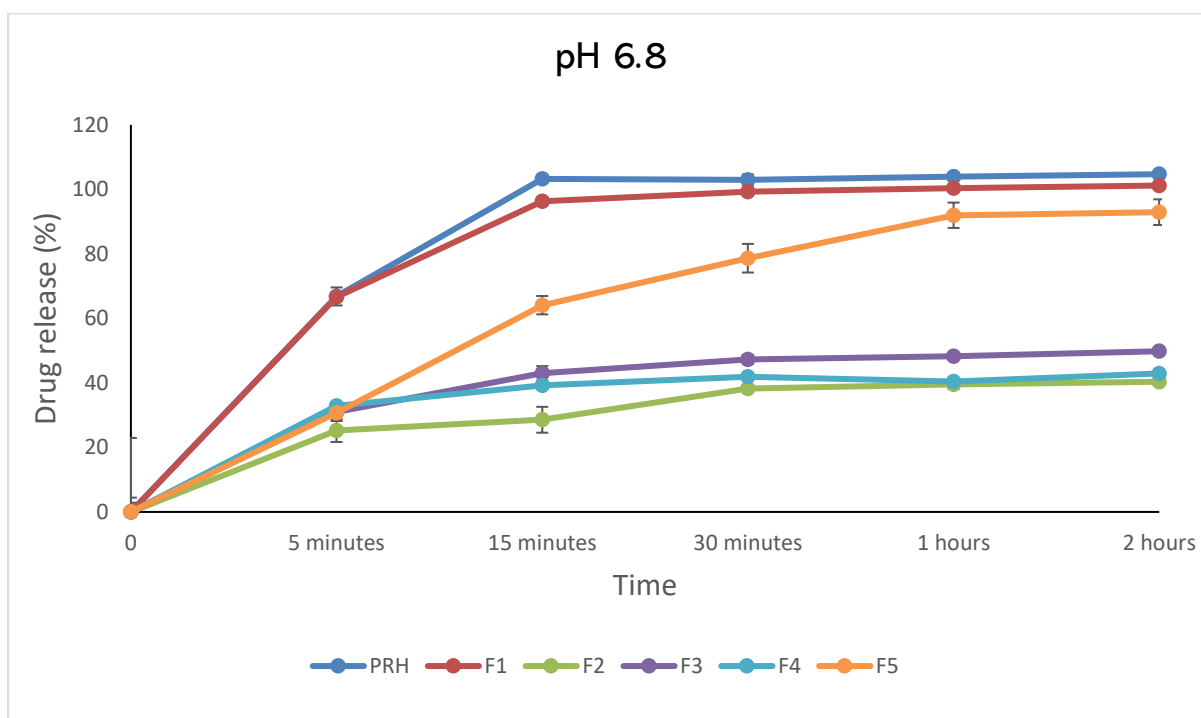


Figure 7.21 The dissolution profiles of ODT formulations PRH, F1, F2, F3, F4 and F5 in buffer media (pH 6.8)

7.6 Conclusion

The physical and mechanical properties of both initial pellets and pellets in the ODTs demonstrated an acceptable range. The results showed that disintegration time was lower than 30 seconds for all batches, and a similar trend was observed with contact angle results indicating a short disintegration time. It can be concluded from the results of PRH release that using either TEC or ATEC as a plasticizer with a coating layer based on time-dependent polymers such as Eudragit RS or Eudragit RL could aid control of PRH (Akhgari, Abbaspour and Moradkhanizadeh, 2013). ATEC of 3% ratio showed a good balance between elasticity and plasticity according to mechanical characterization results of pellets (YM and tensile strength). The batch of sufficient strength for preparation, packing and handling with little imperfection could be achieved using 3% ATEC pellets (1.1 Mpa) without affecting the rapid disintegration time. Hence, according to YM results, the difference between the batches of TEC (3% and 5%) showed no significant difference ($p>0.05$), while pellets of ATEC (3% and 5%) were statistically different ($p<0.05$). In addition to previous findings, the best AR (close to 1) was achieved.

On the other hand, coated pellets with Eudragit RS, Eudragit RL and their combination of RS/RL was successfully prepared. The *in vitro* release studies showed that >75% of PRH releases from batches of uncoated pellets within 30 minutes. In contrast, batches of coated pellets demonstrated a modified PRH release (<54%). The suitable mechanical properties of the pellets were remarkably correlated with the modification of PRH from the coated pellets. The collected data suggested that the reservoir system of good mechanical properties based on time-dependent polymers could protect the drug from burst release, and modification of drug release can be achieved.

Chapter 8 Modelling trials in understanding compression performance of pellets to be used in the orally disintegrating tablet

Scoop of the study

Simulating the preparation process of pellet compression within the ODT matrix using modelling software, namely EDEM®, is crucial to determine the physical and mechanical properties of the obtained formulation with a minimum cost and time. This method is effective to obtain reliable data with minimum lab work.

The study aimed to understand the compression performance of PRH pellets to be used in the orally disintegrating tablet using EDEM.

The pellets of 4 combinations were prepared using the extrusion-spheronisation method. The characterisation data of pellets, including AR, Young's modulus (YM), bulk density, was achieved. The YM and compaction pressure were entered in EDEM 2019 to collect simulation data. The following settings were applied in the type of creator tree the geometry material properties equipment were interaction, geometries were cylindrical for compactors 1 and 2 (top and base), the surface shape around the compaction process was polygon. The number of edges was 32 with specified values centre and radius (1, 0.2 M) for X, and Y with Z was 0. The acceleration was set due to gravity -9.81m/s^2 , and velocity equals 1. The results showed that batch 4 was the most spherical among the other batches, containing 5.4% moisture content.

On the other hand, batch 2 had the highest moisture content of 32%, while the least sphericity was observed for batch 1. YM was the highest in batch 2 and the lowest in batch1. EDEM® simulation demonstrated that pellets could be compressed in the ODT matrix, demonstrating a correlation between the obtained laboratory compression process and simulation data with a maximum compression force of 2537N.

Keywords: particles interaction, compaction, simulation, EDEM®

8.1 Overview

ODTs are solid formulations that dissolve within seconds to 3 minutes once oral contact mucosa (Bandari, Suresh, Rajendar Kumar Mittapalli, 2008; Irfan *et al.*, 2016). The excipients that can be used should be compatible with narrow size distribution and a high ability to swell and disintegrate rapidly in the mouth (Chowdary, Shankar and Suchitra, 2014). There are popular patented technologies for ODT formulations and examples, as summarised in Table 8.1.

Reducing dose frequency and plasma fluctuation to improve patient compliance can be achieved using a multiparticulate system based on polymeric ingredients with the selected drug. Different polymeric systems can be used in the preparation of multiparticulates as in microparticles or pellets based on time or pH-dependent polymers such as Eudragit RS and L100 or based on cellulosic polymers of high viscosity such as microcrystalline cellulose (MCC) (Picker and Hoag, 2002; Arora and Sethi, 2013; Chowdary, Shankar and Suchitra, 2014).

Table 8.1 Examples of significant techniques to prepare orally disintegrating formulations (Badgujar and Mundada, 2011; Ghosh, Ghosh and Prasad, 2011; Arora and Sethi, 2013)

Technique	Properties	Disadvantages	Commercial names	Company
------------------	-------------------	----------------------	-------------------------	----------------

Zydis®	<ul style="list-style-type: none"> • No-water required • Freeze-drying of API in a gelatin matrix • ODTs blister packaging required • Low moisture content allowing long shelf life of the drug with no microbial growth 	<ul style="list-style-type: none"> • Expensive • Sensitive to moisture and temperature 	<ul style="list-style-type: none"> • Zyprexa • Zofran 	Cardinal Health
Orasolv®	<ul style="list-style-type: none"> • Used to prepare OTC (over the counter) drugs with or without water • Consist of effervescent material and coated API powder • API can be loaded from 1 mg to a max of 500 mg 	<ul style="list-style-type: none"> • Low mechanical strength and requires aluminium foil blisters of dome-shaped 	<ul style="list-style-type: none"> • Remeron • Soltab • Tempra firsttabs 	Cima
Durasolv®	<ul style="list-style-type: none"> • Higher mechanical strength than Orasolv® • Time and cost-efficient to manufacture • Packed in both vials and normal blister packs 	<ul style="list-style-type: none"> • Small dose of API • Long disintegration time • Bitter taste 	<ul style="list-style-type: none"> • Zoming ZMT • Nulev 	Cima

Quick-Dis®	<ul style="list-style-type: none"> • API in a thin intraoral dissolving film • Quick dissolving time 5 -10 seconds • Prepared by solvent casting method • Many packaging types: dose-pouches or blister packages 	Suitable for fast dissolving API	Currently under development	Lavipharm
Flashdose®	<ul style="list-style-type: none"> • Sugar matrix consists of API • Orally dissolving tablets 	<ul style="list-style-type: none"> • Bitter taste • Porous and low strength tablet 	<ul style="list-style-type: none"> • Relivia Flashdose 	Fuisz
Wowtab®	<ul style="list-style-type: none"> • Buccal soluble tablet • Based on two types of saccharides • Fast disintegration • High stability compared to ODTs 	<ul style="list-style-type: none"> • Slightly longer disintegration time 	<ul style="list-style-type: none"> • Benadryl Allergy & Sinus Fastmelt 	Yamanouchi Pharma

8.1.1 Pellets in modified release dosage forms

Modified release formulations can be prepared as single or multiple unit dosage forms. Pellets are examples of multi-unit dosage forms filled into capsules or compressed as

tablets. Modify the drug release across ODTs by incorporating pellets in their matrices associated with high patients' compliance. Arguably, by providing ease of ingestion while minimizing dose frequency. The ODT matrix dissolves rapidly upon contacting saliva, and the pellets are released, carrying the active ingredients and modifying the drug release across the GIT (Al-Hashimi et al., 2018).

In order to produce good shape and size pellets with good mechanical properties, the polymer selection is mainly important to possess elastic and plastic properties that can affect the drug release, such as microcrystalline cellulose (MCC) (Figure 8.1) and hydroxypropyl cellulose (HPC). Pellets of an equilibrium tendency between the plasticity and elasticity can withstand compression forces, retaining their shape and integrity upon compaction (Ghosh, Ghosh and Prasad, 2011; Al-Hashimi *et al.*, 2018).

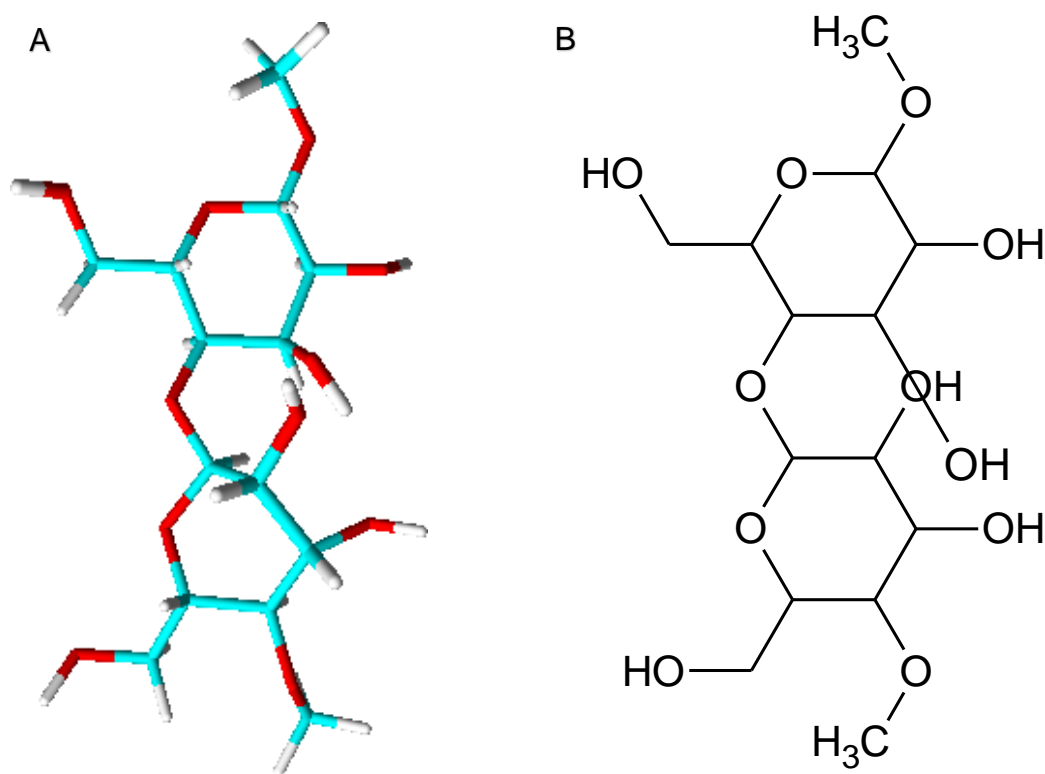


Figure 8.1 Microcrystalline cellulose (MCC) of 370.35 (g/mol) molecular weight showing chemical structure (C₁₄H₂₆O₁₁) in 3D format (A) and normal structure with atomic names (B) by ACDlab software (NCBI, 2015)

8.1.2 Software simulation

Many administrative and economic problems in the pharmaceutical industry are associated with its manufacturing and development (Bandari, Suresh, Rajendar Kumar Mittapalli, 2008).

Providing estimated drug quality and quality by design (QbD) following the international conference on harmonization guidelines (ICH Q8: pharmaceutical development) can be achieved by developing a manufacturing process based on process control and systemic understanding. Consequently, obtaining enough knowledge about the pharmaceutical process is essential to build the drug quality and optimize the process parameters correlation. Moreover, from the economic perspective, improvement of the manufacturing process could be time and resources consuming significantly (Rogers, Hashemi and Ierapetritou, 2013; FB and T, 2015; Devarampally, 2017). Since it is important to develop an efficient and strong manufacturing process with overcoming these challenges, the application of modelling software for the process was necessary from different aspects (Rogers, Hashemi and Ierapetritou, 2013).

Currently, manufacturing process modelling has become an essential step for machine configuration and enhancing process effectiveness in the pharmaceutical industry (Rogers, Hashemi and Ierapetritou, 2013; FB and T, 2015; Devarampally, 2017).

In general, computational fluid dynamics (CFD), finite element method (FEM) and discrete element method (DEM) are commonly used mechanistic models for the simulation of drug manufacturing (Fries *et al.*, 2011; Krok and Wu, 2017). These models work by capturing the physical features using primary information such as mass, size, and energy. Consequently, these models provide accurate estimation for all experimental aspects. Moreover, the mechanistic models provide scientific insight into the manufacturing process (C. Y. Wu *et al.*, 2005).

The FEM and variational method are modelling methods applied to solve partial differential equations of geometrical surfaces from a few variables' information. FEM

is one of the variational methods where it depends on energy minimization. Therefore, it is widely used in different mechanical applications related to civil engineering (Chuan Yu Wu *et al.*, 2005).

This method is a numerical analysis that considers the tablet a continuous medium representing the powders plastic and elastic deformation to analyse powder compaction and its mechanical properties in different pharmaceutical applications (Wu *et al.*, 2008; Klevan, 2011). When specific parameters are applied to a material, this results in various shape arrangements; however, only one layout practically can be attained without depending on the number of simulations performed (Panthi *et al.*, 2007).

FEM simulation was used in a study conducted by Okada *et al.* (2016) to examine the mechanical stress applied on the tablet's surfaces (top and the bottom layer) and evaluate the correlation between the tablet's shape and mechanical properties. This step was done by simulating the distribution of applied stress on the scored tablets. The diametral-compression test was carried out to assess the tensile strength. The results showed that when the depth was low (0.50 mm), the applied force was 79.05 ± 1.13 N, and the tablet's hardness was 33.33 ± 1.53 N which were considered high. The same trend was noticed substantially when the depth increased (0.75, 1.00, 1.50 mm); the applied force along with hardness reduced as their values were 71.21 ± 1.13 , 63.37 ± 2.04 , 32.99 ± 1.5 N and 28.00 ± 1.00 , 25.67 ± 1.53 , 24.00 ± 1.00 N, respectively (Okada *et al.*, 2016).

In addition, the tensile strength was produced on both sides of the tablet's surfaces (top and bottom), with a wide area generated in correlation with score depth. The correlation between FEM and experiments data was detected, indicating the success of FEM in providing more explanation about the properties of the produced tablets. However, some aspects were necessary to further investigate, such as the tablet dimensions, weight, and form, influencing the results and FEM simulation correlation (Okada *et al.*, 2016).

There are limitations in the general application of FEM, such as the representation of mechanics of fluid and wave transmission as it depends on the materials energy and phenomena associated with physical and chemical properties. However, different enhancements have been applied to overcome the drawbacks and improve the model

application. Different types of FEM have been used to cope with the limitations, such as extended, mixed, generalised and hp-finite element methods (Panthi *et al.*, 2007; Frenning, 2010; Jonsson, Gråsjö and Frenning, 2017)

The other mechanistic model is DEM. The use of DEM provides speed, location, and movement simulation of each particle. In addition, it can provide distribution of all particles based on their sizes which is not possible with the Eulerian model that calculates the particles movements or diffusion based on the particle's concentration (Devarampally, 2017; Yeom *et al.*, 2019). Besides, DEM allows examining the impact of process conditions and machine design on the drug quality in the formulation (Ramírez-Aragón *et al.*, 2018). Therefore, DEM can simulate different processes such as granulation and coating (Boikov, Savelev and Payor, 2018).

Furthermore, DEM can be combined with CFD or FEM to simulate other operations-related compaction (Krok and Wu, 2017). Despite the various advantages of DEM, there are some limitations, such as when applying DEM for simulating large numbers of particles, a computational issue is generated. Nevertheless, some computers' hardware was developed to solve the drawbacks using commercially accessible software (Michrafy, Ringenbacher and Tchoreloff, 2002).

In our study, DEM simulation was applied in modelling the multiparticulate system of constructed pellets based on polymeric matrices. The basic components of DEM and its implementations in pharmaceutical methods are comprehensively presented in Table 8.2.

Table 8.2 Examples of simulation software and designed companies (Yeom *et al.*, 2019)

Software name		Designer	Pharmaceutical studies & application	
Commercial	EDEM™	DEM solutions Ltd.	(Ketterhagen, 2011)(Suzzi <i>et al.</i> , 2012)	<ul style="list-style-type: none"> • Motion and orientation of pharmaceutical tablet shapes in a film coating pan • Effects of tablet shape and fill level

				on inter-tablet coating
	Rocky DEMTM	ESSS	(Nyembwe, Cromarty and Garbers-Craig, 2019) (Boikov, Savelev and Payor, 2018) (Jiménez-Herrera, Barrios and Tavares, 2018)	<ul style="list-style-type: none"> • Pressure effect across granulated mixtures • Calibration, design of experiment • Breakage models impact on particle beds
	STAR-CCM+	CD-adapco	(Tamrakar and Ramachandran, 2019) (Devarampally, 2017)(Baran, Han and Aglave, 2016)	<ul style="list-style-type: none"> • Spray fluidized bed wet granulation process • Mixture dry and wet particles inside the rotary mixer
	LS-DYNA®	LSTC	(Jensen, Fraser and Laird, 2014) (Karajan et al., 2014) (Han, Teng and Wang, 2012)	<ul style="list-style-type: none"> • Improving the precision of simulations • Sphere packing
Opensource	YADE	SDEC at Grenoble University	(Wang and Li, 2014)(Lawson, 2008)	<ul style="list-style-type: none"> • Granular materials • Dissolution and content uniformity

8.1.3 Theory of Discrete Element Method

DEM is a simulation method for predicting mechanical dynamics, such as each particle's location, speed, and movement (Ahmat, Ugail and Castro, 2011). The forces generated by particles or boundaries on other particles can be calculated with a specific time using the contact model of DEM. Besides, the position of the particles can be determined with a time step. Simulating the particles bonds, interactions,

particle-particle geometry, or contact is the most critical function in DEM modelling by applying the contact model. Hence, the contact model depends on the physical characteristics of particles, such as elasticity, plasticity, thickness, and density (Papavasileiou et al., 2007)(Baroutaji et al., 2017).

Figure 8.2 lists different contact forces affecting particle interactions and, respectively, their behaviour during compression. The choice of contact model used in the simulation is made based on the contact forces involved, as demonstrated below:

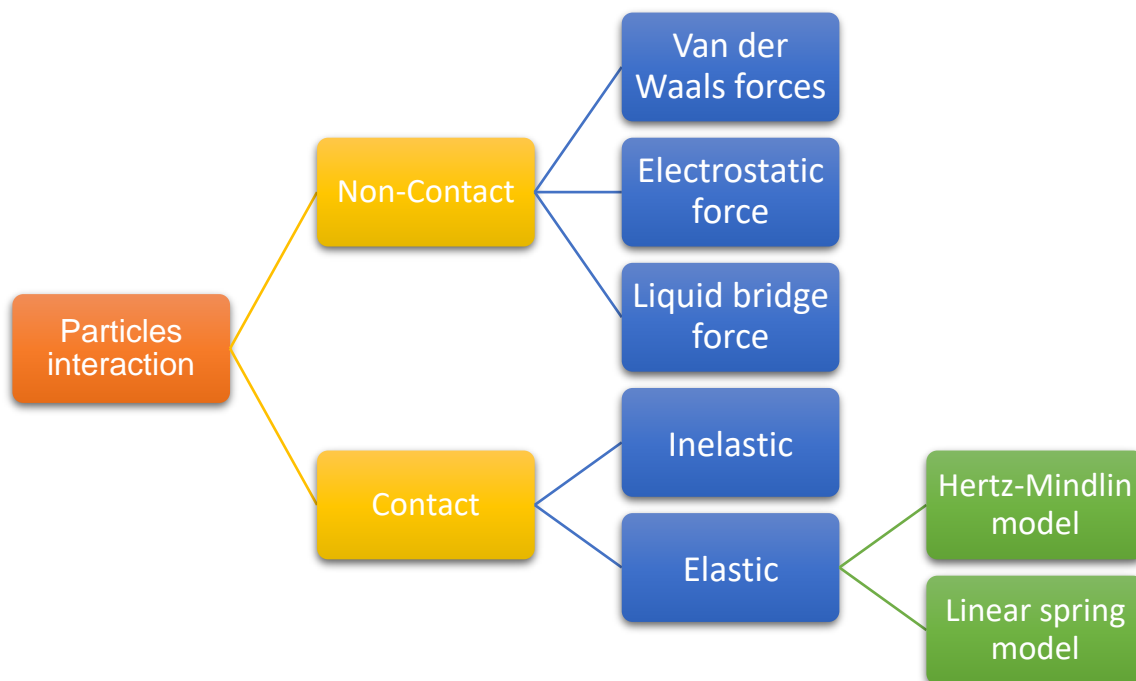


Figure 8.2 Contact forces effect on particles interaction and their behaviour during compression showing the used contact model (Yeom et al., 2019)

Several researchers studied the compaction ability of pharmaceutical ingredients. Michrafy et al. (2002) conducted a study to understand powders mechanical properties and compaction parameters to reduce tableting problems. The results showed that the hypothetical models used to assess powders' mechanical properties agreed with experimental results and previous literature. Also, the method was successful in examining powders compaction behaviour. Hence, different parameters were

examined, including YM, Poisson ratio and angle of friction of lactose powder. Besides, Drucker-Prager Cap (DPC) model based on elastic-plastic theory was applied. Hence, the DPC model was used to consider friction and cohesion between lactose particles (Michrafy, Ringenbacher and Tchoreloff, 2002).

Similarly, Lactose compaction behaviour was analysed by Wu et al. (2005), and the DPC model was applied to assess the yield by FEM software. The results indicated that the simulation results agreed with lab results for the compaction and the relative density, proving the modelling process's success. In addition, examining the stress distribution on the compact showed a local stress band starting at the lowest centre toward the tablet's upper edge, leading to the tablet cracking. These results were confirmed by detecting breaks in the tablets from the X-ray images, showing the harmony with modelling results that predicted dosage form failure under compaction (C. Y. Wu *et al.*, 2005).

Similarly, FEM and the DPC model were used by Krok et al. (2017) to study compaction characteristics of MCC powder and identify the failure aspects in tablet compaction, including the following steps: filling the die, powder compression and tablet ejection. The results of MCC mechanical properties with parameters compaction process were entered into FEM. It was concluded that heat generated during the tableting process was concentrated in the centre of the tablet. Moreover, the distribution of stress produced by FEM was correlated with cracks of tablets in practice (Krok and Wu, 2017).

In this chapter, the elastic-plastic deformation of the particles under compression was examined using EDEM® by applying the contact model according to a modified reported method (Ramírez-Aragón et al., 2018)(Yohannes et al., 2017). The laboratory data of plastic properties and YM were applied using the model for one of the prepared pellets combinations.

8.2 Aim and objective

8.2.1 Aim

This project aims to understand the compaction behaviour of PRH pellets in the ODTs matrix using EDEM

8.2.2 Objectives

- Prepare pellets using the optimum plasticizers ATEC and sorbitol according to previous studies in our project
- Formulate 4 batches with different compositions based on standard recipient MCC
- Determine the physical characteristics of each batch, including dimensions, hardness, and YM
- Produce an extrapolative design of compaction behaviour using EDEM®

8.3 Experimental

8.3.1 Materials

Chemical compounds are explained in detail in the experimental chapter.

EDEM® 2019 is a professional simulation software (DEM Solutions Ltd., Edinburgh).

8.3.2 Methods

8.3.2.1 Pellet preparation

Four batches of pellets were prepared using different combinations of MCC, ATEC and sorbitol with the same amount of PRH as outlined in Table 8.3. Depending on material properties, the amount of water was used to obtain a wet mass with good consistency to be extruded then spheroid into pellets. The method was explained in detail in the experimental chapter.

Table 8.3 Composition of each batch used in the preparation of PRH pellets (% w/w)

Batch	Drug %	MCC %	ATEC %	Sorbitol %	Water (mL)
1	0	100	0	0	12
2	20	80	0	0	10.5
3	20	77	3	0	9
4	20	77	0	3	9

8.3.2.2 Pellet characterization

The pellets were characterised using the general method explained in the experimental chapter and the brief experimental as follow

8.3.2.2.1 Micrometric properties

A.Yield

B.Aspect ratio

C.Bulk density

D.Flowability

The detailed methods were illustrated in the experimental chapter.

8.3.2.2.2 Morphology and shape

The shape of the prepared pellets is an essential factor that affects the physical properties of the pellets, such as porosity and compressibility. The pellets' shape and surface morphology were studied using SEM (Zeiss Evo50- Oxford instrument, UK). Micrographs were collected for pellets showing the morphology, surface, and particles size of all samples. The method was reported in the method chapter.

8.3.2.2.3 Mechanical properties

A.Elastic profiles

The elasticity was measured for each batch (n=3). The results were recorded as a graph of the applied stress (MPa) against deformation, which is the strain (%)(Wang et al., 1996) as expressed in the experimental chapter.

B.Pellets hardness

Pellets (n=30) were examined; hardness was measured according to Cespi et al. method by detecting the first notch of the texture analysis graph(Cespi et al., 2007). The method details were explained in the experimental chapter.

8.3.2.3 Thermal analysis

All samples were thermally analysed, as explained in the experimental chapter, using both of the following techniques:

8.3.2.3.1 Differential Scanning Calorimetry (DSC)

8.3.2.3.2 Thermogravimetric Analysis (TGA)

8.3.2.4 Statistical analysis

The tensile strength results, YM and AR for all batches, were statically analysed using SD, %RSD and one-way ANOVA ($p < 0.05$) via Microsoft excel.

8.3.2.5 Software simulation

The discrete Element Method (DEM) was chosen to prepare the computational data for simulating the pellets behaviour under compression. EDEM® is the commercial version of DEM and offers software without coding. Besides, all the steps of the compression process and pellets behaviour can be modelled. Moreover, the version is available for a three-month free trial, offering a good trial before the full purchase. EDEM® is based on three sections: creator, simulator, and analyst (EDEM, 2016).

8.3.2.5.1 The creator

Once EDEM® started, the first screen starts with the creator section offering a new deck, as seen in Figure 8.3. This section is divided into tree, viewer, and toolbar. The details of the particle are required to be entered in the tree part to start the simulation. The simulated part can be visualized in the viewer. Simulation can be edited using the toolbar, which enables changing parameters such as the simulation opaqueness of the pellets or particles (EDEM, 2016).

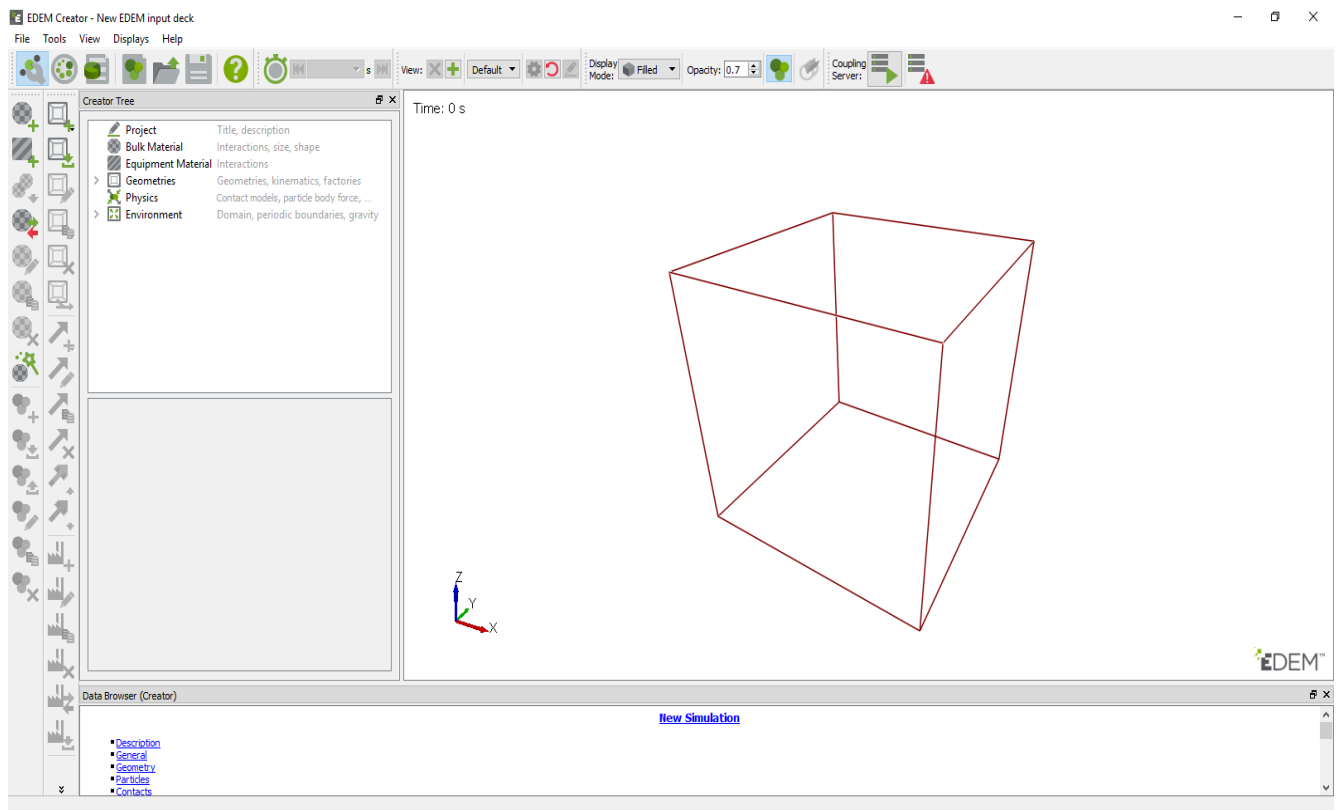


Figure 8.3 Starting window of the EDEM® creator showing tree, viewer, and toolbar

The bulk density, shape and size of particles were entered in the tree part. The groups of particles were produced as small and large particles of a 1 mm and 1.25 mm physical radius, respectively; hence large particles were close to the pellets of the smallest AR.

The correct dynamics can be predicted using a defined particle size. The pharmaceutical materials' particle size was used in the process. However, the micron and submicron particle sizes required a long time to simulate the dynamics of the particles. Therefore, particle size was escalated cautiously within a range showing no impact on the particle movements and other variables following the literature (Adam *et al.*, 2011; Börner *et al.*, 2016; Yeom *et al.*, 2019). Hence, numerous DEM and EDEM-based simulations studies have been computed by scaling up the particle sizes of the pharmaceutical materials (Janda and Ooi, 2016; Pantaleev *et al.*, 2017; Coetzee, 2019; Yeom *et al.*, 2019).

Hassanpour *et al.* studied the simulation of particles blending to detect the flow properties of the particles in the mixer. The size scale for the particles was between

2.26 to 11.40 mm, and the number of particles increased up to 15,000 and 7000. The results showed that the flow properties were similar to the real data for each particle size(Hassanpour *et al.*, 2011; Yeom *et al.*, 2019).

Also, the shear modulus was set to a low value (3.2 MPa) to reduce the computational time, as it does not considerably influence the particle dynamics simulations in pharmaceutical manufacturing processes (Lommen, Schott and Lodewijks, 2014). This part was studied by Lommen *et al.*, showing the effect of reduced shear modulus in three bulk tests to achieve a short simulation time (Lommen, Schott and Lodewijks, 2014). The shear modulus was set within the range of 0.01–100,000 MP and using the Hertz-Mindlin contact model. The shape of the particles was spherical. The results indicated that shear modulus above 100 MPa did not affect the particle dynamics. Therefore, the results showed that reducing the shear modulus was suitable to accelerate simulation since no effect is detectable on particles dynamics(Lommen, Schott and Lodewijks, 2014; Yeom *et al.*, 2019)

In order to define inter-particulate bonds between the small and large particles, a contact model had to be used before running the simulation. The contact model can either be described and generated within the software or chosen from the library of built-in contact models. In this project, Hertz-Mindlin with Bonding Contact Models was applied. Hence, Hertz contact theory applies to the contact between two bodies, including two spherical surfaces or spheres(Wang and Zhu, 2013)(DEM Solutions Ltd., 2014). Hertz-Mindlin with Bonding Contact Models is the appropriate choice for modelling particles compression as the accumulation of energy is detected from both the pellets and particles bonding (Yeom *et al.*, 2019). These bonds can resist indirect and normal movement up to maximum pressure, at which the bond breaks (DEM Solutions Ltd., 2014). In addition, the model can represent the relationship between force and displacement during compression, providing an accurate simulation for all particles(Wang *et al.*, 1996; Yeom *et al.*, 2019).

On the other hand, there is a physical radius and contact radius for each particle. The physical radius is smaller than the contact radius by 20-30%, as depicted in Figure 8.4. Hence, the contact radius can detect the sites where the bonding is starting. Also, bonding occurs when the contact radius is bigger than the distance between two

particles, and there is no bonding if the radius is smaller than the distance (DEM Solutions, 2017).

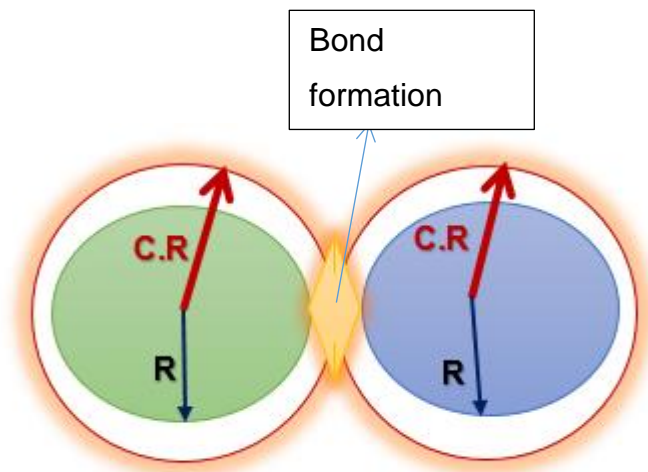


Figure 8.4 Hypothesized illustration of two particles showing the physical radius (R), contact radius (C.R), and bonds formation at the overlap of the contact radius drawn using Microsoft software 2018

The sum of the contact radius between the small and large particles, two small particles and two large particles, was 2.8 mm, 2.6 mm, and 3 mm. In addition, a defined disk radius with a smaller value than that of contact radii is necessary for bond formation when particles are only close to each other. Therefore, according to the Hertz-Mindlin model, the bonded disk radius was set to 0.95 mm to ensure bonds formation only between the overlapped contact radii of particles under compression.

On the other hand, the geometry of the manual tableting compressor in

Figure 8.5 was simulated in Figure 8.6, displaying an upper and a lower press, defining all movements of the particles, dying, and punching through the physics part of the creator. The following settings were applied in the creator tree for the geometry material properties: equipment type was interaction, geometries were cylindrical for compactors 1, and 2 (top and base), the surface shape around the compaction process was polygon. The number of edges was 32 with specified values centre and radius (1, 0.2 M) for X, and Y with Z was 0. The acceleration was set due to gravity - 9.81m/s², and velocity equals 1. The equipment density was set to 7500 kg/m³. The

solid density 1500-2500 g/cm³. The time of the geometry's movement was set with a time difference allowing the suitable compaction process. The start and end times were set to 2.03 – 0.5 for kinematics 1, and kinematics 2 was 0.05 – 0.3, respectively (DEM Solutions, 2017). The simulation set was trialed from 1-10 seconds, similar to the applied pressure time during real compression.

The particles were programmed to fill the die as the first step of the simulation. After that, the punch's movement was initially lowered to compress the particles then elevated after compression.



Figure 8.5 Tableting machine with a manual hydraulic press and upper punch to compress the powders (SPECAC Ltd, UK)

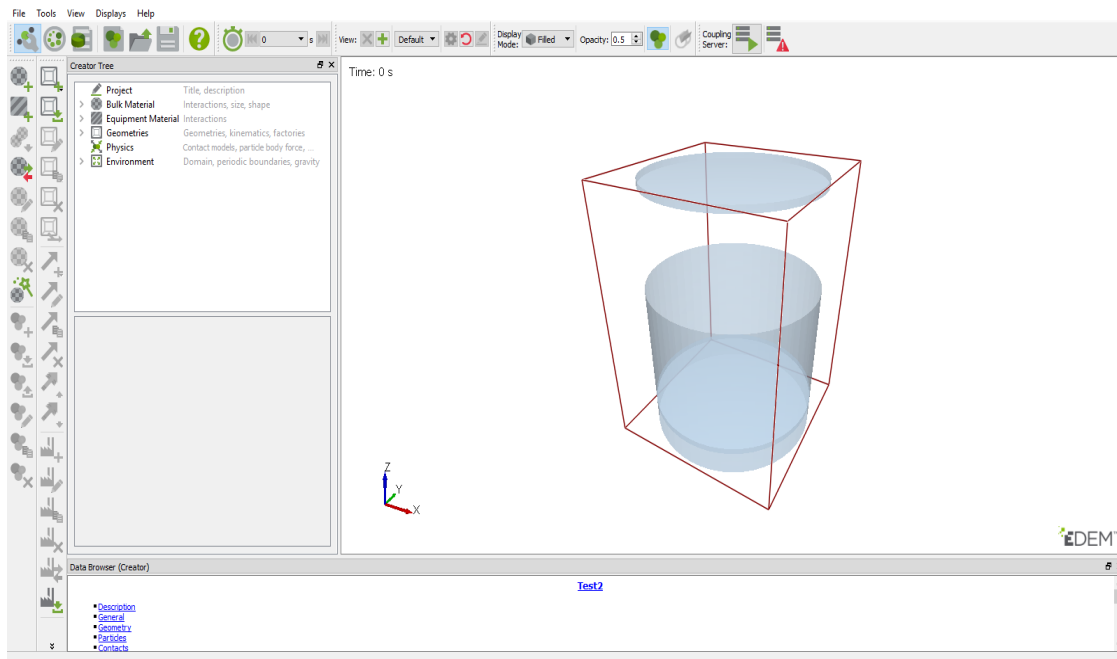


Figure 8.6 Simulated tableting press showing upper and lower punch modelled by EDEM®

8.3.2.5.2 EDEM simulator

The file was saved after preparation for the simulation. Then the creator window switched to the EDEM® simulator section to begin modelling. EDEM® simulator window can be seen in Figure 8.7 showing the simulation settings, including total time of simulation 1.25 seconds for the process, fixed time step 20% of the total simulation time, the smallest grid radius 1 cm and cell size 2.5 cm.

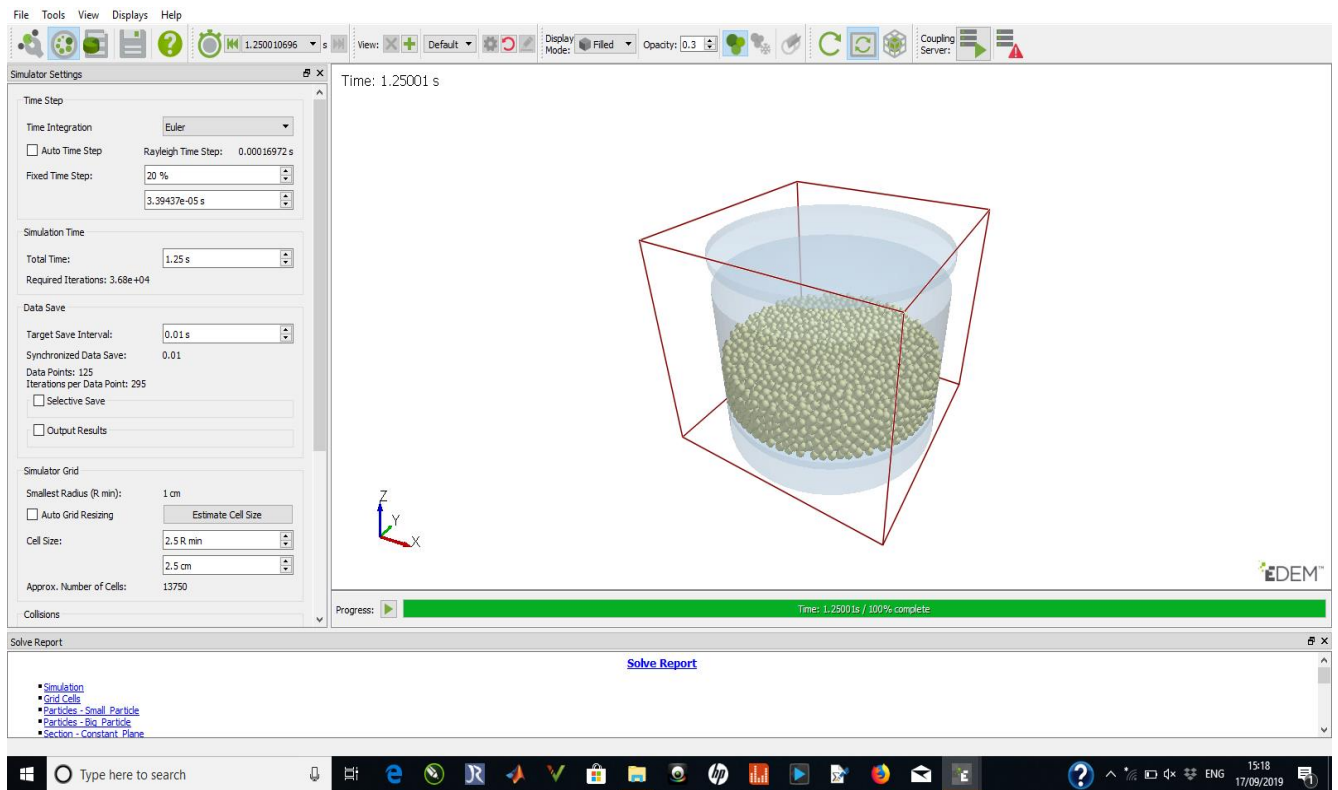


Figure 8.7 EDEM® Simulator, representing the simulation processing of the pellets

8.3.2.5.3 EDEM analyst

In order to analyse the results, the simulation was switched to the EDEM® analyst window shown in Figure 8.8. At this stage, the evaluation of both particles and pellets performance with the equipment was detected. Hence, the analyst window includes the tree, the viewer, and the toolbar for controlling, changing, and analysing simulation. In addition, other options were provided, such as changing opacity and displaying particles in different colours according to particles dimensions, binding energy, density in the viewer section. Moreover, the view of simulations angles and displaying time were controlled in the toolbar options. The video and images of simulations results were recorded. The graphs showed the energy outlines for all particles during the compaction and the compression process of force against time.

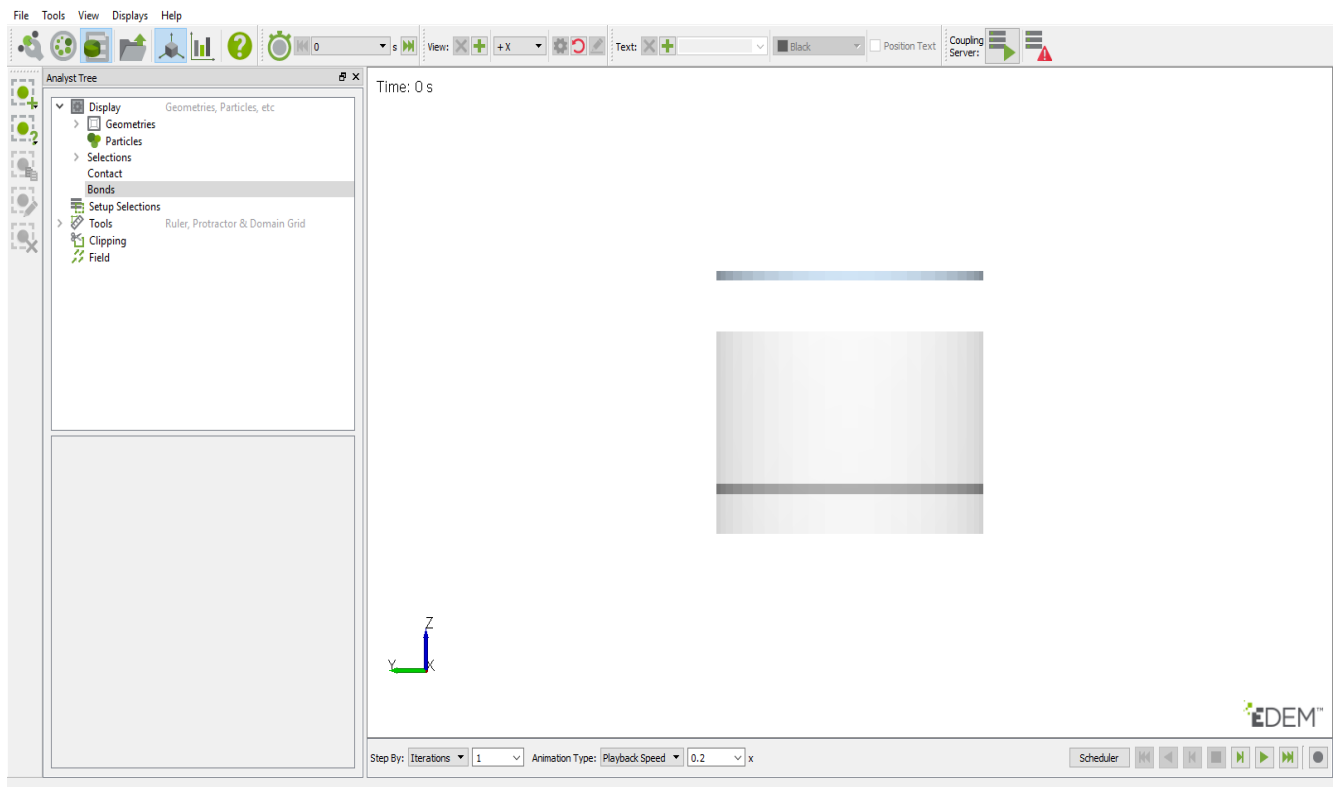


Figure 8.8 EDEM® analyst window showing tree, viewer, and toolbar

8.4 Results and discussion

Pellets were successfully prepared using the extrusion-spheronization technique. The produced batches of different compositions were evaluated to select optimum formulation results. The pellets with good mechanical and rheological properties were tested successfully to obtain the characterization data required for the software simulation.

8.4.1 Micrometric data of pellets

Following the weight measurements of the batches, the yield was calculated and summarized in Table 8.4. The results showed that the yield ranged between 78% - 109% indicating that the method was reproducible. The yield for batch 2 was slightly over 100%. This is possibly due to the high amount of water used. Hence, after drying batch 2, pellets lost 32% of their weight as unbound water (moisture) confirmed by the TGA results.

Table 8.4 Micrometric results showing bulk, tap density and the yield before drying with pellets sphericity in AR (n=30) and moisture content from TGA results

Batch	Yield%	AR mean \pm SD	Moisture content %	%RSD of AR	Bulk density (g/mL)	Tap Density (g/mL)
1	86.8	1.57 \pm 0.3	9.4	19.10	0.71	0.71
2	109.2	1.53 \pm 0.28	32	18.30	0.76	0.76
3	86.8	1.42 \pm 0.20	2.1	14.08	0.71	0.71
4	76	1.31 \pm 0.22	5.4	16.79	0.83	0.83

On the other hand, the bonded water molecules to the MCC particles in batch1 rendered the mixture of high moisture content affecting the formation of extrudates in pellet preparation and ultimately the yield. A similar trend was found by Kaur et al., increasing MCC concentration in the pellets reduced the yield (Kaur et al., 2020).

Batches 1&2 demonstrated high moisture content of 9.4% and 32%, respectively. It can be assumed that the high moisture content was correlated with the amount of water used. Although a higher amount of water was used in batch 1, the porous structure of the pellets (as confirmed in SEM) and the presence of crystalline and amorphous regions in MCC (grade 102) made the pellets retain less water and easily lose the water during the drying process. It was demonstrated by Thoorens et al. that the fraction of amorphous to the crystalline in the MCC structure affects the water sorption within the particles as water is mainly retained in the amorphous part (Thoorens et al., 2014).

On the other hand, the drying parameters could be insufficient to remove the added water (granulation fluid) after adding PRH to the MCC mixture in batch 2. This can be confirmed from the results of other batches (3 and 4) since the water amount (granulation fluid) was less than that in batches 1 and 2. Hence, it was reported that the addition of MCC to the mixture could improve the mixture's ability to hold a large number of water molecules by reducing water molecules migration (Otero-Espinar, Luzardo-Alvarez and Blanco-Méndez, 2010).

Therefore, batch 1 had lower moisture content than batch 2. Moreover, the lowest moisture content was for batch 3 with 2.1%, since ATEC has low water solubility that could render unbounded water molecules in the matrix, thus facilitating water evaporation during the drying stage (Fadda et al., 2008).

The result of batch 4 can confirm this as the moisture content was 5.4%, where the chosen plasticizer was sorbitol with high water solubility and hygroscopic tendency despite using a similar amount of water to batch 3 (Babenko et al., 2019) (National Center for Biotechnology, 2020). It can be stated that the difference in moisture content among the prepared batches was affected by the physical properties of the ingredients (amorphous or crystalline), the quantity of granulation fluid used and drying parameters. The other micrometric examination measured the AR of all batches. It was noticed that batch 4 had the most spherical pellets than other batches as AR was closer to 1 (Hentschel and Page, 2003). Hence, the obtained results using sorbitol as a plasticizer improved the sphericity of the pellets and surface properties (Otero-Espinar, Luzardo-Alvarez and Blanco-Méndez, 2010).

On the contrary, the highest AR was noticed for pellets with only MCC and no plasticizer. Moreover, the high % RSD for pellets of batch 1 and 2 indicated the low shape uniformity compared to batch 3 and 4. This finding happens because many of the pellets had elongated and irregular shapes, as confirmed by SEM. Hence, different factors can affect sphericity, including water amount, excipients, spheronization time and speed. Therefore, adjusting the quantity of added water could also improve sphericity (Muley, Nandgude and Poddar, 2016)(Kaur et al., 2020). This was correlated with the difference between the mechanical properties results as the variance between AR of all batches was significant ($p < 0.05$).

On the other hand, all batches showed low bulk density (< 1 g/ml). Similarly, tap density was low and identical to bulk density, indicating that all batches had good flow properties. Moreover, compressibility index and Hausner ratio results were zero and one for all the batches since there was no volume change between the pellets before and after tapping. This can be attributed to the low AR range of 1.31-1.57 of the pellets resulting in good rheological properties (Tiwari, Agarwal and Tiwari, 2013). This was in harmony with flowability results, as a 2 g sample from every batch had a flow rate of 0.4 seconds.

8.4.2 Mechanical properties

8.4.2.1 Tensile strength

In this preparation, the use of MCC was important to achieve pellets with good strength to maintain their integrity under compression during tableting without affecting the drug release from the pellets. Hence, MCC increases the binding strength between the particles and aids in pellets formation (Thapa et al., 2017). Zeeshan et al. prepared pellets of pseudoephedrine hydrochloride coated with different coating layers, then compressed them into tablets using MCC (Ceolus KG-801) as a tableting excipient. The results showed that increasing MCC content in the tablets from 50% to 60% delayed the drug release rate. Also, increasing the amount of MCC has reduced damage to the coated film. This was related to the distribution of MCC granules within the spaces between the compacted pellets and the cushioning effect of MCC that protected the pellets under compression (Zeeshan, Peh and Tan, 2009).

Therefore, compression of tablets composed of pellets without using MCC either in the coating layer or the matrix might have too low tensile strength. This can be observed in batch 1 as the MCC pellets showed the highest tensile strength compared to other batches. In addition, by reducing the amount of MCC and adding propranolol, as in batch 2, the tensile strength was reduced to the lowest value. This can be related to the effect of its moisture content (9.4%) and the high quantity of water used as a granulation fluid. Despite the higher moisture content in batch 2, this variance could be attributed to the different impacts of water on each ingredient. Hence, water affects MCC properties, enabling hydrogen bonding between the added water molecule and particles during pellet formation, thus increasing the water diffusion coefficient and enhancing the water penetration (Sahputra, Alexiadis and Adams, 2019).

Moreover, the impact of moisture content depends on the state and position of water molecules in the formulation; for instance, moisture content can take the form of anhydrous units bounded either tightly to the particles or absorbed at the surfaces of the particles or as bulk water. Therefore, the tensile strength increased with increasing moisture content since the number of solid bridges between particles increased, reducing the distances between them and allowing particle-particle interaction (Thapa et al., 2017). On the other hand, if bulk water is present in granules, multiple water layers could reside on the particles' surfaces leading to swelling MCC molecules. Thus, the distance between the particles increasingly affects particle bonding by hindering the intermolecular attraction forces, reducing tensile strength (Thapa et al., 2017).

It can be noticed that tensile strength for the batches (2,3 &4) is lower than batch1. Nevertheless, batches 3 & 4 showed higher pellet strength than batch2 after adding the plasticizers ATEC and sorbitol receptively. This can be attributed to two reasons firstly, the low amount of plasticizer used in pellet preparation had an anti-plasticizing effect, thus increasing the tensile strength(Chamarthy and Pinal, 2008). Secondly, the small diameters of batches 3 and 2 offered a large surface area to resist the applied force. On the other hand, the difference in tensile strength values between batch 3 and 4 is related to the type of plasticizers as well as the moisture content effect. Hence, the good moisture content of batch4 (5.4%) allowed water bridges to form between the particles leading to increase pellets strength (4.56 MPa), and the low moisture

content for batch 3 (2.1%) reduced the interparticulate attraction leading to low strength pellets (2.08 MPa) as in Figure 8.9 (Chamarthy and Pinal, 2008).

8.4.2.2 Young's modulus (YM)

The elastic properties of all pellets were evaluated based on the value of YM. Figure 8.9 illustrates the graph of YM and tensile strength values for the four batches.

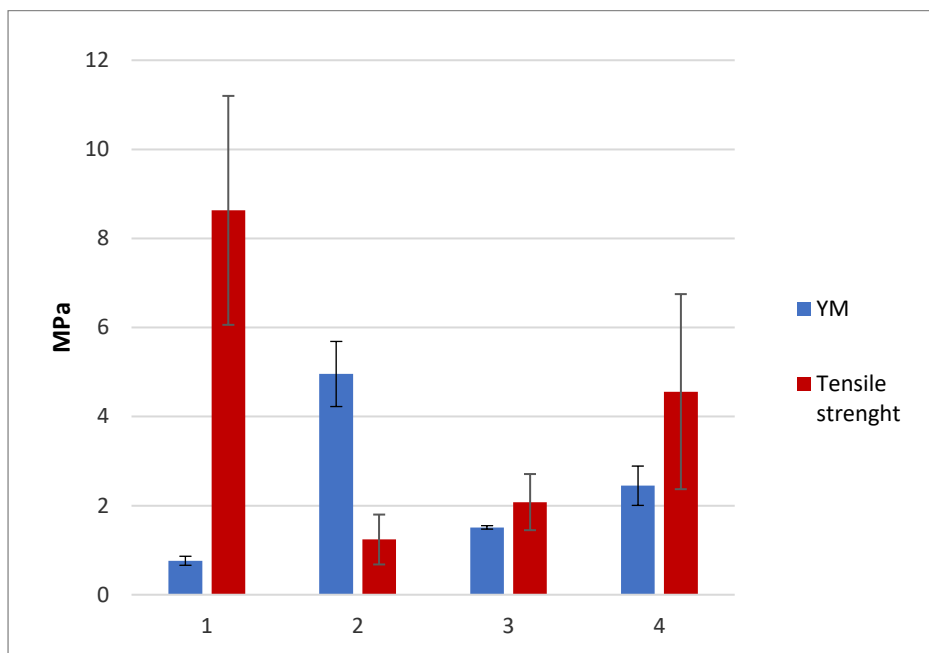


Figure 8.9 Mechanical properties of pellets showing the YM (n=3) and tensile strength (n=30) in mean +/- SD

Pellets with low YM show high elasticity, and those with high values have plastic deformation tendencies (Kubík and Kažimírová, 2015). The results showed that by combining more ingredients with MCC, YM started to change. For example, in batch 2, adding a drug with no plasticizer increased YM value contrary to batch1 of lowest YM, which comprises MCC solely. Regarding batch 2, lower YM was obtained by batch 4 and 3 accordingly, as incorporating sorbitol and ATEC in the pellets rendered the formulation more elastic. A similar trend was noticed with the tensile strength results; for example, using MCC in batch1 resulted in high tensile strength particles. This is related to the impact of water on MCC molecules that exists either bulk or bonded, as discussed earlier. As a result, bulk water presence on the molecules

increased the volume between the particles, thereby enhancing the molecules' mobility and reducing the YM (Thapa et al., 2017).

Moreover, water has a plasticizer effect, which causes the glass transition temperature (T_g) to reduce as moisture content increases; this explains the transition from a glassy to a rubbery state and reduces YM (Snejdrova and Dittrich, 2012). Additionally, batch 2 showed that the addition of the drug could fill these distances or gaps between the swelled particles of MCC, resulting in particles having higher plasticity and reduced mobility. Moreover, the addition of plasticizer, either ATEC or sorbitol, reduced YM values by improving the particles' flexibility by reducing T_g , which was noticed in DSC results (Snejdrova and Dittrich, 2012). Since the difference in mechanical properties results among the batches was significant ($p < 0.05$), the batch of the good properties was selected for simulation studies.

The good batch properties were batch 4 used in EDEM® simulation, including AR, bulk density and YM by applying the basics of a modified reported method. Since experimental data such as AR were mostly in the micron or submicron range, the computational time for simulating the pellets dynamics was significantly long. Therefore, in our study, data numbers were scaled up, since that is not influencing particle or pellets dynamics in general. Similarly, the results were scaled up to obtain less computation time by Yeom et al. and Hassanpour et al. (Hassanpour *et al.*, 2011; Yeom *et al.*, 2019).

8.4.3 Morphological characterization

All batches were examined using SEM analysis, and images were collected in low and high magnification. The images showed a general overview (Figure 8.10) and detailed each pellet with high magnification (Figure 8.11) to determine the pellets' morphology, AR, and surface properties.

SEM showed that pellets of batch1 had rough surfaces and high porosity (Figure 8.10&Figure 8.11 -A). Also, the existence of some MCC crystals in the pellet's surfaces. Although water amount was added in the highest ratio during pellets preparation of batch1, some of the MCC particles retained their crystals shape of the

original powder(Thoorens et al., 2014). Therefore, the high surface roughness and large pores of the pellets increased the mechanical interlocking, leading to high tensile strength recorded in the mechanical properties testing. However, interlocking pellet issues had a minimum effect on pellet flowability as batch1 pellets attained good flowability due to the largest AR. Similarly, Al-Khattawi et al. reported that microfibril and a high number of pores on MCC particles provided a high chance for interlocking mechanism; hence MCC showed 3 times higher surface roughness to d-mannitol particles, which justify the high hardness of MCC compacts (Al-khattawi et al., 2014).

Surprisingly, the MCC micro-strands disappeared from batch 2 surfaces related to the addition of PRH and reducing the amount of MCC (Figure 8.10&Figure 8.11-B). However, batch 2 showed a large AR and rough surface compared to other batches (3 &4), which agreed with physical examinations of AR. It can be assumed that the low tensile strength of batch 2 is attributed to the high surface roughness, which in turn reduced the available binding sites for particle-particle bonding, thus interfering with interparticulate attraction. It was reported that surface roughness is one of the parameters affecting the interparticulate forces between particles (Petean and Aguiar, 2015). On the other hand, batch 4 showed spherical pellets correlated with its small AR. This can be attributed to the addition of sorbitol to MCC and PRH in the pellet matrix, indicating that the good properties of sorbitol improved pellet sphericity, and the incorporation of MCC rendered the pellets with smoother surfaces compared to batch1, 2 and 3.

It was reported that the addition of sorbitol to the pellets could play a significant role in improving the pellets' surface properties by providing a good wet mass consistency for extrusion spheronization (Otero-Espinar, Luzardo-Alvarez and Blanco-Méndez, 2010).

Despite observing smooth surfaces of batch 3, the pellets showed higher AR hence higher diameter than batch 4, leading to a reduction in the surface area under the applied force during tensile strength testing (Figure 8.10&Figure 8.11-D). Therefore, there was a difference in mechanical properties between batch 3 and 4. In addition, the uneven surfaces of the pellets (batch 3), as noticed in image C of Figure 8.11,

could have interfered with the available binding sites between the pellets for forming interparticulate bonding.

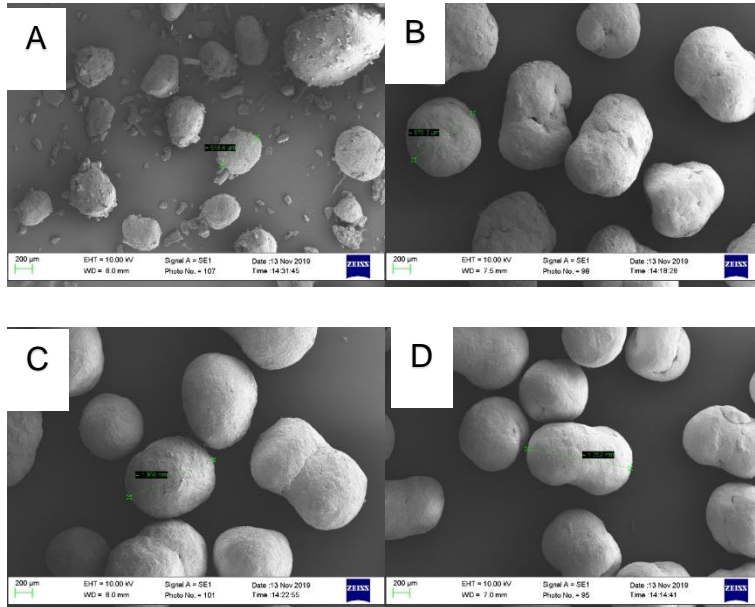


Figure 8.10 SEM images of MCC batches with a general overview of low magnification showing AR batch 1 (A), batch 2 (B), batch 3 (C), batch 4 (D)

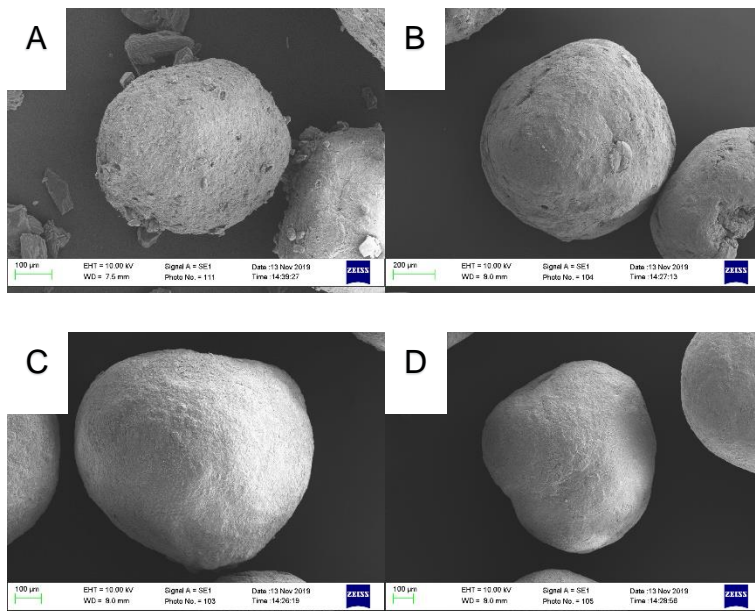


Figure 8.11 SEM images of high magnification showing the surface of each batch1 (A), batch 2 (B), batch 3 (C), batch 4 (D)

8.4.4 Thermal analysis

The four batches were examined to detect the physical changes and melting point after incorporating the drug and the plasticizers within the formulations by DSC (Figure 8.12).

DSC thermogram resulted in an endothermic peak at 167°C representing the propranolol melting point, as 164°C is the PRH melting point according to the British Pharmacopoeia (British Pharmacopoeia, 2020). A similar endothermic peak was noticed in batches 2,3, and 4 (Figure 8.12), showing the presence of the PRH within the formulations. However, the slight peak shifting could be attributed to the reduction of T_g due to the addition of water and plasticizers (Snejdrova and Dittrich, 2012).

Due to the high moisture content, MCC T_g ~133°C was detected in batches 3 and 4 and was less obvious in batches 1 and 2 (Picker and Hoag, 2002). Also, it can be assumed that the sorbed water in the MCC affected the T_g step (Thoorens et al., 2014). Hence, MCC showed almost no T_g indicating that the high moisture content could reduce the T_g step, which was confirmed by the high moisture content in TGA (Figure 8.13). Therefore, the addition of ATEC, sorbitol and water influenced the glass transition of the pellets.

Moreover, all batches showed a decomposition temperature at 271°C, which is the decomposition of MCC (Guo et al., 2012). Also, the wide endothermic peak of batch 2 appeared between 38°C-100°C, indicating that the high moisture content and evaporation of water started after that temperature range. These results agreed with TGA thermograms showing a mass loss at 38°C to 100°C for batch 2.

Moreover, Batch 1, 3 and 4 had 9.4%, 2.1%, and 5.4 % weight loss, respectively, representing the moisture content noticed in DSC starting from 60°C and continuing till 120°C.

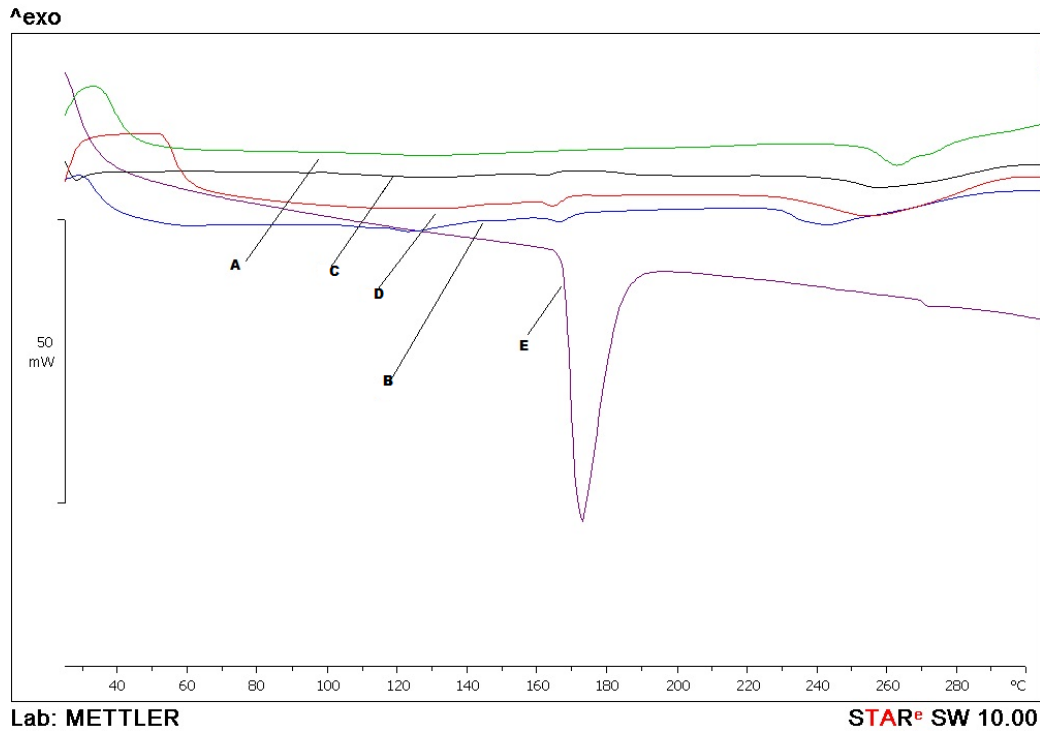


Figure 8.12 DSC thermograms of batches 1 (A), 2 (B), 3(C), 4(D) and drug (E) indicating the presence of the drug melting peak within batches 2,3 and 4

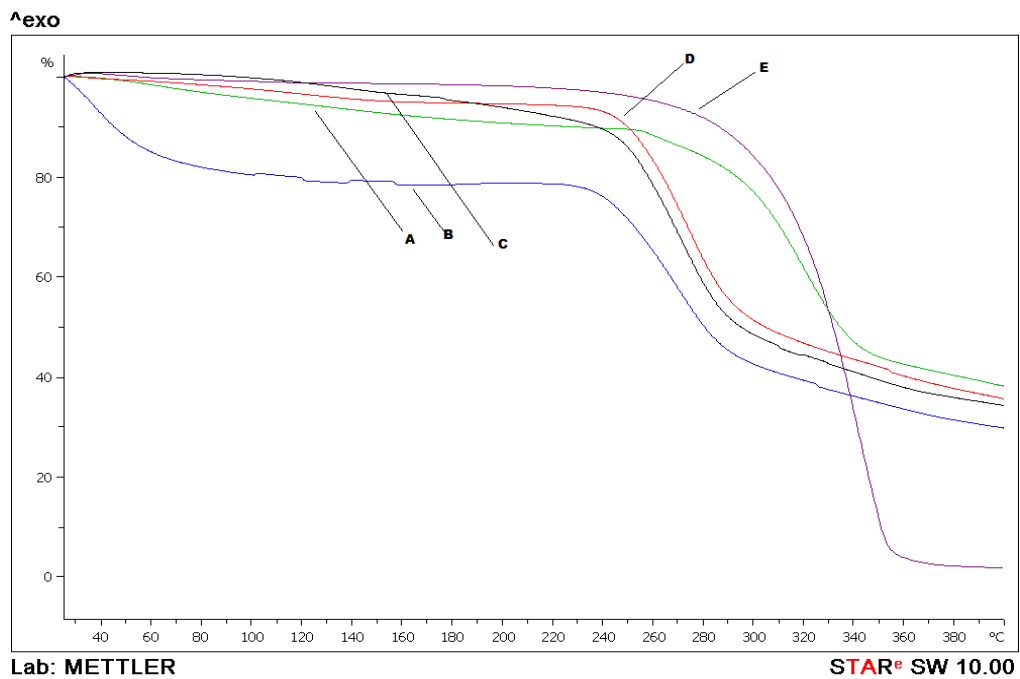


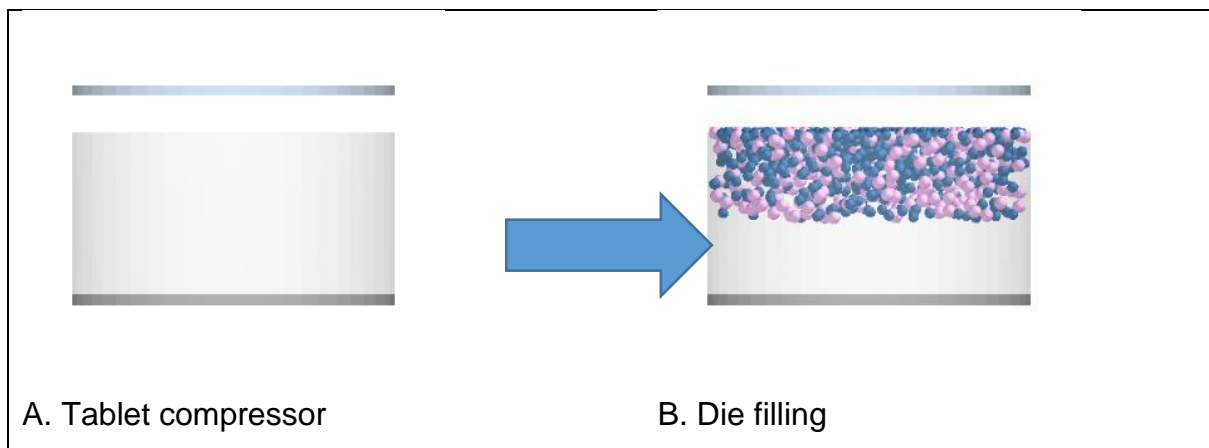
Figure 8.13 TGA results showing the moisture content of all batches 1(A),2(B),3(C),4(D) and the PRH in E

8.4.5 Software simulation

EDEM software is the potential for simulations of pharmaceutical powders and the compression process. This study demonstrates two promising approaches for simulating the compaction process and elastic-plastic compact deformation corresponding to the Hertzian contact model. Hence, different trials were applied to achieve the optimum force to compact the tablet before breaking.

The simulated results generated by EDEM® was obtained by applying the data of the best formulation among the prepared pellets (batch4). The pellets with high tensile strength, low YM and good AR were used. The pellets were simulated to be compressed within the ODTs matrix to examine their behaviour during compression. The initial method was adapted from a reported study to simulate pellet compression (Ramírez-Aragón et al., 2018).

The results were collected in graphs showing the behaviour of pellets under compaction, as in Figure 8.14(A-D).



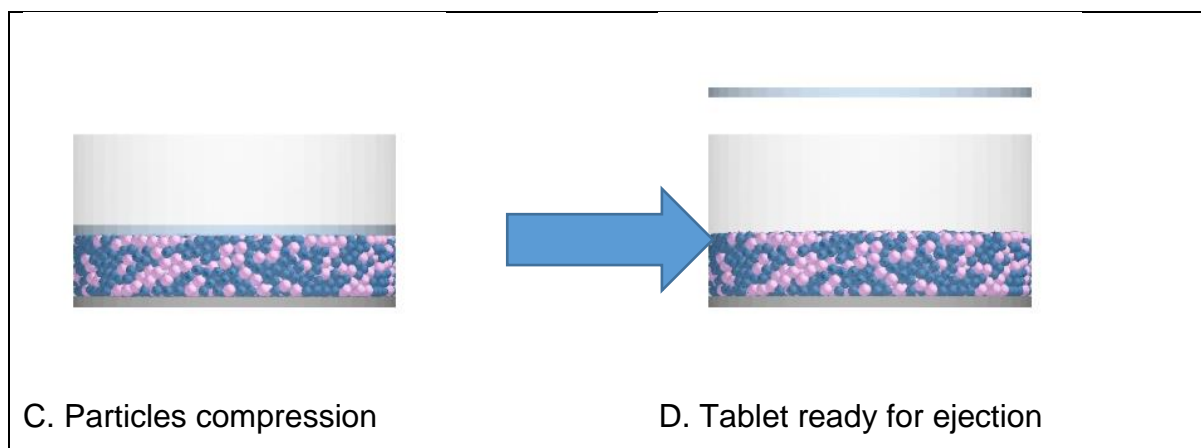


Figure 8.14 Simulation of compaction process demonstrated step by step according to the order of tablet preparations images extracted from EDEM

It can be noticed from the demonstrated simulation steps that the pellets of small AR had good flowability during feeding of the particles into the die owing to improved morphological shape with low surface roughness (Tiwari, Agarwal and Tiwari, 2013). This agreed with the micrometric results as indicated earlier. On the other hand, the good flowing pellets facilitated their compression when the upper punch started to lower; hence at that stage, compaction occurred, and particles-particles bonds started to form, producing a tablet at the end of the compression process. The results demonstrated that the blue particles have small diameters, and the larger particles are shown in pink. In addition, computational results showed that particles were distributed uniformly in the matrix with enough particle-particle interaction producing a sufficient compacted tablet without affecting pellets integrity. This is important as drugs would be protected. Moreover, these results agreed with experimental results as the flowability and bulk density of the pellets were good enough to produce tablets within a short time. The major challenge of the presented results was a long time of the simulation process for particles without scaling up their sizes which was a similar challenge to Yeom et al. (2019) and Hassanpour et al. (2011).

The simulation results (Figure 8.15) detected the strength of the bonds between the tablet's particles and pellets. The results displayed the energy levels of the compaction

forces applied to the particles. The results indicated which tablet's part can tolerate high pressure and how tablet's areas formed strong bonds (

Figure 8.16). The colours indicated the bond strength, as detailed in

Figure 8.16. The blue to cyan was the weakest, $2.77e-0.03$ N and $2.48e+0.0$ N, respectively.

In comparison, the medium strength was in yellow and orange $4.95e+0.0$ N $7.43e+0.0$ N, respectively. The strong bond was formed in red, ranging between $9.9e+0.0$ N to $1.24e+0.01$ N. The results showed that the predominant bonds were on the stronger side of the spectrum ($9.9e+0.0$ to $1.24e+0.01$ N) with a short time of 1.25 seconds and a uniform distribution within the formulation. Although yellow bonds were less generated, their presence indicated the weak interaction between some particles and pellets. However, weaker bonds in cyan were hardly seen in a few places revealing the acceptable particle interaction. On the other hand, the friction between the pellets and the small particles with the compaction wall geometries was difficult to detect.

Nevertheless, detection of the interaction of the materials is complicated to be measured directly (Horabik and Molenda, 2016; Yeom *et al.*, 2019). It was reported by Coetzee (2017), the use of the calibration method based on particles bulk test determine the material properties and interaction issues (Coetzee, 2017). Hence, in Coetzee (2017) study, the test was conducted by simulating the bulk test of the particles by entering randomly used parameters. Then parameters were changed many times, approaching the results of the real laboratory test (Coetzee and Els, 2009; Coetzee, 2017). Although the defined parameters may not be accurate in the reported study and represent a combination of two or more parameters, more experiments could be conducted for each parameter value as trialled by different studies (Coetzee, 2017) (Wang and Alonso-Marroquin, 2009). Hence, researchers applied different approaches to determine each parameter value due to the absence of standardised measuring or calibration methods instead of simulation of laboratory tests (Just *et al.*, 2013; Combarros *et al.*, 2014; Coetzee, 2016, 2017; Marczewska, Rojek and Kačianauskas, 2016).

Although the applied simulation is not completely comparable to our study's experiments, the compact elastic deformation was satisfactorily incorporated, considering the contact and interaction between the particles and pellets. This model

was applicable for the compaction of materials, whereas the fragmentation model would be necessary for future approaches to detecting ductile-brittle materials (Samimi, Hassanpour and Ghadiri, 2005). Therefore, to optimise our simulation method and solve the indicated issues, each parameter can be detected separately to determine the material properties and type of interaction.

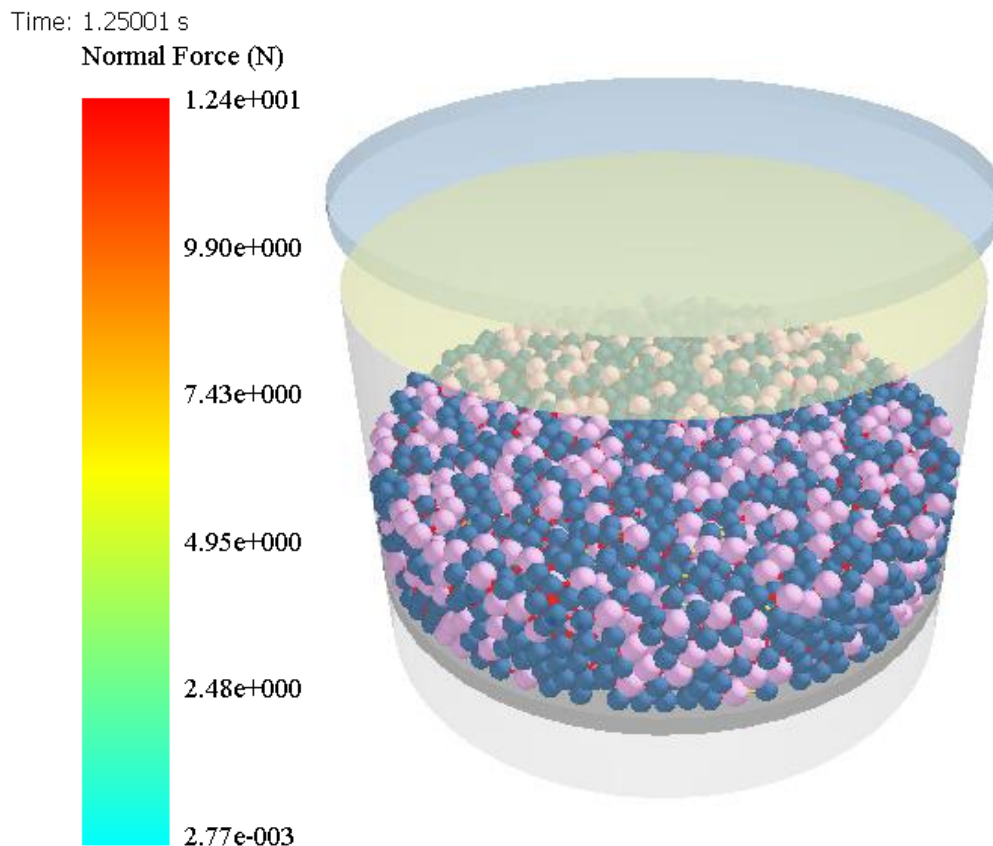


Figure 8.15 Bond strength between particles under compaction (top view)

It can be noticed from the side view image of the simulated compact in Figure 8.15 and

Figure 8.16 that the bonds were distributed and generated across the tablet height showing a uniform scattering of the strong bonds over the top and the bottom, and the weaker bonds were observed mostly at the top.

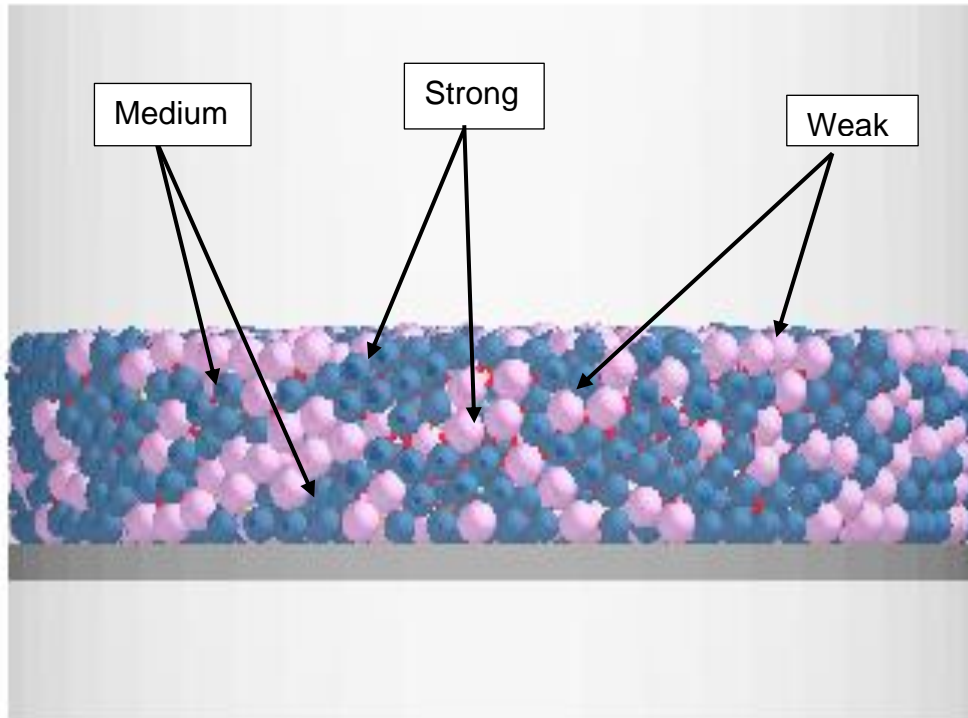


Figure 8.16 Bond formations between particles upon compaction blue and pink particles represent ODT particles and the pellets, respectively, weak bonds are shown in cyan, and those in yellow, orange and red were stronger, orderly

Also, filling the particles in the die showed no bonds formation indicating that the bond formation initiated after starting compression and was affected by particle- pellets distribution within the die. In addition, the number of bonds increased by increasing the compaction pressure. Figure 8.17 shows the pellets after being filled into the dye before being compressed. As seen in the image, there are no bonds among the particles.

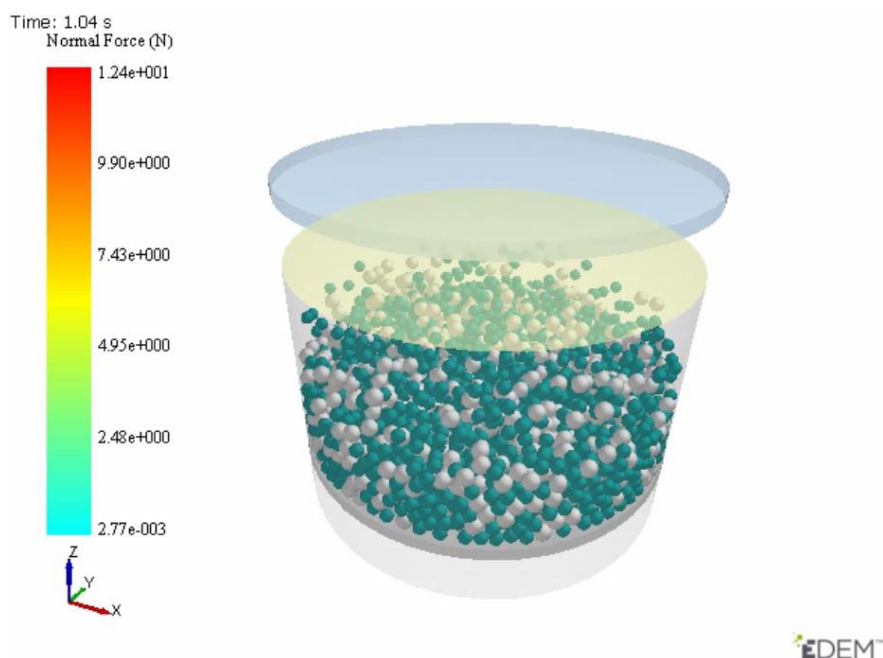


Figure 8.17 EDEM® image showing the particle filling during tablet compression before applying the pressure with no bond's formation

On the other hand, the compression force was measured by EDEM® during tablet compression consisting of the pellets within the ODT matrix. The results showed that a force of 2537 N at a time of 1.15 seconds was the maximum force applied to prepare a good compact (Figure 8.18). Therefore, a good compact without breaking. According to experimental data of the texture analysis, the maximum applied force was around 300 kg (~ 2941.9 N) as the stress was applied to the pellets to test their elasticity. However, further investigation of the laboratory results using simulation is necessary as the experimental YM obtained from the stress-strain slopes is influenced by permanent friction, particle rearrangement, and material elasticity (Agnolin and Roux, 2007). At the same time, tensile strength was inapplicable in this case as the tablet diameter was only detected with no thickness.

Nevertheless, compaction force can be considered high, indicating the tablets and pellets possess plastic to rigid properties without breaking under compression. Moreover, this indicates the even distribution of the pellets within the tablet matrix, which is an important factor to produce a good compact (as confirmed by simulation data). Also, the ejection force was 1040 N, reaching the equilibrium at 1.17 seconds.

Although there was a difference between the shape of the particles and sizes, the data indicated high particle-particle interaction, similar to experimental results. It can be assumed that reaching the force to equilibrium rendered particles to obtain similar pressure on each other hence, after removing the upper punch, there was no pressure applied on particles from the equipment. Therefore, the particles gained enough energy to produce forces to form a good compact with strong bonds after being compressed. In addition, the time between the compaction and the ejection was too short, allowing the particles to retain that energy after ejection.

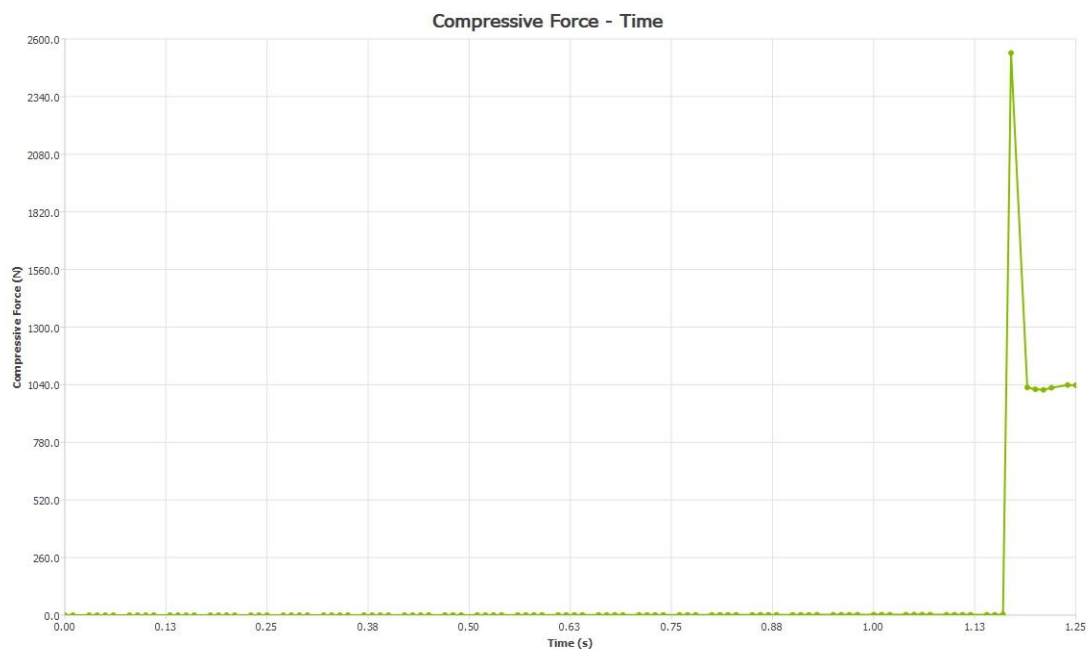


Figure 8.18 Compressive force (N) against time (S) for pellets under compression

On the other hand, during the simulation trials, the interaction forces were cyan colour predominantly showing the weak interaction between the pellets and particles after compression, as in Figure 8.19. Hence, the compression time and strength were insufficient for 0.8 seconds and 57-60 N, respectively, to obtain enough strong compact. This finding indicates that the higher compression force reduces intermolecular voids and increases inter-particle bonding, thus creating good compact formation and tablet densification(Veen *et al.*, 2000). Hence, the bond formation

degree should be high between pellets and powder particles to produce compact with the required strength and maintained structure formed (Mahmoodi, 2012)(Berggren, Frenning and Alderborn, 2004). Therefore, the low compression force resulted in a weak compact formation (Figure 8.20).

The other reason is the elasticity of the compact for both pellets and particles returning to their original phase with relaxation. Therefore, if the compression passes the point of elastic limit, the tablet formation enhances. Hence, when the compaction is controlled by the elastic deformation unloading the pressure leads to the solid relaxation as an elastic recovery(Berggren, Frenning and Alderborn, 2004)(Sun and Grant, 2001). The other trials for simulation examining the compaction force and particles interaction are included in the Appendix.

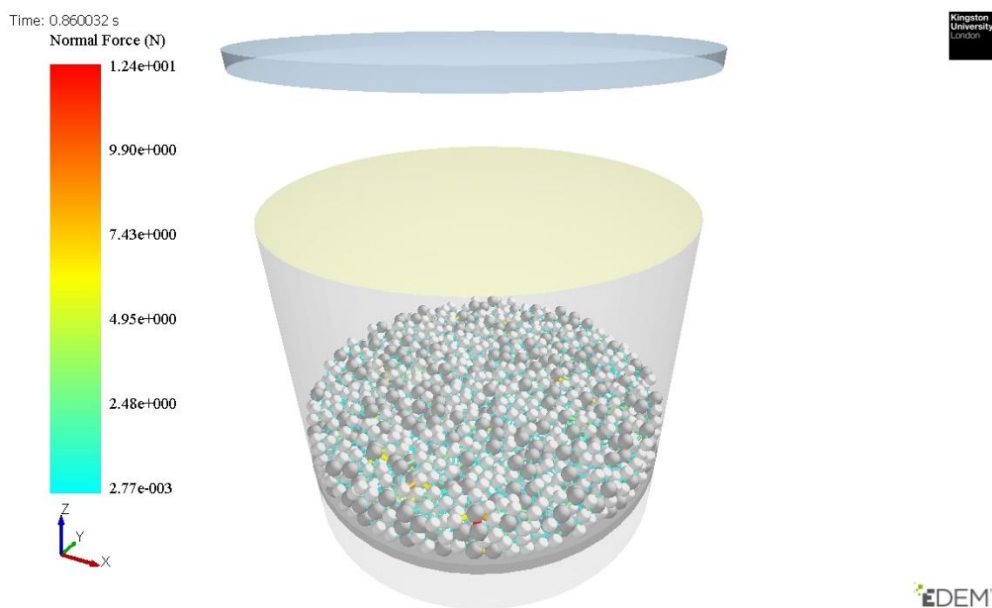


Figure 8.19 Pellets and ODTs particles after compression during simulation trials showing the weak interaction with cyan colour

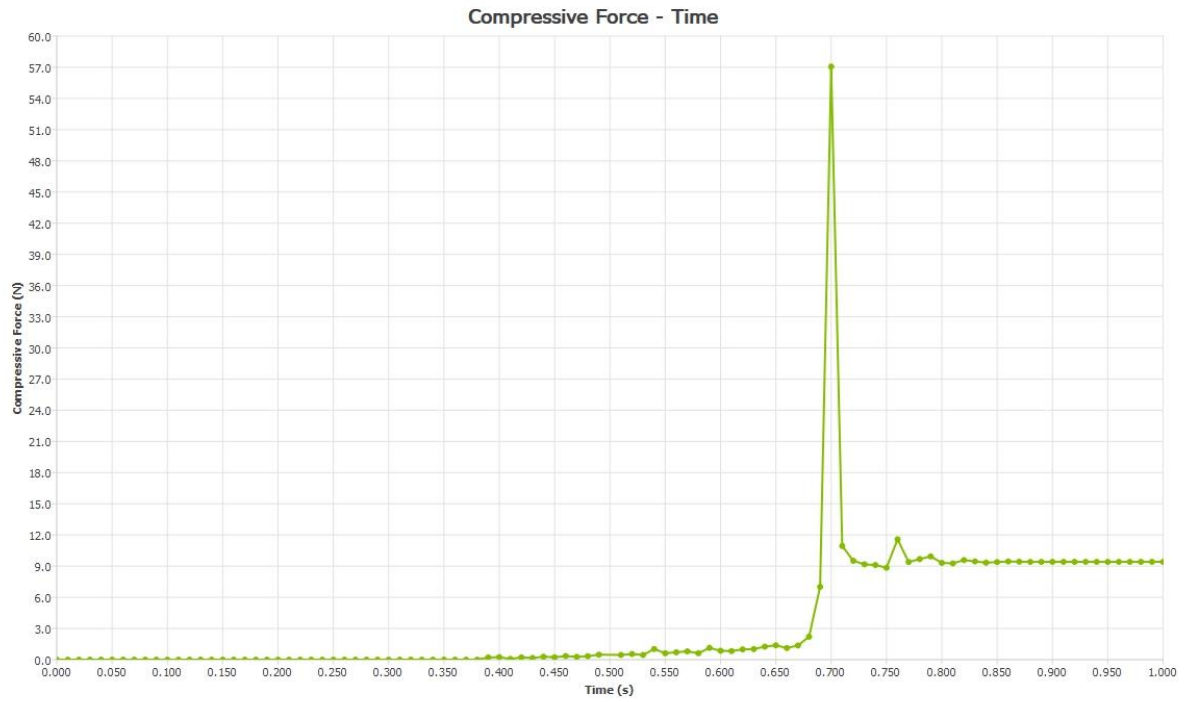


Figure 8.20 Low compaction force during simulation trials represented by force (N) against time (seconds)

8.5 Conclusion

This project successfully manufactured four different batches of PRH pellets. All batches had good rheological properties with a zero-compressibility index and 1 Hausner's ratio. There was a correlation between pellets moisture content, mechanical properties, and the plasticizer type. PRH pellets and ODTs matrix particles were simulated to study the compaction process using EDEM®. The simulation results showed that increasing compression force at the beginning of compression strengthens the interparticulate bonds at the surfaces resulting from the low surface roughness. Also, EDEM® results showed graphs of energy levels generated by particles during compression. Although particle sizes were scaled up, the simulation results followed lab data. This model was applicable for the compaction of materials, while particles fragmentation for the brittle-ductile model would be necessary (Samimi, Hassanpour and Ghadiri, 2005). Finally, this study demonstrated the suitability of EDEM® for pellets- ODT particles compression. Moreover, it provided an increased understanding of the correlation between particle's compression and interaction.

Chapter 9 The summary, conclusions, and future perspectives

9.1 Summary and a general conclusion

Orally disintegrating tablets (ODTs) or orally dispersible tablets are a type of solid dosage that can degrade once they come in touch with the saliva in the mouth (Hannan *et al.*, 2016). ODTs are considered an effective dosage form in delivering the drug for patients suffering from swallowing difficulty called dysphagia (Ghosh and Pfister, 2005). The tablet disintegrates in the mouth, the drug is released and absorbed through the mouth's mucosal tissue, allowing a rapid onset of action because the tissue has a high blood supply (Ghosh and Pfister, 2005). This type of formulation becomes highly important in the pharmaceutical market for prescribed and over the counter medication as this dosage form. The importance of ODTs starts from the ease of manufacturing using the direct compression method and effortless use by patients, leading to a significant increase in patient compliance (Irfan *et al.*, 2016)(Kar *et al.*, 2019). The challenge of using multiple daily doses for long-term medication for patients suffering from chronic diseases affects patient health and compliance(Jimmy and Jose, 2011)(Sadosky *et al.*, 2013). Taking more than one medication multiple times per day leads to forgetting, neglecting, or misunderstanding to take the regular daily dose of each medication (Sadosky *et al.*, 2013). As the patients start to forget to administer the medication, their health deteriorates, causing severe impacts on their health and patient hospitalisation (Martin *et al.*, 2005). This, on the other hand, leads to overwhelming the medical system with the high number of admitted patients and increases the death rate (Martin *et al.*, 2005). The hospitalisation estimation was at 2003 as high as more than \$13 billion annually in the US, and the consequences of health deterioration 125 000 deaths each year(Kane *et al.*, 2003) (Martin *et al.*, 2005). The economic cost for patient noncompliance reached \$949 to \$44190 per patient in the US in 2015. Also, the cost of the annual medication in the US is around US\$290 billion and in Europe is around €1.25 billion (Cutler *et al.*, 2018). In the UK, £930 million is an approximate annual cost of the health deterioration from the patient non-compliance only for asthma, type 2 diabetes, heart diseases and schizophrenia (Elliott, 2013; Cutler *et al.*, 2018). By observing other studies, patients compliance for changing migraine treatment using only a single daily dose of propranolol instead of the twice-daily dose of atenolol raised from 60% to 79.8% within 53 patients (Martin *et al.*, 2005).

Therefore, the use of modified-release formulations (prolonged and delayed-release dosage forms) offers several advantages over the immediate release formulations, including lowering drug-level fluctuations in plasma, minimising the local side effect of drug release, reducing the dose frequency, enhancing patient compliance (Ema, 2013).

The modified release system combined with ODTs offers significant advantages in solving the patient non-compliance issues and poor health outcomes associated with immediate release dosage forms (Ema, 2013). Multiparticulates microparticles and pellets can be the substantial drug carrier to its site of action. Microparticles and pellets offer an effective way to protect the active pharmaceutical ingredient from degradation, allowing control of the drug's release rate over a long duration (Singh *et al.*, 2010) (Goyanes, Souto and Martínez-Pacheco, 2010).

The challenge is associated with compressing ODTs containing multiparticulates without affecting the multiparticulates integrity and potentially distorting the modified drug release property. To prepare multiparticulate with good mechanical properties to be embedded in the ODTs of suitable strength high number of excipients that offer a balance between elastic and plastic properties for optimum compact properties.

9.2 Conclusion

This thesis investigated the use of different polymers to be utilised to prepare a multiparticulate system to be used in the orally disintegrating tablet. Different polymers were initially examined to understand the compaction behaviour of powders in raw and spray-dried form. Sodium alginate, polyacrylic acid and Eudragit L100 were determined to enhance the mechanical properties of the compact. Our preliminary studies found it difficult to prepare adequately shaped pellets from sodium alginate and polyacrylic acid, suggesting the combination of the polymers with reduced ratio with Eudragit L100 for a future approach. The constant behaviour of Eudragit L100 in both forms, raw and spray-dried under compression, suggested the use of that polymer freely with a reduced number of excipients. The spray drying influenced the obtained powder properties. The particles size, shape irregularity, surface smoothness and porosity generated differences in the mechanical properties of the powders before and after spray drying (García Mir *et al.*, 2011). Also, there is a significant relationship

between the particle's hardness and the applied pressure. It was concluded that an adequate balance between the elastic-plastic properties is essential to prepare a good compact maintaining the multiparticulate integrity under compression. The high plastic or elastic material could provide a fragile tablet or low mechanical properties, making it challenging to prepare a suitable formulation.

The model drugs Indomethacin (IND) and propranolol hydrochloride (PRH) were utilised to evaluate their release profile. Both model drugs are widely used by a wide range of patients of different ages, elderly or young (Moise *et al.*, 1988)(Accord, 2020). The IND use is associated with gastric side effects, including heartburn, gastric irritation, stomach pain, and vomiting (FDA, 2008). The side effect of immediate drug release associated with IND could influence patient compliance. On the other hand, as referred to earlier, reducing the dose frequency associated with chronic medication use such as propranolol is significantly essential. Propranolol is a widely used treatment for high blood pressure, irregular heartbeat, migraine or angina 2-3 times a day, depending on the health issue (NHS, 2018).

According to ICH guidelines, the quantification of both model drugs was assessed using a validated method. Accuracy, intermediate precision, and method robustness were detected and achieved for both methods. According to ICH guidelines, the specificity was within the accepted range with no interference to the drug peak, providing the suitability of the applied methods to quantify each of the model drugs in the formulation.

The use of cost and time-efficient preparation was successfully achieved using a few excipients with Eudragit L100 to prepare drug-based multiparticulate.

In the first study, spray-dried IND loaded Eudragit L100 was prepared to study the effect of the spray drying parameters on IND release. The spray-dried particles were embedded in the ODTs to assess the drug release profile in acidic media (pH 1.2) and buffer (6.8). In conclusion, the results showed that the properties of the microparticles were remarkably affected by the spray drying parameters. The solvent and the solid ratio to the solvent influenced IND release. The solvent type affected the behaviour of the spray-dried particles in both acid and buffer medium. The lowest IND release was detected using ethanol solvent with low parameter settings (75°C and 75%) in D1 and high settings in D2 (85°C and 100%) for both temperature and aspiration, respectively.

The shape of the particles and low mechanical strength resulted in a fluctuation of the IND release profile. On the other hand, the consistent release was detected with an acetone batch of high settings in B2. The mechanical properties were correlated with the formulations' release behaviour, indicating the importance of considering the balance between elastic-plastic properties to achieve the optimal formulation.

In conclusion, different factors influenced IND release from the spray-dried particles, including the type of solvent, the shape of the particles, the number of strands, and eventually, the elastic profile. Two solvents, acetone, and ethanol showed notable suitability to prepare accepted shaped microparticles with fewer strands. The balance between elastic and plastic properties offered a significant difference in IND release among other formulations, as in D and B bathes. It is essential to accurately select the parameters along with the type of the polymer, considering increasing the drying temperature to reduce the moisture content in the final product. It can be stated that elastic properties affected by changing the parameters as detected using acetone as a solvent, made it suitable when 5% w/w feed concentration was sprayed. Therefore, the low value of Young's modulus (YM) obtained using the appropriate solvent type and setting feed concentration at 5% w/w was appropriate for achieving IND release modification. Finally, all batches were compatible with the disintegration time, achieving low dispersible time within 21 seconds without significantly affecting the ODTs disintegration properties.

The second study examined the ODTs matrix effect on protecting pellets integrity under compression. The pellets matrices were prepared using Eudragit L100 containing IND to achieve a delayed-release profile passing the gastric medium. The formulation successfully delayed IND release at pH 1.2 and released the drug at a higher pH (6.8). The effect of the cushioning layer using lactose and mannitol in the ODTs was evaluated according to different particles 500, 125 and 63 µg. The development of a consistent system of cushioning agents is essential. The cushioning agents adsorb the applied pressure during tablet compaction, protecting the pellet integrity by limiting crashes between pellet and pellet and pellets with the die or punch surface (Xu, Heng and Liew, 2016)(Tan and Hu, 2016a). The use of both matrixes offered a short disintegration time of fewer than 21 seconds.

The results showed that the particle size and shape of lactose and mannitol influenced the mechanical properties of the final tablets. The amounts of lactose particles were consistent under compression compared to mannitol, which showed variation. It can be concluded that the smaller the particles size, the higher the shapes homogeneity, while the shape of the irregular particles is associated with larger particles. YM was associated with the tensile strength of the same materials. The lactose tablets demonstrated higher plasticity than mannitol. The additive materials performed differently at different particle sizes, and such variance was reduced with increasing the powder particle size. The variation of IND particles shape to lactose particles affected IND distribution within ODTs and thus the necessity of using IND of similar particle size when combined with sieved lactose particles to even drug distribution within ODTs. The dissolution studies indicated that pellets distribution using lactose batches were more homogeneous than mannitol. Finally, lactose was a suitable ingredient for ODTs to retain the pellet's integrity under compression. Also, a small particle size of 63 μm of lactose and mannitol can be beneficial to improve patients compliance with no taste disturbance, i.e. grittiness (Kathpalia *et al.*, 2014)(Patil *et al.*, 2016)(Kakar, 2018).

The third study was applied for further investigation to understand the mechanical behaviour of pellets under compressing, exploring the impact of initial particles properties. As complementary with the second study, it was necessary to investigate similar factors in pellets preparation. Therefore, Eudragit L100 particle size impact on pellets mechanical properties and IND delay was investigated.

The pellets were successfully prepared using different particle sizes 45, 63 and 90 μm of Eudragit L100 and IND as a model drug. The pellets were embedded into the matrix of ODTs. Particle sizes were of good elastic properties as Young's modulus (YM) values were low, and no significant difference between the different sizes ($p>0.05$). Testing the pellets' mechanical properties showed that the tensile strength was directly proportional to YM ($p<0.05$), offering enough support to maintain their integrity under compression. The pellets hardness was associated with initial particles properties in each pellets batch. The pellets prepared from 63 μm Eudragit L100 showed a suitable mechanical properties balance compared to the other sizes. IND delayed-release was achieved in acidic media and immediately released at pH 6.8. The results indicated that the initial powder properties affect remarkably the pellets mechanical properties.

Disintegration time was affected by the porosity of the pellets, and all tablets showed a low disintegration time of lower than 30 seconds. In general, the porosity demonstrated by pellets of 63 and 90 μm batches could preferably have a positive impact for maintaining pellet integrity under compression, thereby retaining IND release compression (Tunón, Gråsjö and Alderborn, 2003).

To conclude, factors affecting the pellets' mechanical properties were powder particle size, pellets' sphericity, and porosity. There was a significant relationship between the morphology and hardness of the pellets. Protecting pellets integrity was essential to delay the release in the acidic media to be immediately released in alkaline media.

The fourth study was conducted using a modified-release system combined with ODTs. The pellets were applied using a matrix system of time-dependent Eudragit polymers. The study examined the propranolol hydrochloride release via pellets of Eudragit RS using three different plasticisers, sorbitol, triethyl citrate (TEC) and acetyl triethyl citrate (ATEC) as plasticisers. The developed method was used successfully to analyse the propranolol release from the prepared ODTs containing pellets. The pellets were successfully prepared using the extrusion spherulisation technique. The suggested ratios and type of the plasticisers influenced the mechanical properties of individual pellets and pellets in the ODTs. The disintegration time achieved rapid disintegration within 30 seconds for all batches. The batch of sufficient strength for preparation, packing and handling with little imperfection could be achieved using 3% ATEC pellets (1.1 Mpa) without affecting the rapid disintegration time. Hence, according to YM results, the difference between the batches of TEC (3% and 5%) showed no significant difference ($p>0.05$), while pellets of ATEC (3% and 5%) were statistically different ($p<0.05$). In addition to previous findings, the best AR (close to 1) was achieved. In conclusion, Eudragit RS as a matrix system could not achieve a remarkable change in the PRH release. The detected variations in both acidic and phosphate buffer media was related to the types of plasticisers used in the pellet's preparation ($P<0.05$), while the change in ratios of plasticisers showed no statistically significant difference ($P>0.05$) according to two-way ANOVA. TEC and ATEC showed a slight modification of PRH release in phosphate buffer media (pH 6.8). In conclusion, utilising ATEC as a plasticiser could be an appropriate additive providing adequate mechanical properties for the compacted pellets in the ODTs. The preparation of

reservoir pellets based on Eudragit RS can be considered for additional examination and analysis.

The fifth study examined the applicability of modification propranolol release from the prepared pellets using time-dependent polymers through the reservoir system instead of the matrix system, which had no effect of modifying the PRH release, as demonstrated earlier. The experiment explored a simple technique to prepare coated pellets saving time and cost. Pellets core matrices contained 77% microcrystalline cellulose (MCC), 3% acetyl triethyl citrate (ATEC), and 20% drug.

The coating process achieved a smooth and continuous coating layer around the coated pellets with Eudragit RS, RL and both polymers in a 1:1 ratio. The coating thickness was necessary for a future approach to consider the effect of the thickness layer on the weights of the prepared pellets. The mechanical properties including remarkably enhanced after coating ($p < 0.05$). Considering the coating process parameters is necessary for developing the prepared pellets. Pellets coated with Eudragit RS and RS/ RL can be optimised to modify the PRH release from ODTs. The uncoated pellets released $> 75\%$ of PRH in acidic and buffer media after 30 minutes, while the coated pellets were able to modify the PRH release to $\leq 53.9\%$ in acidic media and $\leq 47.2\%$ in buffer media. The results were promising, showing the possibility of modifying the PRH release using the reservoir system of Eudragit RS and applying the simile coating method to replace the costly and traditional methods. Future development is necessary to optimise the formulation and the settings parameters.

The proposed studies investigated several factors to approach modification of the drug release using different characterisation techniques, physical, mechanical, and analytical. All the studied and investigated formulations were based on laboratory work and analysis. Therefore, there was necessary to explore a computational method to provide essential laboratory data minimising the time, effort, and cost.

The sixth study was conducted to estimate the formulation development, exploring the obtained results via the simulation software discrete element modelling (EDEM®). The simulation study was an example case that showed the feasibility of using one of the simple measurements obtained in the lab to be used as an indicator for the expected results to avoid any unnecessary mistakes in the lab. Although there was a difference between the shape of the particles and sizes, the data indicated high particle-particle

interaction, similar to experimental results. It can be assumed that reaching the force to equilibrium rendered particles to obtain similar pressure on each other hence, after removing the upper punch, there was no pressure applied on particles from the equipment. Therefore, the particles gained enough energy to produce forces to form a good compact with strong bonds after being compressed. In addition, the time between the compaction and the ejection was too short, allowing the particles to retain that energy after ejection. EDEM® simulation demonstrated that pellets could be compressed in the ODT matrix, demonstrating a correlation between the obtained laboratory compression process and simulation data with a maximum compression force of 2537N. The simulation demonstrated various bond types and their respective strengths with indicated colours. The blue to cyan was the weakest, $2.77e-0.03$ N and $2.48e+0.0$ N, respectively. At the same time, the medium strength was in yellow and orange $4.95e+0.0$ N $7.43e+0.0$ N, respectively. The strong bond was formed in red, ranging between $9.9e+0.0$ N to $1.24e+0.01$ N. The predominant bonds were on the stronger side of the spectrum ($9.9e+0.0$ to $1.24e+0.01$ N) with a short time of 1.25 seconds and a uniform distribution within the formulation.

Additionally, EDEM® generated a compressive force versus time graph depicting the forces that pellets tolerate when they go through compaction. To conclude, the computational method for simulating the tablet compression could potentially minimise the preparation obstacles, costs, and time of laboratory work. Also, optimise the formulation to achieve the target.

The data were limited to show the mechanical properties and could be applied for the future approach to examine other manufacturing parameters. The simulation results showed that increasing compression force at the beginning of compression strengthens the particulates bonds at the surfaces resulting from the low surface roughness. EDEM® showed graphs of energy levels generated by particles during compression. Additionally, it provided a broader understanding of the degree of compression and particles strength. The validity of using EDEM software requires further examination to generate a complete understanding of the mechanical and physical formulation properties.

In conclusion, different analytical techniques and preparation methods were used, starting from preparing microparticles and pellets using spray drying and extrusion spheronisation. The direct compaction method is fundamental for preparing tablets and examining different compaction pressure. The developed HPLC methods analysed, quantified, and detected the model drugs. All batches were compatible with the disintegration time, achieving low dispersible time within 30 seconds. The prepared formulations were examined using inclusive characterisation techniques, including texture analysis, hardness and tensile strength, DSC, TGA, porosity, flowability and disintegration.

To conclude from our project, the multiparticulates system via ODTs is a successful approach to modify the drug release for patients with swallowing difficulties. Eudragit L100 is used to prepare a multiparticulate system as microparticles, and the matrix pellets system was feasible to achieve a delayed IND release profile with a limited number of excipients and low cost. The reservoir system based on Eudragit RS and Eudragit RL was suitable to vary the propranolol release profile rather than using their polymeric matrix, hence providing the burst effect. The multiparticulates of microparticles and pellets based on Eudragit L100 combined with ODTs can offer a flexible dosage form for children and elderly patients, facilitating swallowing with a minimum dose frequency. The computational method showed a successful implementation of simple experimental data, saving time and cost to simulate the compaction behaviour of the multiparticulates within ODTs providing new findings of the binding forces between the particles.

9.3 Future studies

The future investigation can be applied based on the results and findings of this project. The spray drying of sodium alginate particles can be examined in the preparation of pellets since that was challenging using the raw powder. Also, examining the molecular weight of the sodium alginate using spray drying parameters could be further investigated.

Moreover, the combination of Eudragit L100 and sodium alginate after spray drying can be applied to prepare pellets to enhance the shape factor and delay the drug release profile. Similarly, after spray drying, polyacrylic acid combined with Eudragit L100 can be investigated to prepare pellets. Also, further analysis would be accomplished to characterise the obtained microparticulate system.

Additional studies can be carried out by changing the spray drying parameters and changing the type of solvent used during the preparation. Additionally, the particle size of a more elastic polymer needs assessment and characterisation using sieve analysis and texture analysis techniques.

Eudragit L100 spray-dried particles can be examined for the spray drying approach using the optimised parameters with different ratios of less viscosity. The spray drying of Eudragit RS and Eudragit RL applicability can be detected using the same parameters of Eudragit L100. This can be further applied to prepare a multiparticulate system of pH-dependent and time-dependent polymers to combine the beneficial impact of both types on modifying the drug release. Therefore, more than one medication can be combined in one formulation.

For the ODTs matrix study, two approaches can be further investigated. First, the increment of particle size using granulation of the lactose or mannitol for equal distribution of the pellets combine with ODTs matrix. Secondly, spray-dried lactose can be combined with microparticles to examine the fast disintegration and uniformity of microparticles distribution in the spray-dried ODTs matrix. This would allow particle size uniformity between the tablet matrices and the multiparticulate system. Also, a small particle size of ODTs matrix can be beneficial to improve patients compliance with no taste disturbance, i.e. grittiness (Kathpalia *et al.*, 2014)(Patil *et al.*, 2016)(Kakar, 2018), as future approach studies can be applied to test that on patients.

Furthermore, considering the effect of the longer blending time of the multiparticulate and ODTs matrix. Since the longer blending time promotes higher contact between the particles, this can be investigated to provide a higher distribution homogeneity of the multiparticulate system containing medication and the tablet particles.

The use of Eudragit RL and Eudragit RS in the multiparticulate system is promising via reservoir pellets. However, coating parameters such as the rotation speed, the amount of coating liquid and solution temperature require investigation. The content uniformity should be considered while altering the parameters.

Additionally, mixing the pellets with glidant before the coating process can be helpful to reduce the friction between the pellets and the pan. Finally, the use of plasticiser in the coating solution is vital to be further examined. Hence, this can easily facilitate the coating layer's uniformity around the pellets. Nevertheless, developing a control sample using the standard coating method should be unutilised to promote a clear understanding of lab coating method feasibility.

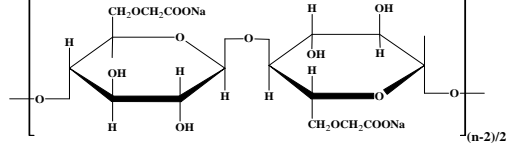
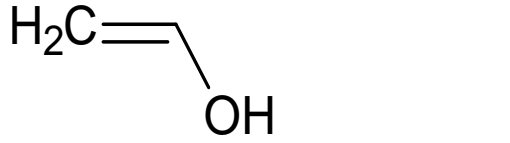
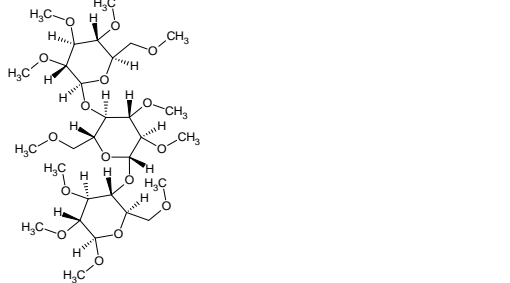
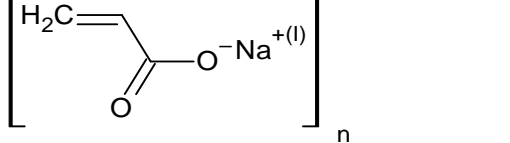
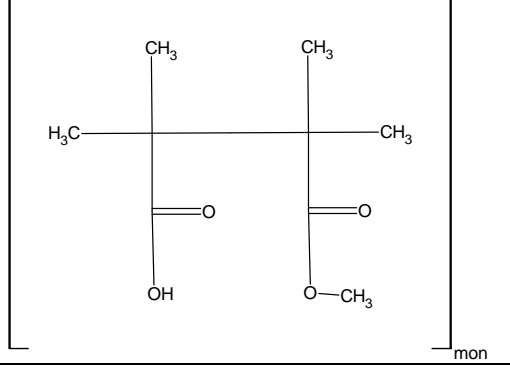
On the other hand, EDEM software can be applied for simulations of flow and compression of powders to prepare ODTs. The particles friction and adhesion forces can interfere with the particles flow. Although the experimental data provided a comprehensive understanding of powder, pellets, and tablets' physical and mechanical properties, the manufacturing and processing parameters must be further investigated to achieve a quantitative agreement. EDEM numerical experimental data can provide agreement with the experimental work. Therefore, estimating the flow for the properties via the simulations system is a promising step. Furthermore, the simulated results can provide the elastic and plastic compact deformation using the truncated-sphere models. This model can accurately detect ductile materials and examine particles shape.

During the project, different skills have been learned, including research skills, analysing techniques, comparing results, and other methods to obtain results from the prepared tablets or spray-dried materials.

Chapter 10 Appendix

10.1 Appendix chapter 3

Table 10.1 Structures of the polymers used in our study according to sigma Aldrich

Name of the polymer	Structure
Sodium alginate	 <p>The structure shows a repeating unit of sodium alginate, which is a linear polysaccharide. It consists of two pyranose rings linked by a 1,3-glycosidic bond. The left ring is in the alpha-D-glucopyranose form, and the right ring is in the alpha-D-galactopyranose form. Both rings have a sodium alginate side chain (-CH₂OCH₂COONa) attached to the C6 position. The entire unit is enclosed in brackets with a subscript (n-2)/2.</p>
PVA	 <p>The structure shows the repeating unit of Polyvinyl Alcohol (PVA), represented as H₂C=CH-OH.</p>
MC	 <p>The structure shows a repeating unit of Methyl Cellulose (MC), which is a cellulose derivative. It consists of a pyranose ring with several hydroxyl groups replaced by methoxy groups (-OCH₃).</p>
PAA	 <p>The structure shows the repeating unit of Polyacrylic Acid (PAA), represented as [H₂C=CH-C(=O)O⁻Na^{+(I)}]_n.</p>
Eudragit L100	 <p>The structure shows the repeating unit of Eudragit L100, which is a methacrylate copolymer. It consists of two methacrylate units: one with a hydroxyl group (-OH) and one with a methoxy group (-OCH₃).</p>

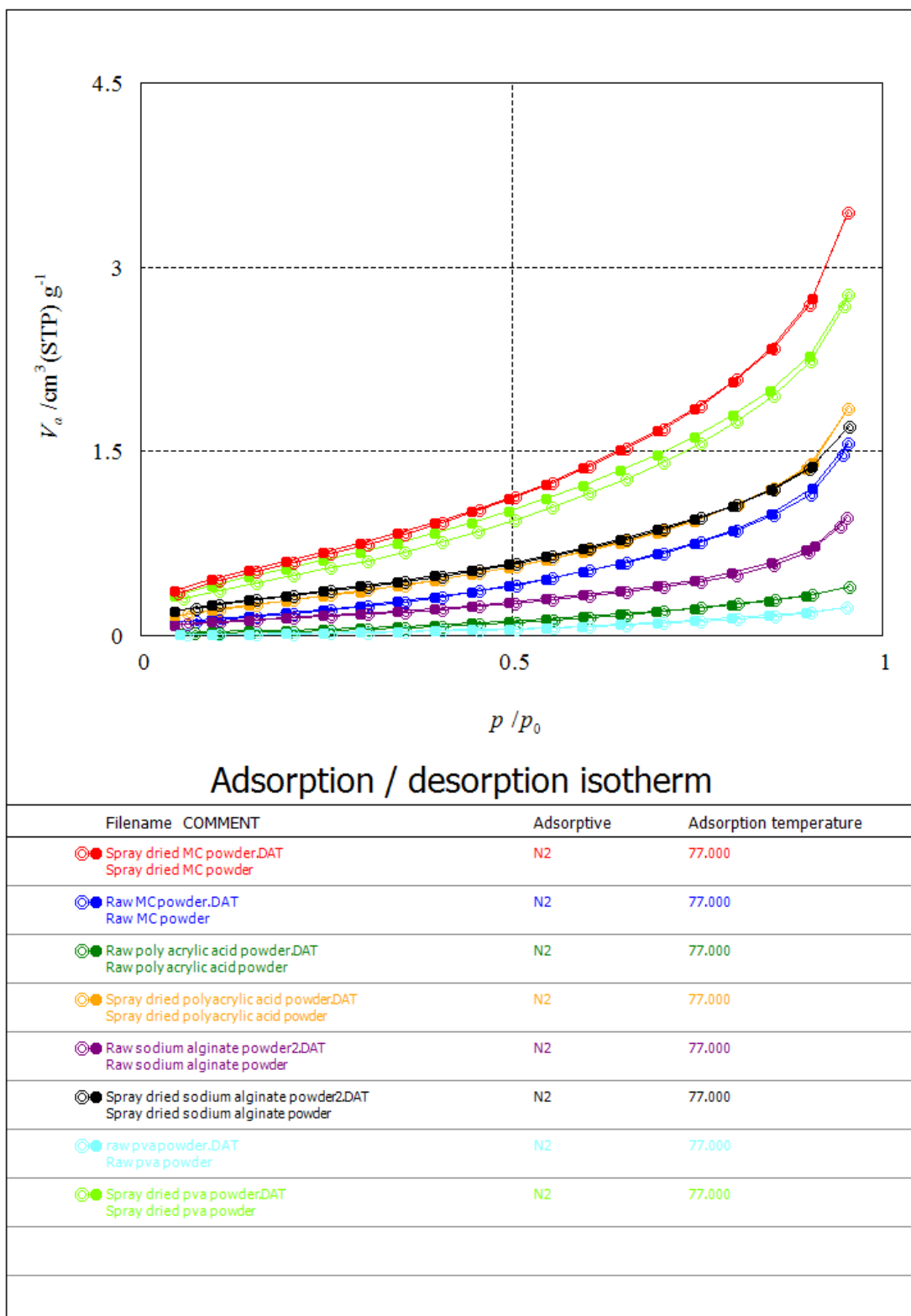


Figure 10.1 Porosity results showing adsorption desorption isotherms for raw and spray dried powders

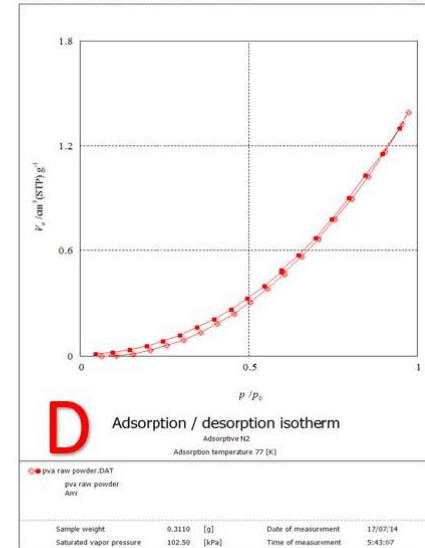
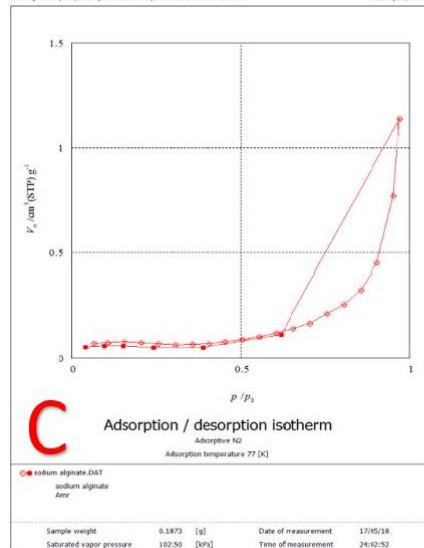
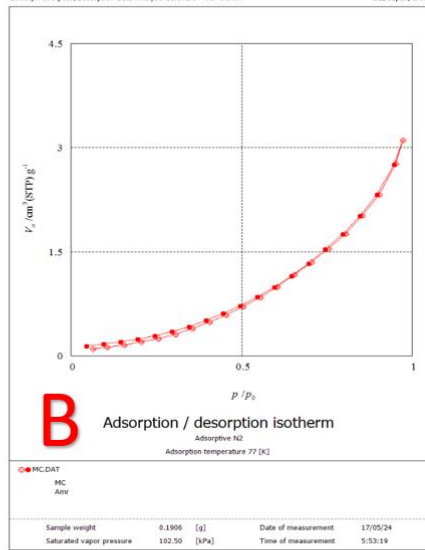
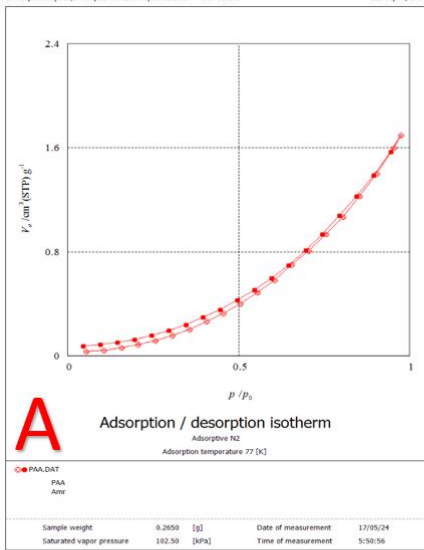


Figure 10.2 The isotherms of the 4 polymers PAA, MC, sodium alginate and MC showing type3 isotherm

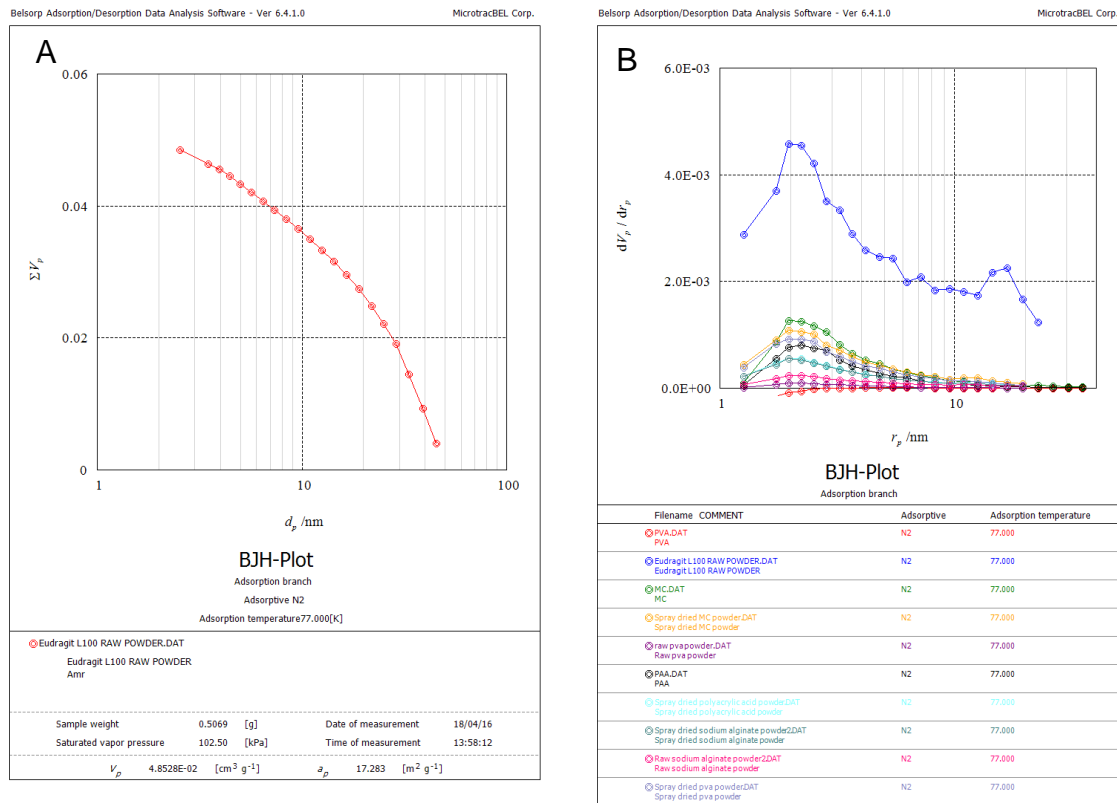


Figure 10.3 A and B BJH- plot from the preliminary studies of the raw and spray dried powder

Polymer	Young's modulus RAV	PAA RAW	Sodium Alg PVA RAW	Eudragit L: MC RAW	T. test	PAA-SALGINATE	PAA-PVA	PAA-Eudr	PAA-MC	
		5.216	8.338	6.374	5.408	14.978	7.32548E-05	0.003058646	0.591803532	9.95E-07
		5.638	8.087	6.557	5.067	14.511				
		5.271	8.471	6.842	5.354	14.726				
Mean		5.375	8.298667	6.591	5.276333	14.73833	0.000641081	4.02775E-05	3.31202E-06	
							PVA-EUD	PVA-MC	MC-EUDR	
							0.00158964	1.83264E-06	6.46049E-07	

Figure 10.4 statistical analysis using t-test (p<0.05) to detect the difference between Young's modulus results of raw powders

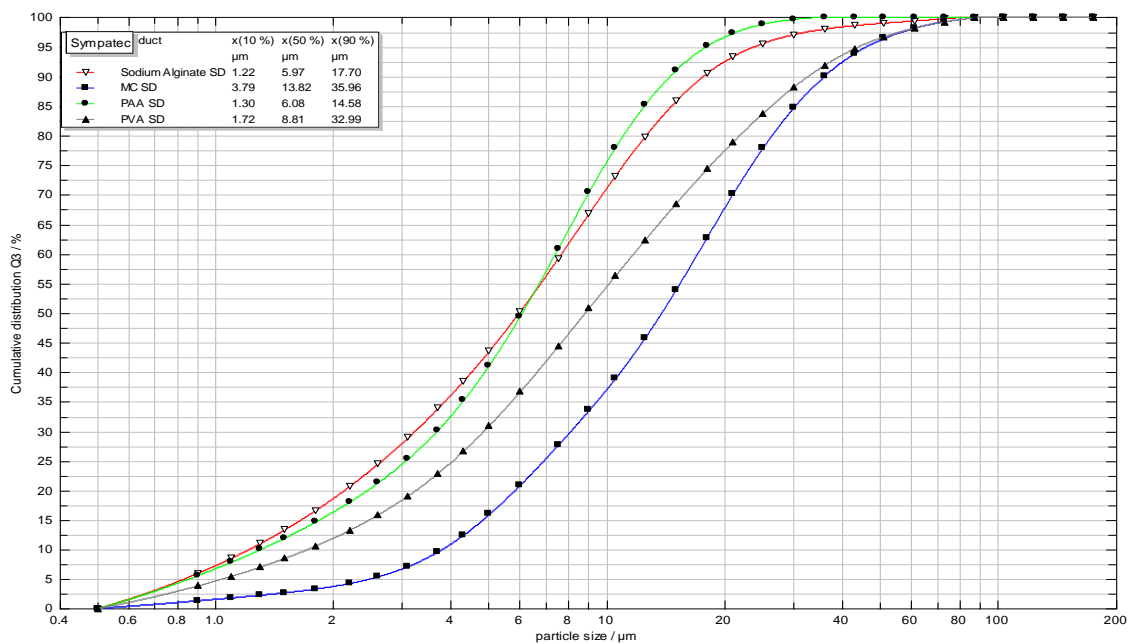


Figure 10.5 one of the particle size results of spray-dried polymers: sodium alginate, PVA, MC, and PAA using Laser diffraction technique showing the cumulative distribution (%) against particle size (μm)

10.2 Appendix chapter 4

Table 10.2 Columns of HPLC used for method development

Specifications			
Product Type	Columns 1	Columns 2	Columns 3
Brand	XTerra	Prodigy™	HyperClone™

Chemistry	C18	C18	C18
Type	Waters	Phenomenex	Phenomenex
Inner Diameter	4.6 mm	4.6 mm	4.6 mm
Length	100 mm	250 mm	150 mm
Particle Size	3.5 µm	5 µm	5 µm
Separation Mode	Reversed Phase	Reversed Phase	Reversed Phase
Pore Size	125 Å (125 x 0.1 nanometre)	150 Å (150 x 0.1 nanometre)	130 Å (130 x 0.1 nanometre)

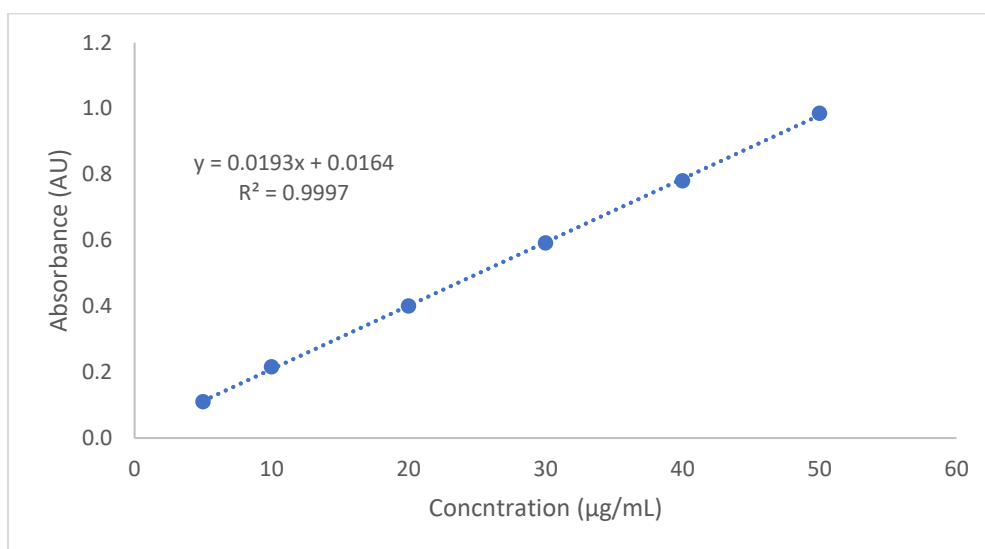


Figure 10.6 PRH UV-vis calibration curve at 291 nm showing good peak linearity 0.9997 and range 5 – 50 µg/mL

Table 10.3 UV-vis accuracy and intra-day precision for PRH (n=6) using wavelength 291 nm

T.C. (µg/mL)	Mean C.C. (µg/mL)	SD	%RSD	%Relative error	%Recovery
16.00	16.15	0.23	1.45	0.96	100.96
20.00	20.25	0.44	2.17	1.23	101.23
30.00	30.06	0.55	1.83	0.19	100.19

Table 10.4 Inter day precision for PRH using UV-vis confirming acceptable wavelength 291 nm showing acceptable rang (n=9)

TC (µg/mL)	Mean N=9	SD	%RSD	%Relative error	%Recover y
16	16.32	0.36	2.19	2.00	102.00
20	20.15	0.35	1.71	0.78	100.78
30	30.18	0.58	1.92	0.60	100.60

Table 10.5 Accuracy and intra-day precision according the HPLC methods for additional quality control 15, 35 and 45 µg/mL (n=3)

T.C µg/mL	C.C Mean± SD µg/mL	%RSD	%Relative error	%Recovery
15	15.1 ± 0.01	0.02	0.72	100.72
35	34.54 ± 0.03	0.09	1.29	98.70
45	43.77 ± 0.03	0.008	2.72	97.27

Table 10.6 Inter-day precision according to proposed HPLC method for quality control 15, 35 and 45 µg/mL for IND (n=9)

T.C µg/mL	Day1	Day2	Day3	C.C Mean ± SD µg/mL	%RSD	%Recovery
15	15.56	15.83	15.46	15.62 ± 0.16	1.07	104.13
35	36.61	34.49	34.75	35.28 ± 1.00	2.83	100.82
45	44.73	44.26	43.91	44.30 ± 0.36	0.81	98.45

Table 10.7 IND method Robustness using 45 µg/mL (n=3) with ± 4 wavelength 248 nm

Sample	TC µg/mL	CC µg/mL	Mean µg/mL	%RSD	%Recovery
252 nm	45	44.03	44.07 ± 0.03	0.07	97.93
		44.10			
		44.07			
244 nm	45	43.30	43.30 ± 0.02	0.03	96.23
		43.30			
		43.32			

Table 10.8 readings of stability for IND HPLC method showing %RSD and %Recovery within the range 80-120% for 100 µg/mL (n=3) as in the peak of Figure 10.7

Area (mAU*S)	C.C	CC (Mean ± SD)	%RSTD	% Recovery
6221.46	106.07	106.36 ± 0.08	0.79	101.15
6271.90	106.93			
6221.46	106.07			

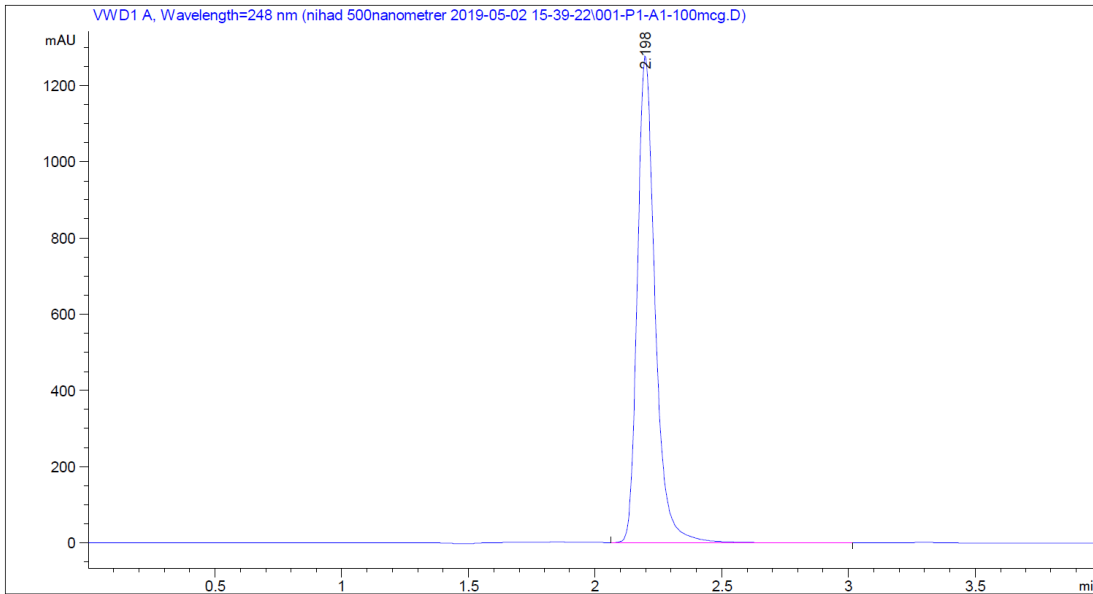


Figure 10.7 IND stability of 100 µg/mL stored at 5 °C – 8 °C for one year from calibration curve points showing method rigidity

Table 10.9 Method suitability and reproducibility using 10 (µg/mL) of the calibration curve points tested on another Agilent HPLC instrument with same conditions and column

Agilent 1 AUC	Agilent 1 C.C (µg/mL)	Agilent 2 AUC	Agilent 2 C.C (µg/mL)	P value	%R SD	%Recovery
225.91	9.44	224.96	9.40	0.66	0.55	94.63
226.23	9.45	227.40	9.50			
228.11	9.53	226.69	9.47			

Table 10.10 Raw data for IND inter day precision and accuracy over three consecutive days (n=9)

Sample	TC (µg/mL)	Day 1 CC (µg/mL)	Day 2 CC (µg/mL)	Day 3 CC (µg/mL)	Mean N=18	%RSD	%Relative error	%Accuracy	%Recovery
Sample A.1	1	0.86	0.87	0.91	0.89±0.02	2.07	10.80	89.20	89.20
Sample A.2		0.88	0.88	0.94					

Sampl e A.3		0.91	0.88	0.91					
Sampl e A.4		0.89	0.88	0.90					
Sampl e A.5		0.89	0.88	0.91					
Sampl e A.6		0.88	0.88	0.91					
Sampl e B.1	3	2.98	2.96	3.05	3.00 ± 0.04	1.17	0.11	99.89	99.89
Sampl e B.2		2.98	2.96	3.04					
Sampl e B.3		2.99	2.98	3.05					
Sampl e B.4		2.98	2.97	3.04					
Sampl e B.5		2.98	2.95	3.03					
Sampl e B.6		2.98	2.97	3.03					
Sampl e C.1	5	4.92	4.87	5.00	4.94 ± 0.05	0.96	1.27	98.73	98.73
Sampl e C.2		4.94	4.92	5.00					
Sampl e C.3		4.94	4.88	4.99					
Sampl e C.4		4.94	4.89	4.98					
Sampl e C.5		4.92	4.87	4.98					
Sampl e C.6		4.94	4.86	5.00					

Table 10.11 Raw data of calibration curve equation for IND showing CC within acceptable range 80-120% according to ICH guidelines

T.C (µg/mL)	Average Area (mAU*S)	C.C (µg/mL)	%RSD	% Recovery
1	55.43	1.17 ± 0.002	0.421	117.32
5	312.00	5.54 ± 0.001	0.073	110.76
10	564.90	9.84 ± 0.03	0.294	98.41
20	1085.34	18.70 ± 0.07	0.359	93.48
30	1713.96	29.39 ± 0.13	0.458	97.97
40	2378.80	40.70 ± 0.13	0.331	101.75
50	2985.37	51.02 ± 0.12	0.236	102.04
100	5843.11	99.64 ± 0.25	0.252	99.64

Table 10.12 Raw data of the calibration curve PRH showing CC within acceptable range 80-120% according to ICH guidelines

T.C µg/mL	Mean Area (mAU*s)	CC Mean ± SD µg/mL	%RSD	%Recovery
1.00	27.24	1.15 ± 0.00	0.12	114.78
5.00	106.95	4.48 ± 0.01	0.00	89.53
10.00	226.75	9.48 ± 0.05	0.00	94.80
20.00	503.01	21.02 ± 0.04	0.06	105.09
30.00	736.85	30.78 ± 0.02	0.00	102.61
40.00	935.94	39.10 ± 0.06	0.00	97.74

Table 10.13 Raw data of Inter day accuracy and precision PRH (n=9)

Sam ple	T.C ($\mu\text{g}/$ mL)	Day 1	Day 2	Day 3	Me an	S D	%R SD	%Rela tive error	%Accur acy	%Reco very
Sam ple A.1	C.C ($\mu\text{g}/$ mL)	C.C ($\mu\text{g}/$ mL)	C.C ($\mu\text{g}/$ mL)							
Sam ple A.2	16	16.2 2	16.1 3	16.0 5	16. 27	0. 37	2.29	1.66	98.34	101.66
Sam ple A.3		16.1 3	16.1 1	16.1 7						
Sam ple A.4		16.1 3	16.1 3	16.2 4						
Sam ple A.5		17.2 0	16.0 0	16.1 9						
Sam ple A.6		17.3 1	16.0 5	16.3 6						
Sam ple B.1		15.9 7	16.1 0	16.3 1						
Sam ple B.2		20	22.0 5	19.5 8						
Sam ple B.3	21.5 9		19.4 5	19.9 2						
Sam ple B.4	20.5 3		19.5 9	19.8 5						

Sam ple B.5		22.2 8	19.5 0	19.7 6						
Sam ple B.6		21.8 5	19.5 3	19.8 9						
Sam ple C.1		20.6 4	19.5 6	19.8 2						
Sam ple C.2	24	25.4 7	23.2 3	23.2 1	24. 01	1. 00	4.17	0.02	99.98	100.02
Sam ple C.3		25.6 3	23.3 2	23.3 8						
Sam ple C.4		26.5 9	23.4 2	23.2 8						
Sam ple C.5		24.5 9	23.5 1	23.3 9						
Sam ple C.6		24.0 0	23.6 4	23.4 5						
		24.8 2	23.8 2	23.3 4						

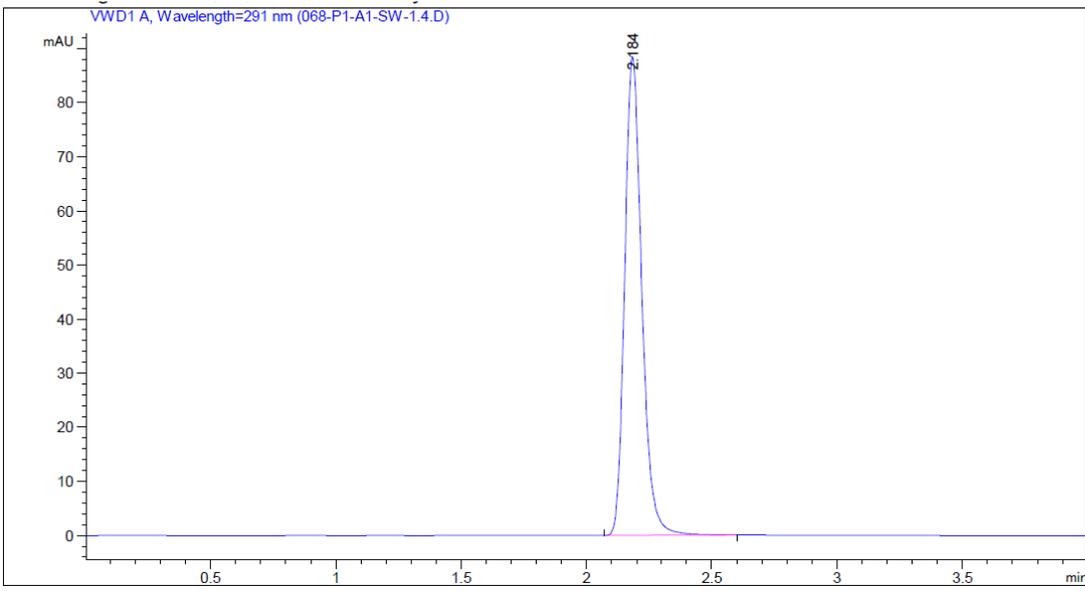


Figure 10.8 PRH HPLC chromatogram 1 µg/mL

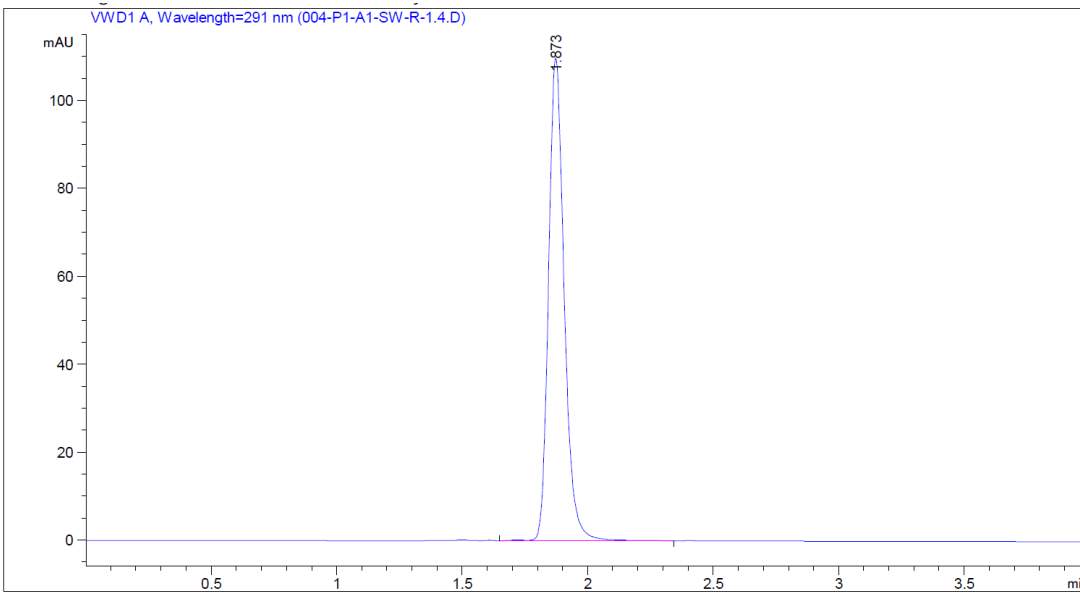


Figure 10.9 Robustness chromatogram of 20 µg/mL PRH showing sharp peak with mobile phase ratio 50:30:20 of acetonitrile, methanol, and buffer respectively

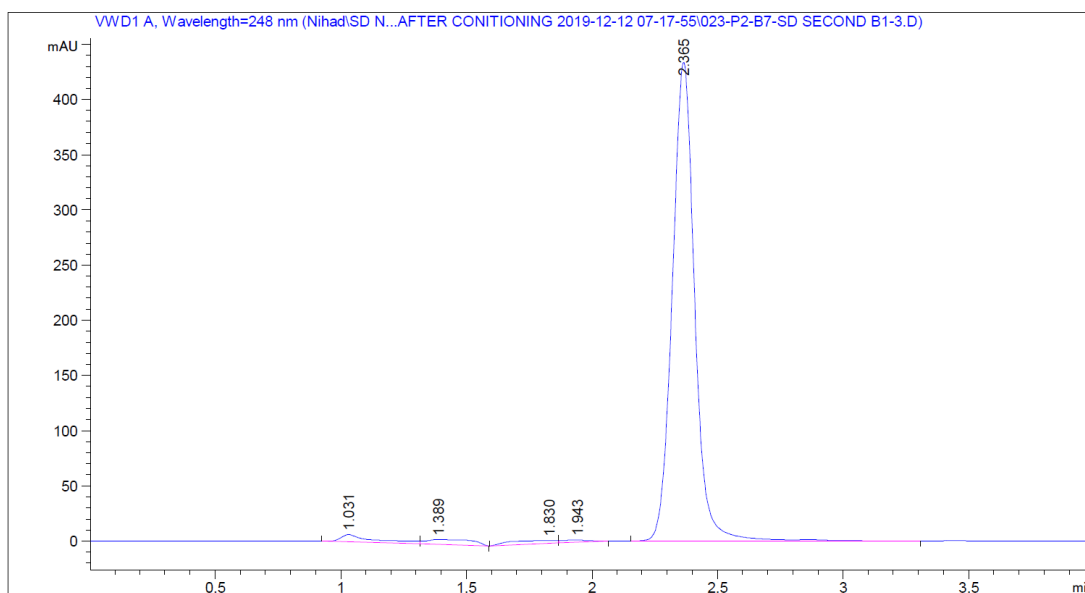


Figure 10.10 Spray dried particles of Eudragit L100 with IND showing the drug release in buffer (pH 6.8) with no interference

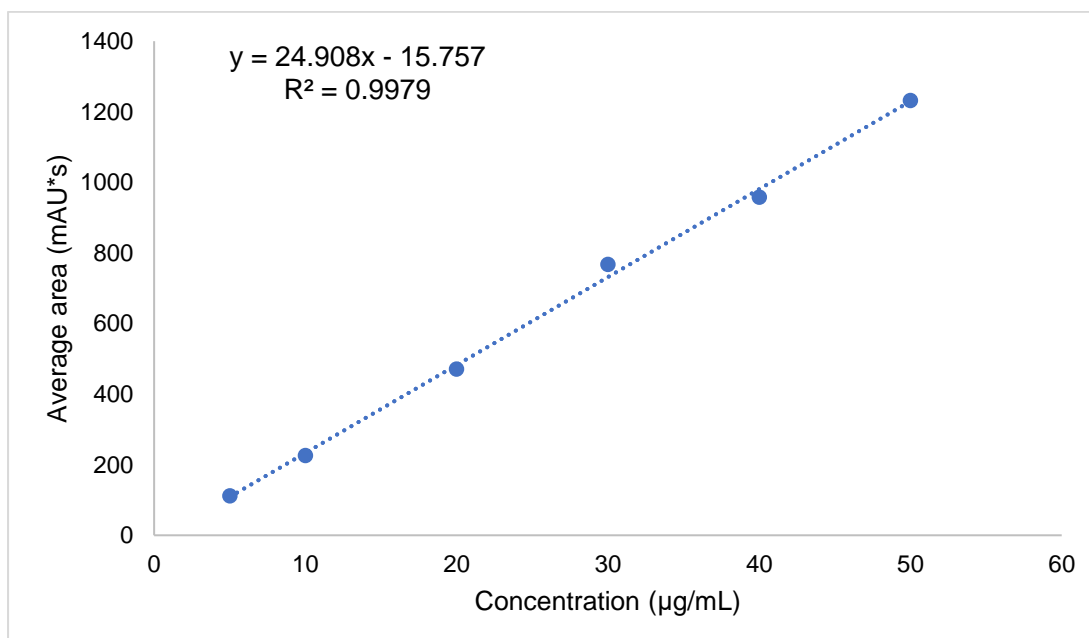


Figure 10.11 Calibration curve concentration and retention time PRH using another Agilent HPLC using same samples of calibration curve contractions with adjusted range 5-50 µg/mL showing high linearity and acceptable absorbance for the 291 nm wavelength

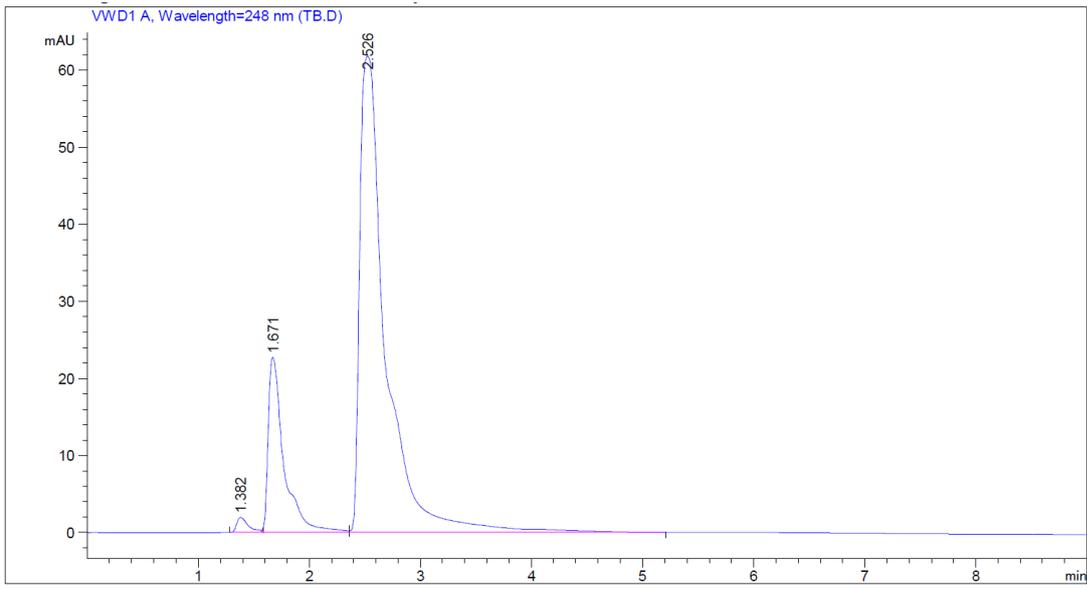


Figure 10.12 One of the trials of HPLC column (1) for IND and unsuitability of detection

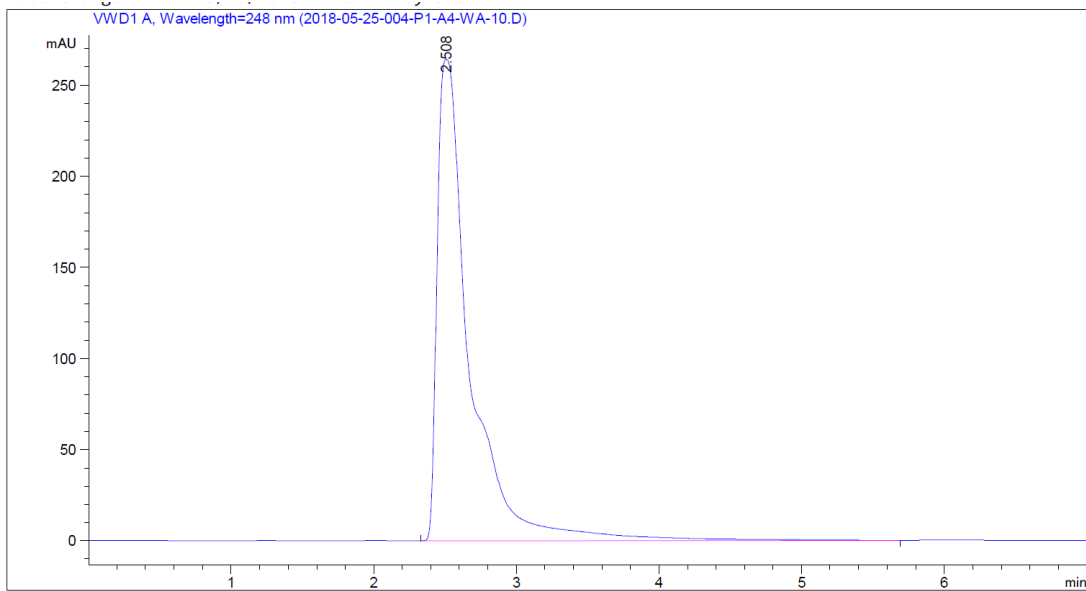


Figure 10.13 Trials of using another C18 column (2) HPLC IND

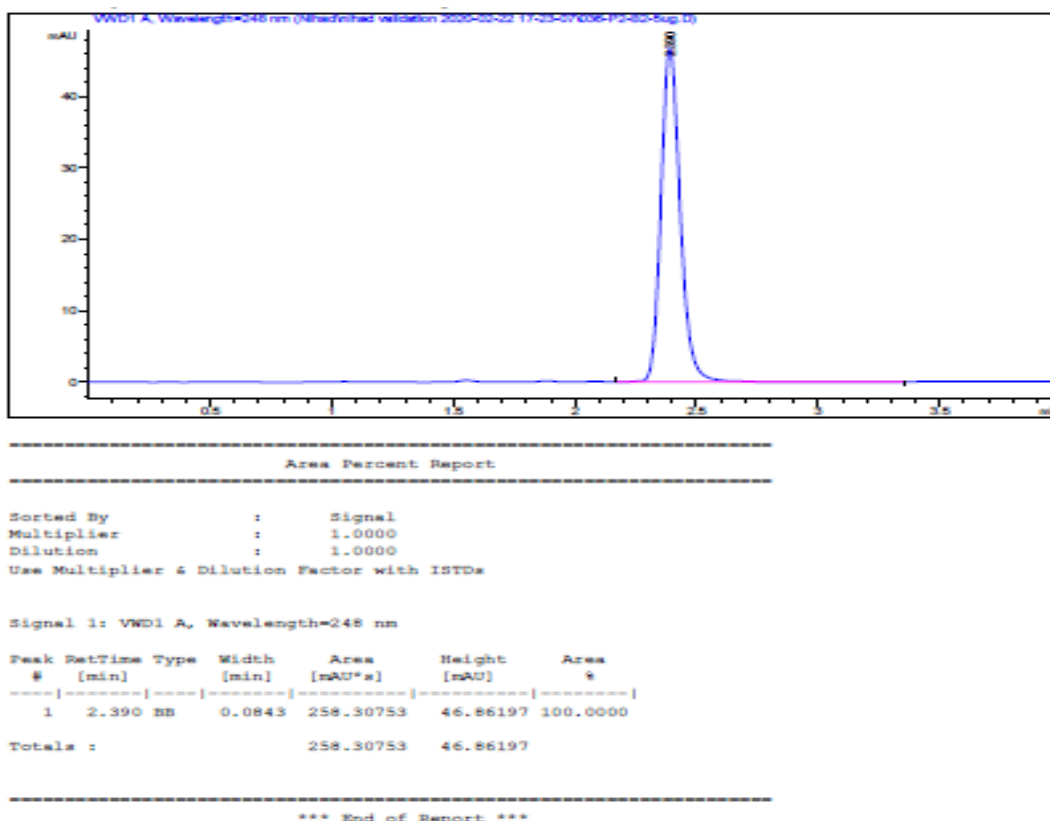


Figure 10.14 One of the calibration curve concentration 5 $\mu\text{g/mL}$ of IND showing peak sharpness and area the run

10.3 Appendix chapter 5

10.3.1 Hot stage microscopy method

This type of microscope was used to detect the polymorphic changes via a video camera and observed events. This technique was correlated with those collected from the DSC. Observations were recorded as captures using eclipse Ni software and camera (Nikon, Japan), with the temperature-controlled stage was used for experiments with 4x and 10x lenses. The heating rate was 10°C per minute. The starting and end temperature was simultaneous with DSC analysis. Before starting the run, a quantity of IND was placed on a slide and placed on the microscopic stage. Small adjustments to the image under a 4000-magnification lens using the filter to enhance the clarity of the observed events.

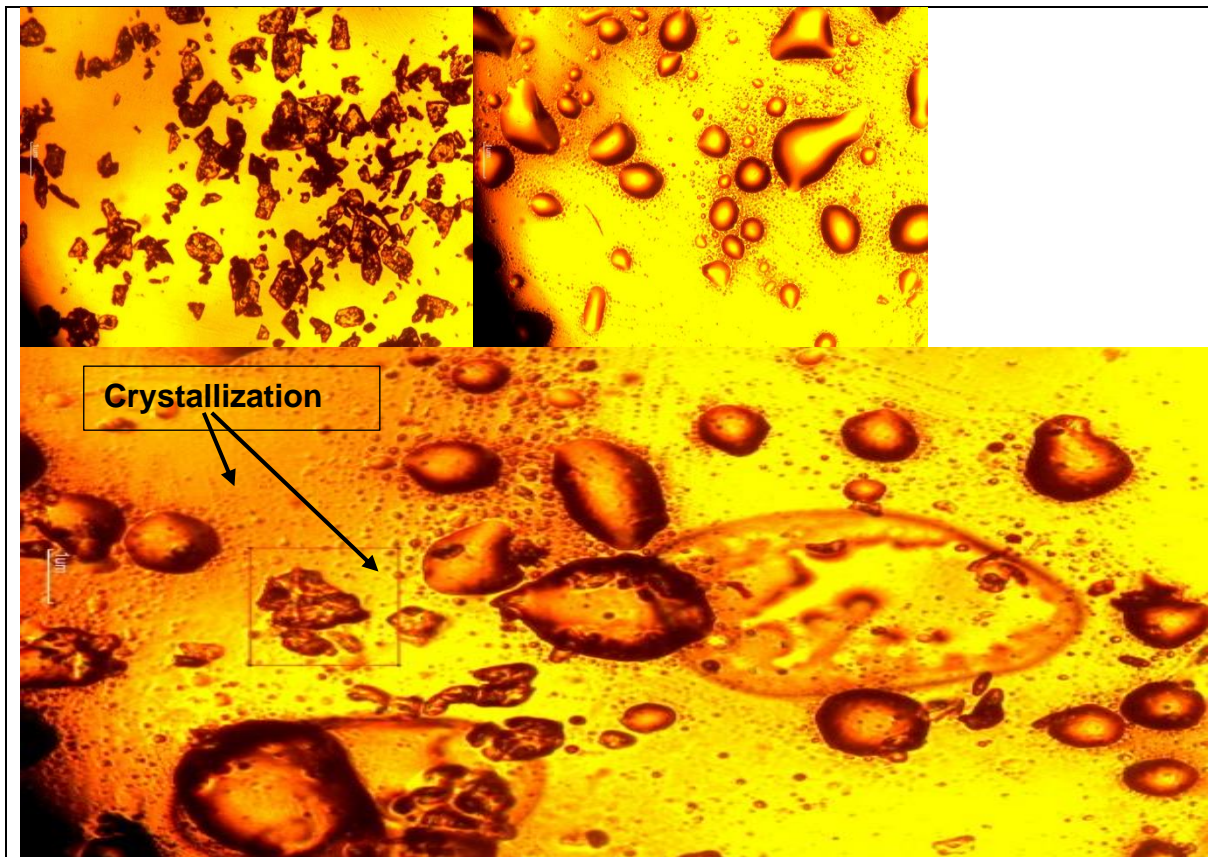


Figure 10.15 Raw IND (a) and melted IND after 165 °C, then slowly cooled melted IND (c) showing start of crystallization at 30°C

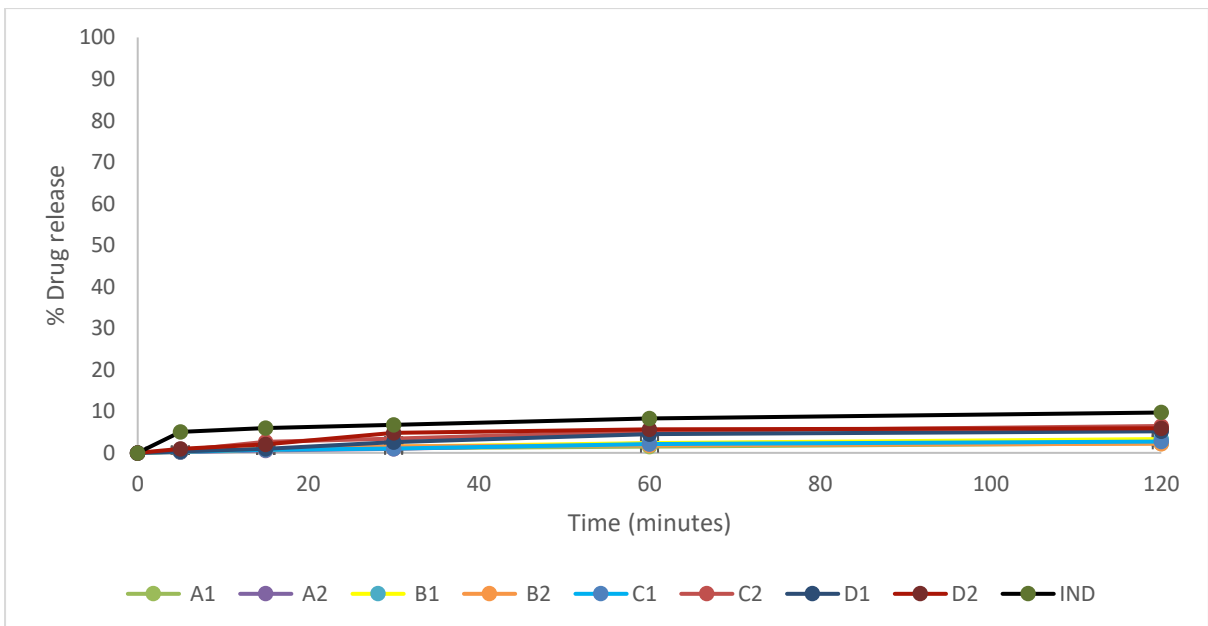


Figure 10.16 IND release from all batches of ODTs with obtained spray dried particles in pH 1.2 media

with 100 bounds in Y axis

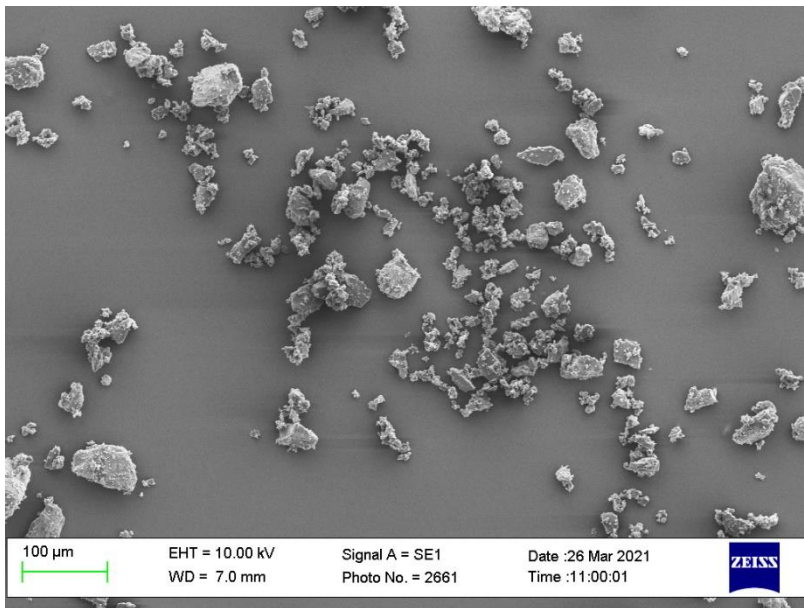


Figure 10.17 Lactose SEM image with low magnification showing a general size of particles

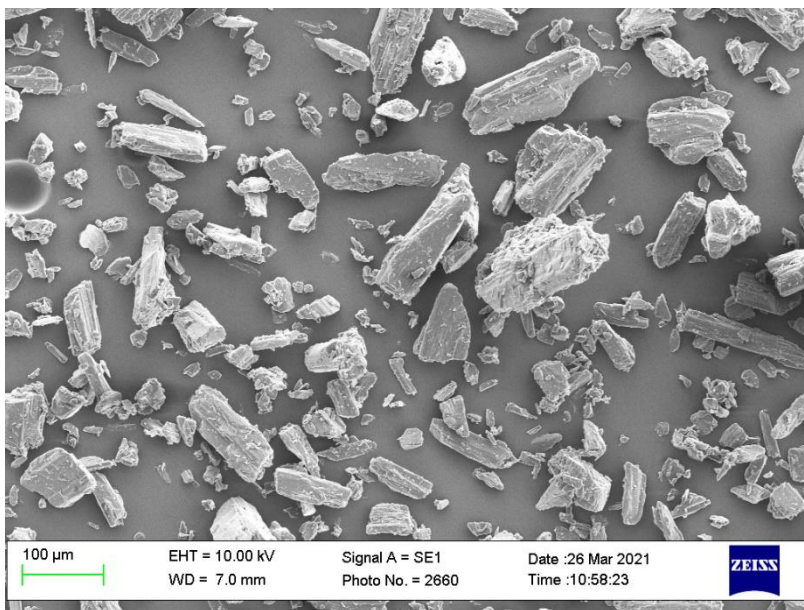


Figure 10.18 Mannitol image of SEM showing the shape and size of the particles

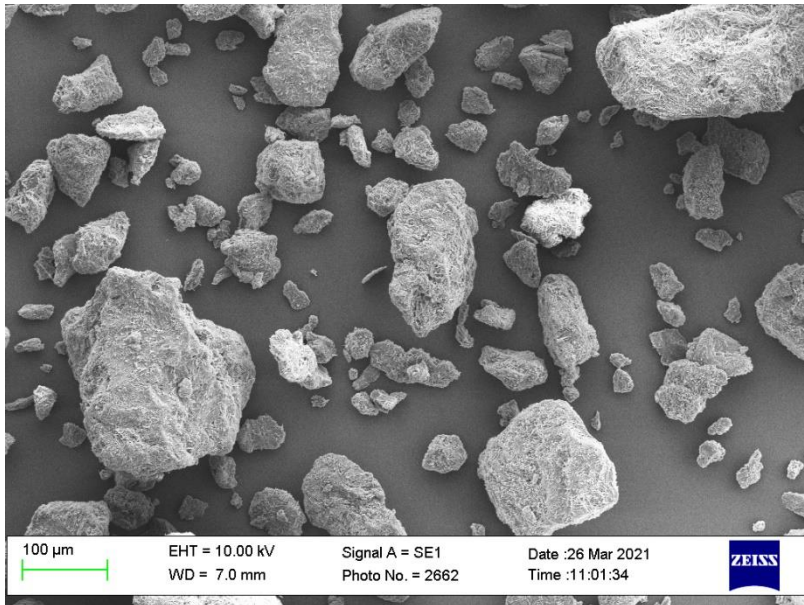


Figure 10.19 Sorbitol SEM image showing shape irregularity and surface roughness

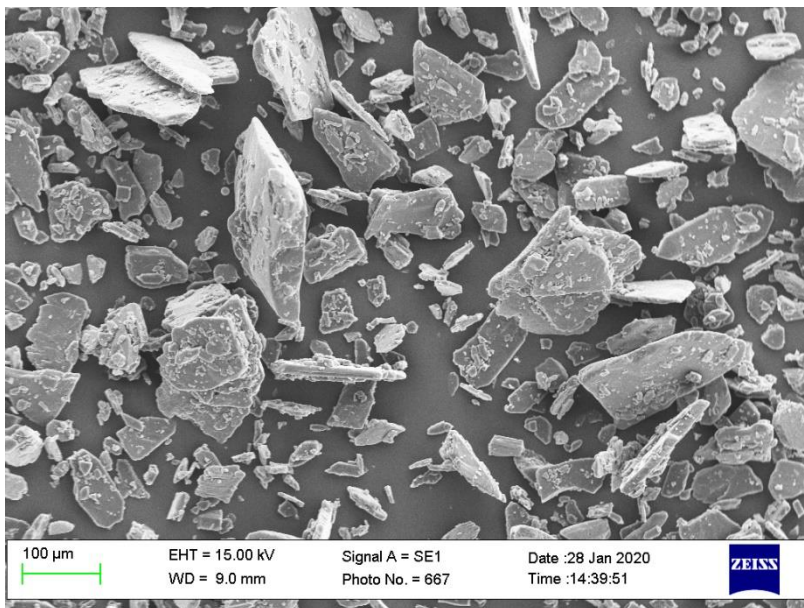


Figure 10.20 IND SEM showing the similarity with mannitol particles

10.4 Appendix chapter 6

Table 10.14 P values obtained from all pellets batches using ANOVA illustrating the significant

differences between the results

Data	p -value for batches (45,63&90)	All P value for two batches (45&90)	P-value for two batches (63&90)	P-value for two batches (45&63)
Hardness	9.47E-11	1.43E-07	1.65E-07	0.66
Tensile strength	2.78E-12	4.66E-08	4.58E-08	0.83
Aspect ratio	4.51E-04	6.65E-04	8.05E-05	0.76
YM	0.03	0.02	0.05	0.56

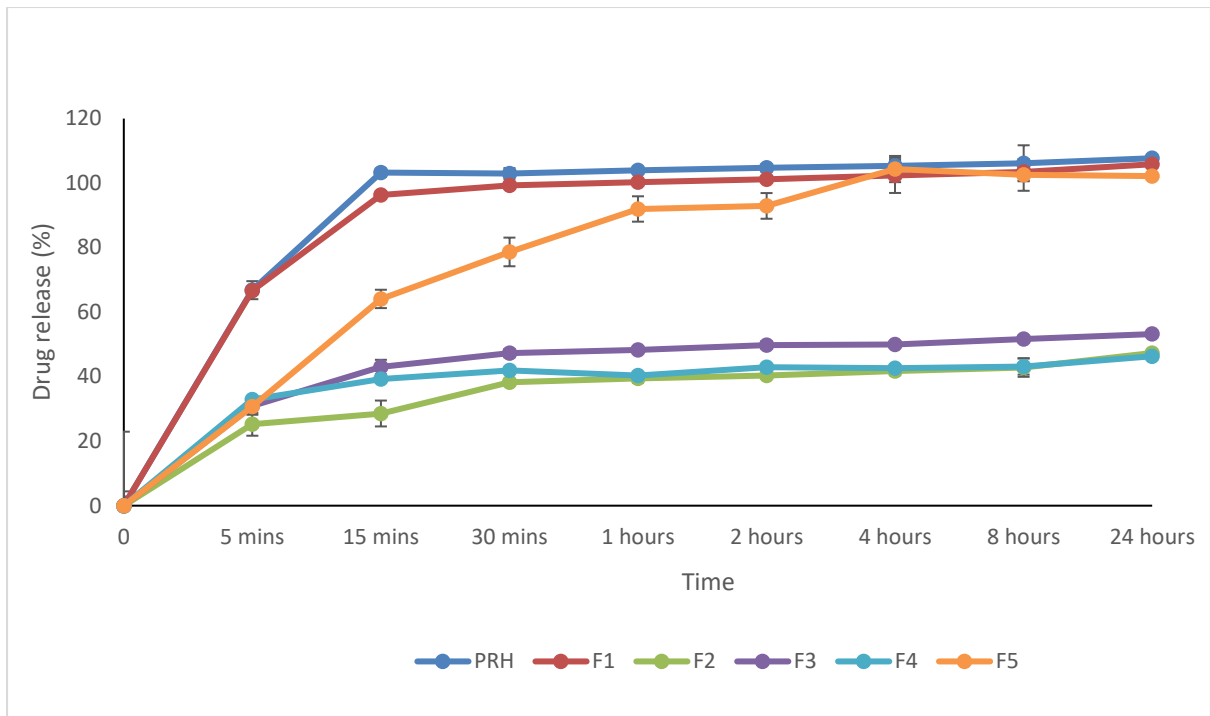


Figure 10.21 PRH release in buffer media pH 6.8 from ODTs of PRH, F1, F2, F3 and F4 for 24 hours

10.5 Appendix chapter 8

10.5.1 Thermography analysis in detail DSC of all batches without PRH

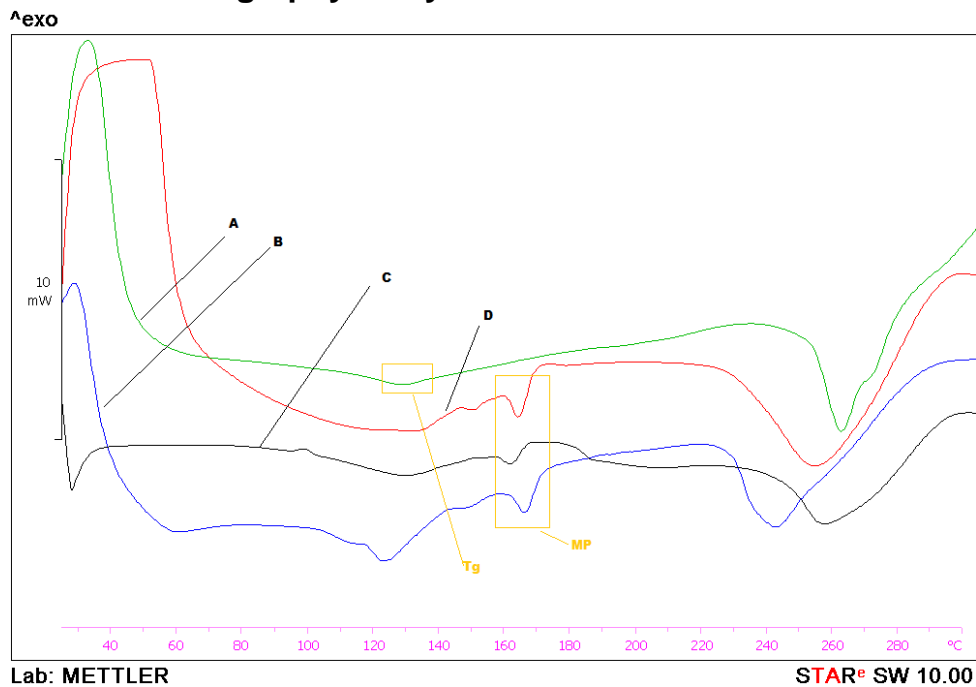


Figure 10.22 DSC thermogram of all batches showing a clear melting point (MP) of PHC in batches 2(B),3(C), 4(D) and missing from the batch1 of MCC only (A) along with a distinct T_g of MCC in all combinations (E)

10.5.2 Simulation trials showing the stages of simulation

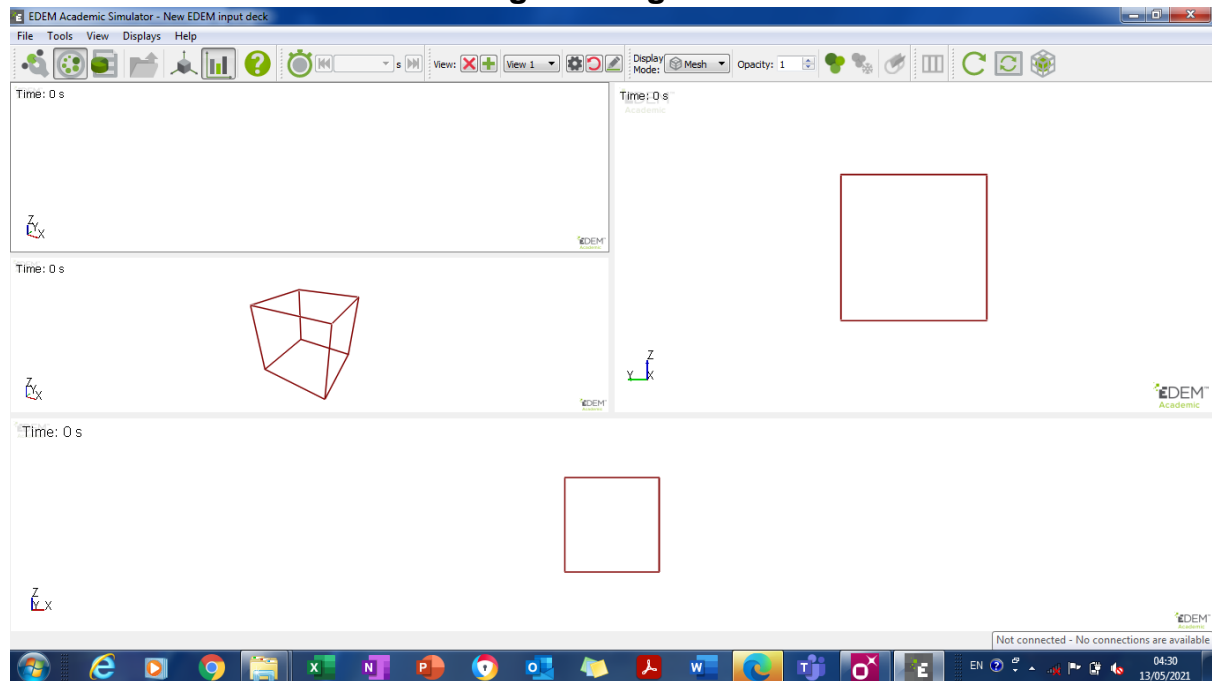


Figure 10.23 Drawing the geometries

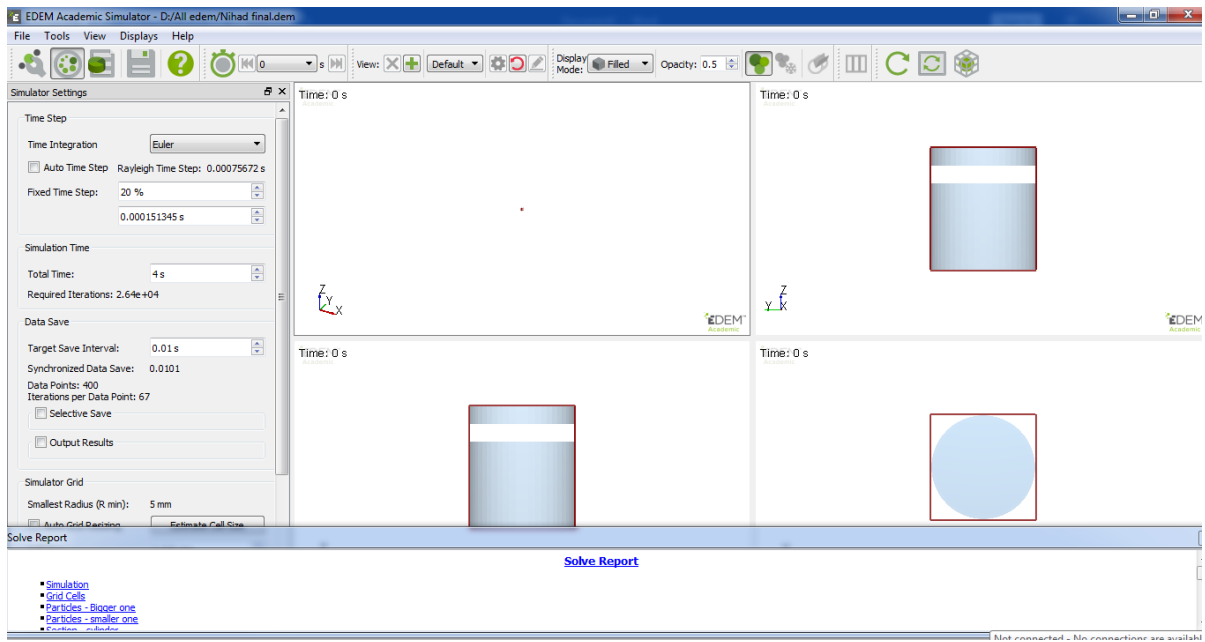


Figure 10.24 Compression simulation

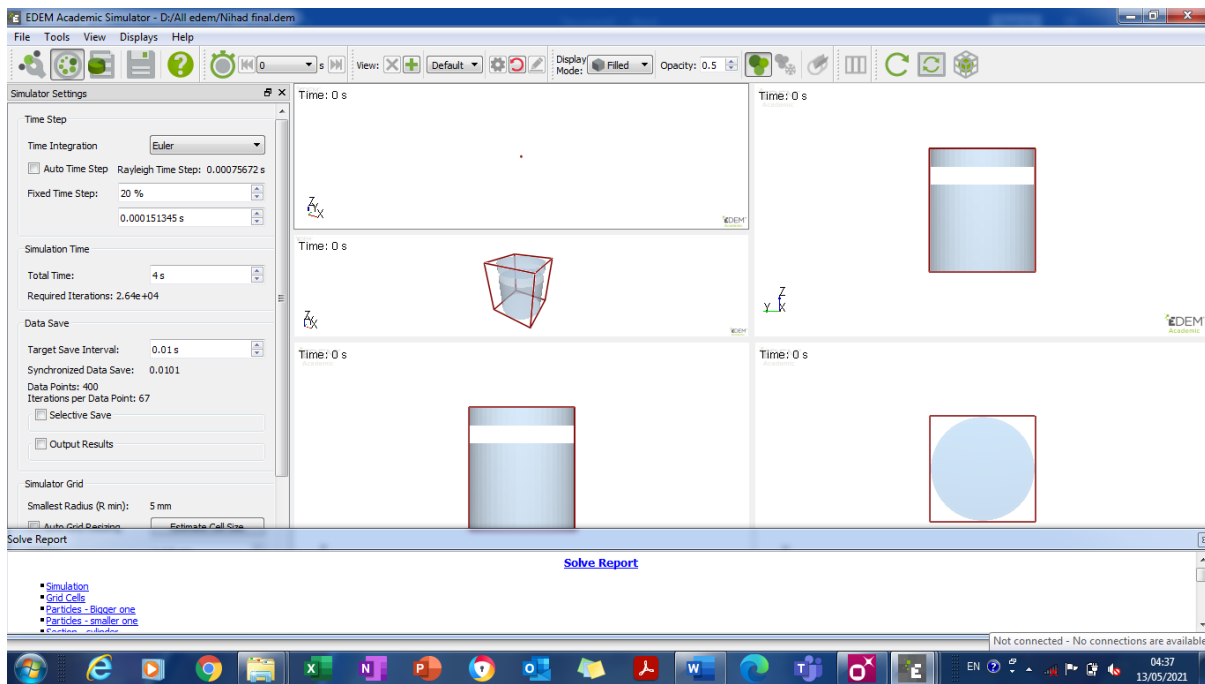


Figure 10.25 Adjusting the cylinders shapes to match the real compression instrument

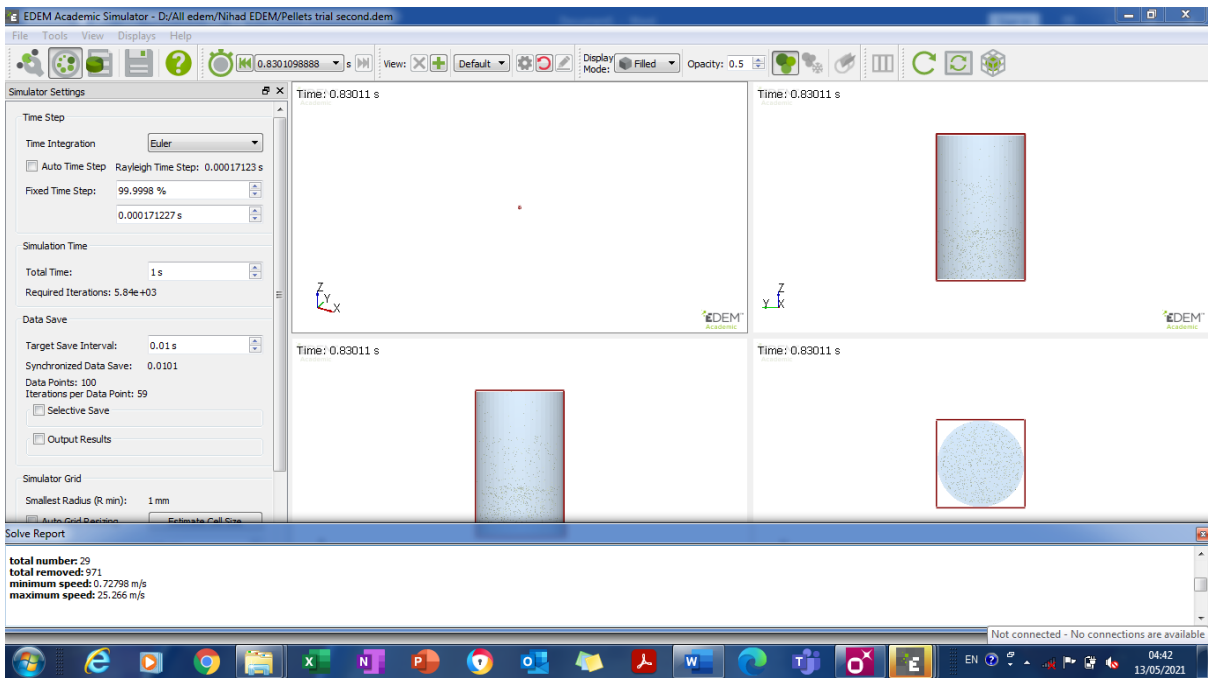


Figure 10.26 Particle's simulation trail without pellets

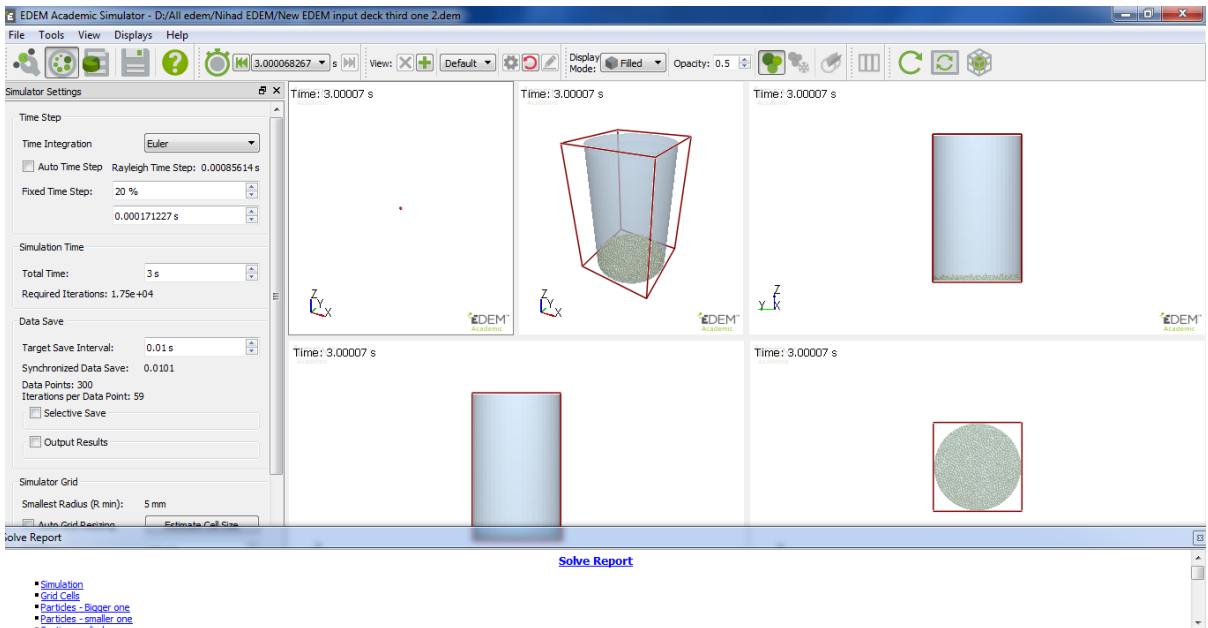


Figure 10.27 The issue with few quantity of particles and small sizes

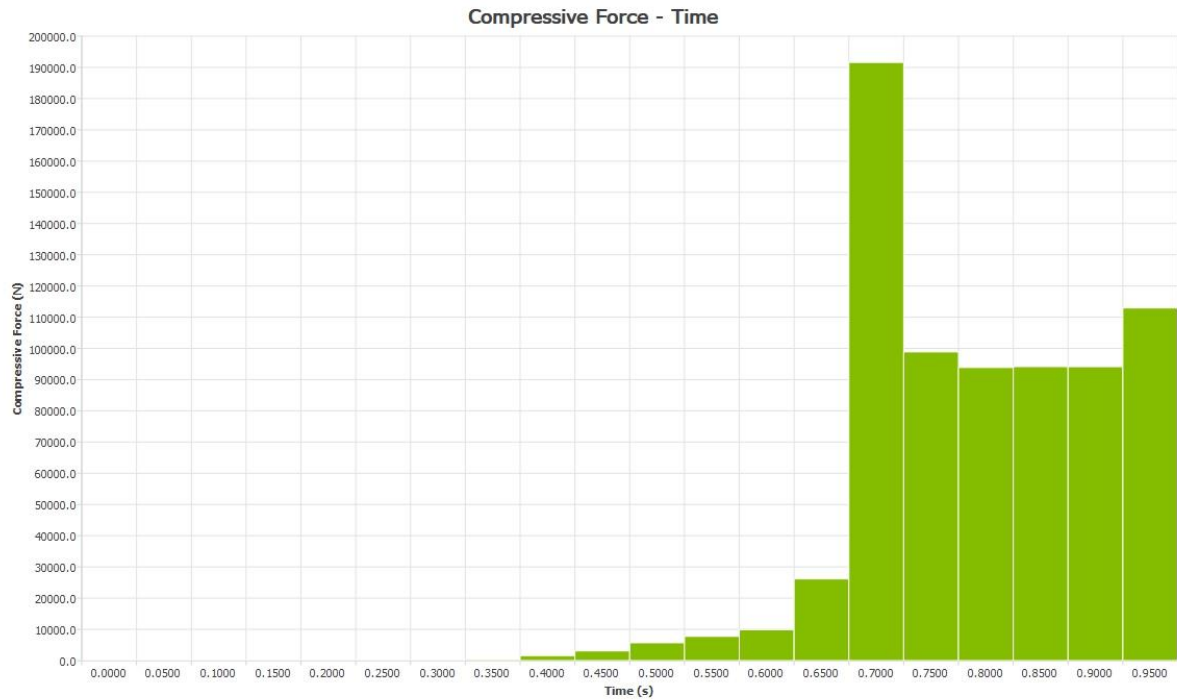


Figure 10.28 The compaction force for compaction fine particles only during the trials

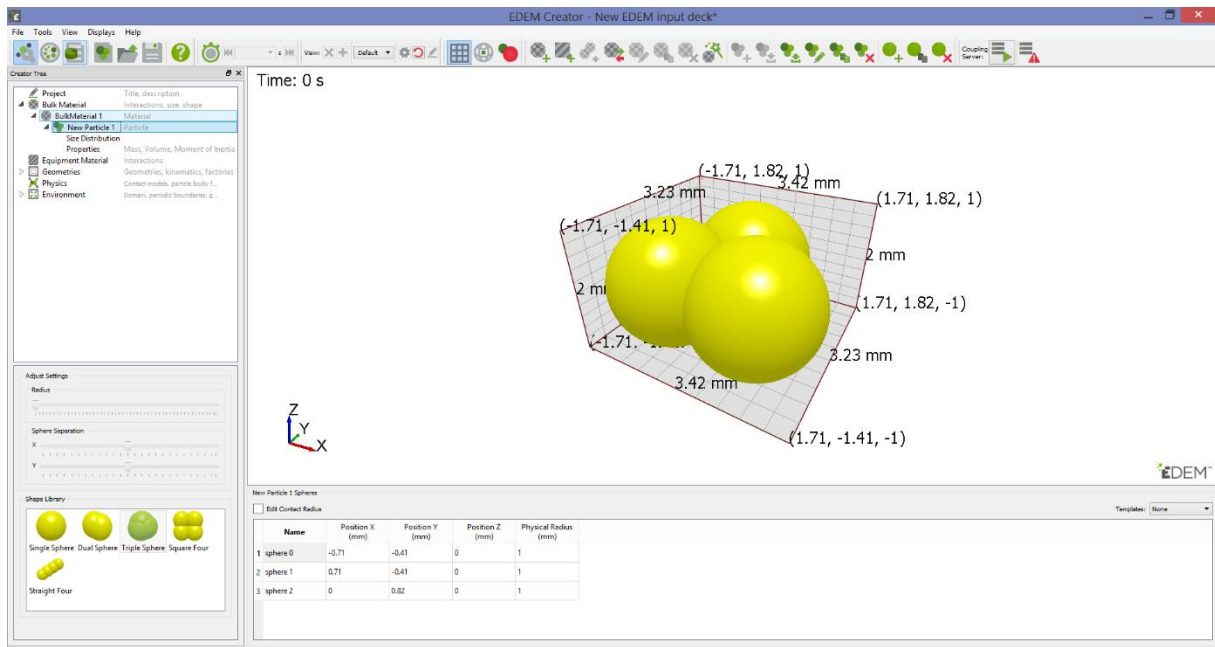


Figure 10.29 Pellet's simulation trial and shape parameters

Chapter 11 References

Abbaspour, M. R., Sadeghi, F. and Afrasiabi Garekani, H. (2007) 'Thermal treating as a tool to produce plastic pellets based on Eudragit RS PO and RL PO aimed for tableting', *European Journal of Pharmaceutics and Biopharmaceutics*, 67(1), pp. 260–267. doi: 10.1016/j.ejpb.2007.01.018.

Abbaspour, M. R., Sadeghi, F. and Afrasiabi Garekani, H. (2008) 'Design and study of ibuprofen disintegrating sustained-release tablets comprising coated pellets', *European Journal of Pharmaceutics and Biopharmaceutics*, 68(3), pp. 747–759. doi: 10.1016/j.ejpb.2007.09.010.

Abbaspour, M. R., Sadeghi, F. and Garekani, H. A. (2005) 'Preparation and characterization of ibuprofen pellets based on Eudragit RS PO and RL PO or their combination', *International Journal of Pharmaceutics*, 303(1–2), pp. 88–94. doi: 10.1016/j.ijpharm.2005.07.016.

Abdel-Hamid, S., Alshihabi, F. and Betz, G. (2011) 'Investigating the effect of particle size and shape on high speed tableting through radial die-wall pressure monitoring', *International Journal of Pharmaceutics*, 413(1), pp. 29–35. doi: <https://doi.org/10.1016/j.ijpharm.2011.04.012>.

Abdelbary, G. *et al.* (2005) 'Determination of the in vitro disintegration profile of rapidly disintegrating tablets and correlation with oral disintegration', *International journal of pharmaceutics*, 292, pp. 29–41. doi: 10.1016/j.ijpharm.2004.08.019.

Abdul, S., Chandewar, A. V. and Jaiswal, S. B. (2010) 'A flexible technology for modified-release drugs: Multiple-unit pellet system (MUPS)', *Journal of Controlled Release*, 147(1), pp. 2–16. doi: 10.1016/j.jconrel.2010.05.014.

Abletshauer, C. B., Schneider, R. and Rupprecht, H. (1993) 'Film coating of pellets with insoluble polymers obtained in situ crosslinking in the fluidized bed', *Journal of Controlled Release*, 27(2), pp. 149–156. doi: [https://doi.org/10.1016/0168-3659\(93\)90218-T](https://doi.org/10.1016/0168-3659(93)90218-T).

Accord (2020) *Propranolol Tablets BP 10mg - Summary of Product Characteristics (SmPC) - (emc), propranolol tablets - Summary of Proud characteristics (SmPC) - (emc)*. Available at: <https://www.medicines.org.uk/emc/medicine/24131#gref> (Accessed: 20 April 2021).

Adam, S. *et al.* (2011) 'An integrated Quality by Design (QbD) approach towards

design space definition of a blending unit operation by Discrete Element Method (DEM) simulation', *European Journal of Pharmaceutical Sciences*, 42(1), pp. 106–115. doi: <https://doi.org/10.1016/j.ejps.2010.10.013>.

AG, E. I. (2020a) *EUDRAGIT® FUNCTIONAL POLYMERS FOR ORAL SOLID DOSAGE FORMS*, *healthcare.evonik.com*. Available at: <https://healthcare.evonik.com/product/health-care/en/products/pharmaceutical-excipients/EUDRAGIT/> (Accessed: 2 July 2020).

AG, E. I. (2020b) *Evonik EUDRAGIT® S 100 Copolymer*, *healthcare.evonik.com*. Available at: https://healthcare.evonik.com/sites/lists/NC/DocumentsHC/Evonik-Eudragit_brochure.pdf (Accessed: 2 July 2020).

Aghbashlo, M. *et al.* (2012) 'Energy and exergy analyses of the spray drying process of fish oil microencapsulation', *Biosystems Engineering*, 111(2), pp. 229–241. doi: 10.1016/j.biosystemseng.2011.12.001.

Agnolin, I. and Roux, J.-N. (2007) 'Internal states of model isotropic granular packings. III. Elastic properties', *Physical Review E*, 76(6), p. 61304. doi: 10.1103/PhysRevE.76.061304.

Aguilar-de-Leyva, Á. *et al.* (2019) 'Study of the critical points in combined matrix tablets containing both inert and swelling excipients', *Journal of Drug Delivery Science and Technology*, 52, pp. 885–894. doi: 10.1016/j.jddst.2019.06.005.

Aher, U., Shelke, T. and Patel, E. (2017) 'Recently used technologies in Pellet Formulation - A Review', *PharmaTutor*, 5(7), pp. 22–30. Available at: <http://www.pharmatutor.org/articles/magazines/articles/july-2017/recently-used-technologiesin-pellet-formulation-a-review> (Accessed: 18 November 2020).

Ahmat, N., Ugail, H. and Castro, G. G. (2011) 'Method of modelling the compaction behaviour of cylindrical pharmaceutical tablets', *International Journal of Pharmaceutics*, 405(1–2), pp. 113–121. doi: 10.1016/j.ijpharm.2010.12.006.

Akhgari, A., Abbaspour, M. and Moradkhanizadeh, M. (2013) 'Combination of pectin and eudargit RS and eudragit RL in the matrix of pellets prepared by extrusion-spheronization for possible colonic delivery of 5-amino salicylic acid', *Jundishapur Journal of Natural Pharmaceutical Products*. 2013/05/04, 8(2), pp. 86–92. doi: 10.5812/jjnpp.8350.

Akhgari, A. and Tavakol, A. (2016) 'Prediction of optimum combination of eudragit RS/eudragit RL/ethyl cellulose polymeric free films based on experimental design for using as a coating system for sustained release theophylline pellets', *Advanced*

Pharmaceutical Bulletin, 6(2), pp. 219–225. doi: 10.15171/apb.2016.030.

Akhter, A. and Kibria, G. (2009) 'Effect of acrylic polymers on physical parameters of spheronized pellets using an aqueous coating system', *Asian Journal of Pharmaceutics*, 3. doi: 10.4103/0973-8398.59953.

Al-Hashimi, N. *et al.* (2018) 'Oral modified release multiple-unit particulate systems: Compressed pellets, microparticles and nanoparticles', *Pharmaceutics*, 10(4). doi: 10.3390/pharmaceutics10040176.

Al-khattawi, A. *et al.* (2014) 'Evidence-based nanoscopic and molecular framework for excipient functionality in compressed orally disintegrating tablets', *PLoS ONE*, 9(7), p. 101369. doi: 10.1371/journal.pone.0101369.

Al-Zoubi, N. *et al.* (2021) 'Spray drying for direct compression of pharmaceuticals', *Processes*. MDPI AG, pp. 1–25. doi: 10.3390/pr9020267.

Alğın Yapar, E. (2014) 'Orally disintegrating tablets: An overview', *Journal of Applied Pharmaceutical Science*, 4(2), pp. 118–125. doi: 10.7324/JAPS.2014.40219.

Allen L.V., J. . b and Ansel, H. C. . (2014) *Ansel's pharmaceutical dosage forms and drug delivery systems: Tenth edition*, *Ansel's Pharmaceutical Dosage Forms and Drug Delivery Systems: Tenth Edition*.

Almaya, A. and Aburub, A. (2008) 'Effect of particle size on compaction of materials with different deformation mechanisms with and without lubricants', *AAPS PharmSciTech*, 9(2), pp. 414–418. doi: 10.1208/s12249-008-9059-3.

Almeida e Sousa, L. *et al.* (2015) 'Assessment of the Amorphous "Solubility" of a Group of Diverse Drugs Using New Experimental and Theoretical Approaches', *Molecular Pharmaceutics*, 12(2), pp. 484–495. doi: 10.1021/mp500571m.

Almeida, H., Amaral, M. H. and Lobão, P. (2012) 'Temperature and pH stimuli-responsive polymers and their applications in controlled and selfregulated drug delivery', *Journal of Applied Pharmaceutical Science*, 2(6), pp. 01–10. doi: 10.7324/JAPS.2012.2609.

Alotaibi, H. F. *et al.* (2019) 'Design of taste masked enteric orodispersible tablets of diclofenac sodium by applying fluid bed coating technology', *Saudi Pharmaceutical Journal*, 27(3), pp. 354–362. doi: <https://doi.org/10.1016/j.jsps.2018.12.003>.

Alyami, H. *et al.* (2017) 'An investigation into the effects of excipient particle size, blending techniques and processing parameters on the homogeneity and content uniformity of a blend containing low-dose model drug', *PloS one*, 12(6), pp. e0178772–e0178772. doi: 10.1371/journal.pone.0178772.

Amador, C. and Martín de Juan, L. (2016) 'Chapter 19 - Strategies for Structured Particulate Systems Design', in Martín, M., Eden, M. R., and Chemmangattuvalappil, N. G. B. T.-C. A. C. E. (eds) *Tools For Chemical Product Design*. Elsevier, pp. 509–579. doi: <https://doi.org/10.1016/B978-0-444-63683-6.00019-8>.

Ambroz, F. *et al.* (2018) 'Evaluation of the BET Theory for the Characterization of Meso and Microporous MOFs', *Small Methods*, 2(11), p. 1800173. doi: <https://doi.org/10.1002/smt.201800173>.

Amidon, G. E. and Houghton, M. E. (1995) 'The Effect of Moisture on the Mechanical and Powder Flow Properties of Microcrystalline Cellulose', *Pharmaceutical Research: An Official Journal of the American Association of Pharmaceutical Scientists*, 12(6), pp. 923–929. doi: 10.1023/A:1016233725612.

Amidon, G. E., Meyer, P. J. and Mudie, D. M. (2017) 'Particle, powder, and compact characterization', in *Developing Solid Oral Dosage Forms: Pharmaceutical Theory and Practice: Second Edition*. Elsevier Inc., pp. 271–293. doi: 10.1016/B978-0-12-802447-8.00010-8.

Amidon, G. E., Seccrest, P. J. and Mudie, D. (2009) 'Chapter 8 - Particle, Powder, and Compact Characterization', in Qiu, Y. *et al.* (eds). San Diego: Academic Press, pp. 163–186. doi: <https://doi.org/10.1016/B978-0-444-53242-8.00008-4>.

Anbalagan, P., Liew, C. V. and Heng, P. W. S. (2017) 'Role of dwell on compact deformation during tableting: an overview', *Journal of Pharmaceutical Investigation*, 47(3), pp. 173–181. doi: 10.1007/s40005-017-0306-z.

Andersson, M. *et al.* (2000) 'Analysis of film coating thickness and surface area of pharmaceutical pellets using fluorescence microscopy and image analysis', *Journal of pharmaceutical and biomedical analysis*, 22, pp. 325–339. doi: 10.1016/S0731-7085(99)00289-7.

Ando, M. *et al.* (2007) 'Evaluation of a novel sugar coating method for moisture protective tablets', *International Journal of Pharmaceutics*, 336(2), pp. 319–328. doi: <https://doi.org/10.1016/j.ijpharm.2006.12.015>.

Ansell, M. P. and Mwaikambo, L. Y. (2009) '2 - The structure of cotton and other plant fibres', in Eichhorn, S. J. *et al.* (eds) *Woodhead Publishing Series in Textiles*. Woodhead Publishing, pp. 62–94. doi: <https://doi.org/10.1533/9781845697310.1.62>.

Anthony Armstrong, N., Patel, A. N. and Jones, T. M. (1988) 'Relationship between porosity and water content of dicalcium phosphate tablets', *International Journal of Pharmaceutics*. doi: 10.1016/0378-5173(88)90261-X.

- Aqil, M. *et al.* (2013) 'A validated RP-HPLC method for simultaneous determination of propranolol and valsartan in bulk drug and gel formulation', *Journal of Pharmacy and Bioallied Sciences*, 5(1), pp. 61–65. doi: 10.4103/0975-7406.106573.
- Arno, E. A. *et al.* (2002) 'Eudragit NE30D Based Metformin/Gliclazide Extended Release Tablets: Formulation, Characterisation and *in Vitro* Release Studies', *Chemical and Pharmaceutical Bulletin*, 50(11), pp. 1495–1498. doi: 10.1248/cpb.50.1495.
- Arora, P. and Sethi, V. A. (2013) 'Orodispersible tablets: A comprehensive review', *International Journal of Research and Development in Pharmacy and Life Sciences*, 2(2), pp. 270–284.
- Arvaniti, E. C. *et al.* (2015) 'Determination of particle size, surface area, and shape of supplementary cementitious materials by different techniques', *Materials and Structures/Materiaux et Constructions*, 48(11), pp. 3687–3701. doi: 10.1617/s11527-014-0431-3.
- Asghar, L. and Chandran, S. (2006) 'Multiparticulate formulation approach to colon specific drug delivery: Current perspectives', *Journal of pharmacy & pharmaceutical sciences : a publication of the Canadian Society for Pharmaceutical Sciences, Société canadienne des sciences pharmaceutiques*, 9, pp. 327–338.
- Ashraf, M. A. *et al.* (2018) 'Effects of Size and Aggregation/Agglomeration of Nanoparticles on the Interfacial/Interphase Properties and Tensile Strength of Polymer Nanocomposites', *Nanoscale Research Letters*, 13(1), p. 214. doi: 10.1186/s11671-018-2624-0.
- Assali, M. *et al.* (2020) 'RP-HPLC Method Development and Validation of Synthesized Codrug in Combination with Indomethacin, Paracetamol, and Famotidine', *International Journal of Analytical Chemistry*. Edited by A. V Herrera-Herrera, 2020, p. 1894907. doi: 10.1155/2020/1894907.
- Atef, E. *et al.* (2012) 'Quantifying Solid-State Mixtures of Crystalline Indomethacin by Raman Spectroscopy Comparison with Thermal Analysis', *ISRN Chromatography*. Edited by R. Nageswara Rao, 2012, p. 892806. doi: 10.5402/2012/892806.
- Aubrey-Medendorp, C., Swadley, M. J. and Li, T. (2008) 'The polymorphism of indomethacin: An analysis by density functional theory calculations', *Pharmaceutical Research*, 25(4), pp. 953–959. doi: 10.1007/s11095-007-9346-9.
- Aulton, M. . and Taylor, K. M. . (2018a) *Aulton's Pharmaceuticals E-Book: The Design and Manufacture of Medicines - Google Books, Elsevier; London, United Kingdom.*

Available at:
<https://books.google.co.uk/books?id=HXfODgAAQBAJ&pg=PA580&lpg=PA580&dq=aulton%27s+Pharmaceutics+coating+is+time+consuming&source=bl&ots=HW0f3nA1nr&sig=ACfU3U1-C5NKHvwF93KdP7BVy-YrQcfr7A&hl=en&sa=X&ved=2ahUKEwiW7-ym7MfqAhWRo3EKHfX4BYsQ6AEwAHoECAoQAQ#v=onep> (Accessed: 12 July 2020).

Aulton, M. . and Taylor, K. M. . (2018b) *Aulton's Pharmaceutics E-Book: The Design and Manufacture of Medicines - Google Books, Elsevier; London, United Kingdom.*

Available at:
https://books.google.co.uk/books?id=SZ43AAAQBAJ&pg=PA473&lpg=PA473&dq=water++increase+the+interparticulates+bonds+of+pellets&source=bl&ots=EK50eYxi-bl&sig=ACfU3U0VTFaIFdEKAhSM_L6FGpgtDNIgdQ&hl=en&sa=X&ved=2ahUKEwjav8Pwy4LqAhUxURUIHak0DBYQ6AEwC3oECA0QAQ#v= (Accessed: 15 June 2020).

Azarmi, S. *et al.* (2002) 'Thermal treating as a tool for sustained release of indomethacin from Eudragit RS and RL matrices', *International Journal of Pharmaceutics*, 246(1), pp. 171–177. doi: [https://doi.org/10.1016/S0378-5173\(02\)00378-2](https://doi.org/10.1016/S0378-5173(02)00378-2).

Babenko, M. *et al.* (2019) '1H NMR quantification of spray dried and spray freeze-dried saccharide carriers in dry powder inhaler formulations', *International Journal of Pharmaceutics*, 564, pp. 318–328. doi: 10.1016/j.ijpharm.2019.03.030.

Badgujar, B. P. and Mundada, A. S. (2011) 'The technologies used for developing orally disintegrating tablets: A review', *Acta Pharmaceutica*, pp. 117–139. doi: 10.2478/v10007-011-0020-8.

Bakalyar, S. R. *et al.* (1997) 'Choosing sample volume to achieve maximum detection sensitivity and resolution with high-performance liquid chromatography columns of 1.0, 2.1 and 4.6 mm I.D.', *Journal of Chromatography A*, 762(1), pp. 167–185. doi: [https://doi.org/10.1016/S0021-9673\(96\)00851-5](https://doi.org/10.1016/S0021-9673(96)00851-5).

van den Ban, S. and Goodwin, D. J. (2017) 'The Impact of Granule Density on Tableting and Pharmaceutical Product Performance', *Pharmaceutical Research*, 34(5), pp. 1002–1011. doi: 10.1007/s11095-017-2115-5.

Bandari, Suresh, Rajendar Kumar Mittapalli, and R. G. (2008) 'Orodispersible tablets: An overview', *Asian Journal of Pharmaceutics*, 2(1). doi: 10.22377/AJP.V2I1.159.

- Bankars, K. *et al.* (2014) 'A review on orodispersible tablets prepared using spray dried sustained release microparticles', *JADD*, 1(2), pp. 82–95.
- Bansal, A. K., Balwani, G. and Sheokand, S. (2019) 'Chapter 12 - Critical Material Attributes in Wet Granulation', in Narang, A. S. and Badawy, S. I. F. B. T.-H. of P. W. G. (eds). Academic Press, pp. 421–453. doi: <https://doi.org/10.1016/B978-0-12-810460-6.00009-9>.
- Bansode, S. *et al.* (2010) 'MICROENCAPSULATION: A REVIEW', *International journal of pharmaceutical sciences review and research*, 1(2), pp. 38–43. Available at: www.globalresearchonline.net (Accessed: 6 May 2021).
- Baran, O., Han, K. and Aglave, R. (2016) 'Dem Simulation of the Mixture of Dry and Wet Particles inside Rotary Mixer', in *Proceedings of the 2016 AIChE Annual Meeting, San Francisco, CA, USA*.
- Barboza, F. *et al.* (2009) 'Differential scanning calorimetry as a screening technique in compatibility studies of acyclovir extended release formulations', *Pharmaceutical Chemistry Journal*, 43, pp. 363–368. doi: 10.1007/s11094-009-0304-1.
- Bardestani, R., Patience, G. S. and Kaliaguine, S. (2019) 'Experimental methods in chemical engineering: specific surface area and pore size distribution measurements—BET, BJH, and DFT', *The Canadian Journal of Chemical Engineering*, 97(11), pp. 2781–2791. doi: <https://doi.org/10.1002/cjce.23632>.
- Barjat, H. *et al.* (2021) 'Demonstration of the Feasibility of Predicting the Flow of Pharmaceutically Relevant Powders from Particle and Bulk Physical Properties', *Journal of Pharmaceutical Innovation*, 16(1), pp. 181–196. doi: 10.1007/s12247-020-09433-5.
- Baroutaji, A. *et al.* (2017) 'Mechanics and Computational Modeling of Pharmaceutical Tableting Process', in *Reference Module in Materials Science and Materials Engineering*. Elsevier. doi: 10.1016/b978-0-12-803581-8.09269-9.
- Barwick, V. J. (1999) 'Sources of uncertainty in gas chromatography and high-performance liquid chromatography', *Journal of Chromatography A*, pp. 13–33. doi: 10.1016/S0021-9673(99)00537-3.
- Bassam, F. *et al.* (1990) 'Young's modulus of powders used as pharmaceutical excipients', *International Journal of Pharmaceutics*, 64(1), pp. 55–60. doi: [https://doi.org/10.1016/0378-5173\(90\)90178-7](https://doi.org/10.1016/0378-5173(90)90178-7).
- Bassam, F. *et al.* (1990) 'Young's modulus of powders used as pharmaceutical excipients', *International Journal of Pharmaceutics*, 64(1), pp. 55–60. doi: 10.1016/0378-5173(90)90178-7.

10.1016/0378-5173(90)90178-7.

Beckert, T. E., Lehmann, K. and Schmidt, P. C. (1998) 'Compression of enteric-coated pellets to disintegrating tablets: Uniformity of dosage units', *Powder Technology*, 96(3), pp. 248–254. doi: 10.1016/S0032-5910(97)03380-9.

Beretzky, Á. *et al.* (2002) 'Pelletization of needle-shaped phenylbutazone crystals', *Journal of Thermal Analysis and Calorimetry - J THERM ANAL CALORIM*, 69, pp. 529–539. doi: 10.1023/A:1019959722975.

Berggren, J., Frenning, G. and Alderborn, G. (2004) 'Compression behaviour and tablet-forming ability of spray-dried amorphous composite particles', *European Journal of Pharmaceutical Sciences*, 22(2), pp. 191–200. doi: <https://doi.org/10.1016/j.ejps.2004.03.008>.

Betancourt, J. and Gottlieb, S. (2018) *Liquid Chromatography - Chemistry LibreTexts, LibreTexts Chemistry*. Available at: https://chem.libretexts.org/Courses/Northeastern_University/12%3A_Chromatographic_and_Electrophoretic_Methods/12.5%3A_High-Performance_Liquid_Chromatography (Accessed: 17 July 2020).

Bhairy, S. *et al.* (2015) 'Pellets and Pelletization as Multiparticulate Drug Delivery Systems (MPDDS): A Conventional and Novel Approach', *International Journal of Institutional Pharmacy and Life Sciences*, 5, pp. 79–126.

Bhairy Srinivas (2015) 'Pellets and pelletization as multiparticulate drug delivery systems (mpdds): a conventional and novel approach', *International journal of institutional pharmacy and life sciences*, 5(August), pp. 79–126. Available at: https://www.researchgate.net/publication/304785086_Pellets_and_Pelletization_as_Multiparticulate_Drug_Delivery_Systems_MPDDS_A_Conventional_and_Novel_Approach (Accessed: 21 March 2020).

Bialleck, S. and Rein, H. (2011) 'Preparation of starch-based pellets by hot-melt extrusion', *European Journal of Pharmaceutics and Biopharmaceutics*, 79(2), pp. 440–448. doi: <https://doi.org/10.1016/j.ejpb.2011.04.007>.

Blasi, P. *et al.* (2005) 'Plasticizing effect of water on poly(lactide-co-glycolide)', *Journal of Controlled Release*, 108(1), pp. 1–9. doi: 10.1016/j.jconrel.2005.07.009.

Bley, O., Siepmann, J. and Bodmeier, R. (2009) 'Importance of glassy-to-rubbery state transitions in moisture-protective polymer coatings', *European Journal of Pharmaceutics and Biopharmaceutics*, 73(1), pp. 146–153. doi: <https://doi.org/10.1016/j.ejpb.2009.05.001>.

- Bodagala, V., Jayaveera, K. N. and Ambati, S. (2016) 'Design and Evaluation of Novel High-load Mesalamine Multi-particulate Formulations for Colon-targeted Controlled Drug Delivery', *Journal of Comprehensive Pharmacy*, 03, pp. 209–219. doi: 10.37483/JCP.2016.3605.
- Bodhmage, A. (2006) 'Correlation between physical properties and flowability indicators for fine powders', *University of Saskatchewan*, (July), pp. 1–122. Available at: <http://www.collectionscanada.gc.ca/obj/s4/f2/dsk3/SSU/TC-SSU-07032006115722.pdf> (Accessed: 15 March 2021).
- Bodmeier, R. (1997) 'Tableting of coated pellets', *European Journal of Pharmaceutics and Biopharmaceutics*, 43(1), pp. 1–8. doi: [https://doi.org/10.1016/S0939-6411\(96\)00028-8](https://doi.org/10.1016/S0939-6411(96)00028-8).
- Böhmer, M. R. *et al.* (2006) 'Preparation of monodisperse polymer particles and capsules by ink-jet printing', *Colloids and Surfaces A: Physicochemical and Engineering Aspects*, 289(1–3), pp. 96–104. doi: 10.1016/j.colsurfa.2006.04.011.
- Boikov, A. V, Savelev, R. V and Payor, V. A. (2018) 'DEM Calibration Approach: Design of experiment', in *Journal of Physics: Conference Series*. Institute of Physics Publishing, p. 32017. doi: 10.1088/1742-6596/1015/3/032017.
- Bolis, V. (2013) 'Fundamentals in Adsorption at the Solid-Gas Interface. Concepts and Thermodynamics', in, pp. 3–50. doi: 10.1007/978-3-642-11954-5_1.
- Bolourchian, N. and Dadashzadeh, S. (2008) 'PH-independent release of propranolol hydrochloride from HPMC-based matrices using organic acids', *Daru*, 16, pp. 136–142.
- Boon, V., Glass, B. and Nimmo, A. (2006) 'High-Performance Liquid Chromatographic Assay of Indomethacin in Porcine Plasma with Applicability to Human Levels', *Journal of Chromatographic Science*, 44(1), pp. 41–44. doi: 10.1093/chromsci/44.1.41.
- Börner, M. *et al.* (2016) 'Impact of impeller design on high-shear wet granulation', *Powder Technology*, 295, pp. 261–271. doi: <https://doi.org/10.1016/j.powtec.2016.03.023>.
- Bornhöft, M., Thommes, M. and Kleinebudde, P. (2005) 'Preliminary assessment of carrageenan as excipient for extrusion/ spheronisation', *European Journal of Pharmaceutics and Biopharmaceutics*, 59(1), pp. 127–131. doi: 10.1016/j.ejpb.2004.05.007.
- Bp, D. *et al.* (2005) 'Safety data sheet Safety data sheet', *Carbon*, 1173(i), pp. 1–8. Available at:

https://www.pharmacopoeia.com/Catalogue/Preview?uri=%2Fcontent%2Ffile%2Fproducts%2Fhealthandsafety%2FCat-1196_GB.pdf (Accessed: 16 March 2020).

Brady, J. *et al.* (2017) 'Chapter 7 - Polymer Properties and Characterization', in Qiu, Y. *et al.* (eds). Boston: Academic Press, pp. 181–223. doi: <https://doi.org/10.1016/B978-0-12-802447-8.00007-8>.

Braia, M. *et al.* (2012) 'Analysis of the interactions between Eudragit® L100 and porcine pancreatic trypsin by calorimetric techniques', *International Journal of Biological Macromolecules*, 50(1), pp. 180–186. doi: <https://doi.org/10.1016/j.ijbiomac.2011.10.016>.

Brika, S. E. *et al.* (2020) 'Influence of particle morphology and size distribution on the powder flowability and laser powder bed fusion manufacturability of Ti-6Al-4V alloy', *Additive Manufacturing*, 31, p. 100929. doi: <https://doi.org/10.1016/j.addma.2019.100929>.

British Heart Foundation (2020) *Beta blockers - how do they work - side effects - types / BHF*. Available at: <https://www.bhf.org.uk/information-support/heart-matters-magazine/medical/drug-cabinet/beta-blockers> (Accessed: 16 July 2020).

British Pharmacopoeia (2017) 'Consultation Dissolution testing in BP finished products monographs for solid oral dosage forms', *British Pharmacopoeia*. Available at: <https://www.pharmacopoeia.com/content/file/Consultation-Dissolution-testing.pdf> (Accessed: 21 February 2021).

British Pharmacopoeia (2020) *Reference Standards Catalogue - British Pharmacopoeia*. Available at: <https://www.pharmacopoeia.com/Catalogue/ProductDetails?productid=1000022099&page=1&pageSize=20&searchText=propranolol&startsWith=> (Accessed: 8 March 2020).

Bruschi, L. *et al.* (2018) 'Adsorption on alumina nanopores with conical shape', *Nanoscale*, 10(38), pp. 18300–18305. doi: 10.1039/c8nr06265j.

Büchi (2002) *Training Papers Spray Drying, Order code 97758*,.

Büchi (2020) 'B-290 Mini Spray Dryer Operation Manual', *Büchi*, pp. 1–82. Available at: https://static1.buchi.com/sites/default/files/downloads/B-290_OM_en_I_0.pdf?b0ba59e782a99211b159d5a83189e1e223038cbe (Accessed: 19 June 2021).

BÜCHI Labortechnik AG (2016) 'Mini Spray Dryer B-290: Technical data sheet', 49, pp. 1–9. Available at: [http://static1.buchi.com/sites/default/files/downloads/B-](http://static1.buchi.com/sites/default/files/downloads/B-399)

290_Data_Sheet_en_D.pdf?83b925aae302a8e76f002d1ce679fa06904d1039

(Accessed: 23 March 2021).

Bürki, K. E. (2016) *Preparation of taste masked orally disintegrating tablets by compression of coated pellets*.

Busignies, V. *et al.* (2011) 'Changes in the specific surface area of tablets composed of pharmaceutical materials with various deformation behaviors', *Drug Development and Industrial Pharmacy*, 37(2), pp. 225–233. doi: 10.3109/03639045.2010.504925.

C. Salas-Bringas¹ *et al.* (2007) 'Measuring physical quality of pelleted feed by texture profile analysis, a new pellet tester and comparisons to other common measurement devices', *Annual Transactions - The Nordic Rheology Society*, 15, pp. 149–157.

Available at:
https://nordicrheologysociety.org/Content/Transactions/2007/Fundamental_research_and_industrial_applications/Salas-Bringas_Measuring_physical_quality_of_pelleted_feed.pdf (Accessed: 25 October 2020).

Cabane, E. *et al.* (2012) 'Stimuli-responsive polymers and their applications in nanomedicine', *Biointerphases*, 7(1–4), pp. 1–27. doi: 10.1007/s13758-011-0009-3.

Cabiscol, R. *et al.* (2018) 'Characterization of Mechanical Property Distributions on Tablet Surfaces', *Pharmaceutics*, 10(4), p. 184. doi: 10.3390/pharmaceutics10040184.

Calatayud-Pascual, M. A. *et al.* (2018) 'Influence of chemical enhancers and iontophoresis on the in vitro transdermal permeation of propranolol: Evaluation by dermatopharmacokinetics', *Pharmaceutics*, 10(4), p. 265. doi: 10.3390/pharmaceutics10040265.

Callard Preedy, E. and Prokopovich, P (2013) '4 - Novel coatings and biotechnology trends in inhaler devices', in Prokopovich, Polina (ed.) *Inhaler Devices*. Woodhead Publishing (Woodhead Publishing Series in Biomaterials), pp. 37–50. doi: <https://doi.org/10.1533/9780857098696.1.37>.

Carnavas, P. C. and Page, N. (1998) 'Elastic Properties of Compacted Metal Powders', *Journal of Materials Science*, 33, pp. 4647–4655. doi: 10.1023/A:1004445527430.

Carvajal, T., Chamorthy, S. P. and Pinal, R. (2006) 'Moisture Induced Antiplasticization of Microcrystalline Cellulose', in. Purdue University, Industrial and Physical Pharmacy, 575 Stadium Mall Dr. doi: 10.1051/iufost:20060236.

Cerchiara, T. *et al.* (2011) 'Eudragit-coated albumin nanospheres carrying inclusion

complexes for oral administration of indomethacin', *Journal of Inclusion Phenomena and Macrocyclic Chemistry*, 71(1–2), pp. 129–136. doi: 10.1007/s10847-010-9916-z.

Cespi, M. *et al.* (2007) 'Stress relaxation test for the characterization of the viscoelasticity of pellets', *European Journal of Pharmaceutics and Biopharmaceutics*, 67(2), pp. 476–484. doi: 10.1016/j.ejpb.2007.03.013.

Cetin, M., Atila, A. and Kadioglu, Y. (2010) 'Formulation and in vitro characterization of Eudragit® L100 and Eudragit® L100-PLGA nanoparticles containing diclofenac sodium', *AAPS PharmSciTech*, 11(3), pp. 1250–1256. doi: 10.1208/s12249-010-9489-6.

Chamarthy, S. P. and Pinal, R. (2008) 'Plasticizer concentration and the performance of a diffusion-controlled polymeric drug delivery system', *Colloids and Surfaces A: Physicochemical and Engineering Aspects*, 331(1–2), pp. 25–30. doi: 10.1016/j.colsurfa.2008.05.047.

Charoo, N. A. (2020) 'Critical Excipient Attributes Relevant to Solid Dosage Formulation Manufacturing', *Journal of Pharmaceutical Innovation*. Springer, pp. 163–181. doi: 10.1007/s12247-019-09372-w.

Chen, Tongkai *et al.* (2017) 'Tablets of multi-unit pellet system for controlled drug delivery', *Journal of Controlled Release*. Elsevier B.V., pp. 222–231. doi: 10.1016/j.jconrel.2017.07.043.

Cheng, S., Huang, J. and He, J. (2007) 'Development and validation of an accurate HPLC method for the quantitative determination of picoside II in tablets', *Pharmazie*, 62(8), pp. 577–579. doi: 10.1691/ph.2007.8.6133.

Chin, W. C., Chan, L. W. and Heng, P. W. S. (2016) 'A mechanistic investigation on the utilization of lactose as a protective agent for multi-unit pellet systems', *Pharmaceutical Development and Technology*, 21(2), pp. 222–230. doi: 10.3109/10837450.2014.991875.

CHMP (2014) 'Committee for Medicinal Products for Human Use (CHMP) assessment report HEMANGIOL International non-proprietary name: propranolol', *European medicines agency*. Available at: www.ema.europa.eu (Accessed: 23 May 2021).

Chopra, R. *et al.* (2002) 'The influence of pellet shape and film coating on the filling of pellets into hard shell capsules', *European Journal of Pharmaceutics and Biopharmaceutics*, 53(3), pp. 327–333. doi: [https://doi.org/10.1016/S0939-6411\(02\)00015-2](https://doi.org/10.1016/S0939-6411(02)00015-2).

Choudhary, N. and Avari, J. (2013) 'Tableting of coated pellets', *International Journal of PharmTech Research*, 5(3), pp. 1355–1359.

Choudhary, N. and Avari, J. (2015) 'Formulation and evaluation of taste mask pellets of granisetron hydrochloride as oro dispersible tablet', *Brazilian Journal of Pharmaceutical Sciences*, 51(3), pp. 569–578. doi: 10.1590/S1984-82502015000300009.

Choudhary, O. P. and Choudhary, P. (2017) 'Scanning Electron Microscope: Advantages and Disadvantages in Imaging Components', *International Journal of Current Microbiology and Applied Sciences*, 6, pp. 1877–1882. doi: 10.20546/ijcmas.2017.605.207.

Chourasia, M. K. and Jain, S. K. (2004) 'Design and Development of Multiparticulate System for Targeted Drug Delivery to Colon', *Drug Delivery*, 11(3), pp. 201–207. doi: 10.1080/10717540490445955.

Chowdary, K. P. R., Shankar, K. R. and Suchitra, B. (2014) 'RECENT RESEARCH ON ORODISPERSIBLE TABLETS – A REVIEW', *Int. Res J Pharm. App Sci. International Research Journal of Pharmaceutical and Applied Sciences (IRJPAS)* www.irjpas.com *Int. Res J Pharm. App Sci*, 4(41), pp. 64–7364. Available at: www.irjpas.com (Accessed: 3 September 2020).

Chuang, J. J. *et al.* (2017) 'Effects of pH on the Shape of Alginate Particles and Its Release Behavior', *International Journal of Polymer Science*, 2017. doi: 10.1155/2017/3902704.

Chvatal, A. *et al.* (2019) 'Formulation and comparison of spray dried non-porous and large porous particles containing meloxicam for pulmonary drug delivery', *International Journal of Pharmaceutics*, 559, pp. 68–75. doi: 10.1016/j.ijpharm.2019.01.034.

Coetzee, C. J. (2016) 'Calibration of the discrete element method and the effect of particle shape', *Powder Technology*, 297, pp. 50–70. doi: <https://doi.org/10.1016/j.powtec.2016.04.003>.

Coetzee, C. J. (2017) 'Review: Calibration of the discrete element method', *Powder Technology*, 310, pp. 104–142. doi: <https://doi.org/10.1016/j.powtec.2017.01.015>.

Coetzee, C. J. (2019) 'Particle upscaling: Calibration and validation of the discrete element method', *Powder Technology*, 344, pp. 487–503. doi: <https://doi.org/10.1016/j.powtec.2018.12.022>.

Coetzee, C. J. and Els, D. N. J. (2009) 'Calibration of granular material parameters for DEM modelling and numerical verification by blade–granular material interaction',

Journal of Terramechanics, 46(1), pp. 15–26. doi: <https://doi.org/10.1016/j.jterra.2008.12.004>.

Cole, G. (1998) 'Evaluating Development and Production Costs: Tablets versus Capsules', *Pharmaceutical Technology Europe*, 5, pp. 17–26.

Combarros, M. *et al.* (2014) 'Segregation of particulate solids: Experiments and DEM simulations', *Particuology*, 12, pp. 25–32. doi: <https://doi.org/10.1016/j.partic.2013.04.005>.

Committee for Human Medicinal Products (2018) 'Information for the package leaflet regarding ethanol used as an excipient in medicinal products for human use', *European Medicines Agency*, 31(September 2018), pp. 1–25. Available at: www.ema.europa.eu/contact (Accessed: 24 April 2021).

Corrigan, O. I. (1995) 'Thermal analysis of spray dried products', *Thermochimica Acta*, 248, pp. 245–258. doi: [https://doi.org/10.1016/0040-6031\(94\)01891-J](https://doi.org/10.1016/0040-6031(94)01891-J).

Coskun, O. (2016) 'Separation Techniques: CHROMATOGRAPHY', *Northern Clinics of Istanbul*, 3(2), p. 156. doi: 10.14744/nci.2016.32757.

Council of Europe (2005) 'Dissolution test for solid dosage forms', *European pharmacopoeia 5.0*, pp. 228–230. Available at: [http://lib.njutcm.edu.cn/yaodian/ep/EP5.0/02_methods_of_analysis/2.9.__pharmaceutical_technical_procedures/2.9.3. Dissolution test for solid dosage forms.pdf](http://lib.njutcm.edu.cn/yaodian/ep/EP5.0/02_methods_of_analysis/2.9.__pharmaceutical_technical_procedures/2.9.3._Dissolution_test_for_solid_dosage_forms.pdf) (Accessed: 21 February 2021).

Crouter, A. and Briens, L. (2014) 'The effect of moisture on the flowability of pharmaceutical excipients', *AAPS PharmSciTech*, 15(1), pp. 65–74. doi: 10.1208/s12249-013-0036-0.

Cutler, R. L. *et al.* (2018) 'Economic impact of medication non-adherence by disease groups: A systematic review', *BMJ Open*, p. 16982. doi: 10.1136/bmjopen-2017-016982.

Daraghmeh, N. H. *et al.* (2011) 'Chapter 2 - Chitin', in *Brittain Excipients and Related Methodology*, H. G. B. T.-P. of D. S. (ed.). Academic Press, pp. 35–102. doi: <https://doi.org/10.1016/B978-0-12-387667-6.00002-6>.

Dashevsky, A., Kolter, K. and Bodmeier, R. (2004) 'Compression of pellets coated with various aqueous polymer dispersions', *International Journal of Pharmaceutics*, 279(1–2), pp. 19–26. doi: 10.1016/j.ijpharm.2004.03.019.

Dave, V. S. *et al.* (2012) 'Eudragit® RS PO/RL PO as rate-controlling matrix-formers via roller compaction: Influence of formulation and process variables on functional

attributes of granules and tablets', *Drug Development and Industrial Pharmacy*, 38(10), pp. 1240–1253. doi: 10.3109/03639045.2011.645831.

Deb, P. K. *et al.* (2018) 'Chapter 5 - Particulate Level Properties and its Implications on Product Performance and Processing', in Tekade, R. K. B. T.-D. F. D. P. (ed.) *Advances in Pharmaceutical Product Development and Research*. Academic Press, pp. 155–220. doi: <https://doi.org/10.1016/B978-0-12-814421-3.00005-1>.

DEM Solutions (2017) *EDEM Tutorial Flexible Plane Copyrights and Trademarks*. Available at: www.dem-solutions.com (Accessed: 5 September 2020).

DEM Solutions Ltd. (2014) *EDEM 2.6 Theory Reference Guide*. Available at: www.dem-solutions.com (Accessed: 13 May 2021).

Dentagama, pure dentistry (2020) *What are orally disintegrating tablets? | News | Dentagama, What are orally disintegrating tablets?* Available at: <https://dentagama.com/news/what-are-orally-disintegrating-tablets> (Accessed: 15 January 2022).

Depeursinge, A. *et al.* (2010) 'Fusing Visual and Clinical Information for Lung Tissue Classification in HRCT Data', *Artificial Intelligence in Medicine*, 10, p. ARTMED1118. doi: 10.1016/j.

Descamps, M. *et al.* (2007) 'Transformation of pharmaceutical compounds upon milling and comilling: The role of Tg', *Journal of Pharmaceutical Sciences*, 96(5), pp. 1398–1407. doi: 10.1002/jps.20939.

Deshmukh, K. *et al.* (2017) '3 - Biopolymer Composites With High Dielectric Performance: Interface Engineering', in Sadasivuni, K. K. *et al.* (eds) *Biopolymer Composites in Electronics*. Elsevier, pp. 27–128. doi: <https://doi.org/10.1016/B978-0-12-809261-3.00003-6>.

Devarampally, D. R. (2017) 'Development of Two-Way Coupled CFD – DEM Model for Top Spray Fluid Bed Granular Using Star CCM +', pp. 1–29. doi: 10.7282/T3474DP6.

Dey, P. and Maiti, S. (2010) 'Orodispersible tablets: A new trend in drug delivery', *Journal of Natural Science, Biology and Medicine*, 1(1), pp. 2–5. doi: 10.4103/0976-9668.71663.

Dimitrov, A. S. *et al.* (1991) 'Contact angle measurements with sessile drops and bubbles', *Journal of Colloid and Interface Science*, 145(1), pp. 279–282. doi: [https://doi.org/10.1016/0021-9797\(91\)90120-W](https://doi.org/10.1016/0021-9797(91)90120-W).

Diós, P. *et al.* (2015) 'Influence of different types of low substituted hydroxypropyl

cellulose on tableting, disintegration, and floating behaviour of floating drug delivery systems', *Saudi Pharmaceutical Journal*, 23(6), pp. 658–666. doi: 10.1016/j.jsps.2014.09.001.

Donohue, M. D. and Aranovich, G. L. (1998) 'Classification of Gibbs adsorption isotherms', *Advances in Colloid and Interface Science*, 76–77, pp. 137–152. doi: 10.1016/S0001-8686(98)00044-X.

van Dooren, A. A. and Müller, B. W. (1984) 'Purity determinations of drugs with differential scanning calorimetry (DSC)—a critical review', *International Journal of Pharmaceutics*, 20(3), pp. 217–233. doi: [https://doi.org/10.1016/0378-5173\(84\)90170-4](https://doi.org/10.1016/0378-5173(84)90170-4).

Dourado, D. (2019) 'Thermal Analysis as a Useful Tool in Drug-Excipient Compatibility Studies: The Impact in Pharmaceuticals Products', *Biomedical Journal of Scientific & Technical Research*, 22(3). doi: 10.26717/bjstr.2019.22.003745.

Dukić-Ott, A. *et al.* (2009) 'Production of pellets via extrusion-spheronisation without the incorporation of microcrystalline cellulose: A critical review', *European Journal of Pharmaceutics and Biopharmaceutics*, 71(1), pp. 38–46. doi: 10.1016/j.ejpb.2008.08.005.

Dukić, A. *et al.* (2007) 'Development of starch-based pellets via extrusion/spheronisation', *European Journal of Pharmaceutics and Biopharmaceutics*, 66(1), pp. 83–94. doi: 10.1016/j.ejpb.2006.08.015.

Easterling, C. S. and Robbins, E. (2008) 'Dementia and Dysphagia', *Geriatric Nursing*, 29(4), pp. 275–285. doi: <https://doi.org/10.1016/j.gerinurse.2007.10.015>.

Echlin, P. (2009) *Handbook of Sample Preparation for Scanning Electron Microscopy and X-Ray Microanalysis*, *Handbook of Sample Preparation for Scanning Electron Microscopy and X-Ray Microanalysis*. doi: 10.1007/978-0-387-85731-2.

EDEM (2016) *EDEM Simulation for Academia*. Available at: <https://www.edemsimulation.com/academia/> (Accessed: 11 September 2020).

EFSA (2004) 'Opinion of the Scientific Panel on Food Additives, Flavourings, Processing Aids and Materials in Contact with Food (AFC) on a request from the Commission related to Ethyl Cellulose as a food additive', *EFSA Journal*, 2(4). doi: 10.2903/j.efsa.2004.35.

Eichie, F. E. and Kudehinbu, A. O. (2009) 'Effect of particle size of granules on some mechanical properties of paracetamol tablets', *African Journal of Biotechnology*, 8(21), pp. 5913–5916. doi: 10.5897/AJB09.859.

- Eisenberg, A., Yokoyama, T. and Sambalido, E. (1969) 'Dehydration kinetics and glass transition of poly(acrylic acid)', *Journal of Polymer Science Part A-1: Polymer Chemistry*, 7(7), pp. 1717–1728. doi: <https://doi.org/10.1002/pol.1969.150070714>.
- El-Badry, M., Fetih, G. and Fathy, M. (2009) 'Improvement of solubility and dissolution rate of indomethacin by solid dispersions in Gelucire 50/13 and PEG4000', *Saudi Pharmaceutical Journal*, 17(3), pp. 217–225. doi: 10.1016/j.jsps.2009.08.006.
- Elliott, R. (2013) 'Nonadherence to medicines: the scale of the problem', *Prescriber*, 24(17), pp. 47–50. doi: <https://doi.org/10.1002/psb.1096>.
- Elsayed, A. *et al.* (2017) 'Thermal energy storage using metal–organic framework materials', *Applied Energy*, 186, pp. 509–519. doi: <https://doi.org/10.1016/j.apenergy.2016.03.113>.
- ElShaer, A. *et al.* (2017) 'Understanding the compaction behaviour of low-substituted HPC: macro, micro, and nano-metric evaluations', *Pharmaceutical Development and Technology*, 23(5), pp. 442–453. doi: 10.1080/10837450.2017.1363775.
- ElShaer, A. *et al.* (2018) 'Understanding the compaction behaviour of low-substituted HPC: macro, micro, and nano-metric evaluations', *Pharmaceutical Development and Technology*, 23(5), pp. 442–453. doi: 10.1080/10837450.2017.1363775.
- Elshaer, A., Hanson, P. and Mohammed, A. R. (2014) 'A novel concentration dependent amino acid ion pair strategy to mediate drug permeation using indomethacin as a model insoluble drug', *European Journal of Pharmaceutical Sciences*, 62, pp. 124–131. doi: 10.1016/j.ejps.2014.05.022.
- ElShaer, A., Hanson, P. and Mohammed, A. R. (2013) 'A systematic and mechanistic evaluation of aspartic acid as filler for directly compressed tablets containing trimethoprim and trimethoprim aspartate', *European Journal of Pharmaceutics and Biopharmaceutics*, 83(3), pp. 468–476. doi: <https://doi.org/10.1016/j.ejpb.2012.11.010>.
- Elwerfalli, A. *et al.* (2015) 'New Generation of Orally Disintegrating Tablets for Sustained Drug Release: A Propitious Outlook', *Current Drug Delivery*, 12(6), pp. 652–667. doi: 10.2174/1567201812666150310151238.
- Elwerfalli, A. M. *et al.* (2015a) 'Nano-engineering chitosan particles to sustain the release of promethazine from orodispersables', *Carbohydrate Polymers*, 131, pp. 447–461. doi: 10.1016/j.carbpol.2015.05.064.
- Elwerfalli, A. M. *et al.* (2015b) 'Nano-engineering chitosan particles to sustain the release of promethazine from orodispersables', *Carbohydrate Polymers*, 131, pp.

447–461. doi: 10.1016/j.carbpol.2015.05.064.

Ema (2013) 'Guideline on the pharmacokinetic and clinical evaluation of modified release dosage forms Guideline on the pharmacokinetic and clinical evaluation of modified release dosage forms (EMA / CPMP / EWP / 280 / 96 Corr1)', *European Medicines Agency (EMA)*, 44(February), pp. 1–38. Available at: www.ema.europa.eu/contact (Accessed: 19 April 2021).

EMA (2008) *European Pharmacopoeia 6.0, chapter 2.9.3 Dissolution Test for Solid Dosage Forms*.

Emam Kassab, S. (2019) 'Indomethacin from Anti-Inflammatory to Anticancer Agent', in *Medicinal Chemistry*. IntechOpen. doi: 10.5772/intechopen.79677.

Emami, F. *et al.* (2018) 'Drying technologies for the stability and bioavailability of biopharmaceuticals', *Pharmaceutics*. MDPI AG, p. 131. doi: 10.3390/pharmaceutics10030131.

EMA (2009) *VICH Topic GL49 at step 4 GUIDELINES FOR THE VALIDATION OF ANALYTICAL METHODS USED IN RESIDUE DEPLETION STUDIES DRAFT AGREED BY VICH STEERING COMMITTEE ADOPTION BY CVMP FOR RELEASE FOR CONSULTATION END OF CONSULTATION (DEADLINE FOR COMMENTS) VICH GL 49 (M, Vet. Med. Insp. Eur. Med. Agency*.

EP (2021) *European Pharmacopoeia (Ph. Eur.) 10th Edition | EDQM - European Directorate for the Quality of Medicines*. Available at: <https://www.edqm.eu/en/european-pharmacopoeia-ph-eur-10th-edition> (Accessed: 26 May 2021).

Esposito, E. *et al.* (2000) 'Production of Eudragit microparticles by spray-drying technique: Influence of experimental parameters on morphological and dimensional characteristics', *Pharmaceutical Development and Technology*, 5(2), pp. 267–278. doi: 10.1081/PDT-100100541.

Fadda, H. M. *et al.* (2008) 'The molecular interactions that influence the plasticizer dependent dissolution of acrylic polymer films', *Journal of Pharmaceutical Sciences*, 97(9), pp. 3957–3971. doi: 10.1002/jps.21292.

Fandino, W. (2019) 'Understanding the physiological changes induced by mannitol: From the theory to the clinical practice in neuroanaesthesia', *Journal of Neuroanaesthesiology and Critical Care*. doi: 10.4103/jnacc-jnacc-31.17.

Faridmehr, I. *et al.* (2014) 'Correlation between Engineering Stress-Strain and True Stress-Strain Curve', *American Journal of Civil Engineering and Architecture*, 2(1), pp.

53–59. doi: 10.12691/ajcea-2-1-6.

Faroongsarng, D., Kadejinda, W. and Sunthornpit, A. (2000) 'Thermal behavior of a pharmaceutical solid acetaminophen doped with p-aminophenol', *AAPS PharmSciTech*, 1(3), p. 23. doi: 10.1208/pt010323.

FB, A. and T, U. (2015) 'Orally Disintegrating Tablets: A Short Review', *Journal of Pharmaceutics and Drug Development*, 3(3). doi: 10.15744/2348-9782.3.303.

FDA/CDER (1997) 'Dissolution Testing of Immediate Release Solid Oral Dosage Forms', *Evaluation*, 4(August), pp. 15–22. Available at: <https://www.fda.gov/media/70936/download> (Accessed: 21 February 2021).

FDA (2008) 'Highlights of prescribing information', *Metabolism Clinical And Experimental*. Available at: www.fda.gov/medwatch. (Accessed: 20 April 2021).

FDA, U. (2008a) *Guidance for Industry Orally Disintegrating Tablets, Federal Register*. Available at: <http://www.fda.gov/cder/guidance/index.htm> (Accessed: 20 November 2020).

FDA, U. (2008b) 'Guidance for Industry Orally Disintegrating Tablets', *Federal Register*, (December), pp. 1–3. Available at: <https://www.fda.gov/regulatory-information/search-fda-guidance-documents/orally-disintegrating-tablets> (Accessed: 26 May 2021).

Felton, L. A. (2013) 'Mechanisms of polymeric film formation', *International Journal of Pharmaceutics*, 457(2), pp. 423–427. doi: <https://doi.org/10.1016/j.ijpharm.2012.12.027>.

FIELDEN, K. E. *et al.* (1988) 'Thermal Studies on the Interaction of Water and Microcrystalline Cellulose', *Journal of Pharmacy and Pharmacology*, 40(10), pp. 674–678. doi: 10.1111/j.2042-7158.1988.tb06993.x.

Fielden, K. E., Newton, J. M. and Rowe, R. C. (1992) 'A comparison of the extrusion and spheronization behaviour of wet powder masses processed by a ram extruder and a cylinder extruder', *International Journal of Pharmaceutics*, 81(2), pp. 225–233. doi: [https://doi.org/10.1016/0378-5173\(92\)90014-S](https://doi.org/10.1016/0378-5173(92)90014-S).

Ford, J. L. (1999) 'Thermal analysis of hydroxypropylmethylcellulose and methylcellulose: powders, gels and matrix tablets', *International Journal of Pharmaceutics*, 179(2), pp. 209–228. doi: [https://doi.org/10.1016/S0378-5173\(98\)00339-1](https://doi.org/10.1016/S0378-5173(98)00339-1).

Frenning, G. (2010) 'Compression mechanics of granule beds: A combined finite/discrete element study', *Chemical Engineering Science*, 65(8), pp. 2464–2471.

doi: <https://doi.org/10.1016/j.ces.2009.12.029>.

Friedman, M. and Donbrow, M. (1978) 'Fluidized bed coating technique for production of sustained release granules', *Drug Development and Industrial Pharmacy*, 4(4), pp. 319–331. doi: 10.3109/03639047809060846.

Friedrich, R. B. *et al.* (2010) 'Tablets containing drug-loaded polymeric nanocapsules: An innovative platform', *Journal of Nanoscience and Nanotechnology*, 10(9), pp. 5885–5888. doi: 10.1166/jnn.2010.2464.

Fries, L. *et al.* (2011) 'DEM-CFD modeling of a fluidized bed spray granulator', *Chemical Engineering Science*, 66(11), pp. 2340–2355. doi: 10.1016/j.ces.2011.02.038.

Frodeson, S. and Berghel, J. (2018) 'Pelletizing pure biomass substances to investigate the mechanical properties and bonding mechanisms', *BioResources*, 13, pp. 1202–1222. doi: 10.15376/biores.13.1.1202-1222.

Fronczek, F., Kamel, H. and Slattery, M. (2003) 'Three polymorphs (alpha, beta and delta) of D-mannitol at 100 K', *Acta crystallographica. Section C, Crystal structure communications*, 59, pp. O567-70. doi: 10.1107/S0108270103018961.

Fu, F., Lin, L. and Xu, E. (2017) '4 - Functional pretreatments of natural raw materials', in Fan, M. and Fu, F. B. T.-A. H. S. N. F. C. in C. (eds). Woodhead Publishing, pp. 87–114. doi: <https://doi.org/10.1016/B978-0-08-100411-1.00004-2>.

Fu, Y. *et al.* (2004) 'Orally fast disintegrating tablets: Developments, technologies, taste-masking and clinical studies', *Critical Reviews in Therapeutic Drug Carrier Systems*, 21(6), pp. 433–475. doi: 10.1615/CritRevTherDrugCarrierSyst.v21.i6.10.

Galland, S., Ruiz, T. and Delalonde, M. (2009) 'Hydro-textural characterisation of wet granular media shaped by extrusion/spheronisation', *Powder Technology*, 190(1–2), pp. 48–52. doi: 10.1016/j.powtec.2008.04.056.

Gandhi, B. R., Badgujar, B. P. and Kasliwal, A. V (2011) 'Development and in vitro evaluation of multiparticulate system using novel coating material for controlled drug delivery system', *International Journal of Pharmacy and Pharmaceutical Sciences*, 3(3), pp. 96–99.

Gang, Z. *et al.* (2010) 'Effect of Operational Conditions on Pellets Settling Velocity', in *2010 International Conference on Challenges in Environmental Science and Computer Engineering*, pp. 197–200. doi: 10.1109/CESCE.2010.127.

García-Triñanes, P., Luding, S. and Shi, H. (2019) 'Tensile strength of cohesive powders', *Advanced Powder Technology*, 30(12), pp. 2868–2880. doi:

10.1016/j.appt.2019.08.017.

García Mir, V. *et al.* (2011) 'Effects of moisture on tablet compression of chitin', *Carbohydrate Polymers*, 86(2), pp. 477–483. doi: <https://doi.org/10.1016/j.carbpol.2011.04.065>.

Ghanam, D. and Kleinebudde, P. (2011) 'Suitability of κ -carrageenan pellets for the formulation of multiparticulate tablets with modified release', *International Journal of Pharmaceutics*, 409(1), pp. 9–18. doi: <https://doi.org/10.1016/j.ijpharm.2011.02.016>.

Ghori, M. and Conway, B. (2016) 'Powder Compaction: Compression Properties of Cellulose Ethers', *British Journal of Pharmacy*, 1. doi: 10.5920/bjpharm.2016.09.

Ghori, M. U. (2016) 'Powder Compaction: Compression Properties of Cellulose Ethers', *British Journal of Pharmacy*, 1(1). doi: 10.5920/bjpharm.2016.09.

Ghosh, T., Ghosh, A. and Prasad, D. (2011) 'A review on new generation orodispersible tablets and its future prospective', *International Journal of Pharmacy and Pharmaceutical Sciences*, 3(1), pp. 1–7. Available at: https://www.researchgate.net/publication/275521790_A_review_on_new_generation_orodispersible_tablets_and_its_future_prospective (Accessed: 4 September 2020).

Ghosh, T. K. and Pfister, W. R. (2005) 'Intraoral delivery systems: An overview, current status, and future trends', in *Drug Delivery to the Oral Cavity: Molecules to Market*, pp. 1–40.

Gibson, N. *et al.* (2020) 'Chapter 4.1 - Volume-specific surface area by gas adsorption analysis with the BET method', in Hodoroaba, V.-D., Unger, W. E. S., and Shard, A. G. (eds) *Characterization of Nanoparticles*. Elsevier (Micro and Nano Technologies), pp. 265–294. doi: <https://doi.org/10.1016/B978-0-12-814182-3.00017-1>.

Giram, P. S. *et al.* (2018) 'Fast dissolving moxifloxacin hydrochloride antibiotic drug from electrospun Eudragit L-100 nonwoven nanofibrous Mats', *Materials Science and Engineering: C*, 92, pp. 526–539. doi: <https://doi.org/10.1016/j.msec.2018.06.031>.

Glatt GmbH (2013) *Extrusion / Spheronization - Glatt Integrated Process Solutions*. Available at: <https://www.glatt.com/en/processes/pelletizing/extrusion-spheronization/> (Accessed: 1 May 2020).

Gochioco, K. (2014) *The Effect of Crystalline and Amorphous Lactose on Mechanical Properties of Roller Compaction Ribbon and Tablets*. Available at: M.Sc. Thesis, University of Kansas (Accessed: 4 October 2020).

Goldstein, J. L. and Cryer, B. (2014) 'Gastrointestinal injury associated with NSAID use: A case study and review of risk factors and preventative strategies', *Drug*,

Healthcare and Patient Safety, 7, pp. 31–41. doi: 10.2147/DHPS.S71976.

Gombotz, W. and Wee, S. (2012) 'Protein release from alginate matrices', *Advanced drug delivery reviews*, 64. doi: 10.1016/j.addr.2012.09.007.

Gómez-Carracedo, A. *et al.* (2008) 'Incidence of drying on microstructure and drug release profiles from tablets of MCC–lactose–Carbopol® and MCC–dicalcium phosphate–Carbopol® pellets', *European Journal of Pharmaceutics and Biopharmaceutics*, 69(2), pp. 675–685. doi: <https://doi.org/10.1016/j.ejpb.2007.11.016>.

Gorain, B. *et al.* (2018) 'Drug–Excipient Interaction and Incompatibilities', in, pp. 363–402. doi: 10.1016/B978-0-12-814421-3.00011-7.

Goula, A. M. and Adamopoulos, K. G. (2008) 'Effect of Maltodextrin Addition during Spray Drying of Tomato Pulp in Dehumidified Air: I. Drying Kinetics and Product Recovery', *Drying Technology*, 26(6), pp. 714–725. doi: 10.1080/07373930802046369.

Gouldson, M. P. and Deasy, P. B. (1997) 'Use of cellulose ether containing excipients with microcrystalline cellulose for the production of pellets containing metformin hydrochloride by the process of extrusion-spheronization', *Journal of Microencapsulation*. doi: 10.3109/02652049709015328.

Govedarica, B. *et al.* (2012) 'The use of single particle mechanical properties for predicting the compressibility of pharmaceutical materials', *Powder Technology*, 225, pp. 43–51. doi: <https://doi.org/10.1016/j.powtec.2012.03.030>.

Goyanes, A., Souto, C. and Martínez-Pacheco, R. (2010) 'Control of drug release by incorporation of sorbitol or mannitol in microcrystalline-cellulose-based pellets prepared by extrusion-spheronization', *Pharmaceutical Development and Technology*, 15(6), pp. 626–635. doi: 10.3109/10837450903419653.

Goyanes, A., Souto, C. and Martínez-Pacheco, R. (2011) 'Co-processed MCC-Eudragit® e excipients for extrusion-spheronization', *European Journal of Pharmaceutics and Biopharmaceutics*, 79(3), pp. 658–663. doi: 10.1016/j.ejpb.2011.07.013.

Greco, K. and Bogner, R. (2010) 'Crystallization of Amorphous Indomethacin during Dissolution: Effect of Processing and Annealing', *Molecular pharmaceutics*, 7. doi: 10.1021/mp1000197.

Grembecka, M. (2015) 'Sugar alcohols—their role in the modern world of sweeteners: a review', *European Food Research and Technology*. Springer Verlag, pp. 1–14. doi:

10.1007/s00217-015-2437-7.

Grosman, A. and Ortega, C. (2005) 'Nature of capillary condensation and evaporation processes in ordered porous materials', *Langmuir*, 21(23), pp. 10515–10521. doi: 10.1021/la051030o.

Grosshans, H. *et al.* (2016) 'A new model for the drying of mannitol-water droplets in hot air above the boiling temperature', *Powder Technology*, 297, pp. 259–265. doi: <https://doi.org/10.1016/j.powtec.2016.04.023>.

Guignon, B., Duquenoy, A. and Dumoulin, E. D. (2002) 'Fluid bed encapsulation of particles: Principles and practice', *Drying Technology*, 20(2), pp. 419–447. doi: 10.1081/DRT-120002550.

Gunjal, S. D. (2020) 'An Overview of Process Parameters and Spray drying agents involved in Spray drying of Herbal Extracts', XIII(Vii), pp. 102–118. Available at: <http://www.paideumajournal.com> (Accessed: 11 April 2021).

Guo, Y. *et al.* (2012) 'Synthesis and characterization of hydrophobic long-chain fatty acylated cellulose and its self-assembled nanoparticles', *Polymer Bulletin*, 69(4), pp. 389–403. doi: 10.1007/s00289-012-0729-7.

Gupta, Simerdeep Singh, Nayan Solanki, and A. T. S. (2016) 'Investigation of thermal and viscoelastic properties of polymers relevant to hot melt extrusion - III: Polymethacrylates and polymethacrylic acid based polymers', *Aaps PharmSciTech* 17.1, pp. 148–17. Available at: https://www.researchgate.net/publication/283809163_Investigation_of_thermal_and_viscoelastic_properties_of_polymers_relevant_to_hot_melt_extrusion_-_III_Polymethacrylates_and_polymethacrylic_acid_based_polymers (Accessed: 11 July 2020).

Gupta, P., Kumar, M. and Sachan, N. (2015a) 'An Overview on Polymethacrylate Polymers in Gastroretentive Dosage Forms', *Open Pharmaceutical Sciences Journal*, 9(1), pp. 31–42. doi: 10.2174/1874844901502010031.

Gupta, P., Kumar, M. and Sachan, N. (2015b) 'An Overview on Polymethacrylate Polymers in Gastroretentive Dosage Forms', *Open Pharmaceutical Sciences Journal*, 9(1), pp. 31–42. doi: 10.2174/1874844901502010031.

Gupta, S. S., Solanki, N. and Serajuddin, A. T. M. (2016) 'Investigation of Thermal and Viscoelastic Properties of Polymers Relevant to Hot Melt Extrusion, IV: Affinisol™ HPMC HME Polymers', *AAPS PharmSciTech*, 17(1), pp. 148–157. doi: 10.1208/s12249-015-0426-6.

Gürsoy, A., Kalkan, F. and Okar, I. (1998) 'Preparation and tableting of dipyridamole alginate-Eudragit microspheres', *Journal of Microencapsulation*, 15(5), pp. 621–628. doi: 10.3109/02652049809008245.

Gutiérrez-Rocca, J. and McGinity, J. W. (1994) 'Influence of water soluble and insoluble plasticizers on the physical and mechanical properties of acrylic resin copolymers', *International Journal of Pharmaceutics*, 103(3), pp. 293–301. doi: [https://doi.org/10.1016/0378-5173\(94\)90180-5](https://doi.org/10.1016/0378-5173(94)90180-5).

Habib, Y. S., Augsburg, L. L. and Shangraw, R. F. (2002) 'Production of inert cushioning beads: effect of excipients on the physicommechanical properties of freeze-dried beads containing microcrystalline cellulose produced by extrusion–spheronization', *International Journal of Pharmaceutics*, 233(1), pp. 67–83. doi: [https://doi.org/10.1016/S0378-5173\(01\)00924-3](https://doi.org/10.1016/S0378-5173(01)00924-3).

Hadi, K. (2015) *Spray Drying of Cocrystals for Engineering Particle Properties*. Available at: <http://www.teknat.uu.se/student%0Ahttp://www.diva-portal.org/smash/get/diva2:866593/FULLTEXT01.pdf>.

Han, Z., Teng, H. and Wang, J. (2012) 'Computer generation of sphere packing for discrete element analysis in Is-dyna', in *Proceedings of the 12th International LS-DYNA Conference, Detroit*.

Hannan, P. A. *et al.* (2016) 'Oral dispersible system: A new approach in drug delivery system', *Indian Journal of Pharmaceutical Sciences*. Medknow Publications, pp. 2–7. doi: 10.4103/0250-474X.180244.

Haq, N. *et al.* (2014) 'An environmentally benign approach for rapid analysis of indomethacin using a stability-indicating RP-HPLC method', *Journal of Liquid Chromatography and Related Technologies*, 37, pp. 878–892. doi: 10.1080/10826076.2012.758150.

Harada, T. *et al.* (2010) 'Effect of physical properties of orally disintegrating tablets on disintegration time as determined by a new apparatus', *Journal of Drug Delivery Science and Technology*, 20(5), pp. 377–383. doi: [https://doi.org/10.1016/S1773-2247\(10\)50062-5](https://doi.org/10.1016/S1773-2247(10)50062-5).

Harshad V. Paithankar (2013) 'HPLC METHOD VALIDATION FOR PHARMACEUTICALS: A REVIEW', *INTERNATIONAL JOURNAL OF UNIVERSAL PHARMACY AND BIO SCIENCES*, 2(4), pp. 229–240. Available at: https://www.researchgate.net/publication/252930849_HPLC_METHOD_VALIDATION_FOR_PHARMACEUTICALS_A_REVIEW (Accessed: 17 July 2020).

- Hart, A. (2015) 'Effect of Particle Size on Detergent Powders Flowability and Tabletability', *Journal of Chemical Engineering & Process Technology*, 06(01), p. 215. doi: 10.4172/2157-7048.1000215.
- Hassanpour, A. *et al.* (2011) 'Analysis of particle motion in a paddle mixer using Discrete Element Method (DEM)', *Powder Technology*, 206(1–2), pp. 189–194. doi: 10.1016/j.powtec.2010.07.025.
- Hay, I. *et al.* (2010) 'Bacterial biosynthesis of alginates', *Journal of Chemical Technology and Biotechnology*, 85, pp. 752–759. doi: 10.1002/jctb.2372.
- Hentschel, M. L. and Page, N. W. (2003) 'Selection of descriptors for particle shape characterization', *Particle and Particle Systems Characterization*, 20(1), pp. 25–38. doi: 10.1002/ppsc.200390002.
- Hess, S. *et al.* (2001) 'Profiling indomethacin impurities using high-performance liquid chromatography and nuclear magnetic resonance', *European Journal of Pharmaceutical Sciences*, 14(4), pp. 301–311. doi: [https://doi.org/10.1016/S0928-0987\(01\)00198-1](https://doi.org/10.1016/S0928-0987(01)00198-1).
- Hillier, K. (2007) 'Methylcellulose', in Enna, S. J. and Bylund, D. B. (eds) *xPharm: The Comprehensive Pharmacology Reference*. New York: Elsevier, pp. 1–3. doi: <https://doi.org/10.1016/B978-008055232-3.62160-9>.
- Himmatagaoglu, A. B. and Erbay, Z. (2019) 'Effects of spray drying process conditions on the quality properties of microencapsulated cream powder', *International Dairy Journal*, 88, pp. 60–70. doi: 10.1016/j.idairyj.2018.08.004.
- Hirani, J. J., Rathod, D. A. and Vadalia, K. R. (2009) 'Orally disintegrating tablets: A review', *Tropical Journal of Pharmaceutical Research*, pp. 161–172. doi: 10.4314/tjpr.v8i2.44525.
- Hiraram Choudhary, N. *et al.* (2012) 'Orally Disintegrating Drug Delivery Systems', *Journal of Pharmacy Research*, 5(7), pp. 3791–3799. Available at: <http://jpr solutions.info> (Accessed: 20 November 2020).
- Hiremath, P., Nuguru, K. and Agrahari, V. (2019) 'Chapter 8 - Material Attributes and Their Impact on Wet Granulation Process Performance', in Narang, A. S. and Badawy, S. I. F. B. T.-H. of P. W. G. (eds). Academic Press, pp. 263–315. doi: <https://doi.org/10.1016/B978-0-12-810460-6.00012-9>.
- Hirjau, M. *et al.* (2020) 'Evaluation of Experimental Multi-Particulate Polymer-Coated Drug Delivery Systems with Meloxicam', *Coatings*, 10, p. 490. doi: 10.3390/coatings10050490.

- Ho, K. Y. *et al.* (2018) 'Nonsteroidal anti-inflammatory drugs in chronic pain: Implications of new data for clinical practice', *Journal of Pain Research*. Dove Press, pp. 1937–1948. doi: 10.2147/JPR.S168188.
- Hoag, S. W. (2017) 'Chapter 27 - Capsules Dosage Form: Formulation and Manufacturing Considerations', in Qiu, Y. *et al.* (eds). Boston: Academic Press, pp. 723–747. doi: <https://doi.org/10.1016/B978-0-12-802447-8.00027-3>.
- Horabik, J. and Molenda, M. (2016) 'Parameters and contact models for DEM simulations of agricultural granular materials: A review', *Biosystems Engineering*, 147, pp. 206–225. doi: <https://doi.org/10.1016/j.biosystemseng.2016.02.017>.
- Hosseini, A., Körber, M. and Bodmeier, R. (2013a) 'Direct compression of cushion-layered ethyl cellulose-coated extended release pellets into rapidly disintegrating tablets without changes in the release profile', *International Journal of Pharmaceutics*, 457(2), pp. 503–509. doi: <https://doi.org/10.1016/j.ijpharm.2013.07.042>.
- Hosseini, A., Körber, M. and Bodmeier, R. (2013b) 'Direct compression of cushion-layered ethyl cellulose-coated extended release pellets into rapidly disintegrating tablets without changes in the release profile', *International Journal of Pharmaceutics*. Elsevier B.V., pp. 503–509. doi: 10.1016/j.ijpharm.2013.07.042.
- Hu, P. *et al.* (2020) 'Effect of Particle Size Ratios on the Physical and Chemical Properties of Surgical-Grade Calcium Sulfate Hemihydrate', *Orthopaedic Surgery*, 12(1), pp. 295–303. doi: 10.1111/os.12569.
- ICH expert working group (1995) *ICH Topic Q 2 (R1) Validation of Analytical Procedures: Text and Methodology Step 5 NOTE FOR GUIDANCE ON VALIDATION OF ANALYTICAL PROCEDURES: TEXT AND METHODOLOGY (CPMP/ICH/381/95) APPROVAL BY CPMP November 1994 DATE FOR COMING INTO OPERATION*. Available at: <http://www.emea.eu.int> (Accessed: 18 July 2020).
- ICH Harmonised Tripartite Guideline (2010) 'EVALUATION AND RECOMMENDATION OF PHARMAPOEIAL TEXTS FOR USE IN THE ICH REGIONS ON ANALYTICAL SIEVING GENERAL CHAPTER Q4B ANNEX 12', (June). Available at: <http://www.emea.europa.eu> (Accessed: 8 July 2020).
- Iglesias, N. *et al.* (2020) 'In-depth study into polymeric materials in low-density gastroretentive formulations', *Pharmaceutics*. MDPI AG, pp. 1–44. doi: 10.3390/pharmaceutics12070636.
- Ikawa, Y. *et al.* (2012) 'Indomethacin antagonizes EP2 prostanoid receptor activation in LS174T human colon cancer cells', *European Journal of Pharmacology*, 680(1), pp.

16–21. doi: <https://doi.org/10.1016/j.ejphar.2012.01.033>.

Instron (2017) *Proportional Limit - Instron*. Available at: <https://www.instron.us/our-company/library/glossary/p/proportional-limit> (Accessed: 21 December 2020).

Irfan, M. *et al.* (2016) 'Orally disintegrating films: A modern expansion in drug delivery system', *Saudi Pharmaceutical Journal*. Elsevier B.V., pp. 537–546. doi: 10.1016/j.jsps.2015.02.024.

Issa, M. G. *et al.* (2017) 'Physical characterization of multiparticulate systems', *Brazilian Journal of Pharmaceutical Sciences*, 53(4), p. 216. doi: 10.1590/s2175-97902017000400216.

Jackcina Stobel Christy, E. *et al.* (2020) 'Chapter 10 - Chitin and chitosan-based aerogels', in Gopi, S., Thomas, S., and Pius, A. B. T.-H. of C. and C. (eds). Elsevier, pp. 285–334. doi: <https://doi.org/10.1016/B978-0-12-817970-3.00010-9>.

Jadhav, N. R. *et al.* (2009) 'Glass transition temperature: Basics and application in pharmaceutical sector', *Asian Journal of Pharmaceutics*, pp. 82–89. doi: 10.4103/0973-8398.55043.

Jain, M. *et al.* (2012) 'Spray Drying in Pharmaceutical Industry: A Review', *Research Journal of Pharmaceutical Dosage Forms and Technology*, 4, pp. 74–79.

Janda, A. and Ooi, J. Y. (2016) 'DEM modeling of cone penetration and unconfined compression in cohesive solids', *Powder Technology*, 293, pp. 60–68. doi: <https://doi.org/10.1016/j.powtec.2015.05.034>.

Jarosz, P. J. and Parrott, E. L. (1982) 'Tensile strengths and hardness of tablets', *Journal of Pharmaceutical Sciences*, 71(6), pp. 705–707. doi: 10.1002/jps.2600710625.

Jelić, D. (2021) 'Thermal Stability of Amorphous Solid Dispersions', *Molecules (Basel, Switzerland)*, 26(1), p. 238. doi: 10.3390/molecules26010238.

Jensen, A., Fraser, K. and Laird, G. (2014) 'Improving the precision of discrete element simulations through calibration models', in *13th International LS-DYNA users conference*, pp. 1–12.

Jess, K. and Steckel, H. (2007) 'The extrusion and spheronization of chitosan', *Pharmaceutical Technology Europe*, 19(7), pp. 21–30. Available at: <https://www.pharmtech.com/view/extrusion-and-spheronization-chitosan> (Accessed: 6 May 2021).

De Jesús, F. *et al.* (2002) 'Relationship between particle size and manufacturing processing and sintered characteristics of iron powders', *Revista Latinoamericana de*

Metalurgia y Materiales, 23, pp. 35–40.

Jezerská, L. *et al.* (2006) 'Particles segregation in pharmaceutical mixtures for direct tablets compression', *CHISA 2006 - 17th International Congress of Chemical and Process Engineering*.

Jiménez-Herrera, N., Barrios, G. K. P. and Tavares, L. M. (2018) 'Comparison of breakage models in DEM in simulating impact on particle beds', *Advanced Powder Technology*, 29(3), pp. 692–706. doi: 10.1016/j.appt.2017.12.006.

Jimmy, B. and Jose, J. (2011) 'Patient medication adherence: Measures in daily practice', *Oman Medical Journal*, 26(3), pp. 155–159. doi: 10.5001/omj.2011.38.

Jivraj, M., Martini, L. G. and Thomson, C. M. (2000) 'An overview of the different excipients useful for the direct compression of tablets', *Pharmaceutical Science & Technology Today*, 3(2), pp. 58–63. doi: [https://doi.org/10.1016/S1461-5347\(99\)00237-0](https://doi.org/10.1016/S1461-5347(99)00237-0).

Jones, D. (2004) *Pharmaceutical Applications of Polymers for Drug Delivery, Polysaccharides for Drug Delivery and Pharmaceutical Applications*. Available at: https://books.google.co.uk/books?id=VQOZ0zrEB9IC&printsec=frontcover&source=gs_b_s_ge_summary_r&cad=0#v=onepage&q&f=false (Accessed: 5 April 2021).

Jonsson, H., Gråsjö, J. and Frenning, G. (2017) 'Mechanical behaviour of ideal elastic-plastic particles subjected to different triaxial loading conditions', *Powder Technology*, 315, pp. 347–355. doi: <https://doi.org/10.1016/j.powtec.2017.04.005>.

Joshi, M. (2013) 'Role of Eudragit in targeted drug delivery', *International Journal of Current Pharmaceutical Research*, 5(2), pp. 58–62.

Ju, X.-J. and Chu, L.-Y. (2019) 'Chapter 9 - Lab-on-a-chip fabrication of polymeric microparticles for drug encapsulation and controlled release', in Santos, H. A., Liu, D., and Zhang, H. (eds) *Microfluidics for Pharmaceutical Applications*. William Andrew Publishing (Micro and Nano Technologies), pp. 217–280. doi: <https://doi.org/10.1016/B978-0-12-812659-2.00009-0>.

Juban, A. *et al.* (2017) 'Experimental study of tensile strength of pharmaceutical tablets: Effect of the diluent nature and compression pressure', in *EPJ Web of Conferences*. doi: 10.1051/epjconf/201714013002.

Just, S. *et al.* (2013) 'Experimental analysis of tablet properties for discrete element modeling of an active coating process', *AAPS PharmSciTech*, 14(1), pp. 402–411. doi: 10.1208/s12249-013-9925-5.

Kadajji, V. and Betageri, G. (2011) 'Water Soluble Polymers for Pharmaceutical

- Applications', *Polymers*, 3. doi: 10.3390/polym3041972.
- Kakar, S. (2018) 'Orodispersible tablets: an overview', *MOJ Proteomics & Bioinformatics*, 7(3). doi: 10.15406/mojpb.2018.07.00230.
- Kalal, A. Y. *et al.* (2018) 'Effect of spray drying and drying aids on bitter gourd juice powder properties', *Agricultural Research Journal*, 55(2), p. 318. doi: 10.5958/2395-146x.2018.00057.1.
- Kállai, N. *et al.* (2010) 'Evaluation of drug release from coated pellets based on isomalt, sugar, and microcrystalline cellulose inert cores', *AAPS PharmSciTech*, 11(1), pp. 383–391. doi: 10.1208/s12249-010-9396-x.
- Kandela, B. *et al.* (2010) 'Study of tablet-coating parameters for a pan coater through video imaging and Monte Carlo simulation', *Powder Technology*, 204(1), pp. 103–112. doi: <https://doi.org/10.1016/j.powtec.2010.07.024>.
- Kane, S. *et al.* (2003) 'Medication nonadherence and the outcomes of patients with quiescent ulcerative colitis', *American Journal of Medicine*, 114(1), pp. 39–43. doi: 10.1016/S0002-9343(02)01383-9.
- Kangulu, I. (2009) 'Sieve Analysis Taking a close look at quality An expert guide to particle size analysis', *Academia.edu*. Available at: https://www.academia.edu/26540270/Sieve_Analysis_Taking_a_close_look_at_quality_An_expert_guide_to_particle_size_analysis (Accessed: 7 July 2020).
- Kanwar, N., Kumar, R. and Sinha, V. R. (2015) 'Preparation and Evaluation of Multi-Particulate System (Pellets) of Prasugrel Hydrochloride', *Open Pharmaceutical Sciences Journal*, 2(1), pp. 74–80. doi: 10.2174/1874844901502010074.
- Kar, M. *et al.* (2019) 'Chapter 2 - Current Developments in Excipient Science: Implication of Quantitative Selection of Each Excipient in Product Development', in Tekade, R. K. (ed.) *Basic Fundamentals of Drug Delivery*. Academic Press (Advances in Pharmaceutical Product Development and Research), pp. 29–83. doi: <https://doi.org/10.1016/B978-0-12-817909-3.00002-9>.
- Karajan, N. *et al.* (2014) 'On the parameter estimation for the discrete-element method in LS-DYNA®', in *Proceedings of the 13th International LS_DYNA Users Conference, Dearborn, MI, USA*, pp. 8–10.
- Karmwar, P. *et al.* (2011) 'Investigation of properties and recrystallisation behaviour of amorphous indomethacin samples prepared by different methods', *International Journal of Pharmaceutics*, 417(1–2), pp. 94–100. doi: 10.1016/j.ijpharm.2010.12.019.
- Kassem, A. *et al.* (2015) 'Development of mucoadhesive microbeads using thiolated

sodium alginate for intrapocket delivery of resveratrol', *International journal of pharmaceuticals*, 487. doi: 10.1016/j.ijpharm.2015.04.010.

Kathpalia, H. *et al.* (2014) 'Controlled release orally disintegrating tablets: A review', *International Journal of Pharmaceutical Sciences Review and Research*, pp. 35–42.

Kaur, V. *et al.* (2020) 'Development and characterization of pellets for targeted delivery of 5-fluorouracil and phytic acid for treatment of colon cancer in Wistar rat', *Heliyon*, 6(1), p. e03125. doi: 10.1016/j.heliyon.2019.e03125.

Keck, C. M. and Müller, R. H. (2008) 'Size analysis of submicron particles by laser diffractometry—90% of the published measurements are false', *International Journal of Pharmaceutics*, 355(1), pp. 150–163. doi: <https://doi.org/10.1016/j.ijpharm.2007.12.004>.

Keleş, Ö. *et al.* (2015) 'Effect of Porosity on Strength Distribution of Microcrystalline Cellulose', *AAPS PharmSciTech*. 2015/05/29, 16(6), pp. 1455–1464. doi: 10.1208/s12249-015-0325-x.

Kelly, J. and Wright, D. (2009) 'Administering medication to adult patients with dysphagia.', *Nursing standard (Royal College of Nursing (Great Britain): 1987)*, 23(29), pp. 62–68. doi: 10.7748/ns2009.03.23.29.62.c6928.

Ketterhagen, W. R. (2011) 'Modeling the motion and orientation of various pharmaceutical tablet shapes in a film coating pan using DEM', *International Journal of Pharmaceutics*, 409(1–2), pp. 137–149. doi: 10.1016/j.ijpharm.2011.02.045.

Khan, A. *et al.* (2019) 'Sintering technique: A novel approach for enhancing mechanical strength of tablets; formulation development and optimization of process variables', *Latin American Journal of Pharmacy*, 38(3), pp. 617–628. Available at: https://www.researchgate.net/publication/332570922_Sintering_Technique_A_Novel_Approach_for_Enhancing_Mechanical_Strength_of_Tablets_Formulation_Development_and_Optimization_of_Process_Variables (Accessed: 12 October 2020).

Khan, M. Z. I., Prebeg, Ž. and Kurjaković, N. (1999) 'A pH-dependent colon targeted oral drug delivery system using methacrylic acid copolymers: I. Manipulation of drug release using Eudragit® L100-55 and Eudragit® S100 combinations', *Journal of Controlled Release*, 58(2), pp. 215–222. doi: [https://doi.org/10.1016/S0168-3659\(98\)00151-5](https://doi.org/10.1016/S0168-3659(98)00151-5).

Khodaverdi, E. *et al.* (2012) 'Comparison of plasticizer effect on thermo-responsive properties of eudragit rs films', *AAPS PharmSciTech*, 13(3), pp. 1024–1030. doi: 10.1208/s12249-012-9827-y.

- Khomane, K. S. and Bansal, A. K. (2013) 'Effect of particle size on in-die and out-of-die compaction behavior of ranitidine hydrochloride polymorphs', *AAPS PharmSciTech*, 14(3), pp. 1169–1177. doi: 10.1208/s12249-013-0008-4.
- Khomane, K. S. and Bansal, A. K. (2014) 'Differential compaction behaviour of roller compacted granules of clopidogrel bisulphate polymorphs', *International Journal of Pharmaceutics*, 472(1), pp. 288–295. doi: <https://doi.org/10.1016/j.ijpharm.2014.06.040>.
- Kibria, G., Akhter, A. and Ariful Islam, K. (2010) 'Formulation and evaluation of domperidone pellets prepared by powder layering technology', *Asian Journal of Pharmaceutics*, 4(1), pp. 41–47. doi: 10.4103/0973-8398.63986.
- Kidokoro, M. *et al.* (2001) 'Properties of tablets containing granulations of ibuprofen and an acrylic copolymer prepared by thermal processes', *Pharmaceutical Development and Technology*, 6(2), pp. 263–275. doi: 10.1081/PDT-100002203.
- Kim, H. *et al.* (2018) 'Pharmacokinetic properties of acetyl tributyl citrate, a pharmaceutical excipient', *Pharmaceutics*, 10(4). doi: 10.3390/pharmaceutics10040177.
- Kim, H. K. *et al.* (2001) 'Determination of propranolol concentration in small volume of rat plasma by HPLC with fluorometric detection', *Biomedical Chromatography*, 15(8), pp. 539–545. doi: <https://doi.org/10.1002/bmc.110>.
- Kim, J. Y. and Ku, Y. S. (2000) 'Enhanced absorption of indomethacin after oral or rectal administration of a self-emulsifying system containing indomethacin to rats', *International Journal of Pharmaceutics*, 194(1), pp. 81–89. doi: [https://doi.org/10.1016/S0378-5173\(99\)00367-1](https://doi.org/10.1016/S0378-5173(99)00367-1).
- Kim, K. *et al.* (2010) 'Investigation of mechanical properties of soft hydrogel microcapsules in relation to protein delivery using a MEMS force sensor', *Journal of Biomedical Materials Research - Part A*, 92(1), pp. 103–113. doi: 10.1002/jbm.a.32338.
- Kiziltas, A. *et al.* (2014) 'Mechanical Properties of Microcrystalline Cellulose (MCC) Filled Engineering Thermoplastic Composites', *Journal of Polymers and the Environment*, 22(3), pp. 365–372. doi: 10.1007/s10924-014-0676-5.
- Kleinebudde, P. (1993) 'Application of low substituted hydroxypropylcellulose (L-HPC) in the production of pellets using extrusion/spheronization', *International Journal of Pharmaceutics*, 96(1–3), pp. 119–128. doi: 10.1016/0378-5173(93)90219-6.
- Klevan, I. (2011) 'Compression Analysis of Pharmaceutical Powders : Assessment of

Mechanical Properties and Tablet Manufacturability Prediction’.

Klose, D. *et al.* (2006) ‘How porosity and size affect the drug release mechanisms from PLIGA-based microparticles’, *International journal of pharmaceutics*, 314, pp. 198–206. doi: 10.1016/j.ijpharm.2005.07.031.

Kojima, Y. *et al.* (2013) ‘Effects of spray drying process parameters on the solubility behavior and physical stability of solid dispersions prepared using a laboratory-scale spray dryer’, *Drug Development and Industrial Pharmacy*, 39(9), pp. 1484–1493. doi: 10.3109/03639045.2012.692378.

Kondo, K. *et al.* (2013) ‘Design of sustained release fine particles using two-step mechanical powder processing: Particle shape modification of drug crystals and dry particle coating with polymer nanoparticle agglomerate’, *International Journal of Pharmaceutics*, 453(2), pp. 523–532. doi: 10.1016/j.ijpharm.2013.06.028.

Koner, J. S. *et al.* (2019) ‘Conceptualisation, Development, Fabrication and In Vivo Validation of a Novel Disintegration Tester for Orally Disintegrating Tablets’, *Scientific Reports*, 9(1), pp. 1–9. doi: 10.1038/s41598-019-48859-x.

KOO, O. M. Y. and HENG, P. W. S. (2001) ‘The Influence of Microcrystalline Cellulose Grade on Shape and Shape Distributions of Pellets Produced by Extrusion-Spheronization’, *Chemical and Pharmaceutical Bulletin*, 49(11), pp. 1383–1387. doi: 10.1248/cpb.49.1383.

Kováčik, J. (1999) ‘Correlation between Young’s Modulus and Porosity in Porous Materials’, *Journal of Materials Science Letters*, 18, pp. 1007–1010. doi: 10.1023/A:1006669914946.

Kraciuk, R. and Sznitowska, M. (2011) ‘Effect of different excipients on the physical characteristics of granules and tablets with carbamazepine prepared with polyethylene glycol 6000 by fluidized hot-melt granulation (FHMg)’, *AAPS PharmSciTech*, 12(4), pp. 1241–1247. doi: 10.1208/s12249-011-9698-7.

Kraisit, P. *et al.* (2017) ‘Preparation and characterization of hydroxypropyl methylcellulose/polycarbophil mucoadhesive blend films using a mixture design approach’, *Chemical and Pharmaceutical Bulletin*, 65(3), pp. 284–294. doi: 10.1248/cpb.c16-00849.

Kranz, H. *et al.* (2009) ‘Drug release from MCC- and carrageenan-based pellets: Experiment and theory’, *European Journal of Pharmaceutics and Biopharmaceutics*, 73(2), pp. 302–309. doi: <https://doi.org/10.1016/j.ejpb.2009.05.007>.

Krause, J. and Breitreutz, J. (2008) ‘Improving drug delivery in paediatric medicine’,

Pharmaceutical Medicine. Springer International Publishing, pp. 41–50. doi: 10.1007/BF03256681.

Krogars, K. *et al.* (2000) 'Extrusion–spheronization of pH-sensitive polymeric matrix pellets for possible colonic drug delivery', *International Journal of Pharmaceutics*, 199(2), pp. 187–194. doi: [https://doi.org/10.1016/S0378-5173\(00\)00382-3](https://doi.org/10.1016/S0378-5173(00)00382-3).

Krok, A. and Wu, C. Y. (2017) 'Finite element modeling of powder compaction', in *NATO Science for Peace and Security Series A: Chemistry and Biology*. Springer Verlag, pp. 451–462. doi: 10.1007/978-94-024-1117-1_28.

Krueger, C., Thommes, M. and Kleinebudde, P. (2013) 'Spheronisation mechanism of MCC II-based pellets', *Powder Technology*, 238, pp. 176–187. doi: <https://doi.org/10.1016/j.powtec.2011.12.052>.

Kubík, L. and Kažimírová, V. (2015) 'Mechanical properties of pellets in compression', *Research in Agricultural Engineering*, 61, pp. S1–S8. doi: 10.17221/17/2015-RAE.

Kudo, Y., Yasuda, M. and Matsusaka, S. (2020) 'Effect of particle size distribution on flowability of granulated lactose', *Advanced Powder Technology*, 31(1), pp. 121–127. doi: 10.1016/j.appt.2019.10.004.

Kuno, H. and Okada, J. (1982) 'The compaction process and deformability of granules', *Powder Technology*, 33(1), pp. 73–79. doi: [https://doi.org/10.1016/0032-5910\(82\)85040-7](https://doi.org/10.1016/0032-5910(82)85040-7).

Kuriyama, A. and Ozaki, Y. (2014) 'Assessment of active pharmaceutical ingredient particle size in tablets by Raman chemical imaging validated using polystyrene microsphere size standards', *AAPS PharmSciTech*, 15(2), pp. 375–387. doi: 10.1208/s12249-013-0064-9.

Kuselman, I. and Pennechi, F. (2016) 'IUPAC/CITAC Guide: Classification, modeling and quantification of human errors in a chemical analytical laboratory (IUPAC Technical Report)', *Pure and Applied Chemistry*, 88(5), pp. 477–515. doi: 10.1515/pac-2015-1101.

Kusumawati, R., Basmal, J. and Utomo, B. (2018) 'Characteristics of Sodium Alginate Extracted from *Turbinaria* sp. and *Sargassum* sp.', *Squalen Bulletin of Marine and Fisheries Postharvest and Biotechnology*, 13, p. 79. doi: 10.15578/squalen.v13i2.297.

Labani, M. M. *et al.* (2013) 'Evaluation of pore size spectrum of gas shale reservoirs using low pressure nitrogen adsorption, gas expansion and mercury porosimetry: A case study from the Perth and Canning Basins, Western Australia', *Journal of Petroleum Science and Engineering*, 112, pp. 7–16. doi:

<https://doi.org/10.1016/j.petrol.2013.11.022>.

Labouffie, F. *et al.* (2013) 'Effect of the plasticizer on permeability, mechanical resistance and thermal behaviour of composite coating films', *Powder Technology*, 238, pp. 14–19. doi: 10.1016/j.powtec.2012.07.035.

De Lange, M. F. *et al.* (2014) 'Adsorptive characterization of porous solids: Error analysis guides the way', *Microporous and Mesoporous Materials*, 200, pp. 199–215. doi: <https://doi.org/10.1016/j.micromeso.2014.08.048>.

Lapham, D. P. and Lapham, J. L. (2019) 'BET surface area measurement of commercial magnesium stearate by krypton adsorption in preference to nitrogen adsorption', *International Journal of Pharmaceutics*, 568, p. 118522. doi: 10.1016/j.ijpharm.2019.118522.

Lassalle, V. and Ferreira, M. L. (2007) 'PLA nano- and microparticles for drug delivery: An overview of the methods of preparation', *Macromolecular Bioscience*, pp. 767–783. doi: 10.1002/mabi.200700022.

Lau, C. L. S. *et al.* (2014) 'The evolution of pellet size and shape during spheronisation of an extruded microcrystalline cellulose paste', *Chemical Engineering Research and Design*, 92(11), pp. 2413–2424. doi: 10.1016/j.cherd.2014.01.018.

Lawson, L. (2008) 'DEVELOPMENT AND VALIDATION OF A COMBINED METHOD FOR QUANTITATIVE DETERMINATION OF DISSOLUTION, ASSAY, AND CONTENT UNIFORMITY IN BISOPROLOL FUMARATE/HYDROCHLOROTHIAZIDE TABLETS USING HPLC AND UPLC', *Department of chemistry and Biochemistry*, 2(2018–6219), pp. 1–124.

Leane, M. *et al.* (2015) 'A proposal for a drug product Manufacturing Classification System (MCS) for oral solid dosage forms', *Pharmaceutical Development and Technology*, pp. 12–21. doi: 10.3109/10837450.2014.954728.

Lechanteur, A. and Evrard, B. (2020) 'Influence of composition and spray-drying process parameters on carrier-free DPI properties and behaviors in the lung: A review', *Pharmaceutics*. MDPI AG. doi: 10.3390/pharmaceutics12010055.

Lee, D. W. *et al.* (2003) 'Preparation and release characteristics of polymer-coated and blended alginate microspheres', *Journal of Microencapsulation*, 20(2), pp. 179–192. doi: 10.3109/02652040309178060.

Lee, E. H. (2014) 'A practical guide to pharmaceutical polymorph screening & selection', *Asian Journal of Pharmaceutical Sciences*, 9(4), pp. 163–175. doi: <https://doi.org/10.1016/j.ajps.2014.05.002>.

- Lee, K. and Mooney, D. (2012) 'Alginate: Properties and biomedical applications', *Progress in polymer science*, 37, pp. 106–126. doi: 10.1016/j.progpolymsci.2011.06.003.
- Lee, S.-W., Kim, M.-H. and Kim, C.-K. (1999) 'Encapsulation of ethanol by spray drying technique: effects of sodium lauryl sulfate', *International Journal of Pharmaceutics*, 187(2), pp. 193–198. doi: [https://doi.org/10.1016/S0378-5173\(99\)00185-4](https://doi.org/10.1016/S0378-5173(99)00185-4).
- Lengyel, M. *et al.* (2019) 'Microparticles, microspheres, and microcapsules for advanced drug delivery', *Scientia Pharmaceutica*. doi: 10.3390/scipharm87030020.
- Lesellier, E. and Tchaplal, A. (2005) 'A simple subcritical chromatographic test for an extended ODS high performance liquid chromatography column classification', *Journal of Chromatography A*, 1100(1), pp. 45–59. doi: <https://doi.org/10.1016/j.chroma.2005.09.016>.
- Li, C. *et al.* (2015) 'Mechanical and thermal properties of microcrystalline cellulose-reinforced soy protein isolate-gelatin eco-friendly films', *RSC Advances*, 5(70), pp. 56518–56525. doi: 10.1039/c5ra04365d.
- Li, F. Q. *et al.* (2011) 'A novel spray-dried nanoparticles-in-microparticles system for formulating scopolamine hydrobromide into orally disintegrating tablets.', *International journal of nanomedicine*, 6, pp. 897–904. doi: 10.2147/ijn.s17900.
- Li, G. U. (2006) *STUDIES ON SPHERONIZATION PROCESSES BY ROTARY AND EXTRUSION*.
- Li, H. (2005) *Impact of cohesion forces on particle mixing and segregation*.
- Li, J. and Wu, Y. M. (2014) 'Lubricants in Pharmaceutical Solid Dosage Forms', *Lubricants*, 2, pp. 21–43. doi: 10.3390/lubricants2010021.
- Li, X. *et al.* (2016) 'Preparation of co-spray dried cushioning agent containing stearic acid for protecting pellet coatings when compressed', *Drug Development and Industrial Pharmacy*, 42(5), pp. 788–795. doi: 10.3109/03639045.2015.1075034.
- Lim, H. and Hoag, S. W. (2013a) 'Plasticizer effects on physical-mechanical properties of solvent cast Soluplus® films', *AAPS PharmSciTech*, 14(3), pp. 903–910. doi: 10.1208/s12249-013-9971-z.
- Lim, H. and Hoag, S. W. (2013b) 'Plasticizer effects on physical-mechanical properties of solvent cast Soluplus® films', *AAPS PharmSciTech*, 14(3), pp. 903–910. doi: 10.1208/s12249-013-9971-z.
- Lin, S. Y., Liao, C. M. and Hsiue, G. H. (1995) 'A reflectance FTIR/DSC microspectroscopic study of the nonisothermal kinetics of anhydride formation in

Eudragit L-100 films', *Polymer Degradation and Stability*, 47(2), pp. 299–303. doi: 10.1016/0141-3910(94)00129-V.

Lin, X. *et al.* (2011) 'Development of potential novel cushioning agents for the compaction of coated multi-particulates by co-processing micronized lactose with polymers', *European Journal of Pharmaceutics and Biopharmaceutics*, 79(2), pp. 406–415. doi: <https://doi.org/10.1016/j.ejpb.2011.03.024>.

Lindgren, S. and Janzon, L. (1991) 'Prevalence of swallowing complaints and clinical findings among 50-79-year-old men and women in an urban population', *Dysphagia*, 6(4), pp. 187–192. doi: 10.1007/BF02493524.

Listiohadi, Y. *et al.* (2009) 'Thermal analysis of amorphous lactose and σ -lactose monohydrate', *Dairy Science and Technology*, 89(1), pp. 43–67. doi: 10.1051/dst:2008027.

Liu, B. *et al.* (2014) 'Effect of moisture content on static compressive elasticity modulus of concrete', *Construction and Building Materials*, 69, pp. 133–142. doi: 10.1016/j.conbuildmat.2014.06.094.

Liu, K. S. (2009) 'Some factors affecting sieving performance and efficiency', *Powder Technology*, 193(2), pp. 208–213. doi: 10.1016/j.powtec.2009.03.027.

Liu, L. X. *et al.* (2008) 'Effect of particle properties on the flowability of ibuprofen powders', *International Journal of Pharmaceutics*, 362(1), pp. 109–117. doi: <https://doi.org/10.1016/j.ijpharm.2008.06.023>.

Loh, Z. H., Samanta, A. K. and Sia Heng, P. W. (2014) 'Overview of milling techniques for improving the solubility of poorly water-soluble drugs', *Asian Journal of Pharmaceutical Sciences*. Shenyang Pharmaceutical University, pp. 255–274. doi: 10.1016/j.ajps.2014.12.006.

Lommen, S., Schott, D. and Lodewijks, G. (2014) 'DEM speedup: Stiffness effects on behavior of bulk material', *Particuology*, 12, pp. 107–112. doi: <https://doi.org/10.1016/j.partic.2013.03.006>.

Lordi, N. and Shiromani, P. (2008) 'Use of sorption isotherms to study the effect of moisture on the hardness of aged compacts', *Drug Development and Industrial Pharmacy*, 9(8), pp. 1399–1416. doi: 10.3109/03639048309052384.

Lou, H. *et al.* (2014) 'Evaluation of Chlorpheniramine Maleate microparticles in orally disintegrating film and orally disintegrating tablet for pediatrics', *Drug Development and Industrial Pharmacy*, 40(7), pp. 910–918. doi: 10.3109/03639045.2013.789907.

Łunio, R. *et al.* (2008) 'Compressibility of gastroretentive pellets coated with Eudragit

NE using a single-stroke and a rotary tablet press', *Pharmaceutical Development and Technology*, 13(4), pp. 323–331. doi: 10.1080/10837450802089206.

Lustig-Gustafsson, C. *et al.* (1999) 'The influence of water content and drug solubility on the formulation of pellets by extrusion and spheronisation', *European Journal of Pharmaceutical Sciences*, 8(2), pp. 147–152. doi: 10.1016/S0928-0987(99)00004-4.

M. Zhang, X.K. Li, D.I. Wilson, T.T. Yao, Y. Y. Z. (2018) 'Influence.pdf'.

Ma, X. *et al.* (2018) 'Effect of sorbitol content on microstructure and thermal properties of chitosan films', *International Journal of Biological Macromolecules*, 119, pp. 1294–1297. doi: 10.1016/j.ijbiomac.2018.08.060.

Maejima, T. and McGinity, J. W. (2001) 'Influence of film additives on stabilizing drug release rates from pellets coated with acrylic polymers', *Pharmaceutical Development and Technology*, 6(2), pp. 211–221. doi: 10.1081/PDT-100002197.

Maganti, L. and Çelik, M. (1994) 'Compaction studies on pellets: II. Coated pellets', *International Journal of Pharmaceutics*, 103(1), pp. 55–67. doi: [https://doi.org/10.1016/0378-5173\(94\)90203-8](https://doi.org/10.1016/0378-5173(94)90203-8).

Mahmoodi, F. (2012) *Compression Mechanics of Powders and Granular Materials Probed by Force Distributions and a Micromechanically Based Compaction Equation*. Acta Universitatis Upsaliensis.

Malamatari, M. *et al.* (2020) 'Spray drying for the preparation of nanoparticle-based drug formulations as dry powders for inhalation', *Processes*, 8(7), p. 788. doi: 10.3390/pr8070788.

Malik, D. J. *et al.* (2017) 'Formulation, stabilisation and encapsulation of bacteriophage for phage therapy', *Advances in Colloid and Interface Science*, 249, pp. 100–133. doi: <https://doi.org/10.1016/j.cis.2017.05.014>.

Mallick, S. *et al.* (2011) 'Study of particle rearrangement, compression behaviour and dissolution properties after melt dispersion of ibuprofen, Avicel and Aerosil', *Results in Pharma Sciences*, 1(1), pp. 1–10. doi: 10.1016/j.rinphs.2011.05.003.

Malvern Panalytical (2015) 'Changing the Properties of Particles to Control Their Rheology', *AZO Materials*, pp. 1–10. Available at: <https://www.azom.com/article.aspx?ArticleID=12304> (Accessed: 15 April 2021).

Malvern Panalytical (2019) *Mastersizer laser diffraction particle size analyzers*. Available at: <https://www.microtrac.com/knowledge/laser-diffraction/> (Accessed: 6 April 2021).

Manda, A., Walker, R. B. and Khamanga, S. M. M. (2019) 'An artificial neural network

approach to predict the effects of formulation and process variables on prednisone release from a multipartite system', *Pharmaceutics*, 11(3), p. 109. doi: 10.3390/pharmaceutics11030109.

Marczewska, I., Rojek, J. and Kačianauskas, R. (2016) 'Investigation of the effective elastic parameters in the discrete element model of granular material by the triaxial compression test', *Archives of Civil and Mechanical Engineering*, 16(1), pp. 64–75. doi: 10.1016/j.acme.2015.09.010.

Martin, L. R. *et al.* (2005) 'The challenge of patient adherence', *Therapeutics and clinical risk management*, 1(3), pp. 189–199. Available at: <https://pubmed.ncbi.nlm.nih.gov/18360559>.

Mathkar, S. *et al.* (2009) 'The use of differential scanning calorimetry for the purity verification of pharmaceutical reference standards', *Journal of Pharmaceutical and Biomedical Analysis*, 49, pp. 627–631. doi: 10.1016/j.jpba.2008.12.030.

Mattsson, S. (2000) 'Pharmaceutical binders and their function in directly compressed tablets : Mechanistic studies on the effect of dry binders on mechanical strength, pore structure and disintegration of tablets'.

McCormick, D. (2005a) 'Evolutions in direct compression', *Pharmaceutical technology (2003)*, 29(4), pp. 52–62.

McCormick, D. (2005b) 'Evolutions in direct compression', *Pharmaceutical Technology*, 29(4), pp. 52–62.

Mehta, S. *et al.* (2012) 'Effect of disintegrants on the properties of multiparticulate tablets comprising starch pellets and excipient granules', *International Journal of Pharmaceutics*, 422(1), pp. 310–317. doi: <https://doi.org/10.1016/j.ijpharm.2011.11.017>.

Meka, V. *et al.* (2012) 'Development and validation of HPLC method for estimation of propranolol HCL in human plasma', *Journal of scientific and industrial research*, 71, pp. 120–123.

Menczel, J. D., & Prime, R. B. (Eds. . (2009) *Thermal analysis of polymers, Thermal analysis of polymers*. Available at: <https://www.wiley.com/engb/Thermal+Analysis+of+Polymers%3A+Fundamentals+and+Applications-p-9780471769170>.

Meng, X. *et al.* (2010) 'Chitosan and alginate polyelectrolyte complex membranes and their properties for wound dressing application', *Journal of Materials Science: Materials in Medicine*, 21(5), pp. 1751–1759. doi: 10.1007/s10856-010-3996-6.

Mettler-Toledo (2015) *Thermal Analysis Excellence Thermogravimetry for Routine Analysis*. Available at: http://my.mt.com/dam/Analytical/ThermalAnalysis/TA-PDF/TGA2_Broch_EN_30247078_V04.15_Original_38299.pdf (Accessed: 11 April 2021).

Mettler-Toledo (2019) 'Thermal Analysis Excellence Unvergleichliche DSC-Leistung', *Mettler-Toledo*, pp. 1–14. Available at: https://www.mt.com/dam/non-indexed/po/ana/thermal-analysis/brochures/30250327B_V03.19_BR_Compotence_STAR_en_LR.pdf (Accessed: 11 April 2021).

Meyer A.S. Hussain, R. J. (2005) 'Awareness topic: Mitigating the risks of ethanol induced dose dumping from oral sustained/controlled release dosage forms', in *ACPS Meeting October*. Available at: <http://www.fda.gov/cder/guidance/5194fnl.pdf> (Accessed: 5 May 2021).

Mezhericher, M., Levy, A. and Borde, I. (2010) 'Theoretical Models of Single Droplet Drying Kinetics: A Review', *Drying Technology*, 28(2), pp. 278–293. doi: 10.1080/07373930903530337.

Michie, H., Podczek, F. and Newton, J. M. (2012) 'The influence of plate design on the properties of pellets produced by extrusion and spheronization', *International Journal of Pharmaceutics*, 434(1), pp. 175–182. doi: <https://doi.org/10.1016/j.ijpharm.2012.05.050>.

Michrafy, A., Ringenbacher, D. and Tchoreloff, P. (2002) 'Modelling the compaction behaviour of powders: Application to pharmaceutical powders', *Powder Technology*, 127(3), pp. 257–266. doi: 10.1016/S0032-5910(02)00119-5.

Miles, S. (2007) 'Ketoprofen', in Enna, S. J. and Bylund, D. B. (eds) *xPharm: The Comprehensive Pharmacology Reference*. New York: Elsevier, pp. 1–7. doi: <https://doi.org/10.1016/B978-008055232-3.61984-1>.

Miyazaki, K. (2000) 'GLYCOPROTEINS: LIQUID CHROMATOGRAPHY', in Wilson, I. D. B. T.-E. of S. S. (ed.). Oxford: Academic Press, pp. 2960–2965. doi: <https://doi.org/10.1016/B0-12-226770-2/06321-3>.

Malacker, S. *et al.* (2016) 'Laser and light-based treatments of venous lakes: a literature review', *Lasers in Medical Science*, 31(7), pp. 1511–1519. doi: 10.1007/s10103-016-1934-7.

Mohammadi, G. *et al.* (2019) 'Preparation and evaluation of Eudragit® L100 nanoparticles loaded impregnated with kt tromethamine loaded PVA-HEC insertions

for ophthalmic drug delivery', *Advanced Pharmaceutical Bulletin*, 9(4), pp. 593–600. doi: 10.15171/apb.2019.068.

Mohan, S. (2012) 'COMPRESSION PHYSICS OF PHARMACEUTICAL POWDERS: A REVIEW | INTERNATIONAL JOURNAL OF PHARMACEUTICAL SCIENCES AND RESEARCH', *INTERNATIONAL JOURNAL OF PHARMACEUTICAL SCIENCES AND RESEARCH*, 1580, pp. 3(6)-1580. Available at: <https://ijpsr.com/bft-article/compression-physics-of-pharmaceutical-powders-a-review/?view=fulltext> (Accessed: 30 April 2021).

Mohanty, C. and Subrahmanyam, K. V. (2017) 'Effect of sintering condition on physio-chemical parameters and drug release characteristics from polymeric matrix tablet of atenolol for controlled release', *International Journal of Pharmaceutical Sciences and Research*, 8(9), pp. 3758–3767. doi: 10.13040/IJPSR.0975-8232.8(9).3758-67.

Moharram, M. A. and Allam, M. A. (2007) 'Study of the interaction of poly(acrylic acid) and poly(acrylic acid-poly acrylamide) complex with bone powders and hydroxyapatite by using TGA and DSC', *Journal of Applied Polymer Science*, 105(6), pp. 3220–3227. doi: 10.1002/app.26267.

Moise, K. J. *et al.* (1988) 'Indomethacin in the Treatment of Premature Labor', *New England Journal of Medicine*, 319(6), pp. 327–331. doi: 10.1056/nejm198808113190602.

Moon, S. and Jang, J. (1999) 'Mechanical interlocking and wetting at the interface between argon plasma treated UHMPE fiber and vinylester resin', *Journal of Materials Science*, 34, pp. 4219–4224. doi: 10.1023/A:1004642500738.

Morin, G. and Briens, L. (2013) 'The effect of lubricants on powder flowability for pharmaceutical application', *AAPS PharmSciTech*, 14(3), pp. 1158–1168. doi: 10.1208/s12249-013-0007-5.

Morishige, K. (2016) 'Nature of adsorption hysteresis in cylindrical pores: Effect of pore corrugation', *Journal of Physical Chemistry C*, 120(39), pp. 22508–22514. doi: 10.1021/acs.jpcc.6b07764.

Morita, R., Honda, R. and Takahashi, Y. (2000) 'Development of oral controlled release preparations, a PVA swelling controlled release system (SCRS). I. Design of SCRS and its release controlling factor', *Journal of Controlled Release*, 63(3), pp. 297–304. doi: 10.1016/S0168-3659(99)00203-5.

Mudie, D. M. *et al.* (2020) 'A novel architecture for achieving high drug loading in amorphous spray dried dispersion tablets', *International Journal of Pharmaceutics: X*,

2. doi: 10.1016/j.ijpx.2020.100042.

Mühlenweg, H. and Dan Hirleman, E. (1998) 'Laser Diffraction Spectroscopy: Influence of Particle Shape and a Shape Adaptation Technique', *Particle and Particle Systems Characterization*, 15(4), pp. 163–169. doi: 10.1002/(SICI)1521-4117(199808)15:4<163::AID-PPSC163>3.0.CO;2-8.

Muley, S., Nandgude, T. and Poddar, S. (2016) 'Extrusion–spheronization a promising pelletization technique: In-depth review', *Asian Journal of Pharmaceutical Sciences*, 11(6), pp. 684–699. doi: 10.1016/j.ajps.2016.08.001.

Murphy, B. M., Prescott, S. W. and Larson, I. (2005) 'Measurement of lactose crystallinity using Raman spectroscopy', *Journal of Pharmaceutical and Biomedical Analysis*, 38(1), pp. 186–190. doi: <https://doi.org/10.1016/j.jpba.2004.12.013>.

Murthy Dwibhashyam, V. S. N. and Ratna, J. (2008) 'Key formulation variables in tableting of coated pellets', *Indian Journal of Pharmaceutical Sciences*. OMICS International, pp. 555–564. doi: 10.4103/0250-474X.45391.

Nachajski, M. J. *et al.* (2019) 'Effect of API on powder flowability, direct compression and properties of orally disintegrating tablets: A preformulation study', *Indian Journal of Pharmaceutical Sciences*, 81(3), pp. 489–495. doi: 10.36468/pharmaceutical-sciences.534.

Nadal, J. M. *et al.* (2016) 'Spray-dried Eudragit® L100 microparticles containing ferulic acid: Formulation, in vitro cytoprotection and in vivo anti-platelet effect', *Materials Science and Engineering C*, 64, pp. 318–328. doi: 10.1016/j.msec.2016.03.086.

Nalamachu, S. and Wortmann, R. (2014) 'Role of Indomethacin in Acute Pain and Inflammation Management: A Review of the Literature', *Postgraduate Medicine*, 126(4), pp. 92–97. doi: 10.3810/pgm.2014.07.2787.

Narayan, P. and Hancock, B. C. (2005) 'The influence of particle size on the surface roughness of pharmaceutical excipient compacts', *Materials Science and Engineering: A*, 407(1), pp. 226–233. doi: <https://doi.org/10.1016/j.msea.2005.06.060>.

Nasatto, P. L. *et al.* (2015) 'Methylcellulose, a cellulose derivative with original physical properties and extended applications', *Polymers*, 7(5), pp. 777–803. doi: 10.3390/polym7050777.

National Center For Biotechnological Information (202AD) *PubChem compound summary for CID3032552*, National Center for Biotechnology Information. Available at: <https://pubchem.ncbi.nlm.nih.gov/compound/Nitrogen-dioxide>.

National Center for Biotechnology information (2020) *PubChem Compound Summary*

for CID 5780, Sorbitol, 2020. Available at: <https://pubchem.ncbi.nlm.nih.gov/compound/Sorbitol> (Accessed: 1 September 2020).

Naveed, A. (2011) 'Pharmaceutical Microencapsulation Technology for Development of Controlled Release Drug Delivery systems'.

NCBI (2015) *PubChem Compound Summary for CID 14055602, Cellulose, microcrystalline.*, *PubChem*. doi: 23673837.

Nežić, I. *et al.* (2018) 'Production of stable amorphous form by means of spray drying', *Particulate Science and Technology*, 37, pp. 1–11. doi: 10.1080/02726351.2017.1417936.

Nguyen, C., Christensen, J. M. and Ayres, J. W. (2014) 'Compression of coated drug beads for sustained release tablet of glipizide: Formulation, and dissolution', *Pharmaceutical Development and Technology*, 19(1), pp. 10–20. doi: 10.3109/10837450.2012.751402.

NHS (2018) *Propranolol: medicine for migraine, anxiety and heart & blood pressure issues - NHS*. Available at: <https://www.nhs.uk/medicines/propranolol/> (Accessed: 20 April 2021).

Nokhodchi, A. *et al.* (2005) 'The effect of type and concentration of vehicles on the dissolution rate of a poorly soluble drug (indomethacin) from liquisolid compacts', *Journal of Pharmacy and Pharmaceutical Sciences*, 8(1), pp. 18–25. Available at: www.cspscanada.org (Accessed: 16 July 2020).

Nokhodchi, A. *et al.* (2012) 'The role of oral controlled release matrix tablets in drug delivery systems', *BioImpacts*, 2(4), pp. 175–187. doi: 10.5681/bi.2012.027.

NOKHODCHI, A. L. I. *et al.* (1996) 'The Effect of Moisture on the Heckel and Energy Analysis of Hydroxypropylmethylcellulose 2208 (HPMC K4M)', *Journal of Pharmacy and Pharmacology*, 48(11), pp. 1122–1127. doi: <https://doi.org/10.1111/j.2042-7158.1996.tb03906.x>.

Nolan, L. M. *et al.* (2011) 'Particle engineering of materials for oral inhalation by dry powder inhalers. II - Sodium cromoglicate', *International Journal of Pharmaceutics*, 405(1–2), pp. 36–46. doi: 10.1016/j.ijpharm.2010.11.040.

Nordström, J. *et al.* (2013) 'The degree of compression of spherical granular solids controls the evolution of microstructure and bond probability during compaction', *International Journal of Pharmaceutics*, 442(1–2), pp. 3–12. doi: 10.1016/j.ijpharm.2012.08.011.

Noronha, C. M. *et al.* (2014) 'Characterization of antioxidant methylcellulose film

incorporated with α -tocopherol nanocapsules', *Food Chemistry*, 159, pp. 529–535. doi: <https://doi.org/10.1016/j.foodchem.2014.02.159>.

Nováková, L. *et al.* (2005) 'Development and validation of HPLC method for determination of indomethacin and its two degradation products in topical gel', *Journal of Pharmaceutical and Biomedical Analysis*, 37(5), pp. 899–905. doi: <https://doi.org/10.1016/j.jpba.2004.09.012>.

Novakovic, D. *et al.* (2018) 'Understanding Dissolution and Crystallization with Imaging: A Surface Point of View', *Molecular Pharmaceutics*, 15(11), pp. 5361–5373. doi: [10.1021/acs.molpharmaceut.8b00840](https://doi.org/10.1021/acs.molpharmaceut.8b00840).

Nyembwe, A. M., Cromarty, R. D. and Garbers-Craig, A. M. (2019) 'Simulation of the pressure drop across granulated mixtures using a coupled DEM – CFD model', *Advanced Powder Technology*, 30(1), pp. 85–97. doi: [10.1016/j.appt.2018.10.010](https://doi.org/10.1016/j.appt.2018.10.010).

Ogolo, N. A. *et al.* (2015) 'Effect of Grain Size on Porosity Revisited', *SPE Nigeria Annual International Conference and Exhibition*. Lagos, Nigeria: Society of Petroleum Engineers, p. 14. doi: [10.2118/178296-MS](https://doi.org/10.2118/178296-MS).

Ohrem, H. L. *et al.* (2014) 'Why is mannitol becoming more and more popular as a pharmaceutical excipient in solid dosage forms?', *Pharmaceutical Development and Technology*, 19(3), pp. 257–262. doi: [10.3109/10837450.2013.775154](https://doi.org/10.3109/10837450.2013.775154).

Ohshima, H. and Makino, K. (2014) *Colloid and Interface Science in Pharmaceutical Research and Development*, *Colloid and Interface Science in Pharmaceutical Research and Development*. Elsevier Inc. doi: [10.1016/C2012-0-00845-9](https://doi.org/10.1016/C2012-0-00845-9).

Okada, N. *et al.* (2016) 'Mechanical Stress Simulation of Scored Tablets Based on the Finite Element Method and Experimental Verification', *CHEMICAL & PHARMACEUTICAL BULLETIN*, 64, pp. 1142–1148. doi: [10.1248/cpb.c16-00177](https://doi.org/10.1248/cpb.c16-00177).

Oliveira, R. *et al.* (2015) 'Synthesis and Characterization of Methylcellulose Produced from Bacterial Cellulose under Heterogeneous Condition', *Journal of the Brazilian Chemical Society*, 26. doi: [10.5935/0103-5053.20150163](https://doi.org/10.5935/0103-5053.20150163).

Oluwabukola, M. and Cheng Shu, C. (2015) 'Silicified microcrystalline cellulose based pellets and their physico-chemical properties', 133, pp. 1–16.

Organization, W. H. (2012a) 'BULK DENSITY AND TAPPED DENSITY OF POWDERS Final text for addition to The International Pharmacopoeia', pp. 1–6. doi: [10.1007/s13398-014-0173-7.2](https://doi.org/10.1007/s13398-014-0173-7.2).

Organization, W. H. (2012b) 'BULK DENSITY AND TAPPED DENSITY OF POWDERS Final text for addition to The International Pharmacopoeia', pp. 1–6.

- Osei-Yeboah, F., Chang, S.-Y. and Sun, C. C. (2016) 'A critical Examination of the Phenomenon of Bonding Area - Bonding Strength Interplay in Powder Tableting', *Pharmaceutical Research*, 33(5), pp. 1126–1132. doi: 10.1007/s11095-016-1858-8.
- Osei-Yeboah, F., Lan, Y. and Sun, C. C. (2017) 'A top coating strategy with highly bonding polymers to enable direct tableting of multiple unit pellet system (MUPS)', *Powder Technology*, 305, pp. 591–596. doi: <https://doi.org/10.1016/j.powtec.2016.10.039>.
- Otero-Espinar, F. J., Luzardo-Alvarez, A. and Blanco-Méndez, J. (2010) 'Non-MCC materials as extrusion-spheronization aids in pellets production', *Journal of Drug Delivery Science and Technology*, pp. 303–318. doi: 10.1016/S1773-2247(10)50047-9.
- Pai, R., Kohli, K. and Shrivastava, B. (2012) 'Compression and evaluation of extended release matrix pellets prepared by the extrusion/spheronization process into disintegrating tablets', *Brazilian Journal of Pharmaceutical Sciences*, 48(1), pp. 117–129. doi: 10.1590/S1984-82502012000100014.
- Pai, S. and Sawant, N. (2017) 'Applications of New Validated RP-HPLC Method for Determination of Indomethacin and its Hydrolytic Degradants using Sodium Acetate Buffer', *Indian Journal of Pharmaceutical Education and Research*, 51, pp. 388–392. doi: 10.5530/ijper.51.3.65.
- Paluch, K. J. *et al.* (2013) 'Impact of alternative solid state forms and specific surface area of high-dose, hydrophilic active pharmaceutical ingredients on tableability', *Molecular Pharmaceutics*, 10(10), pp. 3628–3639. doi: 10.1021/mp400124z.
- Pantaleev, S. *et al.* (2017) 'An experimentally validated DEM study of powder mixing in a paddle blade mixer', *Powder Technology*, 311, pp. 287–302. doi: <https://doi.org/10.1016/j.powtec.2016.12.053>.
- Panthi, S. K. *et al.* (2007) 'An analysis of springback in sheet metal bending using finite element method (FEM)', *Journal of Materials Processing Technology*, 186(1), pp. 120–124. doi: <https://doi.org/10.1016/j.jmatprotec.2006.12.026>.
- Papavasileiou, V. *et al.* (2007) 'Optimize manufacturing of pharmaceutical products with process simulation and production scheduling tools', *Chemical Engineering Research and Design*, 85(7 A), pp. 1086–1097. doi: 10.1205/cherd06240.
- Papich, M. G. and Martinez, M. N. (2015) 'Applying Biopharmaceutical Classification System (BCS) Criteria to Predict Oral Absorption of Drugs in Dogs: Challenges and Pitfalls', *AAPS Journal*, 17(4), pp. 948–964. doi: 10.1208/s12248-015-9743-7.

Parikh, T. *et al.* (2014) 'Investigation of thermal and viscoelastic properties of polymers relevant to hot melt extrusion - III: Polymethacrylates and polymethacrylic acid based polymers', *Journal of Excipients and Food Chemicals*, 5, pp. 56–64.

Park, H. J. *et al.* (2016) 'Multiple-unit tablet of probiotic bacteria for improved storage stability, acid tolerability, and in vivo intestinal protective effect', *Drug Design, Development and Therapy*, 10, pp. 1355–1364. doi: 10.2147/DDDT.S103894.

Particle Analytical - Analysis for the Pharmaceutical Industry (2020) *BET (Brunauer, Emmett and Teller) | Particle Analytical*. Available at: <https://particle.dk/methods-analytical-laboratory/surface-area-bet-2/> (Accessed: 18 November 2020).

Patel, A. *et al.* (2015) 'DEVELOPMENT AND OPTIMIZATION OF EFFERVESCENT TABLETS OF PROMETHAZINE', *International Journal of Pharmaceutical Sciences and Research*, 6, pp. 5077–5084. doi: 10.13040/IJPSR.0975-8232.6(12).5077-84.

Patel, B. B. *et al.* (2015) 'Revealing facts behind spray dried solid dispersion technology used for solubility enhancement', *Saudi Pharmaceutical Journal*, 23(4), pp. 352–365. doi: <https://doi.org/10.1016/j.jsps.2013.12.013>.

Patel, H. P. *et al.* (2010) 'Pellets: A general overview', *International Journal of Current Research and Review*, 2(6), pp. 21–31. Available at: www.ijcrr.com (Accessed: 25 October 2020).

Patel, Hetal *et al.* (2016) 'Dissolution rate improvement of telmisartan through modified MCC pellets using 32 full factorial design', *Saudi Pharmaceutical Journal*, 24(5), pp. 579–587. doi: 10.1016/j.jsps.2015.03.007.

Patel, R. P., Patel, M. P. and Suthar, A. M. (2009) 'Spray drying technology: An overview', *Indian Journal of Science and Technology*, 2(10), pp. 44–47. doi: 10.17485/ijst/2009/v2i10/30719.

Patil, H. G. *et al.* (2016) 'Formulation and development of orodispersible sustained release tablet of domperidone', *Drug Development and Industrial Pharmacy*, 42(6), pp. 906–915. doi: 10.3109/03639045.2015.1088864.

Patra, C. N. *et al.* (2017) 'Pharmaceutical significance of Eudragit: A review', *Future Journal of Pharmaceutical Sciences*, 3(1), pp. 33–45. doi: 10.1016/j.fjps.2017.02.001.

Patterson, J. E. *et al.* (2007) 'Preparation of glass solutions of three poorly water soluble drugs by spray drying, melt extrusion and ball milling', *International Journal of Pharmaceutics*, 336(1), pp. 22–34. doi: <https://doi.org/10.1016/j.ijpharm.2006.11.030>.

Paul, S. *et al.* (2019) 'Tableting performance of various mannitol and lactose grades assessed by compaction simulation and chemometrical analysis', *International*

Journal of Pharmaceutics, 566, pp. 24–31. doi: <https://doi.org/10.1016/j.ijpharm.2019.05.030>.

Payne, R. S. *et al.* (1996) 'The mechanical properties of two forms of primidone predicted from their crystal structures', *International Journal of Pharmaceutics*, 145(1), pp. 165–173. doi: [https://doi.org/10.1016/S0378-5173\(96\)04760-6](https://doi.org/10.1016/S0378-5173(96)04760-6).

Pearnchob, N. and Bodmeier, R. (2003) 'Dry polymer powder coating and comparison with conventional liquid-based coatings for Eudragit® RS, ethylcellulose and shellac', *European Journal of Pharmaceutics and Biopharmaceutics*, 56(3), pp. 363–369. doi: [https://doi.org/10.1016/S0939-6411\(03\)00121-8](https://doi.org/10.1016/S0939-6411(03)00121-8).

Peponi, L. *et al.* (2017) 'Smart Polymers', in, pp. 131–154. doi: 10.1016/B978-0-323-44353-1.00006-3.

Persson, A.-S. *et al.* (2016) 'Compression analysis for assessment of pellet plasticity: Identification of reactant pores and comparison between Heckel, Kawakita, and Adams equations', *Chemical Engineering Research and Design*, 110, pp. 183–191. doi: <https://doi.org/10.1016/j.cherd.2016.01.028>.

Petean, P. G. C. and Aguiar, M. L. (2015) 'Determining the adhesion force between particles and rough surfaces', *Powder Technology*, 274, pp. 67–76. doi: 10.1016/j.powtec.2014.12.047.

Phale, M. D. and Gothoskar, A. V (2011) 'Multiunit particulate systems: A current drug-delivery technology', *Pharmaceutical Technology*, 35(7), pp. 60–66.

Pharmacopoeia, E. (2005) '2.9.26. specific surface area by gas adsorption', *Pharmacopoeia, European*, (1). Available at: http://202.195.214.45/yaodian/ep/EP501E/02_methods_of_analysis/2.9._pharmaceutical_technical_procedures/2.9.26._specific_surface_area_by_gas_adsorption/20926e.pdf (Accessed: 25 May 2021).

Pharmacopoeia, E. (2013) *European Pharmacopoeia 7.0, European Pharmacopoeia 8.0*. Available at: <https://www.edqm.eu/%0Ahttp://www.fptl.ru/biblioteka/farmacop/EP-7.0-2.pdf> (Accessed: 1 May 2021).

Phillips, E. M. (1997) 'An approach to estimate the amorphous content of pharmaceutical powders using calorimetry with no calibration standards', *International Journal of Pharmaceutics*, 149(2), pp. 267–271. doi: [https://doi.org/10.1016/S0378-5173\(96\)04812-0](https://doi.org/10.1016/S0378-5173(96)04812-0).

Picker, K. M. and Hoag, S. W. (2002) 'Characterization of the thermal properties of microcrystalline cellulose by modulated temperature differential scanning calorimetry',

Journal of Pharmaceutical Sciences, 91(2), pp. 342–349. doi: 10.1002/jps.10018.

Pietiläinen, J. (2013) 'Spray Drying Particles from Ethanol-Water Mixtures Intended for Inhalation', p. 97.

Pitt, K. G. and Heasley, M. G. (2013) 'Determination of the tensile strength of elongated tablets', *Powder Technology*, 238, pp. 169–175. doi: <https://doi.org/10.1016/j.powtec.2011.12.060>.

Podczek, F. and Newton, J. M. (2014) 'Influence of the standing time of the extrudate and speed of rotation of the spheroniser plate on the properties of pellets produced by extrusion and spheronization', *Advanced Powder Technology*, 25(2), pp. 659–665. doi: <https://doi.org/10.1016/j.appt.2013.10.011>.

Porter, S., Sackett, G. and Liu, L. (2017) 'Chapter 34 - Development, Optimization, and Scale-Up of Process Parameters: Pan Coating', in Qiu, Y. et al. (eds). Boston: Academic Press, pp. 953–996. doi: <https://doi.org/10.1016/B978-0-12-802447-8.00034-0>.

Prajapati, B., Krunal, P. and Patel, R. (2010) 'Design and in vitro evaluation of novel Nicorandil sustained release matrix tablets based on combination of hydrophilic and hydrophobic matrix system', *International Journal of Pharmaceutical Sciences Review and Research*, 1.

Pretorius, E. and Bouic, P. J. D. (2009) 'Permeation of four oral drugs through human intestinal mucosa', *AAPS PharmSciTech*, 10(1), pp. 270–275. doi: 10.1208/s12249-009-9207-4.

PubChem (2021) *Methylcellulose | C29H54O16 - PubChem, PubChem*. Available at: <https://pubchem.ncbi.nlm.nih.gov/compound/44263857> (Accessed: 13 April 2021).

Pyramides, G., Robinson, J. W. and William Zito, S. (1995) 'The combined use of DSC and TGA for the thermal analysis of atenolol tablets', *Journal of Pharmaceutical and Biomedical Analysis*, 13(2), pp. 103–110. doi: [https://doi.org/10.1016/0731-7085\(94\)00112-F](https://doi.org/10.1016/0731-7085(94)00112-F).

Qiao, M. et al. (2010) 'Sustained release coating of tablets with Eudragit® RS/RL using a novel electrostatic dry powder coating process', *International Journal of Pharmaceutics*, 399(1–2), pp. 37–43. doi: 10.1016/j.ijpharm.2010.07.047.

Quinten, T. et al. (2012) 'Preparation and evaluation of sustained-release matrix tablets based on metoprolol and an acrylic carrier using injection moulding', *AAPS PharmSciTech*, 13(4), pp. 1197–1211. doi: 10.1208/s12249-012-9848-6.

Ragnarsson, G. et al. (2008) 'Development of A New Controlled Release Metoprolol

Product', *Drug Development and Industrial Pharmacy*, 13, pp. 1495–1509. doi: 10.3109/03639048709068677.

Rahim, S. A., Carter, P. A. and Elkordy, A. A. (2015) 'Design and evaluation of effervescent floating tablets based on hydroxyethyl cellulose and sodium alginate using pentoxifylline as a model drug', *Drug Design, Development and Therapy*, 9, pp. 1843–1857. doi: 10.2147/DDDT.S78717.

Rahman, M. and Brazel, C. S. (2004) 'The plasticizer market: an assessment of traditional plasticizers and research trends to meet new challenges', *Progress in Polymer Science*, 29(12), pp. 1223–1248. doi: <https://doi.org/10.1016/j.progpolymsci.2004.10.001>.

Raja, P. M. V. and Barron, A. R. (2019) 2 .3: *BET Surface Area Analysis of Nanoparticles*, *Physical Methods in Chemistry and Nano Science*. Available at: [https://chem.libretexts.org/Bookshelves/Analytical_Chemistry/Book%3A_Physical_Methods_in_Chemistry_and_Nano_Science_\(Barron\)/02%3A_Physical_and_Thermal_Analysis/2.03%3A_BET_Surface_Area_Analysis_of_Nanoparticles](https://chem.libretexts.org/Bookshelves/Analytical_Chemistry/Book%3A_Physical_Methods_in_Chemistry_and_Nano_Science_(Barron)/02%3A_Physical_and_Thermal_Analysis/2.03%3A_BET_Surface_Area_Analysis_of_Nanoparticles) (Accessed: 4 October 2020).

Rajani, C. *et al.* (2018) 'Effects of granule particle size and lubricant concentration on tablet hardness containing large concentration of polymers', *Brazilian Journal of Pharmaceutical Sciences*, 53(3), p. 149. doi: 10.1590/s2175-97902017000300149.

Rajsharad, C. and Kamble, S. (2006) 'Pva based film coating and film coating compositions'. Available at: <https://www.google.com/patents/WO2006111980A2?cl=en> (Accessed: 7 May 2021).

Ramasamy, U. R., Gruppen, H. and Kabel, M. A. (2015) 'Water-holding capacity of soluble and insoluble polysaccharides in pressed potato fibre', *Industrial Crops and Products*, 64, pp. 242–250. doi: <https://doi.org/10.1016/j.indcrop.2014.09.036>.

Ramírez-Aragón, C. *et al.* (2018) 'Comparison of Cohesive models in EDEM and LIGGGHTS for simulating powder compaction', *Materials*, 11(11). doi: 10.3390/ma11112341.

Rani, G. T. *et al.* (2011) 'A Validated RP HPLC Method for Simultaneous Determination of Propranolol Hydrochloride and Alprazolam in Bulk and in Pharmaceutical Formulations', *Journal of Pharmacy Research*, 4(2), pp. 358–360. Available at: <http://jprsolutions.info> (Accessed: 30 March 2021).

Raval, N. *et al.* (2019) 'Chapter 10 - Importance of Physicochemical Characterization of Nanoparticles in Pharmaceutical Product Development', in Tekade, R. K. (ed.) *Basic*

Fundamentals of Drug Delivery. Academic Press (Advances in Pharmaceutical Product Development and Research), pp. 369–400. doi: <https://doi.org/10.1016/B978-0-12-817909-3.00010-8>.

Ré, M. (2007) 'Microencapsulation by Spray Drying', *Drying Technology: An International Journal*, 16, pp. 1195–1236. doi: 10.1080/07373939808917460.

Rengasamy, R. S. (2006) '5 - Wetting phenomena in fibrous materials', in Pan, N. and Gibson, P. (eds) *Thermal and Moisture Transport in Fibrous Materials*. Woodhead Publishing (Woodhead Publishing Series in Textiles), pp. 156–187. doi: <https://doi.org/10.1533/9781845692261.1.156>.

Research, P. M. (2018) *Global Industry Analysis and Forecast 2016-2024. Persistence Market Research. 2015.*", *Global Market Study on Orally Disintegrating Tablets (ODTs): Increasing Number of Clinical Trials to Push Investments*. Available at: <https://www.persistencemarketresearch.com/market-research/orally-disintegrating-tablet-market.asp> (Accessed: 8 June 2021).

Rinaudo, M. (2014) 'Biomaterials based on a natural polysaccharide: alginate', *TIP*, 17(1), pp. 92–96. doi: [https://doi.org/10.1016/S1405-888X\(14\)70322-5](https://doi.org/10.1016/S1405-888X(14)70322-5).

Ritthidej, G. C. (2011) 'Chapter 3 - Nasal Delivery of Peptides and Proteins with Chitosan and Related Mucoadhesive Polymers', in Van Der Walle, C. (ed.) *Peptide and Protein Delivery*. Boston: Academic Press, pp. 47–68. doi: <https://doi.org/10.1016/B978-0-12-384935-9.10003-3>.

Roberts, I. and Smith, I. M. (1987) 'A High Performance Liquid Chromatography Method for the Analysis of Total and Free Indomethacin in Serum', *Annals of Clinical Biochemistry*, 24(2), pp. 167–171. doi: 10.1177/000456328702400207.

ROBERTS, R. J. and ROWE, R. C. (1999) 'Relationships Between the Modulus of Elasticity and Tensile Strength for Pharmaceutical Drugs and Excipients', *Journal of Pharmacy and Pharmacology*, 51(9), pp. 975–977. doi: 10.1211/0022357991773438.

Rodrigues, S. *et al.* (2020) 'Inhalable spray-dried chondroitin sulphate microparticles: Effect of different solvents on particle properties and drug activity', *Polymers*, 12(2), p. 425. doi: 10.3390/polym12020425.

Rogers, A. J., Hashemi, A. and Ierapetritou, M. G. (2013) 'Modeling of particulate processes for the continuous manufacture of solid-based pharmaceutical dosage forms', *Processes*. MDPI AG, pp. 67–127. doi: 10.3390/pr1020067.

Roig, F. *et al.* (2011) 'Influence of hydrogen bonds on glass transition and dielectric relaxations of cellulose', *Journal of Physics D: Applied Physics*, 44(4). doi:

10.1088/0022-3727/44/4/045403.

Ronowicz, J. *et al.* (2015) 'A data mining approach to optimize pellets manufacturing process based on a decision tree algorithm', *European Journal of Pharmaceutical Sciences*, 73, pp. 44–48. doi: 10.1016/j.ejps.2015.03.013.

Rowe, Raymond C., Paul Sheskey, and M. Q. (2009) *Handbook of Pharmaceutical Excipients*. Available at: <https://www.pharmpress.com/files/docs/excipients8e-samplemono1.pdf> (Accessed: 25 October 2020).

Rowe, R. C., Sheskey, P. J. and Fenton, M. E. (2011) *The pain stethoscope: A clinician's guide to measuring pain*, *The pain stethoscope: A clinician's guide to measuring pain*. doi: 10.1007/978-1-908517-43-2.

Roy, J. (2011) '5 - Formulated drugs 1', in Roy, J. (ed.) *An Introduction to Pharmaceutical Sciences*. Woodhead Publishing (Woodhead Publishing Series in Biomedicine), pp. 111–140. doi: <https://doi.org/10.1533/9781908818041.111>.

Rujivipat, S. and Bodmeier, R. (2012) 'Moisture plasticization for enteric Eudragit® L30D-55-coated pellets prior to compression into tablets', *European Journal of Pharmaceutics and Biopharmaceutics*, 81(1), pp. 223–229. doi: 10.1016/j.ejpb.2012.01.003.

Sabri, A. H. *et al.* (2018) 'Understanding tablet defects in commercial manufacture and transfer', *Journal of Drug Delivery Science and Technology*, 46, pp. 1–6. doi: <https://doi.org/10.1016/j.jddst.2018.04.020>.

Sadeghi, F., Hijazi, H. and Garekani, H. A. (2011) 'Production of Ibuprofen Pellets Containing High Amount of Rate Retarding Eudragit RL Using PEG400 and Investigation of Their Physicomechanical Properties', *Iranian journal of basic medical sciences*, 14(4), pp. 383–390. Available at: <https://pubmed.ncbi.nlm.nih.gov/23492856>.

Sadeghi, F., Shahabi, M. and Afrasiabi Garekani, H. (2011) 'Comparison of physicomechanical properties of films prepared from organic solutions and aqueous dispersion of eudragit RL', *DARU, Journal of Pharmaceutical Sciences*, 19(2), pp. 100–106. Available at: [/pmc/articles/PMC3232102/](https://pubmed.ncbi.nlm.nih.gov/23492856) (Accessed: 8 May 2021).

Sadosky, A. *et al.* (2013) 'Impact of reducing dosing frequency on adherence to oral therapies: a literature review and meta-analysis', *Patient Preference and Adherence*, 7, p. 419. doi: 10.2147/ppa.s44646.

Sahoo, J. *et al.* (2008) 'Comparative study of propranolol hydrochloride release from matrix tablets with Kollidon®SR or hydroxy propyl methyl cellulose', *AAPS*

PharmSciTech, 9(2), pp. 577–582. doi: 10.1208/s12249-008-9092-2.

Sahputra, I. H., Alexiadis, A. and Adams, M. J. (2019) 'Effects of Moisture on the Mechanical Properties of Microcrystalline Cellulose and the Mobility of the Water Molecules as Studied by the Hybrid Molecular Mechanics–Molecular Dynamics Simulation Method', *Journal of Polymer Science, Part B: Polymer Physics*, 57(8), pp. 454–464. doi: 10.1002/polb.24801.

Salama, M. *et al.* (2015) 'Formulation and Evaluation of Ketoconazole Polymeric Films for Topical Application', *Journal of Applied Pharmaceutical Science*, 5, pp. 28–32. doi: 10.7324/JAPS.2015.50505.

Salman, S. A. B. *et al.* (2010) 'Quantitative determination of propranolol by ultraviolet HPLC in human plasma', *Toxicology Mechanisms and Methods*, 20(3), pp. 137–142. doi: 10.3109/15376511003602112.

Sambasivam, M., White, R. and Cutting, K. (2016) '12 - Exploring the role of polyurethane and polyvinyl alcohol foams in wound care', in Ågren, M. S. (ed.) *Wound Healing Biomaterials*. Woodhead Publishing, pp. 251–260. doi: <https://doi.org/10.1016/B978-1-78242-456-7.00012-X>.

Samimi, A., Hassanpour, A. and Ghadiri, M. (2005) 'Single and bulk compressions of soft granules: Experimental study and DEM evaluation', *Chemical Engineering Science*, 60(14), pp. 3993–4004. doi: <https://doi.org/10.1016/j.ces.2005.02.036>.

Sandler, N. *et al.* (2010) 'Effect of moisture on powder flow properties of theophylline', *Pharmaceutics*, 2(3), pp. 275–290. doi: 10.3390/pharmaceutics2030275.

Šantl, M. *et al.* (2011) 'A compressibility and compactibility study of real tableting mixtures: The impact of wet and dry granulation versus a direct tableting mixture', *International Journal of Pharmaceutics*, 414(1), pp. 131–139. doi: <https://doi.org/10.1016/j.ijpharm.2011.05.025>.

Santos, D. *et al.* (2018) 'Spray Drying: An Overview', in *Biomaterials - Physics and Chemistry - New Edition*. InTech. doi: 10.5772/intechopen.72247.

Santos, H. *et al.* (2002) 'Physical properties of chitosan pellets produced by extrusion-spheronisation: Influence of formulation variables', *International Journal of Pharmaceutics*, 246(1–2), pp. 153–169. doi: 10.1016/S0378-5173(02)00376-9.

Santos, H. *et al.* (2005) 'Compaction, compression and drug release properties of diclofenac sodium and ibuprofen pellets comprising xanthan gum as a sustained release agent', *International Journal of Pharmaceutics*, 295(1), pp. 15–27. doi: <https://doi.org/10.1016/j.ijpharm.2005.01.014>.

- Sareen, S., Joseph, L. and Mathew, G. (2012) 'Improvement in solubility of poor water-soluble drugs by solid dispersion', *International Journal of Pharmaceutical Investigation*, 2(1), p. 12. doi: 10.4103/2230-973x.96921.
- Saripella, K. K. *et al.* (2016a) 'A Quality by Experimental Design Approach to Assess the Effect of Formulation and Process Variables on the Extrusion and Spheronization of Drug-Loaded Pellets Containing Polyplasdone® XL-10', *AAPS PharmSciTech*, 17(2), pp. 368–379. doi: 10.1208/s12249-015-0345-6.
- Saripella, K. K. *et al.* (2016b) 'A Quality by Experimental Design Approach to Assess the Effect of Formulation and Process Variables on the Extrusion and Spheronization of Drug-Loaded Pellets Containing Polyplasdone® XL-10', *AAPS PharmSciTech*, 17(2), pp. 368–379. doi: 10.1208/s12249-015-0345-6.
- Saripella, K. K., Mallipeddi, R. and Neau, S. H. (2014) 'Crospovidone interactions with water. II. Dynamic vapor sorption analysis of the effect of Polyplasdone particle size on its uptake and distribution of water', *International Journal of Pharmaceutics*, 475(1), pp. 174–180. doi: <https://doi.org/10.1016/j.ijpharm.2014.08.040>.
- Sarkar, S., Ang, B. H. and Liew, C. V. (2014a) 'Influence of starting material particle size on pellet surface roughness', *AAPS PharmSciTech*, 15(1), pp. 131–139. doi: 10.1208/s12249-013-0031-5.
- Sarkar, S., Ang, B. H. and Liew, C. V. (2014b) 'Influence of starting material particle size on pellet surface roughness', *AAPS PharmSciTech*, 15(1), pp. 131–139. doi: 10.1208/s12249-013-0031-5.
- Sastry, S. V., Nyshadham, J. R. and Fix, Joseph A. (2000) 'Recent technological advances in oral drug delivery - A review', *Pharmaceutical Science and Technology Today*. *Pharm Sci Technol Today*, pp. 138–145. doi: 10.1016/S1461-5347(00)00247-9.
- Sastry, S. V., Nyshadham, J. R. and Fix, Joseph A (2000) 'Recent technological advances in oral drug delivery – a review', *Pharmaceutical Science & Technology Today*, 3(4), pp. 138–145. doi: [https://doi.org/10.1016/S1461-5347\(00\)00247-9](https://doi.org/10.1016/S1461-5347(00)00247-9).
- Saunders, M. (2008) 'Thermal Analysis of Pharmaceuticals', in *Principles and Applications of Thermal Analysis*, pp. 286–329. doi: 10.1002/9780470697702.ch8.
- Savjani Ketan, T., Gajjar Anuradha, K. and Savjani Jignasa, K. (2012) 'Drug Solubility: Importance and enhancement techniques', *ISRN pharmaceutics*, 2012. Available at: <https://www.ncbi.nlm.nih.gov/pmc/articles/PMC3399483/> (Accessed: 16 July 2020).
- Sawicki, W. and Łunio, R. (2005) 'Compressibility of floating pellets with verapamil

hydrochloride coated with dispersion Kollicoat SR 30 D', *European Journal of Pharmaceutics and Biopharmaceutics*, 60(1), pp. 153–158. doi: <https://doi.org/10.1016/j.ejpb.2004.11.003>.

Sawicki, W., Mazgalski, J. and Jakubowska, I. (2010) 'Hot tableting of slow-release tramadol hydrochloride microcapsules with cores obtained via compaction Hot tableting of slow-release tramadol microcapsules', *Drug Development and Industrial Pharmacy*, 36(2), pp. 209–217. doi: 10.3109/03639040903517898.

Schmid, W. and Picker-Freyer, K. M. (2009) 'Tableting and tablet properties of alginates: Characterisation and potential for Soft Tableting', *European Journal of Pharmaceutics and Biopharmaceutics*, 72(1), pp. 165–172. doi: <https://doi.org/10.1016/j.ejpb.2008.10.006>.

Schmool, D. S. and Markó, D. (2018) 'Magnetism in Solids: Hysteresis', in *Reference Module in Materials Science and Materials Engineering*. Elsevier. doi: <https://doi.org/10.1016/B978-0-12-803581-8.11413-4>.

Sebhatu, T. and Alderborn, G. (1999) 'Relationships between the effective interparticulate contact area and the tensile strength of tablets of amorphous and crystalline lactose of varying particle size', *European Journal of Pharmaceutical Sciences*, 8(4), pp. 235–242. doi: [https://doi.org/10.1016/S0928-0987\(99\)00025-1](https://doi.org/10.1016/S0928-0987(99)00025-1).

Sedlock, R. and Engineering, N. (2016) *A tableting Tabletability, compactibility, and compressibility: What's the difference?*, CSC publishing.

Seetha, A., Devaraj, H. and Sudhandiran, G. (2020) 'Indomethacin and juglone inhibit inflammatory molecules to induce apoptosis in colon cancer cells', *Journal of Biochemical and Molecular Toxicology*, 34(2), p. e22433. doi: <https://doi.org/10.1002/jbt.22433>.

Seo, J. A. *et al.* (2006) 'The glass transition temperatures of sugar mixtures', *Carbohydrate Research*, 341(15), pp. 2516–2520. doi: 10.1016/j.carres.2006.08.014.

Seo, K. S. *et al.* (2020) 'Pharmaceutical application of tablet film coating', *Pharmaceutics*, 12(9), pp. 1–20. doi: 10.3390/pharmaceutics12090853.

Shabir, G. A. (2011) 'Development and validation of RP-HPLC method for the determination of methamphetamine and propranolol in tablet dosage form', *Indian Journal of Pharmaceutical Sciences*, 73(4), pp. 430–435. doi: 10.4103/0250-474X.95632.

Shah, B., Kakumanu, V. K. and Bansal, A. K. (2006) 'Analytical techniques for quantification of amorphous/crystalline phases in pharmaceutical solids', *Journal of*

Pharmaceutical Sciences, 95(8), pp. 1641–1665. doi: <https://doi.org/10.1002/jps.20644>.

Shah, R. B., Tawakkul, M. A. and Khan, M. A. (2008) 'Comparative evaluation of flow for pharmaceutical powders and granules', *AAPS PharmSciTech*. 2008/02/15, 9(1), pp. 250–258. doi: 10.1208/s12249-008-9046-8.

Shah, R. D. *et al.* (1995) 'Physico-Mechanical Characterization of the Extrusion-Spheronization Process. Part II: Rheological Determinants for Successful Extrusion and Spheronization', *Pharmaceutical Research: An Official Journal of the American Association of Pharmaceutical Scientists*, 12(4), pp. 496–507. doi: 10.1023/A:1016237509740.

Shah, V. P. and Amidon, G. L. (2014) 'G.L. Amidon, H. Lennernas, V.P. Shah, and J.R. Crison. A theoretical basis for a biopharmaceutic drug classification: The correlation of in vitro drug product dissolution and in vivo bioavailability, Pharm Res 12, 413-420, 1995-Backstory of BCS', *AAPS Journal*. Springer New York LLC, pp. 894–898. doi: 10.1208/s12248-014-9620-9.

Shaker, H. *et al.* (2017) 'RP-HPLC–UV method for the quantification of propranolol in rat's serum and Krebs buffer using one-step protein precipitation', *Acta Chromatographica*, 30, pp. 1–6. doi: 10.1556/1326.2017.00018.

Shamma, R. N., Basalious, E. B. and Shoukri, R. A. (2011) 'Development and optimization of a multiple-unit controlled release formulation of a freely water soluble drug for once-daily administration', *International Journal of Pharmaceutics*, 405(1–2), pp. 102–112. doi: 10.1016/j.ijpharm.2010.12.003.

Sharma, M., Sharma, V., Panda, A. K., *et al.* (2011) 'Development of enteric submicron particle formulation of papain for oral delivery.', *International journal of nanomedicine*, 6, pp. 2097–2111. doi: 10.2147/ijn.s23985.

Sharma, M., Sharma, V., Panda, A., *et al.* (2011) 'Enteric Microsphere Formulations of Papain for Oral Delivery', *Yakugaku zasshi: Journal of the Pharmaceutical Society of Japan*, 131, pp. 697–709. doi: 10.1248/yakushi.131.697.

Sheehan, C. (2013) *General Chapters: <1174> Powder flow, Usp29-Nf24*. Available at:

http://www.pharmacopeia.cn/v29240/usp29nf24s0_c1174.html#usp29nf24s0_c1174-t2 (Accessed: 7 July 2020).

Shepard, K. B. *et al.* (2020) 'Impact of process parameters on particle morphology and filament formation in spray dried Eudragit L100 polymer', *Powder Technology*, 362,

pp. 221–230. doi: 10.1016/j.powtec.2019.12.013.

Shi, H. *et al.* (2018) 'Effect of particle size and cohesion on powder yielding and flow', *KONA Powder and Particle Journal*, 2018(35), pp. 226–250. doi: 10.14356/kona.2018014.

Shiga, H. *et al.* (2014) 'Encapsulation of alcohol dehydrogenase in mannitol by spray drying', *Pharmaceutics*, 6(1), pp. 185–194. doi: 10.3390/pharmaceutics6010185.

Šibanc, R. *et al.* (2013) 'Physical properties of pharmaceutical pellets', *Chemical Engineering Science*, 86, pp. 50–60. doi: <https://doi.org/10.1016/j.ces.2012.04.037>.

Siegel, R. A. and Rathbone, M. J. (2012) 'Overview of controlled release mechanisms', in *Fundamentals and Applications of Controlled Release Drug Delivery*. Springer US, pp. 19–43. doi: 10.1007/978-1-4614-0881-9_2.

Sigma-Aldrich (2021) *Poly(acrylic acid sodium salt) average Mw ~5,100 by GPC, powder* | Sigma-Aldrich. Available at: <https://www.sigmaaldrich.com/catalog/product/aldrich/447013?lang=en®ion=GB> (Accessed: 31 March 2021).

Silva, C. M. *et al.* (2006) 'Insulin encapsulation in reinforced alginate microspheres prepared by internal gelation', *European Journal of Pharmaceutical Sciences*, 29(2), pp. 148–159. doi: 10.1016/j.ejps.2006.06.008.

Sing, K. (2001) 'The use of nitrogen adsorption for the characterisation of porous materials', in *Colloids and Surfaces A: Physicochemical and Engineering Aspects*. Elsevier, pp. 3–9. doi: 10.1016/S0927-7757(01)00612-4.

Sing, K. S. W. (1982) 'Reporting physisorption data for gas/solid systems', *Pure and Applied Chemistry*, 54(11), pp. 2201–2218. doi: 10.1351/pac198254112201.

Singaraju, A. B. *et al.* (2016) 'Aggregate elasticity, crystal structure, and tableting performance for p-aminobenzoic acid and a series of its benzoate esters', *Molecular Pharmaceutics*, 13(11), pp. 3794–3806. doi: 10.1021/acs.molpharmaceut.6b00598.

Singh, A. and Van den Mooter, G. (2016) 'Spray drying formulation of amorphous solid dispersions', *Advanced Drug Delivery Reviews*, 100, pp. 27–50. Available at: <https://doi.org/10.1016/j.addr.2015.12.010>.

Singh, G., Pai, R. S. and Kusum Devi, V. (2012) 'Optimization of pellets containing solid dispersion prepared by extrusion/spheronization using central composite design and desirability function', *Journal of Young Pharmacists*, 4(3), pp. 146–156. doi: 10.4103/0975-1483.100020.

Singh, M. N. *et al.* (2010) 'Microencapsulation: A promising technique for controlled

drug delivery', *Research in pharmaceutical sciences*, 5(2), pp. 65–77. Available at: <https://pubmed.ncbi.nlm.nih.gov/21589795>.

Singh, S. *et al.* (2015) 'An overview of multifaceted significance of eudragit polymers in drug delivery systems', *Asian Journal of Pharmaceutical and Clinical Research*, pp. 1–6.

Singh, S. and SI, H. (2009) 'Eudragit and its Pharmaceutical Significance', <http://www.pharmainfo.net/satishsinghkadian/publications/eudragit-and-its-pharmaceutical-significance>, 247667(OCTOBER 2009), p. 17. Available at: http://www.farmavita.net/component/option,com_repository/Itemid,88/func,fileinfo/id,108/ (Accessed: 8 June 2021).

Sinha, P. *et al.* (2019) 'Surface Area Determination of Porous Materials Using the Brunauer–Emmett–Teller (BET) Method: Limitations and Improvements', *The Journal of Physical Chemistry C*, 123(33), pp. 20195–20209. doi: 10.1021/acs.jpcc.9b02116.

Sinha, V. *et al.* (2007) 'Influence of operational variables on properties of piroxicam pellets prepared by extrusion-spheronization: A technical note', *AAPS PharmSciTech*, 8, p. 20. doi: 10.1208/pt0801020.

Sinha, V. R. *et al.* (2009) 'Extrusion-spheronization: Process variables and characterization', *Critical Reviews in Therapeutic Drug Carrier Systems*, pp. 275–331. doi: 10.1615/CritRevTherDrugCarrierSyst.v26.i3.20.

Siow, C. R. S., Heng, P. W. S. and Chan, L. W. (2020) 'A study on the impact of HPMC viscosity grade and proportion on the functional properties of co-freeze-dried mannitol-HPMC cushioning excipients for compacted MUPS', *European Journal of Pharmaceutics and Biopharmaceutics*, 151, pp. 98–107. doi: <https://doi.org/10.1016/j.ejpb.2020.04.001>.

Smith, C. (2014) *What are the Main Benefits of Reversed Phase HPLC? Chromatography Today*. Available at: <https://www.chromatographytoday.com/news/hplc-uhplc/31/breaking-news/what-are-the-main-benefits-of-reversed-phase-hplc/30467> (Accessed: 30 March 2021).

Snejdrova, E. and Dittrich, M. (2012) 'Pharmaceutical Applications of Plasticized Polymers', in *Recent Advances in Plasticizers*. InTech. doi: 10.5772/39190.

Soares, J. P. *et al.* (2004) 'Thermal behavior of alginic acid and its sodium salt', *Ecletica Quimica*, 29(2), pp. 57–63. doi: 10.1590/s0100-46702004000200009.

Soni, V. *et al.* (2019) 'Chapter 13 - Design and Evaluation of Ophthalmic Delivery Formulations', in Tekade, R. K. (ed.) *Basic Fundamentals of Drug Delivery*. Academic

Press (Advances in Pharmaceutical Product Development and Research), pp. 473–538. doi: <https://doi.org/10.1016/B978-0-12-817909-3.00013-3>.

Sosnik, A. (2014) 'Alginate Particles as Platform for Drug Delivery by the Oral Route: State-of-the-Art', *ISRN Pharmaceuticals*. Edited by S. Raic-Malic et al., 2014, p. 926157. doi: 10.1155/2014/926157.

Sosnik, A. and Seremeta, K. (2015) 'Advantages and challenges of the spray-drying technology for the production of pure drug particles and drug-loaded polymeric carriers', *Advances in Colloid and Interface Science*, 223. doi: 10.1016/j.cis.2015.05.003.

Sosnik, A. and Seremeta, K. P. (2015) 'Advantages and challenges of the spray-drying technology for the production of pure drug particles and drug-loaded polymeric carriers', *Advances in Colloid and Interface Science*, 223, pp. 40–54. doi: 10.1016/j.cis.2015.05.003.

Srikanth, M. V. et al. (2012) 'Development and validation of HPLC method for estimation of propranolol HCL in human plasma', *Journal of Scientific and Industrial Research*, 71(2), pp. 120–123. Available at: https://www.researchgate.net/publication/227943908_Development_and_validation_of_HPLC_method_for_estimation_of_propranolol_HCL_in_human_plasma?enrichId=rgreq-e0dc08313928b0a3cb5b4ddef2571eb3-XXX&enrichSource=Y292ZXJQYWdlOzlyNzk0MzkwODtBUzozNDA1MzYzMzEzOTA (Accessed: 16 July 2020).

Staurt, C. (2008) *Overview of pharmaceutical excipients used in tablets and capsules*, *Drug Topics*. Available at: <https://www.drugtopics.com/view/overview-pharmaceutical-excipients-used-tablets-and-capsules> (Accessed: 24 April 2021).

Steckel, H. and Mindermann-Nogly, F. (2004) 'Production of chitosan pellets by extrusion/spheronization', *European Journal of Pharmaceutics and Biopharmaceutics*, 57(1), pp. 107–114. doi: [https://doi.org/10.1016/S0939-6411\(03\)00156-5](https://doi.org/10.1016/S0939-6411(03)00156-5).

Strasser, C. (2018) *Thermal Stability of Pharmaceuticals: Eudragit®, NETZSCH – the Thermal Analysis*. Available at: <https://ta-netzsch.com/thermal-stability-of-pharmaceuticals-eudragit> (Accessed: 3 June 2021).

Stulzer, H. K. et al. (2008) 'Development of controlled release captopril granules coated with ethylcellulose and methylcellulose by fluid bed dryer', *Drug Delivery*, 15(1), pp. 11–18. doi: 10.1080/10717540701827196.

Su, W. et al. (2017) 'Polymorphism of D-mannitol: Crystal structure and the crystal

growth mechanism', *Chinese Journal of Chemical Engineering*. Chemical Industry Press, pp. 358–362. doi: 10.1016/j.cjche.2016.09.002.

Sukul, A. *et al.* (2017) 'Comparative physicochemical, anti-inflammatory, and analgesic activity assay of synthesized chromium and nickel complexes of indomethacin', *Cogent Chemistry*. Edited by Y. Mehellou, 3(1), p. 1302312. doi: 10.1080/23312009.2017.1302312.

Sun, C. C. (2008) 'Mechanism of moisture induced variations in true density and compaction properties of microcrystalline cellulose', *International Journal of Pharmaceutics*, 346(1), pp. 93–101. doi: <https://doi.org/10.1016/j.ijpharm.2007.06.017>.

Sun, C. C. (2017) 'Microstructure of Tablet—Pharmaceutical Significance, Assessment, and Engineering', *Pharmaceutical Research*, 34(5), pp. 918–928. doi: 10.1007/s11095-016-1989-y.

Sun, C. and Grant, D. J. W. (2001) 'Influence of elastic deformation of particles on Heckel analysis', *Pharmaceutical Development and Technology*, 6(2), pp. 193–200. doi: 10.1081/PDT-100000738.

Sun, J. *et al.* (2012) 'Preparation and in vitro/in vivo evaluation of sustained-release venlafaxine hydrochloride pellets', *International Journal of Pharmaceutics*, 426(1–2), pp. 21–28. doi: 10.1016/j.ijpharm.2011.12.053.

Sun, W. J., Kothari, S. and Sun, C. C. (2018) 'The relationship among tensile strength, Young's modulus, and indentation hardness of pharmaceutical compacts', *Powder Technology*, 331, pp. 1–6. doi: 10.1016/j.powtec.2018.02.051.

Suresh Kumar, P. *et al.* (2019) 'Effect of pore size distribution and particle size of porous metal oxides on phosphate adsorption capacity and kinetics', *Chemical Engineering Journal*, 358, pp. 160–169. doi: 10.1016/j.cej.2018.09.202.

Suzzi, D. *et al.* (2012) 'DEM simulation of continuous tablet coating: Effects of tablet shape and fill level on inter-tablet coating variability', *Chemical Engineering Science*, 69(1), pp. 107–121. doi: 10.1016/j.ces.2011.10.009.

Swartz, M. E. and Krull, I. S. (2012) *Handbook of Analytical Validation, Handbook of Analytical Validation*. CRC Press. doi: 10.1201/b12039.

Swift, T. *et al.* (2016) 'The pH-responsive behaviour of poly(acrylic acid) in aqueous solution is dependent on molar mass', *Soft Matter*, 12(9), pp. 2542–2549. doi: 10.1039/c5sm02693h.

Szalay, A. (2015) *A few aspects on the importance of particle size enabling proper*

tableting. (Doctoral dissertation, szte).

Szumilo, M. *et al.* (2017) 'Assessment of physical properties of granules with paracetamol and caffeine', *Saudi Pharmaceutical Journal*, 25(6), pp. 900–905. doi: <https://doi.org/10.1016/j.jsps.2017.02.009>.

Taghe, S. *et al.* (2020) 'Polymeric inserts containing eudragit® L100 nanoparticle for improved ocular delivery of azithromycin', *Biomedicines*, 8(11), pp. 1–21. doi: [10.3390/biomedicines8110466](https://doi.org/10.3390/biomedicines8110466).

Taha, A. S. *et al.* (1996) 'Famotidine for the Prevention of Gastric and Duodenal Ulcers Caused by Nonsteroidal Antiinflammatory Drugs', *New England Journal of Medicine*, 334(22), pp. 1435–1439. doi: [10.1056/nejm199605303342204](https://doi.org/10.1056/nejm199605303342204).

Takeuchi, H. *et al.* (1998) 'Spray-dried composite particles of lactose and sodium alginate for direct tableting and controlled releasing', *International Journal of Pharmaceutics*, 174(1), pp. 91–100. doi: [https://doi.org/10.1016/S0378-5173\(98\)00248-8](https://doi.org/10.1016/S0378-5173(98)00248-8).

Tamrakar, A. and Ramachandran, R. (2019) 'CFD–DEM–PBM coupled model development and validation of a 3D top-spray fluidized bed wet granulation process', *Computers and Chemical Engineering*, 125, pp. 249–270. doi: [10.1016/j.compchemeng.2019.01.023](https://doi.org/10.1016/j.compchemeng.2019.01.023).

Tan, X. and Hu, J. (2016a) 'Investigation for the quality factors on the tablets containing medicated pellets', *Saudi Pharmaceutical Journal*, 24(5), pp. 507–514. doi: <https://doi.org/10.1016/j.jsps.2015.01.020>.

Tan, X. and Hu, J. (2016b) 'Investigation for the quality factors on the tablets containing medicated pellets', *Saudi Pharmaceutical Journal*, 24(5), pp. 507–514. doi: [10.1016/j.jsps.2015.01.020](https://doi.org/10.1016/j.jsps.2015.01.020).

Tanabe, S. *et al.* (2019) 'Influence of particle size and blender size on blending performance of bi-component granular mixing: A dem and experimental study', *European Journal of Pharmaceutical Sciences*, 134, pp. 205–218.

Tanaka, M. and Iizuka, H. (1991) 'Effects of grain size and microstructures on the internal friction and Young's modulus of a high-strength steel HT-80', *Journal of Materials Science*, 26(16), pp. 4389–4393. doi: [10.1007/BF00543656](https://doi.org/10.1007/BF00543656).

Tang, X. *et al.* (no date) 'Development and Validation of HPLC Methods for the Determination of Propranolol Hydrochloride and Hydrochlorothiazid Related Substances in'.

Tank, D. *et al.* (2018) 'Investigate the Effect of Solvents on Wet granulation of

Microcrystalline Cellulose using Hydroxypropyl methylcellulose as a binder and evaluation of rheological and thermal characteristics of granules', *Saudi Pharmaceutical Journal*, 26. doi: 10.1016/j.jsps.2018.02.007.

Thakral, S., Thakral, N. K. and Majumdar, D. K. (2013a) 'Eudragit®: A technology evaluation', *Expert Opinion on Drug Delivery*, 10(1), pp. 131–149. doi: 10.1517/17425247.2013.736962.

Thakral, S., Thakral, N. K. and Majumdar, D. K. (2013b) 'Eudragit®: A technology evaluation', *Expert Opinion on Drug Delivery*, 10(1), pp. 131–149. doi: 10.1517/17425247.2013.736962.

Thapa, P. *et al.* (2017) 'Effects of moisture content and compression pressure of various deforming granules on the physical properties of tablets', *Powder Technology*, 310, pp. 92–102. doi: 10.1016/j.powtec.2017.01.021.

Thirugnanasambandham, K. and Sivakumar, V. (2017) 'Influence of process conditions on the physicochemical properties of pomegranate juice in spray drying process: Modelling and optimization', *Journal of the Saudi Society of Agricultural Sciences*, 16(4), pp. 358–366. doi: <https://doi.org/10.1016/j.jssas.2015.11.005>.

Thiry, J., Krier, F. and Evrard, B. (2015) 'A review of pharmaceutical extrusion: Critical process parameters and scaling-up', *International Journal of Pharmaceutics*. Elsevier B.V., pp. 227–240. doi: 10.1016/j.ijpharm.2014.12.036.

Tho, I. and Bauer-Brandl, A. (2011) 'Quality by design (QbD) approaches for the compression step of tableting', *Expert opinion on drug delivery*, 8, pp. 1631–1644. doi: 10.1517/17425247.2011.633506.

Thomas, D. *et al.* (2018) 'Fundamental thermal properties of polyvinyl alcohol by fast scanning calorimetry', *Polymer*, 137. doi: 10.1016/j.polymer.2018.01.004.

Thomas, D. and Cebe, P. (2017) 'Self-nucleation and crystallization of polyvinyl alcohol', *Journal of Thermal Analysis and Calorimetry*, 127(1), pp. 885–894. doi: 10.1007/s10973-016-5811-1.

Thomas, L. C. (2001) 'Use of multiple heating rate DSC and modulated temperature DSC to detect and analyze temperature-time-dependent transitions in materials', *American Laboratory*, 33(1).

Thommes, M. *et al.* (2009) 'Improved bioavailability of darunavir by use of κ -carrageenan versus microcrystalline cellulose as pelletisation aid', *European Journal of Pharmaceutics and Biopharmaceutics*, 72(3), pp. 614–620. doi: 10.1016/j.ejpb.2009.03.004.

- Thommes, M. *et al.* (2015) 'Physisorption of gases, with special reference to the evaluation of surface area and pore size distribution (IUPAC Technical Report)', *Pure and Applied Chemistry*, 87(9–10), pp. 1051–1069. doi: 10.1515/pac-2014-1117.
- Thommes, M. and Kleinebudde, P. (2006) 'Use of κ -carrageenan as alternative pelletisation aid to microcrystalline cellulose in extrusion/spheronisation. II. Influence of drug and filler type', *European Journal of Pharmaceutics and Biopharmaceutics*, 63(1), pp. 68–75. doi: <https://doi.org/10.1016/j.ejpb.2005.10.003>.
- Thommes, M. and Kleinebudde, P. (2007) 'Properties of Pellets Manufactured by Wet Extrusion / Spheronization Process Using κ -Carrageenan: Effect of Process Parameters', *AAPS PharmSciTech* 2007, 8(4), pp. 4–11.
- Thoorens, G. *et al.* (2014) 'Microcrystalline cellulose, a direct compression binder in a quality by design environment - A review', *International Journal of Pharmaceutics*. Elsevier, pp. 64–72. doi: 10.1016/j.ijpharm.2014.06.055.
- Tiefenbacher, K. F. (2017) 'Chapter Six - Wafer Sheet Manufacturing: Technology and Products', in Tiefenbacher, K. F. (ed.) *Wafer and Waffle*. Academic Press, pp. 405–486. doi: <https://doi.org/10.1016/B978-0-12-809438-9.00006-5>.
- Tiwari, R., Agarwal, S. K. and Tiwari, S. (2013) 'Formulation and multivariate optimization of Microcrystalline Cellulose pellets of highly water soluble drug', *International Journal of Drug Delivery*, 5(2), pp. 206–213. doi: 10.5138/ijdd.v5i2.1156.
- Tjipangandjara, K. F. and Somasundaran, P. (1992) 'Effects of the conformation of polyacrylic acid on the dispersion-flocculation of alumina and kaolinite fines', *Advanced Powder Technology*, 3(2), pp. 119–127. doi: 10.1016/S0921-8831(08)60678-0.
- Tomer, G. *et al.* (2001) 'Measuring the water retention capacities (MRC) of different microcrystalline cellulose grades', *European Journal of Pharmaceutical Sciences*, 12(3), pp. 321–325. doi: 10.1016/S0928-0987(00)00188-3.
- Torrado, J. J. and Augsburger, L. L. (1994) 'Effect of different excipients on the tableting of coated particles', *International Journal of Pharmaceutics*, 106(2), pp. 149–155. doi: [https://doi.org/10.1016/0378-5173\(94\)90313-1](https://doi.org/10.1016/0378-5173(94)90313-1).
- Trasi, N. S. *et al.* (2011) 'Investigating the effect of dehydration conditions on the compactability of glucose', *International Journal of Pharmaceutics*, 406(1), pp. 55–61. doi: <https://doi.org/10.1016/j.ijpharm.2010.12.042>.
- Tripathi, R. and Mishra, B. (2012) 'Development and evaluation of sodium alginate-polyacrylamide graft-co-polymer-based stomach targeted hydrogels of famotidine',

AAPS PharmSciTech, 13(4), pp. 1091–1102. doi: 10.1208/s12249-012-9824-1.

Tseng, H.-W. *et al.* (2018) 'Effect of molecular weight of poly(acrylic acid) on the interaction of oppositely charged ionic surfactant–polyelectrolyte mixtures', *Journal of the Taiwan Institute of Chemical Engineers*, 92, pp. 50–57. doi: <https://doi.org/10.1016/j.jtice.2018.02.030>.

Tsvetkova, B. *et al.* (2012) 'High performance liquid chromatographic assay of indomethacin and its related substances in tablet dosage forms', *International Journal of Pharmacy and Pharmaceutical Sciences*, 4, pp. 549–552.

Tunón, Å. (2003) *Preparation of Tablets from Reservoir Pellets with an Emphasis on the Compression Behaviour and Drug Release, Comprehensive Summaries of Uppsala Dissertations from the Faculty of Pharmacy NV - 288*. Acta Universitatis Upsaliensis. Available at: <http://uu.diva-portal.org/smash/get/diva2:162716/FULLTEXT01.pdf>.

Tunón, Å., Gråsjö, J. and Alderborn, G. (2003) 'Effect of intragranular porosity on compression behaviour of and drug release from reservoir pellets', *European Journal of Pharmaceutical Sciences*, 19(5), pp. 333–344. doi: 10.1016/S0928-0987(03)00106-4.

Umemoto, Y. *et al.* (2020) 'An effective polyvinyl alcohol for the solubilization of poorly water-soluble drugs in solid dispersion formulations', *Journal of Drug Delivery Science and Technology*, 55, p. 101401. doi: <https://doi.org/10.1016/j.jddst.2019.101401>.

United Nations Office on Drugs and Crime (UNODC) (2009) *Guidance for the validation of analytical methodology and calibration of equipment used for testing of illicit drugs in seized materials and biological specimens : a commitment to quality and continuous improvement*, United Nations Office on Drugs and Crime. Available at: www.unodc.org (Accessed: 2 April 2021).

Urakami, K. *et al.* (2002) 'A Novel Method for Estimation of Transition Temperature for Polymorphic Pairs in Pharmaceuticals Using Heat of Solution and Solubility Data', *Chemical & pharmaceutical bulletin*, 50, pp. 263–267. doi: 10.1248/cpb.50.263.

USP (2014) 'Chapter 616 Bulk Density and Tapped Density of Powders', *The United States Pharmacopeial Convention*, 06(2012), pp. 2014–2016. Available at: <https://www.usp.org/harmonization-standards/pdg/general-chapters/bulk-density-and-tapped-density-of-powers> (Accessed: 1 May 2021).

USP37-NF32 (2014) 'Tablet Breaking Force', *U.S. Pharmacopeia*. Available at: https://www.drugfuture.com/pharmacopoeia/usp32/pub/data/v32270/usp32nf27s0_c

1217.html (Accessed: 11 April 2021).

USPC, U. S. P. C. (2014) 'Method II-Measurement in a Volumeter', *The United States Pharmacopeial Convention*, 06(2012), pp. 2014–2016. Available at: https://www.usp.org/sites/default/files/usp/document/harmonization/gen-chapter/bulk_density.pdf (Accessed: 1 May 2021).

Vanhoorne, V. *et al.* (2016) 'Improved tableability after a polymorphic transition of delta-mannitol during twin screw granulation', *International Journal of Pharmaceutics*, 506(1), pp. 13–24. doi: <https://doi.org/10.1016/j.ijpharm.2016.04.025>.

Varshosaz, J. *et al.* (2012) 'Development and Evaluation of a Novel Pellet-Based Tablet System for Potential Colon Delivery of Budesonide', *Journal of Drug Delivery*. Edited by J. Y. Fang, 2012, p. 905191. doi: 10.1155/2012/905191.

Veen, B. *et al.* (2000) 'Tensile strength of tablets containing two material with a different compaction behaviour', *International journal of pharmaceutics*, 203, pp. 71–79. doi: 10.1016/S0378-5173(00)00450-6.

Velmurugan, S., and S. V. (2010) 'Oral disintegrating tablets: An overview', *Int. J. Chem. Pharm. Sci.*, 1(2), pp. 1–12. Available at: www.ijcps.com.

Venkata Srikanth, M. *et al.* (2012) 'Statistical design and evaluation of a propranolol HCl gastric floating tablet', *Acta Pharmaceutica Sinica B*, 2(1), pp. 60–69. doi: 10.1016/j.apsb.2011.12.008.

Vervaeet, C., Baert, L. and Remon, J. P. (1995) 'Extrusion-spheronisation A literature review', *International Journal of Pharmaceutics*, 116(2), pp. 131–146. doi: 10.1016/0378-5173(94)00311-R.

Vhora, I., Khatri, N. and Misra, A. (2021) 'Chapter 8 - Applications of Polymers in Parenteral Drug Delivery', in Misra, A. and Shahiwala, A. B. T.-A. of P. in D. D. (Second E. (eds). Elsevier, pp. 221–261. doi: <https://doi.org/10.1016/B978-0-12-819659-5.00008-2>.

Villetti, M. *et al.* (2011) 'Physicochemical Properties of Methylcellulose and Dodecyltrimethylammonium Bromide in Aqueous Medium', *The journal of physical chemistry. B*, 115, pp. 5868–5876. doi: 10.1021/jp110247r.

Vlachou, M. *et al.* (2019) 'Development and characterization of eudragit®-based electrospun nanofibrous mats and their formulation into nanofiber tablets for the modified release of furosemide', *Pharmaceutics*, 11(9), p. 480. doi: 10.3390/pharmaceutics11090480.

Voogt, B. *et al.* (2019) 'Film Formation of High Tg Latex Using Hydroplasticization:

- Explanations from NMR Relaxometry', *Langmuir*, 35(38), pp. 12418–12427. doi: 10.1021/acs.langmuir.9b01353.
- Wagner, K. G. and McGinity, J. W. (2002) 'Influence of chloride ion exchange on the permeability and drug release of Eudragit RS 30 D films', *Journal of Controlled Release*, 82(2–3), pp. 385–397. doi: 10.1016/S0168-3659(02)00145-1.
- Walters-Salas, T. (2012) 'The challenge of patient adherence', *Bariatric Nursing and Surgical Patient Care*, 7(4), p. 186. doi: 10.1089/bar.2012.9960.
- Walton, D. E. (2000) 'THE MORPHOLOGY OF SPRAY-DRIED PARTICLES A QUALITATIVE VIEW', *Drying Technology*, 18(9), pp. 1943–1986. doi: 10.1080/07373930008917822.
- Wang, C. C. *et al.* (1996) 'Mechanical properties of single pellets containing acrylic polymers', *Pharmaceutical Development and Technology*, 1(2), pp. 213–222. doi: 10.3109/10837459609029896.
- Wang, C. C. *et al.* (1997) 'Influence of plasticizers on the mechanical properties of pellets containing eudragit® RS 30 d', *International Journal of Pharmaceutics*, 152(2), pp. 153–163. doi: 10.1016/S0378-5173(97)00080-X.
- Wang, Q. J. and Zhu, D. (2013) 'Hertz Theory: Contact of Spherical Surfaces', in Wang, Q. J. and Chung, Y.-W. (eds) *Encyclopedia of Tribology*. Boston, MA: Springer US, pp. 1654–1662. doi: 10.1007/978-0-387-92897-5_492.
- Wang, W., Dufour, C. and Zhou, W. (2015) 'Impacts of spray-drying conditions on the physicochemical properties of soy sauce powders using maltodextrin as auxiliary drying carrier', *CyTA - Journal of Food*, 13(4), pp. 548–555. doi: 10.1080/19476337.2015.1014430.
- Wang, X. *et al.* (2007) 'Phase characterization of indomethacin in binary solid dispersions with PVP VA64 or Myrj 52', *International Journal of Pharmaceutics*, 345(1–2), pp. 95–100. doi: 10.1016/j.ijpharm.2007.05.046.
- Wang, X. and Li, J. (2014) 'Simulation of triaxial response of granular materials by modified DEM', *Science China Physics, Mechanics & Astronomy*, 57(12), pp. 2297–2308.
- Wang, Y. and Alonso-Marroquin, F. (2009) 'A finite deformation method for discrete modeling: Particle rotation and parameter calibration', *Granular Matter*, 11(5), pp. 331–343. doi: 10.1007/s10035-009-0146-2.
- Waters (2018) 'HPLC Separation Modes: Waters', *Technology*. Available at: https://www.waters.com/waters/en_GB/HPLC-Separation-

Modes/nav.htm?cid=10049076&locale=en_GB (Accessed: 17 July 2020).

Wei, Q., Yang, F. and Luan, L. (2013) 'Preparation and in vitro/in vivo evaluation of a ketoprofen orally disintegrating/sustained release tablet', *Drug Development and Industrial Pharmacy*, 39(6), pp. 928–934. doi: 10.3109/03639045.2012.664146.

Welling, G. W. and Welling-Wester, S. (2000) 'Chapter 12 - Integral Membrane Proteins', in Kastner, M. B. T.-J. of C. L. (ed.) *Protein Liquid Chromatography*. Elsevier, pp. 527–556. doi: [https://doi.org/10.1016/S0301-4770\(08\)60540-0](https://doi.org/10.1016/S0301-4770(08)60540-0).

Wen, H. and Park, K. (2010) *Oral Controlled Release Formulation Design and Drug Delivery: Theory to Practice*, *Oral Controlled Release Formulation Design and Drug Delivery: Theory to Practice*. doi: 10.1002/9780470640487.

Westermarck, S. *et al.* (1998) 'Pore structure and surface area of mannitol powder, granules and tablets determined with mercury porosimetry and nitrogen adsorption', *European Journal of Pharmaceutics and Biopharmaceutics*, 46(1), pp. 61–68. doi: [https://doi.org/10.1016/S0939-6411\(97\)00169-0](https://doi.org/10.1016/S0939-6411(97)00169-0).

Wiącek, J. and Stasiak, M. (2018) 'Effect of the particle size ratio on the structural properties of granular mixtures with discrete particle size distribution', *Granular Matter*, 20(2), p. 31. doi: 10.1007/s10035-018-0800-7.

Wu, C.-Y. *et al.* (2008) 'Numerical and experimental investigation of capping mechanisms during pharmaceutical tablet compaction', *Powder Technology*, 181(2), pp. 121–129. doi: <https://doi.org/10.1016/j.powtec.2006.12.017>.

Wu, C. and McGinity, J. W. (2000) 'Influence of relative humidity on the mechanical and drug release properties of theophylline pellets coated with an acrylic polymer containing methylparaben as a non-traditional plasticizer', *European Journal of Pharmaceutics and Biopharmaceutics*, 50(2), pp. 277–284. doi: 10.1016/S0939-6411(99)00088-0.

Wu, Chuan Yu *et al.* (2005) 'Finite element analysis of capping mechanisms during pharmaceutical powder compaction', in *Advances in Powder Metallurgy and Particulate Materials - 2005, Proceedings of the 2005 International Conference on Powder Metallurgy and Particulate Materials, PowderMet 2005*, pp. 62–73.

Wu, C. Y. *et al.* (2005) 'Modelling the mechanical behaviour of pharmaceutical powders during compaction', *Powder Technology*, 152(1–3), pp. 107–117. doi: 10.1016/j.powtec.2005.01.010.

Wu, Y. *et al.* (2011) 'Reactive impurities in excipients: Profiling, identification and mitigation of drug-excipient incompatibility', *AAPS PharmSciTech*, 12(4), pp. 1248–

1263. doi: 10.1208/s12249-011-9677-z.

Wulff, R. and Leopold, C. S. (2014) 'Coatings from blends of Eudragit® RL and L55: A novel approach in pH-controlled drug release', *International Journal of Pharmaceutics*, 476(1), pp. 78–87. doi: <https://doi.org/10.1016/j.ijpharm.2014.09.023>.

Xu, M., Heng, P. W. S. and Liew, C. V. (2016) 'Formulation and process strategies to minimize coat damage for compaction of coated pellets in a rotary tablet press: A mechanistic view', *International Journal of Pharmaceutics*, 499(1), pp. 29–37. doi: <https://doi.org/10.1016/j.ijpharm.2015.12.068>.

Yadav, N. and Verma, A. (2016) 'Pharmaceutical Pellets: A Versatile Carrier for Oral Controlled Delivery of Drugs', *Indian journal of pharmaceutical education*, 50. doi: 10.5530/ijper.50.3.27.

Yadav, P. and Majee, C. (2015) 'Method development and validation for quantification of propranolol HCL in pharmaceutical dosage form by RP-UPLC', *International Journal of PharmTech Research*, 7, pp. 197–203.

Yang, B. *et al.* (2018) 'Evaluation about wettability, water absorption or swelling of excipients through various methods and the correlation between these parameters and tablet disintegration', *Drug Development and Industrial Pharmacy*, 44(9), pp. 1417–1425. doi: 10.1080/03639045.2018.1453519.

Yang, L. and Alexandridis, P. (2000) 'Physicochemical aspects of drug delivery and release from polymer-based colloids', *Current Opinion in Colloid & Interface Science*, 5(1), pp. 132–143. doi: [https://doi.org/10.1016/S1359-0294\(00\)00046-7](https://doi.org/10.1016/S1359-0294(00)00046-7).

Yang, Z. *et al.* (2016) 'A method for the preparation of sustained release-coated Metoprolol Succinate pellet-containing tablets', *Pharmaceutical Development and Technology*, 21(8), pp. 943–950. doi: 10.3109/10837450.2015.1081612.

Yassin, S. *et al.* (2015) 'The Disintegration Process in Microcrystalline Cellulose Based Tablets, Part 1: Influence of Temperature, Porosity and Superdisintegrants', *Journal of Pharmaceutical Sciences*, 104(10), pp. 3440–3450. doi: 10.1002/jps.24544.

Yeom, S. Bin *et al.* (2019) 'Application of the discrete element method for manufacturing process simulation in the pharmaceutical industry', *Pharmaceutics*. MDPI AG. doi: 10.3390/pharmaceutics11080414.

Yohana Chaerunisaa, A., Sriwidodo, S. and Abdassah, M. (2020) 'Microcrystalline Cellulose as Pharmaceutical Excipient', in *Pharmaceutical Formulation Design - Recent Practices*. IntechOpen. doi: 10.5772/intechopen.88092.

Yohannes, B. *et al.* (2017) 'Discrete particle modeling and micromechanical

characterization of bilayer tablet compaction', *International Journal of Pharmaceutics*, 529(1–2), pp. 597–607. doi: 10.1016/j.ijpharm.2017.07.032.

Yoshinari, T. *et al.* (2003) 'The improved compaction properties of mannitol after a moisture-induced polymorphic transition', *International journal of pharmaceutics*, 258, pp. 121–131. doi: 10.1016/S0378-5173(03)00157-1.

Yoshioka, M., Hancock, B. C. and Zografi, G. (1994) 'Crystallization of indomethacin from the amorphous state below and above its glass transition temperature', *Journal of Pharmaceutical Sciences*, 83(12), pp. 1700–1705. doi: 10.1002/jps.2600831211.

Younes, M. *et al.* (2018) 'Safety of low-substituted hydroxypropyl cellulose (L-HPC) to be used as a food additive in food supplements in tablet form', *EFSA Journal*, 16(1), p. 5062. doi: 10.2903/j.efsa.2018.5062.

Yuan, Y. and Lee, T. R. (2013) 'Contact Angle and Wetting Properties'.

Zainuddin, M. *et al.* (2014) 'Effect of Moisture Content on Physical Properties of Animal Feed Pellets from Pineapple Plant Waste', *Agriculture and Agricultural Science Procedia*, 2, pp. 224–230. doi: 10.1016/j.aaspro.2014.11.032.

Zarmpi, P. *et al.* (2020) 'Impact of Magnesium Stearate Presence and Variability on Drug Apparent Solubility Based on Drug Physicochemical Properties', *AAPS Journal*, 22(4). doi: 10.1208/s12248-020-00449-w.

Zeeshan, F., Peh, K. K. and Tan, Y. T. F. (2009) 'Exploring the potential of a highly compressible microcrystalline cellulose as novel tableting excipient in the compaction of extended-release coated pellets containing an extremely water-soluble model drug', *AAPS PharmSciTech*, 10(3), pp. 850–857. doi: 10.1208/s12249-009-9278-2.

Zhang, J. *et al.* (2017) 'On identification of critical material attributes for compression behaviour of pharmaceutical diluent powders', *Materials*, 10(7). doi: 10.3390/ma10070845.

Zhang, P. (2016) 'Adsorption and Desorption Isotherms', *KE Group*. Available at: http://www.kererearchgroup.com/uploads/4/8/4/5/48456521/160903_introduction_to_bet_isotherms.pdf (Accessed: 28 March 2021).

Zhang, T. and Youan, B. B. C. (2010) 'Analysis of process parameters affecting spray-dried oily core nanocapsules using factorial design', *AAPS PharmSciTech*, 11(3), pp. 1422–1431. doi: 10.1208/s12249-010-9516-7.

Zhou, M. *et al.* (2018) 'Development on porous particles of: Pueraria lobatae Radix for improving its compactibility and dissolution', *RSC Advances*, 8(43), pp. 24250–24260. doi: 10.1039/c8ra04125c.

- Zhu, Y. *et al.* (2002) 'Solid-state plasticization of an acrylic polymer with chlorpheniramine maleate and triethyl citrate', *International Journal of Pharmaceutics*, 241(2), pp. 301–310. doi: [https://doi.org/10.1016/S0378-5173\(02\)00244-2](https://doi.org/10.1016/S0378-5173(02)00244-2).
- Ziaee, A. *et al.* (2019) 'Spray drying of pharmaceuticals and biopharmaceuticals: Critical parameters and experimental process optimization approaches', *European Journal of Pharmaceutical Sciences*, 127, pp. 300–318. doi: [10.1016/j.ejps.2018.10.026](https://doi.org/10.1016/j.ejps.2018.10.026).
- Zielinski, J. M. and Kettle, L. (2013) 'Pharmaceutical Physical Characterization: Surface Area and Porosity', *White paper, Intertek Chemicals and Pharmaceuticals*. Intertek Chemicals and Pharmaceuticals. Available at: <https://docplayer.net/17669226-Pharmaceutical-physical-characterization-surface-area-and-porosity.html>.
- Ziffels, S. and Steckel, H. (2010) 'Influence of amorphous content on compaction behaviour of anhydrous α -lactose', *International Journal of Pharmaceutics*, 387(1), pp. 71–78. doi: <https://doi.org/10.1016/j.ijpharm.2009.12.009>.
- Zimper, U. *et al.* (2010) 'Quantification of process induced disorder in milled samples using different analytical techniques', *Pharmaceutics*, 2(1), pp. 30–49. doi: [10.3390/pharmaceutics2010030](https://doi.org/10.3390/pharmaceutics2010030).
- Zoubari, G., Ali, R. and Dashevskiy, A. (2019) 'Water-soluble and -insoluble polymers as binders for pellet preparation by extrusion/spheronization', *Journal of Drug Delivery Science and Technology*, 49, pp. 1–5. doi: <https://doi.org/10.1016/j.jddst.2018.10.030>.